

REGULATION OF ENDOPLASMIC RETICULUM AND MITOCHONDRIA IN CELLULAR HOMEOSTASIS

EDITED BY: Yongye Huang, Jianguang Ji, Jun Song and Qi Zhao
PUBLISHED IN: *Frontiers in Cell and Developmental Biology*



frontiers

Frontiers eBook Copyright Statement

The copyright in the text of individual articles in this eBook is the property of their respective authors or their respective institutions or funders. The copyright in graphics and images within each article may be subject to copyright of other parties. In both cases this is subject to a license granted to Frontiers.

The compilation of articles constituting this eBook is the property of Frontiers.

Each article within this eBook, and the eBook itself, are published under the most recent version of the Creative Commons CC-BY licence.

The version current at the date of publication of this eBook is CC-BY 4.0. If the CC-BY licence is updated, the licence granted by Frontiers is automatically updated to the new version.

When exercising any right under the CC-BY licence, Frontiers must be attributed as the original publisher of the article or eBook, as applicable.

Authors have the responsibility of ensuring that any graphics or other materials which are the property of others may be included in the CC-BY licence, but this should be checked before relying on the CC-BY licence to reproduce those materials. Any copyright notices relating to those materials must be complied with.

Copyright and source acknowledgement notices may not be removed and must be displayed in any copy, derivative work or partial copy which includes the elements in question.

All copyright, and all rights therein, are protected by national and international copyright laws. The above represents a summary only. For further information please read Frontiers' Conditions for Website Use and Copyright Statement, and the applicable CC-BY licence.

ISSN 1664-8714

ISBN 978-2-83250-189-4

DOI 10.3389/978-2-83250-189-4

About Frontiers

Frontiers is more than just an open-access publisher of scholarly articles: it is a pioneering approach to the world of academia, radically improving the way scholarly research is managed. The grand vision of Frontiers is a world where all people have an equal opportunity to seek, share and generate knowledge. Frontiers provides immediate and permanent online open access to all its publications, but this alone is not enough to realize our grand goals.

Frontiers Journal Series

The Frontiers Journal Series is a multi-tier and interdisciplinary set of open-access, online journals, promising a paradigm shift from the current review, selection and dissemination processes in academic publishing. All Frontiers journals are driven by researchers for researchers; therefore, they constitute a service to the scholarly community. At the same time, the Frontiers Journal Series operates on a revolutionary invention, the tiered publishing system, initially addressing specific communities of scholars, and gradually climbing up to broader public understanding, thus serving the interests of the lay society, too.

Dedication to Quality

Each Frontiers article is a landmark of the highest quality, thanks to genuinely collaborative interactions between authors and review editors, who include some of the world's best academicians. Research must be certified by peers before entering a stream of knowledge that may eventually reach the public - and shape society; therefore, Frontiers only applies the most rigorous and unbiased reviews.

Frontiers revolutionizes research publishing by freely delivering the most outstanding research, evaluated with no bias from both the academic and social point of view. By applying the most advanced information technologies, Frontiers is catapulting scholarly publishing into a new generation.

What are Frontiers Research Topics?

Frontiers Research Topics are very popular trademarks of the Frontiers Journals Series: they are collections of at least ten articles, all centered on a particular subject. With their unique mix of varied contributions from Original Research to Review Articles, Frontiers Research Topics unify the most influential researchers, the latest key findings and historical advances in a hot research area! Find out more on how to host your own Frontiers Research Topic or contribute to one as an author by contacting the Frontiers Editorial Office: frontiersin.org/about/contact

REGULATION OF ENDOPLASMIC RETICULUM AND MITOCHONDRIA IN CELLULAR HOMEOSTASIS

Topic Editors:

Yongye Huang, Northeastern University, China

Jianguang Ji, Lund University, Sweden

Jun Song, University of Michigan, United States

Qi Zhao, University of Science and Technology Liaoning, China

Citation: Huang, Y., Ji, J., Song, J., Zhao, Q., eds. (2022). Regulation of Endoplasmic Reticulum and Mitochondria in Cellular Homeostasis. Lausanne: Frontiers Media SA. doi: 10.3389/978-2-83250-189-4

Table of Contents

- 05 Editorial: Regulation of Endoplasmic Reticulum and Mitochondria in Cellular Homeostasis**
Yongye Huang, Jianguang Ji, Qi Zhao and Jun Song
- 08 Therapeutic Effects of Natural Compounds and Small Molecule Inhibitors Targeting Endoplasmic Reticulum Stress in Alzheimer's Disease**
Xun Gao and Yuanyuan Xu
- 16 Immune Cell Infiltration Landscape of Ovarian Cancer to Identify Prognosis and Immunotherapy-Related Genes to Aid Immunotherapy**
Xiushen Li, Weizheng Liang, Huanyi Zhao, Zheng Jin, Guoqi Shi, Wanhua Xie, Hao Wang and Xueqing Wu
- 27 Mitochondrial Defects in Fibroblasts of Pathogenic MAPT Patients**
Vinita Bharat, Chung-Han Hsieh and Xinnan Wang
- 37 Endoplasmic Reticulum-Mitochondria Contacts: A Potential Therapy Target for Cardiovascular Remodeling-Associated Diseases**
Yu Wang, Xinrong Zhang, Ya Wen, Sixuan Li, Xiaohui Lu, Ran Xu and Chao Li
- 62 Mitochondria Endoplasmic Reticulum Contact Sites (MERCs): Proximity Ligation Assay as a Tool to Study Organelle Interaction**
Sara Benhammouda, Anjali Vishwakarma, Priya Gatti and Marc Germain
- 68 5-Hydroxymethylfurfural Alleviates Inflammatory Lung Injury by Inhibiting Endoplasmic Reticulum Stress and NLRP3 Inflammasome Activation**
Hang Zhang, Zheyi Jiang, Chuanbin Shen, Han Zou, Zhiping Zhang, Kaitao Wang, Renren Bai, Yanhua Kang, Xiang-Yang Ye and Tian Xie
- 85 FUNDC1: A Promising Mitophagy Regulator at the Mitochondria-Associated Membrane for Cardiovascular Diseases**
Guoyong Li, Junli Li, Ruochen Shao, Jiahao Zhao and Mao Chen
- 96 MFG-E8 Maintains Cellular Homeostasis by Suppressing Endoplasmic Reticulum Stress in Pancreatic Exocrine Acinar Cells**
Yifan Ren, Wuming Liu, Jia Zhang, Jianbin Bi, Meng Fan, Yi Lv, Zheng Wu, Yuanyuan Zhang and Rongqian Wu
- 110 Deep Learning-Based Morphological Classification of Endoplasmic Reticulum Under Stress**
Yuanhao Guo, Di Shen, Yanfeng Zhou, Yutong Yang, Jinzhao Liang, Yating Zhou, Ningning Li, Yu Liu, Ge Yang and Wenjing Li
- 123 Calcium Signaling Regulated by Cellular Membrane Systems and Calcium Homeostasis Perturbed in Alzheimer's Disease**
Dong-Xu Huang, Xin Yu, Wen-Jun Yu, Xin-Min Zhang, Chang Liu, Hong-Ping Liu, Yue Sun and Zi-Ping Jiang
- 136 Intracellular Cholesterol Synthesis and Transport**
Qingyang Shi, Jiahuan Chen, Xiaodong Zou and Xiaochun Tang
- 148 Mitochondrial ROS in Slc4a11 KO Corneal Endothelial Cells Lead to ER Stress**
Rajalekshmy Shyam, Diego G. Ogando and Joseph A. Bonanno

158 *The ER-Mitochondria Interface as a Dynamic Hub for T Cell Efficacy in Solid Tumors*

Elizabeth G. Hunt, Alex M. Andrews, Sydney R. Larsen and
Jessica E. Thaxton

174 *Mitochondrial-Dependent and Independent Functions of PINK1*

Xiusheng Chen, Qi Wang, Shihua Li, Xiao-Jiang Li and Weili Yang



OPEN ACCESS

EDITED AND REVIEWED BY
Ana Cuenda,
Spanish National Research Council
(CSIC), Spain

*CORRESPONDENCE

Yongye Huang,
huangyongye88@163.com
Jianguang Ji,
jianguang.ji@med.lu.se
Qi Zhao,
zhaoqi@lnu.edu.cn
Jun Song,
songjun@neau.edu.cn

SPECIALTY SECTION

This article was submitted to Signaling,
a section of the journal
Frontiers in Cell and Developmental
Biology

RECEIVED 27 July 2022

ACCEPTED 01 August 2022

PUBLISHED 30 August 2022

CITATION

Huang Y, Ji J, Zhao Q and Song J (2022),
Editorial: Regulation of endoplasmic
reticulum and mitochondria in
cellular homeostasis.
Front. Cell Dev. Biol. 10:1004376.
doi: 10.3389/fcell.2022.1004376

COPYRIGHT

© 2022 Huang, Ji, Zhao and Song. This is
an open-access article distributed
under the terms of the [Creative
Commons Attribution License \(CC BY\)](#).
The use, distribution or reproduction in
other forums is permitted, provided the
original author(s) and the copyright
owner(s) are credited and that the
original publication in this journal is
cited, in accordance with accepted
academic practice. No use, distribution
or reproduction is permitted which does
not comply with these terms.

Editorial: Regulation of endoplasmic reticulum and mitochondria in cellular homeostasis

Yongye Huang^{1*}, Jianguang Ji^{2*}, Qi Zhao^{3*} and Jun Song^{4*}

¹College of Life and Health Sciences, Northeastern University, Shenyang, China, ²Center for Primary Health Care Research, Department of Clinical Sciences, Lund University, Lund, Sweden, ³School of Computer Science and Software Engineering, University of Science and Technology Liaoning, Anshan, China, ⁴College of Life Science, Northeast Agriculture University, Harbin, China

KEYWORDS

endoplasmic reticulum, mitochondria, homeostasis, redox, cell death, aging

Editorial on the Research Topic

[Regulation of endoplasmic reticulum and mitochondria in cellular homeostasis](#)

Hub: Endoplasmic reticulum centers in a variety of essential pathways

Endoplasmic reticulum (ER) is an interconnected single membrane-bound network and the largest organelle in the eukaryotic cell. The major function of ER includes the synthesis of proteins and lipids, protein folding and maturation, membrane biogenesis, xenobiotic detoxification, and cellular Ca²⁺ storage. Various mechanisms are conducted to help ER to complete these functions. ER-associated protein degradation (ERAD) mechanism is a conserved protein quality control pathway to erase misfolded, mistargeted and unassembled proteins to maintain ER homeostasis. ER stress, another critical mechanism to regulate ER homeostasis, is induced by the accumulation of misfolded proteins in the ER and triggers the unfolded protein response. Besides recovering cellular homeostasis to maintain cell survival, persistent or intense ER stress could also result in apoptosis, autophagic cell death, or ferroptosis. Altogether, targeting ER *via* modulating ERAD or ER stress would be beneficial for organism development and disease therapy.

Powerhouse: Mitochondria serve as an energetic and metabolic center

Mitochondrion is a complex double-membraned cellular organelle that harbors their own genome. Mitochondrion acts as the energy-producing center in cells for producing ATP *via* the oxidative phosphorylation system. The mitochondrion also serves as a powerful center for the precursors of macromolecules, such as DNA, RNA, proteins, and lipids. Besides the well-known roles in cell metabolism and energy conversion, mitochondria also participate in redox homeostasis, Ca^{2+} homeostasis, stress response, metabolite transport, cell signaling, cell cycle distribution, differentiation, cell death, embryonic development, and aging. Emerging evidence has shown that mitochondrial malfunction is closely related to a broad spectrum of human diseases, including cancer and neurological disorder. Mitochondria execute these functions *via* various molecular and cellular mechanisms. For example, mitophagy, a tightly regulated biological process defined as autophagy-dependent selective degradation of damaged or excessive mitochondria, acts an important role in the quality and quantity control of mitochondria to maintain ultimate cellular homeostasis. Mitochondria-mediated intrinsic apoptosis, regulated by caspases, Bcl-2 family of proteins, Smac/DIABLO, death receptors, IAPs, Omi/HtrA2 and cytochrome c, is one of the major apoptotic pathways. In sum, modulating mitochondria-mediated cell apoptosis, mitochondrial dynamics, mitochondrial energy metabolism, and some other mitochondrial physiological processes would be critical for cells to rebuild homeostasis.

Offensive and defensive alliance: Crosstalk between endoplasmic reticulum and mitochondria

ER and mitochondria are all essential for maintaining cellular homeostasis. To fulfill the goal, an efficient and fast exchange of materials between the ER and mitochondria is required. In addition, there are physical interactions between ER and mitochondria at specific sites (named mitochondria-associated ER membrane, MAMs) in which the surfaces of the two organelles juxtapose at a constant distance, for several nm in length. The unique contact sites serve as the platform for communication between the two organelles and are critical for the regulation of cellular homeostasis, including Ca^{2+} homeostasis, proteostasis, and ER redox homeostasis. Different pathways and numerous mediators participate in the cross-talk between ER and mitochondria. For example, Mitofusin 2 (Mfn2), fission protein 1 homologue (Fis1) and B-cell receptor-associated protein 31 (BAP31) play a crucial role in mitochondrial fusion and fission (Barazzuol et al., 2021). Among them, BAP31, a polytopic integral membrane protein

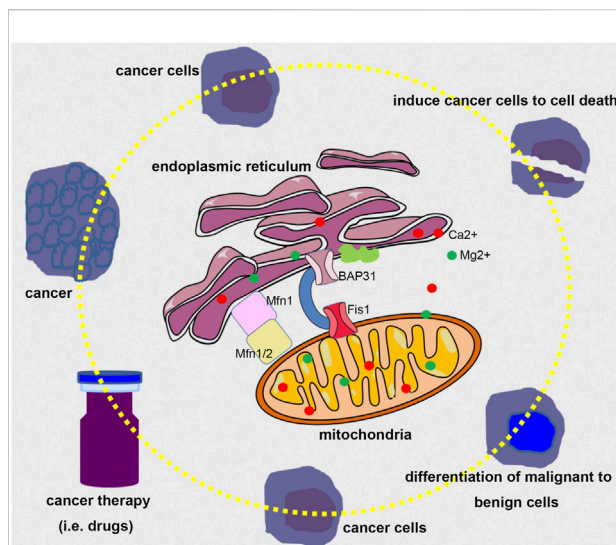


FIGURE 1

A bold assumption for modulating the crosstalk between ER and mitochondria in cancer therapy. Considering the significant role of ER and mitochondria in determining cells to restore cellular homeostasis or induce programmed cell death, it would be possible that tuning the interplay between ER and mitochondria using proper therapeutic means could guide cancer cells to death or differentiate malignant to benign cells.

of ER, functions in apoptosis and participates in several kinds of diseases, including cancers (Li et al., 2022a). BAP31 interacting with Fis1 in MAMs generates an essential platform for the procaspase eight recruitment and transduces apoptotic signal from mitochondria to ER. BAP31 could be cleaved into proapoptotic p20BAP31 in case procaspase eight is recruited and activated to transmit ER calcium signals to mitochondria rapidly. Certainly, there are also some other proteins interacting in MAMs to bridge the crosstalk between ER and mitochondria.

Bumper harvest and future perspective

In this Research Topic, we have published 14 papers. Excitedly, there are many novel findings regarding the mechanism and/or application associated with ER and mitochondria. 5-hydroxymethylfurfural, a furan-containing aldehyde widely presented in various sacchariferous foods, is shown to alleviate inflammatory lung injury by suppressing ER stress (Zhang et al.). In another study, a lipophilic glycoprotein named milk fat globule EGF factor 8 (MFG-E8) is reported to inhibit ER stress to maintain cellular homeostasis in pancreatic exocrine acinar cells during acute pancreatitis (Ren et al.). These studies convey a message that ER stress acts as an important mediator in the various physiological and pathological processes. In our previous studies, we also found that modulating ER stress could be

beneficial for inhibiting cancer development (Huang et al., 2021; Li et al., 2022b). Since the existence of the ER-mitochondria interface, the stress from ER could also send a signal to mitochondria and even further receive feedback from mitochondria. In this Research Topic, Rajalekshmy Shyam etc. report that there was dilated ER and elevated expression of ER stress markers BIP and CHOP in mouse *Slc4a11*^{-/-} corneal endothelial tissue, and concludes that mitochondrial ROS could induce ER stress (Shyam et al.). Furthermore, the Research Topic also collected several review articles deciphering the role of ER and mitochondria in many biological events.

However, it is a pity that we just received limited papers about the mechanisms of ER and mitochondria regulating cellular homeostasis, the contribution of modulating these two organelles to embryo and disease development, and novel methods to assess the crosstalk between ER and mitochondria. In addition, we consider that it would be wonderful to investigate the crosstalk between ER and mitochondria in future research using editing techniques, such as CRISPR-Cas9 and DdCBE. It would also be interesting to study the molecular mechanism between ER and mitochondria interplay and novel cell death modes, such as ferroptosis, NETosis, pyroptosis, and cuproptosis. Expectedly, it would have great significance for regulating the ER and mitochondria to maintain cellular homeostasis to prevent the occurrence of disease (Figure 1).

Author contributions

YH drafted the manuscript, JJ revised the draft, QZ and JS made substantial contributions to the work through in-depth discussion. All the authors proposed the Research Topic theme,

made a direct and intellectual contribution to the work, and approved the final version for publication.

Funding

This study was funded by the National Natural Science Foundation of China (No. 81502582). Funding was also provided by the Fundamental Research Funds for the Central Universities (N182004002), Natural Science Foundation of Liaoning Province (2021-MS-104, 2022-YGJC-39), and Fundamental Scientific Research Fund of Liaoning Provincial Education Department (LJKQZ2021002).

Conflict of interest

The authors declare that the research was conducted in the absence of any commercial or financial relationships that could be construed as a potential conflict of interest.

Publisher's note

All claims expressed in this article are solely those of the authors and do not necessarily represent those of their affiliated organizations, or those of the publisher, the editors and the reviewers. Any product that may be evaluated in this article, or claim that may be made by its manufacturer, is not guaranteed or endorsed by the publisher.

References

- Barazzuol, L., Giamogante, F., and Cali, T. (2021). Mitochondria associated membranes (MAMs): Architecture and physiopathological role. *Cell Calcium* 94, 102343. doi:10.1016/j.ceca.2020.102343
- Huang, Y., Yuan, K., Tang, M., Yue, J., Bao, L., Wu, S., et al. (2021). Melatonin inhibiting the survival of human gastric cancer cells under ER stress involving autophagy and Ras-Raf-MAPK signalling. *J. Cell. Mol. Med.* 25 (3), 1480–1492. doi:10.1111/jcmm.16237
- Li, T., Hao, Z., Tang, Z., Li, C., Cheng, L., Wang, T., et al. (2022a). BAP31 regulates wnt signaling to modulate cell migration in lung cancer. *Front. Oncol.* 12, 859195. doi:10.3389/fonc.2022.859195
- Li, T., Zhang, X., Cheng, L., Li, C., Wu, Z., Luo, Y., et al. (2022b). Modulation of lncRNA H19 enhances resveratrol-inhibited cancer cell proliferation and migration by regulating endoplasmic reticulum stress. *J. Cell. Mol. Med.* 26 (8), 2205–2217. doi:10.1111/jcmm.17242



Therapeutic Effects of Natural Compounds and Small Molecule Inhibitors Targeting Endoplasmic Reticulum Stress in Alzheimer's Disease

Xun Gao and Yuanyuan Xu*

Key Laboratory of Zoonosis Research, Ministry of Education, College of Animal Science, Jilin University, Changchun, China

OPEN ACCESS

Edited by:

Yongye Huang,
Northeastern University, China

Reviewed by:

Cláudia Pereira,
University of Coimbra, Portugal
Tu Zhuchi,
Jinan University, China

*Correspondence:

Yuanyuan Xu
xuyuan@jlu.edu.cn

Specialty section:

This article was submitted to
Signaling,
a section of the journal
Frontiers in Cell and Developmental
Biology

Received: 21 July 2021

Accepted: 13 August 2021

Published: 01 September 2021

Citation:

Gao X and Xu Y (2021)
Therapeutic Effects of Natural
Compounds and Small Molecule
Inhibitors Targeting Endoplasmic
Reticulum Stress in Alzheimer's
Disease.
Front. Cell Dev. Biol. 9:745011.
doi: 10.3389/fcell.2021.745011

Alzheimer's disease (AD) is the most common neurodegenerative disease, characterized by progressive cognitive impairment and memory loss. So far, the pathogenesis of AD has not been fully understood. Research have shown that endoplasmic reticulum (ER) stress and unfolded protein response (UPR) participate in the occurrence and development of AD. Furthermore, various studies, both *in vivo* and *in vitro*, have shown that targeting ER stress and ER stress-mediated apoptosis contribute to the recovery of AD. Thus, targeting ER stress and ER stress-mediated apoptosis may be effective for treating AD. In this review, the molecular mechanism of ER stress and ER stress-mediated apoptosis, as well as the therapeutic effects of some natural compounds and small molecule inhibitors targeting ER stress and ER stress-mediated apoptosis in AD will be introduced.

Keywords: Alzheimer's disease, apoptosis, endoplasmic reticulum stress, neuroprotection, unfolded protein response

INTRODUCTION

The endoplasmic reticulum (ER) is a crucial organelle of eukaryotic cells, whose functions include protein synthesis and folding, lipid biogenesis and calcium metabolism (Schwarz and Blower, 2016). Numerous cellular stresses, such as disequilibrium of calcium homeostasis, redox imbalance, changes in protein glycosylation, or protein folding defects in the ER, can trigger ER stress response, causing accumulation of unfolded or misfolded proteins in the ER lumen (Senft and Ronai, 2015). In order to maintain the homeostasis of the ER, the unfolded protein response (UPR), an integrated signal transduction pathway, is activated (Walter and Ron, 2011). UPR can inhibit protein transcription and translation, promote the degradation of misfolded proteins and increase the ability of correct protein folding (Hetz, 2012). However, under chronic or excessive ER stress, UPR fails to maintain the homeostasis of ER, then the apoptosis signaling pathway is activated, leading to a variety of diseases, including Alzheimer's disease (AD) (Uddin et al., 2020).

AD is the most common neurodegenerative disease, characterized by progressive cognitive impairment and memory loss. Besides, abnormal accumulation of misfolded proteins in the brain, such as β -amyloid (A β) peptide and hyperphosphorylated tau protein, is the main neuropathological hallmark of AD (Villain and Dubois, 2019; Ghemrawi and Khair, 2020). So far, the pathogenesis of AD has not been fully understood, and there is no effective treatment for this

disease. The existing treatments can only relieve the symptoms or slow down the progression of the disease, but the patients can't be cured (Morris et al., 2018). Therefore, it is necessary to find a novel and effective treatment for AD.

Recently, research have shown that ER stress and UPR participate in the occurrence and development of AD (Hoozemans et al., 2009; Salminen et al., 2009; Uddin et al., 2020). Furthermore, various studies, both *in vivo* and *in vitro*, have shown that targeting ER stress and ER stress-mediated apoptosis contribute to the recovery of AD (Xu et al., 2018; Zhu et al., 2019; Song et al., 2020; Oliveira et al., 2021). Thus, targeting ER stress and ER stress-mediated apoptosis may be effective for treating AD. In this review, the molecular mechanism of ER stress and ER stress-mediated apoptosis, as well as the therapeutic effects of some natural compounds and small molecule inhibitors targeting ER stress and ER stress-mediated apoptosis in AD will be introduced.

ER STRESS, UPR, AND APOPTOSIS

ER Stress-Mediated UPR Signaling Pathways

Early ER stress will induce UPR, which might be protective to cells (Walter and Ron, 2011). Three ER transmembrane proteins are involved in UPR signaling pathways: PERK (protein kinase RNA-like ER kinase), IRE1 (inositol-requiring enzyme 1) and ATF6 (activating transcription factor 6) (Chen and Brandizzi, 2013; Hillary and FitzGerald, 2018; Rozpedek et al., 2019). Under physiological conditions, these proteins are combined with ER chaperone BiP (immunoglobulin binding protein, also called glucose-regulated protein 78, GRP78), and located in the ER membrane in an inactive state (Carrara et al., 2015; Ghemrawi and Khair, 2020). However, under ER stress, when a misfolded or unfolded protein binds to BiP, BiP is dissociated from these transmembrane proteins, then downstream signaling pathways of UPR are initiated (Figure 1; Ron and Walter, 2007; Parmar and Schroder, 2012). These three transmembrane proteins play a key role in the three signaling pathways of UPR, promoting the correct folding of unfolded and misfolded proteins, thus maintaining ER homeostasis.

PERK is a type I ER transmembrane protein with a serine/threonine protein kinase domain (Rozpedek et al., 2019). Under mild ER stress, PERK first undergoes autophosphorylation, and then eukaryotic initiation factor 2 α (eIF2 α) is activated by phosphorylation. Phosphorylated eIF2 α can block protein synthesis and reduce the protein load of ER (Cnop et al., 2017).

IRE1 is also a type I ER transmembrane protein with endonuclease activities, which can be divided into two isoforms, IRE1 α and IRE1 β (Chen and Brandizzi, 2013). When ER stress occurs, IRE1 α is first activated by autophosphorylation and dimerization (Hetz et al., 2011). Then, through unconventional splicing of X-box binding protein 1 (XBP1) mRNA, an active transcription factor, XBP1s, is produced. XBP1s can promote the correct folding of unfolded and misfolded proteins, thereby restore ER homeostasis (Hollien et al., 2009).

ATF6 is a type II transmembrane protein, which encodes a basic leucine zipper (bZIP) transcription factor (Hillary and FitzGerald, 2018). In conditions of ER stress, ATF6 moves from the ER to the Golgi, where it undergoes proteolytic cleavage. Subsequently, the active transcription factor, ATF6 α , is produced and transferred to the nucleus, where it regulates the expression of UPR related genes, such as CHOP, BiP, and XBP1 (Wu et al., 2007; Ghemrawi and Khair, 2020).

Chronic or Excessive ER Stress-Mediated Apoptosis Signaling Pathways

On the contrary, under chronic or excessive ER stress, UPR fails to maintain the homeostasis of ER, then the apoptosis signaling pathways are activated, even resulting in cell death (Senft and Ronai, 2015; Iurlaro and Munoz-Pinedo, 2016). ER stress can induce apoptosis through three major signaling pathways: CHOP pathway, JNK pathway and caspase-12 pathway (Figure 1; Hu et al., 2018).

PERK-CHOP Pathway

Phosphorylated eIF2 α allows the translation of activating transcription factor 4 (ATF4), an activator of apoptosis-related genes (Hu et al., 2018). Subsequently, ATF4 up-regulates the expression of several apoptosis-related genes, for example, C/EBP homologous protein (CHOP) (Oyadomari and Mori, 2004). CHOP can regulate the expression of some BCL-2 family members, including the down-regulation of anti-apoptotic proteins like BCL-2 and BCL-XL, and the up-regulation of pro-apoptotic proteins like BIM, BAK, and BAX (Hata et al., 2015). Furthermore, the oligomerization of BAK-BAX will lead to the release of cytochrome c, which causes apoptosis through the mitochondrial pathway (Brenner and Mak, 2009).

IRE1-JNK Pathway

Activated IRE1 can activate apoptotic-signaling kinase-1 (ASK1) (Ron and Hubbard, 2008). Then downstream kinases, such as Jun-N-terminal kinase (JNK) and p38 mitogen-activated protein kinase (p38 MAPK), are activated (Urano et al., 2000). JNK can up-regulate the expression of pro-apoptotic proteins, such as BIM and PUMA, leading to the activation of BAX and subsequent apoptosis (Deng et al., 2001). Meanwhile, p38 MAPK can promote the transcription of CHOP, as well as regulate the expression of some BCL-2 family members (Oyadomari and Mori, 2004; Hata et al., 2015).

Caspase-12 Pathway

ER stress can activate caspase-12, and then the caspase cascade is activated (Iurlaro and Munoz-Pinedo, 2016). Activated caspase-12 moves from the ER to the cytosol, where it cleaves procaspase-9 to form caspase-9 (Szegezdi et al., 2003). Caspase-9 in turn activates caspase-3, the main executioner of apoptosis (Lossi et al., 2018).

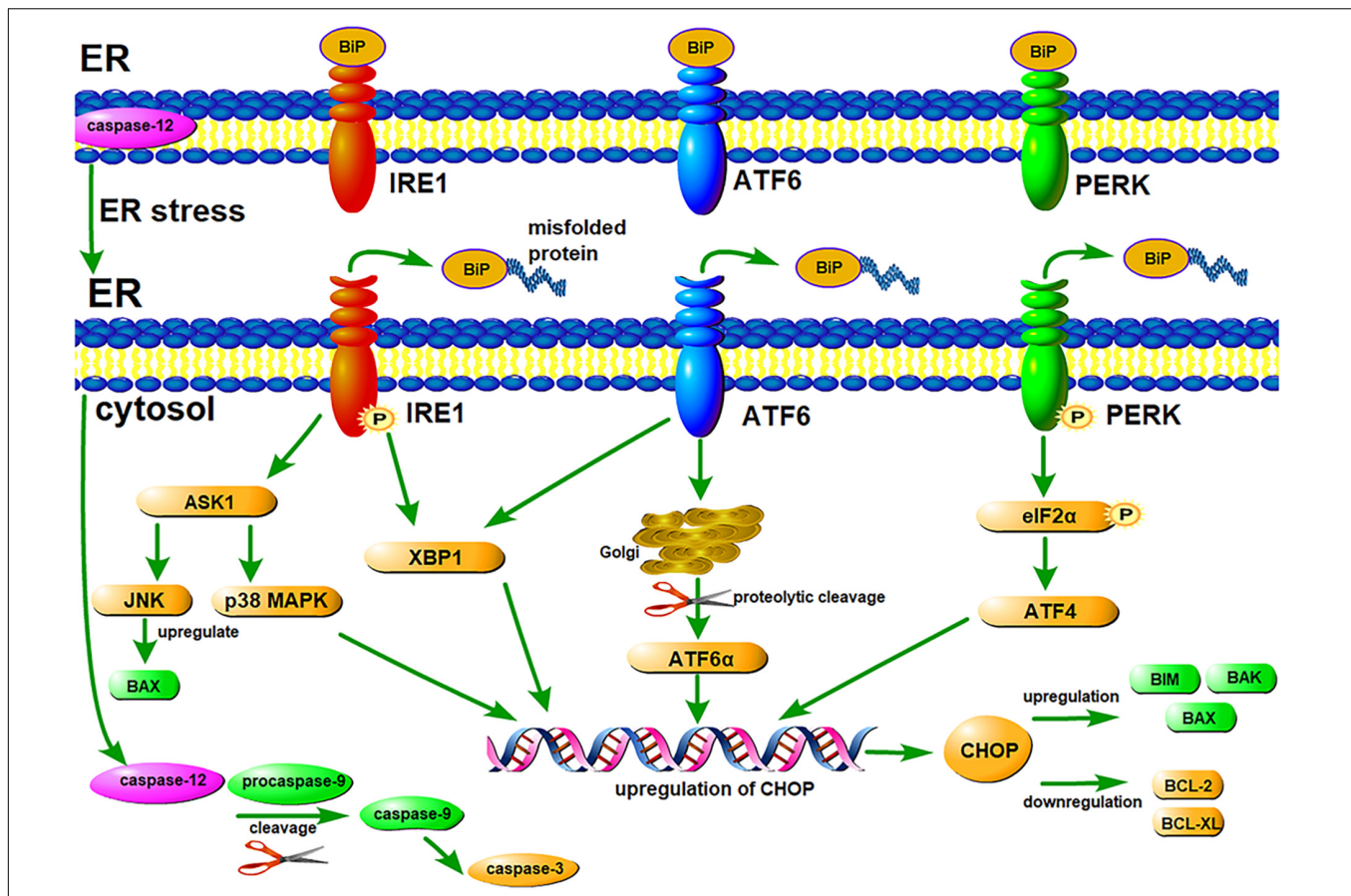


FIGURE 1 | ER stress-mediated UPR signaling pathways and apoptosis signaling pathways. Three ER transmembrane proteins, IRE1, ATF6, and PERK, are involved in UPR signaling pathways. Under normal conditions, these proteins are combined with ER chaperone BiP, and located in the ER membrane in an inactive state. Under ER stress, when a misfolded protein binds to BiP, BiP dissociates from IRE1, ATF6, and PERK. Subsequently, PERK and IRE1 undergo autophosphorylation, and ATF6 undergoes proteolytic cleavage. Downstream signaling pathways of UPR are initiated, thereby maintaining ER homeostasis. However, under chronic or excessive ER stress, UPR fails to maintain the homeostasis of ER, then apoptosis signaling pathways are activated. All the three ER transmembrane proteins can up-regulate CHOP, leading to apoptosis by regulating the expression of some BCL-2 family members. Activated IRE1 can activate JNK, inducing apoptosis by up-regulating the expression of some pro-apoptotic proteins. Caspase-12 can induce apoptosis by activating the caspase cascade reaction.

APPLICATIONS OF NATURAL COMPOUNDS AND SMALL MOLECULE INHIBITORS TARGETING ER STRESS AND ER STRESS-MEDIATED APOPTOSIS IN TREATING ALZHEIMER'S DISEASE

Researches have shown that ER stress and UPR participate in the occurrence and development of AD (Hoozemans et al., 2009; Salminen et al., 2009; Uddin et al., 2020). During AD, the continuous accumulation of A β or p-tau leads to unbalanced ER calcium homeostasis, abnormal protein folding and ER stress (Sobow et al., 2004; Mondragon-Rodriguez et al., 2012). Neuronal cells are especially sensitive to protein misfolding, therefore, the excessive accumulation of A β or p-tau will result in synaptic dysfunction and apoptosis, even neuronal death (Remondelli and Renna, 2017; Ghemrawi and Khair, 2020). In addition, some UPR-related proteins, such as phosphorylated PERK, eIF2 α

and IRE1 were found in AD brains (Devi and Ohno, 2014; Duran-Aniotz et al., 2017; Uddin et al., 2020). Meanwhile, ER stress markers, including GRP78, CHOP and caspase-12, are up-regulated in AD patients (Santos and Ferreira, 2018).

Recently, various studies, both *in vivo* and *in vitro*, have shown that targeting ER stress and ER stress-mediated apoptosis contribute to the recovery of AD (Xu et al., 2018; Zhu et al., 2019; Song et al., 2020; Oliveira et al., 2021). Several active components extracted from the plants and small molecule inhibitors of UPR signaling pathways and other signaling pathways have displayed good therapeutic effects on AD models. A brief summary of some natural compounds and small molecule inhibitors targeting ER stress in AD studies is shown in Table 1.

Targeting PERK-CHOP Signaling Pathway

The PERK-CHOP signaling pathway plays an essential role in inducing cell apoptosis. In the early stage of ER stress, activated

TABLE 1 | Natural compounds and small molecule inhibitors targeting ER stress and ER stress-mediated apoptosis in treating Alzheimer's disease.

Agents	AD models	Mechanisms	References
Natural compounds			
Schisandrin	Streptozotocin-induced rat model	GRP78↓ CHOP↓ caspase-12↓	Song et al., 2020
Resveratrol and crocin	A β_{25-35} -induced rat model	GRP78↓ CHOP↓ caspase-3↓ BAX↓ BCL-2↑	Lin et al., 2019
Gas	Tg2576 mouse model	eIF2 α ↓	Zhang et al., 2016
Quercetin	APP23 mouse model	p-eIF2 α ↓ ATF4↓	Hayakawa et al., 2015
Bajijiasu	A β_{25-35} -induced PC12 cell model; APP/PS1 mouse model	IRE1 α ↓ PERK↓ eIF α ↓ CHOP↓	Chen et al., 2013; Xu et al., 2018
Ginsenoside Rg1	APP/PS1 rat model	GRP78↓ IRE1↓ TRAF2↓ p-JNK↓ caspase-3↓	Mu et al., 2015
GE and its pure compounds	A β -induced BV2 cell model	IRE1 α ↓ XBP1↓ PERK↓ p-eIF2 α ↓ CHOP↓ caspase-3↓	Lee et al., 2012
Taurine	H ₂ O ₂ -induced PC12 cell model; hypoxia- and glutamate-induced primary neuronal cell model; APP/PS1 mouse model; A β -infusion mouse model	Cleaved ATF6↓ p-IRE1↓ GRP78↓ CHOP↓ BIM↓ BCL-2↑	Pan et al., 2010, 2012
SAC	A β -induced cell models (PC12 cells; hippocampal neurons; rat organotypic hippocampal slice cultures)	Unknown	Kim et al., 2014; Jang et al., 2017
Small molecule inhibitors			
LDN-0060609	Thapsigargin-induced DI TNC1 cell model	p-eIF2 α ↓	Rozpedek et al., 2019
ISRIB	APP ^{SWE} /PS1 Δ E9 mouse model	ATF4↓	Oliveira et al., 2021
Xestospongion C	APP/PS1 mouse model	GRP78↓ CHOP↓ caspase-12↓	Wang et al., 2019
DA-CH3	APP ^{SWE} /PS1 Δ E9 mouse model	Akt↑	Panagaki et al., 2018
Bpv	APP/PS1 mouse model	GRP78↓ CHOP↓ BAX↓ p-AKT/AKT↑	Cui et al., 2017
ATAN	A β -induced cell model (rat organotypic hippocampal slice cultures)	Caspase-12↓	Imai et al., 2007

BAX, BCL-2-associated X protein; BCL-2, B-cell lymphoma 2; BiP, immunoglobulin heavy chain-binding protein; CHOP, C/EBP homologous protein; eIF2, eukaryotic initiation factor 2; GRP78, glucose-regulated Protein 78; PERK, protein kinase RNA-like ER kinase; IRE1, inositol-requiring protein 1; JNK, Jun-N-terminal kinase; p38 MAPK, p38 mitogen-activated protein kinase; TRAF2, tumor necrosis factor receptor-associated 2.

PERK can further activate eIF2 α , which can block protein synthesis and exert a protective effect on cells (Rozpedek et al., 2019). However, under chronic or excessive ER stress, PERK-CHOP signaling pathway will be activated, leading to apoptosis (Hu et al., 2018).

Schisandrin (Sch)

Schisandrin (Sch) is an active component extracted from schisandra chinensis Baill (Zhu et al., 2019). In the Streptozotocin (STZ)-induced AD rats, after the treatment of Sch, the

expression of ER stress markers, including GRP78, CHOP, and cleaved caspase-12, was obviously decreased (Song et al., 2020). Moreover, Sch also improved the learning and memory capacity of STZ-induced AD rats, by enhancing the activity of Sirtuin 1 (SIRT1, an enzyme contributes to the acquisition and maintenance of memory) (Song et al., 2020).

Resveratrol and Crocin

In the A β_{25-35} -induced AD rats, both enhanced expression of GRP78, CHOP, caspase-3, BAX and attenuated expression of

BCL-2 were observed in the hippocampal CA1 region (Hippo) and prefrontal cortical (PFC), while the situation was reversed by treatment with resveratrol (a polyphenolic stilbenoid, present in grapes, mulberries, peanuts and other plants; Malaguarnera, 2019) and crocin (a non-tetraquinone pigment extracted from *Crocus sativus* L.; Shafahi et al., 2018). Furthermore, improved learning and memory ability and decreased number of apoptotic neurons were also detected in AD rats (Lin et al., 2019).

Gastrodin (Gas)

Tg2576 transgenic mouse is an AD model with high expression of β -site APP-cleaving enzyme 1 (BACE1), which is a rate-limiting enzyme for A β generation and could aggravate the process of AD (O'Connor et al., 2008). Gastrodin (Gas), an active component of *Gastrodia elata* Blume, was found to improve learning and memory abilities and attenuate intracellular oxidative stress of Tg2576 mice (Zhang et al., 2016). Moreover, Gas down-regulated BACE1 expression via inhibiting activation of PKR and eIF2 α (Zhang et al., 2016).

Quercetin

In the APP23 AD model mice, after long-term feeding with quercetin, a polyhydroxylated flavonoid, the expression of growth arrest and DNA damaged-inducible gene 34 (GADD34) was induced, leading to the down-regulation of phosphorylated-eIF2 α and ATF4 (Ohta et al., 2011; Hayakawa et al., 2015). This resulted in improvement of memory in aged AD mice, and delayed deterioration in memory of the mice at the early stage of AD (Hayakawa et al., 2015).

LDN-0060609

Compound LDN-0060609 is a small molecule PERK inhibitor (Rozpedek et al., 2019). In rat astrocytic DI TNC1 cell line, LDN-0060609 pretreatment attenuated the pro-apoptotic, PERK-dependent signaling pathway induced by thapsigargin (Th) treatment. It significantly inhibited eIF2 α phosphorylation and increased cell survival *in vitro*. Notably, LDN-0060609 has no cytotoxicity to DI TNC1 cells and also has no influence on cell cycle progression (Rozpedek et al., 2019; Rozpedek-Kaminska et al., 2020). Therefore, it may contribute to prevention against apoptosis and neurodegeneration in AD without the cytotoxic effect.

ISRIB

ISRIB is a small molecule integrated stress response (ISR) inhibitor, which can reverse the phosphorylation of eIF2 α and inhibit the downstream targets of eIF2 α , such as ATF4, CHOP, and GADD34 (Sidrauski et al., 2015). In an AD mouse model induced by intracerebroventricular injection of amyloid- β oligomers (A β Os), ISRIB treatment counteracted the increase in ATF4 protein level, protecting mice from long-term memory impairment (Oliveira et al., 2021). Furthermore, ISRIB was shown to attenuate translational repression, restore synaptic plasticity and memory in transgenic APP_{SWE}/PS1 Δ E9 AD mice (Oliveira et al., 2021).

Xestospongine C (XeC)

Xestospongine C (XeC), a compound isolated from the *Xestospongia* species, is a reversible IP₃ receptor antagonist (Gafni et al., 1997). It was found that XeC could improve the cognitive behavior of APP/PS1 AD mice. XeC also reduced the number of A β plaques and down-regulated the expression of GRP78, CHOP and caspase-12 in APP/PS1 mice (Wang et al., 2019). In addition, XeC significantly ameliorated A β _{1–42}-induced neuronal apoptosis and intracellular Ca²⁺ overload in primary cultured hippocampal neurons (Wang et al., 2019).

Targeting IRE1-JNK Signaling Pathway

Activated IRE1 can activate JNK, leading to the up-regulation of pro-apoptotic proteins and subsequent apoptosis (Urano et al., 2000; Deng et al., 2001). Activation of IRE1-JNK signaling pathway plays a key role in ER stress-mediated apoptosis.

Bajijiasu

Bajijiasu (also known as bajisu) is a natural active ingredient isolated from *Morinda officinalis* (Chen et al., 2014). It was shown to play a protective role against A β _{25–35}-induced neurotoxicity in PC12 cells (Chen et al., 2013). In a double transgenic APP/PS1 mouse model of AD, oral administration of bajijiasu improved learning and memory abilities of APP/PS1 mice. Also, Bajijiasu protected neurons from apoptosis by down-regulating the expression of IRE1 α , PERK, eIF2 α , and CHOP. Moreover, reduced ROS and MDA levels in both the hippocampus and cortex were detected (Xu et al., 2018).

Ginsenoside Rg1

Ginsenoside Rg1 is a steroidal saponin highly abundant in ginseng (Wu et al., 2013). In a APP/PS1 rat model, AD rats were fed with 0.5% Rg1-enriched food to investigate the neuroprotective effects of Rg1. After Rg1 treatment, the accumulation of A β plaque and neurofibrillary tangles (NFTs) was significantly decreased in the AD rats, as well as the reduced expression of caspase-3 and the number of apoptotic cells. Furthermore, down-regulation of GRP78, IRE1, and p-JNK was observed in the AD rats, indicating that Rg1 exhibited neuroprotective effects by inhibiting the ER stress-mediated JNK apoptotic pathway (Mu et al., 2015).

Gastrodia Elata (GE) and Its Pure Compounds

In the BV2 mouse microglial cells, A β not only induced cytotoxicity and apoptosis but also promoted the expression of IRE1 α , XBP1, PERK, phosphorylated eIF2 α , CHOP, caspase-3 (Lee et al., 2012). However, after treatment with *Gastrodia elata* (GE) and its pure compounds, gastrodin (Gas) and 4-hydroxybenzyl alcohol (4HBA), these ER stress-relevant proteins were down-regulated. Moreover, Gas and 4HBA inhibited the neurotoxicity induced by A β and increased cells viability (Lee et al., 2012).

Targeting ATF6-AKT Signaling Pathway

Under ER stress, the ATF6 pathway can mediate cell survival by regulating the activation of Akt and the expression of GRP78 and CHOP (Cui et al., 2017).

Taurine

Taurine, a free amino acid, is abundant in the brain and plays an important role in the central nervous system (Seidel et al., 2019). It was found that taurine can protect PC12 cells against H₂O₂-induced ER stress, leading to the increase in cell viability, as well as the down-regulation of GRP78, CHOP, and BIM (Pan et al., 2010). Meanwhile, in primary neuronal cultures, taurine can also modulate hypoxia- and glutamate-induced ER stress by down-regulating the expression of caspase-12, CHOP, cleaved ATF6 and p-IRE1 (Pan et al., 2012). Later, in APP/PS1 transgenic AD mouse model, oral administration of taurine significantly ameliorated cognitive deficits of the adult AD mice (Kim et al., 2014). Further study conducted in the oligomeric A β -infusion AD mouse model showed that taurine can ameliorate cognitive impairment by directly binding to oligomeric A β (Jang et al., 2017). Nevertheless, mechanisms underlying taurine mediated cognitive improvement still need further elucidation.

Dipotassium Bisperoxo-(5-Hydroxypyridine-2-Carboxyl)-Oxovanadate (bpv)

Phosphatase and tensin homolog deleted on chromosome ten (PTEN) is a tumor suppressor, which plays an essential role in regulating neuronal survival or apoptosis (Kitagishi and Matsuda, 2013). Dipotassium bisperoxo-(5-hydroxypyridine-2-carboxyl)-oxovanadate (bpv), a PTEN inhibitor, could decrease apoptosis and suppress the expression of ER stress related protein GRP78, CHOP, and Bax in APP/PS1 transgenic AD mice. Further study showed that the neuroprotective role of bpv in APP/PS1 mice was mediated by activation of PI3K/AKT signaling pathways (Cui et al., 2017).

DA-CH3

Chronic treatment with DA-CH3, a novel dual GLP-1/GIP receptor agonist (Holscher, 2018), could rescue the spatial acquisition and memory impairments of APP_{SWE}/PS1 Δ E9 mice. Additionally, excessive plaque deposition, gliosis and synaptic damage was ameliorated in the APP_{SWE}/PS1 Δ E9 brain. Further research found that the alleviated ER stress and autophagy impairments in the APP_{SWE}/PS1 Δ E9 mouse brain might be attributed to the up-regulation of the Akt activation (Panagaki et al., 2018).

Targeting Caspase-12 Signaling Pathway

ER stress can induce mitochondrial apoptosis by regulating Bcl-2 family members, such as Bcl-2 and Bcl-XL. However, persistent ER stress will activate caspase-12, and further activate caspase-3, finally triggering cell apoptosis (Iurlaro and Munoz-Pinedo, 2016).

S-allyl-L-cysteine (SAC) is an organosulfur compound extracted from aged garlic (Moriguchi et al., 1996). It was shown that SAC could prevent neuronal death induced by A β in PC12 cells (Ito et al., 2003), cultured hippocampal neurons (Kosuge et al., 2003), and rat organotypic hippocampal slice cultures (OHCs) (Imai et al., 2007). Besides, A β -induced increase in caspase-12 protein expression was suppressed by SAC in cultured hippocampal neurons and OHCs. Furthermore, SAC

also decreased the A β -induced intracellular reactive oxygen species (ROS) levels in hippocampal neurons (Kosuge et al., 2003). In addition, Z-ATAN-fmk (ATAN), a specific caspase-12 inhibitor, could markedly suppress neurotoxicity induced by A β in OHCs (Imai et al., 2007).

DISCUSSION

It is proved that ER stress and UPR play an essential role in the occurrence and development of AD (Devi and Ohno, 2014; Duran-Aniotz et al., 2017; Uddin et al., 2020). The related findings, both *in vivo* and *in vitro*, have shown that many natural compounds and small molecular inhibitors targeting ER stress and ER stress-mediated neuronal apoptosis contribute to the recovery of AD (Xu et al., 2018; Zhu et al., 2019; Song et al., 2020; Oliveira et al., 2021). However, there are still a lot of questions to be considered if we want to convert these agents into a safe and reliable drug for clinical application, such as the safety, efficacy, and applicability.

Nevertheless, due to the species differences between humans and mice, the existing AD mouse models cannot fully simulate the pathologic and clinical features of human AD, which limits their application in preclinical studies of AD (de Bem et al., 2020). Therefore, it is necessary to develop animal models more similar to human AD to test the safety and efficacy of these agents (Medina and Avila, 2014). Recently, with the development of efficient genome editing technology, larger animals, such as rabbits, pigs and non-human primates, can be used to construct models of AD (Bosze et al., 2003; Chan, 2013; Yang and Wu, 2018). By using the CRISPR/Cas9 system and base editing system, these animal models can accurately simulate the gene mutation sites of human AD, and provide an ideal platform for AD pathogenesis research and preclinical evaluation (Tu et al., 2015; Gaudelli et al., 2017). In the near future, more unknown mechanisms between ER stress and AD will be clarified, which will offer more safe and effective therapeutic strategies to AD.

AUTHOR CONTRIBUTIONS

XG and YX initiated the project, wrote, revised, and finalized the manuscript. XG searched the database. Both authors contributed to the article and approved the submitted version.

FUNDING

This work was financially supported by the National Key Research and Development Program of China Stem Cell and Translational Research (2017YFA0105101). The Program for Changjiang Scholars and Innovative Research Team in University (No. IRT_16R32). The Strategic Priority Research Program of the Chinese Academy of Sciences (XDA16030501 and XDA16030503), Key Research and Development Program of Guangzhou Regenerative Medicine and Health Guangdong Laboratory (2018GZR110104004).

REFERENCES

- Bosze, Z., Hiripi, L., Carnwath, J. W., and Niemann, H. (2003). The transgenic rabbit as model for human diseases and as a source of biologically active recombinant proteins. *Transgenic Res.* 12, 541–553.
- Brenner, D., and Mak, T. W. (2009). Mitochondrial cell death effectors. *Curr. Opin. Cell Biol.* 21, 871–877. doi: 10.1016/j.ceb.2009.09.004
- Carrara, M., Prisch, F., Nowak, P. R., Kopp, M. C., and Ali, M. M. (2015). Noncanonical binding of BiP ATPase domain to Ire1 and Perk is dissociated by unfolded protein CH1 to initiate ER stress signaling. *Elife* 4:e03522.
- Chan, A. W. (2013). Progress and prospects for genetic modification of nonhuman primate models in biomedical research. *ILAR J.* 54, 211–223. doi: 10.1093/ilar/ilt035
- Chen, D. L., Zhang, P., Lin, L., Shuai, O., Zhang, H. M., Liu, S. H., et al. (2013). Protective effect of Bajjiasu against beta-amyloid-induced neurotoxicity in PC12 cells. *Cell. Mol. Neurobiol.* 33, 837–850. doi: 10.1007/s10571-013-9950-7
- Chen, D. L., Zhang, P., Lin, L., Zhang, H. M., Deng, S. D., Wu, Z. Q., et al. (2014). Protective effects of bajjiasu in a rat model of Abeta(2)(5)(-)(3)(5)-induced neurotoxicity. *J. Ethnopharmacol.* 154, 206–217. doi: 10.1016/j.jep.2014.04.004
- Chen, Y., and Brandizzi, F. (2013). IRE1: ER stress sensor and cell fate executor. *Trends Cell Biol.* 23, 547–555.
- Cnop, M., Toivonen, S., Igoillo-Esteve, M., and Salpea, P. (2017). Endoplasmic reticulum stress and eIF2alpha phosphorylation: the Achilles heel of pancreatic beta cells. *Mol. Metab.* 6, 1024–1039. doi: 10.1016/j.molmet.2017.06.001
- Cui, W., Wang, S., Wang, Z., Wang, Z., Sun, C., and Zhang, Y. (2017). Inhibition of PTEN Attenuates Endoplasmic Reticulum Stress and Apoptosis via Activation of PI3K/AKT Pathway in Alzheimer's Disease. *Neurochem. Res.* 42, 3052–3060. doi: 10.1007/s11064-017-2338-1
- de Bem, A. F., Krolow, R., Farias, H. R., De Rezende, V. L., Gelain, D. P., Moreira, J. C. F., et al. (2020). Animal Models of Metabolic Disorders in the Study of Neurodegenerative Diseases: an Overview. *Front. Neurosci.* 14:604150. doi: 10.3389/fnins.2020.604150
- Deng, X., Xiao, L., Lang, W., Gao, F., Ruvolo, P., and May, W. S. Jr. (2001). Novel role for JNK as a stress-activated Bcl2 kinase. *J. Biol. Chem.* 276, 23681–23688. doi: 10.1074/jbc.m100279200
- Devi, L., and Ohno, M. (2014). PERK mediates eIF2alpha phosphorylation responsible for BACE1 elevation, CREB dysfunction and neurodegeneration in a mouse model of Alzheimer's disease. *Neurobiol. Aging* 35, 2272–2281. doi: 10.1016/j.neurobiolaging.2014.04.031
- Duran-Aniotz, C., Cornejo, V. H., Espinoza, S., Ardiles, A. O., Medinas, D. B., Salazar, C., et al. (2017). IRE1 signaling exacerbates Alzheimer's disease pathogenesis. *Acta Neuropathol.* 134, 489–506. doi: 10.1007/s00401-017-1694-x
- Gafni, J., Munsch, J. A., Lam, T. H., Catlin, M. C., Costa, L. G., Molinski, T. F., et al. (1997). Xestospingins: potent membrane permeable blockers of the inositol 1,4,5-trisphosphate receptor. *Neuron* 19, 723–733. doi: 10.1016/s0896-6273(00)80384-0
- Gaudelli, N. M., Komor, A. C., Rees, H. A., Packer, M. S., Badran, A. H., Bryson, D. I., et al. (2017). Programmable base editing of AT to GC in genomic DNA without DNA cleavage. *Nature* 551, 464–471. doi: 10.1038/nature24644
- Ghemrawi, R., and Khair, M. (2020). Endoplasmic Reticulum Stress and Unfolded Protein Response in Neurodegenerative Diseases. *Int. J. Mol. Sci.* 21:6127. doi: 10.3390/ijms21176127
- Hata, A. N., Engelman, J. A., and Faber, A. C. (2015). The BCL2 Family: key Mediators of the Apoptotic Response to Targeted Anticancer Therapeutics. *Cancer Discov.* 5, 475–487. doi: 10.1158/2159-8290.cd-15-0011
- Hayakawa, M., Itoh, M., Ohta, K., Li, S., Ueda, M., Wang, M. X., et al. (2015). Quercetin reduces eIF2alpha phosphorylation by GADD34 induction. *Neurobiol. Aging* 36, 2509–2518. doi: 10.1016/j.neurobiolaging.2015.05.006
- Hetz, C. (2012). The unfolded protein response: controlling cell fate decisions under ER stress and beyond. *Nat. Rev. Mol. Cell Biol.* 13, 89–102. doi: 10.1038/nrm3270
- Hetz, C., Martinon, F., Rodriguez, D., and Glimcher, L. H. (2011). The unfolded protein response: integrating stress signals through the stress sensor IRE1alpha. *Physiol. Rev.* 91, 1219–1243. doi: 10.1152/physrev.00001.2011
- Hillary, R. F., and FitzGerald, U. (2018). A lifetime of stress: ATF6 in development and homeostasis. *J. Biomed. Sci.* 25:48.
- Hollien, J., Lin, J. H., Li, H., Stevens, N., Walter, P., and Weissman, J. S. (2009). Regulated Ire1-dependent decay of messenger RNAs in mammalian cells. *J. Cell Biol.* 186, 323–331. doi: 10.1083/jcb.200903014
- Holscher, C. (2018). Novel dual GLP-1/GIP receptor agonists show neuroprotective effects in Alzheimer's and Parkinson's disease models. *Neuropharmacology* 136, 251–259. doi: 10.1016/j.neuropharm.2018.01.040
- Hoozemans, J. J., Van Haastert, E. S., Nijholt, D. A., Rozemuller, A. J., Eikelenboom, P., and Scheper, W. (2009). The unfolded protein response is activated in pretangle neurons in Alzheimer's disease hippocampus. *Am. J. Pathol.* 174, 1241–1251. doi: 10.2353/ajpath.2009.080814
- Hu, H., Tian, M., Ding, C., and Yu, S. (2018). The C/EBP Homologous Protein (CHOP) Transcription Factor Functions in Endoplasmic Reticulum Stress-Induced Apoptosis and Microbial Infection. *Front. Immunol.* 9:3083. doi: 10.3389/fimmu.2018.03083
- Imai, T., Kosuge, Y., Ishige, K., and Ito, Y. (2007). Amyloid beta-protein potentiates tunicamycin-induced neuronal death in organotypic hippocampal slice cultures. *Neuroscience* 147, 639–651. doi: 10.1016/j.neuroscience.2007.04.057
- Ito, Y., Kosuge, Y., Sakikubo, T., Horie, K., Ishikawa, N., Obokata, N., et al. (2003). Protective effect of S-allyl-L-cysteine, a garlic compound, on amyloid beta-protein-induced cell death in nerve growth factor-differentiated PC12 cells. *Neurosci. Res.* 46, 119–125. doi: 10.1016/s0168-0102(03)00037-3
- Iurlaro, R., and Munoz-Pinedo, C. (2016). Cell death induced by endoplasmic reticulum stress. *FEBS J.* 283, 2640–2652.
- Jang, H., Lee, S., Choi, S. L., Kim, H. Y., Baek, S., and Kim, Y. (2017). Taurine Directly Binds to Oligomeric Amyloid-beta and Recovers Cognitive Deficits in Alzheimer Model Mice. *Adv. Exp. Med. Biol.* 975, 233–241. doi: 10.1007/978-94-024-1079-2_21
- Kim, H. Y., Kim, H. V., Yoon, J. H., Kang, B. R., Cho, S. M., Lee, S., et al. (2014). Taurine in drinking water recovers learning and memory in the adult APP/PS1 mouse model of Alzheimer's disease. *Sci. Rep.* 4:7467.
- Kitagishi, Y., and Matsuda, S. (2013). Diets involved in PPAR and PI3K/AKT/PTEN pathway may contribute to neuroprotection in a traumatic brain injury. *Alzheimers Res. Ther.* 5:42. doi: 10.1186/alzrt208
- Kosuge, Y., Koen, Y., Ishige, K., Minami, K., Urasawa, H., Saito, H., et al. (2003). S-allyl-L-cysteine selectively protects cultured rat hippocampal neurons from amyloid beta-protein- and tunicamycin-induced neuronal death. *Neuroscience* 122, 885–895. doi: 10.1016/j.neuroscience.2003.08.026
- Lee, G. H., Kim, H. R., Han, S. Y., Bhandary, B., Kim, D. S., Kim, M. G., et al. (2012). Gastrodia elata Blume and its pure compounds protect BV-2 microglial-derived cell lines against beta-amyloid: the involvement of GRP78 and CHOP. *Biol. Res.* 45, 403–410. doi: 10.4067/s0716-97602012000400013
- Lin, L., Liu, G., and Yang, L. (2019). Crocin Improves Cognitive Behavior in Rats with Alzheimer's Disease by Regulating Endoplasmic Reticulum Stress and Apoptosis. *Biomed. Res. Int.* 2019:9454913.
- Lossi, L., Castagna, C., and Merighi, A. (2018). Caspase-3 Mediated Cell Death in the Normal Development of the Mammalian Cerebellum. *Int. J. Mol. Sci.* 19:3999. doi: 10.3390/ijms19123999
- Malaguarnera, L. (2019). Influence of Resveratrol on the Immune Response. *Nutrients* 11:946. doi: 10.3390/nu11050946
- Medina, M., and Avila, J. (2014). The need for better AD animal models. *Front. Pharmacol.* 5:227. doi: 10.3389/fphar.2014.00227
- Mondragon-Rodriguez, S., Perry, G., Zhu, X., and Boehm, J. (2012). Amyloid Beta and tau proteins as therapeutic targets for Alzheimer's disease treatment: rethinking the current strategy. *Int. J. Alzheimers Dis.* 2012:630182.
- Moriguchi, T., Saito, H., and Nishiyama, N. (1996). Aged garlic extract prolongs longevity and improves spatial memory deficit in senescence-accelerated mouse. *Biol. Pharm. Bull.* 19, 305–307. doi: 10.1248/bpb.19.305
- Morris, G., Puri, B. K., Walder, K., Berk, M., Stubbs, B., Maes, M., et al. (2018). The Endoplasmic Reticulum Stress Response in Neuroprogressive Diseases: emerging Pathophysiological Role and Translational Implications. *Mol. Neurobiol.* 55, 8765–8787. doi: 10.1007/s12035-018-1028-6
- Mu, J. S., Lin, H., Ye, J. X., Lin, M., and Cui, X. P. (2015). Rgl exhibits neuroprotective effects by inhibiting the endoplasmic reticulum stress-mediated c-Jun N-terminal protein kinase apoptotic pathway in a rat model of Alzheimer's disease. *Mol. Med. Rep.* 12, 3862–3868. doi: 10.3892/mmr.2015.3853

- O'Connor, T., Sadleir, K. R., Maus, E., Velliquette, R. A., Zhao, J., Cole, S. L., et al. (2008). Phosphorylation of the translation initiation factor eIF2 α increases BACE1 levels and promotes amyloidogenesis. *Neuron* 60, 988–1009. doi: 10.1016/j.neuron.2008.10.047
- Ohta, K., Mizuno, A., Li, S., Itoh, M., Ueda, M., Ohta, E., et al. (2011). Endoplasmic reticulum stress enhances gamma-secretase activity. *Biochem. Biophys. Res. Commun.* 416, 362–366. doi: 10.1016/j.bbrc.2011.11.042
- Oliveira, M. M., Lourenco, M. V., Longo, F., Kasica, N. P., Yang, W., Ureta, G., et al. (2021). Correction of eIF2-dependent defects in brain protein synthesis, synaptic plasticity, and memory in mouse models of Alzheimer's disease. *Sci. Signal* 14:eabc5429. doi: 10.1126/scisignal.abc5429
- Oyadomari, S., and Mori, M. (2004). Roles of CHOP/GADD153 in endoplasmic reticulum stress. *Cell Death Differ.* 11, 381–389. doi: 10.1038/sj.cdd.4401373
- Pan, C., Giraldo, G. S., Prentice, H., and Wu, J. Y. (2010). Taurine protection of PC12 cells against endoplasmic reticulum stress induced by oxidative stress. *J. Biomed. Sci.* 17:S17.
- Pan, C., Prentice, H., Price, A. L., and Wu, J. Y. (2012). Beneficial effect of taurine on hypoxia- and glutamate-induced endoplasmic reticulum stress pathways in primary neuronal culture. *Amino Acids* 43, 845–855. doi: 10.1007/s00726-011-1141-6
- Panagaki, T., Gengler, S., and Holscher, C. (2018). The Novel DA-CH3 Dual Incretin Restores Endoplasmic Reticulum Stress and Autophagy Impairments to Attenuate Alzheimer-Like Pathology and Cognitive Decrements in the APPSWE/PS1DeltaE9 Mouse Model. *J. Alzheimers Dis.* 66, 195–218. doi: 10.3233/jad-180584
- Parmar, V. M., and Schroder, M. (2012). Sensing endoplasmic reticulum stress. *Adv. Exp. Med. Biol.* 738, 153–168.
- Remondelli, P., and Renna, M. (2017). The Endoplasmic Reticulum Unfolded Protein Response in Neurodegenerative Disorders and Its Potential Therapeutic Significance. *Front. Mol. Neurosci.* 10:187. doi: 10.3389/fnmol.2017.010187
- Ron, D., and Hubbard, S. R. (2008). How IRE1 reacts to ER stress. *Cell* 132, 24–26. doi: 10.1016/j.cell.2007.12.017
- Ron, D., and Walter, P. (2007). Signal integration in the endoplasmic reticulum unfolded protein response. *Nat. Rev. Mol. Cell Biol.* 8, 519–529. doi: 10.1038/nrm2199
- Rozpedek, W., Pytel, D., Poplawski, T., Walczak, A., Gradzik, K., Wawrzynkiewicz, A., et al. (2019). Inhibition of the PERK-Dependent Unfolded Protein Response Signaling Pathway Involved in the Pathogenesis of Alzheimer's Disease. *Curr. Alzheimer Res.* 16, 209–218. doi: 10.2174/1567205016666190228121157
- Rozpedek-Kaminska, W., Siwecka, N., Wawrzynkiewicz, A., Wojtczak, R., Pytel, D., Diehl, J. A., et al. (2020). The PERK-Dependent Molecular Mechanisms as a Novel Therapeutic Target for Neurodegenerative Diseases. *Int. J. Mol. Sci.* 21:2108. doi: 10.3390/ijms21062108
- Salminen, A., Kauppinen, A., Suuronen, T., Kaarniranta, K., and Ojala, J. (2009). ER stress in Alzheimer's disease: a novel neuronal trigger for inflammation and Alzheimer's pathology. *J. Neuroinflammation* 6:41. doi: 10.1186/1742-2094-6-41
- Santos, L. E., and Ferreira, S. T. (2018). Crosstalk between endoplasmic reticulum stress and brain inflammation in Alzheimer's disease. *Neuropharmacology* 136, 350–360. doi: 10.1016/j.neuropharm.2017.11.016
- Schwarz, D. S., and Blower, M. D. (2016). The endoplasmic reticulum: structure, function and response to cellular signaling. *Cell Mol. Life Sci.* 73, 79–94. doi: 10.1007/s00018-015-2052-6
- Seidel, U., Huebbe, P., and Rimbach, G. (2019). Taurine: a Regulator of Cellular Redox Homeostasis and Skeletal Muscle Function. *Mol. Nutr. Food Res.* 63:e1800569.
- Senft, D., and Ronai, Z. A. (2015). UPR, autophagy, and mitochondria crosstalk underlies the ER stress response. *Trends Biochem. Sci.* 40, 141–148. doi: 10.1016/j.tibs.2015.01.002
- Shafahi, M., Vaezi, G., Shajee, H., Sharafi, S., and Khaksari, M. (2018). Crocin Inhibits Apoptosis and Astroglialosis of Hippocampus Neurons Against Methamphetamine Neurotoxicity via Antioxidant and Anti-inflammatory Mechanisms. *Neurochem. Res.* 43, 2252–2259. doi: 10.1007/s11064-018-2644-2
- Sidrauski, C., Tsai, J. C., Kampmann, M., Hearn, B. R., Vedantham, P., Jaishankar, P., et al. (2015). Pharmacological dimerization and activation of the exchange factor eIF2B antagonizes the integrated stress response. *Elife* 4:e07314.
- Sobow, T., Flirski, M., and Liberski, P. P. (2004). Amyloid-beta and tau proteins as biochemical markers of Alzheimer's disease. *Acta Neurobiol. Exp. (Wars)* 64, 53–70.
- Song, L., Piao, Z., Yao, L., Zhang, L., and Lu, Y. (2020). Schisandrin ameliorates cognitive deficits, endoplasmic reticulum stress and neuroinflammation in streptozotocin (STZ)-induced Alzheimer's disease rats. *Exp. Anim.* 69, 363–373. doi: 10.1538/expanim.19-0146
- Szegezdi, E., Fitzgerald, U., and Samali, A. (2003). Caspase-12 and ER-stress-mediated apoptosis: the story so far. *Ann. N. Y. Acad. Sci.* 1010, 186–194. doi: 10.1196/annals.1299.032
- Tu, Z., Yang, W., Yan, S., Guo, X., and Li, X. J. (2015). CRISPR/Cas9: a powerful genetic engineering tool for establishing large animal models of neurodegenerative diseases. *Mol. Neurodegener.* 10:35.
- Uddin, M. S., Tewari, D., Sharma, G., Kabir, M. T., Barreto, G. E., Bin-Jumah, M. N., et al. (2020). Molecular Mechanisms of ER Stress and UPR in the Pathogenesis of Alzheimer's Disease. *Mol. Neurobiol.* 57, 2902–2919. doi: 10.1007/s12035-020-01929-y
- Urano, F., Wang, X., Bertolotti, A., Zhang, Y., Chung, P., Harding, H. P., et al. (2000). Coupling of stress in the ER to activation of JNK protein kinases by transmembrane protein kinase IRE1. *Science* 287, 664–666. doi: 10.1126/science.287.5453.664
- Villain, N., and Dubois, B. (2019). Alzheimer's Disease Including Focal Presentations. *Semin. Neurol.* 39, 213–226. doi: 10.1055/s-0039-1681041
- Walter, P., and Ron, D. (2011). The unfolded protein response: from stress pathway to homeostatic regulation. *Science* 334, 1081–1086. doi: 10.1126/science.1209038
- Wang, Z. J., Zhao, F., Wang, C. F., Zhang, X. M., Xiao, Y., Zhou, F., et al. (2019). Xestospingon C, a Reversible IP3 Receptor Antagonist, Alleviates the Cognitive and Pathological Impairments in APP/PS1 Mice of Alzheimer's Disease. *J. Alzheimers Dis.* 72, 1217–1231. doi: 10.3233/jad-190796
- Wu, J., Pan, Z., Cheng, M., Shen, Y., Yu, H., Wang, Q., et al. (2013). Ginsenoside Rg1 facilitates neural differentiation of mouse embryonic stem cells via GR-dependent signaling pathway. *Neurochem. Int.* 62, 92–102. doi: 10.1016/j.neuint.2012.09.016
- Wu, J., Rutkowski, D. T., Dubois, M., Swathirajan, J., Saunders, T., Wang, J., et al. (2007). ATF6 α optimizes long-term endoplasmic reticulum function to protect cells from chronic stress. *Dev. Cell* 13, 351–364. doi: 10.1016/j.devcel.2007.07.005
- Xu, T. T., Zhang, Y., He, J. Y., Luo, D., Luo, Y., Wang, Y. J., et al. (2018). Bajijiasu Ameliorates beta-Amyloid-Triggered Endoplasmic Reticulum Stress and Related Pathologies in an Alzheimer's Disease Model. *Cell Physiol. Biochem.* 46, 107–117. doi: 10.1159/000488414
- Yang, H., and Wu, Z. (2018). Genome Editing of Pigs for Agriculture and Biomedicine. *Front. Genet.* 9:360. doi: 10.3389/fgene.2018.00360
- Zhang, J. S., Zhou, S. F., Wang, Q., Guo, J. N., Liang, H. M., Deng, J. B., et al. (2016). Gastrodin suppresses BACE1 expression under oxidative stress condition via inhibition of the PKR/eIF2 α pathway in Alzheimer's disease. *Neuroscience* 325, 1–9. doi: 10.1016/j.neuroscience.2016.03.024
- Zhu, P., Li, J., Fu, X., and Yu, Z. (2019). Schisandra fruits for the management of drug-induced liver injury in China: a review. *Phytomedicine* 59:152760. doi: 10.1016/j.phymed.2018.11.020

Conflict of Interest: The authors declare that the research was conducted in the absence of any commercial or financial relationships that could be construed as a potential conflict of interest.

Publisher's Note: All claims expressed in this article are solely those of the authors and do not necessarily represent those of their affiliated organizations, or those of the publisher, the editors and the reviewers. Any product that may be evaluated in this article, or claim that may be made by its manufacturer, is not guaranteed or endorsed by the publisher.

Copyright © 2021 Gao and Xu. This is an open-access article distributed under the terms of the Creative Commons Attribution License (CC BY). The use, distribution or reproduction in other forums is permitted, provided the original author(s) and the copyright owner(s) are credited and that the original publication in this journal is cited, in accordance with accepted academic practice. No use, distribution or reproduction is permitted which does not comply with these terms.



Immune Cell Infiltration Landscape of Ovarian Cancer to Identify Prognosis and Immunotherapy-Related Genes to Aid Immunotherapy

Xiushen Li^{1,2,3†}, Weizheng Liang^{4†}, Huanyi Zhao^{5†}, Zheng Jin⁶, Guoqi Shi⁵, Wanhua Xie⁷, Hao Wang^{1,2,3*} and Xueqing Wu^{1,2,8*}

OPEN ACCESS

Edited by:

Yongye Huang,
Northeastern University, China

Reviewed by:

Xingzhou Peng,
Hainan University, China
Xueman Ma,
Qinghai University, China

*Correspondence:

Hao Wang
haowang0806@gmail.com
Xueqing Wu
wuxueqing.37@hotmail.com

[†]These authors have contributed
equally to this work

Specialty section:

This article was submitted to
Signaling,
a section of the journal
Frontiers in Cell and Developmental
Biology

Received: 29 July 2021

Accepted: 19 October 2021

Published: 03 November 2021

Citation:

Li X, Liang W, Zhao H, Jin Z, Shi G,
Xie W, Wang H and Wu X (2021)
Immune Cell Infiltration Landscape of
Ovarian Cancer to Identify Prognosis
and Immunotherapy-Related Genes to
Aid Immunotherapy.
Front. Cell Dev. Biol. 9:749157.
doi: 10.3389/fcell.2021.749157

¹Department of Obstetrics and Gynecology, Shenzhen University General Hospital, Shenzhen, China, ²Guangdong Key Laboratory for Biomedical Measurements and Ultrasound Imaging, School of Biomedical Engineering, Shenzhen University Health Science Center, Shenzhen, China, ³Shenzhen Key Laboratory, Shenzhen University General Hospital, Shenzhen, China, ⁴Harbin Institute of Technology, Harbin, China, ⁵Guangzhou University of Chinese Medicine, Guangzhou, China, ⁶Zhujiang Hospital of Southern Medical University, Guangzhou, China, ⁷The Precise Medicine Center, Department of Basic Medical College, Shenyang Medical College, Shenyang, China, ⁸Clinical Medical Academy, Shenzhen University, Shenzhen, China

Ovarian cancer (OC) is the second leading cause of death in gynecological cancer. Multiple study have shown that the efficacy of tumor immunotherapy is related to tumor immune cell infiltration (ICI). However, so far, the Immune infiltration landscape of tumor microenvironment (TME) in OC has not been elucidated. In this study, We organized the transcriptome data of OC in the Cancer Genome Atlas (TCGA) and Gene Expression Omnibus (GEO) databases, evaluated the patient's TME information, and constructed the ICI scores to predict the clinical benefits of patients undergoing immunotherapy. Immune-related genes were further used to construct the prognostic model. After clustering analysis of ICI genes, we found that patients in ICI gene cluster C had the best prognosis, and their tumor microenvironment had the highest proportion of macrophage M1 and T cell follicular helper cells. This result was consistent with that of multivariate cox (multi-cox) analysis. The prognostic model constructed by immune-related genes had good predictive performance. By estimating Tumor mutation burden (TMB), we also found that there were multiple genes with statistically different mutation frequencies in the high and low ICI score groups. The model based on the ICI score may help to screen out patients who would benefit from immunotherapy. The immune-related genes screened may be used as biomarkers and therapeutic targets.

Keywords: ovarian cancer, immune cell infiltration, tumor mutation burden, immunotherapy, prognosis

Abbreviations: OC, ovarian cancer; ICI, immune cell infiltration; TME, tumor microenvironment; TCGA, the cancer genome atlas; GEO, gene expression omnibus; multi-cox, multivariate cox; TMB, tumor mutation burden; TPM, transcripts per kilobase of exon model per million mapped reads; GO, gene ontology; GSEA, gene set enrichment analysis; ROC, receiver operating characteristic; uni-cox, univariate cox; KEGG, kyoto encyclopedia of genes and genomes; PCA, principal component analysis; ICB, immune checkpoint blocking.

INTRODUCTION

Ovarian cancer (OC) is one of the deadliest gynecological malignancies. Owing to the lack of specific symptoms and early detection methods, approximately three-quarters of patients are already in stage III/IV at the time of diagnosis (Cheng et al., 2021). OC is the second most common cause of death in gynecological cancer. Globally, the number of deaths due to OC each year is nearly 152,000, accounting for 4.3% of all cancer deaths (Lheureux et al., 2019). In the past 30 years, the 5-year relative survival rate of most cancers has increased by one-fifth, but that of OC has not changed significantly (Siegel et al., 2018).

Cancer immunotherapy, based on the mechanism of immune escape, was rated as Breakthrough of the Year by Science (Xiang et al., 2019). Immunotherapy, including adoptive cell and checkpoint inhibitor therapy, which is often applied in the treatment lymphoma, melanoma, lung cancer, breast cancer and others, has become an indispensable method for the treatment of many cancer types (Lauss et al., 2017; Hirayama et al., 2019; Chalabi et al., 2020; Melosky et al., 2020). Tumor mutation burden (TMB), also known as tumor mutational load, is an emerging feature of cancer, which represents the number of somatic mutations (per one million bases) (Zehir et al., 2017). A growing body of literature has suggested that TMB can be used as a biomarker to identify patients suitable for immunotherapy (Steuer and Ramalingam, 2018; Klebanov et al., 2019). The tumor microenvironment (TME), composed of a variety of immune and non-immune cell populations, plays an crucial role during tumor initiation and progression. Many factors secreted within TME drive tumor biological processes such as immune suppression, pro-angiogenesis, and chronic inflammation (Pitt et al., 2016; Bader et al., 2020). The changes in the proportion of different immune cell populations and stromal cell populations in TME are related to the occurrence, metastasis, chemoresistance and progression of tumors (Turley et al., 2015). However, the overall landscape of immune cells and non-immune cells in the TME of OC is not yet clear.

In this study, we analyzed OC transcriptome data from The Cancer Genome Atlas (TCGA) and Gene Expression Omnibus databases to obtain the comprehensive outlook on 22 types of immune-related cells in the TME of OC patients through “CIBERSORT” and “estimate” packages. According to the immune cell infiltration (ICI) landscape, we divided patients with OC into 8 independent subtypes, and further established the ICI scores and immune-related gene prognosis model to predict the prognosis.

MATERIALS AND METHODS

OV Datasets and Samples

Through the TCGA database (<https://portal.gdc.cancer.gov/>) and GEO array express database (<https://www.ncbi.nlm.nih.gov/geo/>), we obtained six data sets (GSE18520, GSE26193, GSE19829, GSE30161, GSE63885, and TCGA-OV), and collected a total of

723 OC patient samples' transcriptome data. In order to perform unified analysis of data sets from different databases, we converted the expression value of the TCGA-OV data set into TPM (Transcripts Per Kilobase of exon model per Million mapped reads) value (Wagner et al., 2012). Furthermore, we reduced the possibility of batch effects between data sets due to non-biotechnology biases through the “ComBat” algorithm (Johnson et al., 2007).

Consensus Clustering

We used the leukocyte signature matrix gene signature and the “CIBERSORT” algorithm to quantify the proportion of 22 immune cells in OC samples. Through the “ESTIMATE” R package, the immune and matrix cell content of each OC sample was evaluated (Yoshihara et al., 2013). We performed the “ConsensusClusterPlus” R software package based on the unsupervised clustering method to perform ICI cluster analysis on the OC data set to determine the appropriate number of clusters.

DEGs Associated With the ICI Subgroup

With absolute multiple change > 1.5 and adjusted $p < 0.05$ as the screening conditions, the Differentially expressed genes (DEGs) between ICI subgroups were identified through the “limma” R package (Ritchie et al., 2015).

Dimensionality Reduction and Generation of ICI Score

First, according to the expression value of DEGs of the sample, the patients in the data set were classified by the unsupervised clustering method. DEGs contained in ICI feature gene sets A and B that were positively correlated and negatively correlated with patient classification, respectively. Next, the dimensionality reduction analysis of ICI feature gene sets A and B was performed by the “Boruta” R package (Kursa and Rudnicki, 2010). Then, we obtain feature scores through principal component analysis. Finally, the ICI score of each patient was obtained through the algorithm similar to the gene expression grade index. The specific calculation formula is as follows:

$$\text{ICI score} = \sum \text{PC1}_A - \sum \text{PC1}_B$$

This formula was based on the Gene expression grade index algorithm, which was used to summarize the similarity between expression profile and tumor grade (Sotiriou et al., 2006).

Functional and Pathway Enrichment Analysis

The genes in different ICI feature gene sets were respectively subjected to Gene Ontology (GO) enrichment analysis. Then, we observed the difference of the signal pathways enriched in different ICI score groups through gene set enrichment analysis (GSEA).

Collection of Somatic Alteration Data

We downloaded and calculated the number of non-synonymous mutations in TCGA-OV patients. According to the ICI scores, the somatic mutations of the driver genes in different groups of patients were evaluated accordingly. We identified the driver genes in OC patients by “maftool” package. The top 20 driver genes with the highest mutation frequency were analyzed, respectively.

Analyze the Predictive Performance of the ICI Scores and TMB Model

We constructed the Receiver Operating Characteristic (ROC) curve to analyze the predictive performance of the ICI score model. The TMB and ICI score models were combined through univariate cox (uni-cox), lasso, and multivariate cox (multi-cox) analysis, and ROC curve and Kaplan-Meier curve were used to analyze its prediction performance.

Construction and External Verification of Prognostic Models of Immune-Related Genes

Uni-cox analysis was used to screen out the ICI characteristic genes related to the patient’s prognosis. The lasso regression algorithm was used to delete the genes with higher correlation to prevent overfitting. We constructed the prognostic model through multi-cox analysis. The OC data (GSE140082) was used for external verification. The ICI scores, TMB and immune genes were used to construct a prognostic model (uni-cox, lasso, multi-cox).

Statistical Analyses

All statistical analyses were performed by SPSS Version 21.0 software. The data comparison between the two groups used unpaired Student’s *t* test for statistical significance, and the non-normally distributed variables used Mann-Whitney *U* test. For the data comparison between the above two groups, the parametric method and the non-parametric method used one-way analysis of variance and Kruskal-Wallis test, respectively. The correlation coefficient was calculated by Spearman correlation analysis and distance correlation analysis. The survival curve of each subgroup was drawn by Kaplan-Meier method. The log-rank test was used to evaluate whether the difference is statistically significant. Only when the two-tailed *p*-value is < 0.05, the difference is considered to be statistically significant.

RESULTS

Landscape of OC TME

We converted the expression value of the TCGA-OV data set to TPM value and merged the data of GSE18520, GSE26193, GSE19829, GSE30161, and GSE63885 (Supplementary Table S1). The ratio of 22 immune cells in OC samples was calculated by executing the CIBERSORT algorithms (Supplementary Table S2). The “ConsensusClusterPlus” R package clustered OC patients into 8 subtypes through an unsupervised clustering method (Supplementary Figure S1).

Figure 1 In order to clarify the inherent biological differences of different clinical phenotypes of OC samples, We divided patients into 8 ICI subgroups (Figure 2A). Figure 2B showed the distribution of 22 types of tumor cells in 8 ICI subgroups through the heat map. The correlation between the 22 types of tumor cells was further analyzed, and a map of correlation coefficient was constructed (Figure 2C). As shown in Figure 2D, the median survival time of each subtype was different. ICI subtype D patients had the longest median survival period, which was characterized by high infiltration of T cells regulatory, NK cells activated, plasma cells, and T cells follicular helper. The median survival time of patients with ICI subtype G was the shortest, which was characterized by the highly infiltrating cells Macrophages M2, Neutrophils, and Monocytes. Further analysis of the differences in the proportion of 22 types of tumor cells among the 8 ICI subtypes revealed that only in the four types of cells were no statistical difference between the subgroups (Figure 2E).

Identify Immune Gene Subtypes and GO Enrichment Analysis

We screened the differentially expressed genes among eight immune subtypes by “limma” R software. According to the obtained 817 differentially expressed genes, the OC patients were divided into five gene subgroups by using the “ConsensusClusterPlus” R package based on the unsupervised clustering algorithm (Supplementary Figure S2, Figure 3A). As shown in Figure 3C, we found patients in the ICI gene C group had the best prognosis, while those in the E group had the worst.

The 205 genes positively related to the gene subgroup were called ICI gene signature set A, while the 612 genes positively related to the gene subgroup were called ICI gene signature set B (Supplementary Table S3). Draw the expression of these 817 characteristic genes in OC samples through the “pheatmap” R package (Figure 3B). We performed dimensionality reduction analysis to reduce redundant genes, and finally got 37 and 237 genes, respectively (Supplementary Table S4). Through “clusterProfiler” R package we performed GO and Kyoto Encyclopedia of Genes and Genomes (KEGG) enrichment analysis on the ICI gene signature sets A and B after dimensionality reduction analysis (Figures 3D,E, Supplementary Figures S3E–F). Supplementary Table S5 provides detailed GO and KEGG enrichment analysis results. As shown in Figure 3F, the ICI gene subgroup C with the best prognosis showed the highest proportion of T cell follicular helper, monocytes, and macrophages M1, while the ICI gene subgroup E with the worst prognosis showed the highest proportion of naive B cells and the lowest proportion of regulatory T cells.

Construction of the ICI Score

We used principal component analysis (PCA) algorithm to analyze the ICI landscape of patients with OC. After calculation, we finally got the ICI prognostic landmark score. According to the ICI scores of patients with OC, we used the “survminer” R package to find the best cut-off value, and divided the patients into two groups with high and low scores. Then, the

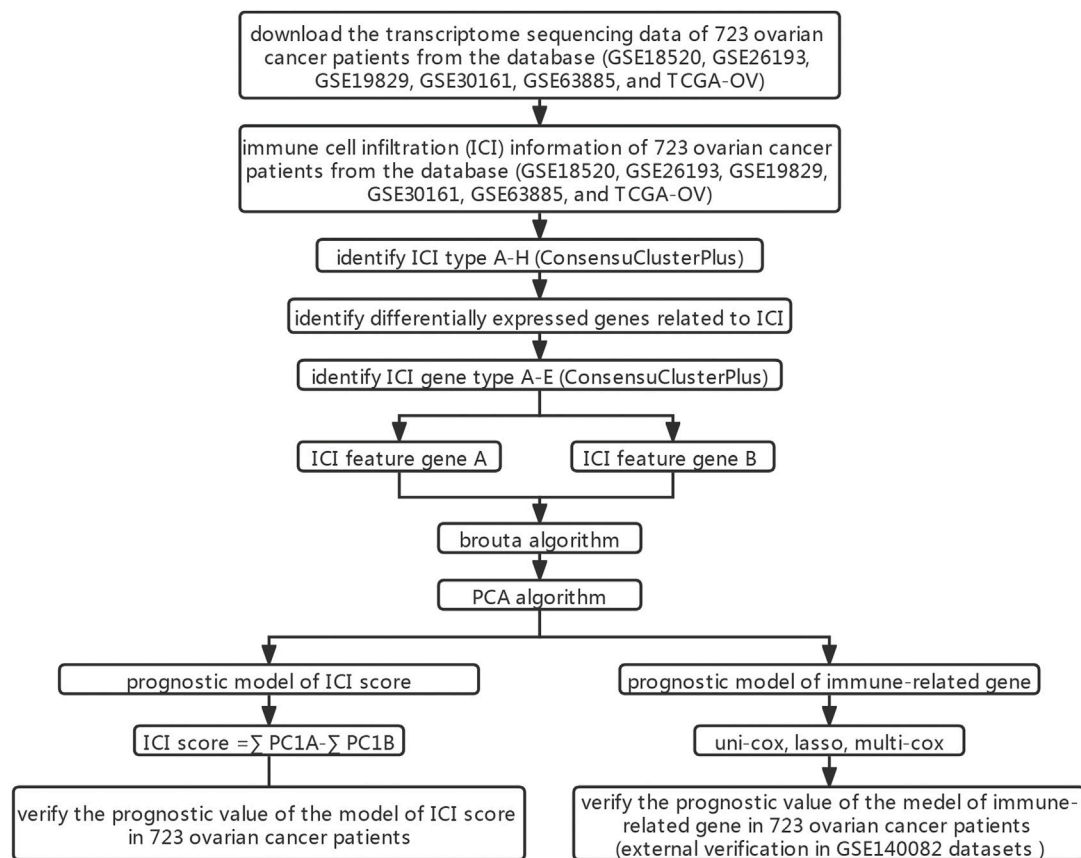


FIGURE 1 | Flow chart.

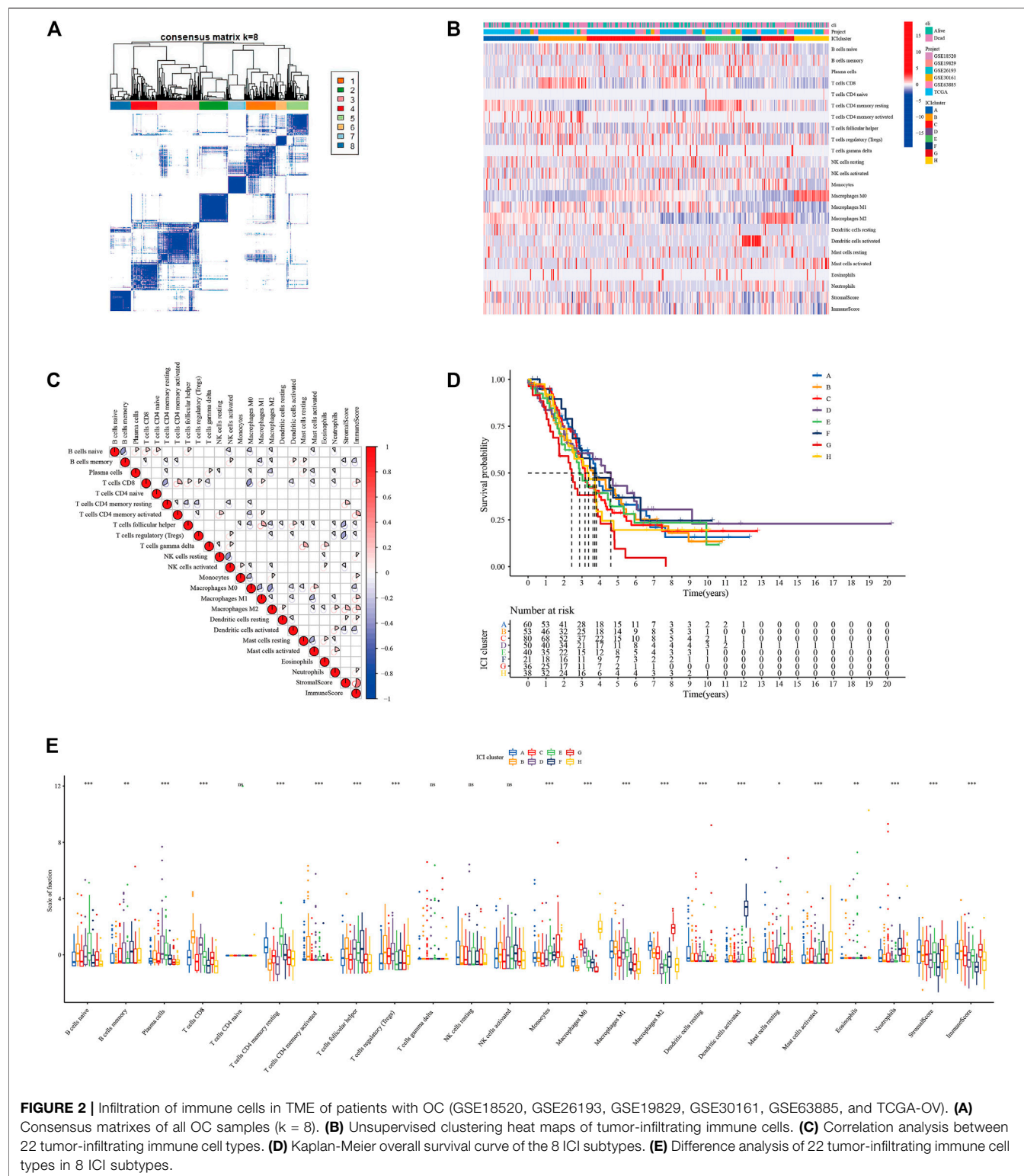
expression of immune-related genes in the two groups with high and low ICI scores was searched. The distribution of patients in five gene clusters was represented in **Figure 4A**. In this study, we selected the immune checkpoint-related genes and the immune activity-related genes for display. As shown in **Figure 4B**, the expressions of these 15 genes were statistically different between the two groups. In addition, the results of GSEA showed that in the high ICI group, jak-stat and chemokine signaling pathways were significantly enriched, while in the low ICI group, RNA polymerase and ribosome signaling pathways were significantly enriched (**Figure 4C**; **Supplementary Table S6**). We analyzed the relationship between the patient's ICI scores and survival time through the "survival" R package, and found that in the OC patient cohort of the TCGA database, patients with high ICI scores had poorer prognosis (**Figure 4D**). Further we analyzed the relationship between the ICI scores and prognosis of all OC patients included in this study and found that was consistent with the relationship obtained by TCGA-OC patients (**Figure 4E**).

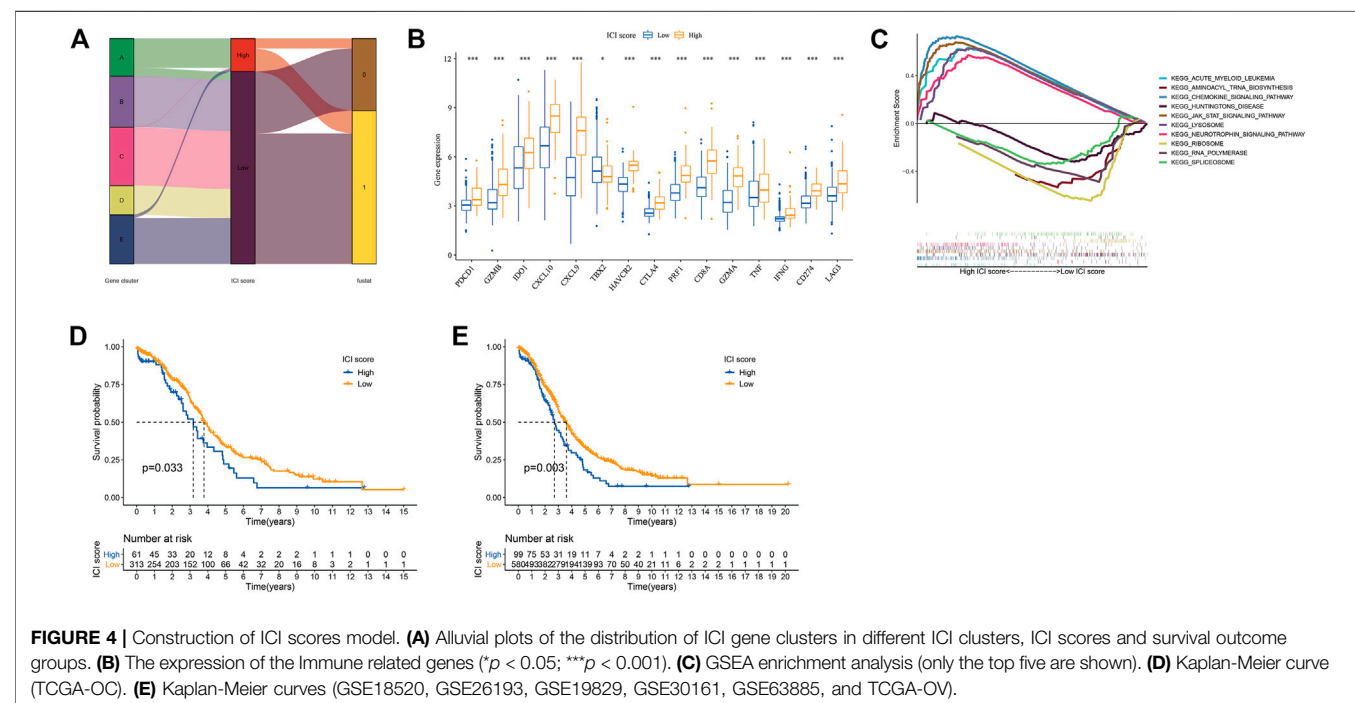
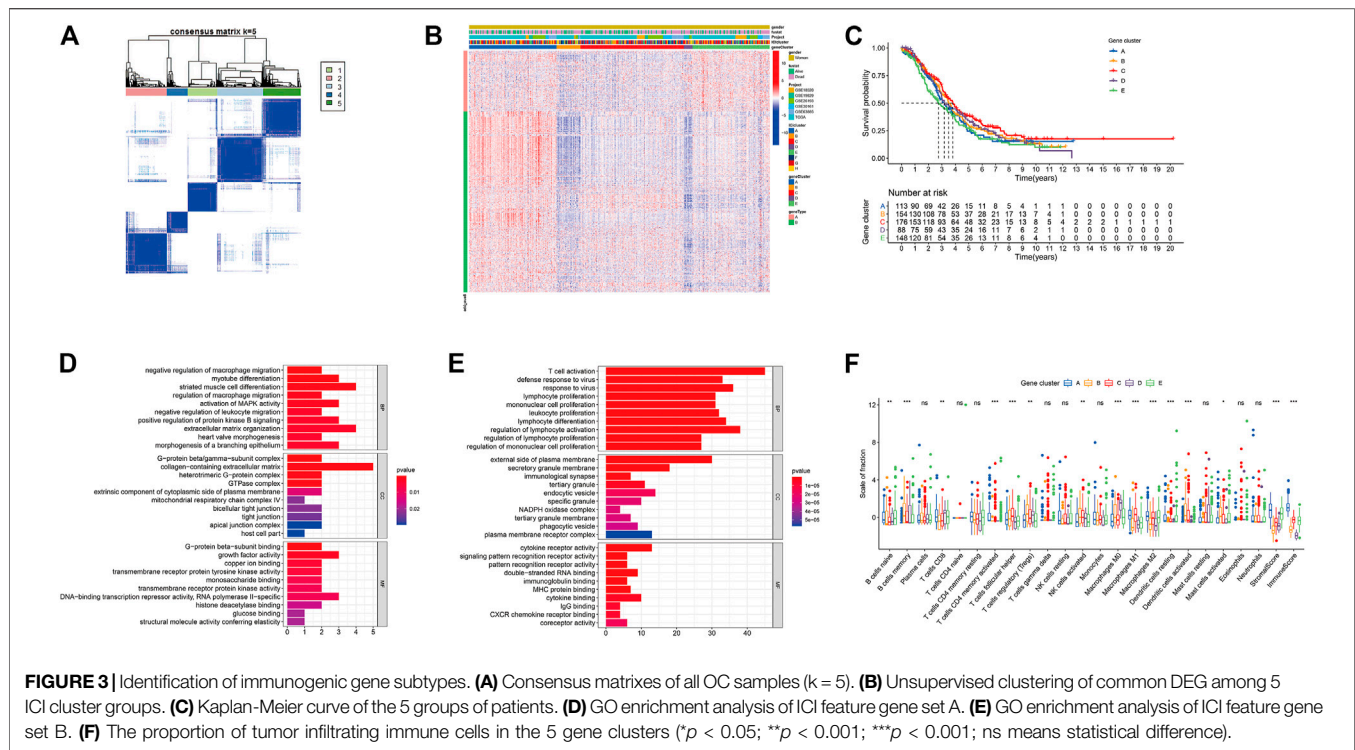
TME Characteristics of the TCGA Subtype and Cancer Somatic Genome

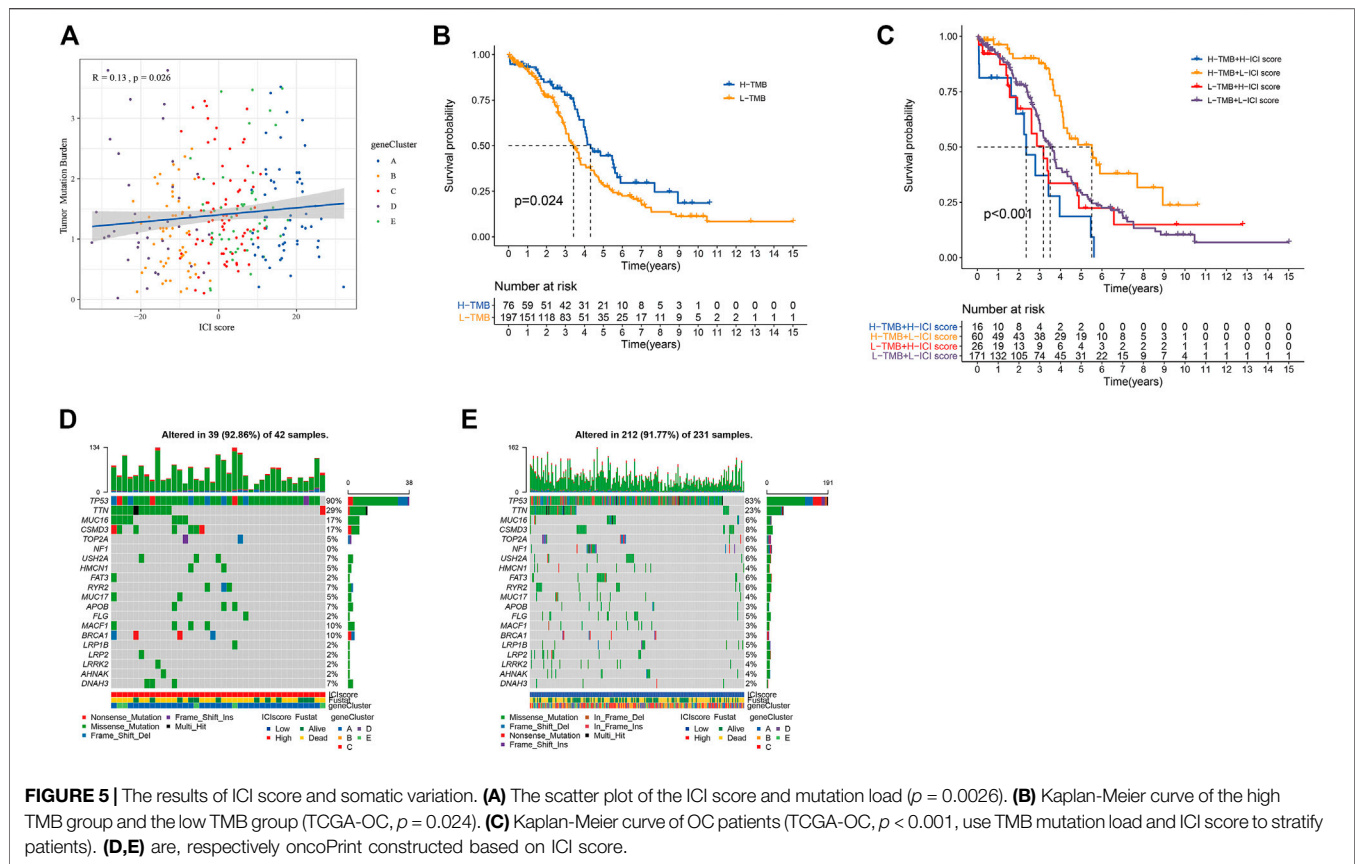
At present, Immune Checkpoint Blocking (ICB) therapy had been applied to a variety of tumor diseases, improving the overall survival rate of patients (Hodi, 2010; Borghaei et al., 2015; Nghiem et al.,

2016; Tom, 2018). A number of studies had shown that to mutation. Tumor mutation burden (TMB) could be used to predict the efficacy of ICB, and it has become a biomarker for various cancer types to identify patients who will benefit from immunotherapy (Rizvi et al., 2015; Timothy et al., 2015; Hugo et al., 2016; Carbone et al., 2017; Chan et al., 2019). Based on the important clinical significance of TMB for immunotherapy (**Supplementary Table S7**), we further explored the inner link between TMB and ICI scores to clarify the genetic information of ICI subgroups. Correlation analysis revealed a positive correlation between TMB and ICI scores (Spearman coefficient: $r = 0.13$, $p = 0.026$; **Figure 5A**). We found the best cutoff value by "survminer" R package, and divided the patients into high and low groups. By analyzing the relationship between TMB and patient prognosis, we found that the prognosis of patients in the high TMB group was better ($p = 0.024$; **Figure 5B**). We combined the patient's TMB and ICI scores information for analysis. It was found that patients with high ICI score and low TMB group had the best prognosis, while patients with high ICI score and high TMB group had the worst ($p < 0.001$; **Figure 5C**).

We obtained the driver genes of OC and evaluated the somatic mutations of patients in different ICI subgroup. **Figures 5D,E** showed respectively the mutation distributions of the 20 driver genes with the highest frequency of changes in the high and low ICI subgroups. These results might provide new directions for studying the mechanisms of immunotherapy, gene mutations, and tumor ICI distribution.







The Predictive Performance of the ICI Scores and TMB Model

We found that the prediction performance of the ICI scores model was poor by establishing the ROC curve (Supplementary Figures S3A,B). Further analysis of the predictive performance of the ICI scores and TMB combined model, through ROC curve and Kaplan-Meier curve found that its predictive performance was average (Supplementary Figures S3C,D).

Construction and External Verification of Prognostic Models of Immune-Related Genes

Through uni-cox analysis, a total of 44 genes related to the prognosis of OC patients and immunity were obtained (Figure 6A). In order to prevent overfitting, the lasso analysis was used to further screen the genes related to the patient's prognosis. As shown in Figures 6B,C, the value of the intersection point corresponding to the $\log(\lambda)$ of -3.5 was the smallest, and the corresponding values were 18. Therefore, we screened out 18 genes for subsequent analysis. The multi-cox analysis was performed on these 18 genes, and the results were shown in Figure 6D. The results of the multi-cox analysis were displayed in the nomogram (Figure 6E). The results of each step of the analysis were saved in Supplementary Table S8.

We tested the prognostic model of immune-related genes. The survival curve showed that the prognosis of patients in the low-

risk group was better, and there were statistical differences between the groups (Figure 7A). We observed the forecasting performance of the model through the ROC curve. As the forecasting time increased, the forecasting effect of the model showed an upward trend (Figure 7B). We sorted the samples of OC patients according to the risk score and found that as the score increased, the risk of death was higher (Figure 7C). We also obtained good prediction performance in the externally verified GSE140082 data set (Figures 7D–F; Supplementary Table S9).

Combining ICI scores, TMB, and immune genes (uni-cox, lasso, multi-cox), we further built a prognostic model (Supplementary Figure S4), and found that the prediction performance of this model was basically the same as that of immune-related gene models. The results of each step of the analysis were saved in Supplementary Table S10.

DISCUSSION

Cancer is a global public health problem and the second leading cause of death (Siegel et al., 2020; Huang et al., 2021b). In the last few years, a variety of specific immunotherapy drugs have been used in the clinical treatment of cancer patients. Immunotherapy, which uses the patient's immune capacity to treat cancer and prevent recurrence, has become the first-line treatment for some types of tumors (Kruger et al., 2019; Szeto and Finley, 2019). Immunotherapy has made remarkable

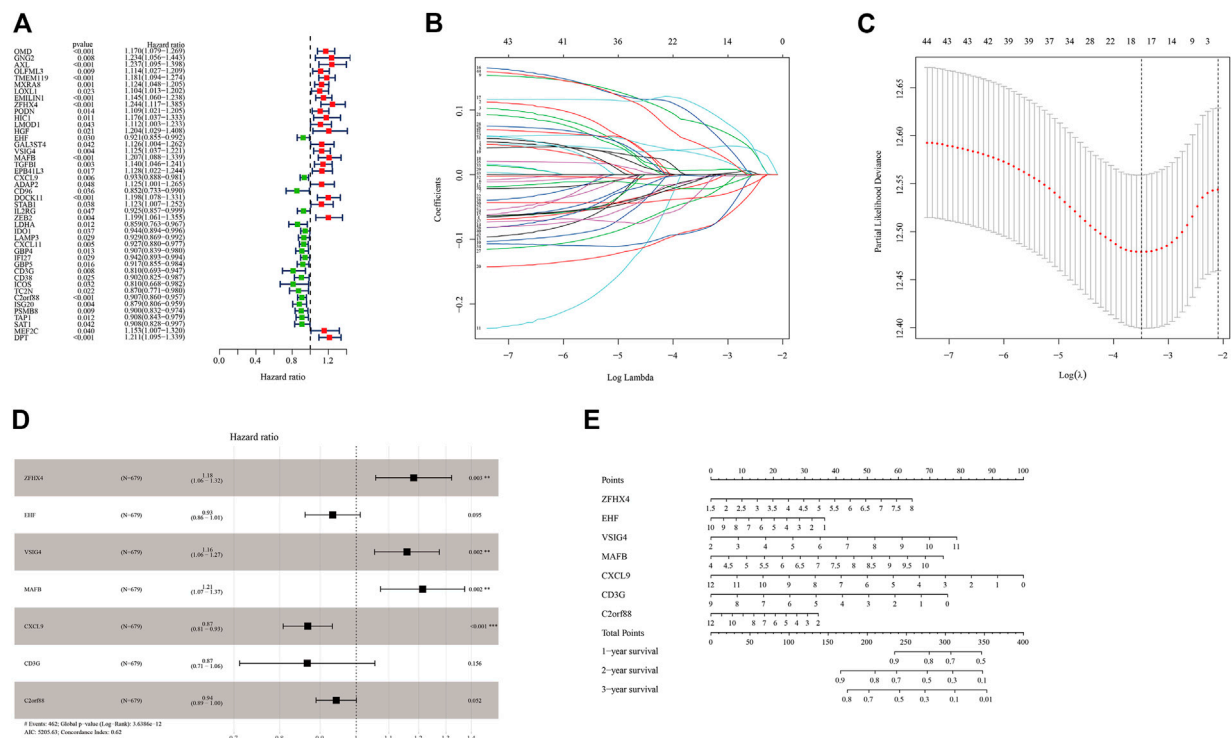


FIGURE 6 | Construction of the prognostic model of immune-related genes. **(A)** Uni-cox variance analysis of ICI feature gene set. **(B,C)** Lasso regression analysis results for genes obtained from uni-cox analysis. **(D)** Multi-cox analysis results of genes obtained from lasso regression analysis. **(E)** The nomogram of the prognostic model.

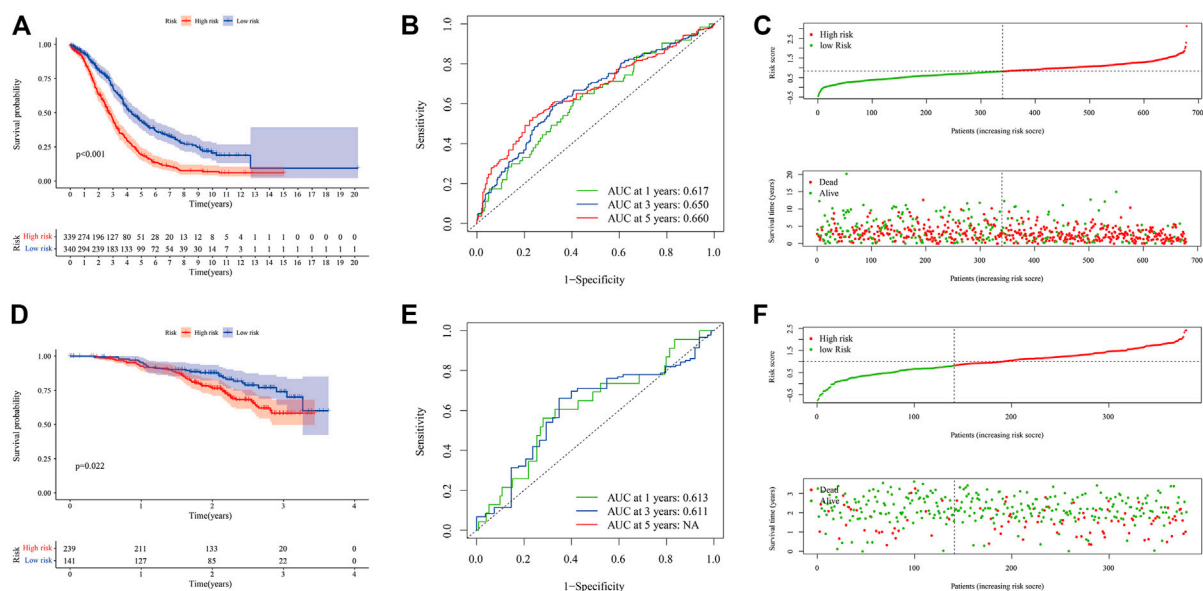


FIGURE 7 | Evaluation and external verification of prognostic models of immune-related genes. **(A–C)** show the analysis result of GSE18520, GSE26193, GSE19829, GSE30161, GSE63885, and TCGA-OV data set. **(A)** Kaplan-Meier curve (6 independent OC data sets). **(B)** ROC curves. **(C)** Scatter plot of the risk score and overall survival. **(D–F)** show the analysis result of GSE140082. **(D)** Kaplan-Meier curve (external verification). **(E)** ROC curves (external verification). **(F)** Scatter plot of patient risk score and overall survival (external verification).

progress in the treatment of tumors, but it still faces many challenges. The first obstacle is that only a few patients can benefit from immunotherapy. In 2018, it was estimated that two-fifths of the United States patients treated tumors with immune checkpoint inhibitor-related drugs, but the immune response rate was only 13% (Haslam and Prasad, 2019). Drug resistance might appear during chemotherapy, which greatly reduces the efficacy of treatment (Huang et al., 2021a). In this study, we established the model for predicting the immune benefit of OV patients and the immune prognosis evaluation model, which may provide help for immunotherapy of patients with ovarian cancer.

OC is classified as “immunogenic tumor”. Immune cell populations in tumors, peripheral blood and ascites fluid, including T and B lymphocytes, natural killer cells, etc., have great significance in the treatment of OC (Santoiemma et al., 2016; Yang et al., 2020). Non-immune cells in the TME may also have an impact on the efficacy of immunotherapy (Rodriguez et al., 2018). We divide the samples into eight different immune subtypes based on the content of 22 immune cells in OC patients. Further analysis found that the proportion of 18 immune cell populations between immune subtypes was statistically different. The proportion of follicular helper T cells, M1 macrophages, M2 macrophages, mast cells activated and the established ICI score model had the strong correlation with prognosis (**Supplementary Figure S5**). The tumor suppressor effect of follicular helper T cells was related to its ability to promote B cell maturation, affinity maturation and antibody secretion (Bindea et al., 2013; Crotty, 2014; Gu-Trantien et al., 2017). In addition, follicular helper T cells could promote the survival of CD8 T cells related to the prognosis of OC patients by secreting IL-21 (Zeng et al., 2005; Søndergaard et al., 2010; Kroeger et al., 2016). M1 macrophages could promote T cell immunity and played an anti-cancer effect, while M2 macrophages had the anti-inflammatory effect and played the cancer-promoting effect (Galli et al., 2011; Tamura et al., 2018). The relative proportion of M1 and M2 macrophages were closely related to the immunity of T cells, which had a major influence in the immune checkpoint blocking therapy of tumors (Galli et al., 2011). Mast cells in the tumor mass could inhibit tumor proliferation and angiogenesis, but their presence in the area around the tumor might promote tumor progression (Johansson et al., 2010). The positive and negative regulatory relationships between these four types of cells and tumor progression were opposite to the coefficient of multi-cox analysis, which was consistent with the conclusion that patients with low ICI scores in this study had a better prognosis.

Differences in gene expression during tumor formation might lead to changes in information transmission between immune cells, thereby affecting the occurrence of immune responses in the human body (Chen and Mellman, 2017). In this study, in order to have more in-depth understanding of the gene characteristics related to the immune system in patients with OC, we first extracted immune-related genes

and performed the cluster analysis on patients with OC. ICI gene cluster C with the highest Macrophages M1 and T cells follicular helper content had the best prognosis. We speculated that OC patients with ICI gene cluster C could benefit from immunotherapy, and the gene cluster used in this study may provide new targets for precision immunotherapy. ICI gene cluster E with higher Macrophages M2 and lower T cells follicular helper content had the worst prognosis. These were consistent with the results of the previous multi-cox analysis of the proportion of 22 immune cells. Therefore, we speculated that macrophage M1, macrophage M2, and T cell follicular helper cells might have important implications for the immunotherapy of OC.

Due to the large differences in individual immune environments, we quantified the ICI score of patients with OC. We used dimensionality reduction analysis on ICI gene feature sets A and B. The GO enrichment analysis results of ICI gene feature sets A and B were related to macrophages and T cells, respectively, which played extremely important roles in immunotherapy. Through GSEA, we discovered that chemokine, neurotrophin, and jak-stat signaling pathway might play significant roles in the occurrence and development of OC. Clinical studies have found that gene mutations were related to the clinical benefits of immunotherapy and could be used as potential biomarkers for immunotherapy (Wang et al., 2019; Pan et al., 2021). Recently, the United States Food and Drug Administration approved pembrolizumab as a clinical drug for high TMB-H solid tumors (≥ 10). Survival analysis found that TMB was related to patient prognosis. The joint analysis of TMB and ICI scores found that patients with high TMB and low ICI score had the best prognosis, while patients with H-TMB and high ICI score had the worst. It meant that ICI score and TMB might play a role in different aspects of OC immunotherapy. The low correlation between ICI score and TMB also confirmed this statement.

CONCLUSION

By analyzing the ICI characteristics of OC patients, we found that follicular helper T cells, mast cell activation, M1 macrophages and M2 macrophages may affect the patient's immunotherapy, and established an ICI score to predict the patient's clinical benefit. Provide a basis. We have further identified immune-related genes, which can be used as biomarkers for immunotherapy evaluation and targets for personalized immunotherapy.

DATA AVAILABILITY STATEMENT

The datasets presented in this study can be found in online repositories. The names of the repository/repositories and accession number(s) can be found in the article/**Supplementary Material**.

AUTHOR CONTRIBUTIONS

XL, WL, and HZ collected and analyzed the data, ZJ, GS, and WX conducted experiments and wrote the manuscript. XL, WL, and HZ contributed to find references. XL, WL, and HZ contributed equally, so they are the co-first authors. HW and XW are the guarantors of this study.

FUNDING

This study was supported by the Research fund of Shenzhen University General Hospital (SUGH2018QD042), Shenzhen Science and Technology Innovation Committee

REFERENCES

- Bader, J. E., Voss, K., and Rathmell, J. C. (2020). Targeting Metabolism to Improve the Tumor Microenvironment for Cancer Immunotherapy. *Mol. Cell* 78 (6), 1019–1033. doi:10.1016/j.molcel.2020.05.034
- Bindea, G., Mlecnik, B., Tosolini, M., Kirilovsky, A., Waldner, M., Obenaus, A. C., et al. (2013). Spatiotemporal Dynamics of Intratumoral Immune Cells Reveal the Immune Landscape in Human Cancer. *Immunity* 39 (4), 782–795. doi:10.1016/j.immuni.2013.10.003
- Borghaei, H., Paz-Ares, L., Horn, L., Spigel, D. R., Steins, M., Ready, N. E., et al. (2015). Nivolumab versus Docetaxel in Advanced Nonsquamous Non-small-cell Lung Cancer. *N. Engl. J. Med.*, 123–135.
- Carbone, D. P., Reck, M., Paz-Ares, L., Creelan, B., Horn, L., Steins, M., et al. (2017). First-Line Nivolumab in Stage IV or Recurrent Non-small-cell Lung Cancer. *N. Engl. J. Med.* 376 (25), 2415–2426. doi:10.1056/nejmoa1613493
- Chalabi, M., Fanchi, L. F., Dijkstra, K. K., Van den Berg, J. G., Aalbers, A. G., Sikorska, K., et al. (2020). Neoadjuvant Immunotherapy Leads to Pathological Responses in MMR-Proficient and MMR-Deficient Early-Stage colon Cancers. *Nat. Med.* 26 (4), 566–576. doi:10.1038/s41591-020-0805-8
- Chan, T. A., Yarchoan, M., Jaffee, E., Swanton, C., Quezada, S. A., Stenzinger, A., et al. (2019). Development of Tumor Mutation burden as an Immunotherapy Biomarker: Utility for the Oncology Clinic. *Ann. Oncol.* 30 (1), 44–56. doi:10.1093/annonc/mdy495
- Chen, D. S., and Mellman, I. (2017). Elements of Cancer Immunity and the Cancer-Immune Set point. *Nature* 541 (7637), 321–330. doi:10.1038/nature21349
- Cheng, X., Wang, J., Liu, C., Jiang, T., Yang, N., Liu, D., et al. (2021). Zinc Transporter SLC39A13/ZIP13 Facilitates the Metastasis of Human Ovarian Cancer Cells via Activating Src/FAK Signaling Pathway. *J. Exp. Clin. Cancer Res.* 40 (1), 199. doi:10.1186/s13046-021-01999-3
- Crotty, S. (2014). T Follicular Helper Cell Differentiation, Function, and Roles in Disease. *Immunity* 41 (4), 529–542. doi:10.1016/j.immuni.2014.10.004
- Galli, S. J., Borregaard, N., and Wynn, T. A. (2011). Phenotypic and Functional Plasticity of Cells of Innate Immunity: Macrophages, Mast Cells and Neutrophils. *Nat. Immunol.* 12 (11), 1035–1044. doi:10.1038/ni.2109
- Gu-Trantien, C., Migliori, E., Buisseret, L., de Wind, A., Brohée, S., Garaud, S., et al. (2017). CXCL13-producing TFH Cells Link Immune Suppression and Adaptive Memory in Human Breast Cancer. *JCI Insight* 2 (11). doi:10.1172/jci.insight.91487
- Haslam, A., and Prasad, V. (2019). Estimation of the Percentage of US Patients with Cancer Who Are Eligible for and Respond to Checkpoint Inhibitor Immunotherapy Drugs. *JAMA Netw. Open* 2 (5), e192535. doi:10.1001/jamanetworkopen.2019.2535
- Hirayama, A. V., Gauthier, J., Hay, K. A., Voutsinas, J. M., Wu, Q., Pender, B. S., et al. (2019). High Rate of Durable Complete Remission in Follicular Lymphoma after CD19 CAR-T Cell Immunotherapy. *Blood* 134 (7), 636–640. doi:10.1182/blood.2019000905
- (JCYJ20190808120807379), National Natural Science Foundation of China (81873822), and The grant of 2019 Guangdong Recruitment Program of Foreign experts (project name: Long-term effects of obesity on hypothalamic-pituitary-ovarian axis in women and mechanism study). Shenzhen Key Laboratory Foundation (ZDSYS20200811143757022).
- ## SUPPLEMENTARY MATERIAL
- The Supplementary Material for this article can be found online at: <https://www.frontiersin.org/articles/10.3389/fcell.2021.749157/full#supplementary-material>
- Hodi, F. S., O'Day, S. J., McDermott, D. F., Weber, R. W., Sosman, J. A., and Haanen, J. B. (2010). Improved Survival with Ipilimumab in Patients with Metastatic Melanoma. *N. Engl. J. Med.* 363 (8), 711–723. doi:10.1056/NEJMoa1003466
- Huang, Y., Yuan, K., Tang, M., Yue, J., Bao, L., Wu, S., et al. (2021a). Melatonin Inhibiting the Survival of Human Gastric Cancer Cells under ER Stress Involving Autophagy and Ras-Raf-MAPK Signalling. *J. Cel Mol Med.* 25 (3), 1480–1492. doi:10.1111/jcmm.16237
- Huang, Y., Zhou, Z., Zhang, J., Hao, Z., He, Y., Wu, Z., et al. (2021b). lncRNA MALAT1 Participates in Metformin Inhibiting the Proliferation of Breast Cancer Cell. *J. Cel Mol Med.* 25, 7135–7145. doi:10.1111/jcmm.16742
- Hugo, W., Zaretsky, J. M., Sun, L., Song, C., Moreno, B. H., Hu-Lieskovan, S., et al. (2016). Genomic and Transcriptomic Features of Response to Anti-PD-1 Therapy in Metastatic Melanoma. *Cell* 165, 35–44. doi:10.1016/j.cell.2016.02.065
- Johansson, A., Rudolphsson, S., Hammarsten, P., Halin, S., Pietras, K., Jones, J., et al. (2010). Mast Cells Are Novel Independent Prognostic Markers in Prostate Cancer and Represent a Target for Therapy. *Am. J. Pathol.* 177 (2), 1031–1041. doi:10.2353/ajpath.2010.100070
- Johnson, W. E., Li, C., and Rabinovic, A. (2007). Adjusting Batch Effects in Microarray Expression Data Using Empirical Bayes Methods. *Biostatistics* 8 (1), 118–127. doi:10.1093/biostatistics/kxj037
- Klebanov, N., Artomov, M., Goggins, W. B., Daly, E., Daly, M. J., and Tsao, H. (2019). Burden of Unique and Low Prevalence Somatic Mutations Correlates with Cancer Survival. *Sci. Rep.* 9 (1), 4848. doi:10.1038/s41598-019-41015-5
- Kroeger, D. R., Milne, K., and Nelson, B. H. (2016). Tumor-Infiltrating Plasma Cells Are Associated with Tertiary Lymphoid Structures, Cytolytic T-Cell Responses, and Superior Prognosis in Ovarian Cancer. *Clin. Cancer Res.* 22 (12), 3005–3015. doi:10.1158/1078-0432.Ccr-15-2762
- Kruger, S., Ilmer, M., Kobold, S., Cadilha, B. L., Endres, S., Ormanns, S., et al. (2019). Advances in Cancer Immunotherapy 2019 - Latest Trends. *J. Exp. Clin. Cancer Res.* 38 (1), 268. doi:10.1186/s13046-019-1266-0
- Kursa, M. B., and Rudnicki, W. R. (2010). Feature Selection with the Boruta Package. *J. Stat. Soft.* 36 (11), 1–13. doi:10.18637/jss.v036.i11
- Lauss, M., Donia, M., Harbst, K., Andersen, R., Mitra, S., Rosengren, F., et al. (2017). Mutational and Putative Neoantigen Load Predict Clinical Benefit of Adoptive T Cell Therapy in Melanoma. *Nat. Commun.* 8 (1), 1738. doi:10.1038/s41467-017-01460-0
- Lheureux, S., Braunstein, M., and Oza, A. M. (2019). Epithelial Ovarian Cancer: Evolution of Management in the Era of Precision Medicine. *CA Cancer J. Clin.* 69 (4), 280–304. doi:10.3322/caac.21559
- Melosky, B., Juergens, R., Hirsh, V., McLeod, D., Leigh, N., Tsao, M. S., et al. (2020). Amplifying Outcomes: Checkpoint Inhibitor Combinations in First-Line Non-Small Cell Lung Cancer. *Oncol.* 25 (1), 64–77. doi:10.1634/theoncologist.2019-0027
- Nghiem, P. T., Bhatia, S., Lipson, E. J., Kudchadkar, R. R., Miller, N. J., Annamalai, L., et al. (2016). PD-1 Blockade with Pembrolizumab in Advanced Merkel-Cell Carcinoma. *N. Engl. J. Med.* 374, 2542–2552. doi:10.1056/nejmoa1603702

- Pan, D., Hu, A. Y., Antonia, S. J., and Li, C.-Y. (2021). A Gene Mutation Signature Predicting Immunotherapy Benefits in Patients with NSCLC. *J. Thorac. Oncol.* 16 (3), 419–427. doi:10.1016/j.jtho.2020.11.021
- Pitt, J. M., Marabelle, A., Eggermont, A., Soria, J.-C., Kroemer, G., and Zitvogel, L. (2016). Targeting the Tumor Microenvironment: Removing Obstruction to Anticancer Immune Responses and Immunotherapy. *Ann. Oncol.* 27 (8), 1482–1492. doi:10.1093/annonc/mdw168
- Ritchie, M. E., Phipson, B., Wu, D., Hu, Y., Law, C. W., Shi, W., et al. (2015). Limma powers Differential Expression Analyses for RNA-Sequencing and Microarray Studies. *Nucleic Acids Res.* 43 (7), e47. doi:10.1093/nar/gkv007
- Rizvi, N. A., Hellmann, M. D., Snyder, A., Kvistborg, P., Makarov, V., Havel, J. J., et al. (2015). Cancer Immunology. Mutational Landscape Determines Sensitivity to PD-1 Blockade in Non-small Cell Lung Cancer. *Science* 348 (6230), 124–128. doi:10.1126/science.aaa1348
- Rodriguez, G., Galpin, K., McCloskey, C., and Vanderhyden, B. (2018). The Tumor Microenvironment of Epithelial Ovarian Cancer and its Influence on Response to Immunotherapy. *Cancers* 10 (8), 242. doi:10.3390/cancers10080242
- Santoemma, P. P., Reyes, C., Wang, L.-P., McLane, M. W., Feldman, M. D., Tanyi, J. L., et al. (2016). Systematic Evaluation of Multiple Immune Markers Reveals Prognostic Factors in Ovarian Cancer. *Gynecol. Oncol.* 143 (1), 120–127. doi:10.1016/j.ygyno.2016.07.105
- Siegel, R. L., Miller, K. D., and Jemal, A. (2020). Cancer Statistics, 2020. *CA A. Cancer J. Clin.* 70 (1), 7–30. doi:10.3322/caac.21590
- Siegel, R. L., Miller, K. D., and Jemal, A. J. C. A. C. J. f. C. (2018). Cancer Statistics. 60 (s 12), 277–300.
- Søndergaard, H., Galsgaard, E. D., Bartholomaeussen, M., Straten, P. T., Ødum, N., and Skak, K. (2010). Intratumoral Interleukin-21 Increases Antitumor Immunity, Tumor-Infiltrating CD8+ T-Cell Density and Activity, and Enlarges Draining Lymph Nodes. *J. Immunother.* 33 (3), 236–249. doi:10.1097/CJI.0b013e3181c0c1cb
- Sotiriou, C., Wirapati, P., Loi, S., Harris, A., Fox, S., Smeds, J., et al. (2006). Gene Expression Profiling in Breast Cancer: Understanding the Molecular Basis of Histologic Grade to Improve Prognosis. *J. Natl. Cancer Inst.* 98 (4), 262–272. doi:10.1093/jnci/djj052
- Steuer, C. E., and Ramalingam, S. S. (2018). Tumor Mutation Burden: Leading Immunotherapy to the Era of Precision Medicine. *Jco* 36 (7), 631–632. doi:10.1200/jco.2017.76.8770
- Szeto, G. L., and Finley, S. D. (2019). Integrative Approaches to Cancer Immunotherapy. *Trends Cancer* 5 (7), 400–410. doi:10.1016/j.trecan.2019.05.010
- Tamura, R., Tanaka, T., Yamamoto, Y., Akasaki, Y., and Sasaki, H. (2018). Dual Role of Macrophage in Tumor Immunity. *Immunotherapy* 10 (10), 899–909. doi:10.2217/imt-2018-0006
- Timothy, A., Chan Jedd, D., and Wolchok, A. (2015). medicine, S.J.T.N.E.j.o: Genetic Basis for Clinical Response to CTLA-4 Blockade in Melanoma..
- Tom, P. J. E. (2018). Urology Re: Nivolumab Plus Ipilimumab versus Sunitinib in Advanced Renal-Cell Carcinoma..
- Turley, S. J., Cremasco, V., and Astarita, J. L. (2015). Immunological Hallmarks of Stromal Cells in the Tumour Microenvironment. *Nat. Rev. Immunol.* 15 (11), 669–682. doi:10.1038/nri3902
- Wagner, G. P., Kin, K., and Lynch, V. J. (2012). Measurement of mRNA Abundance Using RNA-Seq Data: RPKM Measure Is Inconsistent Among Samples. *Theor. Biosci.* 131 (4), 281–285. doi:10.1007/s12064-012-0162-3
- Wang, Z., Duan, J., Cai, S., Han, M., Dong, H., Zhao, J., et al. (2019). Assessment of Blood Tumor Mutational Burden as a Potential Biomarker for Immunotherapy in Patients with Non-small Cell Lung Cancer with Use of a Next-Generation Sequencing Cancer Gene Panel. *JAMA Oncol.* 5 (5), 696–702. doi:10.1001/jamaoncol.2018.7098
- Xiang, Y., Guo, Z., Zhu, P., Chen, J., and Huang, Y. (2019). Traditional Chinese Medicine as a Cancer Treatment: Modern Perspectives of Ancient but Advanced Science. *Cancer Med.* 8 (5), 1958–1975. doi:10.1002/cam4.2108
- Yang, C., Xia, B.-R., Zhang, Z.-C., Zhang, Y.-J., Lou, G., and Jin, W.-L. (2020). Immunotherapy for Ovarian Cancer: Adjuvant, Combination, and Neoadjuvant. *Front. Immunol.* 11, 577869. doi:10.3389/fimmu.2020.577869
- Yoshihara, K., Shahmoradgoli, M., Martínez, E., Vegesna, R., Kim, H., Torres-Garcia, W., et al. (2013). Inferring Tumour Purity and Stromal and Immune Cell Admixture from Expression Data. *Nat. Commun.* 4, 2612. doi:10.1038/ncomms3612
- Zehir, A., Benayed, R., Shah, R. H., Syed, A., Middha, S., Kim, H. R., et al. (2017). Erratum: Mutational Landscape of Metastatic Cancer Revealed from Prospective Clinical Sequencing of 10,000 Patients. *Nat. Med.* 23 (8), 1004. doi:10.1038/nm0817-1004c
- Zeng, R., Spolski, R., Finkelstein, S. E., Oh, S., Kovanen, P. E., Hinrichs, C. S., et al. (2005). Synergy of IL-21 and IL-15 in Regulating CD8+ T Cell Expansion and Function. *J. Exp. Med.* 201 (1), 139–148. doi:10.1084/jem.20041057

Conflict of Interest: The authors declare that the research was conducted in the absence of any commercial or financial relationships that could be construed as a potential conflict of interest.

Publisher's Note: All claims expressed in this article are solely those of the authors and do not necessarily represent those of their affiliated organizations, or those of the publisher, the editors and the reviewers. Any product that may be evaluated in this article, or claim that may be made by its manufacturer, is not guaranteed or endorsed by the publisher.

Copyright © 2021 Li, Liang, Zhao, Jin, Shi, Xie, Wang and Wu. This is an open-access article distributed under the terms of the Creative Commons Attribution License (CC BY). The use, distribution or reproduction in other forums is permitted, provided the original author(s) and the copyright owner(s) are credited and that the original publication in this journal is cited, in accordance with accepted academic practice. No use, distribution or reproduction is permitted which does not comply with these terms.



Mitochondrial Defects in Fibroblasts of Pathogenic *MAPT* Patients

Vinita Bharat, Chung-Han Hsieh and Xinnan Wang*

Department of Neurosurgery, Stanford University School of Medicine, Stanford, CA, United States

OPEN ACCESS

Edited by:

Yongye Huang,
Northeastern University, China

Reviewed by:

Tiziana Alberio,
University of Insubria, Italy
Giuseppe Arena,
University of Luxembourg,
Luxembourg
Yuzuru Imai,
Juntendo University, Japan

*Correspondence:

Xinnan Wang
xinnanw@stanford.edu

Specialty section:

This article was submitted to
Signaling,
a section of the journal
Frontiers in Cell and Developmental
Biology

Received: 27 August 2021

Accepted: 14 October 2021

Published: 03 November 2021

Citation:

Bharat V, Hsieh C-H and Wang X
(2021) Mitochondrial Defects
in Fibroblasts of Pathogenic *MAPT*
Patients.
Front. Cell Dev. Biol. 9:765408.
doi: 10.3389/fcell.2021.765408

Mutations in *MAPT* gene cause multiple neurological disorders, including frontal temporal lobar degeneration and parkinsonism. Increasing evidence indicates impaired mitochondrial homeostasis and mitophagy in patients and disease models of pathogenic *MAPT*. Here, using *MAPT* patients' fibroblasts as a model, we report that disease-causing *MAPT* mutations compromise early events of mitophagy. By employing biochemical and mitochondrial assays we discover that upon mitochondrial depolarization, the recruitment of LRRK2 and Parkin to mitochondria and degradation of the outer mitochondrial membrane protein Miro1 are disrupted. Using high resolution electron microscopy, we reveal that the contact of mitochondrial membranes with ER and cytoskeleton tracks is dissociated following mitochondrial damage. This membrane dissociation is blocked by a pathogenic *MAPT* mutation. Furthermore, we provide evidence showing that tau protein, which is encoded by *MAPT* gene, interacts with Miro1 protein, and this interaction is abolished by pathogenic *MAPT* mutations. Lastly, treating fibroblasts of a *MAPT* patient with a small molecule promotes Miro1 degradation following depolarization. Altogether, our results show molecular defects in a peripheral tissue of patients and suggest that targeting mitochondrial quality control may have a broad application for future therapeutic intervention.

Keywords: ER, mitochondria, Miro, parkinsonism, FTL, mitophagy, tau, *MAPT*

INTRODUCTION

Mitochondria are a vital organelle to support neuronal function and survival. Emerging evidence has revealed mitochondrial malfunction in a broad spectrum of neurological disorders (Misgeld and Schwarz, 2017). One such neurological condition is tauopathy, which is shared by multiple neurodegenerative diseases such as Alzheimer's disease (AD), progressive supranuclear palsy (PSP), frontal temporal lobar degeneration (FTLD), and parkinsonism (Spillantini and Goedert, 2013; Medina, 2018). Tauopathy is featured with intracellular neurofibrillary tangles. The main constituent of those filaments is tau protein, which is encoded by *MAPT* gene. Mutations in *MAPT* gene result in production of abnormal tau protein and promote tangle formation. Therefore, pathogenic *MAPT* mutations are detrimental to neuronal integrity and function (Fuster-Matanzo et al., 2018). In several mouse models, overexpression of tau affects mitochondrial distribution, transport, and clearance (Thies and Mandelkow, 2007; Zempel and Mandelkow, 2015; Hu et al., 2016). Recent reports have shown that mutant tau impairs mitophagy (Hu et al., 2016; Cummins et al., 2019; Fang et al., 2019), a mitochondria-specific autophagy process, likely by

inhibiting Parkin recruitment to damaged mitochondria (Hu et al., 2016; Cummins et al., 2019). Further characterization of mitophagy steps affected by pathogenic *MAPT* would help us understand better the underlying mechanisms and potential implications for disease pathogenesis.

Upon mitochondrial damage, outer mitochondrial membrane (OMM) proteins rapidly undergo proteasome degradation, prior to lysosomal digestion of the remaining mitochondrion (Chan et al., 2011). This initial step is thought to facilitate the dissociation of a damaged mitochondrion from the rest of the healthy mitochondrial network to halt the spread of damage. Particularly, the removal of Mitofusin protein has been shown to promote mitochondrial fragmentation and the separation of mitochondria-ER tethering (Poole et al., 2010; Tanaka et al., 2010; Hsieh et al., 2016; McLelland et al., 2018); this step can sever a damaged part from a large, otherwise healthy mitochondrion and block ER contact with mitochondrial damage. In addition, the removal of Miro protein uncouples mitochondria from motors and microtubule tracks to prevent mitochondria from moving around (Wang et al., 2011). Importantly, we have recently found that removing Miro is also essential for static mitochondria to undergo mitophagy (Hsieh et al., 2016, 2019; Shaltouki et al., 2018), pinpointing a role for Miro in additional steps of mitophagy. The degradation of these OMM proteins following mitochondrial depolarization is mediated by at least two pathways – LRRK2 and the PINK1-Parkin axis (Wang et al., 2011; Chen and Dorn, 2013; Hsieh et al., 2016; **Figure 1A**). Mutations in *LRRK2*, *PINK1*, or *Parkin* cause familial Parkinson's disease (PD) (Kitada et al., 1998; Bonifati, 2002; Valente et al., 2004; Zimprich et al., 2004). However, whether the removal of these OMM proteins from damaged mitochondria is affected by pathogenic *MAPT* mutations remains largely elusive.

Skin fibroblast cells cultured directly from patients have emerged as an outstanding model to study disease-relevant molecular defects, because these cells retain the identical genetic backgrounds of patients and contain molecular and mitochondrial pathologies (Smith et al., 2016; Di Nottia et al., 2017; Fitzgerald et al., 2017; Garcia-Sanz et al., 2017; Teves et al., 2017; Verma et al., 2017; Juarez-Flores et al., 2018; Bonello et al., 2019; Korecka et al., 2019). In addition, skin fibroblasts can be obtained from patients by a minimally invasive, painless procedure (Le et al., 2017), and thus are a convenient source for developing biomarkers and diagnostic assays. A biomarker in biopsied skin tissues may originate from an alternative biological process to that in body fluids, providing an additional and possibly more reliable (Le et al., 2017) predicative value. In this study, we examined several mitochondrial behaviors in fibroblasts of *MAPT* patients, and found clear evidence of impairments in these molecular and cellular processes.

MATERIALS AND METHODS

Cell Culture and Biochemistry

Fibroblasts were obtained under an MTA from the National Institute of Neurological Disorders and Stroke (NINDS) human

and cell repository or the Parkinson's Progression Markers Initiative (PPMI), which is in a partnership with multiple institutions that approved study protocols, ensured consent from donors, and deposited fibroblasts. All available lines were acquired from NINDS at the time of purchase. Fibroblast and HEK cell culture, immunoprecipitation (IP), and mitochondrial purification were described in Hsieh et al. (2016). Briefly, CCCP in DMSO or the same volume of DMSO treated fibroblasts were lifted by a cell scraper, and mechanically homogenized with a Dounce homogenizer in 750 μ l isolation buffer (200 mM sucrose, 10 mM TRIS/MOPS, pH 7.4). After centrifugation at 500 g for 10 min, crude supernatant was spun at 10,000 g for 10 min to pellet intact mitochondria. Mitochondrial pellet was washed twice with isolation buffer. After this step, supernatant was named "cytosolic fraction (Cyto)," and pellet was resuspended in 50 μ l lysis buffer (50 mM Tris pH 8.0, 150 mM NaCl, and 1% Triton X-100-T8787, Sigma-Aldrich) with 0.25 mM phenylmethanesulfonyl fluoride (P7626, Sigma-Aldrich) and protease inhibitors (Roche) named "mitochondrial fraction (Mito)." Samples were mixed 1:1 with 2 \times Laemmli buffer (4% SDS, 20% Glycerol, 120 mM Tris-HCl, 0.02% bromophenol blue, 700 mM 2-mercaptoethanol) and boiled for 5 min prior to being loaded (Mito: Cyto = 25:1) into an SDS-PAGE. pRK5-EGFP-tau (#46904, addgene), pRK5-EGFP-tau-P301L, pRK5-EGFP-tau-N279K, and pRK5-EGFP-tau-R406W (the latter three were custom-made by SynBio Technology) were used for transfection by the calcium phosphate transfection protocol (Wang and Schwarz, 2009). Transferred membranes were first blocked overnight in phosphate-buffered saline (PBS) containing 5% fat-free milk and 0.1% tween-20 at 4°C, and then incubated with the following primary antibodies: mouse anti-Miro1 (WH0055288M1, Sigma-Aldrich) at 1:1,000, rabbit anti-Miro1 (HPA010687, Sigma-Aldrich) at 1:1,000, rabbit anti-VDAC (4661S, Cell Signaling Technology) at 1:1,000, mouse anti-Mitofusin2 (H00009927-M01, Abnova) at 1:1,000, mouse anti-Parkin (sc32282, Santa Cruz Biotechnology) at 1:500, rabbit anti-LRRK2 (NB300-268, Novus Biologicals) at 1:500, rabbit anti-GAPDH (5174S, Cell Signaling Technology) at 1:3,000, rabbit anti- β -actin (4967S, Cell Signaling Technology) at 1:1,000, rabbit anti-GFP (A11122, Invitrogen) at 1:750, mouse anti-ATP5 β (ab14730, Abcam) at 1:100, rabbit anti-Calreticulin (2891, Cell Signaling Technology) at 1:1,000, mouse anti-Golgi (NB600-412, Novus Biologicals) at 1:100, or mouse anti-Myc (9E10/sc-40, Santa Cruz Biotechnology) at 1:100, at 4°C overnight in blocking buffer. HRP-conjugated goat anti-mouse or rabbit IgG (Jackson ImmunoResearch Laboratories) were used at 1:5,000–10,000. West Dura ECL Reagents (34075, GE Healthcare) were used for ECL immunoblotting. Membranes were exposed to UltraCruz autoradiography films (Santa Cruz Biotechnology) and developed on a Konica Minolta SRX-101A developer or scanned using a Bio-Rad ChemiDoc XRS system.

All experiments were performed in a blinded format, and the identities of the lines were un-blinded after the experiments. For **Figure 1C**, the intensities of protein bands were measured by ImageJ (ver. 1.48V, NIH). The intensity of each band in the mitochondrial fraction was normalized to that of the

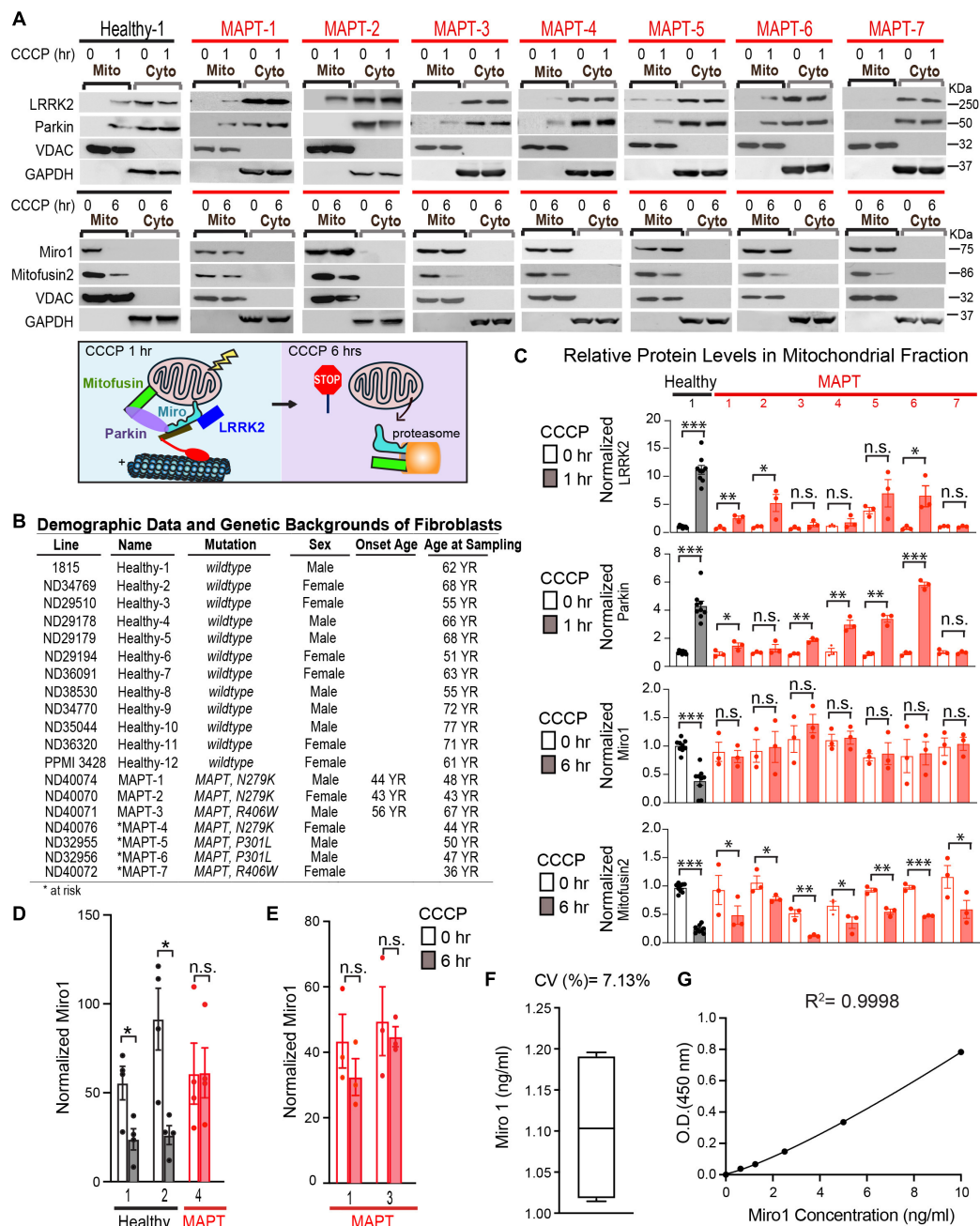


FIGURE 1 | Mitochondrial protein changes following CCCP treatment in fibroblasts. **(A)** Mitochondrial (Mito) and cytosolic (Cyto) fractions were immunoblotted as indicated. Below: Schematic representation of our readouts. **(B)** Demographic and genetic information of all cell lines used in this study or described in Text. **(C)** Quantifications of mitochondrial protein levels. The intensity of each band in the mitochondrial fraction is normalized to that of the mitochondrial loading control VDAC from the same blot and expressed as a fraction of Mean of Healthy-1 with DMSO treatment; this control was included in every experiment. Student *T* Test is performed for comparing normalized band intensities within the same subject (DMSO vs. CCCP). *N* = 3–9 independent experiments. Please note that Healthy-2 to 12 show similar mitochondrial protein responses to CCCP as Healthy-1, previously published in Hsieh et al. (2019). **(D,E)** ELISA of Miro1 protein. Comparison within the same subject. Mann-Whitney *U* Test. **(D)** *N* = 4 with duplicates each time. **(E)** *N* = 3. **(F)** Intra-plate variability of ELISA shown in **(E)**, measured by running the same fibroblast sample 4 times in the same plate. **(G)** The standard curve for **(E)** is shown. Sigmoidal 4PL is used. **P* < 0.05, ***P* < 0.01, ****P* < 0.001. n.s.: not significant.

mitochondrial loading control VDAC from the same blot, and expressed as a fraction of Mean of Healthy-1 with DMSO treatment (Hsieh et al., 2016); this control was included in every

independent experiment. The band intensities of VDAC were not significantly different among all fibroblast lines and conditions (*P* > 0.8, One-Way ANOVA Post Hoc Tukey Test).

Enzyme-Linked Immunosorbent Assay (ELISA)

All experiments were performed as blinded tests. A 40 μ M CCCP in DMSO or the same volume of DMSO alone was applied to fibroblasts for 6 h, and then cells were lysed in lysis buffer (100 mM Tris, 150 mM NaCl, 1 mM EGTA, 1 mM EDTA, 1% Triton X-100, 0.5% Sodium deoxycholate) with protease inhibitor cocktail (539134, Calbiochem). Cell debris was removed by centrifugation at 17,000 *g* for 10 min at 4°C. Details of ELISA are in **Supplementary Methods**.

Transmission Electron Microscopy (TEM)

Cells were grown on ~10 mm Aclar discs in 37°C incubator with 5% CO₂ till 95–100% confluent. Each Aclar disc was then transferred separately into an Eppendorf tube with 1 ml of fixative solution (2% glutaraldehyde and 4% paraformaldehyde in 0.1 M sodium cacodylate buffer) and incubated for an hour. These cells were kept on ice until processed for imaging. Fixative was removed and 1% OsO₄ in ddH₂O was added. Samples were then gently shaken and incubated for 1 h at 4°C. Incubated samples were washed three times with cold ddH₂O for 5 min each. Samples were then stained with 1% uranyl acetate for 2 h at 4°C. Stained samples were dehydrated, first with 50% EtOH for 10 min, next 70% EtOH for 10 min, and lastly 95% EtOH for 10 min. Samples were allowed to warm up to room temperature before two more dehydration procedures with 100% EtOH for 10 min each. The final dehydration was performed with acetonitrile for 15 min. The dehydration mixture was then replaced with Embed 812 medium (44% Embed 812, 35% DDSA, 18% NMA, 3% BDMA) and acetonitrile (1:1 ratio) for 1 h. The ratio was then increased to 2:1 (Embed 812 medium to acetonitrile) for overnight incubation. Next, the mixture was replaced with 100% Embed 812 medium and incubated for 2 h before samples were placed in molds for overnight settling. Settled samples were polymerized in a 65°C oven for 24 h before being sectioned for imaging. Imaging was performed using a Jeol TEM 1400 microscope, and images were acquired at 5,000 \times . Images were saved as .dc3 files. Analysis of .dc3 images was performed using ImageJ.

Statistics

Throughout the paper, the distribution of data points was expressed as box-whisker, or dot-plot with Mean \pm SEM, except otherwise stated. Box center line is median and box limits are upper and lower quartiles. One-Way or Two-Way ANOVA Post Hoc Tukey Test was performed for comparing multiple groups. Mann-Whitney *U* or *T* Test was performed for comparing two groups. Chi-Square Test was performed for **Figure 3B** because the data was categorical. Statistical analyses were performed using the Prism software (ver. 8.01, GraphPad) or Excel (ver. 16.51). The number of experimental replications (*n*) can be found in Figure Legends. No statistical methods were used to predetermine sample sizes, but the number of experiments and biological replicates was chosen based on the nature of the experiments (it is usually difficult to assess an outcome that follows a normal distribution in our experiments), degree of

variations, and published papers describing similar experiments. We did not exclude any data. **P* < 0.05, ***P* < 0.01, ****P* < 0.001, for all Figures.

RESULTS

The LRRK2 and PINK1-Parkin Pathways Are Affected in Selective Fibroblast Lines of Pathogenic *MAPT* Patients

We have identified two parallel molecular pathways essential for removing Miro from the OMM of depolarized mitochondria—LRRK2 and the PINK1-Parkin axis (Wang et al., 2011; Hsieh et al., 2016, 2019). In addition, the OMM protein Mitofusin2 is a target of the PINK1-Parkin pathway, but not of LRRK2, for depolarization-triggered degradation (Poole et al., 2010; Tanaka et al., 2010; Hsieh et al., 2016). We have previously found that in 12 healthy control fibroblast lines, CCCP treatment, which depolarizes the mitochondrial membrane potential ($\Delta\Psi$ m), for only 1 h triggers the recruitment of a small fraction of cytosolic LRRK2 and Parkin to mitochondria, prior to Miro1 and Mitofusin2 removal at 6 h detected by Western blotting (**Figures 1A–C**; **Supplementary Figure 1A**; Hsieh et al., 2016, 2019). Antibodies against LRRK2, Parkin, and Miro1 have been validated in human cells lacking the corresponding genes (Hsieh et al., 2016). We then examined whether LRRK2 and Parkin recruitment to damaged mitochondria was impaired in 7 fibroblast lines of FTL and parkinsonism patients or at-risk individuals with *MAPT* mutations, obtained from the NINDS human and cell repository (**Figure 1B**; **Supplementary Table 1**). At-risk subjects are younger asymptomatic family members of probands and carry the same genetic mutations. In contrast to healthy controls, 4 *MAPT* lines failed to significantly recruit LRRK2 to mitochondria, and 2 lines failed to recruit Parkin (**Figures 1A–C**). One line (MAPT-7, R406W) failed to recruit both proteins (**Figures 1A–C**). Basal levels of LRRK2 and Parkin were comparable among all lines (*P* > 0.8). Collectively, our results provide evidence indicating that the LRRK2 and PINK1-Parkin pathways are affected in selective *MAPT* patients' fibroblast lines.

Miro1 Is Resistant to Removal From Depolarized Mitochondria in Fibroblasts of *MAPT* Patients

Because the failure to relocate LRRK2 or Parkin to damaged mitochondria disrupts the following removal of Miro1 or Mitofusin2 (Hsieh et al., 2016), we next examined Miro1 and Mitofusin2 protein levels in the mitochondrial fractions of these cells upon depolarization. In healthy controls at 6 h following CCCP treatment, both Miro1 and Mitofusin2 are removed from damaged mitochondria detected by Western blotting (**Figures 1A–C**); this time point is earlier than the completion of mitophagy when multiple mitochondrial markers are degraded (**Figure 1A**; Hsieh et al., 2016, 2019). Notably, we discovered a unifying impairment in removing

Miro1 from the mitochondrial fractions at 6 h after CCCP treatment in all 7 *MAPT* lines (Figures 1A–C). By contrast, Mitofusin2 was significantly degraded in the mitochondrial fractions after CCCP treatment in all *MAPT* lines, just as in control cells (Figures 1A–C). Basal protein levels of Miro1 and Mitofusin2 were largely comparable among all lines (Figure 1C; $P > 0.09$). For all experiments, the cell passaging numbers were within the range of 5–19 which had no influence on the phenotypes (Hsieh et al., 2019). We next validated the result from Western blotting by an alternative assay: ELISA (Hsieh et al., 2019; Nguyen et al., 2021). We tested 3 *MAPT* lines and consistently observed the resistance of Miro1 to degradation upon CCCP treatment (Figures 1D–G;

Hsieh et al., 2019). Taken together, our results show that the failure to remove Miro1 from damaged mitochondria is a common molecular defect associated with pathogenic *MAPT* mutations.

The Dissociation of Mitochondria From ER and Cytoskeleton Tracks Is Impaired in Pathogenic *MAPT* Fibroblasts

In order to examine mitochondrial changes at the ultrastructural level, we performed TEM on a healthy and a *MAPT* fibroblast line used in Figure 1, with or without CCCP treatment for 6 h (Figure 2A). We found that the mitochondrial size, perimeter,

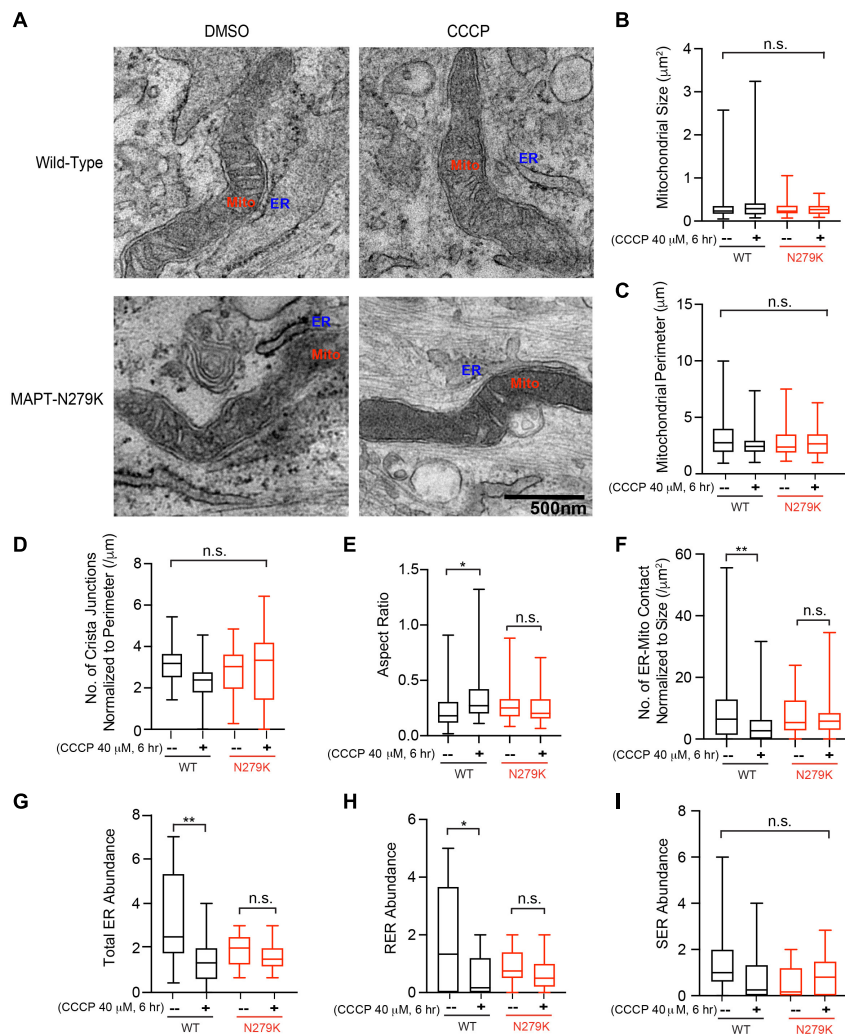


FIGURE 2 | Ultrastructural changes of mitochondria in fibroblasts. **(A)** Representative TEM images of Healthy-6 (WT) and MAPT-1 (MAPT-N279K) with and without CCCP treatment. Scale bar: 500 nm. **(B–I)** Quantifications from images as in **(A)**. **(B)** Quantification of mitochondrial size (minor × major diameter). **(C)** Quantification of mitochondrial perimeter. **(D)** Quantification of cristae junction number normalized to mitochondrial perimeter. **(E)** Quantification of aspect ratio (minor/major diameter). **(F)** Quantification of ER-mitochondrial contact number normalized to mitochondrial size (contact is defined where the distance between ER and mitochondrial membranes is less than 10 nm). **(G)** Quantification of total ER abundance (the total number of ER-mitochondrial contact divided by the total number of mitochondria per image). **(H)** Quantification of rough ER (RER) abundance. Similar to **(G)** but only RER is counted. **(I)** Quantification of smooth ER (SER) abundance. Similar to **(G)** but only SER is counted. $N = 57$ (WT, DMSO), 51 (WT, CCCP), 53 (MAPT-N279K, DMSO), and 64 (MAPT-N279K, CCCP) mitochondria from 15 different images from 3 independent cultures. Two-Way ANOVA Post Hoc Tukey Test. * $P < 0.05$, ** $P < 0.01$. n.s.: not significant.

and crista junction number were indistinguishable among all conditions (**Figures 2B–D**), whereas the aspect ratio (minor to major diameter) was increased in healthy control with CCCP treatment (**Figure 2E**), indicating mitochondrial rounding in this condition. Strikingly, we found that following CCCP treatment the ER-mitochondrial contact number, particularly for rough ER (RER), was significantly reduced in healthy fibroblasts; however, it was not altered at the same time point in *MAPT* fibroblasts (**Figures 2A,F–I**). This result suggests that mitochondrial depolarization causes the separation of mitochondria and ER contact, consistent with a previous report (McLelland et al., 2018). This study also implicates that the mitochondrial and ER separation is essential for the following mitophagy, and blocking their dissociation, as seen in *MAPT* fibroblasts (**Figure 2**), could lead to mitophagy impairment (McLelland et al., 2018), observed in other tau models as well (Hu et al., 2016; Cummins et al., 2019; Fang

et al., 2019). In addition, we saw mitochondria frequently juxtaposed with cytoskeleton (actin or microtubule) tracks in healthy control fibroblasts and this association was significantly reduced following CCCP treatment (**Figures 3A,B**), showing that damaged mitochondria are sequestered from cytoskeleton networks. However, *MAPT* fibroblasts failed to exhibit this response (**Figures 3A,B**). Furthermore, *MAPT* fibroblasts displayed the widespread presence of structures resembling lamellar bodies (LB) and multivesicular bodies (MV) under both basal and depolarized conditions (**Figure 3C**), indicating possible imbalance in proteostasis and lipid homeostasis. The global mitochondrial network or $\Delta\Psi_m$ visualized by TMRM staining was indistinguishable among healthy and *MAPT* fibroblasts at baseline (**Figure 4A**). Together, our results show that the dissociation of damaged mitochondria from ER and cytoskeleton networks is blocked in fibroblasts of a *MAPT* patient.

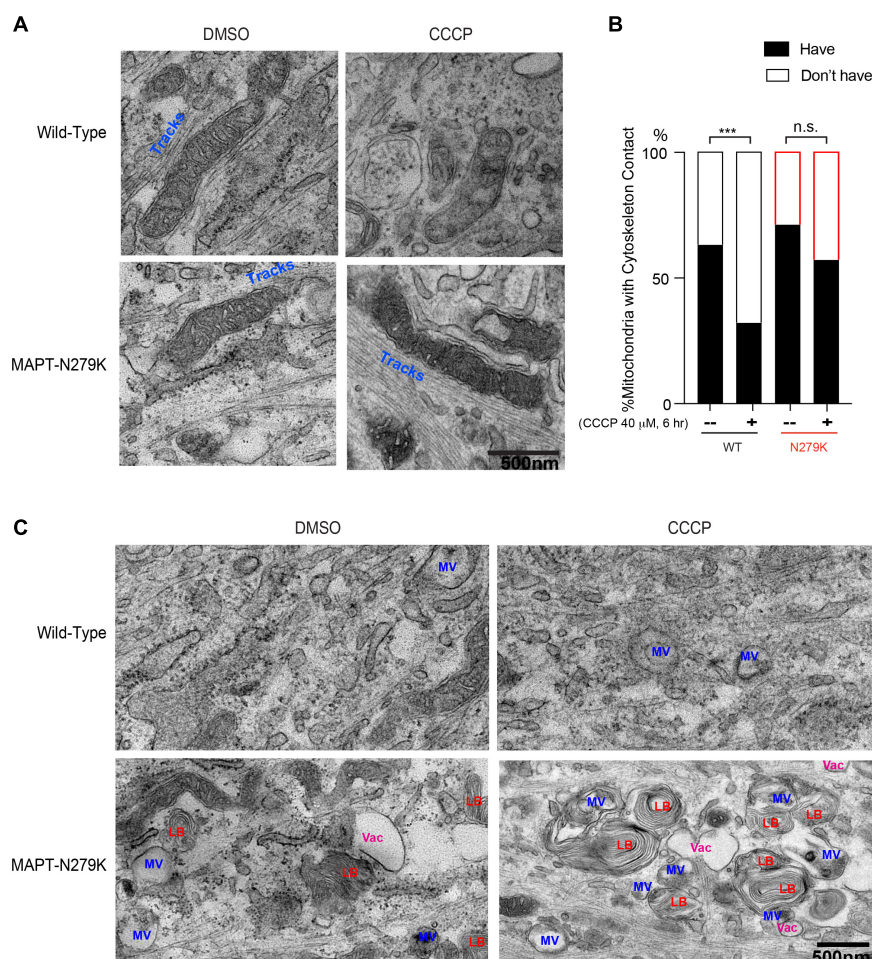
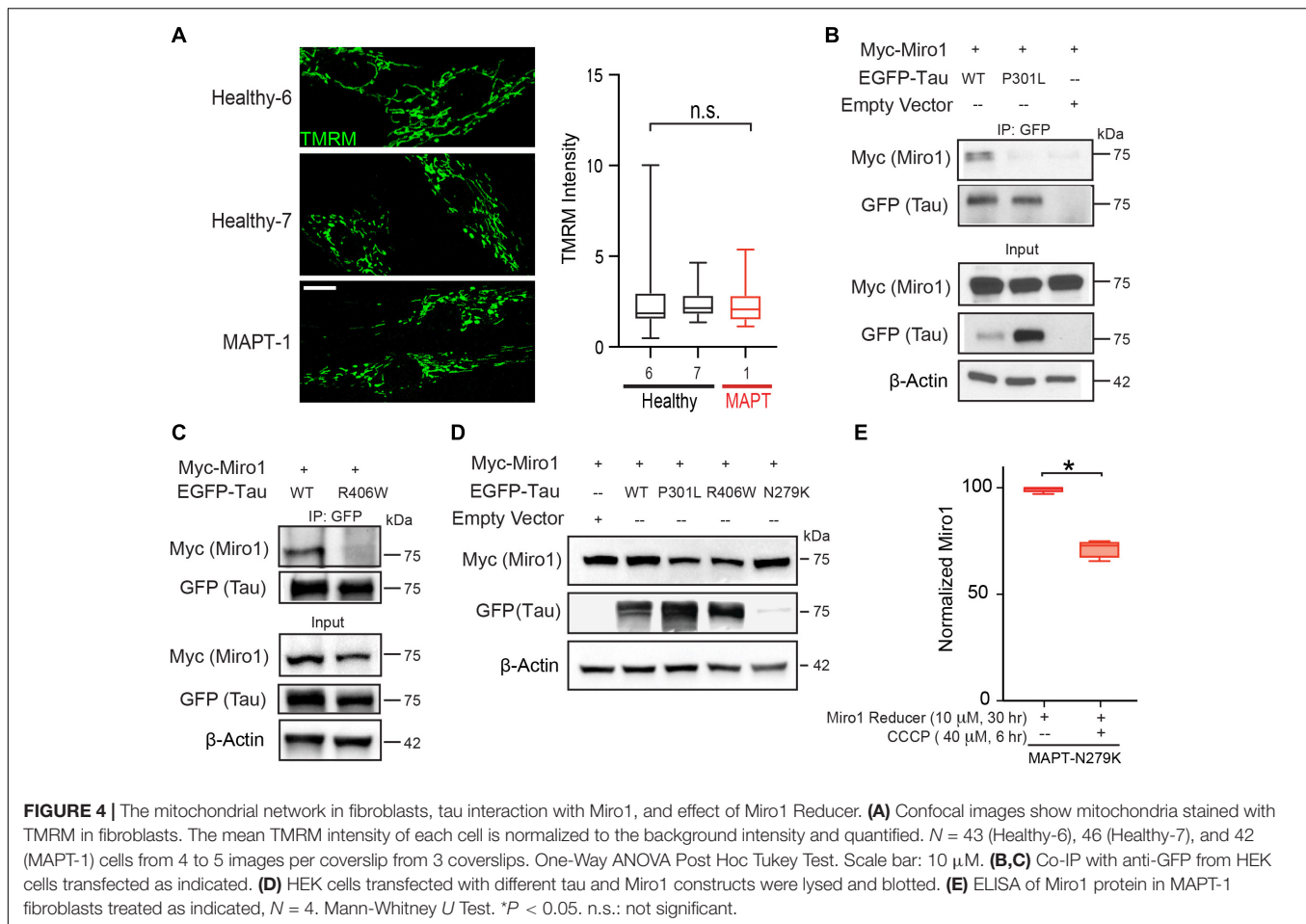


FIGURE 3 | Phenotypes of cytoskeleton and other organelles in fibroblasts. **(A)** Representative TEM images of Healthy-6 (WT) and MAPT-1 (MAPT-N279K) with and without CCCP treatment, showing cytoskeleton tracks (Tracks) next to mitochondria. **(B)** From images as in **(A)**, the percentage of total mitochondria with or without adjacent cytoskeleton tracks is counted. $N = 30$ (WT, DMSO), 28 (WT, CCCP), 31 (MAPT-N279K, DMSO), and 36 (MAPT-N279K, CCCP) mitochondria from 15 images from 3 independent cultures. Chi Square Test. **(C)** Representative TEM images of Healthy-6 (WT) and MAPT-1 (MAPT-N279K) with and without CCCP treatment, showing vacuole-like structures (Vac), structures similar to multi-vesicular bodies (MV), and structures similar to lamellar bodies (LB). Scale bars: 500 nm. *** $P < 0.001$. n.s.: not significant.



MAPT Mutations Disrupt Tau Interaction With Miro1

One hypothesis that could explain our TEM observations is that normal *MAPT* is essential to facilitate the separation of mitochondria from ER and cytoskeleton at the early stage of mitophagy. Interestingly, Miro can localize to the ER-mitochondrial contact sites (Kornmann et al., 2011; Stroud et al., 2011) and anchors mitochondria to microtubule and actin tracks (Stowers et al., 2002; Glater et al., 2006; Wang and Schwarz, 2009; Morlino et al., 2014; Lopez-Domenech et al., 2018; Oeding et al., 2018). Notably, Miro is quickly removed from depolarized mitochondria (Chan et al., 2011; Wang et al., 2011; Birsa et al., 2014), and our earlier results showed a unifying impairment in removing Miro1 from damaged mitochondria in all 7 *MAPT* lines (Figure 1), suggesting that Miro1 and tau may coordinate to ensure an efficient mitophagy process. We next determined whether tau could physically interact with Miro1. By performing co-immunoprecipitation (co-IP) from HEK cells transfected with tau and Miro1 constructs, we found that wild-type tau, but not tau-P301L or tau-R406W, interacted with Miro1 (Figures 4B,C; Supplementary Figure 1B). Tau-N279K protein was not well-expressed in HEK cells (Figure 4D)

though the same amount of DNA was transfected as tau-P301L or tau-R406W, which did not allow reliable co-IP experiments. Therefore, mutant tau compromises its ability to bind to Miro1.

Miro1 Reducer Rescues the Phenotype of Miro1 Retention in Pathogenic MAPT Fibroblasts

The failure to remove Miro1 from damaged mitochondria in fibroblasts of *MAPT* patients (Figure 1) is reminiscent of that observed in fibroblasts of PD patients (Hsieh et al., 2019). We have previously discovered a small molecule (named Miro1 Reducer or MR3) that binds to and destabilizes human Miro1 protein (Hsieh et al., 2019; Li et al., 2021). Treating fibroblasts of PD patients with Miro1 Reducer rescues the phenotype of Miro1 accumulation on damaged mitochondria, and applying Miro1 Reducer to human neuron and fly models of PD ameliorates Parkinson's relevant phenotypes, without affecting Miro1's overall GTPase activity or other mitochondrial proteins including Miro2, Mitofusin, OPA1, VDAC, and ATP5B (Hsieh et al., 2019). We examined whether Miro1 Reducer could also promote Miro1 degradation in *MAPT* fibroblasts. We

administered Miro1 Reducer to MAPT-1 line which exhibited the phenotype of Miro1's resistance to degradation upon CCCP treatment, shown earlier (**Figure 1**). We found that Miro1 Reducer treatment caused significant Miro1 degradation following CCCP treatment detected by ELISA (**Figure 4E**), just like the response of Miro1 in healthy control fibroblasts (**Figure 1**). These results suggest that pharmacologically targeting Miro1 could be tested as a therapeutic approach in tauopathy models.

DISCUSSION

In this study, we have revealed mitochondrial molecular and membrane dynamic defects upon depolarization in fibroblasts of pathogenic *MAPT* patients. The failure to recruit LRRK2 or Parkin to damaged mitochondria and to remove Miro1 from the OMM could slow or impair the following mitophagy leading to an accumulation of damaged mitochondria (Hsieh et al., 2016, 2019; Shaltouki et al., 2018). In addition, the failure to separate mitochondria from ER and cytoskeleton networks could also hinder the mitophagy process (Wang et al., 2011; McLelland et al., 2018). The discovery of these mitochondrial defects in a peripheral tissue of patients may aid in biomarker development, as well as shed light on pathogenic processes in tauopathy.

Our work points to a crucial role for tau in maintaining dynamics of ER-mitochondrial contact sites. Consistently, a previous study has shown that mutant tau stabilizes ER-mitochondrial tethering in mouse models (Perreault et al., 2009). Mechanistically, tau may conduct this role via Miro. Here, we have shown that wild-type tau physically interacts with Miro1 and mutant tau disrupts this interaction. Both tau and Miro can reside at the ER-mitochondrial contact sites (Perreault et al., 2009; Kornmann et al., 2011; Stroud et al., 2011; Cieri et al., 2018). Importantly, Miro is quickly detached from the OMM of depolarized mitochondria to facilitate the following mitophagy (Chan et al., 2011; Wang et al., 2011; Birsa et al., 2014). Because the classical role of Miro is to anchor mitochondria to microtubule motors to mediate mitochondrial transport, eliminating Miro stops damaged mitochondrial motility and limits the spread of damage. It is highly possible that in addition to halting mitochondrial transport, removing Miro from damaged mitochondria helps the dissociation of ER and mitochondrial tethering, which is similarly essential to ensure efficient mitophagy (McLelland et al., 2018). This hypothesis is in line with our previous observations that Miro degradation is required for all mitochondria, both motile and static, to undergo mitophagy (Hsieh et al., 2016, 2019; Shaltouki et al., 2018). Therefore, our studies suggest that Miro may have multiple roles in mitophagy: on one hand ablating Miro uncouples damaged mitochondria from microtubules, and on the other hand deleting Miro separates damaged mitochondria from ER, resulting in the quarantine of mitochondrial damage. Wild-type tau might help remove Miro from these mitochondrial contact sites and mutant tau might lose this function. Further work is warranted to reveal

the underlying molecular mechanisms. For example, how exactly does tau facilitate Miro removal from the mitochondrial surface? Do other mitophagy players such as Mitofusin, Parkin, and LRRK2 play a part? Parkin and Mitofusin are also important for the integrity of ER-mitochondrial contact sites (Basso et al., 2018; McLelland et al., 2018), and LRRK2 interplays with tau (Bardai et al., 2018). Our results have shown that LRRK2 or Parkin relocation to damaged mitochondria is compromised in selective fibroblast lines of *MAPT* (**Figure 1**). However, this defect seems to be cell line-specific, rather than mutation-specific. For example, LRRK2 recruitment is normal in two *MAPT* lines with the N279K mutation, but impaired in a third *MAPT* line with the same mutation (**Figure 1C**). In addition, MAPT-1 or MAPT-6 cell line is able to recruit both LRRK2 and Parkin, but still fails to degrade Miro1 (**Figure 1C**). Perhaps normal tau is essential for the enzymatic activities of LRRK2 and Parkin, rather than their relocation to damaged mitochondria. Or LRRK2 and Parkin function in parallel to tau to mediate Miro removal.

Detecting endogenous LRRK2 in human fibroblasts has yielded variable results among different laboratories. It is possible that different antibodies, experimental procedures, and handlings may have contributed to the discrepancies. It is important to validate the specificity of an antibody using a knockout cell line. The interaction of LRRK2 with mitochondria needs further investigations. State-of-art techniques such as super-resolution microscopy, immunogold TEM, and mitochondrial sub-fractionation et cetera can help us understand the nature of their interaction. Although we have observed robust phenotypes with TEM in one patient's cell line, future work is required to extend the TEM study to additional *MAPT* patients' lines. Fibroblasts provide a great value for biomarker studies, yet employing neuronal models is essential to understand disease mechanisms. Given the wide involvement of these mitophagy players including LRRK2, Parkin, tau, and Miro1 in age-dependent neurodegenerative diseases, it would be imperative to examine whether the failure to disconnect damaged mitochondria from ER and cytoskeleton tracks underlies additional diseases including AD and PSP. Testing Miro1 reducers in human neuron and *in vivo* models of tauopathy would be crucial to determine the therapeutic potential of Miro1. Together, our results support a convergent role of mitochondrial quality control in age-dependent neurodegeneration (Menzies et al., 2015; Pickrell and Youle, 2015; Hsieh et al., 2016, 2019; Shaltouki et al., 2018; Fang et al., 2019; Lautrup et al., 2019; Lou et al., 2020), and indicate that targeting mitophagy may have a broad application for disease intervention.

DATA AVAILABILITY STATEMENT

The original contributions presented in the study are included in the article/**Supplementary Material**, further inquiries can be directed to the corresponding author.

AUTHOR CONTRIBUTIONS

VB and C-HH designed and performed the experiments, analyzed the data, made the figures, and wrote the manuscript. XW conceived and supervised the project, designed the experiments, and wrote the manuscript. All authors contributed to the article and approved the submitted version.

FUNDING

This work was supported by NINDS (RO1NS089583, XW), NIGMS (RO1GM143258, XW), Stanford Parkinson's Disease Seed Grant (XW), and in part National Center for Research Resources (ARRA, 1S10RR026780-01). PPMI is funded by the Michael J. Fox Foundation (MJFF) and funding partners, including Abbvie, Avid, Biogen, Bristol-Myers Squibb, COVANCE, GE Healthcare, Genentech, GlaxoSmithKline, Lilly,

Lundbeck, Merck, Meso Scale Discovery, Pfizer, Piramal, Roche, Servier, and UCB.

ACKNOWLEDGMENTS

We thank Aarooran Sivakumaran Durairaj for technical support, MJFF for providing cell lines, and J. Perrino and Stanford Cell Science Imaging EM Facility (RRID:SCR_017787) for support with TEM.

SUPPLEMENTARY MATERIAL

The Supplementary Material for this article can be found online at: <https://www.frontiersin.org/articles/10.3389/fcell.2021.765408/full#supplementary-material>

REFERENCES

- Bardai, F. H., Ordonez, D. G., Bailey, R. M., Hamm, M., Lewis, J., and Feany, M. B. (2018). Lrrk promotes tau neurotoxicity through dysregulation of actin and mitochondrial dynamics. *PLoS Biol.* 16:e2006265. doi: 10.1371/journal.pbio.2006265
- Basso, V., Marchesan, E., Peggion, C., Chakraborty, J., von Stockum, S., Giacomello, M., et al. (2018). Regulation of ER-mitochondria contacts by Parkin via Mfn2. *Pharmacol. Res.* 138, 43–56. doi: 10.1016/j.phrs.2018.09.006
- Birsa, N., Norkett, R., Wauer, T., Mevissen, T. E., Wu, H. C., Foltynie, T., et al. (2014). Lysine 27 ubiquitination of the mitochondrial transport protein Miro is dependent on serine 65 of the Parkin ubiquitin ligase. *J. Biol. Chem.* 289, 14569–14582. doi: 10.1074/jbc.M114.563031
- Bonello, F., Hassoun, S. M., Mouton-Liger, F., Shin, Y. S., Muscat, A., Tesson, C., et al. (2019). LRRK2 impairs PINK1/Parkin-dependent mitophagy via its kinase activity: pathologic insights into Parkinson's disease. *Hum. Mol. Genet.* 28, 1645–1660. doi: 10.1093/hmg/ddz004
- Bonifati, V. (2002). Deciphering Parkinson's disease—PARK8. *Lancet Neurol.* 1:83.
- Chan, N. C., Salazar, A. M., Pham, A. H., Sweredoski, M. J., Kolawa, N. J., Graham, R. L., et al. (2011). Broad activation of the ubiquitin-proteasome system by Parkin is critical for mitophagy. *Hum. Mol. Genet.* 20, 1726–1737. doi: 10.1093/hmg/ddr048
- Chen, Y., and Dorn, G. W. II (2013). PINK1-phosphorylated mitofusin 2 is a Parkin receptor for culling damaged mitochondria. *Science* 340, 471–475. doi: 10.1126/science.1231031
- Cieri, D., Vicario, M., Vallesse, F., D'Orsi, B., Berto, P., Grinzato, A., et al. (2018). Tau localises within mitochondrial sub-compartments and its caspase cleavage affects ER-mitochondria interactions and cellular Ca(2+) handling. *Biochim. Biophys. Acta Mol. Basis Dis.* 1864, 3247–3256. doi: 10.1016/j.bbdis.2018.07.011
- Cummins, N., Tweedie, A., Zuryn, S., Bertran-Gonzalez, J., and Gotz, J. (2019). Disease-associated tau impairs mitophagy by inhibiting Parkin translocation to mitochondria. *EMBO J.* 38:e99360. doi: 10.15252/embj.201899360
- Di Nottia, M., Masciullo, M., Verrigni, D., Petrillo, S., Modoni, A., Rizzo, V., et al. (2017). DJ-1 modulates mitochondrial response to oxidative stress: clues from a novel diagnosis of PARK7. *Clin. Genet.* 92, 18–25. doi: 10.1111/cge.12841
- Fang, E. F., Hou, Y., Palikaras, K., Adriaanse, B. A., Kerr, J. S., Yang, B., et al. (2019). Mitophagy inhibits amyloid-beta and tau pathology and reverses cognitive deficits in models of Alzheimer's disease. *Nat. Neurosci.* 22, 401–412. doi: 10.1038/s41593-018-0332-9
- Fitzgerald, J. C., Zimprich, A., Carvajal Berrio, D. A., Schindler, K. M., Maurer, B., Schulte, C., et al. (2017). Metformin reverses TRAP1 mutation-associated alterations in mitochondrial function in Parkinson's disease. *Brain* 140, 2444–2459. doi: 10.1093/brain/awx202
- Fuster-Matanzo, A., Hernandez, F., and Avila, J. (2018). Tau spreading mechanisms; implications for dysfunctional tauopathies. *Int. J. Mol. Sci.* 19:645. doi: 10.3390/ijms19030645
- Garcia-Sanz, P., Orgaz, L., Bueno-Gil, G., Espadas, I., Rodriguez-Traver, E., Kulisevsky, J., et al. (2017). N370S-GBA1 mutation causes lysosomal cholesterol accumulation in Parkinson's disease. *Mov. Disord.* 32, 1409–1422. doi: 10.1002/mds.27119
- Glater, E. E., Megeath, L. J., Stowers, R. S., and Schwarz, T. L. (2006). Axonal transport of mitochondria requires milton to recruit kinesin heavy chain and is light chain independent. *J. Cell Biol.* 173, 545–557. doi: 10.1083/jcb.200601067
- Hsieh, C. H., Li, L., Vanhauwaert, R., Nguyen, K. T., Davis, M. D., Bu, G., et al. (2019). Miro1 marks Parkinson's disease subset and miro1 reducer rescues neuron loss in Parkinson's models. *Cell Metab.* 30, 1131–1140 e1137. doi: 10.1016/j.cmet.2019.08.023
- Hsieh, C. H., Shaltouki, A., Gonzalez, A. E., Bettencourt da Cruz, A., Burbulla, L. F., St Lawrence, E., et al. (2016). Functional impairment in miro degradation and mitophagy is a shared feature in familial and sporadic Parkinson's disease. *Cell Stem Cell* 19, 709–724. doi: 10.1016/j.stem.2016.08.002
- Hu, Y., Li, X. C., Wang, Z. H., Luo, Y., Zhang, X., Liu, X. P., et al. (2016). Tau accumulation impairs mitophagy via increasing mitochondrial membrane potential and reducing mitochondrial Parkin. *Oncotarget* 7, 17356–17368. doi: 10.18632/oncotarget.7861
- Juarez-Flores, D. L., Gonzalez-Casacuberta, I., Ezquerro, M., Bano, M., Carmona-Pontaque, F., Catalan-Garcia, M., et al. (2018). Exhaustion of mitochondrial and autophagic reserve may contribute to the development of LRRK2 (G2019S)-Parkinson's disease. *J. Transl. Med.* 16:160. doi: 10.1186/s12967-018-1526-3
- Kitada, T., Asakawa, S., Hattori, N., Matsumine, H., Yamamura, Y., Minoshima, S., et al. (1998). Mutations in the parkin gene cause autosomal recessive juvenile Parkinsonism. *Nature* 392, 605–608. doi: 10.1038/33416
- Korecka, J. A., Thomas, R., Christensen, D. P., Hinrich, A. J., Ferrari, E. J., Levy, S. A., et al. (2019). Mitochondrial clearance and maturation of autophagosomes are compromised in LRRK2 G2019S familial Parkinson's disease patient fibroblasts. *Hum. Mol. Genet.* 28, 3232–3243. doi: 10.1093/hmg/ddz126
- Kornmann, B., Osman, C., and Walter, P. (2011). The conserved GTPase Gem1 regulates endoplasmic reticulum-mitochondria connections. *Proc. Natl. Acad. Sci. U.S.A.* 108, 14151–14156. doi: 10.1073/pnas.1111314108
- Lautrup, S., Sinclair, D. A., Mattson, M. P., and Fang, E. F. (2019). NAD(+) in brain aging and neurodegenerative disorders. *Cell Metab.* 30, 630–655. doi: 10.1016/j.cmet.2019.09.001
- Le, W., Dong, J., Li, S., and Korczyn, A. D. (2017). Can biomarkers help the early diagnosis of Parkinson's disease? *Neurosci. Bull.* 33, 535–542. doi: 10.1007/s12264-017-0174-6

- Li, L., Conradson, D. M., Bharat, V., Kim, M. J., Hsieh, C. H., Minhas, P. S., et al. (2021). A mitochondrial membrane-bridging machinery mediates signal transduction of intramitochondrial oxidation. *Nat. Metab.* 3, 1242–1258. doi: 10.1038/s42255-021-00443-2
- Lopez-Domench, G., Covill-Cooke, C., Ivankovic, D., Half, E. F., Sheehan, D. F., Norkett, R., et al. (2018). Miro proteins coordinate microtubule- and actin-dependent mitochondrial transport and distribution. *EMBO J.* 37, 321–336. doi: 10.15252/embj.201696380
- Lou, G., Palikaras, K., Lautrup, S., Scheibye-Knudsen, M., Tavernarakis, N., and Fang, E. F. (2020). Mitophagy and neuroprotection. *Trends Mol. Med.* 26, 8–20. doi: 10.1016/j.molmed.2019.07.002
- McLelland, G. L., Goiran, T., Yi, W., Dorval, G., Chen, C. X., Lauinger, N. D., et al. (2018). Mfn2 ubiquitination by PINK1/parkin gates the p97-dependent release of ER from mitochondria to drive mitophagy. *Elife* 7:e32866. doi: 10.7554/eLife.32866
- Medina, M. (2018). An overview on the clinical development of tau-based therapeutics. *Int. J. Mol. Sci.* 19:1160. doi: 10.3390/ijms19041160
- Menzies, F. M., Fleming, A., and Rubinstein, D. C. (2015). Compromised autophagy and neurodegenerative diseases. *Nat. Rev. Neurosci.* 16, 345–357. doi: 10.1038/nrn3961
- Misgeld, T., and Schwarz, T. L. (2017). Mitostasis in neurons: maintaining mitochondria in an extended cellular architecture. *Neuron* 96, 651–666. doi: 10.1016/j.neuron.2017.09.055
- Morlino, G., Barreiro, O., Baiauli, F., Robles-Valero, J., Gonzalez-Granado, J. M., Villa-Bellosta, R., et al. (2014). Miro-1 links mitochondria and microtubule Dynein motors to control lymphocyte migration and polarity. *Mol. Cell Biol.* 34, 1412–1426. doi: 10.1128/MCB.01177-13
- Nguyen, D., Bharat, V., Conradson, D. M., Nandakishore, P., and Wang, X. (2021). Miro1 impairment in a Parkinson's at-risk cohort. *Front. Mol. Neurosci.* 14:734273. doi: 10.3389/fnmol.2021.734273
- Oeding, S. J., Majstrowicz, K., Hu, X. P., Schwarz, V., Freitag, A., Honnert, U., et al. (2018). Identification of Miro1 and Miro2 as mitochondrial receptors for myosin XIX. *J. Cell Sci.* 131:jcs219469. doi: 10.1242/jcs.219469
- Perreault, S., Bousquet, O., Lauzon, M., Paiement, J., and Leclerc, N. (2009). Increased association between rough endoplasmic reticulum membranes and mitochondria in transgenic mice that express P301L tau. *J. Neuropathol. Exp. Neurol.* 68, 503–514. doi: 10.1097/NEN.0b013e3181a1fc49
- Pickrell, A. M., and Youle, R. J. (2015). The roles of PINK1, parkin, and mitochondrial fidelity in Parkinson's disease. *Neuron* 85, 257–273. doi: 10.1016/j.neuron.2014.12.007
- Poole, A. C., Thomas, R. E., Yu, S., Vincow, E. S., and Pallanck, L. (2010). The mitochondrial fusion-promoting factor mitofusin is a substrate of the PINK1/parkin pathway. *PLoS One* 5:e10054. doi: 10.1371/journal.pone.0010054
- Shaltouki, A., Hsieh, C. H., Kim, M. J., and Wang, X. (2018). Alpha-synuclein delays mitophagy and targeting Miro rescues neuron loss in Parkinson's models. *Acta Neuropathol.* 136, 607–620. doi: 10.1007/s00401-018-1873-4
- Smith, G. A., Jansson, J., Rocha, E. M., Osborn, T., Hallett, P. J., and Isacson, O. (2016). Fibroblast biomarkers of sporadic Parkinson's Disease and LRRK2 kinase inhibition. *Mol. Neurobiol.* 53, 5161–5177. doi: 10.1007/s12035-015-9435-4
- Spillantini, M. G., and Goedert, M. (2013). Tau pathology and neurodegeneration. *Lancet Neurol.* 12, 609–622. doi: 10.1016/S1474-4422(13)70090-5
- Stowers, R. S., Megeath, L. J., Gorska-Andrzejak, J., Meinertzhagen, I. A., and Schwarz, T. L. (2002). Axonal transport of mitochondria to synapses depends on Milton, a novel *Drosophila* protein. *Neuron* 36, 1063–1077.
- Stroud, D. A., Oeljeklaus, S., Wiese, S., Bohnert, M., Lewandrowski, U., Sickmann, A., et al. (2011). Composition and topology of the endoplasmic reticulum-mitochondria encounter structure. *J. Mol. Biol.* 413, 743–750. doi: 10.1016/j.jmb.2011.09.012
- Tanaka, A., Cleland, M. M., Xu, S., Narendra, D. P., Suen, D. F., Karbowski, M., et al. (2010). Proteasome and p97 mediate mitophagy and degradation of mitofusins induced by Parkin. *J. Cell Biol.* 191, 1367–1380. doi: 10.1083/jcb.2010.07013
- Teves, J. M. Y., Bhargava, V., Kirwan, K. R., Corenblum, M. J., Justiniano, R., Wondrak, G. T., et al. (2017). Parkinson's disease skin fibroblasts display signature alterations in growth, redox homeostasis, mitochondrial function, and autophagy. *Front. Neurosci.* 11:737. doi: 10.3389/fnins.2017.00737
- Thies, E., and Mandelkow, E. M. (2007). Misrouting of tau in neurons causes degeneration of synapses that can be rescued by the kinase MARK2/Par-1. *J. Neurosci.* 27, 2896–2907. doi: 10.1523/JNEUROSCI.4674-06.2007
- Valente, E. M., Abou-Sleiman, P. M., Caputo, V., Muqit, M. M., Harvey, K., Gispert, S., et al. (2004). Hereditary early-onset Parkinson's disease caused by mutations in PINK1. *Science* 304, 1158–1160. doi: 10.1126/science.1096284
- Verma, M., Callio, J., Otero, P. A., Sekler, I., Wills, Z. P., and Chu, C. T. (2017). Mitochondrial calcium dysregulation contributes to dendrite degeneration mediated by PD/LBD-associated LRRK2 mutants. *J. Neurosci.* 37, 11151–11165. doi: 10.1523/JNEUROSCI.3791-16.2017
- Wang, X., and Schwarz, T. L. (2009). The mechanism of Ca²⁺-dependent regulation of kinesin-mediated mitochondrial motility. *Cell* 136, 163–174. doi: 10.1016/j.cell.2008.11.046
- Wang, X., Winter, D., Ashrafi, G., Schlehe, J., Wong, Y. L., Selkoe, D., et al. (2011). PINK1 and Parkin target Miro for phosphorylation and degradation to arrest mitochondrial motility. *Cell* 147, 893–906. doi: 10.1016/j.cell.2011.10.018
- Zempel, H., and Mandelkow, E. M. (2015). Tau misrouting and spastin-induced microtubule disruption in neurodegeneration: Alzheimer disease and hereditary spastic paraplegia. *Mol. Neurodegener.* 10:68. doi: 10.1186/s13024-015-0064-1
- Zimprich, A., Biskup, S., Leitner, P., Lichtner, P., Farrer, M., Lincoln, S., et al. (2004). Mutations in LRRK2 cause autosomal-dominant parkinsonism with pleomorphic pathology. *Neuron* 44, 601–607. doi: 10.1016/j.neuron.2004.11.005

Conflict of Interest: XW is a co-founder, adviser, and shareholder of AcureX Therapeutics Inc., and a shareholder of Mitokinin Inc. C-HH is a shareholder of AcureX Therapeutics Inc.

The remaining author declares that the research was conducted in the absence of any commercial or financial relationships that could be construed as a potential conflict of interest.

Publisher's Note: All claims expressed in this article are solely those of the authors and do not necessarily represent those of their affiliated organizations, or those of the publisher, the editors and the reviewers. Any product that may be evaluated in this article, or claim that may be made by its manufacturer, is not guaranteed or endorsed by the publisher.

Copyright © 2021 Bharat, Hsieh and Wang. This is an open-access article distributed under the terms of the Creative Commons Attribution License (CC BY). The use, distribution or reproduction in other forums is permitted, provided the original author(s) and the copyright owner(s) are credited and that the original publication in this journal is cited, in accordance with accepted academic practice. No use, distribution or reproduction is permitted which does not comply with these terms.



Endoplasmic Reticulum-Mitochondria Contacts: A Potential Therapy Target for Cardiovascular Remodeling-Associated Diseases

Yu Wang^{1,2†}, Xinrong Zhang^{1†}, Ya Wen¹, Sixuan Li¹, Xiaohui Lu^{2*}, Ran Xu^{3*} and Chao Li^{1*}

OPEN ACCESS

Edited by:

Yongye Huang,
Northeastern University, China

Reviewed by:

Melanie Paillard,
INSERM U1060 Laboratoire
de Recherche en Cardiovasculaire,
Métabolisme, Diabétologie et
Nutrition, France
Ming Yang,
Central South University, China

*Correspondence:

Chao Li
lichao71795@hotmail.com
Xiaohui Lu
lxhtcm@126.com
Ran Xu
xuran9129@163.com

[†] These authors have contributed
equally to this work

Specialty section:

This article was submitted to
Signaling,
a section of the journal
Frontiers in Cell and Developmental
Biology

Received: 13 September 2021

Accepted: 08 October 2021

Published: 10 November 2021

Citation:

Wang Y, Zhang X, Wen Y, Li S,
Lu X, Xu R and Li C (2021)
Endoplasmic Reticulum-Mitochondria
Contacts: A Potential Therapy Target
for Cardiovascular
Remodeling-Associated Diseases.
Front. Cell Dev. Biol. 9:774989.
doi: 10.3389/fcell.2021.774989

¹ Innovation Research Institute of Traditional Chinese Medicine, Shandong University of Traditional Chinese Medicine, Jinan, China, ² Emergency Department, Affiliated Hospital of Shandong University of Traditional Chinese Medicine, Jinan, China, ³ Jinan Tianqiao People's Hospital, Jinan, China

Cardiovascular remodeling occurs in cardiomyocytes, collagen meshes, and vascular beds in the progress of cardiac insufficiency caused by a variety of cardiac diseases such as chronic ischemic heart disease, chronic overload heart disease, myocarditis, and myocardial infarction. The morphological changes that occur as a result of remodeling are the critical pathological basis for the occurrence and development of serious diseases and also determine morbidity and mortality. Therefore, the inhibition of remodeling is an important approach to prevent and treat heart failure and other related diseases. The endoplasmic reticulum (ER) and mitochondria are tightly linked by ER-mitochondria contacts (ERMCs). ERMCs play a vital role in different signaling pathways and provide a satisfactory structural platform for the ER and mitochondria to interact and maintain the normal function of cells, mainly by involving various cellular life processes such as lipid metabolism, calcium homeostasis, mitochondrial function, ER stress, and autophagy. Studies have shown that abnormal ERMCs may promote the occurrence and development of remodeling and participate in the formation of a variety of cardiovascular remodeling-associated diseases. This review focuses on the structure and function of the ERMCs, and the potential mechanism of ERMCs involved in cardiovascular remodeling, indicating that ERMCs may be a potential target for new therapeutic strategies against cardiovascular remodeling-induced diseases.

Keywords: endoplasmic reticulum, mitochondria, cardiovascular remodeling, calcium transfer, therapeutic strategies

INTRODUCTION

With an aging society and the change in people's lifestyles, on a global scale, the incidence and mortality of cardiovascular disease (CVD) have been increasing for decades (Bansilal et al., 2015). In 2019, there were nearly 523 million new cases of cardiovascular disease and 18.6 million deaths from cardiovascular disease worldwide (Andersson and Vasan, 2018; Roth et al., 2020). The World Health Organization (WHO) has classified CVD, as well as cancer and rheumatic immune diseases (Capewell and Lloyd-Jones, 2010), as a threat to human health.

Cardiovascular remodeling plays a crucial role in the pathological process of CVD (Porter and Turner, 2009), and it constitutes a pathological change in the structure and function of cardiovascular tissue produced under a series of physiological stimuli (such as exercise or pregnancy) and pathological stimuli (such as hypertension, diabetes, or myocardial infarction) (Sekaran et al., 2017). The molecular mechanisms involved in cardiovascular remodeling are multi-angular and multi-dimensional, and include various inflammatory pathways and other molecular biological dimensions (Martinez-Martinez et al., 2015), autophagy mechanisms (Shi et al., 2021; Sciarretta et al., 2018a), angiogenesis mechanisms (Mentzer and Konerding, 2014; Saraf et al., 2016), and gene transcription regulation (Van Guilder et al., 2021; Zhang C. et al., 2021). Moreover, in abnormal cellular energy metabolism (Akhmedov et al., 2015; Kimball and Vondriska, 2020), oxidative stress (Münzel et al., 2017), autophagy defects (Sciarretta et al., 2018b), calcium homeostasis imbalance (Chaanine et al., 2013), ER stress (Lebeau et al., 2018), and apoptotic activation (Intengan and Schiffrin, 2001), remodeling may occur (Yang Y. et al., 2019). An increasing number of studies has begun to focus on cardiovascular remodeling from the overall functional level of organelles and organelle interaction, especially the mitochondria (Nunnari and Suomalainen, 2012) and ER/sarcoplasmic reticulum (SR) (Reddish et al., 2017). ERMCs are architecture and ultrastructural organization that exist between mitochondria and the ER which involve various cellular life processes (Szymański et al., 2017). Accumulating evidences (Zhou et al., 2018a; Gao et al., 2020; Silva-Palacios et al., 2020; Yang et al., 2020) has demonstrated that abnormal ERMCs may be pivotal in the development of cardiovascular remodeling because they are involved in the development of a variety of cardiovascular remodeling-related diseases.

In recent years, researchers have found that during their physiological functions, mitochondria and the ER are not isolated and do not act divisively (Gomez-Suaga et al., 2017b). On the contrary, there is a very close relationship between mitochondria and the ER in structure and function (Kornmann, 2013). They jointly exercise the responsibility of maintaining the stability of the intracellular environment (Lee and Min, 2018). In the past decade, there has been an explosive growth in knowledge regarding the role of ERMCs in cardiovascular remodeling (Lee and Min, 2018; Vannuvel et al., 2013), and clinical studies have found that energy-intensive and calcium signal-regulated dependent cells such as cardiomyocytes are very susceptible to mitochondrial and ER dysfunction, especially ERMCs (Kho et al., 2012; Chan, 2020). Mitochondria are the main productive organelles and the second largest calcium pool in eukaryotic cells (Ruan et al., 2020). They are also multifunctional and dynamically plastic organelles (Kummer and Ban, 2021) that are involved in various biological processes such as steroid synthesis (Chow et al., 2017), lipid metabolism (Benador et al., 2019), calcium signal transduction (De Stefani et al., 2016) and apoptosis (Bhola and Letai, 2016). As the largest intracellular calcium store (Raffaello et al., 2016), the ER is a multifunctional organelle that is the main site of protein synthesis, folding, transport (Guerriero and Brodsky, 2012),

calcium homeostasis regulation (Stutzmann and Mattson, 2011) and lipid biosynthesis (Yousuf et al., 2020). The ER has the most extensive intracellular membrane structure and forms structural and functional coupling regions with a variety of intracellular organelles (Wang and Kaufman, 2016), of which the most important coupling organelle is the mitochondria, and their binding sites are known as mitochondria-associated ER membranes (MAMs) (Cheng et al., 2020). ERMCs and MAMs are sometime used as synonyms, but they do not mean the same thing. ERMCs are architecture and ultrastructural organization that exist between mitochondria and the ER and involve various cellular life processes (Giacomello and Pellegrini, 2016; Szymański et al., 2017). The term MAMs, instead, are the product of the biophysical enrichment of mitochondria and ER membranes tethered together, and describes the repertoire of proteins and lipids that form the ERMCs (Giacomello and Pellegrini, 2016; Szymański et al., 2017). MAMs are the binding sites and structural basis of ERMCs. In some papers, ERMCs were also written as “mitochondria-endoplasmic reticulum contacts (MERCs) (Giacomello and Pellegrini, 2016; Cheng et al., 2020).

Under physiological conditions, mitochondria and the ER are physiologically interconnected through MAMs to participate in basic cell biological processes including lipid (Tatsuta et al., 2014) and calcium (Ca^{2+}) homeostasis (Bagur and Hajnóczky, 2017), mitochondrial dynamics (Kleckner et al., 2014), and other related cellular behaviors such as autophagy (Senft and Ronai, 2015), ER stress (Murphy, 2013), inflammation (Roca et al., 2019), and apoptosis (Rosati et al., 2010). The complex functional regulatory structure is involved in the development of various cardiovascular diseases, including cardiac hypertrophy (Tuncay et al., 2019), heart failure (Liu et al., 2014), metabolic cardiomyopathy (Liu et al., 2014), ischemic heart disease (Li et al., 2016), and arrhythmia (Silva-Palacios et al., 2020).

Dysfunction of ERMCs is involved in the homeostasis reconstruction of cardiomyocytes (Chen J. et al., 2021), protection against oxidative stress (Grings et al., 2019), Ca^{2+} signaling (Bagur and Hajnóczky, 2017), lipid metabolism (Biczko et al., 2018), energy metabolism (Szymański et al., 2017), and cell survival (Zhou et al., 2018a). Therefore, in this review, we will summarize the structure and function of the ERMCs, and then we will discuss how ERMCs are associated with the high prevalence of cardiovascular diseases such as cardiac hypertrophy, heart failure, and systemic vascular diseases, as well as the potential use of ERMCs as therapeutic targets for cardiovascular remodeling.

STRUCTURE OF ENDOPLASMIC RETICULUM-MITOCHONDRIA CONTACTS

Formation of Mitochondria-Associated Endoplasmic Reticulum Membranes

In 1956, an intimate relationship between mitochondria and ergastoplasm was discovered in rat liver cells (Bernhard and Rouiller, 1956). In 1990, MAMs were interpreted as a point of contact between ER membranes and mitochondria by

Vance (1990). Electron tomography has shown that the ER and mitochondria are connected by tethers (9–16 nm for smooth ER and 19–30 nm for rough ER) (Simmen and Herrera-Cruz, 2018; Zhao et al., 2020). Further studies showed that MAMs are formed when the ER is close to the mitochondria by approximately 20 nm on 20% of the mitochondrial surface (Csordas et al., 2006). The presence of MAMs promotes communication between the ER and mitochondria, and also endows both with new properties and functions. MAMs are structurally heterogeneous, and according to the size of the ER and mitochondrial contact areas observed under electron microscopy, MAMs can be divided into three types: in type I, the contact area between the ER and mitochondria is approximately 10%, and in the case of mitochondrial elongation, only a portion of the mitochondria is anchored to the ER, and the rest can move independently. Most human intracellular MAMs are of this type. In type II, the contact area between the ER and mitochondria is approximately 50%, and this type is often present in brown adipose tissue. In type III, the ER completely covers the mitochondria (Fujimoto and Hayashi, 2011).

Proteomics indicate the presence of specific molecules in specific sites on ERs that form different ER domains, which is also one of the sources of structural heterogeneity of MAMs (Xu H. et al., 2020). The ER has a universal pluripotent fusion property, leading to active formation of physical contacts between two different membranes (Nguyen et al., 2020). Active extension of ER protrusions to other organelles is frequently observed (Gagnon et al., 2002). The ER may facilitate interactions with mitochondria if proteins necessary for membrane association are present on both sides. Thus, as the ER establishes a large monolayer membrane network, ERMCS may occur during ER maturation (Nam and Jeon, 2019). Moreover, the trafficking between the ER and Golgi apparatus appears to be pivotal and the structural integrity of the ER and the normal ER-Golgi vesicle transport function are essential for the structural maintenance of mitochondria and their formation with MAMs (Coutinho et al., 2004).

Recent studies have shown that the regulation of ERMCS and mitochondrial dynamics are two closely intertwined processes (Friedman et al., 2011). Studies have shown that the sites of MAMs in rat heart cells coincide with the outer mitochondrial membrane (OMM) – inner mitochondrial membrane (IMM) contact sites, and therefore, MAMs may form calcium channel complexes to regulate Ca^{2+} transport between the endoplasmic reticulum and mitochondria (Jin et al., 2021). The inositol 1,4,5-triphosphate receptor (IP3R) is located in the ER membrane and regulates Ca^{2+} release, and voltage-dependent anion selective channel protein (VDAC) 1 is a Ca^{2+} uptake channel on the OMM (Szabadkai et al., 2006). Similarly, another important Ca^{2+} release channel, the ryanodine receptor (RyR), is also expressed at MAMs and plays a key role in Ca^{2+} transport (Jakob et al., 2014; Yang et al., 2018).

Proteins involved in mitochondrial fusion also regulate ER morphology and MAMs. Mitochondrial fusion protein 2 (Mfn2) is located on the surface of the OMM, connecting adjacent mitochondria, and also on the surface of the ER, which can form dimers with Mfn1 or Mfn2 located on the surface of

mitochondria, thereby connecting the ER to mitochondria and promoting mitochondrial Ca^{2+} transport (de Brito and Scorrano, 2008). Silencing Mfn2 in mouse embryonic fibroblasts and HeLa cells not only disrupts the ER, but it can also alter the normal structure of MAMs (Wang et al., 2012).

Composition of Mitochondria-Associated Endoplasmic Reticulum Membranes

A series of proteins constitutes the tether of MAMs, which are expressed on the ER membrane and the OMM, thus connecting the two organelles. The protein components on MAMs are classified according to the functions performed by the protein complexes (Li et al., 2020a): (1) Ca^{2+} regulatory proteins, such as IP3Rs/GRP75/VDAC1 complexes and Sigma-1 receptors (Sig1Rs); (2) lipid synthesis and transport proteins; (3) MAM tethers proteins, such as VAPB-PTPIP51; (4) MAM controlled proteins, such as phosphofurin acidic cluster sorting protein-2 (PACS-2) and Mfn2. Depletion of certain proteins or interruption of certain protein-protein interactions on MAMs can lead to disruption of the structure and function of MAMs (as shown in Table 1).

Ca^{2+} Regulatory Proteins

IP3Rs are highly expressed at MAMs. IP3Rs are spatially specific, and certain isoforms of IP3Rs, such as IP3R3, are specifically concentrated at MAMs. Earlier studies found that IP3Rs/GRP75/VDAC1 can form complexes in MAMs, and IP3Rs are expressed in the ER membrane (Bartok et al., 2019). VDAC1 is expressed in the OMM, and GRP75 connects IP3Rs with VDAC1, thereby connecting the ER membrane with the mitochondrial membrane to promote the formation of MAMs, and mediate ER-mitochondrial calcium transfer and affect mitochondrial function (Szabadkai et al., 2006). There is evidence that GRP75 deficiency leads to reduced Ca^{2+} exchange at ERMCS. Because disruption of the bridge perturbs Ca^{2+} flux into mitochondria but does not alter the close proximity of the ER and mitochondria, the IP3R/GRP75/VDAC1 protein complex is specialized for Ca^{2+} transfer at MAMs (Honrath et al., 2017). Thymocyte-expressed, positive selection-associated 1 (Tesp1) is expressed in MAMs and binds to GRP75, affecting IP3R/GRP75/VDAC1 complex interactions. Silencing Tesp1 expression reduces T cell receptor (TCR)-mediated mitochondrial and cytoplasmic calcium influx (Matsuzaki et al., 2013). Pyruvate dehydrogenase kinase 4 (PDK4) (Thoudam et al., 2019), glycogen synthase kinase-3 β (GSK-3 β) (Klec et al., 2019), and transglutaminase 2 (TG2) (D'Eletto et al., 2018) are also involved in the regulation of the IP3R/GRP75/VDAC complex, which affects MAM formation and ERMCS calcium transfer. We found that Nogo-B affects the binding of GRP75 and may regulate the formation of MAMs through the protein interactions of this complex (Yang Y. D. et al., 2019).

Sig1Rs are integral membrane proteins that possess two transmembrane domains and localize to the C-terminus of the ER. They are involved in multiple functions of brain tissue and other organs and play an important role

TABLE 1 | Summary of the functional proteins at mitochondria-associated endoplasmic reticulum membranes (MAMs).

Components	Roles	Interactions	Functions and mechanisms	References
(1) Ca²⁺ regulatory proteins				
IP3Rs	ER-resident Ca ²⁺ receptors	Forming IP3Rs/GRP75/VDAC1 complex	Interaction with GRP75 and VDAC1, promoting Ca ²⁺ release from ER in MAMs	Bartok et al., 2019
GRP75	Cytosolic molecular chaperone		Linking IP3Rs to VDACs, fostering MAMs formation, and Ca ²⁺ transfer	Szabadkai et al., 2006
VDACs	OMM porins		Interaction with GRP75 and IP3Rs, promoting Ca ²⁺ uptake of mitochondria in MAMs	Maurya and Mahalakshmi, 2016
Tespa1	Regulator of Ca ²⁺ flux in MAMs	Binding to GRP75	Maintaining MAMs integrity and affecting IP3R/GRP75/VDAC1 complex interactions	Matsuzaki et al., 2013
Sig1R	Chaperon at the ER	Forming complexes with BIP	Resulting in continuous mitochondrial Ca ²⁺ influx via stabilizing IP3R at MAMs in case of separation from BIP by stimuli	Hayashi and Su, 2007
SERCA	Ca ²⁺ uptake pump at the ER	Interacting with calnexin	Maintaining intracellular calcium homeostasis	Bollo et al., 2010
RyRs	Ca ²⁺ uptake pump at the SR in cardiomyocytes	Forming RyR2-VDAC2 complex	Promoting the Ca ²⁺ transfer of ERMCS in heart	Min et al., 2012
(2) Lipid synthesis and transport proteins				
ORP 5/8	PTPIP51 binding proteins in ER	Forming ORP5-PTPIP51; Competition with VAPB-PTPIP51	Mediating PS transfer; Expanding the ERMCS with PTPIP51	Pulli et al., 2018
ACAT	Regulate the balance of intracellular cholesterol	Synergizing with HMGCS and HMG-CoA reductase	Catalyzing the connection of long-chain fatty acids with free cholesterol to form cholesteryl esters	Li et al., 2021
DGAT	A major triacylglycerol biosynthetic enzyme	Interacting tightly with mitochondria	Catalyzing the final step of TG synthesis	Kornmann, 2020
PSS	Enzymes involved in PE biosynthesis	PSS-1 is highly enriched in MAM	Catalyzing PC and PE to generate PS	Vance and Steenbergen, 2005
StAR	OMM proteins	Binding to Tom22, VDAC2 and Sig1R	Mediating cholesterol transport; Undergoing steroidogenesis	Garay et al., 2017
(3) MAM tethers proteins				
VAPB	Tethers	Forming VAPB-PTPIP51; Suppressing ORP5-PTPIP51	Interacting with PTPIP51 to ensure the formation of MAMs; Regulating autophagy via Ca ²⁺ transfer	Stoica et al., 2014
PTPIP51		Binding to VAPB and ORP5; Interaction with PTP1B	Ensuring the formation of MAMs as the linker complex; Modulating mitochondrial structure and function with ORP5/8	Gomez-Suaga et al., 2017a
VPS13A		Interacting with the ER protein VAPA	Promoting MAM formation and mitochondria stability; Involved in mitophagy	Yeshaw et al., 2019
El-24		Forming a quaternary complex with IP3R/GRP75/VDAC1	Promoting MAM formation; Regulating calcium transfer; Cause apoptosis	Yuan L. et al., 2020
BAP31		Interacting with Tom40	Maintaining the integrity of ERMCS and regulating the mitochondrial respiration by BAP31-Tom40 complex	Namba, 2019
ERMES		Consisting of Mmm1, Mdm10, Mdm12, and Mdm34	Promoting phospholipid biosynthesis and calcium-signaling genes	Kornmann et al., 2009
(4) MAM controlled proteins				
PACS-2	MAM regulatory protein	Stabilizing BAP31	Required for MAM stabilization; Regulation of Ca ²⁺ transfer and phospholipid synthesis; Inhibiting apoptosis	Moulis et al., 2019
Mfn2	GTPase located in ERMCS	Interacting with Mfn1/2 to form homo- or heterodimeric complexes	Promoting fusion of mitochondria and structural stabilization of MAMs; Facilitating Ca ²⁺ transfer	Larrea et al., 2019
FUNDC1	Autophagy regulatory protein	Interacting with calnexin; Binding to IP3Rs	Promoting DRP1-dependent mitochondrial fission and mitophagy; Increasing the Ca ²⁺ concentration in both the cytoplasm and the mitochondria	Wu et al., 2016
DsbA-L	Antioxidant enzyme	Forming DsbA-L/FATE1 complex	Maintaining the integrity of MAMs; Reducing ER stress and apoptosis of ERMCS	Yang M. et al., 2019
FATE-1	Uncoupler of MAMs		Increasing the distance between mitochondria and ER and decreasing Ca ²⁺ transfer of ERMCS	Doghman-Bouguerra et al., 2016

ER, endoplasmic reticulum; ERMCS, ER-mitochondria contacts; MAM, mitochondria-associated ER membrane; OMM, outer mitochondrial membrane; IP3R, inositol 1,4,5-triphosphate receptor; GRP75, glucose-regulated protein 75 kDa in size; VDAC, voltage-dependent anion selective channel protein; Sig1R, Sigma-1 receptor; BIP, binding immunoglobulin protein; Tespa1, Thymocyte-expressed, positive selection-associated 1; SERCA, sarco/endoplasmic reticulum Ca²⁺-ATPase; RyRs, ryanodine receptors; ORP5/8, oxysterol-binding protein-related protein 5/8; PTPIP51, protein tyrosine phosphatase interacting protein 51; VAPB, Vesicle-associated membrane protein-associated protein B; BAP31, B-cell receptor-association protein 31; Tom40, translocase of the outer mitochondrial membrane 40; ERMES, The ER-mitochondria encounter structure; ACAT, acyl CoA-cholesterol acyl transferase; HMG-CoA, hydroxymethylglutaryl coenzyme A; HMGCS, HMG-CoA synthase; DGAT, diglyceride acyltransferase; TG, triglyceride; PSS, phosphatidylserine synthase; PS, phosphatidylethanolamine; PE, phosphatidylcholine; PC, phosphatidylcholine; StAR, steroidogenic acute regulatory protein; Tom22, translocon of the outer membrane 22; VPS13A, Vacuolar protein sorting 13A; El-24, etoposide-induced protein 2.4; PACS-2, phosphofurin acidic cluster sorting protein-2; BAP31, B-cell receptor-association protein 31; Mfn1/2, mitochondrial fusion protein 1/2; FUNDC1, FUN14 domain-containing 1; DRP1, dynamin-related protein 1; DsbA-L, disulphide-bond A oxidoreductase-like protein; FATE-1, fetal and adult testis-expressed 1.

in neuropsychiatric disorders, pain disorders, and tumor progression (Penke et al., 2018). Sig1Rs can form complexes with binding immunoglobulin protein (BIP) at MAMs, and after the ER receives a stimulating signal, Sig-1Rs separate from BIP and bind IP3Rs to stabilize their expression, which causes continuous mitochondrial calcium influx (Hayashi and Su, 2007). Other binding partners of Ca^{2+} such as calnexin and calreticulin are similarly expressed in MAMs and are involved in the regulation of ER-mitochondrial calcium signaling (Stahon et al., 2016).

RyR is a calcium release channel on ER/SRs. In mammals, there are three isoforms, namely skeletal muscle type (RyR1), cardiac muscle type (RyR2), and brain type (RyR3), which are encoded by the *ryr1*, *ryr2*, and *ryr3* genes, respectively (Ogawa, 1994). It has previously been shown that RyRs are not only present on the ER/SRs, but also localized to the IMM and may be involved in Ca^{2+} uptake of mitochondria. The structural and functional properties of mitochondrial RyR (mRyR) are similar to those of RyR1 in skeletal muscles and different from those of RyR2 in cardiomyocytes, which were almost absent in the heart by immunoprecipitation and liquid chromatography-tandem mass spectrometry (LC-MS/MS) techniques (Beutner et al., 2005).

RyR2 is a 560 kDa molecule responsible for Ca^{2+} release from SR. RyR2 plays an important role in the Ca^{2+} at ERMCS in cardiomyocytes. Typically, VDAC1 physically interacts with IP3Rs via the GRP75 to mediate Ca^{2+} transport. In addition, RyR2 and VDAC2 are two key proteins for the functional ERMCS in cardiomyocytes, and RyR2-VDAC2 coupling may be indispensable. Previous study found that RyR2 was physically coupled to VDAC2 in the heart and co-localized with RyR2 in the subsarcolemmal region of cardiomyocytes (Min et al., 2012). In brief, RyR2-VDAC2 complex could also promote the uptake of mitochondrial Ca^{2+} and the function of ERMCS in cardiomyocytes.

Lipid Synthesis and Transport Proteins

Enzymes involved in various types of lipid metabolism are enriched in MAMs, such as phosphatidylserine synthase (PSS), phosphatidylserine decarboxylase (PSD), phosphatidylethanolamine N-methyl transferase (PEMT), long chain acyl-CoA synthase 4 (ACSL4/FACL4), acyl CoA-cholesterol acyl transferase (ACAT), lysophosphatidylinositol-acyltransferase-1 (LPIAT1), steroidogenic acute regulatory protein (StAR), diglyceride acyltransferase (DGAT), and glucose-6-phosphatase (G-6-Pase) (Kornmann, 2020).

Synthetases abundant on MAMs can locally synthesize phosphatidylserine (PS), phosphatidylethanolamine (PE), and phosphatidylcholine (PC), which are all major structural components of membranes. PSS-1 and PSS-2 are involved in PS biosynthesis in mammalian cells. Experiments revealed that PSS-1 was highly enriched in rat liver MAMs (Stone and Vance, 2000). PS transport is achieved through oxysterol-binding protein-related protein (ORP) 5 and ORP8, which are abundantly expressed in MAMs. These enzymes enriched in MAMs may support the direct transfer of lipids between the ER and mitochondria (Pulli et al., 2018). The PS generated by the ER is transferred to the mitochondria and converted

to PE by a decarboxylation reaction. This process is the main source of mitochondrial PE, and mice lacking PSD activity develop abnormal mitochondrial function or even death during the embryonic period (Zhao and Wang, 2020). In addition to enzymes involved in phospholipid synthesis, the enzymes required for triacylglycerol, cholesterol, and glycosphingolipid synthesis are also enriched in MAMs, and thus, they are a core regulatory link in the balance of lipid metabolism (Vance, 2014).

Mitochondria-Associated Endoplasmic Reticulum Membranes Tethers Proteins

Vesicle-associated membrane protein-associated protein (VAP) B and protein tyrosine phosphatase interacting protein 51 (PTPIP51) are expressed in MAMs and interact to form linker complexes, ensure the formation of MAM structures, and mediate calcium transfer from ERMCS (Stoica et al., 2014). Knockdown of VAPB and PTPIP51 expression reduced calcium transfer levels by 86% (Gomez-Suaga et al., 2017a). VAPB and PTPIP51 are expressed at neuronal synapses, and after stimulation, VAPB-PTPIP51 interaction is enhanced and MAM formation is increased. Deficiency of VAPB and PTPIP51 reduced the number of dendritic spines and synaptic activity (Gomez-Suaga et al., 2019).

Vacuolar protein sorting (VPS) 13A is expressed in MAMs, and its FFAT domain interacts with the ER protein VAPA, which binds mitochondria via its C-terminus and anchors the ER and mitochondria (Park et al., 2016). After knockdown of VPS13A, MAM formation was reduced, mitochondria appeared fragmented, and mitophagy was inhibited (Yeshaw et al., 2019). The DNA damage response activates p53-mediated transcription of a variety of ER morphology proteins (Zheng et al., 2018). Among them, etoposide-induced protein 2.4 (EI24) forms an ER-mitochondrial linker with VDAC to promote MAM formation, mediate ER-mitochondrial calcium transfer, and cause apoptosis (Yuan L. et al., 2020).

B cell receptor-associated protein 31 (BAP31) is an integral ER membrane protein (Namba et al., 2013), which also plays a pivotal role in the constitution of the ERMCS by interacting with translocase of the outer mitochondrial membrane 40 (Tom40) to stimulate the translocation of ubiquinone oxidoreductase (mitochondrial complex I) core subunit 4 (NDUFS4), the component of complex I from the cytoplasm to the mitochondria. BAP31 is a key factor in maintaining the integrity of ERMCS with Tom40, and the BAP31-Tom40 complex is essential for activating mitochondrial respiration by stimulating NDUFS4 translocation in mitochondria by regulating the activity of the mitochondrial respiratory chain complex I. After loss of BAP31 function, it can affect the metabolism of cells, followed by a decrease in mitochondrial aerobic respiration-dependent ATP levels, triggering AMPK signaling and ultimately leading to autophagy (Namba, 2019).

The ER-mitochondria encounter structure (ERMES) is a complex which consists of mitochondrial morphology protein 1 (Mmm1), mitochondrial distribution and morphology protein 10 (Mdm10), Mdm12 and Mdm34 in yeast that reside in both the ER and the OMM except that Mdm12 is cytoplasmic. Mdm12, Mdm34, and Mmm1 possess a common SMP domain,

which maintains ER contact with the mitochondrial membrane, promotes MAMs formation, and mediates ERMCs functions (Burgess et al., 1994). With the use of genome-wide mapping of genetic interactions, a study showed that the ERMES were functionally connected to phospholipid biosynthesis and calcium-signaling genes. In addition, phospholipid biosynthesis was impaired in mutant cells (Kornmann et al., 2009).

Mitochondria-Associated Endoplasmic Reticulum Membrane Controlled Proteins

Phosphofurin Acidic Cluster Sorting Protein-2

Phosphofurin acidic cluster sorting protein-2 was identified as the first MAM regulatory protein with a number of functions that can mediate ERMCs. Overall, PACS-2 regulates ER homeostasis and MAM formation (Simmen et al., 2005). Both PACS-2 and B-cell receptor-association protein 31 (BAP31) are located in the MAMs. Experiments have demonstrated that knockdown of PACS-2 resulted in BAP31-dependent mitochondrial fragmentation, deregulated synthesis of lipids, and translocation of BH3-interacting domain death agonists (Bid) to mitochondria, indicating that PACS-2 is required for MAM stabilization (Iwasawa et al., 2011). Mechanistically, PACS-2 depletion induces BAP31 cleavage to form P20. P20 triggers the release of Ca^{2+} from the ER to the mitochondria while regulating calcium homeostasis in the cell, which then recruits DRP1 to the mitochondria and subsequently induces mitochondrial fragmentation. Upon apoptotic stimulation, Bid translocates into the mitochondria via PACS-2 to initiate apoptosis (Simmen et al., 2005). Mammalian target of rapamycin (mTOR) complex 2 (mTORC2) located in MAMs phosphorylates PACS-2 by activating Akt to maintain the integrity of MAMs, indicating that phosphorylated PACS-2 is involved in the maintenance of the MAM structure. In addition, mTORC2-Akt-regulated phosphorylation at Ser437 of PACS-2 maintains the formation of MAMs (Betz et al., 2013). PACS-2 also regulates the transport of calnexin and transient receptor potential channel P2 (TRPP2) from MAMs to the plasma membrane (Kottgen et al., 2005). PACS-2 similarly mediates MAMs-regulated phospholipid synthesis (Hamasaki et al., 2013).

Mfn2

Mfn2 is a GTPase located on the OMM that stabilizes interactions between adjacent mitochondria and promotes fusion of mitochondria (de Brito and Scorrano, 2008). In recent years, it has been found that within the ER-mitochondrial membrane contact interface, Mfn2 localized in the ER interacts with Mfn2 or Mfn1 in mitochondria to form homo- or heterodimeric complexes and promote the structural stabilization of MAMs. Mutation of Mfn2 resulted in the dissociation of both membranes, morphological changes in the ER and mitochondria, and corresponding functional alterations in some patients but not all (Larrea et al., 2019).

A previous study found that ERMCs are approximately two times more abundant in Mfn2 KO cells than in wild-type (WT) cells examined by electron microscopy, which suggested that Mfn2 did not play a critical role in the ERMCs (Cosson et al., 2012). Not only the structural ERMCs but also the functions of them including Ca^{2+} transfer increased due to the Mfn2

reduction using a multiple study approaches (Filadi et al., 2015). Gp78/autocrine motility factor receptor (AMFR) is an E3 ubiquitin ligase in the ER that promotes MAM formation, where it can cause degradation of Mfn2 (Li L. et al., 2015). Based on these results, another perspective for ERMCs was proposed in which Mfn2 works as a tethering antagonist rather than a tether. In order to further determine the regulation of MAMs by Mfn2, it was experimentally found that MAM formation was reduced after knockdown of Mfn2, while the calcium transfer of ERMCs was inhibited, which demonstrated the positive regulation of MAM formation by Mfn2 (Zorzano et al., 2010). Other regulators such as mitochondrial ubiquitin ligase (MITOL) (Takeda et al., 2019) and trichoplein/mitostatin (TpMs), a keratin-binding protein, can also affect the integrity of MAMs and mitochondrial function by affecting the assembly and degradation of Mfn2 (Cerqua et al., 2010).

Disulphide-Bond A Oxidoreductase-Like Protein and Fetal and Adult Testis-Expressed 1

As previously reported, disulphide-bond A oxidoreductase-like protein (DsbA-L) and fetal and adult testis-expressed 1 (FATE-1) were expressed in MAMs. DsbA-L, an antioxidant enzyme, showed the function of reducing ER stress and maintained MAMs integrity while FATE-1 can regulate mitochondrial Ca^{2+} uptake and dissociate the MAMs (Doghman-Bouguerra et al., 2016; Tubbs et al., 2018; Yang M. et al., 2019). One study has showed that the MAMs was reduced in the kidneys of diabetic DsbA-L gene-deficient mice (DsbA-L^{-/-}). Importantly, the overexpression of DsbA-L in HK-2 cells restored the high-glucose induced dysfunction of MAMs and reduced apoptosis. Interestingly, these beneficial effects were partially abolished by overexpression of FATE-1 (Yang M. et al., 2019). Previous studies implicated that FATE-1 is a cancer-testis antigen which has been identified as an uncoupler of MAMs (Doghman-Bouguerra et al., 2016; Tubbs et al., 2018). Under the control of steroidogenic factor-1 (SF-1), FATE1 upregulation increased the distance between mitochondria and ER and decreased mitochondrial Ca^{2+} uptake (Doghman-Bouguerra et al., 2016).

Lipids

After MAMs were treated with proteinase K, nearly 50% of their function remained (Kobuchi et al., 2012). Upon removal of cholesterol from membranes using methyl- β -cyclodextrin (M β C), the expression of Sig1Rs was reduced in the lipid raft regions of MAMs and would lead to calcium overload. Further experiments revealed that M β C inhibits PS lyases expressed in MAMs, the *de novo* synthesis function of PS is disturbed, and MAM formation is reduced (Fujimoto et al., 2012). The above results suggest that cholesterol may affect the function of ERMCs by altering the structure of biofilms at MAMs.

THE FUNCTION OF ENDOPLASMIC RETICULUM-MITOCHONDRIA CONTACTS

Studies have shown that core proteins and signaling pathways involved in various life activities of cells are expressed in

ERMCs. In addition to earlier findings of calcium transfer and phospholipid metabolism, ERMCS are also involved in steroid synthesis, ER stress, mitochondrial dynamics, autophagy, and apoptosis (Figure 1).

Endoplasmic Reticulum-Mitochondria Contacts and Calcium Transfer

Earlier studies revealed that mitochondrial calcium levels and the Ca^{2+} concentration of ERMCS significantly increased after HeLa cells were stimulated with IP3 (Lao and Chang, 2008). Subsequent studies confirmed that the IP3Rs/GRP75/VDAC1 protein complex is expressed in ERMCS and mediates the transfer of calcium (Moshkforoush et al., 2019). IP3Rs mainly regulate ER calcium efflux and exist in three isoforms. IP3R1 is widely distributed and particularly abundant in the brain, oocytes, and eggs. IP3R2 is expressed in the epithelium, myocardium, and skeletal muscle. However, IP3R3 is highly expressed in different cells and tissues. IP3R3 mainly mediates the release of ER calcium, while IP3R1 is mainly involved in the stabilization of cytosolic calcium (Bartok et al., 2019). Recently, it has been shown that Akt can phosphorylate IP3R3 at ERMCS and inhibit calcium release, thereby reducing the level of mitochondrial calcium and promoting cell proliferation (Marchi et al., 2008). mTORC2, promyelocytic leukemia protein (PML), and protein phosphatase 2A (PP2A) can activate Akt, promote its phosphorylation, and regulate calcium transfer in ERMCS, on

the contrary, PTEN can counteract Akt activation and thus can inhibit the Akt-mediated phosphorylation of IP3R3 that protects from Ca^{2+} mediated apoptosis (Ando et al., 2018).

A variety of oxidoreductases are involved in the regulation of calcium transfer at ERMCS. Endoplasmic reticulum oxidoreductin 1 α (Ero1 α) is expressed in ERMCS and regulates calcium release from IP3Rs (Anelli et al., 2012). Endoplasmic reticulum resident protein (ERP) 44 belongs to the thioredoxin family and is localized in the ER lumen. ERP44 can directly bind IP3R1 and inhibit Ca^{2+} efflux, and this interaction is regulated by hydrogen ion concentration, Ca^{2+} concentration, and redox state (Higo et al., 2005). ER glutathione peroxidase 8 (GPX8) is expressed in ERMCS and can scavenge hydrogen peroxide generated by Ero1 α mediation (Ramming et al., 2014).

Calnexin is associated with chaperones that bind newly synthesized glycoproteins and delay the process of protein folding. After detachment from the formed complex, the glycoprotein is transported to the Golgi when correctly folded. If misfolded, it is glycosylated again and enters into the calnexin cycle (Gutierrez et al., 2020). ERP57 in the protein disulfide isomerase (PDI) family is involved in this cycling process through binding to calnexin. Thus, calnexin prevents the accumulation of misfolded proteins within the ER (Lynes et al., 2013). At the ERMCS interface, calnexin interacts with sarco/endoplasmic reticulum Ca^{2+} -ATPase (SERCA) 2b to maintain intracellular calcium homeostasis. Phosphorylation at S562 in the cytoplasmic domain of calnexin promotes binding to SERCA2b. This site is

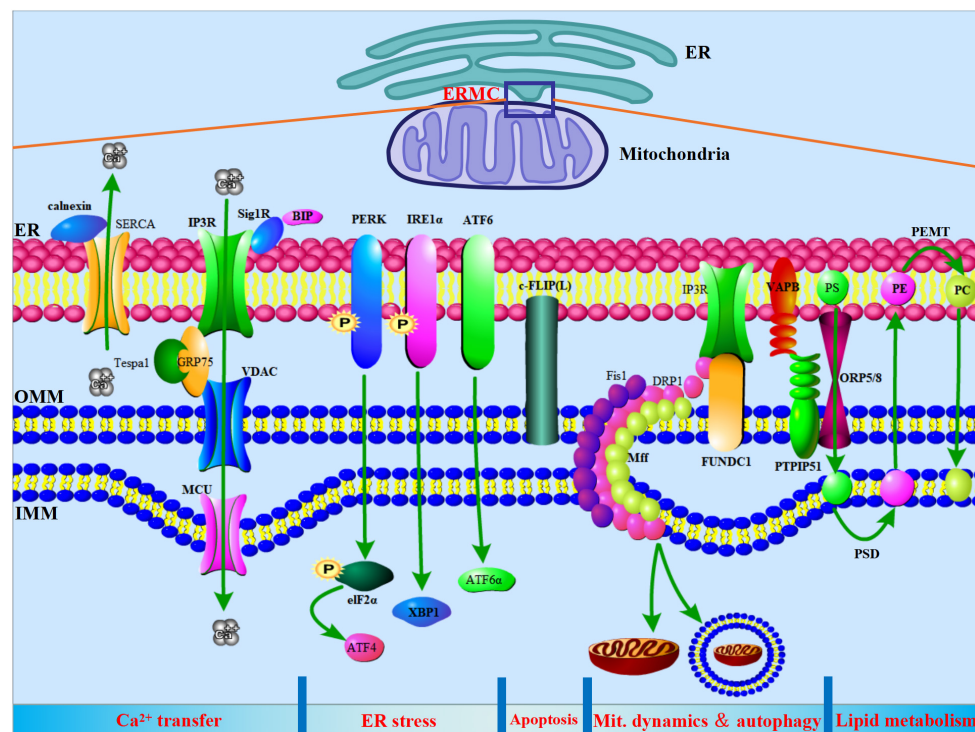


FIGURE 1 | ER-mitochondria contacts (ERMCS) are involved in the regulation of Ca^{2+} transfer, ER stress, apoptosis, mitochondria dynamics, autophagy, and lipid metabolism. Top, a schematic diagram to show the ERMCS. Below, on a schematized segment of MAMs, the molecular contributors to the main known functions of ERMCS are summarized.

dephosphorylated during IP₃-mediated ER calcium release, and the interaction of calnexin with SERCA2b is inhibited (Bollo et al., 2010). Alternatively, the phosphorylation status of calnexin and its interaction with PACS-2 also determine the distribution of calnexin protein in MAMs (Myhill et al., 2008).

Endoplasmic Reticulum-Mitochondria Contacts and Lipid Metabolism

Lipids in the IMM and OMM cannot be synthesized in mitochondria. The close contact of the ER membrane with the mitochondrial membrane allows the rapid exchange of lipids between mitochondria and the ER. Studies have shown that enzymes involved in lipid metabolism are expressed in ERMCS and are involved in the metabolism of phospholipids, triglycerides, fatty acids, and steroids.

Phospholipid Metabolism

Earlier studies found that most of the mitochondrial PE is derived from the decarboxylation of PS after labeling serine or ethanolamine using [³H], and radiolabeled PS accumulates in ERMCS after administration of PS decarboxylation inhibitors (Steenbergen et al., 2005). PS was significantly increased in ERMCS after ATP deprivation. The above results indicate that PS can enter mitochondria through ERMCS after synthesis, and ATP is involved in this transport process (Vance and Steenbergen, 2005). Subsequent studies confirmed that PSS-1 and PSS-2 are expressed in ERMCS and catalyze PC and PE to generate PS. Subsequently, PS is transferred into the mitochondria, where it is decarboxylated by PSD1 at the IMM to generate PE. PE returns to the ER and methylates via PEMT2 at ERMCS to generate PC (Vance, 2015). It is the ERMCS that produce several major components that enable phospholipids to be efficiently synthesized and transported to the appropriate position (Vance, 1990; Stone and Vance, 2000; Voelker, 2000).

Steroid Synthesis

Recent studies have shown that ACAT1 is expressed in ERMCS. Intracellularly, ACAT1 is the only enzyme that catalyzes the connection of long-chain fatty acids with free cholesterol to form cholesterol esters, which together with hydroxymethylglutaryl coenzyme A (HMG-CoA) synthase (HMGCS) and HMG-CoA reductase maintain and regulate the balance of intracellular cholesterol metabolism and play a key role in the development and progression of atherosclerosis (Rusinol et al., 1994; Li et al., 2021). The StAR protein transports cholesterol to undergo steroidogenesis, where it binds to VDAC2 at the OMM to mediate cholesterol trafficking to the IMM (Liu et al., 2006). Subsequently, cholesterol is catalyzed by cytochrome P450 side-chain cleavage (SCC) enzymes to generate pregnenolone. Pregnenolone returns to the ER to generate other classes of steroids. StAR is expressed in ERMCS and mediates cholesterol transport (Garay et al., 2017). In ERMCS, StAR binds the mitochondrial proteins Tom22 and VDAC2, and conversely, VDAC2 regulates the process of StAR entry into mitochondria. Upon knockdown of VDAC2, StAR is expressed but fails to bind ERMCS interface proteins in the mature protein form and enter the mitochondria, thereby inhibiting steroid synthesis (Prasad et al., 2015). In addition, StAR can bind to Sig1R and

GRP78 before transferring cholesterol to mitochondria, which regulate the expression and activity of StAR. After knockdown of Sig1R, the synthesis of pregnenolone was decreased by 75–95% (Marriott et al., 2012). GRP78, a chaperone in the ER, is expressed in ERMCS and folds at the interface of ERMCS to activate StAR and promote its trafficking to the OMM. After knockdown of GRP78 expression, the expression and activity of StAR were significantly reduced (Prasad et al., 2017).

Endoplasmic Reticulum-Mitochondria Contacts and Endoplasmic Reticulum Stress

The ER is involved in protein folding, lipid synthesis, and calcium storage. Under ER stress, misfolded proteins accumulate in the ER. Chaperones such as GRP78/BIP and three ER stress-sensing proteins, which are PKR-like ER kinase (PERK), activating transcription factor (ATF) 6, and inositol-requiring enzyme 1 α (IRE1 α), initiate unfolded protein response (UPR) after activation of recognition to repair misfolded proteins and maintain proteostasis (Oakes and Papa, 2015). Appropriate UPR levels can promote cell survival, whereas when ER stress is sustained or excessive, the ER apoptotic pathway is activated and promotes apoptosis.

The PKR-Like Endoplasmic Reticulum Kinase-Mediated Signaling Pathway

PKR-like endoplasmic reticulum kinase is a type I transmembrane protein, and its cytoplasmic fraction contains a serine/threonine kinase domain (Wang et al., 2020a). Under physiological conditions, heat shock protein (HSP) 90 and BIP bind the cytoplasmic and ER domains of PERK and stabilize PERK. Under ER stress, BIP binds misfolded proteins, thereby releasing PERK and causing PERK dimerization and autophosphorylation activation. Subsequently, PERK activates eukaryotic initiation factor 2 (eIF2) to inhibit translation initiation. PERK phosphorylation ensures cell survival, and results in differentiation and metabolism-related substances, such as nuclear factor E2-related factor 2 (Nrf2), forkhead box O (FOXO), and diacylglycerol (DAG) (Xu Y. et al., 2020). In addition to inhibiting total mRNA translation, PERK activates the transcription of some genes, including ATF4, ATF5, and amino acid transport carriers. ATF4 enters the nucleus to activate the transcription of genes related to antioxidant response and amino acid synthesis and transport and promote cell survival. However, ATF4 can also activate the expression of pro-apoptotic transcription factor C/EBP homologous protein (CHOP) and mediate the ER stress apoptotic pathway (Verfaillie et al., 2012). Recent studies have found that PERK is expressed in ERMCS and rapidly transfers lipid peroxides from the ER into mitochondria, causing oxidation of cardiolipin in mitochondria and release of cytochrome *c*, and then promotes apoptosis (Rozpedek et al., 2016). In addition, the PERK-eIF2 α -ATF4 pathway activates the expression of SERCA1 in ERMCS, which can promote ERMCS formation and feedback enhancement of the PERK-eIF2 α -ATF4 pathway. Knockdown of SERCA1 expression can inhibit ER stress-induced mitochondrial calcium overload and apoptosis (Guo et al., 2016).

The ATF6-Mediated Signaling Pathway

ATF6 is a type II transmembrane protein containing the cytoplasmic cAMP response binding protein domain. Under ER stress, ATF6 is released from the ATF6/BIP protein complex and further processed by proteases site-1/2 protease (S1P/S2P) in the Golgi apparatus to produce active ATF6. The cleaved ATF6 α activates adaptive responses, whereas ATF6 β may inhibit ATF6 α function (Huang et al., 2018). During ER stress, ATF6 expression increases, which can promote the formation of ERMCs, increase ER-mitochondrial calcium transfer, and enhance mitochondrial respiration, thereby inhibiting cell proliferation and promoting apoptosis (Burkewitz et al., 2020).

The Inositol-Requiring Enzyme 1 α -Mediated Signaling Pathway

Inositol-requiring enzyme 1 α is an endonuclease in the ER that is widely distributed and binds HSP72/HSP90/BIP under physiological conditions (Shemorry et al., 2019). ER stress can cause IRE1 α oligomerization and phosphorylation, activating its kinase and endoribonuclease activities. Subsequently, IRE1 α activates cleavage to generate X-box binding protein 1 (XBP1), which enters the nucleus to promote gene transcription for protein folding, trafficking, and degradation of ER-associated proteins (Zhang et al., 2018). Recently, it was shown that IRE1 α is expressed in ERMCs, and MITOL can mediate K63 chain ubiquitination at Lys481 of IRE1 α , thereby inhibiting the polymerization reaction of IRE1 α . Under ER stress, reduced expression of MITOL can increase the endonuclease activity of IRE1 α and promote apoptosis development (Takeda et al., 2019).

Endoplasmic Reticulum-Mitochondria Contacts and Mitochondrial Dynamics

Mitochondria are highly motile organelles in cells that continuously fuse and divide. The fusion of two adjacent mitochondria causes the redistribution of mitochondrial DNA and protein, forming an evenly distributed mitochondrial network (Chen et al., 2003). Mitochondrial fission and fusion are precisely regulated by calcium and calcium-dependent kinases, phosphatases, metabolism, and intracellular oxidative status. A series of proteins is involved in the regulation of mitochondrial dynamics, such as Mfn1, Mfn2, and OPA1, as well as mitochondrial fission protein 1 (Fis1) and DRP1. Mfn1 mediates fusion of the OMM with Mfn2, whereas OPA1 integrates the inner mitochondrial membrane (Tilokani et al., 2018). Upon phosphorylation of Mfn1 by extracellular regulated protein kinase (ERK), mitochondria appear fragmented and BAK oligomerizes, which increases mitochondrial membrane permeability and initiates apoptosis (Pyakurel et al., 2015). Cyclin B1/cyclin-dependent kinase (CDK) 1 activates DRP-1 in response to growth factors and promotes DRP-1 phosphorylation to initiate the intracellular transfer of DRP1. DRP1 is located in the cytoplasm in the inactive state and translocates to the OMM upon activation. Subsequently, DRP1 assembles to form multimers that bind and divide mitochondria, and DRP1 phosphorylation inhibits mitochondrial fission (Kizaki et al., 1988).

The initiating role of ERMCs on mitochondrial fission is more evident. The ERMCs sites determine the location

of the bound and divided mitochondria (Friedman et al., 2011). DRP1 assembles and recruits other split proteins Fis1, mitochondrial fission factor (Mff), and mitochondrial dynamics proteins of 49 and 51 kDa (MiD49/MiD51) at the ERMCs to form mitochondrial split protein polymers, which tighten mitochondria and initiate fission (Ji et al., 2017). In a real-time observational study, 84% of mitochondrial fission events occurred at sites of ERMCs. During mitochondrial segmentation, ERMCs points persist. After mitochondrial fission, the progeny mitochondria move distally, and the other maintains tight junctions with the ERMC points and remains relatively quiescent. Subsequently, the mitochondrial membrane elongates at the site of fission to form a tubular intermediate form until mitochondrial fission is complete (Guo et al., 2018). The above results indicate that the ERMCs not only mark the mitochondrial fission site but also act to stabilize mitochondria during mitochondrial fission. In addition, ERMCs proteins can regulate the activation of DRP1. The activity of DRP1 is reduced after phosphorylation of DRP1 by PKA, which expands the ER lumen, promotes the elongation of mitochondria, and increases ERMCs formation (Bravo-Sagua et al., 2019).

In addition to its involvement in mitochondrial fission, it was recently reported that ERMCs are similarly involved in mitochondrial fusion (Basso et al., 2018). Fifty-nine percent of mitochondrial fusion events occur at the ERMCs, with the ER being between two adjacent mitochondria. It was found that without the involvement of the ER, mitochondrial membrane fusion is a lengthier process as compared to having the involvement of the ERMCs (Guo et al., 2018). The results showed that ERMCs can accelerate the process of mitochondrial fusion, although the molecular mechanism requires further elucidation. ERMCs are similarly involved in mitochondrial DNA replication and predate mitochondrial fission (Qin et al., 2020).

Endoplasmic Reticulum-Mitochondria Contacts and Autophagy

Autophagy is a process whereby intracellular components are degraded and recycled (Mizushima and Komatsu, 2011). After wrapping damaged organelles or proteins, lysosomes degrade their contents. The unc-51-like autophagy activating kinase (ULK) 1/2 complex initiates and activates the VPS34 complex. Subsequently, LC3-II which produced from cleavage of microtubule-associated protein light chain 3 (LC3) by ATG family proteins mediates the extension of isolated membranes (Parzych and Klionsky, 2014). Isolated membranes encapsulate damaged organelles, and cytoplasmic components continuously extend to produce phagocytic vacuoles, which form autophagosomes after blocking. In addition, p62 protein can bind LC3, enter autophagosomes, and undergo degradation by fused lysosomes. It was observed that total intracellular p62 protein levels were inversely correlated with autophagic flux (Seibenhenner et al., 2013).

With adequate nutrition, ATG14 complexes are diffusely distributed in the ER membrane. In starvation-induced autophagy, ATG14 is specifically recruited in ERMCs by the ER-resident SNARE proteinsyntaxin17 (STX17)

(Hamasaki et al., 2013). Other early autophagy marker proteins such as beclin-1 and zinc finger FYVE domain-containing protein 1 (ZFYVE1)/double FYVE-containing protein 1 (DFCP1) are also similarly expressed at ERMCs (Hamasaki et al., 2013). Knocking down ERMCs linkers such as PACS-2 or Mfn2 can inhibit the expression of autophagic proteins in ERMCs and prevent autophagy initiation (Hamasaki et al., 2013; Hu et al., 2021). In addition to autophagic proteins expressed in ERMCs, ganglioside (GD3) is similarly involved in the initiation of autophagy (Matarrese et al., 2014). GD3 interacts with the cytoskeletal network and can be rapidly transferred from the cell membrane to various components within the cell, including ERMCs. GD3 not only binds the conventional class III phosphatidylinositol-3-kinase (PI3K) complex to initiate autophagy, but also can interact with LC3 after autophagy initiation. Inhibition of ceramide synthase and GD3 synthase significantly inhibited the formation of autophagosomes. Upon autophagy induction, calnexin expression increased in ERMCs and promoted autophagy (Garofalo et al., 2016).

Mitophagy can selectively remove damaged mitochondria, improve mitochondrial energy metabolism disorders, and prevent the release of pro-apoptotic proteins in mitochondria, which is essential for the quality maintenance of mitochondria (Bravo-San Pedro et al., 2017). After mitochondrial damage, PTEN induced putative kinase 1 (PINK1) can accumulate on the membrane surface of damaged mitochondria as well as recruit and phosphorylate ubiquitin and parkin RBR E3 ubiquitin protein ligase (PARK2), which mediate ubiquitination labeling of OMM proteins and proteasomal degradation, and inhibit the fusion of damaged mitochondria (Tang et al., 2018). Subsequently, these organelles form autophagosomes by activation of specific ubiquitin-binding receptor proteins such as sequestosome 1 (SQSTM1)/p62, which fuse with lysosomes to complete mitophagy (Yamada et al., 2019). Upon stimulation with the mitophagy agonist carbonyl cyanide 3-chlorophenylhydrazone (CCCP), PINK1 and beclin-1 are expressed in ERMCs, and promote the formation of omegasomes produced by ERMCs. At the same time, PARK2 expression at the ERMCs increased (Gelmetti et al., 2017). However, knockdown of PINK1 expression mediated reduced beclin-1 expression in ERMCs through the non-PARK2 pathway (Erpapazoglou and Corti, 2015). FUN14 domain-containing 1 (FUNDC1) is expressed in ERMCs and interacts with calnexin. Upon stimulation, FUNDC1 detaches from the calnexin complex and recruits dynamin-1-like protein (DNM1L)/DRP1 to initiate mitochondrial fission. Knockdown of FUNDC1, DNM1L, and CANX increased mitochondrial length, inhibited the binding of autophagosomes to mitochondria, and inhibited mitophagy under hypoxia (Wu et al., 2016).

Endoplasmic Reticulum-Mitochondria Contacts and Apoptosis

Regulation of calcium levels in ERMCs plays a pivotal role in apoptosis. Numerous proteins are involved in the regulation of the calcium transfer axis in ERMCs, thereby precisely regulating cell survival and death (Suresh, 2019). The long form of

c-FLIP (c-FLIP_L) is an isoform of cellular FLICE-like inhibitory protein (c-FLIP) that is expressed in the ERMCs. Knockdown of c-FLIP_L caused ER fragmentation and expansion of peripheral tubular ERs, and inhibited the formation of ERMCs (Jeong et al., 2015). Further studies showed that c-FLIP_L knockdown suppressed reticulon 4 (RTN-4) expression, and c-FLIP_L can inhibit apoptosis by inhibiting calcium transfer in ERMCs (Marini et al., 2015). Bcl-xl belongs to the Bcl-2 family of proteins, which are expressed in ERMCs and bind to each other with IP3R3. The overexpression of Bcl-xl promotes calcium transfer in ERMCs, decreases the NAD/NADH ratio, and enhances the oxidase activity of the electron transport chain (Bessou et al., 2020). BCL2-like 10 (Bcl2l10) binds to the IP3R and inhibits calcium release from the ER. IP3R binding protein released with IP3 (IRBIT) requires regulation of the IP3R through Bcl-2l10 binding. Cell fraction separation revealed that both Bcl2l10 and IRBIT are expressed in ERMCs, regulate the formation of ERMCs, and synergistically inhibit IP3R-mediated calcium release (Bonneau et al., 2016).

Studies have shown that cell necrosis is similarly regulated and is known as necroptosis. Necroptosis is involved in host defensive responses, chronic inflammation, and tissue damage, such as inflammation, hemolysis, and atherosclerosis (Frank and Vince, 2019). The formation of receptor interacting protein kinase-1 and -3/mixed lineage kinase domain-like protein (RIP1/RIP3/MLKL)-containing complexes in necrotic bodies can initiate the necroptosis pathway (Zhou et al., 2021). RIP1/RIP3/MLKL is expressed in ERMCs, and its content is higher than that in mitochondria. The process is mediated by the interaction of RIP3 and MLKL (Chen et al., 2013). The above results suggest that ERMCs may be the initiation site for accumulation of necrosomes and initiation of necroptosis, and further studies are needed to investigate the mechanism involved.

In conclusion, a growing body of studies has shown that core proteins involved in cellular biological processes are enriched in ERMCs, thereby exerting biological functions. Therefore, in pathological conditions, ERMCs can also participate in the development and progression of diseases.

THE CRITICAL ROLE OF ENDOPLASMIC RETICULUM-MITOCHONDRIA CONTACTS IN REMODELING AND CARDIOVASCULAR REMODELING-ASSOCIATED DISEASES

Endoplasmic Reticulum-Mitochondria Contacts in Remodeling of the Heart

Endoplasmic Reticulum-Mitochondria Contacts and the Pathophysiology of Cardiac Remodeling

Myocardial remodeling refers to the pathological changes such as myocardial hypertrophy, myocardial apoptosis, and interstitial fibrosis induced by various pathological stimuli such as inflammation, oxidative stress, ischemia-reperfusion, and mechanical tension in the heart (Huang et al., 2020). Additionally, progressive damage to mitochondrial function,

imbalance of energy homeostasis, and alteration of cardiac metabolism are important characteristics of cardiac remodeling (Sekaran et al., 2017; Ding et al., 2020).

The complex network formed by mitochondrial remodeling and the calcium buffer maintained by the ER and mitochondria are the premise for the maintenance of cardiomyocyte physiological function (Eisner et al., 2017). Based on the particularity of cardiomyocytes, there are essential differences in ERMCS compared with other types of cells, and they are especially prominent in the regulation of calcium homeostasis and calcium buffering involved in the ER and mitochondria (Chaanine et al., 2020). Calcium is a key second messenger regulating mitochondrial redox and energy metabolism, and during cardiomyocyte contraction, spontaneous Ca^{2+} oscillations evoked by the endoplasmic reticulum and cytoplasmic Ca^{2+} spikes propagate to the mitochondrial matrix to stimulate oxidative energy production (Jouaville et al., 1999). It has also been suggested that Ca^{2+} release via the IP3R-GRP75-VDAC1 complex is necessary to maintain the bioenergy of cardiomyocytes (Cárdenas et al., 2010). A massive release of ER Ca^{2+} into the cytoplasm causes mitochondrial Ca^{2+} overload as well as persistent opening of the mitochondrial permeability transition pore (mPTP), which can activate the mitochondrial apoptotic pathway and lead to cardiomyocyte apoptosis (Eisner et al., 2013). Moreover, continuous studies have confirmed that MAM-associated proteins are widely involved in multiple links of cardiovascular remodeling, and ERMCS is an important mechanism in the pathogenesis of heart diseases such as heart failure, myocardial hypertrophy, arrhythmia, and cardiomyopathy (Lopez-Crisosto et al., 2017; Silva-Palacios et al., 2020) (Figure 2).

Endoplasmic Reticulum-Mitochondria Contacts in Cardiomyocyte Hypertrophy and Heart Failure

Cardiac hypertrophy is a common type of remodeling that occurs in the heart under physiological and pathological overload. In sustained pathological overload, cardiomyocytes and the heart undergo enlargement that is accompanied by a decrease in the ventricular wall as well as interventricular septal stress and cardiac remodeling, leading to heart failure (Oka et al., 2014; Nakamura and Sadoshima, 2018). Studies have shown that the topology of mitochondria and the ER in cardiomyocytes is the center of signal transduction and calcium homeostasis, and crosstalk and alterations between the SR/ER and mitochondria have been involved in the pathogenesis of myocardial hypertrophy and heart failure (Reddish et al., 2017; Wacquier et al., 2019).

Overactivation of endoplasmic reticulum stress (ERS) and perturbation of mitochondrial function play a significant role in compensatory cardiac hypertrophy and progression to overt systolic heart failure (Chaanine et al., 2013; Ma et al., 2021). Intraperitoneal injection of tunicamycin (TN) is an interesting model that can be used to study the functional effects of cardiac ER stress. Prola et al. (2019) evaluated the exact physiological effect of TN-induced ER stress in mice, and the study found that TN injection resulted in a reduction of cardiac contractility and ultrastructural cytoarchitectural alterations in

cardiomyocytes after 72 h. The expression of ER stress markers GRP78, CHOP, and growth arrest and DNA damage-inducible protein 34 (GADD34) increased, while the expression of peroxisome proliferator-activated receptor- γ co-activator-1 α (PGC-1 α), a major regulator of mitochondrial biogenesis, and its downstream target Nrf1 were significantly inhibited. Mitochondria showed metabolic remodeling, slowed oxidative rate, and impaired Ca^{2+} uptake (Prola et al., 2019). These results provide evidence that the ER stress induced significant impairment of cardiac energy metabolism and function. In addition, SR as a modified ER, and mitochondrial-SR calcium crosstalk and cardiomyocyte Ca^{2+} transfer are closely linked to the development of heart failure (Eisner et al., 2013). The efficiency of Ca^{2+} transfer is affected by the distance between the ER and mitochondria, and in norepinephrine (NE)-induced hypertrophic cardiomyocytes, IP3R is dysfunctional. Mitochondrial Ca^{2+} uptake capacity is generally decreased, the average distance between the ER and mitochondria is increased, and ERMCS are decreased (Gutierrez et al., 2014).

Recently, MAM dysfunction was also implicated in the onset and progression of heart failure (HF) (Luan et al., 2021). Disruption of ERMCS has been found in Sig-1R, Mfn1/2, and FUNDC1-related HF (Silva-Palacios et al., 2020). The studies focused on the involvement of these proteins in HF pathogenesis are summarized below:

Duchenne muscular dystrophy (DMD) is a fatal disease featuring progressive cardiomyopathy, and compelling evidence supports the central role of mitochondrial dysfunction and impaired Ca^{2+} homeostasis in the pathogenesis of DMD (Meyers and Townsend, 2019). In dystrophin-deficient mice (mdx mice), IP3R1-VDAC1 interaction as well as GRP75-VDAC1 ligation were significantly enhanced, IP3R1 and its regulatory subunit Sig-1R were significantly increased, and the mitochondrial Ca^{2+} content was also significantly increased. It was shown that in mdx cardiomyocytes, IP3R1 and VDAC enhanced the physical interconnection of SR/ER-mitochondria. Additionally, increased IP3R1-GRP75-VDAC1 interaction is thought to enhance the direct channel of Ca^{2+} from SR/ER to the mitochondria (Angebault et al., 2020).

Mfn1/2-related proteins and VDAC2 probably have a role in stabilizing SR-mitochondrial interactions in cardiac muscle. Mfn1/2 is the protein most likely to be involved in tethering between SR and cardiac mitochondria (Chen et al., 2012; Hall et al., 2016). In the hearts of Mfn1 and Mfn2 cardiac knockout mice, reduced mitochondrial size and contact length of ERMCS, as well as severe cardiomyopathy and impaired cardiac function, were observed (Papanicolaou et al., 2011, 2012a,b).

The OMM protein FUNDC1 mediates the formation of MAMs (Wang C. et al., 2021). One study has shown that interruption of FUNDC1 and IPR2 interaction reduces the level of Ca^{2+} in the mitochondria and cytoplasm, triggering abnormal mitochondrial fission and cardiac dysfunction. In heart tissue from patients with heart failure, it has also been demonstrated that the FUNDC1/MAMs/CREB/Fis1 signaling axis is significantly inhibited. FUNDC1 can degrade IP3R3 through FBXL2 to maintain Ca^{2+} homeostasis and mitochondrial function, and FUNDC1 knockout exacerbates

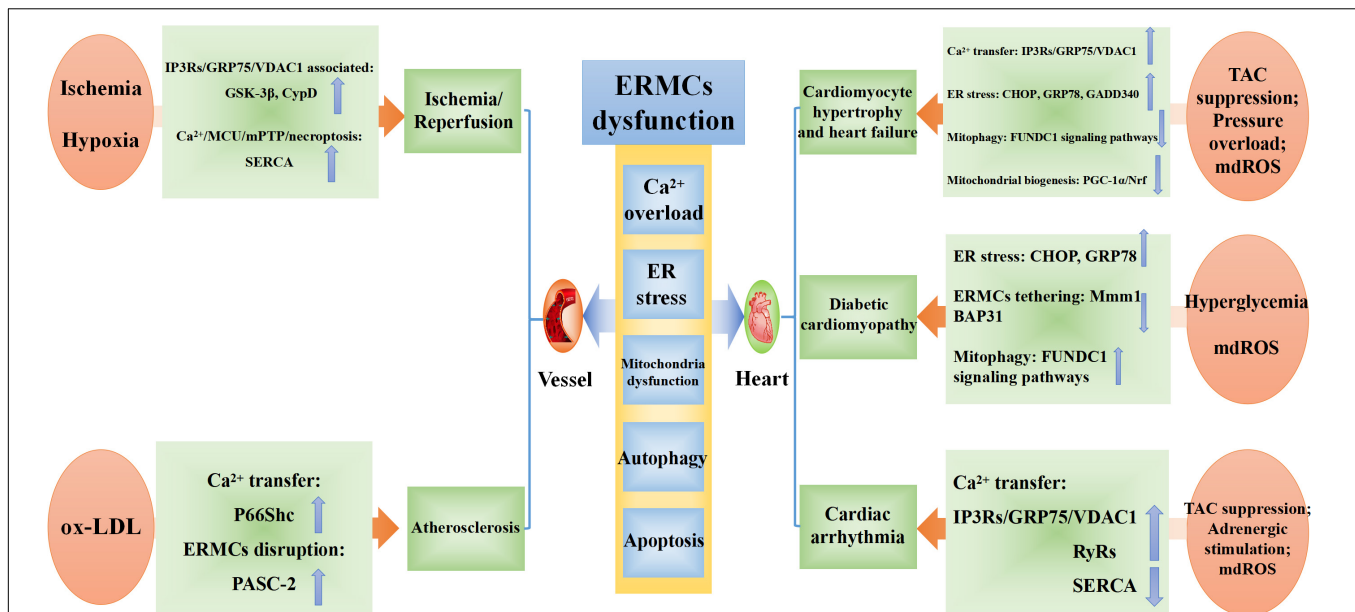


FIGURE 2 | The pathophysiology and underlying mechanisms of ERMCS dysfunction in pathogenesis of cardiovascular remodeling.

high-fat diet-induced IP3R3 elevation, calcium overload, mitochondrial dysfunction, and cardiac remodeling in FUNDC1-KO mice (Ren et al., 2020).

Overall, ERMCS seem to have a strong role in cardiomyocyte hypertrophy and heart failure. First, mitochondrial dysfunction induced by excessive ER stress can affect myocardial energy metabolism and aggravate HF. In addition, the structure and dysfunction of MAMs overlap with the pathophysiological mechanism of HF. In particular, MAM-related proteins such as IP3R1, VDAC1, Mfn1/2, and FUNDC1 are directly involved in the pathophysiological process of cardiac remodeling. In summary, inhibiting the over-activation of ERS and the disturbance of mitochondrial function, decreasing the disorder of SR/ER-mitochondrial Ca²⁺ crosstalk, and correcting the abnormal expression of key proteins of MAMs will contribute to the prevention and treatment of pathological myocardial remodeling. Therefore, ERMCS are considered to be a key factor in the onset of cardiac hypertrophy and heart failure, and a potential therapeutic target.

Endoplasmic Reticulum-Mitochondria Contacts in Diabetic Cardiomyopathy

At present, the pathogenesis of DCM remains unclear, and studies have shown that it is mainly related to glucose metabolism disorders, lipotoxicity, myocardial fibrosis, oxidative stress, and insulin resistance (Liu et al., 2015; Tate et al., 2017; Zhao et al., 2019; Luo et al., 2020; Xiong et al., 2020). In recent years, studies have found that ER stress and mitochondrial apoptosis pathways may be involved in the progression of DCM, and myocardial cells in DCM patients are accompanied by glucose and lipid metabolism disorders, producing large amounts of reactive oxygen species (ROS). This leads to ER swelling and mitochondrial structure and function disorders, which in turn

cause myocardial hypertrophy, interstitial fibrosis, myocardial necrosis, and apoptosis (Zhou et al., 2018b; Ljubkovic et al., 2019; Zhang J. et al., 2021).

In addition, MAMs' constitutive proteins may be involved in the pathogenesis of diabetic cardiomyopathy, for example, Mfn2 and FUNDC1. These protein bridges of MAMs could be potential therapeutic targets for DCM in the future (Wu et al., 2019; Zhang J. et al., 2021). A recent work showed that Mfn2 promotes ERMCS in cardiomyocytes subjected to hyperglycemic conditions. Mfn2 siRNA significantly attenuated mitochondrial Ca²⁺ overload, increased mitochondrial membrane potential, and decreased ER swelling-induced cardiomyocyte death. Transmission electron microscopy micrographs suggested that Mfn2 silencing markedly increased the mean distance between the ER and the OMM (Yuan M. et al., 2020). Additionally, Mfn2 deficiency decreased the production of mitochondrial ROS and the frequency of mitochondria-dependent apoptosis in cardiomyocytes (Zhang J. et al., 2021). Therefore, the regulation of Mfn2-related MAMs may represent a potential therapeutic pathway for the treatment of DCM.

It has been observed that disruption of MAM integrity affects insulin signaling *in vivo* and *in vitro*, and ER-mitochondrial miscommunication was found to be an early event that induced insulin resistance before mitochondrial dysfunction occurred in type 2 diabetes (T2D) mice (Tubbs et al., 2018). For example, FUNDC1 is a highly conserved outer-membrane protein in mitochondria, and mediates the formation of MAMs (Zhang, 2021). Wu et al. (2019) observed that the level of FUNDC1 was increased in cardiac tissue from diabetic patients and Type 1 diabetic mice model. FUNDC1 overexpression promoted MAM formation, mitochondrial Ca²⁺ increase, and mitochondrial dysfunction (Wu et al., 2019). Moreover, cardiomyocyte-specific FUNDC1 knockdown eliminated diabetes-induced

MAM formation, resulting in reduction of mitochondrial Ca^{2+} overload, mitochondrial fragmentation, and apoptosis, and increased mitochondrial functional capacity and cardiac function (Wu et al., 2019). This evidence indicated that FUNDC1 may serve an important role in diabetes-induced cardiac MAM formation. In addition, cardiac-specific FUNDC1 suppression prevented streptozotocin-induced cardiac abnormalities in diabetic mice and protected the function of the heart (Wu et al., 2019). It can be speculated that hyperglycemia-driven FUNDC1-related MAM formation was implicated in the mitochondrial Ca^{2+} overload and mitochondrial dysfunction. Interestingly, the reticulum-mitochondria Ca^{2+} miscoupling was found to disrupt the mitochondrial bioenergetics and cardiomyocyte contraction in an obesogenic T2D mouse model (Dia et al., 2020).

These findings suggest that the interaction between the ER and mitochondria via MAMs is hindered in the initiation and development of DCM, and this promotes Ca^{2+} overload, oxidative stress, mitochondrial dysfunction, and apoptosis, which eventually leads to myocardial remodeling and cardiac dysfunction.

Endoplasmic Reticulum-Mitochondria Contacts in Cardiac Arrhythmia

The mechanism of arrhythmia (including atrial arrhythmia) includes trigger activity and reentry, of which trigger activity is closely related to calcium cycle disorder and abnormalities of Ca^{2+} homeostasis (Sipido, 2006; Peyronnet et al., 2016). Ca^{2+} is a signaling ion in the heart, and is one of the most prevalent signal transduction molecules. It mediates a diverse array of biological functions including mitochondrial energy production, cardiomyocyte excitation-contraction (ECC), and triggering of programmed cellular death (Landstrom et al., 2017). Recent studies demonstrate that in the fast-paced HL-1 atrial muscle cell model for atrial tachycardia remodeling, ER stress induces activation of the MAPK pathway through mitochondrial-related apoptosis, which may be a mechanism involved in the occurrence of atrial fibrillation (Shi et al., 2015).

The ER and mitochondria act as intracellular calcium stores involved in Ca^{2+} storage and flow. RyR, IP3R, and SERCA2a are major channel proteins for Ca^{2+} release and uptake on the SR (Connell et al., 2020; Zhihao et al., 2020). In addition, IP3R1 and its chaperone protein GRP75, and the calcium transport channel VDAC1 of the OMM comprise the IP3R1-GRP75-VDAC1 complex involved in regulating ER-mitochondrial calcium flow (Pedriali et al., 2017). The presence of specialized proteins that connect the SR to the mitochondria ensures local calcium flux between these organelles. Recent evidence suggests that acquired modifications of ER-mitochondrial Ca^{2+} -handling proteins cause abnormal calcium flow between organelles, and their resulting disturbed calcium balance is associated with arrhythmias (Salazar-Ramirez et al., 2020). The altered SR Ca^{2+} handling proteins, such as RyRs and IP3R, play an important role in maintaining appropriate cardiomyocyte excitability, which may be initiated and intensified when mitochondria are dysfunctional (Salazar-Ramirez et al., 2020). Moreover, the junctional sarcoplasmic reticulum (jSR) is an important and specialized ER subdomain that concentrates resident proteins to

regulate Ca^{2+} release in adult cardiomyocytes (Sleiman et al., 2015), jSR, mitochondria, and transverse-tubules (TTs), which are specialized sarcolemma invaginations, are tightly regulated and form an important and highly repetitive functional structure along the cell (De la Fuente and Sheu, 2019). Mitochondrial Ca^{2+} targeted fluorescent probes have revealed that mitochondria Ca^{2+} transients are synchronized with SR Ca^{2+} fluxes (Salazar-Ramirez et al., 2020). Different research groups provided evidence indicating that erratic abnormal action potential (AP) generation relies on pathological mitochondria-derived ROS (mdROS), and interaction between mitochondria and the SR (Salazar-Ramirez et al., 2020). Li Q. et al. (2015) developed a multiscale guinea pig cardiomyocyte model that included the mitochondria-SR microdomain for the first time. Simulations showed that mdROS bursts increased the cytosolic Ca^{2+} by inhibiting SERCA and stimulating RyRs, which elicited Ca^{2+} overload and abnormal AP (Li Q. et al., 2015). Therefore, it is important to evaluate the specific role of the interaction between mitochondria and the SR in Ca^{2+} overload-mediated cardiac arrhythmogenesis. This underscores the importance of considering SR-mitochondrial targets in designing new antiarrhythmic therapies.

Endoplasmic Reticulum-Mitochondria Contacts in the Remodeling of the Vasculature

Endoplasmic Reticulum-Mitochondria Contacts and the Pathophysiology of Vasculature Remodeling

Vascular remodeling refers to the adaptive changes in structure and function that occur in response to various physiological and pathophysiological changes closely related to aging and vascular diseases (Ma et al., 2020). The concept of vascular remodeling was first proposed by Baumbach and Heistad (1992), and vascular remodeling is not only an important pathological basis for the progression of related diseases such as hypertension and atherosclerosis, but it is also the cause of the development of such diseases (Cai et al., 2021). Analyzing the process of vasculature remodeling at the cellular level is, therefore, of vital importance to more thoroughly understand the underlying mechanisms that lead to its development and elucidate new potential therapeutic targets to prevent it. Vascular remodeling is the production of a variety of cellular and molecular pathways, and the vascular wall is mainly composed of endothelial cells, smooth muscle cells, extracellular matrix, and adventitial fibroblasts (Méndez-Barbero et al., 2021). Functional changes in endothelial cells, and changes in proliferation, hypertrophy, and apoptosis of vascular smooth muscle cells as well as changes in adventitia and extracellular matrix are the cytological basis of vascular remodeling (Tanaka and Laurindo, 2017). More and more studies suggested an association between ERMCs and cardiovascular remodeling pathogenesis, thus implicating the participation of the SR/ER-mitochondria axis (Gomez et al., 2016; Garrido-Moreno et al., 2019; Yuan M. et al., 2020). Endoplasmic reticulum stress, Ca^{2+} homeostasis imbalance, and mitochondrial dysfunction are involved in vascular cell proliferation and apoptosis by regulating redox balance, intracellular ion homeostasis, and

cellular metabolism (Lebiedzinska et al., 2009). A recent study demonstrated that Mfn2 overexpression causes mitochondrial fusion into tubular networks and attachment to the ER, which in turn prevents proliferation of vascular smooth muscle cells (VSMCs) (Li D. et al., 2015). A 2015 study found that ERMCS plays a critical role in the endothelium during reperfusion injury, and may be a new molecular target for endothelial protection. In this context, acetylcholine attenuates both intracellular and mitochondrial Ca^{2+} overload and protects endothelial cells from hypoxia/reoxygenation (H/R) injury, through disrupting the ER-mitochondria interaction. Importantly, inhibition of VDAC1 or Mfn2 reduced mitochondrial Ca^{2+} overload and endothelial cell death after H/R (He et al., 2015). Therefore, it is very important to understand the regulatory mechanism and targeted proteins involved in maintaining vascular remodeling related to ERMCS in order to explore new targets for the prevention or treatment of cardiovascular diseases.

Endoplasmic Reticulum-Mitochondria Contacts in Ischemia/Reperfusion

Myocardial ischemia/reperfusion (I/R) injury is defined as a pathophysiological phenomenon in which the structural damage and dysfunction of cells or tissues are instead progressively aggravated after the ischemic myocardium returns to normal perfusion (Zhao et al., 2020). Studies on the mechanism of myocardial I/R injury have been conducted for decades, and it is mainly considered to be related to cellular redox imbalance, calcium overload, ER stress, mitochondrial injury, energy depletion, and programmed cell death (Toth et al., 2007; Consolini et al., 2017; Gong et al., 2021).

An effective Ca^{2+} -dependent mitochondrial energy supply is crucial for proper cardiac contractile activity, while disruption of Ca^{2+} homeostasis contributes to the pathogenesis of cardiac diseases (Gong et al., 2021). Additional evidence has suggested that several SR-mitochondria tethering complex components that regulate the calcium exchange mechanism are involved in the pathological process of I/R injury. Additionally, SR-mitochondria Ca^{2+} transfer is considered detrimental in I/R injury, for example, that of the IP3R1/GGP75/VDAC1 complex (Zhou et al., 2018a). For instance, a 2016 report showed that GSK-3 β is a new Ca^{2+} regulator located in the SR/ER and MAMs, and it can specifically interact with the IP3R Ca^{2+} -channeling complex. Gomez et al. (2016) reported that GSK3 β inhibition diminished cytosolic and mitochondrial Ca^{2+} overload and decreased the cardiomyocyte apoptosis caused by I/R.

Recent reports have confirmed that during hypoxia-reoxygenation, Ca^{2+} overload and the excessive opening of the mPTP is an important mediator of cell death in cardiomyocytes during I/R injury (Paillard et al., 2013). It is well accepted that mitochondrial chaperone cyclophilin D (CypD), which is a component of mPTP, and accumulation of Ca^{2+} in the mitochondrial matrix can activate CypD and trigger permeability transition pore opening (Di Lisa et al., 2007). Paillard et al. (2013) found that CypD acts synergistically with the VDAC1/Grp75/IP3R1 complex, which localizes to MAMs to promote ER calcium efflux to the mitochondria. Remarkably, during H/R, this interaction is amplified with

increased mitochondrial Ca^{2+} load and induces apoptosis. Inhibition of CypD or GRP75 expression and reduction of the interaction of CypD and VDAC1-IP3R1 prevented mitochondrial Ca^{2+} overload and cell death in an adult mouse cardiomyocyte H/R model (Paillard et al., 2013). Thus far, coronary microcirculation remains a difficult and neglected aspect in the treatment of myocardial I/R injury (Pries et al., 2018; Wang et al., 2020b). The latest research in 2020 demonstrated that SERCA plays an important role in this pathological process. For instance, SERCA overexpression inhibited calcium overload by regulating calcium/XO/ROS signaling and preserving the mitochondrial quality control (MQC) system to increase endothelium-dependent vasodilation, attenuate lumen stenosis, and target cardiac microvascular I/R damage (Tan et al., 2020). Likewise, overexpression of SERCA reduced reperfusion-mediated cardiac microvascular injury through inhibition of the calcium/mitochondrial calcium uniporter (MCU)/mPTP/necroptosis signaling pathways (Li et al., 2020b). These observations suggested that controlling SR-mitochondria interaction can protect cardiomyocytes against lethal reperfusion injury through the reduction of mPTP and thereby identifies new molecular targets for cardiac protection.

Excessive mitochondrial division is a predominant cause of cardiac I/R injury (Maneechote et al., 2018). Mechanistically, the Mfn1-Mfn2 heteromultimer is crucial for regulating mitochondrial fission and stabilizing ER-mitochondria microdomain formation (de Brito and Scorrano, 2008). *In vitro* studies showed that acute ablation of Mfn1 and Mfn2 (DKO) reduced the mitochondrial uptake of Ca^{2+} and decreased oxidative stress production through uncoupling the SR from mitochondria. Electron microscopy revealed predominantly fragmented interfibrillar mitochondria with loss of cristae structure in DKO intact cardiomyocytes (Papanicolaou et al., 2011; Hall et al., 2016). Importantly, the authors demonstrated that despite apparent mitochondrial dysfunction, acute deletion of Mfn1 and Mfn2 protected against cardiomyocytes I/R injury due to impaired mitochondria/ER tethering in DKO mice hearts. In conclusion, ERMCS may have beneficial roles in regulating cardiac I/R injury through modulating malignant mitochondrial fission, oxidative stress, calcium overload, and programmed cell death.

Endoplasmic Reticulum-Mitochondria Contacts in Atherosclerosis

Atherosclerosis is a lipid-driven chronic inflammatory disease that leads to the formation of lipid-rich and immune cell-rich plaques in the arterial intima lesions (Finney et al., 2017). The remodeling of the vascular endothelium during atherosclerosis involves alteration of the vascular cell phenotype, modulation of cell migration and proliferation, and propagation of local extracellular matrix remodeling (Perrotta, 2020).

There is evidence that the communication imbalance between the ER and mitochondria affects the function of MAMs, which leads to cardiac diseases (Safiedeen et al., 2016; Perrotta, 2020). Recent research suggested that changes in phospholipids, glucose, and key proteins located in MAMs can cause the occurrence

and development of atherosclerosis (Moulis et al., 2019; Perrotta, 2020; Wang X. et al., 2021).

A 2020 study defined the role of protein p66Shc in atherosclerosis. The adaptor protein p66Shc located in the MAMs is considered as a sensor of oxidative stress-induced apoptosis (Mishra et al., 2019). Experiments with a p66Shc knockout mouse showed that a reduced number of atherosclerotic plaques formed (Napoli et al., 2003; Gil-Hernández and Silva-Palacios, 2020).

Likewise, oxidized low-density lipoprotein (ox-LDL) contributing to endothelial cell (EC) apoptosis is the first step of atherogenesis and is related to Ca^{2+} overload. The phosphofurin acid cluster classification protein 2 (PACS2) is a multifunctional tethering protein that is essential for mitochondrial Ca^{2+} overload because it mediates ER-mitochondria Ca^{2+} transfer (Yu et al., 2019). In an ox-LDL-induced apoptosis model of human umbilical vein endothelial cells (HUVECs), silencing PACS-2 inhibited ox-LDL-induced cell apoptosis and mitochondrial localization of PACS-2 and MAMs formation. Thus, this finding indicated that PACS-2 may become a promising therapeutic target for atherosclerosis by regulating MAM formation and increasing levels of mitochondrial Ca^{2+} (Yu et al., 2019).

Despite recent evidence underlining the role of ERMCs in cardiac tissue physiology, little is known about the role of ERMCs in vascular cells, including in VSMCs (Lopez-Crisosto et al., 2017; Moulis et al., 2019; Wang X. et al., 2021). However, a study published in 2019 suggested that in the VSMC apoptosis model, high-resolution confocal microscopy and adjacent ligation analysis found that the molecular changes in MAMs play a critical role in the balance between cell survival and death through modulating the interaction between autophagy and apoptosis (Moulis et al., 2019). Moulis et al. (2019) first reported that PACS-2 deletion induced MAM disruption and potentiated VSMC apoptosis. These findings suggest that MAMs-associated PACS-2 is a crucial regulator of VSMC fate during oxidized LDL-induced mitophagy. These findings reveal new insights regarding the significance of ERMCs in cell vascular pathophysiology, which indicates that manipulating ERMCs can supply new strategies to selectively improve VSMC fate and stabilize atherosclerotic plaque (Moulis et al., 2019).

As a platform to modify the phenotypic transformation of VSMCs and ECs, p66Shc and PACS-2 located on ERMCs participate in the pathological process of atherosclerosis by modifying the mitochondrial Ca^{2+} overload and apoptosis, which contributes to the survival of VSMCs and ECs. However, further research is warranted to conclusively elucidate how the molecular mechanisms in the regulation of ERMCs contribute to atherosclerosis.

THERAPY TARGETING ENDOPLASMIC RETICULUM-MITOCHONDRIA CONTACTS FOR CARDIOVASCULAR REMODELING-INDUCED DISEASES

As discussed above, alterations in the contacts between the SR/ER-mitochondria may induce cardiovascular tissue

remodeling and cardiac disease. Therefore, therapeutic interventions to improve ERMCs may conserve cardiac function and represent possible promising strategies to delay cardiac aging, and to delay or prevent cardiac disease (Table 2).

Pharmacological Interventions

One option to improve the ER-mitochondrial contacts is by means of metformin, a traditional anti-diabetic drug with pleiotropic properties associated with its mitochondrial effects (Pries et al., 2018). Administration of metformin decreased MICU1 expression and mitochondrial Ca^{2+} content, and enhanced complex I-driven respiration in a cardiomyopathy mouse model of dystrophin-deficiency, suggesting that metformin has a cardioprotective role in impaired Ca^{2+} homeostasis and aberrant SR/ER-mitochondria interaction (Angebault et al., 2020). Moreover, metformin decreased the infarct size during cardiac I/R through attenuating CHOP expression and subsequently protecting the mitochondria (Chen Q. et al., 2021).

In a phase IV randomized controlled trial (NCT 00473876) with metformin in patients with chronic heart failure, it was reported that metformin treatment significantly improved the VE/ VCO_2 slope but had no effect on peak VO_2 , which reflected exercise capacity (Das et al., 2019). A phase II randomized, placebo-controlled study in chronic heart failure (CHF) patients with metformin (NCT 03514108), which was designed to determine whether metformin reduces the incidence of worsening heart failure and acute myocardial infarction in patients with diabetes, is still in progress (Wiggers et al., 2021).

Another option is the utilization of tauroursodeoxycholic acid (TUDCA) and 4-phenylbutyric acid (4-PBA), which are ER stress inhibitors. This proved to be beneficial in ameliorating mitochondrial oxidative injury and ER stress-mediated cerebrovascular VSMC phenotypic transition through the PERK-eIF2 α -ATF4-CHOP pathway in a rat model. A randomized, placebo-controlled study of type 2 diabetes mellitus patients with TUDCA (NCT 03331432) aimed to evaluate the effect of TUDCA administration on enhancement of vascular function in humans, and the trial is currently still in progress (Wiggers et al., 2021). Additionally, a phase II open label trial with TUDCA (NCT 01855360), which was designed to evaluate the safety and tolerability of the combination of TUDCA and doxycycline in familial and senile amyloidosis patients, has not yet been completed.

Moreover, in H_2O_2 -induced apoptosis of neonatal rat cardiomyocytes, ibutilide, a class III antiarrhythmic agent, attenuated ER stress (GRP78, GRP94, and CHOP), mitochondrial oxidative stress, and mitochondrial-dependent apoptosis (Bax, Bcl-2, and caspase-3/9/12) (Wang et al., 2017). A prospective, non-randomized, un-blinded, observational trial (NCT 03370536) investigating the effectiveness of ibutilide on atrial fibrillation (AF) source location and organization is under advanced development.

The therapeutic contribution of melatonin reversed changes in mitochondrial dynamics, ameliorated ER stress, and prevented the disassembly of the cardiomyocyte cytoskeleton by repressing RIPK3 in a septic cardiomyopathy mouse model. This study

showed that melatonin simultaneously modulated mitochondrial homeostasis and ER function (Zhong et al., 2019). In brief, this finding highlights the role of melatonin, which may be considered as an ideal agent for the targeted therapy of septic cardiomyopathy via modulating mitochondrial homeostasis and ER function. An attempt at therapy in a randomized placebo-controlled phase II trial (NCT 03894683) is currently ongoing to determine the effect of melatonin on cardiovascular and muscle mass and function in patients with CHF (Sadeghi et al., 2020). Another randomized, placebo-controlled trial (NCT 01172171), which was designed to determine whether administration of melatonin reduces infarct size in patients with acute myocardial infarction, is proceeding (Dominguez-Rodriguez et al., 2007). If successful, these findings would support the therapeutic use of melatonin for cardiac disease.

Finally, in a rat model of cardiac hypertrophy induced by isoproterenol, administration of difluoromethylornithine (DFMO) attenuated cardiac hypertrophy through downregulating the MAM signaling pathway (cleaved caspase-3/9, GRP75, Mfn2, CypD, and VDAC1) and upregulating the autophagy pathway in heart tissue (Zhao et al., 2021). These findings suggested that DFMO treatment could provide a potential strategy for preventing ISO-induced cardiac hypertrophy.

Several clinical medicines may improve ERMCs, thereby having a beneficial effect on cardiovascular

remodeling-induced diseases. However, further research is required to elucidate compounds that directly target the ERMCs (Li et al., 2019).

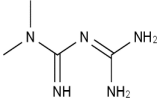
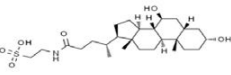
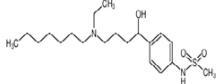
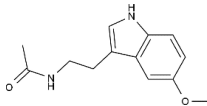
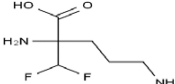
Lifestyle Interventions

Lifestyle change consisting of regular physical activity and caloric restriction (CR) demonstrated protection against cardiac risk factors and improved cardiorespiratory fitness in humans (Makar and Siabrenko, 2018; Kumar et al., 2020).

In peripheral blood mononuclear cells (PBMCs) from healthy elderly subjects, 8-week resistance-training (RT) exercise-induced UPR activation counteracted ERS and led to mitochondrial improvement and prevention of mitophagy activation through increased ATF4, XBP1, PGC-1 α , and Mfn1 protein levels (Estebanez et al., 2019). The results showed that RT resulted in the UPR, as a protective mechanism, and mitochondrial biogenesis to adapt to the exercise demands. In addition, in a diabetic mouse model, it was found that high-intensity training improved cardiac function and reduced cardiac infarction by downregulating GRP78, phosphorylated PERK, phosphorylated eIF2 α , ATF4, ATF6, XBP1, CHOP, and cleaved caspase-3 (Bourdier et al., 2016; Bozi et al., 2016).

Finally, a study suggested that an 8-week diet reversal alleviated the T2D-induced cardiac dysfunction via reestablishing the functional Ca²⁺ coupling of the ER-mitochondria interface and a normal Ca²⁺ transfer in the high-fat high-sucrose

TABLE 2 | Pharmacological interventions for cardiovascular remodeling-associated diseases.

Medicine	Chemical structure	Preclinical studies	Current clinical status	References
Metformin		Cardiomyopathy mouse model of dystrophin-deficient; Cardiac injury in murine model during ischemia-reperfusion.	Phase IV for CHF (NCT 00473876); Phase II for CHF (NCT 03514108)	Angebault et al., 2020; Chen Q. et al., 2021
TUDCA		Simulated microgravity induced ER stress in rats.	Phase IV for vascular function of Type 2 DM humans (NCT 03331432); Phase II for SSA (NCT 01855360)	Zhang et al., 2020
Ibutilide		Murine model of cardiomyocytes apoptosis.	Phase I for AF (NCT 03370536)	Wang et al., 2017
Melatonin		Septic cardiomyopathy in mice.	Phase II for CHF (NCT 03894683); Phase II for AMI (NCT 01172171)	Zhong et al., 2019
DFMO		Rodent models of cardiac hypertrophy.	NA	Zhao et al., 2021

TUDCA, tauroursodeoxycholic acid; I/R, ischemia-reperfusion; CHF, chronic heart failure; DFMO, difluoromethylornithine; DM, diabetes mellitus; SSA, senile systemic amyloidosis; AMI, acute myocardial infarction.

diet (HFHSD)-induced obesogenic T2D mouse model (Dia et al., 2020).

The impact of lifestyle interventions on ERMCS modification remains an open question (Li et al., 2019; Kumar et al., 2020; Sun and Ding, 2020). Much input is required to understand whether and how alterations in ERMCS are involved in cardiovascular remodeling-induced disease enhancement, and how different types of lifestyle interventions counteract this.

CONCLUSION

As outlined in this review, cardiovascular disease caused by cardiovascular remodeling is still the main cause of the disease incidence rate and mortality worldwide. An increasing amount of evidence has shown that ERMCS play an important role in the pathologic process of cardiovascular remodeling. The functional balance and interaction between the ER and mitochondria are prerequisites for a healthy heart and optimal vascular function, and loss of this interaction can exacerbate cardiovascular remodeling and cardiovascular disease.

Here, we describe the concept, structure, and function of the interaction between the ER and mitochondria, and discuss how the imbalance of interaction exacerbates cardiovascular diseases such as heart failure and atherosclerosis. However, more studies are required to define the role that alterations in ERMCS have in the pathogenesis of cardiovascular remodeling-associated diseases (Li et al., 2019). Obviously, due to the different substrates and mechanisms of the energy metabolism of cardiomyocytes, vascular ECs, and VSMCs, the effects of ERMCS in these cell types are not identical (Gao et al., 2020).

The relationship between ERMCS regulation and cardiovascular remodeling is two-sided. The journey that calcium must take between the ER and its mitochondrial

destination requires several regulatory steps and molecular checkpoints, and any alterations result in dramatic metabolic or apoptotic defects. However, any increase in ER-mitochondrial proximity enhances mitochondrial Ca^{2+} uptake, thus activating an excitation-contraction coupling process and ATP synthesis of cardiomyocytes (Safiedeen et al., 2016; Marchi et al., 2018). Therefore, a deeper understanding and precise regulation of ERMCS may be a promising method to develop more specific treatment strategies and selectively inhibit the progression of remodeling. Finally, we enumerated some drugs: Metformin, TUDCA, Ibutilide, Melatonin and DFMO, which have the potential to preserve this ER-mitochondrial interaction, but also need further study to identify the exactly effect on ERMCS. Further well-designed clinical trials are required to explore the underlying mechanism and prove their efficacy in cardiovascular remodeling-induced diseases.

AUTHOR CONTRIBUTIONS

CL, XL, and YuW conceived the project. CL, YuW, XZ, YaW, and RX wrote the manuscript. XZ and RX prepared the figure. SL finished the table. All authors have reviewed the manuscript.

FUNDING

This study was supported by the National Natural Science Foundation of China (82004276), Natural Science Foundation of the Shandong Province (ZR2020KH034), China Postdoctoral Science Foundation (2020M672125 and 2021T140429), Shandong Postdoctoral Innovation Project (202003027), and Medical and Health Science and Technology Development Project of Shandong Province (2019WS553 and 202003011161).

REFERENCES

- Akhmedov, A., Rybin, V., and Marín-García, J. (2015). Mitochondrial oxidative metabolism and uncoupling proteins in the failing heart. *Heart Fail. Rev.* 20, 227–249. doi: 10.1007/s10741-014-9457-4
- Andersson, C., and Vasan, R. (2018). Epidemiology of cardiovascular disease in young individuals. *Nat. Rev. Cardiol.* 15, 230–240. doi: 10.1038/nrcardio.2017.154
- Ando, H., Kawaai, K., Bonneau, B., and Mikoshiba, K. (2018). Remodeling of Ca^{2+} signaling in cancer: regulation of inositol 1,4,5-trisphosphate receptors through oncogenes and tumor suppressors. *Adv. Biol. Regul.* 68, 64–76. doi: 10.1016/j.jbior.2017.12.001
- Anelli, T., Bergamelli, L., Margittai, E., Rimessi, A., Fagioli, C., Malgaroli, A., et al. (2012). Ero1alpha regulates Ca^{2+} fluxes at the endoplasmic reticulum-mitochondria interface (MAM). *Antioxid. Redox Signal.* 16, 1077–1087. doi: 10.1089/ars.2011.4004
- Angebault, C., Panel, M., Lacote, M., Rieusset, J., Lacampagne, A., and Fauconnier, J. (2020). Metformin reverses the enhanced myocardial SR/ER-mitochondria interaction and impaired complex I-driven respiration in dystrophin-deficient mice. *Front. Cell Dev. Biol.* 8:609493. doi: 10.3389/fcell.2020.609493
- Bagur, R., and Hajnóczy, G. (2017). Intracellular Ca^{2+} sensing: its role in calcium homeostasis and signaling. *Mol. Cell* 66, 780–788. doi: 10.1016/j.molcel.2017.05.028
- Bansilal, S., Castellano, J., and Fuster, V. (2015). Global burden of CVD: focus on secondary prevention of cardiovascular disease. *Int. J. Cardiol.* 201(Suppl. 1), S1–S7. doi: 10.1016/s0167-5273(15)31026-3
- Bartok, A., Weaver, D., Golenar, T., Nichtova, Z., Katona, M., Bansaghi, S., et al. (2019). IP3 receptor isoforms differently regulate ER-mitochondrial contacts and local calcium transfer. *Nat. Commun.* 10:3726. doi: 10.1038/s41467-019-11646-3
- Basso, V., Marchesan, E., Peggion, C., Chakraborty, J., von Stockum, S., Giacomello, M., et al. (2018). Regulation of ER-mitochondria contacts by Parkin via Mfn2. *Pharmacol. Res.* 138, 43–56. doi: 10.1016/j.phrs.2018.09.006
- Baumbach, G., and Heistad, D. (1992). Drug-induced changes in mechanics and structure of cerebral arterioles. *J. Hypertens. Suppl.* 10, S137–S140.
- Benador, I., Veliova, M., Liesa, M., and Shiriha, O. (2019). Mitochondria bound to lipid droplets: where mitochondrial dynamics regulate lipid storage and utilization. *Cell Metab.* 29, 827–835. doi: 10.1016/j.cmet.2019.02.011
- Bernhard, W., and Rouiller, C. (1956). Close topographical relationship between mitochondria and ergastoplasm of liver cells in a definite phase of cellular activity. *J. Biophys. Biochem. Cytol.* 2(4 Suppl.), 73–78. doi: 10.1083/jcb.2.4.73
- Bessou, M., Lopez, J., Gadet, R., Deygas, M., Popgeorgiev, N., Poncet, D., et al. (2020). The apoptosis inhibitor Bcl-xL controls breast cancer

- cell migration through mitochondria-dependent reactive oxygen species production. *Oncogene* 39, 3056–3074. doi: 10.1038/s41388-020-1212-9
- Betz, C., Stracka, D., Prescianotto-Baschong, C., Frieden, M., Demaux, N., and Hall, M. N. (2013). Feature article: mTOR complex 2-Akt signaling at mitochondria-associated endoplasmic reticulum membranes (MAM) regulates mitochondrial physiology. *Proc. Natl. Acad. Sci. U.S.A.* 110, 12526–12534. doi: 10.1073/pnas.1302455110
- Beutner, G., Sharma, V. K., Lin, L., Ryu, S. Y., Dirksen, R. T., and Sheu, S. S. (2005). Type 1 ryanodine receptor in cardiac mitochondria: transducer of excitation-metabolism coupling. *Biochim. Biophys. Acta* 1717, 1–10. doi: 10.1016/j.bbame.2005.09.016
- Bhola, P., and Letai, A. (2016). Mitochondria-judges and executioners of cell death sentences. *Mol. Cell* 61, 695–704. doi: 10.1016/j.molcel.2016.02.019
- Biczko, G., Vegh, E., Shalbuva, N., Mareninova, O., Elperin, J., Lotshaw, E., et al. (2018). Mitochondrial dysfunction, through impaired autophagy, leads to endoplasmic reticulum stress, deregulated lipid metabolism, and pancreatitis in animal models. *Gastroenterology* 154, 689–703. doi: 10.1053/j.gastro.2017.10.012
- Bollo, M., Paredes, R. M., Holstein, D., Zheleznova, N., Camacho, P., and Lechleiter, J. D. (2010). Calcineurin interacts with PERK and dephosphorylates calnexin to relieve ER stress in mammals and frogs. *PLoS One* 5:e11925. doi: 10.1371/journal.pone.0011925
- Bonneau, B., Ando, H., Kawaai, K., Hirose, M., Takahashi-Iwanaga, H., and Mikoshiba, K. (2016). IRE1 controls apoptosis by interacting with the Bcl-2 homolog, Bcl2l10, and by promoting ER-mitochondria contact. *Elife* 5:e19896. doi: 10.7554/eLife.19896
- Bourdier, G., Flore, P., Sanchez, H., Pepin, J., Belaidi, E., and Arnaud, C. (2016). High-intensity training reduces intermittent hypoxia-induced ER stress and myocardial infarct size. *Am. J. Physiol. Heart Circ. Physiol.* 310, H279–H289. doi: 10.1152/ajpheart.00448.2015
- Bozi, L., Jannig, P., Rolim, N., Voltarelli, V., Dourado, P., Wisløff, U., et al. (2016). Aerobic exercise training rescues cardiac protein quality control and blunts endoplasmic reticulum stress in heart failure rats. *J. Cell. Mol. Med.* 20, 2208–2212. doi: 10.1111/jcmm.12894
- Bravo-Sagua, R., Parra, V., Ortiz-Sandoval, C., Navarro-Marquez, M., Rodriguez, A. E., Diaz-Valdivia, N., et al. (2019). Caveolin-1 impairs PKA-DRP1-mediated remodeling of ER-mitochondria communication during the early phase of ER stress. *Cell Death Differ.* 26, 1195–1212. doi: 10.1038/s41418-018-0197-1
- Bravo-San Pedro, J. M., Kroemer, G., and Galluzzi, L. (2017). Autophagy and mitophagy in cardiovascular disease. *Circ. Res.* 120, 1812–1824. doi: 10.1161/CIRCRESAHA.117.311082
- Burgess, S. M., Delannoy, M., and Jensen, R. E. (1994). MAM1 encodes a mitochondrial outer membrane protein essential for establishing and maintaining the structure of yeast mitochondria. *J. Cell Biol.* 126, 1375–1391. doi: 10.1083/jcb.126.6.1375
- Burkewitz, K., Feng, G., Dutta, S., Kelley, C. A., Steinbaugh, M., Cram, E. J., et al. (2020). Atf-6 regulates lifespan through ER-mitochondrial calcium homeostasis. *Cell Rep.* 32:108125. doi: 10.1016/j.celrep.2020.108125
- Cai, Z., Gong, Z., Li, Z., Li, L., and Kong, W. (2021). Vascular extracellular matrix remodeling and hypertension. *Antioxid. Redox Signal.* 34, 765–783. doi: 10.1089/ars.2020.8110
- Capewell, S., and Lloyd-Jones, D. (2010). Optimal cardiovascular prevention strategies for the 21st century. *JAMA* 304, 2057–2058. doi: 10.1001/jama.2010.1641
- Cárdenas, C., Miller, R., Smith, I., Bui, T., Molgó, J., Müller, M., et al. (2010). Essential regulation of cell bioenergetics by constitutive Inp3 receptor Ca²⁺ transfer to mitochondria. *Cell* 142, 270–283. doi: 10.1016/j.cell.2010.06.007
- Cerqua, C., Anesti, V., Pyakurel, A., Liu, D., Naon, D., Wiche, G., et al. (2010). Trichoplein/mitostatin regulates endoplasmic reticulum-mitochondria juxtaposition. *EMBO Rep.* 11, 854–860. doi: 10.1038/embor.2010.151
- Chaanine, A. H., Gordon, R. E., Kohlbrenner, E., Benard, L., Jeong, D., and Hajjar, R. J. (2013). Potential role of BNP3 in cardiac remodeling, myocardial stiffness, and endoplasmic reticulum: mitochondrial calcium homeostasis in diastolic and systolic heart failure. *Circ. Heart Fail.* 6, 572–583. doi: 10.1161/CIRCHEARTFAILURE.112.000200
- Chaanine, A. H., Lejemtel, T. H., and Delafontaine, P. (2020). Mitochondrial pathology and metabolic remodeling in progression to overt systolic heart failure. *J. Clin. Med.* 9:3582. doi: 10.3390/jcm9113582
- Chan, D. C. (2020). Mitochondrial dynamics and its involvement in disease. *Annu. Rev. Pathol.* 15, 235–259. doi: 10.1146/annurev-pathmechdis-012419-032711
- Chen, H., Detmer, S. A., Ewald, A. J., Griffin, E. E., Fraser, S. E., and Chan, D. C. (2003). Mitofusins Mfn1 and Mfn2 coordinately regulate mitochondrial fusion and are essential for embryonic development. *J. Cell Biol.* 160, 189–200. doi: 10.1083/jcb.200211046
- Chen, J., Li, L., Bai, X., Xiao, L., Shangguan, J., Zhang, W., et al. (2021). Inhibition of autophagy prevents panax notoginseng saponins (PNS) protection on cardiac myocytes against endoplasmic reticulum (ER) stress-induced mitochondrial injury, Ca homeostasis and associated apoptosis. *Front. Pharmacol.* 12:620812. doi: 10.3389/fphar.2021.620812
- Chen, Q., Thompson, J., Hu, Y., and Lesnfsky, E. J. (2021). Chronic metformin treatment decreases cardiac injury during ischemia-reperfusion by attenuating endoplasmic reticulum stress with improved mitochondrial function. *Aging* 13, 7828–7845.
- Chen, W., Zhou, Z., Li, L., Zhong, C. Q., Zheng, X., Wu, X., et al. (2013). Diverse sequence determinants control human and mouse receptor interacting protein 3 (RIP3) and mixed lineage kinase domain-like (MLKL) interaction in necroptotic signaling. *J. Biol. Chem.* 288, 16247–16261. doi: 10.1074/jbc.M112.435545
- Chen, Y., Csordas, G., Jowdy, C., Schneider, T. G., Csordas, N., Wang, W., et al. (2012). Mitofusin 2-containing mitochondrial-reticular microdomains direct rapid cardiomyocyte bioenergetic responses via interorganelle Ca(2+) crosstalk. *Circ. Res.* 111, 863–875. doi: 10.1161/CIRCRESAHA.112.266585
- Cheng, H., Gang, X., He, G., Liu, Y., Wang, Y., Zhao, X., et al. (2020). The molecular mechanisms underlying mitochondria-associated endoplasmic reticulum membrane-induced insulin resistance. *Front. Endocrinol.* 11:592129. doi: 10.3389/fendo.2020.592129
- Chow, J., Rahman, J., Achermann, J., Dattani, M., and Rahman, S. (2017). Mitochondrial disease and endocrine dysfunction. *Nat. Rev. Endocrinol.* 13, 92–104. doi: 10.1038/nrendo.2016.151
- Connell, P., Word, T., and Wehrens, X. (2020). Targeting pathological leak of ryanodine receptors: preclinical progress and the potential impact on treatments for cardiac arrhythmias and heart failure. *Expert Opin. Ther. Targets* 24, 25–36. doi: 10.1080/14728222.2020.1708326
- Consolini, A., Ragone, M., Bonazzola, P., and Colareda, G. (2017). Mitochondrial bioenergetics during ischemia and reperfusion. *Adv. Exp. Med. Biol.* 982, 141–167. doi: 10.1007/978-3-319-55330-6_8
- Cosson, P., Marchetti, A., Ravazzola, M., and Orci, L. (2012). Mitofusin-2 independent juxtaposition of endoplasmic reticulum and mitochondria: an ultrastructural study. *PLoS One* 7:e46293. doi: 10.1371/journal.pone.0046293
- Coutinho, P., Parsons, M. J., Thomas, K. A., Hirst, E. M., Saude, L., Campos, I., et al. (2004). Differential requirements for COPI transport during vertebrate early development. *Dev. Cell* 7, 547–558. doi: 10.1016/j.devcel.2004.07.020
- Csordas, G., Renken, C., Varnai, P., Walter, L., Weaver, D., Buttle, K. F., et al. (2006). Structural and functional features and significance of the physical linkage between ER and mitochondria. *J. Cell Biol.* 174, 915–921. doi: 10.1083/jcb.200604016
- Das, A., Kalra, S., Tiwaskar, M., Bajaj, S., Seshadri, K., Chowdhury, S., et al. (2019). Expert group consensus opinion: role of anti-inflammatory agents in the management of type-2 diabetes (T2D). *J. Assoc. Physicians India* 67, 65–74.
- de Brito, O. M., and Scorrano, L. (2008). Mitofusin 2 tethers endoplasmic reticulum to mitochondria. *Nature* 456, 605–610. doi: 10.1038/nature07534
- De la Fuente, S., and Sheu, S. (2019). SR-mitochondria communication in adult cardiomyocytes: a close relationship where the Ca has a lot to say. *Arch. Biochem. Biophys.* 663, 259–268. doi: 10.1016/j.abb.2019.01.026
- De Stefani, D., Rizzuto, R., and Pozzan, T. (2016). Enjoy the trip: calcium in mitochondria back and forth. *Annu. Rev. Biochem.* 85, 161–192. doi: 10.1146/annurev-biochem-060614-034216
- D'Eletto, M., Rossin, F., Occhigrossi, L., Farrace, M. G., Faccenda, D., Desai, R., et al. (2018). Transglutaminase type 2 regulates ER-mitochondria contact sites by interacting with GRP75. *Cell Rep.* 25, 3573–3581.e4. doi: 10.1016/j.celrep.2018.11.094
- Di Lisa, F., Canton, M., Menabò, R., Kaludercic, N., and Bernardi, P. (2007). Mitochondria and cardioprotection. *Heart Fail. Rev.* 12, 249–260. doi: 10.1007/s10741-007-9028-z
- Dia, M., Gomez, L., Thibault, H., Tessier, N., Leon, C., Chouabe, C., et al. (2020). Reduced reticulum-mitochondria Ca(2+) transfer is an early and reversible

- trigger of mitochondrial dysfunctions in diabetic cardiomyopathy. *Basic Res. Cardiol.* 115:74. doi: 10.1007/s00395-020-00835-7
- Ding, W., Feng, H., Li, W. J., Liao, H. H., and Tang, Q. Z. (2020). Research progress on the interaction between autophagy and energy homeostasis in cardiac remodeling. *Front. Pharmacol.* 11:587438. doi: 10.3389/fphar.2020.587438
- Doghman-Bouguerra, M., Granatiero, V., Sbiera, S., Sbiera, I., Lacas-Gervais, S., Brau, F., et al. (2016). FATE1 antagonizes calcium- and drug-induced apoptosis by uncoupling ER and mitochondria. *EMBO Rep.* 17, 1264–1280. doi: 10.15252/embr.201541504
- Dominguez-Rodriguez, A., Abreu-Gonzalez, P., Garcia-Gonzalez, M. J., Kaski, J. C., Reiter, R. J., and Jimenez-Sosa, A. (2007). A unicenter, randomized, double-blind, parallel-group, placebo-controlled study of melatonin as an adjunct in patients with acute myocardial infarction undergoing primary angioplasty the melatonin adjunct in the acute myocardial infarction treated with angioplasty (MARIA) trial: study design and rationale. *Contemp. Clin. Trials* 28, 532–539. doi: 10.1016/j.cct.2006.10.007
- Eisner, D. A., Caldwell, J. L., Kistamas, K., and Trafford, A. W. (2017). Calcium and excitation-contraction coupling in the heart. *Circ. Res.* 121, 181–195. doi: 10.1161/CIRCRESAHA.117.310230
- Eisner, V., Csordas, G., and Hajnoczky, G. (2013). Interactions between sarcoplasmic reticulum and mitochondria in cardiac and skeletal muscle – pivotal roles in Ca(2+)(+) and reactive oxygen species signaling. *J. Cell Sci.* 126(Pt 14), 2965–2978. doi: 10.1242/jcs.093609
- Erpapazoglou, Z., and Corti, O. (2015). The endoplasmic reticulum/mitochondria interface: a subcellular platform for the orchestration of the functions of the PINK1-Parkin pathway? *Biochem. Soc. Trans.* 43, 297–301. doi: 10.1042/BST20150008
- Estebanez, B., Moreira, O. C., Almar, M., de Paz, J. A., Gonzalez-Gallego, J., and Cuevas, M. J. (2019). Effects of a resistance-training programme on endoplasmic reticulum unfolded protein response and mitochondrial functions in PBMCs from elderly subjects. *Eur. J. Sport Sci.* 19, 931–940. doi: 10.1080/17461391.2018.1561950
- Filadi, R., Greotti, E., Turacchio, G., Luini, A., Pozzan, T., and Pizzo, P. (2015). Mitofusin 2 ablation increases endoplasmic reticulum-mitochondria coupling. *Proc. Natl. Acad. Sci. U.S.A.* 112, E2174–E2181. doi: 10.1073/pnas.1504880112
- Finney, A., Stokes, K., Pattillo, C., and Orr, A. (2017). Integrin signaling in atherosclerosis. *Cell. Mol. Life Sci.* 74, 2263–2282. doi: 10.1007/s00018-017-2490-4
- Frank, D., and Vince, J. E. (2019). Pyroptosis versus necroptosis: similarities, differences, and crosstalk. *Cell Death Differ.* 26, 99–114. doi: 10.1038/s41418-018-0212-6
- Friedman, J. R., Lackner, L. L., West, M., DiBenedetto, J. R., Nunnari, J., and Voeltz, G. K. (2011). ER tubules mark sites of mitochondrial division. *Science* 334, 358–362. doi: 10.1126/science.1207385
- Fujimoto, M., and Hayashi, T. (2011). New insights into the role of mitochondria-associated endoplasmic reticulum membrane. *Int. Rev. Cell Mol. Biol.* 292, 73–117. doi: 10.1016/B978-0-12-386033-0.00002-5
- Fujimoto, M., Hayashi, T., and Su, T. P. (2012). The role of cholesterol in the association of endoplasmic reticulum membranes with mitochondria. *Biochem. Biophys. Res. Commun.* 417, 635–639. doi: 10.1016/j.bbrc.2011.12.022
- Gagnon, E., Duclos, S., Rondeau, C., Chevet, E., Cameron, P. H., Steele-Mortimer, O., et al. (2002). Endoplasmic reticulum-mediated phagocytosis is a mechanism of entry into macrophages. *Cell* 110, 119–131. doi: 10.1016/S0092-8674(02)00797-3
- Gao, P., Yan, Z., and Zhu, Z. (2020). Mitochondria-associated endoplasmic reticulum membranes in cardiovascular diseases. *Front. Cell Dev. Biol.* 8:604240. doi: 10.3389/fcell.2020.604240
- Garay, L., Gonzalez Giqueaux, P., Guennoun, R., Schumacher, M., Gonzalez Deniselle, M. C., and De Nicola, A. F. (2017). Progesterone treatment modulates mRNA OF neurosteroidogenic enzymes in a murine model of multiple sclerosis. *J. Steroid Biochem. Mol. Biol.* 165(Pt B), 421–429. doi: 10.1016/j.jsmbm.2016.09.001
- Garofalo, T., Matarrese, P., Manganelli, V., Marconi, M., Tinari, A., Gambardella, L., et al. (2016). Evidence for the involvement of lipid rafts localized at the ER-mitochondria associated membranes in autophagosome formation. *Autophagy* 12, 917–935. doi: 10.1080/15548627.2016.1160971
- Garrido-Moreno, V., Diaz-Vegas, A., Lopez-Crisosto, C., Troncoso, M. F., Navarro-Marquez, M., Garcia, L., et al. (2019). GDF-11 prevents cardiomyocyte hypertrophy by maintaining the sarcoplasmic reticulum-mitochondria communication. *Pharmacol. Res.* 146:104273. doi: 10.1016/j.phrs.2019.104273
- Gelmetti, V., De Rosa, P., Torosantucci, L., Marini, E. S., Romagnoli, A., Di Rienzo, M., et al. (2017). PINK1 and BECN1 relocate to mitochondria-associated membranes during mitophagy and promote ER-mitochondria tethering and autophagosome formation. *Autophagy* 13, 654–669. doi: 10.1080/15548627.2016.1277309
- Giacomello, M., and Pellegrini, L. (2016). The coming of age of the mitochondria-ER contact: a matter of thickness. *Cell Death Differ.* 23, 1417–1427. doi: 10.1038/cdd.2016.52
- Gil-Hernández, A., and Silva-Palacios, A. (2020). Relevance of endoplasmic reticulum and mitochondria interactions in age-associated diseases. *Ageing Res. Rev.* 64:101193. doi: 10.1016/j.arr.2020.101193
- Gomez, L., Thiebaut, P., Paillard, M., Ducreux, S., Abrial, M., Crola Da Silva, C., et al. (2016). The SR/ER-mitochondria calcium crosstalk is regulated by GSK3 β during reperfusion injury. *Cell Death Differ.* 23, 313–322. doi: 10.1038/cdd.2015.101
- Gomez-Suaga, P., Paillusson, S., Stoica, R., Noble, W., Hanger, D., and Miller, C. (2017b). The ER-mitochondria tethering complex VAPB-PTPIP51 regulates autophagy. *Curr. Biol.* 27, 371–385. doi: 10.1016/j.cub.2016.12.038
- Gomez-Suaga, P., Paillusson, S., and Miller, C. C. J. (2017a). ER-mitochondria signaling regulates autophagy. *Autophagy* 13, 1250–1251. doi: 10.1080/15548627.2017.1317913
- Gomez-Suaga, P., Perez-Nievas, B. G., Glennon, E. B., Lau, D. H. W., Paillusson, S., Morotz, G. M., et al. (2019). The VAPB-PTPIP51 endoplasmic reticulum-mitochondria tethering proteins are present in neuronal synapses and regulate synaptic activity. *Acta Neuropathol. Commun.* 7:35. doi: 10.1186/s40478-019-0688-4
- Gong, Y., Lin, J., Ma, Z., Yu, M., Wang, M., Lai, D., et al. (2021). Mitochondria-associated membrane-modulated Ca transfer: a potential treatment target in cardiac ischemia reperfusion injury and heart failure. *Life Sci.* 278:119511. doi: 10.1016/j.lfs.2021.119511
- Grings, M., Seminotti, B., Karunanidhi, A., Ghaloul-Gonzalez, L., Mohsen, A., Wipf, P., et al. (2019). ETHE1 and MOC1 deficiencies: disruption of mitochondrial bioenergetics, dynamics, redox homeostasis and endoplasmic reticulum-mitochondria crosstalk in patient fibroblasts. *Sci. Rep.* 9:12651. doi: 10.1038/s41598-019-49014-2
- Guerriero, C., and Brodsky, J. (2012). The delicate balance between secreted protein folding and endoplasmic reticulum-associated degradation in human physiology. *Physiol. Rev.* 92, 537–576. doi: 10.1152/physrev.00027.2011
- Guo, H., Cao, A., Chu, S., Wang, Y., Zang, Y., Mao, X., et al. (2016). Astragaloside IV attenuates podocyte apoptosis mediated by endoplasmic reticulum stress through upregulating sarco/endoplasmic reticulum Ca(2+)-ATPase 2 expression in diabetic nephropathy. *Front. Pharmacol.* 7:500. doi: 10.3389/fphar.2016.00500
- Guo, Y., Li, D., Zhang, S., Yang, Y., Liu, J. J., Wang, X., et al. (2018). Visualizing intracellular organelle and cytoskeletal interactions at nanoscale resolution on millisecond timescales. *Cell* 175, 1430–1442.e17. doi: 10.1016/j.cell.2018.09.057
- Gutierrez, T., Parra, V., Troncoso, R., Pennanen, C., Contreras-Ferrat, A., Vasquez-Trincado, C., et al. (2014). Alteration in mitochondrial Ca(2+) uptake disrupts insulin signaling in hypertrophic cardiomyocytes. *Cell Commun. Signal.* 12:68. doi: 10.1186/s12964-014-0068-4
- Gutierrez, T., Qi, H., Yap, M. C., Tahbaz, N., Milburn, L. A., Lucchinetti, E., et al. (2020). The ER chaperone calnexin controls mitochondrial positioning and respiration. *Sci. Signal.* 13:eaax6660. doi: 10.1126/scisignal.aax6660
- Hall, A. R., Burke, N., Dongworth, R. K., Kalkhoran, S. B., Dyson, A., Vicencio, J. M., et al. (2016). Hearts deficient in both Mfn1 and Mfn2 are protected against acute myocardial infarction. *Cell Death Dis.* 7:e2238. doi: 10.1038/cddis.2016.139
- Hamasaki, M., Furuta, N., Matsuda, A., Nezu, A., Yamamoto, A., Fujita, N., et al. (2013). Autophagosomes form at ER-mitochondria contact sites. *Nature* 495, 389–393. doi: 10.1038/nature11910
- Hayashi, T., and Su, T. P. (2007). Sigma-1 receptor chaperones at the ER-mitochondrion interface regulate Ca(2+) signaling and cell survival. *Cell* 131, 596–610. doi: 10.1016/j.cell.2007.08.036
- He, X., Bi, X. Y., Lu, X. Z., Zhao, M., Yu, X. J., Sun, L., et al. (2015). Reduction of mitochondria-endoplasmic reticulum interactions by acetylcholine protects human umbilical vein endothelial cells from hypoxia/reoxygenation injury.

- Arterioscler. Thromb. Vasc. Biol.* 35, 1623–1634. doi: 10.1161/ATVBAHA.115.305469
- Higo, T., Hattori, M., Nakamura, T., Natsume, T., Michikawa, T., and Mikoshiba, K. (2005). Subtype-specific and ER luminal environment-dependent regulation of inositol 1,4,5-trisphosphate receptor type 1 by ERp44. *Cell* 120, 85–98. doi: 10.1016/j.cell.2004.11.048
- Honrath, B., Metz, I., Bendridi, N., Rieusset, J., Culmsee, C., and Dolga, A. M. (2017). Glucose-regulated protein 75 determines ER-mitochondrial coupling and sensitivity to oxidative stress in neuronal cells. *Cell Death Discov.* 3:17076. doi: 10.1038/cddiscovery.2017.76
- Hu, Y., Chen, H., Zhang, L., Lin, X., Li, X., Zhuang, H., et al. (2021). The AMPK-MFN2 axis regulates MAM dynamics and autophagy induced by energy stresses. *Autophagy* 17, 1142–1156. doi: 10.1080/15548627.2020.1749490
- Huang, J., Wan, L., Lu, H., and Li, X. (2018). High expression of active ATF6 aggravates endoplasmic reticulum stress-induced vascular endothelial cell apoptosis through the mitochondrial apoptotic pathway. *Mol. Med. Rep.* 17, 6483–6489. doi: 10.3892/mmr.2018.8658
- Huang, Y., Zhang, K., Jiang, M., Ni, J., Chen, J., Li, L., et al. (2020). Regulation of energy metabolism by combination therapy attenuates cardiac metabolic remodeling in heart failure. *Int. J. Biol. Sci.* 16, 3133–3148. doi: 10.7150/ijbs.49520
- Intengan, H., and Schiffrin, E. (2001). Vascular remodeling in hypertension: roles of apoptosis, inflammation, and fibrosis. *Hypertension* 38, 581–587. doi: 10.1161/hy09t1.096249
- Iwasawa, R., Mahul-Mellier, A. L., Datler, C., Pazarentzos, E., and Grimm, S. (2011). Fis1 and Bap31 bridge the mitochondria-ER interface to establish a platform for apoptosis induction. *EMBO J.* 30, 556–568. doi: 10.1038/emboj.2010.346
- Jakob, R., Beutner, G., Sharma, V. K., Duan, Y., Gross, R. A., Hurst, S., et al. (2014). Molecular and functional identification of a mitochondrial ryanodine receptor in neurons. *Neurosci. Lett.* 575, 7–12. doi: 10.1016/j.neulet.2014.05.026
- Jeong, S. A., Kim, I. Y., Lee, A. R., Yoon, M. J., Cho, H., Lee, J. S., et al. (2015). Ca²⁺ influx-mediated dilation of the endoplasmic reticulum and c-FLIPL downregulation trigger CDDO-Me-induced apoptosis in breast cancer cells. *Oncotarget* 6, 21173–21192. doi: 10.18632/oncotarget.4065
- Ji, W. K., Chakrabarti, R., Fan, X., Schoenfeld, L., Strack, S., and Higgs, H. N. (2017). Receptor-mediated Drp1 oligomerization on endoplasmic reticulum. *J. Cell Biol.* 216, 4123–4139. doi: 10.1083/jcb.201610057
- Jin, C., Kumar, P., Gracia-Sancho, J., and Dufour, J. F. (2021). Calcium transfer between endoplasmic reticulum and mitochondria in liver diseases. *FEBS Lett.* 595, 1411–1421. doi: 10.1002/1873-3468.14078
- Jouaville, L., Pinton, P., Bastianutto, C., Rutter, G., and Rizzuto, R. (1999). Regulation of mitochondrial ATP synthesis by calcium: evidence for a long-term metabolic priming. *Proc. Natl. Acad. Sci. U.S.A.* 96, 13807–13812. doi: 10.1073/pnas.96.24.13807
- Kho, C., Lee, A., and Hajjar, R. (2012). Altered sarcoplasmic reticulum calcium cycling—targets for heart failure therapy. *Nat. Rev. Cardiol.* 9, 717–733. doi: 10.1038/nrcardio.2012.145
- Kimball, T., and Vondriska, T. (2020). Metabolism, epigenetics, and causal inference in heart failure. *Trends Endocrinol. Metab.* 31, 181–191. doi: 10.1016/j.tem.2019.11.009
- Kizaki, H., Shimada, H., Ohsaka, F., and Sakurada, T. (1988). Adenosine, deoxyadenosine, and deoxyguanosine induce DNA cleavage in mouse thymocytes. *J. Immunol.* 141, 1652–1657.
- Klec, C., Madreiter-Sokolowski, C. T., Stryeck, S., Sachdev, V., Duta-Mare, M., Gottschalk, B., et al. (2019). Glycogen synthase kinase 3 beta controls presenilin-1-mediated endoplasmic reticulum Ca²⁺(+) leak directed to mitochondria in pancreatic islets and beta-cells. *Cell. Physiol. Biochem.* 52, 57–75. doi: 10.33594/000000005
- Klecker, T., Böckler, S., and Westermann, B. (2014). Making connections: interorganelle contacts orchestrate mitochondrial behavior. *Trends Cell Biol.* 24, 537–545. doi: 10.1016/j.tcb.2014.04.004
- Kobuchi, H., Moriya, K., Ogino, T., Fujita, H., Inoue, K., Shuin, T., et al. (2012). Mitochondrial localization of ABC transporter ABCG2 and its function in 5-aminolevulinic acid-mediated protoporphyrin IX accumulation. *PLoS One* 7:e50082. doi: 10.1371/journal.pone.0050082
- Kornmann, B. (2013). The molecular hug between the ER and the mitochondria. *Curr. Opin. Cell Biol.* 25, 443–448. doi: 10.1016/j.ccb.2013.02.010
- Kornmann, B. (2020). The endoplasmic reticulum-mitochondria encounter structure: coordinating lipid metabolism across membranes. *Biol. Chem.* 401, 811–820. doi: 10.1515/hsz-2020-0102
- Kornmann, B., Currie, E., Collins, S. R., Schuldiner, M., Nunnari, J., Weissman, J. S., et al. (2009). An ER-mitochondria tethering complex revealed by a synthetic biology screen. *Science* 325, 477–481. doi: 10.1126/science.1175088
- Kottgen, M., Benzing, T., Simmen, T., Tauber, R., Buchholz, B., Feliciani, S., et al. (2005). Trafficking of TRPP2 by PACS proteins represents a novel mechanism of ion channel regulation. *EMBO J.* 24, 705–716. doi: 10.1038/sj.emboj.7600566
- Kumar, V. K., Lackey, A., Snyder, J., Karhadkar, S., Rao, A. D., DiCarlo, A., et al. (2020). Mitochondrial membrane intracellular communication in healthy and diseased myocardium. *Front. Cell Dev. Biol.* 8:609241. doi: 10.3389/fcell.2020.609241
- Kummer, E., and Ban, N. (2021). Mechanisms and regulation of protein synthesis in mitochondria. *Nat. Rev. Mol. Cell Biol.* 22, 307–325. doi: 10.1038/s41580-021-00332-2
- Landstrom, A. P., Dobrev, D., and Wehrens, X. H. T. (2017). Calcium signaling and cardiac arrhythmias. *Circ. Res.* 120, 1969–1993. doi: 10.1161/CIRCRESAHA.117.310083
- Lao, Y., and Chang, D. C. (2008). Mobilization of Ca²⁺ from endoplasmic reticulum to mitochondria plays a positive role in the early stage of UV- or TNF α -induced apoptosis. *Biochem. Biophys. Res. Commun.* 373, 42–47. doi: 10.1016/j.bbrc.2008.05.172
- Larrea, D., Pera, M., Gonnelli, A., Quintana-Cabrera, R., Akman, H. O., Guardia-Laguarta, C., et al. (2019). MFN2 mutations in Charcot-Marie-Tooth disease alter mitochondria-associated ER membrane function but do not impair bioenergetics. *Hum. Mol. Genet.* 28, 1782–1800. doi: 10.1093/hmg/ddz008
- Lebeau, J., Saunders, J., Moraes, V., Madhavan, A., Madrazo, N., Anthony, M., et al. (2018). The PERK arm of the unfolded protein response regulates mitochondrial morphology during acute endoplasmic reticulum stress. *Cell Rep.* 22, 2827–2836. doi: 10.1016/j.celrep.2018.02.055
- Lebiedzinska, M., Szabadkai, G., Jones, A., Duszynski, J., and Wieckowski, M. (2009). Interactions between the endoplasmic reticulum, mitochondria, plasma membrane and other subcellular organelles. *Int. J. Biochem. Cell Biol.* 41, 1805–1816. doi: 10.1016/j.biocel.2009.02.017
- Lee, S., and Min, K. (2018). The interface between ER and mitochondria: molecular compositions and functions. *Mol. Cells* 41, 1000–1007. doi: 10.14348/molcells.2018.0438
- Li, C., Li, L., Yang, M., Zeng, L., and Sun, L. (2020a). PACS-2: a key regulator of mitochondria-associated membranes (MAMs). *Pharmacol. Res.* 160:105080. doi: 10.1016/j.phrs.2020.105080
- Li, C., Ma, Q., Toan, S., Wang, J., Zhou, H., and Liang, J. (2020b). SERCA overexpression reduces reperfusion-mediated cardiac microvascular damage through inhibition of the calcium/MCU/mPTP/necroptosis signaling pathways. *Redox Biol.* 36:101659. doi: 10.1016/j.redox.2020.101659
- Li, D., Li, X., Guan, Y., and Guo, X. (2015). Mitofusin-2-mediated tethering of mitochondria and endoplasmic reticulum promotes cell cycle arrest of vascular smooth muscle cells in G0/G1 phase. *Acta Biochim. Biophys. Sin.* 47, 441–450. doi: 10.1093/abbs/gmv035
- Li, J., Meng, Q., Fu, Y., Yu, X., Ji, T., Chao, Y., et al. (2021). Novel insights: dynamic foam cells derived from the macrophage in atherosclerosis. *J. Cell. Physiol.* 236, 6154–6167. doi: 10.1002/jcp.30300
- Li, J., Zhang, D., Brundel, B., and Wiersma, M. (2019). Imbalance of ER and mitochondria interactions: prelude to cardiac ageing and disease? *Cells* 8:1617. doi: 10.3390/cells8121617
- Li, L., Gao, G., Shankar, J., Joshi, B., Foster, L. J., and Nabi, I. R. (2015). p38 MAP kinase-dependent phosphorylation of the Gp78 E3 ubiquitin ligase controls ER-mitochondria association and mitochondria motility. *Mol. Biol. Cell* 26, 3828–3840. doi: 10.1091/mbc.E15-02-0120
- Li, Q., Su, D., O'Rourke, B., Pogwizd, S. M., and Zhou, L. (2015). Mitochondria-derived ROS bursts disturb Ca²⁺(+) cycling and induce abnormal automaticity in guinea pig cardiomyocytes: a theoretical study. *Am. J. Physiol. Heart Circ. Physiol.* 308, H623–H636. doi: 10.1152/ajpheart.00493.2014
- Li, Y., Wang, X., and Lou, C. (2016). Gastrodin pretreatment impact on sarcoplasmic reticulum calcium transport ATPase (SERCA) and calcium phosphate (PLB) expression in rats with myocardial ischemia reperfusion. *Med. Sci. Monit.* 22, 3309–3315. doi: 10.12659/msm.896835

- Liu, F., Song, R., Feng, Y., Guo, J., Chen, Y., Zhang, Y., et al. (2015). Upregulation of MG53 induces diabetic cardiomyopathy through transcriptional activation of peroxisome proliferation-activated receptor alpha. *Circulation* 131, 795–804. doi: 10.1161/CIRCULATIONAHA.114.012285
- Liu, J., Rone, M. B., and Papadopoulos, V. (2006). Protein-protein interactions mediate mitochondrial cholesterol transport and steroid biosynthesis. *J. Biol. Chem.* 281, 38879–38893. doi: 10.1074/jbc.M608820200
- Liu, X., Kwak, D., Lu, Z., Xu, X., Fassett, J., Wang, H., et al. (2014). Endoplasmic reticulum stress sensor protein kinase R-like endoplasmic reticulum kinase (PERK) protects against pressure overload-induced heart failure and lung remodeling. *Hypertension* 64, 738–744. doi: 10.1161/hypertensionaha.114.03811
- Ljubkovic, M., Gressette, M., Bulat, C., Cavar, M., Bakovic, D., Fabijanic, D., et al. (2019). Disturbed fatty acid oxidation, endoplasmic reticulum stress, and apoptosis in left ventricle of patients with type 2 diabetes. *Diabetes* 68, 1924–1933. doi: 10.2337/db19-0423
- Lopez-Crisosto, C., Pennanen, C., Vasquez-Trincado, C., Morales, P., Bravo-Sagua, R., Quest, A., et al. (2017). Sarcoplasmic reticulum-mitochondria communication in cardiovascular pathophysiology. *Nat. Rev. Cardiol.* 14, 342–360. doi: 10.1038/nrcardio.2017.23
- Luan, Y., Luan, Y., Yuan, R. X., Feng, Q., Chen, X., and Yang, Y. (2021). Structure and function of mitochondria-associated endoplasmic reticulum membranes (MAMs) and their role in cardiovascular diseases. *Oxid. Med. Cell. Longev.* 2021:4578809. doi: 10.1155/2021/4578809
- Luo, J., Yan, D., Li, S., Liu, S., Zeng, F., Cheung, C. W., et al. (2020). Allopurinol reduces oxidative stress and activates Nrf2/p62 to attenuate diabetic cardiomyopathy in rats. *J. Cell Mol. Med.* 24, 1760–1773. doi: 10.1111/jcmm.14870
- Lynes, E. M., Raturi, A., Shenkman, M., Ortiz Sandoval, C., Yap, M. C., Wu, J., et al. (2013). Palmitoylation is the switch that assigns calnexin to quality control or ER Ca²⁺ signaling. *J. Cell Sci.* 126(Pt 17), 3893–3903. doi: 10.1242/jcs.125856
- Ma, M., Chen, W., Hua, Y., Jia, H., Song, Y., and Wang, Y. (2021). Aerobic exercise ameliorates cardiac hypertrophy by regulating mitochondrial quality control and endoplasmic reticulum stress through M2 AChR. *J. Cell Physiol.* 236, 6581–6596. doi: 10.1002/jcp.30342
- Ma, Z., Mao, C., Jia, Y., Fu, Y., and Kong, W. (2020). Extracellular matrix dynamics in vascular remodeling. *Am. J. Physiol. Cell Physiol.* 319, C481–C499. doi: 10.1152/ajpcell.00147.2020
- Makar, O., and Siabrenko, G. (2018). Influence of physical activity on cardiovascular system and prevention of cardiovascular diseases (review). *Georgian Med. News* 69–74.
- Maneechote, C., Palee, S., Kerdphoo, S., Jaiwongkam, T., Chattipakorn, S. C., and Chattipakorn, N. (2018). Differential temporal inhibition of mitochondrial fission by Mdivi-1 exerts effective cardioprotection in cardiac ischemia/reperfusion injury. *Clin. Sci.* 132, 1669–1683. doi: 10.1042/CS20180510
- Marchi, S., Patergnani, S., Missiroli, S., Morciano, G., Rimessi, A., Wieckowski, M. R., et al. (2018). Mitochondrial and endoplasmic reticulum calcium homeostasis and cell death. *Cell Calcium* 69, 62–72. doi: 10.1016/j.ceca.2017.05.003
- Marchi, S., Rimessi, A., Giorgi, C., Baldini, C., Ferroni, L., Rizzuto, R., et al. (2008). Akt kinase reducing endoplasmic reticulum Ca²⁺ release protects cells from Ca²⁺-dependent apoptotic stimuli. *Biochem. Biophys. Res. Commun.* 375, 501–505. doi: 10.1016/j.bbrc.2008.07.153
- Marini, E. S., Giampietri, C., Petrunaro, S., Conti, S., Filippini, A., Scorrano, L., et al. (2015). The endogenous caspase-8 inhibitor c-FLIPL regulates ER morphology and crosstalk with mitochondria. *Cell Death Differ.* 22, 1131–1143. doi: 10.1038/cdd.2014.197
- Marriott, K. S., Prasad, M., Thapliyal, V., and Bose, H. S. (2012). sigma-1 receptor at the mitochondrial-associated endoplasmic reticulum membrane is responsible for mitochondrial metabolic regulation. *J. Pharmacol. Exp. Ther.* 343, 578–586. doi: 10.1124/jpet.112.198168
- Martinez-Martinez, E., Lopez-Andres, N., Jurado-Lopez, R., Rousseau, E., Bartolome, M. V., Fernandez-Celis, A., et al. (2015). Galectin-3 participates in cardiovascular remodeling associated with obesity. *Hypertension* 66, 961–969. doi: 10.1161/HYPERTENSIONAHA.115.06032
- Matarrese, P., Garofalo, T., Manganeli, V., Gambardella, L., Marconi, M., Grasso, M., et al. (2014). Evidence for the involvement of GD3 ganglioside in autophagosome formation and maturation. *Autophagy* 10, 750–765. doi: 10.4161/auto.27959
- Matsuzaki, H., Fujimoto, T., Tanaka, M., and Shirasawa, S. (2013). Tespa1 is a novel component of mitochondria-associated endoplasmic reticulum membranes and affects mitochondrial calcium flux. *Biochem. Biophys. Res. Commun.* 433, 322–326. doi: 10.1016/j.bbrc.2013.02.099
- Maurya, S. R., and Mahalakshmi, R. (2016). VDAC-2: mitochondrial outer membrane regulator masquerading as a channel? *FEBS J.* 283, 1831–1836. doi: 10.1111/febs.13637
- Méndez-Barbero, N., Gutiérrez-Muñoz, C., and Colio, L. (2021). Cellular crosstalk between endothelial and smooth muscle cells in vascular wall remodeling. *Int. J. Mol. Sci.* 22:7284. doi: 10.3390/ijms22147284
- Mentzer, S., and Konerding, M. (2014). Intussusceptive angiogenesis: expansion and remodeling of microvascular networks. *Angiogenesis* 17, 499–509. doi: 10.1007/s10456-014-9428-3
- Meyers, T., and Townsend, D. (2019). Cardiac pathophysiology and the future of cardiac therapies in duchenne muscular dystrophy. *Int. J. Mol. Sci.* 20:4098. doi: 10.3390/ijms20174098
- Min, C. K., Yeom, D. R., Lee, K. E., Kwon, H. K., Kang, M., Kim, Y. S., et al. (2012). Coupling of ryanodine receptor 2 and voltage-dependent anion channel 2 is essential for Ca(2)+ transfer from the sarcoplasmic reticulum to the mitochondria in the heart. *Biochem. J.* 447, 371–379. doi: 10.1042/BJ20120705
- Mishra, M., Duraisamy, A., Bhattacharjee, S., and Kowluru, R. (2019). Adaptor protein p66Shc: a link between cytosolic and mitochondrial dysfunction in the development of diabetic retinopathy. *Antioxid. Redox Signal.* 30, 1621–1634. doi: 10.1089/ars.2018.7542
- Mizushima, N., and Komatsu, M. (2011). Autophagy: renovation of cells and tissues. *Cell* 147, 728–741. doi: 10.1016/j.cell.2011.10.026
- Moshkforoush, A., Ashenagar, B., Tsoukias, N. M., and Alevriadou, B. R. (2019). Modeling the role of endoplasmic reticulum-mitochondria microdomains in calcium dynamics. *Sci. Rep.* 9:17072. doi: 10.1038/s41598-019-53440-7
- Moulis, M., Grousset, E., Faccini, J., Richetin, K., Thomas, G., and Vindis, C. (2019). The multifunctional sorting protein PACS-2 controls mitophagosome formation in human vascular smooth muscle cells through mitochondria-ER contact sites. *Cells* 8:638. doi: 10.3390/cells8060638
- Münzel, T., Camici, G., Maack, C., Bonetti, N., Fuster, V., and Kovacic, J. (2017). Impact of oxidative stress on the heart and vasculature: part 2 of a 3-part series. *J. Am. Coll. Cardiol.* 70, 212–229. doi: 10.1016/j.jacc.2017.05.035
- Murphy, M. (2013). Mitochondrial dysfunction indirectly elevates ROS production by the endoplasmic reticulum. *Cell Metab.* 18, 145–146. doi: 10.1016/j.cmet.2013.07.006
- Myhill, N., Lynes, E. M., Nanji, J. A., Blagoveshchenskaya, A. D., Fei, H., Carmine Simmen, K., et al. (2008). The subcellular distribution of calnexin is mediated by PACS-2. *Mol. Biol. Cell* 19, 2777–2788. doi: 10.1091/mbc.E07-10-0995
- Nakamura, M., and Sadoshima, J. (2018). Mechanisms of physiological and pathological cardiac hypertrophy. *Nat. Rev. Cardiol.* 15, 387–407. doi: 10.1038/s41569-018-0007-y
- Nam, S. M., and Jeon, Y. J. (2019). Proteostasis in the endoplasmic reticulum: road to cure. *Cancers* 11:1793. doi: 10.3390/cancers11111793
- Namba, T. (2019). BAP31 regulates mitochondrial function via interaction with Tom40 within ER-mitochondria contact sites. *Sci. Adv.* 5:eaa1386. doi: 10.1126/sciadv.aaw1386
- Namba, T., Tian, F., Chu, K., Hwang, S. Y., Yoon, K. W., Byun, S., et al. (2013). CDIP1-BAP31 complex transduces apoptotic signals from endoplasmic reticulum to mitochondria under endoplasmic reticulum stress. *Cell Rep.* 5, 331–339. doi: 10.1016/j.celrep.2013.09.020
- Napoli, C., Martin-Padura, I., de Nigris, F., Giorgio, M., Mansueto, G., Somma, P., et al. (2003). Deletion of the p66Shc longevity gene reduces systemic and tissue oxidative stress, vascular cell apoptosis, and early atherogenesis in mice fed a high-fat diet. *Proc. Natl. Acad. Sci. U.S.A.* 100, 2112–2116. doi: 10.1073/pnas.0336359100
- Nguyen, C. C., Domma, A. J., Zhang, H., and Kamil, J. P. (2020). Endoplasmic reticulum (ER) reorganization and intracellular retention of CD58 are functionally independent properties of the human cytomegalovirus ER-resident glycoprotein UL148. *J. Virol.* 94:e01435-19. doi: 10.1128/JVI.01435-19
- Nunnari, J., and Suomalainen, A. (2012). Mitochondria: in sickness and in health. *Cell* 148, 1145–1159. doi: 10.1016/j.cell.2012.02.035

- Oakes, S. A., and Papa, F. R. (2015). The role of endoplasmic reticulum stress in human pathology. *Annu. Rev. Pathol.* 10, 173–194. doi: 10.1146/annurev-pathol-012513-104649
- Ogawa, Y. (1994). Role of ryanodine receptors. *Crit. Rev. Biochem. Mol. Biol.* 29, 229–274. doi: 10.3109/10409239409083482
- Oka, T., Akazawa, H., Naito, A. T., and Komuro, I. (2014). Angiogenesis and cardiac hypertrophy: maintenance of cardiac function and causative roles in heart failure. *Circ. Res.* 114, 565–571. doi: 10.1161/CIRCRESAHA.114.300507
- Paillass, M., Tubbs, E., Thiebaut, P., Gomez, L., Fauconnier, J., Da Silva, C., et al. (2013). Depressing mitochondria-reticulum interactions protects cardiomyocytes from lethal hypoxia-reoxygenation injury. *Circulation* 128, 1555–1565. doi: 10.1161/circulationaha.113.001225
- Papanicolaou, K., Khairallah, R., Ngoh, G., Chikando, A., Luptak, I., O'Shea, K., et al. (2011). Mitofusin-2 maintains mitochondrial structure and contributes to stress-induced permeability transition in cardiac myocytes. *Mol. Cell. Biol.* 31, 1309–1328. doi: 10.1128/mcb.00911-10
- Papanicolaou, K., Kikuchi, R., Ngoh, G., Coughlan, K., Dominguez, I., Stanley, W., et al. (2012a). Mitofusins 1 and 2 are essential for postnatal metabolic remodeling in heart. *Circ. Res.* 111, 1012–1026. doi: 10.1161/circresaha.112.274142
- Papanicolaou, K., Ngoh, G., Dabkowski, E., O'Connell, K., Ribeiro, R., Stanley, W., et al. (2012b). Cardiomyocyte deletion of mitofusin-1 leads to mitochondrial fragmentation and improves tolerance to ROS-induced mitochondrial dysfunction and cell death. *Am. J. Physiol. Heart Circ. Physiol.* 302, H167–H179. doi: 10.1152/ajpheart.00833.2011
- Park, J. S., Thorsness, M. K., Policastro, R., McGoldrick, L. L., Hollingsworth, N. M., Thorsness, P. E., et al. (2016). Yeast Vps13 promotes mitochondrial function and is localized at membrane contact sites. *Mol. Biol. Cell* 27, 2435–2449. doi: 10.1091/mbc.E16-02-0112
- Parzych, K. R., and Klionsky, D. J. (2014). An overview of autophagy: morphology, mechanism, and regulation. *Antioxid. Redox Signal.* 20, 460–473. doi: 10.1089/ars.2013.5371
- Pedriali, G., Rimessi, A., Sbrano, L., Giorgi, C., Wieckowski, M., Previati, M., et al. (2017). Regulation of endoplasmic reticulum-mitochondria Ca transfer and its importance for anti-cancer therapies. *Front. Oncol.* 7:180. doi: 10.3389/fonc.2017.00180
- Penke, B., Fulop, L., Szucs, M., and Frecka, E. (2018). The role of sigma-1 receptor, an intracellular chaperone in neurodegenerative diseases. *Curr. Neuropharmacol.* 16, 97–116. doi: 10.2174/1570159X15666170529104323
- Perrotta, I. (2020). The microscopic anatomy of endothelial cells in human atherosclerosis: focus on ER and mitochondria. *J. Anat.* 237, 1015–1025. doi: 10.1111/joa.13281
- Peyronnet, R., Nerbonne, J., and Kohl, P. (2016). Cardiac mechano-gated ion channels and arrhythmias. *Circ. Res.* 118, 311–329. doi: 10.1161/circresaha.115.305043
- Porter, K., and Turner, N. (2009). Cardiac fibroblasts: at the heart of myocardial remodeling. *Pharmacol. Ther.* 123, 255–278. doi: 10.1016/j.pharmthera.2009.05.002
- Prasad, M., Kaur, J., Pawlak, K. J., Bose, M., Whittall, R. M., and Bose, H. S. (2015). Mitochondria-associated endoplasmic reticulum membrane (MAM) regulates steroidogenic activity via steroidogenic acute regulatory protein (StAR)-voltage-dependent anion channel 2 (VDAC2) interaction. *J. Biol. Chem.* 290, 2604–2616. doi: 10.1074/jbc.M114.605808
- Prasad, M., Pawlak, K. J., Burak, W. E., Perry, E. E., Marshall, B., Whittall, R. M., et al. (2017). Mitochondrial metabolic regulation by GRP78. *Sci. Adv.* 3:e1602038. doi: 10.1126/sciadv.1602038
- Pries, A., Kuebler, W., and Habazettl, H. (2018). Coronary microcirculation in ischemic heart disease. *Curr. Pharm. Des.* 24, 2893–2899. doi: 10.2174/1381612824666180625142341
- Prola, A., Nichtova, Z., Pires Da Silva, J., Piquereau, J., Monceaux, K., Guilbert, A., et al. (2019). Endoplasmic reticulum stress induces cardiac dysfunction through architectural modifications and alteration of mitochondrial function in cardiomyocytes. *Cardiovasc. Res.* 115, 328–342. doi: 10.1093/cvr/cvy197
- Pulli, L., Lassila, T., Pan, G., Yan, D., Olkkonen, V. M., and Tornquist, K. (2018). Oxysterol-binding protein related-proteins (ORPs) 5 and 8 regulate calcium signaling at specific cell compartments. *Cell Calcium* 72, 62–69. doi: 10.1016/j.ceca.2018.03.001
- Pyakurel, A., Savoia, C., Hess, D., and Scorrano, L. (2015). Extracellular regulated kinase phosphorylates mitofusin 1 to control mitochondrial morphology and apoptosis. *Mol. Cell* 58, 244–254. doi: 10.1016/j.molcel.2015.02.021
- Qin, J., Guo, Y., Xue, B., Shi, P., Chen, Y., Su, Q. P., et al. (2020). ER-mitochondria contacts promote mtDNA nucleoids active transportation via mitochondrial dynamic tubulation. *Nat. Commun.* 11:4471. doi: 10.1038/s41467-020-18202-4
- Raffaello, A., Mammucari, C., Gherardi, G., and Rizzuto, R. (2016). Calcium at the center of cell signaling: interplay between endoplasmic reticulum, mitochondria, and lysosomes. *Trends Biochem. Sci.* 41, 1035–1049. doi: 10.1016/j.tibs.2016.09.001
- Ramming, T., Hansen, H. G., Nagata, K., Ellgaard, L., and Appenzeller-Herzog, C. (2014). GPx8 peroxidase prevents leakage of H₂O₂ from the endoplasmic reticulum. *Free Radic. Biol. Med.* 70, 106–116. doi: 10.1016/j.freeradbiomed.2014.01.018
- Reddish, F. N., Miller, C. L., Gorkhali, R., and Yang, J. J. (2017). Calcium dynamics mediated by the endoplasmic/sarcoplasmic reticulum and related diseases. *Int. J. Mol. Sci.* 18:1024. doi: 10.3390/ijms18051024
- Ren, J., Sun, M., Zhou, H., Ajoalabady, A., Zhou, Y., Tao, J., et al. (2020). FUNDC1 interacts with FBXL2 to govern mitochondrial integrity and cardiac function through an IP3R3-dependent manner in obesity. *Sci. Adv.* 6:eabc8561. doi: 10.1126/sciadv.abc8561
- Roca, F., Whitworth, L., Redmond, S., Jones, A., and Ramakrishnan, L. (2019). TNF induces pathogenic programmed macrophage necrosis in tuberculosis through a mitochondrial-lysosomal-endoplasmic reticulum circuit. *Cell* 178, 1344–1361.e11. doi: 10.1016/j.cell.2019.08.004
- Rosati, E., Sabatini, R., Rampino, G., De Falco, F., Di Ianni, M., Falzetti, F., et al. (2010). Novel targets for endoplasmic reticulum stress-induced apoptosis in B-CLL. *Blood* 116, 2713–2723. doi: 10.1182/blood-2010-03-275628
- Roth, G., Mensah, G., Johnson, C., Addolorato, G., Ammirati, E., Baddour, L., et al. (2020). Global burden of cardiovascular diseases and risk factors, 1990–2019: update from the GBD 2019 study. *J. Am. Coll. Cardiol.* 76, 2982–3021. doi: 10.1016/j.jacc.2020.11.010
- Rozpedek, W., Pytel, D., Mucha, B., Leszczynska, H., Diehl, J. A., and Majsterek, I. (2016). The role of the PERK/eIF2alpha/ATF4/CHOP signaling pathway in tumor progression during endoplasmic reticulum stress. *Curr. Mol. Med.* 16, 533–544. doi: 10.2174/1566524016666160523143937
- Ruan, L., Wang, Y., Zhang, X., Tomaszewski, A., McNamara, J., and Li, R. (2020). Mitochondria-associated proteostasis. *Annu. Rev. Biophys.* 49, 41–67. doi: 10.1146/annurev-biophys-121219-081604
- Rusinol, A. E., Cui, Z., Chen, M. H., and Vance, J. E. (1994). A unique mitochondria-associated membrane fraction from rat liver has a high capacity for lipid synthesis and contains pre-Golgi secretory proteins including nascent lipoproteins. *J. Biol. Chem.* 269, 27494–27502.
- Sadeghi, M., Khosrawi, S., Heshmat-Ghahdarijani, K., Gheisari, Y., Roohafza, H., Mansoorian, M., et al. (2020). Effect of melatonin on heart failure: design for a double-blinded randomized clinical trial. *ESC Heart Fail.* 7, 3142–3150. doi: 10.1002/ehf2.12829
- Safiedeen, Z., Andriantsitohaina, R., and Martinez, M. C. (2016). Dialogue between endoplasmic reticulum and mitochondria as a key actor of vascular dysfunction associated to metabolic disorders. *Int. J. Biochem. Cell Biol.* 77(Pt A), 10–14. doi: 10.1016/j.biocel.2016.05.011
- Salazar-Ramirez, F., Ramos-Mondragon, R., and Garcia-Rivas, G. (2020). Mitochondrial and sarcoplasmic reticulum interconnection in cardiac arrhythmia. *Front. Cell Dev. Biol.* 8:623381. doi: 10.3389/fcell.2020.623381
- Saraf, R., Mahmood, F., Amir, R., and Matyal, R. (2016). Neuropeptide Y is an angiogenic factor in cardiovascular regeneration. *Eur. J. Pharmacol.* 776, 64–70. doi: 10.1016/j.ejphar.2016.02.033
- Sciarretta, S., Forte, M., Frati, G., and Sadoshima, J. (2018a). New insights into the role of mTOR signaling in the cardiovascular system. *Circ. Res.* 122, 489–505. doi: 10.1161/circresaha.117.311147
- Sciarretta, S., Maejima, Y., Zablocki, D., and Sadoshima, J. (2018b). The role of autophagy in the heart. *Annu. Rev. Physiol.* 80, 1–26. doi: 10.1146/annurev-physiol-021317-121427
- Seibenhener, M. L., Du, Y., Diaz-Meco, M. T., Moscat, J., Wooten, M. C., and Wooten, M. W. (2013). A role for sequestosome 1/p62 in mitochondrial dynamics, import and genome integrity. *Biochim. Biophys. Acta* 1833, 452–459. doi: 10.1016/j.bbamcr.2012.11.004

- Sekaran, N. K., Crowley, A. L., de Souza, F. R., Resende, E. S., and Rao, S. V. (2017). The role for cardiovascular remodeling in cardiovascular outcomes. *Curr. Atheroscler. Rep.* 19:23. doi: 10.1007/s11883-017-0656-z
- Senft, D., and Ronai, Z. (2015). UPR, autophagy, and mitochondria crosstalk underlies the ER stress response. *Trends Biochem. Sci.* 40, 141–148. doi: 10.1016/j.tibs.2015.01.002
- Shemorry, A., Harnoss, J. M., Guttman, O., Marsters, S. A., Komuves, L. G., Lawrence, D. A., et al. (2019). Caspase-mediated cleavage of IRE1 controls apoptotic cell commitment during endoplasmic reticulum stress. *Elife* 8:e47084. doi: 10.7554/eLife.47084
- Shi, J., Jiang, Q., Ding, X., Xu, W., Wang, D. W., and Chen, M. (2015). The ER stress-mediated mitochondrial apoptotic pathway and MAPKs modulate tachypacing-induced apoptosis in HL-1 atrial myocytes. *PLoS One* 10:e0117567. doi: 10.1371/journal.pone.0117567
- Shi, Y., Liu, L., Deng, C., Zhao, T., Shi, Z., Yan, J., et al. (2021). Celastrol ameliorates vascular neointimal hyperplasia through Wnt5a-involved autophagy. *Int. J. Biol. Sci.* 17, 2561–2575. doi: 10.7150/ijbs.58715
- Silva-Palacios, A., Zazueta, C., and Pedraza-Chaverri, J. (2020). ER membranes associated with mitochondria: possible therapeutic targets in heart-associated diseases. *Pharmacol. Res.* 156:104758. doi: 10.1016/j.phrs.2020.104758
- Simmen, T., and Herrera-Cruz, M. S. (2018). Plastic mitochondria-endoplasmic reticulum (ER) contacts use chaperones and tethers to mould their structure and signaling. *Curr. Opin. Cell Biol.* 53, 61–69. doi: 10.1016/jceb.2018.04.014
- Simmen, T., Aslan, J. E., Blagoveshchenskaya, A. D., Thomas, L., Wan, L., Xiang, Y., et al. (2005). PACS-2 controls endoplasmic reticulum-mitochondria communication and Bid-mediated apoptosis. *EMBO J.* 24, 717–729. doi: 10.1038/sj.emboj.7600559
- Sipido, K. (2006). Calcium overload, spontaneous calcium release, and ventricular arrhythmias. *Heart Rhythm* 3, 977–979. doi: 10.1016/j.hrthm.2006.01.013
- Sleiman, N., McFarland, T., Jones, L., and Cala, S. (2015). Transitions of protein traffic from cardiac ER to junctional SR. *J. Mol. Cell. Cardiol.* 81, 34–45. doi: 10.1016/j.yjmcc.2014.12.025
- Stahon, K. E., Bastian, C., Griffith, S., Kidd, G. J., Brunet, S., and Baltan, S. (2016). Age-related changes in axonal and mitochondrial ultrastructure and function in white matter. *J. Neurosci.* 36, 9990–10001. doi: 10.1523/JNEUROSCI.1316-16.2016
- Steenbergen, R., Nanowski, T. S., Beigneux, A., Kulinski, A., Young, S. G., and Vance, J. E. (2005). Disruption of the phosphatidylserine decarboxylase gene in mice causes embryonic lethality and mitochondrial defects. *J. Biol. Chem.* 280, 40032–40040. doi: 10.1074/jbc.M506510200
- Stoica, R., De Vos, K. J., Paillusson, S., Mueller, S., Sancho, R. M., Lau, K. F., et al. (2014). ER-mitochondria associations are regulated by the VAPB-PTPIP51 interaction and are disrupted by ALS/FTD-associated TDP-43. *Nat. Commun.* 5:3996. doi: 10.1038/ncomms4996
- Stone, S. J., and Vance, J. E. (2000). Phosphatidylserine synthase-1 and -2 are localized to mitochondria-associated membranes. *J. Biol. Chem.* 275, 34534–34540. doi: 10.1074/jbc.M002865200
- Stutzmann, G., and Mattson, M. (2011). Endoplasmic reticulum Ca(2+) handling in excitable cells in health and disease. *Pharmacol. Rev.* 63, 700–727. doi: 10.1124/pr.110.003814
- Sun, Y., and Ding, S. (2020). ER-mitochondria contacts and insulin resistance modulation through exercise intervention. *Int. J. Mol. Sci.* 21:9587. doi: 10.3390/ijms21249587
- Suresh, S. N. (2019). Endoplasmic reticulum mitochondria contacts modulate apoptosis of renal cells and its implications in diabetic neuropathy. *EBioMedicine* 44, 24–25. doi: 10.1016/j.ebiom.2019.05.061
- Szabadkai, G., Bianchi, K., Varnai, P., De Stefani, D., Wieckowski, M. R., Cavagna, D., et al. (2006). Chaperone-mediated coupling of endoplasmic reticulum and mitochondrial Ca²⁺ channels. *J. Cell Biol.* 175, 901–911. doi: 10.1083/jcb.200608073
- Szymański, J., Janikiewicz, J., Michalska, B., Patalas-Krawczyk, P., Perrone, M., Ziolkowski, W., et al. (2017). Interaction of mitochondria with the endoplasmic reticulum and plasma membrane in calcium homeostasis, lipid trafficking and mitochondrial structure. *Int. J. Mol. Sci.* 18:1576. doi: 10.3390/ijms18071576
- Takeda, K., Nagashima, S., Shiiba, I., Uda, A., Tokuyama, T., Ito, N., et al. (2019). MITOL prevents ER stress-induced apoptosis by IRE1α ubiquitylation at ER-mitochondria contact sites. *EMBO J.* 38:e100999. doi: 10.15252/emboj.2018100999
- Tan, Y., Mui, D., Toan, S., Zhu, P., Li, R., and Zhou, H. (2020). SERCA overexpression improves mitochondrial quality control and attenuates cardiac microvascular ischemia-reperfusion injury. *Mol. Ther. Nucleic Acids* 22, 696–707. doi: 10.1016/j.omtn.2020.09.013
- Tanaka, L., and Laurindo, F. (2017). Vascular remodeling: a redox-modulated mechanism of vessel caliber regulation. *Free Radic. Biol. Med.* 109, 11–21. doi: 10.1016/j.freeradbiomed.2017.01.025
- Tang, C., Han, H., Yan, M., Zhu, S., Liu, J., Liu, Z., et al. (2018). PINK1-PRKN/PARK2 pathway of mitophagy is activated to protect against renal ischemia-reperfusion injury. *Autophagy* 14, 880–897. doi: 10.1080/15548627.2017.1405880
- Tate, M., Deo, M., Cao, A. H., Hood, S. G., Huynh, K., Kiriazis, H., et al. (2017). Insulin replacement limits progression of diabetic cardiomyopathy in the low-dose streptozotocin-induced diabetic rat. *Diab. Vasc. Dis. Res.* 14, 423–433. doi: 10.1177/1479164117710390
- Tatsuta, T., Scharwey, M., and Langer, T. (2014). Mitochondrial lipid trafficking. *Trends Cell Biol.* 24, 44–52. doi: 10.1016/j.tcb.2013.07.011
- Thoudam, T., Ha, C. M., Leem, J., Chanda, D., Park, J. S., Kim, H. J., et al. (2019). PDK4 augments ER-mitochondria contact to dampen skeletal muscle insulin signaling during obesity. *Diabetes* 68, 571–586. doi: 10.2337/db18-0363
- Tilokani, L., Nagashima, S., Paupe, V., and Prudent, J. (2018). Mitochondrial dynamics: overview of molecular mechanisms. *Essays Biochem.* 62, 341–360. doi: 10.1042/EBC20170104
- Toth, A., Nickson, P., Mandl, A., Bannister, M., Toth, K., and Erhardt, P. (2007). Endoplasmic reticulum stress as a novel therapeutic target in heart diseases. *Cardiovasc. Hematol. Disord. Drug Targets* 7, 205–218. doi: 10.2174/187152907781745260
- Tabbs, E., Chanon, S., Robert, M., Bendridi, N., Bidaux, G., Chauvin, M., et al. (2018). Disruption of mitochondria-associated endoplasmic reticulum membrane (MAM) integrity contributes to muscle insulin resistance in mice and humans. *Diabetes* 67, 636–650. doi: 10.2337/db17-0316
- Tuncay, E., Bitirim, C. V., Olgar, Y., Durak, A., Rutter, G. A., and Turan, B. (2019). Zn(2+)-transporters ZIP7 and ZnT7 play important role in progression of cardiac dysfunction via affecting sarco(endo)plasmic reticulum-mitochondria coupling in hyperglycemic cardiomyocytes. *Mitochondrion* 44, 41–52. doi: 10.1016/j.mito.2017.12.011
- Van Guilder, G., Preston, C., Munce, T., and Faustino, R. (2021). Impacts of circulating microRNAs in exercise-induced vascular remodeling. *Am. J. Physiol. Heart Circ. Physiol.* 320, H2401–H2415. doi: 10.1152/ajpheart.00894.2020
- Vance, J. E. (1990). Phospholipid synthesis in a membrane fraction associated with mitochondria. *J. Biol. Chem.* 265, 7248–7256.
- Vance, J. E. (2014). MAM (mitochondria-associated membranes) in mammalian cells: lipids and beyond. *Biochim. Biophys. Acta* 1841, 595–609. doi: 10.1016/j.bbalip.2013.11.014
- Vance, J. E. (2015). Phospholipid synthesis and transport in mammalian cells. *Traffic* 16, 1–18. doi: 10.1111/tra.12230
- Vance, J. E., and Steenbergen, R. (2005). Metabolism and functions of phosphatidylserine. *Prog. Lipid Res.* 44, 207–234. doi: 10.1016/j.plipres.2005.05.001
- Vannuvel, K., Renard, P., Raes, M., and Arnould, T. (2013). Functional and morphological impact of ER stress on mitochondria. *J. Cell. Physiol.* 228, 1802–1818. doi: 10.1002/jcp.24360
- Verfaillie, T., Rubio, N., Garg, A. D., Bultynck, G., Rizzuto, R., Decuypere, J. P., et al. (2012). PERK is required at the ER-mitochondrial contact sites to convey apoptosis after ROS-based ER stress. *Cell Death Differ.* 19, 1880–1891. doi: 10.1038/cdd.2012.74
- Voelker, D. R. (2000). Interorganelle transport of aminoglycerophospholipids. *Biochim. Biophys. Acta* 1486, 97–107. doi: 10.1016/s1388-1981(00)00051-2
- Wacquier, B., Combettes, L., and Dupont, G. (2019). Cytoplasmic and mitochondrial calcium signaling: a two-way relationship. *Cold Spring Harb. Perspect. Biol.* 11:a035139. doi: 10.1101/cshperspect.a035139
- Wang, C., Dai, X., Wu, S., Xu, W., Song, P., and Huang, K. (2021). FUNDC1-dependent mitochondria-associated endoplasmic reticulum membranes are involved in angiogenesis and neoangiogenesis. *Nat. Commun.* 12:2616. doi: 10.1038/s41467-021-22771-3

- Wang, J., Lu, L., Chen, S., Xie, J., Lu, S., Zhou, Y., et al. (2020a). PERK overexpression-mediated Nrf2/HO-1 pathway alleviates hypoxia/reoxygenation-induced injury in neonatal murine cardiomyocytes via improving endoplasmic reticulum stress. *Biomed. Res. Int.* 2020:6458060. doi: 10.1155/2020/6458060
- Wang, J., Toan, S., and Zhou, H. (2020b). Mitochondrial quality control in cardiac microvascular ischemia-reperfusion injury: new insights into the mechanisms and therapeutic potentials. *Pharmacol. Res.* 156:104771. doi: 10.1016/j.phrs.2020.104771
- Wang, M., and Kaufman, R. (2016). Protein misfolding in the endoplasmic reticulum as a conduit to human disease. *Nature* 529, 326–335. doi: 10.1038/nature17041
- Wang, S., Xiao, W., Shan, S., Jiang, C., Chen, M., Zhang, Y., et al. (2012). Multi-patterned dynamics of mitochondrial fission and fusion in a living cell. *PLoS One* 7:e19879. doi: 10.1371/journal.pone.0019879
- Wang, X., Luo, D., and Wu, S. (2021). Molecular dysfunctions of mitochondria-associated endoplasmic reticulum contacts in atherosclerosis. *Oxid. Med. Cell. Longev.* 2021:2424509. doi: 10.1155/2021/2424509
- Wang, Y., Wang, Y. L., Huang, X., Yang, Y., Zhao, Y. J., Wei, C. X., et al. (2017). Ibutilide protects against cardiomyocytes injury via inhibiting endoplasmic reticulum and mitochondrial stress pathways. *Heart Vessels* 32, 208–215. doi: 10.1007/s00380-016-0891-1
- Wiggers, H., Køber, L., Gislason, G., Schou, M., Poulsen, M., Vraa, S., et al. (2021). The DANish randomized, double-blind, placebo controlled trial in patients with chronic HEART failure (DANHEART): a 2 × 2 factorial trial of hydralazine-isosorbide dinitrate in patients with chronic heart failure (H-HeFT) and metformin in patients with chronic heart failure and diabetes or prediabetes (Met-HeFT). *Am. Heart J.* 231, 137–146. doi: 10.1016/j.ahj.2020.09.020
- Wu, S., Lu, Q., Ding, Y., Wu, Y., Qiu, Y., Wang, P., et al. (2019). Hyperglycemia-driven inhibition of AMP-activated protein kinase α 2 induces diabetic cardiomyopathy by promoting mitochondria-associated endoplasmic reticulum membranes in vivo. *Circulation* 139, 1913–1936. doi: 10.1161/CIRCULATIONAHA.118.033552
- Wu, S., Lu, Q., Wang, Q., Ding, Y., Ma, Z., Mao, X., et al. (2017). Binding of FUN14 domain containing 1 with inositol 1,4,5-trisphosphate receptor in mitochondria-associated endoplasmic reticulum membranes maintains mitochondrial dynamics and function in hearts in vivo. *Circulation* 136, 2248–2266. doi: 10.1161/CIRCULATIONAHA.117.030235
- Wu, W., Li, W., Chen, H., Jiang, L., Zhu, R., and Feng, D. (2016). FUNDC1 is a novel mitochondrial-associated-membrane (MAM) protein required for hypoxia-induced mitochondrial fission and mitophagy. *Autophagy* 12, 1675–1676. doi: 10.1080/15548627.2016.1193656
- Xiong, Z., Li, Y., Zhao, Z., Zhang, Y., Man, W., Lin, J., et al. (2020). Mst1 knockdown alleviates cardiac lipotoxicity and inhibits the development of diabetic cardiomyopathy in db/db mice. *Biochim. Biophys. Acta Mol. Basis Dis.* 1866:165806. doi: 10.1016/j.bbadis.2020.165806
- Xu, H., Zhou, W., Zhan, L., Sui, H., Zhang, L., Zhao, C., et al. (2020). The ZiBuPiYin recipe regulates proteomic alterations in brain mitochondria-associated ER membranes caused by chronic psychological stress exposure: Implications for cognitive decline in Zucker diabetic fatty rats. *Aging* 12, 23698–23726. doi: 10.18632/aging.103894
- Xu, Y., Yuan, H., Luo, Y., Zhao, Y. J., and Xiao, J. H. (2020). Ganoderic acid D protects human amniotic mesenchymal stem cells against oxidative stress-induced senescence through the PERK/NRF2 signaling pathway. *Oxid. Med. Cell. Longev.* 2020:8291413. doi: 10.1155/2020/8291413
- Yamada, T., Dawson, T. M., Yanagawa, T., Iijima, M., and Sesaki, H. (2019). SQSTM1/p62 promotes mitochondrial ubiquitination independently of PINK1 and PRKN/parkin in mitophagy. *Autophagy* 15, 2012–2018. doi: 10.1080/15548627.2019.1643185
- Yang, J., Zhang, R., Jiang, X., Lv, J., Li, Y., Ye, H., et al. (2018). Toll-like receptor 4-induced ryanodine receptor 2 oxidation and sarcoplasmic reticulum Ca^{2+} leakage promote cardiac contractile dysfunction in sepsis. *J. Biol. Chem.* 293, 794–807. doi: 10.1074/jbc.M117.812289
- Yang, M., Li, C., Yang, S., Xiao, Y., Xiong, X., Chen, W., et al. (2020). Mitochondria-associated ER membranes – the origin site of autophagy. *Front. Cell Dev. Biol.* 8:595. doi: 10.3389/fcell.2020.00595
- Yang, M., Zhao, L., Gao, P., Zhu, X., Han, Y., Chen, X., et al. (2019). DsbA-L ameliorates high glucose induced tubular damage through maintaining MAM integrity. *EBioMedicine* 43, 607–619. doi: 10.1016/j.ebiom.2019.04.044
- Yang, Y. D., Li, M. M., Xu, G., Feng, L., Zhang, E. L., Chen, J., et al. (2019). Nogo-B receptor directs mitochondria-associated membranes to regulate vascular smooth muscle cell proliferation. *Int. J. Mol. Sci.* 20:2319. doi: 10.3390/ijms20092319
- Yang, Y., Gao, H., Zhou, H., Liu, Q., Qi, Z., Zhang, Y., et al. (2019). The role of mitochondria-derived peptides in cardiovascular disease: recent updates. *Biomed. Pharmacother.* 117:109075. doi: 10.1016/j.biopha.2019.109075
- Yeshaw, W. M., van der Zwaag, M., Pinto, F., Lahaye, L. L., Faber, A. I., Gomez-Sanchez, R., et al. (2019). Human VPS13A is associated with multiple organelles and influences mitochondrial morphology and lipid droplet motility. *Elife* 8:e43561. doi: 10.7554/eLife.43561
- Yousuf, M. S., Maguire, A. D., Simmen, T., and Kerr, B. J. (2020). Endoplasmic reticulum-mitochondria interplay in chronic pain: the calcium connection. *Mol. Pain* 16:1744806920946889. doi: 10.1177/1744806920946889
- Yu, S., Zhang, L., Liu, C., Yang, J., Zhang, J., and Huang, L. (2019). PACS2 is required for ox-LDL-induced endothelial cell apoptosis by regulating mitochondria-associated ER membrane formation and mitochondrial Ca^{2+} elevation. *Exp. Cell Res.* 379, 191–202. doi: 10.1016/j.yexcr.2019.04.002
- Yuan, L., Liu, Q., Wang, Z., Hou, J., and Xu, P. (2020). EI24 tethers endoplasmic reticulum and mitochondria to regulate autophagy flux. *Cell. Mol. Life Sci.* 77, 1591–1606. doi: 10.1007/s00018-019-03236-9
- Yuan, M., Gong, M., Zhang, Z., Meng, L., Tse, G., Zhao, Y., et al. (2020). Hyperglycemia induces endoplasmic reticulum stress in atrial cardiomyocytes, and mitofusin-2 downregulation prevents mitochondrial dysfunction and subsequent cell death. *Oxid. Med. Cell. Longev.* 2020:6569728. doi: 10.1155/2020/6569728
- Zhang, C., Niu, K., Lian, P., Hu, Y., Shuai, Z., Gao, S., et al. (2021). Pathological bases and clinical application of long noncoding RNAs in cardiovascular diseases. *Hypertension* 78, 16–29. doi: 10.1161/hypertensionaha.120.16752
- Zhang, J., Zhang, F., and Wang, Y. (2021). Mitofusin-2 enhances mitochondrial contact with the endoplasmic reticulum and promotes diabetic cardiomyopathy. *Front. Physiol.* 12:707634. doi: 10.3389/fphys.2021.707634
- Zhang, L., Cheng, X., Xu, S., Bao, J., and Yu, H. (2018). Curcumin induces endoplasmic reticulum stress-associated apoptosis in human papillary thyroid carcinoma BCPAP cells via disruption of intracellular calcium homeostasis. *Medicine* 97:e11095. doi: 10.1097/MD.00000000000011095
- Zhang, R., Jiang, M., Zhang, J., Qiu, Y., Li, D., Li, S., et al. (2020). Regulation of the cerebrovascular smooth muscle cell phenotype by mitochondrial oxidative injury and endoplasmic reticulum stress in simulated microgravity rats via the PERK-eIF2 α -ATF4-CHOP pathway. *Biochim. Biophys. Acta Mol. Basis Dis.* 1866:165799. doi: 10.1016/j.bbadis.2020.165799
- Zhang, W. (2021). The mitophagy receptor FUN14 domain-containing 1 (FUNDC1): a promising biomarker and potential therapeutic target of human diseases. *Genes Dis.* 8, 640–654. doi: 10.1016/j.gendis.2020.08.011
- Zhao, H. H., Han, Q. X., Ding, X. N., Yan, J. Y., Li, Q., Zhang, D., et al. (2020). Critical hubs of renal ischemia-reperfusion injury: endoplasmic reticulum-mitochondria tethering complexes. *Chin. Med. J.* 133, 2599–2609. doi: 10.1097/CM9.0000000000001091
- Zhao, H., and Wang, T. (2020). PE homeostasis rebalanced through mitochondria-ER lipid exchange prevents retinal degeneration in *Drosophila*. *PLoS Genet.* 16:e1009070. doi: 10.1371/journal.pgen.1009070
- Zhao, T., Chen, H., Xu, F., Wang, J., Liu, Y., Xing, X., et al. (2019). Liraglutide alleviates cardiac fibrosis through inhibiting P4 α 1 expression in STZ-induced diabetic cardiomyopathy. *Acta Biochim. Biophys. Sin.* 51, 293–300. doi: 10.1093/abbs/gmy177
- Zhao, Y., Jia, W. W., Ren, S., Xiao, W., Li, G. W., Jin, L., et al. (2021). Difluoromethylornithine attenuates isoproterenol-induced cardiac hypertrophy by regulating apoptosis, autophagy and the mitochondria-associated membranes pathway. *Exp. Ther. Med.* 22:870. doi: 10.3892/etm.2021.10302
- Zheng, P., Chen, Q., Tian, X., Qian, N., Chai, P., Liu, B., et al. (2018). DNA damage triggers tubular endoplasmic reticulum extension to promote apoptosis by facilitating ER-mitochondria signaling. *Cell Res.* 28, 833–854. doi: 10.1038/s41422-018-0065-z

- Zhihao, L., Jingyu, N., Lan, L., Michael, S., Rui, G., Xiyun, B., et al. (2020). SERCA2a: a key protein in the Ca cycle of the heart failure. *Heart Fail. Rev.* 25, 523–535. doi: 10.1007/s10741-019-09873-3
- Zhong, J., Tan, Y., Lu, J., Liu, J., Xiao, X., Zhu, P., et al. (2019). Therapeutic contribution of melatonin to the treatment of septic cardiomyopathy: a novel mechanism linking Ripk3-modified mitochondrial performance and endoplasmic reticulum function. *Redox Biol.* 26:101287. doi: 10.1016/j.redox.2019.101287
- Zhou, H., Liu, L., Ma, X., Wang, J., Yang, J., Zhou, X., et al. (2021). RIP1/RIP3/MLKL-mediated necroptosis contributes to vinblastine-induced myocardial damage. *Mol. Cell. Biochem.* 476, 1233–1243. doi: 10.1007/s11010-020-03985-3
- Zhou, H., Wang, S., Hu, S., Chen, Y., and Ren, J. (2018a). ER-mitochondria microdomains in cardiac ischemia-reperfusion injury: a fresh perspective. *Front. Physiol.* 9:755. doi: 10.3389/fphys.2018.00755
- Zhou, H., Yue, Y., Wang, J., Ma, Q., and Chen, Y. (2018b). Melatonin therapy for diabetic cardiomyopathy: a mechanism involving Syk-mitochondrial complex I-SERCA pathway. *Cell. Signal.* 47, 88–100. doi: 10.1016/j.cellsig.2018.03.012
- Zorzano, A., Liesa, M., Sebastian, D., Segales, J., and Palacin, M. (2010). Mitochondrial fusion proteins: dual regulators of morphology and metabolism. *Semin. Cell Dev. Biol.* 21, 566–574. doi: 10.1016/j.semcdb.2010.01.002

Conflict of Interest: The authors declare that the research was conducted in the absence of any commercial or financial relationships that could be construed as a potential conflict of interest.

Publisher's Note: All claims expressed in this article are solely those of the authors and do not necessarily represent those of their affiliated organizations, or those of the publisher, the editors and the reviewers. Any product that may be evaluated in this article, or claim that may be made by its manufacturer, is not guaranteed or endorsed by the publisher.

Copyright © 2021 Wang, Zhang, Wen, Li, Lu, Xu and Li. This is an open-access article distributed under the terms of the Creative Commons Attribution License (CC BY). The use, distribution or reproduction in other forums is permitted, provided the original author(s) and the copyright owner(s) are credited and that the original publication in this journal is cited, in accordance with accepted academic practice. No use, distribution or reproduction is permitted which does not comply with these terms.



Mitochondria Endoplasmic Reticulum Contact Sites (MERCs): Proximity Ligation Assay as a Tool to Study Organelle Interaction

Sara Benhammouda^{1,2†}, Anjali Vishwakarma^{1,2†}, Priya Gatti^{1,2} and Marc Germain^{1,2*}

¹Groupe de Recherche en Signalisation Cellulaire and Département de Biologie Médicale, Université Du Québec à Trois-Rivières, Trois-Rivières, QC, Canada, ²Centre D'Excellence en Recherche sur les Maladies Orphelines - Fondation Courtois, Université du Québec à Montréal, Montréal, QC, Canada

OPEN ACCESS

Edited by:

Yongye Huang,
Northeastern University, China

Reviewed by:

Hua Han,
Institute of Automation (CAS), China
Alenka Lovy,
Universidad Mayor, Chile

*Correspondence:

Marc Germain
marc.germain1@uqtr.ca

[†]These authors have contributed
equally to this work

Specialty section:

This article was submitted to
Signaling,
a section of the journal
Frontiers in Cell and Developmental
Biology

Received: 05 October 2021

Accepted: 18 November 2021

Published: 03 December 2021

Citation:

Benhammouda S, Vishwakarma A,
Gatti P and Germain M (2021)
Mitochondria Endoplasmic Reticulum
Contact Sites (MERCs): Proximity
Ligation Assay as a Tool to Study
Organelle Interaction.
Front. Cell Dev. Biol. 9:789959.
doi: 10.3389/fcell.2021.789959

Organelles cooperate with each other to regulate vital cellular homeostatic functions. This occurs through the formation of close connections through membrane contact sites. Mitochondria-Endoplasmic-Reticulum (ER) contact sites (MERCs) are one of such contact sites that regulate numerous biological processes by controlling calcium and metabolic homeostasis. However, the extent to which contact sites shape cellular biology and the underlying mechanisms remain to be fully elucidated. A number of biochemical and imaging approaches have been established to address these questions, resulting in the identification of a number of molecular tethers between mitochondria and the ER. Among these techniques, fluorescence-based imaging is widely used, including analysing signal overlap between two organelles and more selective techniques such as *in-situ* proximity ligation assay (PLA). While these two techniques allow the detection of endogenous proteins, preventing some problems associated with techniques relying on overexpression (FRET, split fluorescence probes), they come with their own issues. In addition, proper image analysis is required to minimise potential artefacts associated with these methods. In this review, we discuss the protocols and outline the limitations of fluorescence-based approaches used to assess MERCs using endogenous proteins.

Keywords: mitochondria, endoplasmic reticulum, organelle contact sites, organelle, contact sites methodologies

INTRODUCTION

Organelles are responsible for many of the anabolic and catabolic processes required for the proper functioning of eukaryotic cells. For decades, organelle research has centred on identifying each compartment and their distinct properties with the thought that transfer of material between organelles occurred through diffusion of soluble metabolites or vesicular trafficking (Dennis and Kennedy, 1972). However, in recent years, the subject has undergone a revolution as we realised that cells use a network of contact sites between membranes of different organelles, termed membrane contact sites (MCS), to communicate and transfer metabolites (Schrader et al., 2015; Cohen et al., 2018; Scorrano et al., 2019). MCS are defined as areas of close apposition (typically less than 30 nm) between two organelles in the absence of membrane fusion. It is becoming clear that most, if not all, organelles interact via MCS. In addition, a growing number of proteins have been shown to be required for these MCS (Eisenberg-Bord et al., 2016; Simmen and Tagaya, 2017; Cohen et al., 2018; Scorrano et al., 2019).

Mitochondria-Endoplasmic-Reticulum (ER) contact sites (MERCS) play a central role in calcium signalling (Ca^{2+}), phospholipid synthesis and transfer, regulation of oxidative stress and inflammatory responses, mitochondrial dynamics, bioenergetic and cell survival (Tubbs and Rieusset, 2017) (Patergnani et al., 2011; Kroes et al., 2016; Martinvalet, 2018; Missiroli et al., 2018; Perrone et al., 2020; Xu et al., 2020). MERCS require proteins on both the ER and mitochondria to bridge the two organelles. While the nature of these protein tethers has not been fully characterized and likely varies depending on cellular conditions and cell types, several MERCS tethering complexes have been identified. This includes the interaction between ER-resident Inositol 1,4,5-triphosphate receptor (IP3R) and mitochondrial voltage-gated anion channel (VDAC) that is bridged by glucose-regulated protein 75 (GRP75), and the mitochondrial fusion protein Mitofusin-2 (MFN2) which localizes to both the ER and mitochondria (De Brito and Scorrano, 2008; Basso et al., 2018). Vesicle-associated membrane protein B (VAPB) and protein tyrosine phosphatase interacting protein 51 (PTPIP51) are other reported ER-mitochondria tethering proteins (Gomez-Suaga et al., 2017).

The size of a MERCS area and the width of the gap between the two organelles are critical structural characteristics of MERCS that are tightly regulated. While the underlying mechanisms are still being elucidated, it is clear that disruption of MERCS structure and/or activity is a crucial factor that promotes or contributes to oncogenesis, neurodegeneration, and a variety of other diseases (Kisby et al., 2011; López-Crisosto et al., 2015; Rodríguez-Arribas et al., 2017; Annunziata et al., 2018; Pinton, 2018; Eysert et al., 2020; Gao et al., 2020). Several imaging techniques have been used to study MERCS and, in general, MCS (recently reviewed by (Giamogante et al., 2020)). These techniques include electron microscopy (EM), the gold standard for MCS identification, and fluorescence-based techniques that, while having a lower resolution, allow a more dynamic assessment of MCS and MERCS. Here, we will briefly review these techniques, focussing on proximity ligation assay (PLA), one of the most recent techniques used to study MERCS.

TECHNIQUES FOR ER-MITOCHONDRIA INTERACTION

Electron Microscopy

EM is the oldest tool for morphological examination of intracellular structures and provided the first evidence that ER and mitochondria interact (Copeland and Dalton, 1959). It allows the measure of both the distance between the organelles and the length of the extension. Also, EM provides strong membrane contrast and nanometer-scale resolution for observing cellular organelles. EM can also be combined with light microscopy using correlative light-electron microscopy (CLEM). Combining CLEM and 3D electron microscopy can also enhance the detailed structural studies of mitochondria and ER (Jung and Mun, 2019). Yet, EM analysis is extremely time-consuming. In addition, the fundamental restriction of EM is tissue fixation,

which prohibits live cell imaging and monitoring MERCS dynamics. Another serious challenge with EM is quantifying apparent changes in organelle morphology. Point counting can be used to analyse mitochondria or ER morphology (Howard, 2004) but it has limited ability to quantify finer structural elements such as mito-ER interactions and cristae measurements. A simple method has recently been described using open source software ImageJ (Lam et al., 2021), but EM analysis remains time-consuming. Overall, while EM remains the gold standard for quantifying ER-mitochondria interaction, several techniques based on fluorescence have been developed to circumvent the limitation of EM.

Fluorescent Microscopy

Fluorescence-based techniques to study MERCS are based on the use of antibodies that recognize the proteins of interest or the expression of proteins genetically tagged with Green Fluorescent Protein (GFP) or other fluorescent proteins and are easily available. The use of a combination of fluorescent-tagged proteins with distinct emission spectrums also allows dynamic interactions to be resolved in real time (Huang et al., 2020).

The simplest approach with fluorescence-based microscopy is to measure the co-localisation/overlap of fluorescent signals from cells co-transfected with fluorescence proteins targeted to ER and mitochondria. This has been used to demonstrate that ER-mitochondria interactions regulate calcium signaling (Rizzuto et al., 1998) and that mitochondrial fission occurs at MERCS (Friedman et al., 2011). The key advantages of this technology are its simplicity, fast processing, and compatibility with live imaging. The primary constraint of this technique is the resolution, which significantly limits our ability to distinguish organelles that are close to each other from those that actually interact. The use of live cell imaging can partially alleviate this by measuring the coordinated movement of the organelles on both sides of the MCS (Yang et al., 2018) or a functional consequence of this interaction (for example mitochondrial fission in the case of MERCS (Friedman et al., 2011)). Alternatively, it is possible to use a super-resolution fluorescence microscope that transcends traditional epi-fluorescence and confocal microscopy diffraction limits (Giamogante et al., 2020). Super-resolution microscopy can also be amenable to live cell imaging but requires a highly specialized microscope.

Generally, fluorescent images are processed to conduct a colocalization analysis that measures the amount of signal overlap between the two tagged organelles. While this colocalization does not necessarily represent the actual colocalization of two probes due to resolution limits, it can provide a useful estimate of changes occurring under the experimental conditions tested. To address this, most image processing software includes specific correlation measures: Pearson correlation coefficient (PCC) and Manders' coefficients (Adler and Parmryd, 2010).

PCC measures how well the variation in pixel intensities between two signals can be explained by a simple, linear correlation between the two. As such, PCC is appropriate to measure the colocalization of two probes localized to the same cellular structure. However, the situation is more complex when

measuring MCS because only a fraction of the signal is correlated (the MCS). In such situations, PCC measurements are ambiguous, if not misleading (Dunn et al., 2011). Manders' coefficients provide an alternative to PCC by considering the co-occurrence of the signals (the fraction of pixels with positive values for both channels) independently of relative pixel intensity. There are two types of Manders' coefficient: Manders' overlap coefficient, which provides a global estimate of the overlap between the two signals akin to the PCC, and Manders' colocalization coefficients that specifically assess the fraction of signal 1 overlapping with signal 2 and the fraction of signal 2 overlapping with signal 1. These coefficients can provide a useful measure of colocalization but require the proper determination of what constitutes the signal to measure, which is not trivial. Different strategies can be used to eliminate background signal, but these usually involve applying a global threshold to the image. Importantly, none of these methods (including the Costes automated method that is usually used when calculating Manders' coefficients) are effective in all situations. The selected strategy (global thresholding, local thresholding, use of preprocessing tools such as ImageJ's Tubeness (Almutawa et al., 2019), etc.) needs to be carefully selected and validated so that the pixels that are selected as signal correspond to the actual signal. Changes in organelle structure can also affect Manders' coefficients, as exemplified by the conflicting role of MFN2 in MERCS regulation as determined by fluorescence microscopy and EM (De Brito and Scorrano, 2008; Cosson et al., 2012; Filadi et al., 2015). A thorough discussion of the limitations of PCC and Manders' coefficients can be found in (Dunn et al., 2011).

Other Fluorescent Techniques

While the analysis of tagged organelles described above provides a rapid assessment of organelle colocalization that can be used to measure the dynamic interaction between organelles, its limitations have led to the development of more specific methods to probe MCS. These involve the transfection of fluorescent probes that can be detected only when two organelles are in close proximity or the use of antibodies for two distinct proteins that will be detected only when in close proximity.

Fluorescence-based techniques to selectively detect MCS are based on energy transfer (Förster energy transfer (FRET), bioluminescence resonance emission transfer (BRET)) or biomolecular fluorescence complementation (BiFC). FRET consists of energy transfer from an excitable fluorophore donor to a suited fluorophore acceptor (Shrestha et al., 2015). BRET provides an alternative to FRET where the donor fluorophore is replaced by luciferase which serves as the source of light for energy transfer to the acceptor (Pfleger and Eidne, 2006). In either case, donor/acceptor pairs are fused to resident ER and mitochondrial proteins and used to detect MERCS in an interaction-free approach (Naon et al., 2016). While FRET and BRET measure the energy transfer between to probes in close proximity, BiFC is based on the reconstitution of two fragments of a fluorescent protein (or luciferase) into a functional fluorophore. This technique requires the targeting of

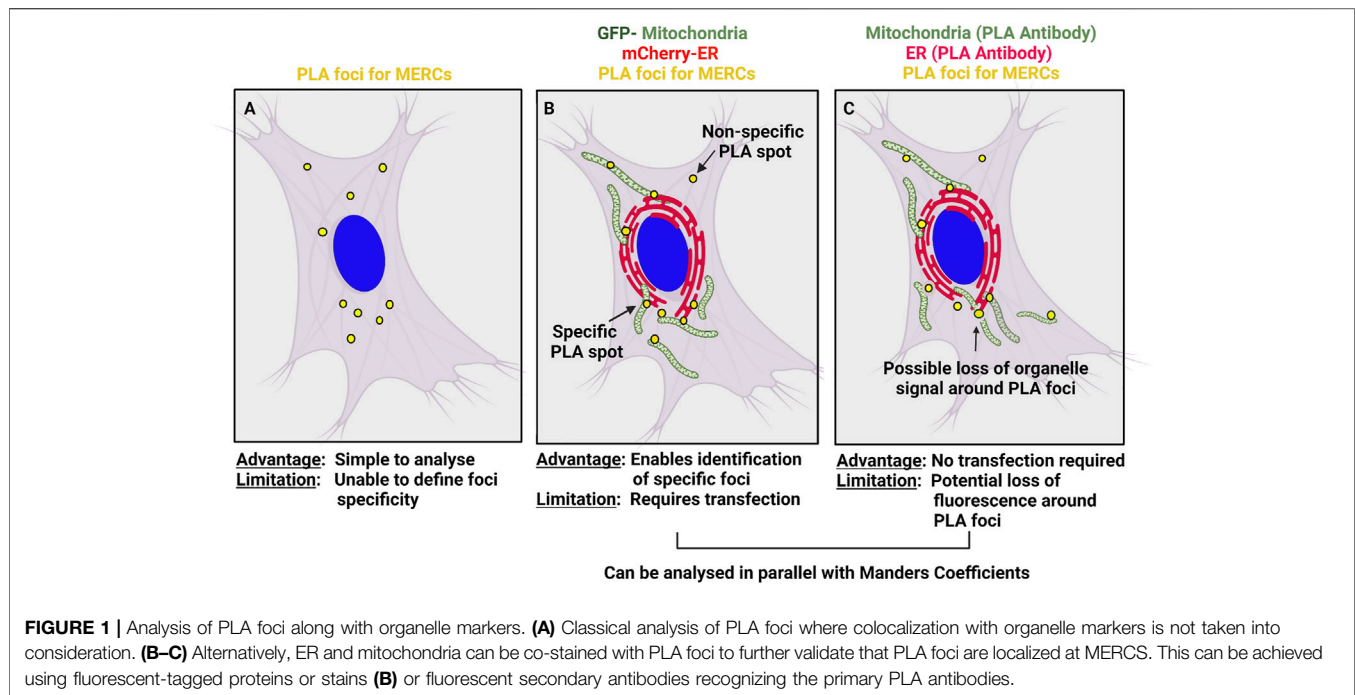
each fragment of the protein to a distinct organelle. Fluorescence is then observed at sites where the two organelles are in close proximity (MCS). In addition, because BiFC components have to assemble across membranes to be active, they can possibly promote MCS assembly.

In situ Proximity Ligation Assay

Most of the approaches cited above require the overexpression of tagged proteins which is not amenable to all experimental systems. In addition, the overexpressed proteins can potentially affect the behaviour of target organelles. A highly sensitive approach recently being used to investigate endogenous protein interactions is *in situ* Proximity Ligation Assay (PLA) (Söderberg et al., 2006). This is a probe-based method in which endogenous proteins of interest are targeted by primary antibodies, followed by secondary antibodies fused to oligonucleotides. When the proteins are in close proximity, there is complementary base pairing and the creation of circular DNA when a third oligonucleotide is added. The circular DNA can then be amplified and visualised using complementary fluorophore-labeled probes. PLA has a reported detection range of 40–60 nm, which is larger than the size of most MERCS. Nonetheless, this is greater than the resolution obtained by a typical fluorescence microscope and simple co-localisation analysis. The method's advantage are its robustness and relative simplicity, as commercial kits are accessible (Söderberg et al., 2006; Hegazy et al., 2020). PLA also has the advantage of not requiring the expression of tagged proteins. However, it cannot be used in live cells and is limited by the availability of good antibodies for the proteins of interest.

ER-Mitochondria Contact Assessment Using PLA

Though the PLA technique was established in 2006, its application in the investigation of MERCS emerged extensively in the last decade. ER-mitochondrial coupling was shown by PLA using several pairs of proteins (VDAC/IP3R, Grp75/IP3R, and CypD/IP3R) (Tubbs et al., 2014), while overexpression of VAPB (ER) and PTPIP51 (mitochondria) altered MERCS assembly, facilitating Ca^{2+} exchange and autophagy. (Gomez-Suaga et al., 2017). Furthermore, PLA has been widely utilized to study ER-mitochondria interactions in disease. Decreased MERCS were observed in cardiomyopathy caused by phospholamban p. Arg14del mutation (Cuello et al., 2021), in Charcot-Marie-Tooth type 2A (CMT2A, a dominant axonal form of peripheral neuropathy due to mutation in MFN2 (Bernard-Marissal et al., 2019)) and also in conditions such as amyotrophic lateral sclerosis and frontal dementia (ALS/FTD) due to defects in fused in sarcoma (FUS) (Stoica et al., 2016). In addition, overexpression of α -Synuclein, a protein that accumulates in patients with Parkinson's disease, disrupts binding between tethering proteins VAPB and PTPIP5 at MERCS (Paillusson et al., 2017). Overall, while supporting an important role for MERCS in cell physiology, the studies highlighted the usefulness of PLA in the study of MERCS.



Considerations for the Analysis of PLA Foci

PLA has several advantages: 1) It allows the measurement of endogenous proteins at MERCS. 2) It provides dual-binder specificity for detecting organelle contacts *in situ* and exposes protein proximity in normal cells without being influenced by overexpression artefacts. (Söderberg et al., 2006). 3) Because the *in-situ* PLA signal can be amplified, the approach is extremely sensitive, allowing transient and weak interactions to be viewed and quantified as a single spot; and 4) The tool itself and its analysis (by examining the number of interacting spots) is very simple to perform and may be used to test multiple conditions.

Nevertheless, PLA has several shortcomings in addition to requiring fixed cells. The common procedure for studying the interaction of organelles is to count the number of PLA spots (Figure 1A). However, while ER or mitochondrial structures are easy to identify by immunofluorescence, the foci produced by the PLA signal can potentially be difficult to separate from non-specific signal. Non-specific PLA signal can come from two sources, the PLA procedure itself and the primary antibodies used. Isotype antibody controls are usually used to detect background fluorescence related to the PLA procedure. Further, to avoid background signals created by non-bound probes in close vicinity, the concentration of proximity probes must be kept low (Weibrecht et al., 2010; Jalili et al., 2018).

A second approach to validate PLA spots is to stain the organelles of interest along with PLA foci (Figures 1B,C). This allows to colocalize PLA spots with sites of overlap between the two organelles (Alpy et al., 2013; Gomez-Suaga et al., 2017; Sharma et al., 2021), thus identifying real PLA foci and allowing further assessment of organelle colocalization using Mander's coefficients. Co-staining of PLA and organelles can be achieved by expressing fluorescently tagged

organelles markers, using fixable stains such as mitotracker or labelling the primary antibodies used for the PLA. A large array of ER- or mitochondria-targeted fluorescent proteins (GFP, mCherry, etc.) as well as some fixable mitochondria stains (mitotracker) are readily available and can be used to label organelles prior fixation and PLA (Figure 1B). However, it does require cells to be transfected, which is not always possible.

Alternatively, the primary antibodies chosen to produce PLA spots can simply be labeled with fluorescent secondary antibodies, which will allow visualization of the organelles in addition to PLA foci and thus facilitate colocalization studies (Figure 1C). However, the presence of the amplified circular DNA could locally prevent the recognition of the primary antibodies by the fluorescent secondary antibodies. Nonetheless, examining for the presence and absence of organelles in the vicinity of the signal location will ensure that the PLA spots correspond to true contact sites.

Obtaining a clear, distinct, and quantifiable PLA signal also requires using quality antibodies that bind only the organelles of interest without background staining. It is thus critical to validate the antibodies used for PLA by first co-marking them with proper mitochondrial or ER markers (antibodies of fluorescent proteins) and only use antibodies that show highly specific staining of the organelle of interest. The choice of good PLA antibodies for the detection of MERCS can also be extended to proteins present within the contact site but that do not necessarily form a tethering pair. This is because PLA defines the proximity of the proteins, not necessarily their physical interaction. This means that while most PLA studies use protein pairs that have been shown to physically interact (for example VDAC1-IP3R), other pairs including membrane proteins could also be selected based on different criteria (i.e. availability of good antibodies).

CONCLUSION

MERCs are signalling hubs consisting of structural components that play a critical role in a variety of pathways, ranging from the regulation of organelle homeostasis to a variety of cellular activities or signalling pathways, all of which ultimately affect cellular metabolism. In the last decade, the recognition of MERCS and more generally MCS as crucial controllers of cellular functions has led to the application of novel tools to study organelle interaction. These methods have significantly expedited recent developments in the field but come with their drawbacks. PLA in particular has the potential to simplify the quantification of MCS but requires careful validation of the antibodies used and the result. Ultimately, it is important to validate results using different approaches that investigate MERCS functions (like

calcium transport) or performing complementary biochemical, fluorescent, and EM approaches.

AUTHOR CONTRIBUTIONS

SB, AV, and PG structured and wrote the manuscript. MG guided, provided insights in writing the review and edited the manuscript.

FUNDING

This work was supported by a grant from the Natural Sciences and Engineering Research Council of Canada. PG is a recipient of a Queen Elizabeth II Diamond Jubilee scholarship and a Fonds du Québec-Santé scholarship.

REFERENCES

- Adler, J., and Parmryd, I. (2010). Quantifying Colocalization by Correlation: the Pearson Correlation Coefficient Is superior to the Mander's Overlap Coefficient. *Cytometry* 77A, 733–742. doi:10.1002/cyto.a.20896
- Almutawa, W., Smith, C., Sabouny, R., Smit, R. B., Zhao, T., Wong, R., et al. (2019). The R941L Mutation in MYH14 Disrupts Mitochondrial Fission and Associates with Peripheral Neuropathy. *EBioMedicine* 45, 379–392. doi:10.1016/j.ebiom.2019.06.018
- Alpy, F., Rousseau, A., Schwab, Y., Legueux, F., Stoll, L., Wendling, C., et al. (2013). STARD3 or STARD3NL and VAP Form a Novel Molecular Tether between Late Endosomes and the ER. *J. Cell Sci* 126, 5500–5512. doi:10.1242/jcs.139295
- Annuziata, I., Sano, R., and d'Azzo, A. (2018). Mitochondria-associated ER Membranes (MAMs) and Lysosomal Storage Diseases. *Cell Death Dis* 9, 328. doi:10.1038/s41419-017-0025-4
- Basso, V., Marchesan, E., Peggion, C., Chakraborty, J., Von Stockum, S., Giacomello, M., et al. (2018). Regulation of ER-Mitochondria Contacts by Parkin via Mfn2. *Pharmacol. Res.* 138, 43–56. doi:10.1016/j.phrs.2018.09.006
- Bernard-Marissal, N., Van Hameren, G., Juneja, M., Pellegrino, C., Louhivuori, L., Bartsaghi, L., et al. (2019). Altered Interplay between Endoplasmic Reticulum and Mitochondria in Charcot-Marie-Tooth Type 2A Neuropathy. *Proc. Natl. Acad. Sci. USA* 116, 2328–2337. doi:10.1073/pnas.1810932116
- Cohen, S., Valm, A. M., and Lippincott-Schwartz, J. (2018). Interacting Organelles. *Curr. Opin. Cell Biol.* 53, 84–91. doi:10.1016/j.cob.2018.06.003
- Copeland, D. E., and Dalton, A. J. (1959). An Association between Mitochondria and the Endoplasmic Reticulum in Cells of the Pseudobranch Gland of a Teleost. *J. Biophys. Biochem. Cytol.* 5, 393–396. doi:10.1083/jcb.5.3.393
- Cosson, P., Marchetti, A., Ravazzola, M., and Orci, L. (2012). Mitofusin-2 Independent Juxtaposition of Endoplasmic Reticulum and Mitochondria: an Ultrastructural Study. *PLoS One* 7, e46293. doi:10.1371/journal.pone.0046293
- Cuello, F., Knaust, A., Saleem, U., Loos, M., Raabe, J., Mosqueira, D., et al. (2021). Impairment of the ER/mitochondria compartment in human cardiomyocytes with PLN p.Arg14del mutation. *EMBO Mol. Med.* 13, e13074. doi:10.15252/emmm.202013074
- De Brito, O. M., and Scorrano, L. (2008). Mitofusin 2 Tethers Endoplasmic Reticulum to Mitochondria. *Nature* 456, 605–610. doi:10.1038/nature07534
- Dennis, E. A., and Kennedy, E. P. (1972). Intracellular Sites of Lipid Synthesis and the Biogenesis of Mitochondria. *J. Lipid Res.* 13, 263–267. doi:10.1016/s0022-2275(20)39421-9
- Dunn, K. W., Kamocka, M. M., and McDonald, J. H. (2011). A Practical Guide to Evaluating Colocalization in Biological Microscopy. *Am. J. Physiology-Cell Physiol.* 300, C723–C742. doi:10.1152/ajpcell.00462.2010
- Eisenberg-Bord, M., Shai, N., Schuldiner, M., and Bohnert, M. (2016). A Tether Is a Tether: Tethering at Membrane Contact Sites. *Dev. Cell* 39, 395–409. doi:10.1016/j.devcel.2016.10.022
- Eysert, F., Kinoshita, P., Mary, A., Vaillant-Beuchot, L., Checler, F., and Chami, M. (2020). Molecular Dysfunctions of Mitochondria-Associated Membranes (MAMs) in Alzheimer's Disease. *Int. J. Mol. Sci.* 21, 9521. doi:10.3390/ijms21249521
- Filadi, R., Greotti, E., Turacchio, G., Luini, A., Pozzan, T., and Pizzo, P. (2015). Mitofusin 2 Ablation Increases Endoplasmic Reticulum-Mitochondria Coupling. *Proc. Natl. Acad. Sci. USA* 112, E2174–E2181. doi:10.1073/pnas.1504880112
- Friedman, J. R., Lackner, L. L., West, M., Dibenedetto, J. R., Nunnari, J., and Voeltz, G. K. (2011). ER Tubules Mark Sites of Mitochondrial Division. *Science* 334, 358–362. doi:10.1126/science.1207385
- Gao, P., Yang, W., and Sun, L. (2020). Mitochondria-Associated Endoplasmic Reticulum Membranes (MAMs) and Their Prospective Roles in Kidney Disease. *Oxid. Med. Cell Longev* 2020, 3120539. doi:10.1155/2020/3120539
- Giamogante, F., Barazzuol, L., Brini, M., and Cali, T. (2020). ER-mitochondria Contact Sites Reporters: Strengths and Weaknesses of the Available Approaches. *Int. J. Mol. Sci.* 21, 8157. doi:10.3390/ijms21218157
- Gomez-Suaga, P., Paillusson, S., Stoica, R., Noble, W., Hanger, D. P., and Miller, C. J. (2017). The ER-Mitochondria Tethering Complex VAPB-PTPIP51 Regulates Autophagy. *Curr. Biol.* 27, 371–385. doi:10.1016/j.cub.2016.12.038
- Hegazy, M., Cohen-Barak, E., Koetsier, J., Najor, N., Arvanitis, C., Sprecher, E., et al. (2020). Proximity Ligation Assay for Detecting Protein-Protein Interactions and Protein Modifications in Cells and Tissues *In Situ*. *Curr. Protoc. Cell Biol.* 89, e115. doi:10.1002/cpcb.115
- Howard, V. R. M. (2004). *Unbiased Stereology: Three-Dimensional Measurement in Microscopy*. New York, NY, USA: Garland Science.
- Huang, X., Jiang, C., Yu, L., and Yang, A. (2020). Current and Emerging Approaches for Studying Inter-organelle Membrane Contact Sites. *Front. Cell Dev. Biol.* 8, 195. doi:10.3389/fcell.2020.00195
- Jalili, R., Horecka, J., Swartz, J. R., Davis, R. W., and Persson, H. H. J. (2018). Streamlined Circular Proximity Ligation Assay Provides High Stringency and Compatibility with Low-Affinity Antibodies. *Proc. Natl. Acad. Sci. USA* 115, E925–E933. doi:10.1073/pnas.1718283115
- Jung, M., and Mun, J. Y. (2019). Mitochondria and Endoplasmic Reticulum Imaging by Correlative Light and Volume Electron Microscopy. *J. Vis. Exp* 149, e59750. doi:10.3791/59750
- Kisby, G. E., Fry, R. C., Lasarev, M. R., Bammler, T. K., Beyer, R. P., Churchwell, M., et al. (2011). The Cycad Genotoxin MAM Modulates Brain Cellular Pathways Involved in Neurodegenerative Disease and Cancer in a DNA Damage-Linked Manner. *PLoS One* 6, e20911. doi:10.1371/journal.pone.0020911
- Krols, M., Bultynck, G., and Janssens, S. (2016). ER-mitochondria Contact Sites: A New Regulator of Cellular Calcium Flux Comes into Play. *J. Cell Biol* 214, 367–370. doi:10.1083/jcb.201607124
- Lam, J., Katti, P., Biete, M., Mungai, M., Ashshareef, S., Neikirk, K., et al. (2021). A Universal Approach to Analyzing Transmission Electron Microscopy with ImageJ. *Cells* 10, 2177. doi:10.3390/cells10092177

- López-Crisosto, C., Bravo-Sagua, R., Rodríguez-Peña, M., Mera, C., Castro, P. F., Quest, A. F. G., et al. (2015). ER-to-mitochondria Miscommunication and Metabolic Diseases. *Biochim. Biophys. Acta (Bba) - Mol. Basis Dis.* 1852, 2096–2105. doi:10.1016/j.bbdis.2015.07.011
- Martinvalet, D. (2018). The Role of the Mitochondria and the Endoplasmic Reticulum Contact Sites in the Development of the Immune Responses. *Cel Death Dis* 9, 336. doi:10.1038/s41419-017-0237-7
- Missiroli, S., Patergnani, S., Caroccia, N., Pedriali, G., Perrone, M., Prevati, M., et al. (2018). Mitochondria-associated Membranes (MAMs) and Inflammation. *Cel Death Dis* 9, 329. doi:10.1038/s41419-017-0027-2
- Naon, D., Zaninello, M., Giacomello, M., Varanita, T., Grespi, F., Lakshminarayanan, S., et al. (2016). Critical Reappraisal Confirms that Mitofusin 2 Is an Endoplasmic Reticulum-Mitochondria Tether. *Proc. Natl. Acad. Sci. USA* 113, 11249–11254. doi:10.1073/pnas.1606786113
- Paillusson, S., Gomez-Suaga, P., Stoica, R., Little, D., Gissen, P., Devine, M. J., et al. (2017). α -Synuclein Binds to the ER-Mitochondria Tethering Protein VAPB to Disrupt Ca^{2+} Homeostasis and Mitochondrial ATP Production. *Acta Neuropathol.* 134, 129–149. doi:10.1007/s00401-017-1704-z
- Patergnani, S., Suski, J. M., Agnoletto, C., Bononi, A., Bonora, M., De Marchi, E., et al. (2011). Calcium Signaling Around Mitochondria Associated Membranes (MAMs). *Cell Commun Signal* 9, 19. doi:10.1186/1478-811x-9-19
- Perrone, M., Caroccia, N., Genovese, I., Missiroli, S., Modesti, L., Pedriali, G., et al. (2020). The Role of Mitochondria-Associated Membranes in Cellular Homeostasis and Diseases. *Int. Rev. Cel Mol Biol* 350, 119–196. doi:10.1016/b.sircmb.2019.11.002
- Pfleger, K. D. G., and Eidne, K. A. (2006). Illuminating Insights into Protein-Protein Interactions Using Bioluminescence Resonance Energy Transfer (BRET). *Nat. Methods* 3, 165–174. doi:10.1038/nmeth841
- Pinton, P. (2018). Mitochondria-associated Membranes (MAMs) and Pathologies. *Cel Death Dis* 9, 413. doi:10.1038/s41419-018-0424-1
- Rizzuto, R., Pinton, P., Carrington, W., Fay, F. S., Fogarty, K. E., Lifshitz, L. M., et al. (1998). Close Contacts with the Endoplasmic Reticulum as Determinants of Mitochondrial Ca^{2+} Responses. *Science* 280, 1763–1766. doi:10.1126/science.280.5370.1763
- Rodríguez-Arribas, M., Yakhine-Diop, S. M. S., Pedro, J. M. B.-S., Gómez-Suaga, P., Gómez-Sánchez, R., Martínez-Chacón, G., et al. (2017). Mitochondria-Associated Membranes (MAMs): Overview and its Role in Parkinson's Disease. *Mol. Neurobiol.* 54, 6287–6303. doi:10.1007/s12035-016-0140-8
- Schrader, M., Godinho, L. F., Costello, J. L., and Islinger, M. (2015). The Different Facets of Organelle Interplay-An Overview of Organelle Interactions. *Front. Cel Dev. Biol.* 3, 56. doi:10.3389/fcell.2015.00056
- Scorrano, L., De Matteis, M. A., Emr, S., Giordano, F., Hajnóczky, G., Kornmann, B., et al. (2019). Coming Together to Define Membrane Contact Sites. *Nat. Commun.* 10, 1287. doi:10.1038/s41467-019-09253-3
- Sharma, G., Saubouny, R., Joel, M. M., Martens, K., Martino, D., De Koning, A. P. J., et al. (2021). Characterization of a Novel Variant in the HR1 Domain of MFN2 in a Patient with Ataxia, Optic Atrophy and Sensorineural Hearing Loss [version 1; peer review: 2 approved with reservations]. *F1000Research* 10 606 doi:10.12688/f1000research.53230.1
- Shrestha, D., Jenei, A., Nagy, P., Vereb, G., and Szöllösi, J. (2015). Understanding FRET as a Research Tool for Cellular Studies. *Ijms* 16, 6718–6756. doi:10.3390/ijms16046718
- Simmen, T., and Tagaya, M. (2017). Organelle Communication at Membrane Contact Sites (MCS): From Curiosity to Center Stage in Cell Biology and Biomedical Research. *Adv. Exp. Med. Biol.* 997, 1–12. doi:10.1007/978-981-10-4567-7_1
- Söderberg, O., Gullberg, M., Jarvius, M., Ridderstråle, K., Leuchowius, K.-J., Jarvius, J., et al. (2006). Direct Observation of Individual Endogenous Protein Complexes *In Situ* by Proximity Ligation. *Nat. Methods* 3, 995–1000. doi:10.1038/nmeth947
- Stoica, R., Paillusson, S., Gomez-Suaga, P., Mitchell, J. C., Lau, D. H., Gray, E. H., et al. (2016). ALS/FTD-associated FUS Activates GSK-3 β to Disrupt the VAPB - PTPIP 51 Interaction and ER -mitochondria Associations. *EMBO Rep.* 17, 1326–1342. doi:10.15252/embr.201541726
- Tubbs, E., and Rieusset, J. (2017). Metabolic Signaling Functions of ER-Mitochondria Contact Sites: Role in Metabolic Diseases. *J. Mol. Endocrinol.* 58, R87–R106. doi:10.1530/jme-16-0189
- Tubbs, E., Theurey, P., Vial, G., Bendridi, N., Bravard, A., Chauvin, M.-A., et al. (2014). Mitochondria-associated Endoplasmic Reticulum Membrane (MAM) Integrity Is Required for Insulin Signaling and Is Implicated in Hepatic Insulin Resistance. *Diabetes* 63, 3279–3294. doi:10.2337/db13-1751
- Weibrecht, I., Leuchowius, K.-J., Clausson, C.-M., Conze, T., Jarvius, M., Howell, W. M., et al. (2010). Proximity Ligation Assays: a Recent Addition to the Proteomics Toolbox. *Expert Rev. Proteomics* 7, 401–409. doi:10.1586/epr.10.10
- Xu, L., Wang, X., and Tong, C. (2020). Endoplasmic Reticulum-Mitochondria Contact Sites and Neurodegeneration. *Front. Cel Dev. Biol.* 8, 428. doi:10.3389/fcell.2020.00428
- Yang, Z., Zhao, X., Xu, J., Shang, W., and Tong, C. (2018). A Novel Fluorescent Reporter Detects Plastic Remodeling of Mitochondria-ER Contact Sites. *J. Cel Sci* 131, jcs208686. doi:10.1242/jcs.208686

Conflict of Interest: The authors declare that the research was conducted in the absence of any commercial or financial relationships that could be construed as a potential conflict of interest.

Publisher's Note: All claims expressed in this article are solely those of the authors and do not necessarily represent those of their affiliated organizations, or those of the publisher, the editors and the reviewers. Any product that may be evaluated in this article, or claim that may be made by its manufacturer, is not guaranteed or endorsed by the publisher.

Copyright © 2021 Benhammouda, Vishwakarma, Gatti and Germain. This is an open-access article distributed under the terms of the Creative Commons Attribution License (CC BY). The use, distribution or reproduction in other forums is permitted, provided the original author(s) and the copyright owner(s) are credited and that the original publication in this journal is cited, in accordance with accepted academic practice. No use, distribution or reproduction is permitted which does not comply with these terms.



5-Hydroxymethylfurfural Alleviates Inflammatory Lung Injury by Inhibiting Endoplasmic Reticulum Stress and NLRP3 Inflammasome Activation

Hang Zhang^{1,2,3,4}, Zheyi Jiang⁵, Chuanbin Shen¹, Han Zou¹, Zhiping Zhang¹, Kaitao Wang¹, Renren Bai^{2,3,4,6}, Yanhua Kang^{1*}, Xiang-Yang Ye^{2,3,4,6*} and Tian Xie^{2,3,4,6*}

¹School of Basic Medical Science, Hangzhou Normal University, Hangzhou, China, ²School of Pharmacy, Hangzhou Normal University, Hangzhou, China, ³Key Laboratory of Elemene Class Anti-cancer Chinese Medicine of Zhejiang Province, Hangzhou Normal University, Hangzhou, China, ⁴Engineering Laboratory of Development and Application of Traditional Chinese Medicine from Zhejiang Province, Hangzhou Normal University, Hangzhou, China, ⁵Department of Cardiology, Shanghai Ninth People's Hospital, Shanghai Jiaotong University School of Medicine, Shanghai, China, ⁶Collaborative Innovation Center of Traditional Chinese Medicines from Zhejiang Province, Hangzhou Normal University, Hangzhou, China

OPEN ACCESS

Edited by:

Yongye Huang,
Northeastern University, China

Reviewed by:

Tao Zhang,
Anhui Agricultural University, China
Xiaonan Zhang,
Bengbu Medical College, China

*Correspondence:

Yanhua Kang
20117024@hznu.edu.cn
Xiang-Yang Ye
xyye@hznu.edu.cn
Tian Xie
xbs@dljg.sina.net

Specialty section:

This article was submitted to
Signaling,
a section of the journal
Frontiers in Cell and Developmental
Biology

Received: 24 September 2021

Accepted: 26 November 2021

Published: 13 December 2021

Citation:

Zhang H, Jiang Z, Shen C, Zou H,
Zhang Z, Wang K, Bai R, Kang Y,
Ye X-Y and Xie T (2021) 5-
Hydroxymethylfurfural Alleviates
Inflammatory Lung Injury by Inhibiting
Endoplasmic Reticulum Stress and
NLRP3 Inflammasome Activation.
Front. Cell Dev. Biol. 9:782427.
doi: 10.3389/fcell.2021.782427

5-Hydroxymethylfurfural (5-HMF) is a common reaction product during heat processing and the preparation of many types of foods and Traditional Chinese Medicine formulations. The aim of this study was to evaluate the protective effect of 5-HMF on endotoxin-induced acute lung injury (ALI) and the underlying mechanisms. Our findings indicate that 5-HMF attenuated lipopolysaccharide (LPS)-induced ALI in mice by mitigating alveolar destruction, neutrophil infiltration and the release of inflammatory cytokines. Furthermore, the activation of macrophages and human monocytes in response to LPS was remarkably suppressed by 5-HMF *in vitro* through inhibiting the NF- κ B signaling pathway, NLRP3 inflammasome activation and endoplasmic reticulum (ER) stress. The inhibitory effect of 5-HMF on NLRP3 inflammasome was reversed by overexpressing ATF4 or CHOP, indicating the involvement of ER stress in the negative regulation of 5-HMF on NLRP3 inflammasome-mediated inflammation. Consistent with this, the ameliorative effect of 5-HMF on *in vivo* pulmonary dysfunction were reversed by the ER stress inducer tunicamycin. In conclusion, our findings elucidate the anti-inflammatory and protective efficacy of 5-HMF in LPS-induced acute lung injury, and also demonstrate the key mechanism of its action against NLRP3 inflammasome-related inflammatory disorders via the inhibition of ER stress.

Keywords: 5-hydroxymethylfurfural, acute lung injury, NLRP3 inflammasome, endoplasmic reticulum stress, inflammation

INTRODUCTION

Acute lung injury (ALI) is a debilitating disease characterized by severe pulmonary lung inflammation and air leak in the upper lobe, which typically lead to hypoxemic respiratory failure in critically ill patients (Moazed and Calfee, 2014). Multiple endogenous inflammatory mediators and exogenous agents can trigger inflammatory response and vascular leak in the lungs (Wu et al., 2018), including pneumonia and pulmonary contusion sepsis, inhalation of noxious gases, and reperfusion (Moazed and Calfee, 2014). Lipopolysaccharide (LPS, also known as endotoxin) is

the major toxic component present in the outer membrane of Gram-negative bacteria that causes considerable tissue injury and accelerates ALI pathogenesis (Xu et al., 2014; Kim et al., 2015a). It is a typical macrophage activator that stimulates the innate immune system through multiple downstream signaling pathways (Xu et al., 2014). Given the lack of effective drugs against ALI, it is crucial to develop novel therapeutic strategies and explore the molecular pharmacological mechanisms.

LPS-induced ALI is mediated by proinflammatory cytokines and mediators such as nitric oxide (NO), interleukin-6 (IL-6), tumor necrosis factor- α (TNF- α), IL-1 β and IL-8, which are produced by the alveolar macrophages (Wu et al., 2018) following activation of the mitogen activated protein kinases (MAPK) and NF- κ B signaling pathways (Xu et al., 2014; Kim et al., 2015a). LPS is recognized by toll-like receptor 4 (TLR4) that is expressed on the cell membrane of various immune cells (Lu et al., 2008), and the ensuing stimulation of TLR4 activates the NF- κ B and MAPKs (ERK, JNK and p38 kinases) signaling pathways. Therefore, inhibiting these pathways may alleviate LPS-induced inflammation and pulmonary dysfunction.

Studies show that the nucleotide-binding domain (NOD)-like receptor protein 3 (NLRP3) inflammasome plays a pivotal role in the pathogenesis of ALI. The NLRP3 inflammasome is a protein complex consisting of NLRP3, pro-caspase-1 and apoptosis-associated speck-like protein containing a C-terminal caspase recruitment domain (ASC). ASC promotes activation of the NLRP3 inflammasome (Lamkanfi et al., 2010) by mediating caspase-1 maturation. The activated caspase-1 cleaves pro-IL-1 β and pro-IL-18 to their respective mature forms, eventually triggering cytokine secretion and inflammatory responses (Compan et al., 2015). Since inactivation of NLRP3 inflammasome has been shown to protect against hyperoxia-induced ALI (Fukumoto et al., 2013), NLRP3 inflammasome may be a viable target for developing potential candidate drugs to treat ALI.

Endoplasmic reticulum (ER) stress is a process wherein misfolded or unfolded proteins accumulate in the ER and trigger the unfolded protein response (UPR). In mammalian cells, ER stress involves three signaling cascades mediated by pancreatic endoplasmic reticulum kinase (PERK), inositol-requiring enzyme 1 (IRE1) and activating transcription factor 6 (ATF6), which is activated by the ER chaperone glucose regulated protein 78 (GRP78). These UPR sensors regulate multiple downstream components, such as the alternative mRNA splicing of X-box binding protein 1 (XBP1), and the expression of eukaryotic translation initiation factor 2 subunit alpha (eIF2 α) and C/EBP-homologous protein (CHOP), which upregulate several target genes to restore ER homeostasis (Zhang and Kaufman, 2008). There is evidence indicating that ER stress is involved in LPS-induced lung inflammation and ALI. For instance, the ER stress components GRP78 and CHOP are upregulated in an LPS-induced ALI rodent model (Kim et al., 2013). In addition, stimulation of the alveolar epithelial cell line A549 with LPS enhanced PERK and eIF2 α phosphorylation, and the nuclear translocation of ATF4 (Ye et al., 2015). Studies increasingly show that ER stress is associated with the activation of NLRP3 inflammasome, and its suppression can

inactivate the NLRP3 inflammasome (Oslowski et al., 2012). In addition, inhibition of ER stress can attenuate LPS-induced ALI *in vivo* and *in vitro* (Kim et al., 2015b; Zeng et al., 2017). Taken together, the ER stress pathway is a promising therapeutic target in NLRP3 inflammasome-related inflammatory diseases.

Common heterocyclic Maillard reaction of sugars at high temperatures produces 5-hydroxymethylfurfural (5-HMF, **Figure 1A**), a furan-containing aldehyde which is present in various sacchariferous foods such as honey, coffee, fruit juices, dried fruits and baked foods that typically undergo thermal processing and long-term storage (Anese et al., 2013; Zirbes et al., 2013). 5-HMF has also been detected in various heat-processed Traditional Chinese Medicine (TCM) formulations including black garlic extracts (Kim et al., 2011) and *Codonopsis pilosula* (Feng et al., 2017). Studies have reported antioxidant (Zhao et al., 2013), anti-proliferative (Zhao et al., 2013) and cardioprotective effects (Wölkart et al., 2017) of 5-HMF. In addition, 5-HMF protects against alcoholic liver oxidative injury (Li et al., 2015), and exerts an anti-inflammatory effect on human umbilical vein endothelial cells (Kim et al., 2011) and LPS-stimulated RAW 264.7 macrophages (Kong et al., 2019). However, no study so far has reported a therapeutic role of 5-HMF in ALI. In this study, we analyzed the protective effect of 5-HMF against lung inflammation and injury, and found that 5-HMF inhibited the TLR-driven inflammatory response in macrophages by inactivating the NF- κ B signaling pathway. Moreover, 5-HMF treatment significantly inhibited NLRP3 inflammasome activation in LPS-primed macrophages in response to ATP or nigericin stimulation. ER stress was identified as the central signaling cascade regulated by 5-HMF in LPS-stimulated macrophages, which was essential for its inhibitory effect on NLRP3 inflammasome activation. Our data suggests that 5-HMF suppresses the LPS-induced inflammatory response by blocking the NF- κ B/NLRP3 inflammasome cascade through attenuation of ER stress. These findings provide insights into the mechanisms underlying the potential therapeutic effect of 5-HMF in ALI and related diseases.

MATERIALS AND METHODS

Reagents and Antibodies

5-HMF (purity >99.5%), LPS (055:B5), Griess reagent, 4', 6-diamidino-2-phenylindole (DAPI) and Fluo-3 AM were purchased from Sigma-Aldrich Co. (St. Louis, MO, United States). The anti- β -actin antibody (A5441) was purchased from Sigma Aldrich (St. Louis, MO, United States). Antibodies against NLRP3 (#15101), mouse IL-1 β (#12242), human IL-1 β (#12703), mouse ASC (#67824), human ASC (#13833), GPR78 (#3177), ATF4 (#11815), CHOP (#2895, for western blotting), eIF2 α (#5324), phosphorylated eIF α (#3398) and PERK (#3192) were purchased from Cell Signaling Technology (Danvers, MA, United States). Antibodies against phosphorylated PERK (PA5-40294) and CHOP (MA5-32571, for immunohistochemistry) were purchased from Invitrogen (Carlsbad, CA, United States), and those specific for caspase-1 (ab179515), IRE1 α (ab37073) and phosphorylated IRE1 α

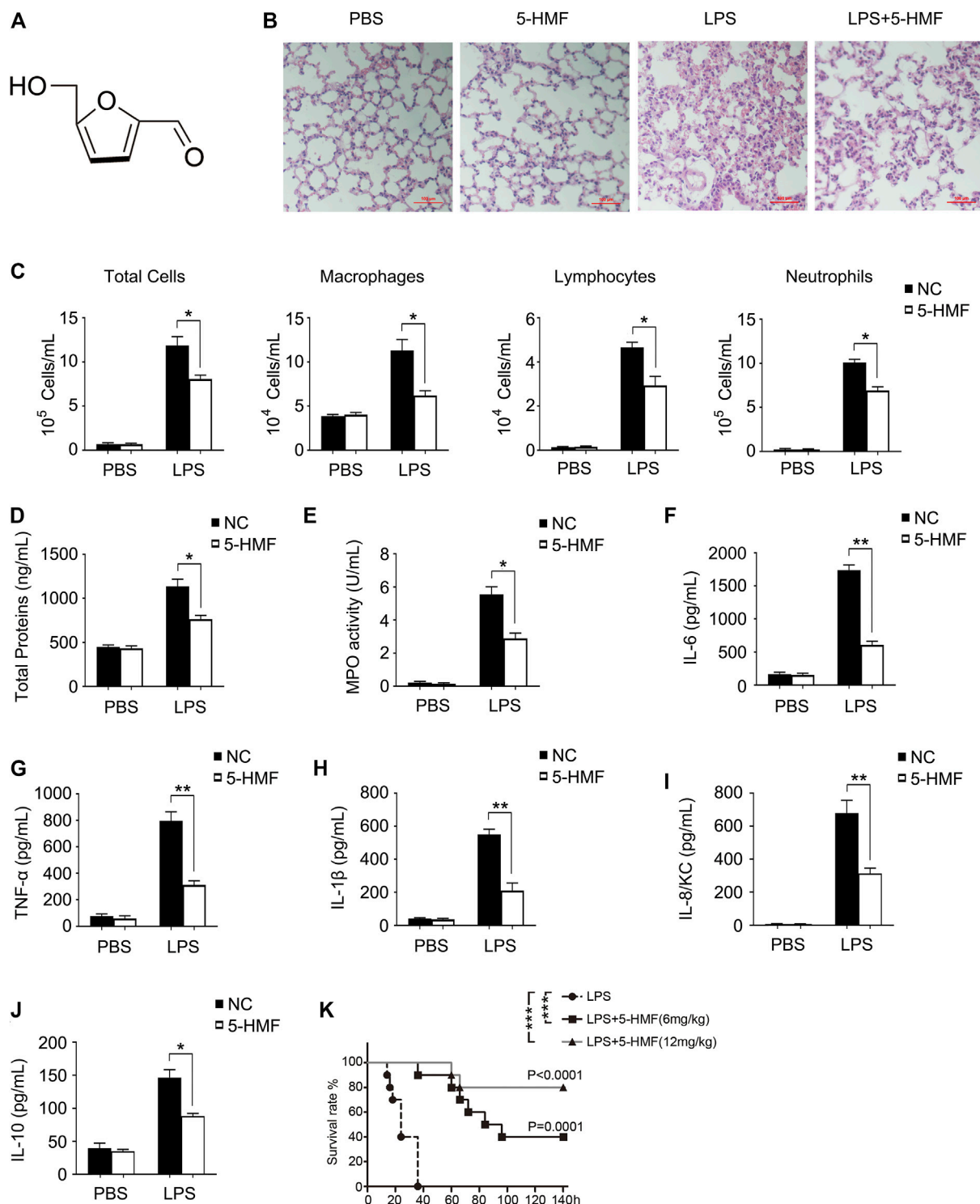


FIGURE 1 | 5-HMF attenuates organ damage, serum cytokine secretion and mortality in LPS-challenged mice. **(A)** Chemical structure of 5-HMF. **(B–J)** C57BL/6J mice (5 mice/group) pretreated with 5-HMF (12 mg/kg, i. p.) or PBS were injected intraperitoneally with LPS (1 mg/kg) or PBS. **(B)** Representative images of H&E stained lung tissue sections from the indicated groups (x200). Scale bar, 100 μ m. **(C)** Cellular changes in BALF. **(D)** Protein content in BALF. **(E)** MPO activity of lung tissues. **(F–J)** Serum levels of IL-6 **(F)**, TNF- α **(G)**, IL-1 β **(H)**, IL-8/KC **(I)** and IL-10 **(J)**. All results are expressed as the mean \pm SD. * and ** indicate $p < 0.05$ and $p < 0.01$ respectively by Student's t-test. **(K)** Kaplan–Meier survival plots of C57BL/6J mice (10 mice/group) injected intraperitoneally with LPS (25 mg/kg). Survival status was recorded for 6 days and data were analyzed using the Log-Rank test ($n = 10$ mice per group; ** $p < 0.01$).

(ab48187) were purchased from Abcam (Cambridge, UK). DyLight488-conjugated anti-rabbit IgG, horseradish peroxidase (HRP)-conjugated goat anti-mouse IgG and HRP-conjugated goat anti-rabbit IgG antibodies were purchased from MultiSciences Biotech (Hangzhou, China).

Animals and Experimental Protocol

C57BL/6J mice (6–8 weeks old, weighing 20 ± 3 g, male) were purchased from SLAC Laboratory Experimental Animal Co. (Shanghai, China) and housed at the Animal Center of Hangzhou Normal University. All animal experiments were approved by the ethics committee for Animal Care and the Use of Laboratory Animals, Hangzhou Normal University. To assess the effect of 5-HMF on LPS-induced septic shock, the mice were randomly divided into the PBS control, 5-HMF, LPS and LPS+5-HMF groups ($n = 5$ each). The mice were injected intraperitoneally with 200 μ L PBS or 100 μ L 12 mg/kg 5-HMF as appropriate, followed by 100 μ L PBS or LPS (1 mg/kg) i. p. after 1 h. The mice were sacrificed 16 h after the LPS challenge, and blood sera, broncho-alveolar lavage fluid (BALF) and lung tissues were harvested for further analysis of cytokine production, cell infiltration and MPO activity in BALF, and histological staining. The cytokines level in sera and the MPO activity were measured by ELISA. For cell differentials examination, total cell numbers were counted with a Nucleocounter (Thermo Fisher). Smears of BALF cells were prepared by cytospin, and stained with Diff-Quik solution (Saint-bio co., Shanghai, China) to examine cell differentials. To determine the role of ER stress in the above model, tunicamycin (TM)-treated groups were also included. The mice were randomly divided into the PBS control, LPS, LPS+5-HMF, LPS+5-HMF + TM and LPS + TM ($n = 5$ each). The mice were injected with PBS/5-HMF as described, and 0.2 mg/kg TM was injected i. p. 1 h before LPS induction. The mice were sacrificed 16 h after the LPS challenge, and samples were collected for the followed examinations as above.

For survival analysis, the mice were injected with 5-HMF (6 or 12 mg/kg, i. p.) or PBS, followed by LPS (25 mg/kg), and the survival statuses of each group was recorded at different time points as described previously (Kang et al., 2018).

Cell Culture

The BMDMs were isolated from C57BL/6J mice as previously described (Kang et al., 2018). Briefly, the bone marrow was flushed out from the femurs and centrifuged at 1,000 rpm for 5 min. The harvested cells were resuspended and cultured in Dulbecco's Modified Eagle Medium (DMEM, Life Technologies) supplemented with 10% (v/v) heat-inactivated FBS and 20% conditioned medium of L929 cells. The cells were harvested 6 days later for subsequent experiments. The THP-1 and RAW264.7 cell lines were obtained from the American Type Culture Collection (ATCC, Manassas, VA). THP-1 cells were cultured in RPMI-1640 supplemented with 10% heat-inactivated FBS and 50 μ M 2-mercaptoethanol, and differentiated into macrophages by incubating with 10 ng/ml PMA for 16 h. RAW264.7 was cultured in DMEM with 10% (v/v) heat-inactivated FBS. All cells were maintained at 37°C in a humidified incubator under 5% CO₂.

Cell Viability Assay

The viability of the suitably treated cells was determined using the CellTiter 96 Aqueous Non-Radioactive Cell Proliferation Assay kit (MTS; Promega, Madison, WI, United States) (Lou et al., 2021). The cells were seeded into 96-well microplates and treated with 0, 5, 10, 25, 50 and 100 μ g/ml 5-HMF for 48 h. After adding 20 μ L MTS reagent per well, the cells were further incubated for 2 h. The absorbance of each well was measured at 490 nm and the inhibition rate was calculated from three independent experiments.

Ribonucleic Acid Isolation, Real Time-Polymerase Chain Reaction and Quantitative Real Time Polymerase Chain Reaction

RNA was isolated from the cells using TRIzol reagent (Invitrogen, Carlsbad, CA) according to the manufacturer's instructions. Complementary DNA (cDNA) was synthesized from 0.5 μ g total RNA by reverse transcriptase (Takara, Dalian, China). SYBR Green PCR Master Mix (Bio-Rad) was used for quantitative real time PCR, and relative gene expression levels were determined with the $\Delta\Delta$ Ct method using GAPDH as the endogenous control. The following primers were used: mouse IL-6 forward 5'-CTGCAAGAGACTTCCATCCAG-3' and reverse 5'-AGTGCATCATCGTTGTTTCATAC-3'; human IL-6 forward 5'-ACTCACCTCTTCAGAACGAATTG-3' and reverse 5'-CCA TCTTTGGAAGGTTTCAGGTTG-3'; mouse TNF- α forward 5'-AAGGCCGGGGTGTCCTGGAG-3' and reverse 5'-AGGCCA GGTGGGGACAGCTC-3'; human TNF- α forward 5'-GAG GCCAAGCCCTGGTATG-3' and reverse 5'-CGGGCCGAT TGATCTCAGC-3'; mouse IL-1 β forward 5'-AACCTCACC TACAGGGCGGACTTCA-3' and reverse 5'-TGTAATGAA AGACGGCACACC-3'; human IL-1 β forward 5'-ATGATG GCTTATTACAGTGGCAA-3' and reverse 5'-GTCGGAGAT TCGTAGCTGGA-3'; mouse inducible nitric oxide synthase (iNOS) forward 5'-GTTCTCAGCCCAACAATACAAGA-3' and reverse 5'-GTGGACGGGTCGATGTCAC-3' human iNOS forward 5'-AGGGACAAGCCTACCCCTC-3' and reverse 5'-CTCATCTCCCCTCAGTTGGT-3' mouse IL-10 forward 5'-CTTACTGACTGGCATGAGGATCA-3' and reverse 5'-GCA GCTCTAGGAGCATGTGG-3'; human IL-10 forward 5'-CTT ACTGACTGGCATGAGGATCA-3' and reverse 5'-TCACAT GCGCCTTGATGTCTG-3'; mouse C-X-C motif chemokine ligand 1 (Cxcl1) forward 5'-TGAGAGTGATTGAGAGTG GAC-3' and reverse 5'-AACCCTCTGCACCCAGTTTTC-3'; mouse CHOP forward 5'-AAGCCTGGTATGAGGATCTGC-3' and reverse 5'-TTCCTGGGGATGAGATATAGGTG-3'; mouse GPR78 forward 5'-ACTTGGGGACCACCTATTCCT-3' and reverse 5'-GTTGCCCTGATCGTTGGCTA-3'; mouse GAPDH forward 5'-AGGTCGGTGTGAACGGATTG-3' and reverse 5'-TGTAGACCATGTAGTTGAGGTCA-3'; human GAPDH forward 5'-GGAGTCAACGGATTGTTG-3' and reverse 5'-GTGATGGGATTTCATTGAT-3'.

To evaluate relative expression levels of XBP1u/XBP1s, RT-PCR analysis was performed using Primerstar PCR Mix (Takara) as described previously (Mimura et al., 2012). Murine XBP1

primer sequences were as follows: forward 5'-ACACGCTTG GGAATGGACAC-3' and reverse 5'-CCATGGGAAGATGTT CTGGG-3'. GAPDH was used as a loading control and PCR products were analyzed on a 3.5% agarose gel.

Detection of Myeloperoxidase Levels, Enzyme-Linked Immunosorbent Assay and Western Blotting

Lung myeloperoxidase (MPO) levels were determined using mouse MPO ELISA kit (Hycult Biotech) according to the manufacturer's instructions (Yu et al., 2014). The levels of different cytokines in the culture supernatants and sera were measured using specific ELISA kits according to the manufacturer's instructions. ELISA kits for murine and human IL-6 and TNF- α were purchased from Invitrogen (Carlsbad, CA), ELISA kits for murine and human IL-1 β were purchased from R&D Systems (Minneapolis, MN), ELISA kits for murine and human IL-10, murine KC/IL-8 and human IL-10 were purchased from Neobioscience (Shenzhen, China). For western blotting, equivalent amounts of protein were separated by SDS-PAGE, transferred to polyvinylidene fluoride membranes, and incubated with specific antibodies to analyze the specific protein levels as described previously (Dong et al., 2020).

Over Expression of ATF4 and CHOP in BMDMs

Murine ATF4 and CHOP mRNAs were transfected into the BMDMs following the procedure described by Herb et al. (2019). The total mRNA of the BMDMs were reverse transcribed into cDNAs using a Reverse Transcription kit (Takara), and the ORF sequences of ATF4 and CHOP were amplified by PCR using the following primers: ATF4: forward: 5'-TCAGAATTCATGACCGAGATGAGCTTCCT-3' and reverse 5'-TATCTCGAGTTACGGAAGTCTCTTCTTCC-3'; CHOP: forward: 5'-TCAGAATTCATGGCAGCTGAGTCCCTGCCT TT-3'; and reverse 5'-TATCTCGAGTCATGCTTGGTGCAG GCTGAC-3'. The respective ORFs were cloned into the pcDNA3.1 vector downstream of the T7 promoter. The plasmids were then linearized by XhoI digestion, and were used as a template to generate the fragment DNA containing the T7 promoter and the ORFs of ATF4 or CHOP by PCR amplification, the following primers specific for the flanking sequences were used: forward: 5'-AAATTAATACGACTCACT ATAGGGAG-3'; reverse: 5'-GCTGATCAGCGGGTTAAACG G-3'. The PCR product was purified and transcribed *in vitro* using the HiScribe T7 *in vitro* mRNA transcription kit (New England Biolabs). The mRNA was purified using MEGAclear transcription clean-up kit (ThermoFisher Scientific) and transfected into BMDMs at the dose of 200 ng/10⁵ cells using the jetMESSENGER mRNA transfection buffer and reagent (Polyplus transfection) according to manufacturers' instructions.

Luciferase Reporter Gene Assay

To determine NF- κ B reporter activity, the pGL3-NF- κ B reporter plasmid and the pRL-TK-Renilla-luciferase plasmid

were co-transfected into RAW264.7 cells using X-tremeGENE DNA transfection reagent (Roche). After 24 h, the cells were treated with PBS or different concentrations of 5-HMF (0, 10, 25 and 50 μ g/ml), followed by stimulation with LPS (100 ng/ml) for 6 h. The cells were harvested and lysed for dual luciferase assays (Promega) according to the manufacturer's instructions.

Immunofluorescence Staining

ASC-speck formation was detected by immunofluorescence staining. Briefly, 10-mm cell culture slides were placed at the bottom of 6-well cell culture plates, and BMDMs or PMA-primed THP-1 cells were seeded at the density of 5 \times 10⁶/ml per well. After the suitable treatments, the cells were fixed overnight in 4% paraformaldehyde, and incubated sequentially with anti-mouse or anti-human ASC antibody (1:100), followed by staining with AlexaFluor488-conjugated goat-anti-mouse IgG antibody (1:1,000). The nuclei were counterstained with DAPI (2.5 μ g/ml). The ASC speck formation were observed and counted under a fluorescence microscope (Nikon, Tokyo, Japan) controlled with ZEN software (Carl Zeiss).

Intracellular Free Ca²⁺ Detection

Free Ca²⁺ levels in the BMDMs were measured by staining with the Ca²⁺-binding dye Fluo-3 AM. Briefly, the cells harvested after the specific treatments were washed twice with ice-cold PBS, and incubated with 5 μ M Fluo-3 AM at 37°C for 30 min. The stained samples were washed three times with PBS and analyzed by flow cytometry on FACS Calibur (Beckman Coulter, United States).

ASC Oligomerization

ASC oligomerization was determined as described previously with minor modifications (Lugrin and Martinon, 2017). Briefly, BMDMs or PMA-primed THP-1 cells were stimulated with LPS (500 ng/ml) for 6 h and then with ATP (5 mM) or nigericin (10 μ M) for 1 h. The suitably treated cells were harvested by scraping in cold PBS containing 2 mM EDTA, and centrifuged at 1,500 \times g. The cells were then lysed in Cold Buffer A (20 mM HEPES-KOH, pH 7.5, 10 mM KCl, 1.5 mM MgCl₂, 1 mM EDTA, 1 mM EGTA, 320 mM sucrose) by repeatedly (20 times) passing through a 21-gauge needle, and the lysates were centrifuged at 3,300 \times g to pellet the inflammasome complexes. The precipitate was resuspended in CHAPS buffer (20 mM HEPES-KOH, pH 7.5, 5 mM MgCl₂, 0.5 mM EGTA, 0.1 mM PMSF, 0.1% CHAPS) containing 4 mM disuccinimidyl, and incubated for 30 min at room temperature with constant rotation to cross link the proteins. The samples were centrifuged at 5,000 \times g for 10 min, and the pellets were harvested for western blotting.

Histopathological Staining and Immunohistochemistry

The lung tissue paraffin sections were cleared in xylene and rehydrated through an alcohol gradient. After antigen retrieval, the slides were blocked using 20% normal goat

serum and then incubated overnight with anti-CHOP and anti-GPR78 antibodies at 4°C. The slides were washed three times with PBS and incubated with HRP-linked secondary antibodies at room temperature. Diaminobenzidine-hydrogen peroxide (Sigma-Aldrich) was used to develop color and the nuclei were counterstained with 0.5% hematoxylin (Li et al., 2021).

Statistical Analysis

The data from three independent experiments are presented as means \pm SD. Statistical significance was determined using Student's t-test and indicated as * $p < 0.05$ and ** $p < 0.01$. All statistical analyses were performed using the GraphPad Prism software.

RESULTS

5-HMF Protects Mice Against Lung Injury and Inflammation Induced by Lipopolysaccharide

The chemical structure of 5-HMF is shown in **Figure 1A**. To evaluate the cytotoxicity of 5-HMF, we treated BMDMs and THP-1 cells with different concentrations of 5-HMF for 24 h and measured cell viability using MTS assay. As shown in **Supplementary Figure S1**, 5-HMF did not significantly affect the viability of BMDMs and THP-1 cells even at the high concentration of 100 μ g/ml. To determine the therapeutic role of 5-HMF on LPS-induced pneumonia, we established a mouse model of ALI via intraperitoneal injection of LPS (10 mg/kg). H&E staining of the lung tissues indicated that compared to the untreated LPS-challenged mice, 5-HMF pre-treatment effectively reduced peri-bronchial wall thickening, infiltration of inflammatory cells into the alveolar space, and vascular congestion (**Figure 1B**). Furthermore, 5-HMF also attenuated the LPS-induced increase in the number of inflammatory cells such as macrophages, lymphocytes and neutrophils (**Figure 1C**), as well as the total protein concentration and cell count (**Figure 1D**) in the BALF. MPO is released by activated neutrophils and is considered as a specific marker of neutrophil infiltration. As shown in **Figure 1E**, MPO activity in the lung tissues of the LPS-challenged mice was also reduced in 5-HMF treatment group. Consistent with this, the serum levels of proinflammatory cytokines including IL-6, TNF- α , IL-1 β and mouse IL-8 homologue, keratinocyte-derived cytokine (KC) were significantly lower in the 5-HMF-treated versus untreated mice (**Figures 1F–I**). Unexpectedly, the serum level of anti-inflammatory cytokine IL-10 was repressed in 5-HMF treatment group (**Figure 1J**). To further assess the therapeutic effect of 5-HMF during acute inflammation, we monitored the survival of the LPS-challenged mice pre-treated with 5-HMF (6 or 12 mg/kg, i. p.) or PBS. As shown in **Figure 1K**, the overall survival of the mice pre-treated with 5-HMF was significantly prolonged over a 6-day period, and a greater protective effect was observed with the

higher dose. Taken together, 5-HMF protected mice against LPS-induced lung inflammation and injury.

5-HMF Inhibits the Lipopolysaccharide-Induced Inflammatory Response in Mouse Macrophages and Human Monocytes

Macrophages mediate both innate and adaptive immune response by producing inflammatory cytokines and presenting antigens, and also play a central role during lung inflammation and injury. To determine whether 5-HMF regulated the LPS-induced inflammatory response in macrophages, we treated murine BMDMs with different concentrations of 5-HMF (0–50 μ g/ml) and stimulated them with LPS (100 ng/ml) for 6 h. As shown in **Figures 2A–H**, in BMDMs, 5-HMF treatment significantly decreased the LPS-induced production of IL-6, TNF- α , IL-1 β and IL-8/KC, which was encoded by *Cxcl1* gene in mice (**Figures 2A–H**). Since nitric oxide (NO) is a critical mediator of ALI pathogenesis, we next analyzed the expression of inducible nitric oxide synthase (iNOS) and found that the *iNOS* mRNA levels were markedly lower in the 5-HMF-treated macrophages (**Figure 2I**). Unexpectedly, the mRNA level and the production of the anti-inflammatory cytokine IL-10 were also reduced following 5-HMF treatment (**Figures 2J,K**). Similar pharmacological effects of 5-HMF were observed in the THP-1 cells as well with a significant inhibition of LPS-induced IL-6, TNF- α , IL-1 β , IL-8 (encoded by *CXCL8* gene in human), iNOS and IL-10 (**Supplementary Figure S2**). Taken together, 5-HMF suppressed the LPS-induced inflammatory response by reducing the production of inflammation-related chemokines and cytokines.

5-HMF Inhibits Lipopolysaccharide-Induced NF- κ B Signaling Pathway

Pro-inflammatory cytokines are produced following activation of NF- κ B and MAPK signaling in response to TLR stimulation (Ko et al., 2020). To further elucidate the molecular mechanisms underlying the anti-inflammatory effects of 5-HMF, therefore, we analyzed the expression and phosphorylation levels of NF- κ B and MAPK signal pathway mediators in the LPS-stimulated macrophages. The BMDMs were treated with 5-HMF, and thereafter with LPS for varying durations. 5-HMF treatment reduced the levels of phosphorylated IKK α / β , I κ B α and p65 in the LPS-stimulated BMDMs (**Figures 3A–D**). We also performed a reporter gene assay by transfecting RAW264.7 cells with the NF- κ B luciferase reporter plasmid, and found that 5-HMF repressed NF- κ B-induced transcriptional activity in a dose-dependent manner (**Figure 3M**). However, 5-HMF did not affect the activation of the MAPK signaling molecules ERK, JNK and p38 (**Figures 3E–H**). The AKT/mTOR signaling pathway is also crucial to initiate and mediate the NF- κ B

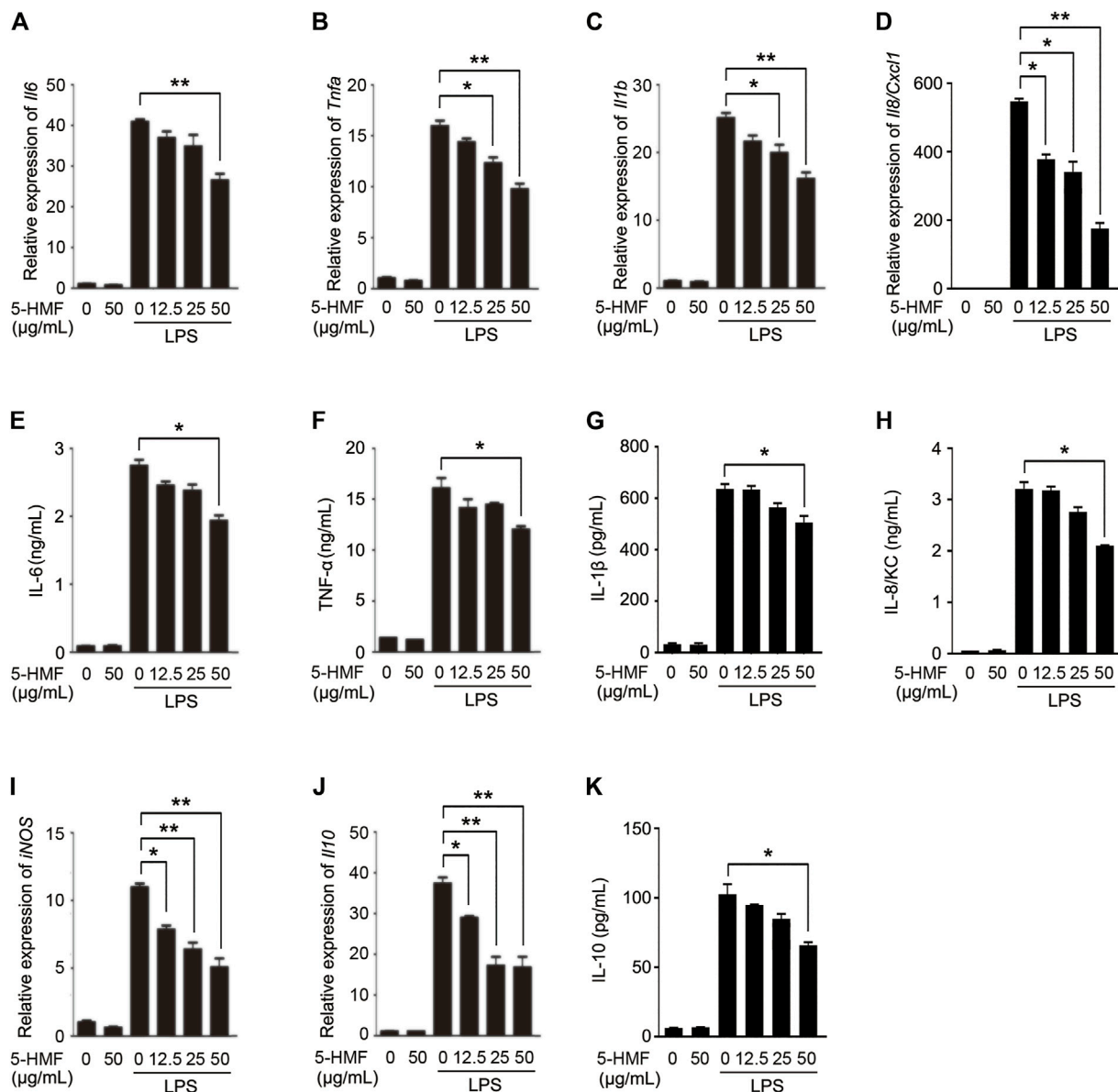


FIGURE 2 | 5-HMF inhibits the production of LPS-triggered proinflammatory cytokines in BMDMs. BMDMs were pretreated with PBS or 5-HMF and stimulated with LPS (100 ng/ml). (A–D) *Il6* (A), *Tnfa* (B), *Il1b* (C) and *Il8/Cxcl1* (D) mRNA levels. (E–H) IL-6 (E), TNF-α (F), IL-1β (G) and IL-8/KC (H) levels in the culture supernatant. (I, J) *iNOS* (I) and *Il10* (J) mRNA levels. (K) IL-10 levels in the culture supernatant. Data are the mean ± SD of three independent experiments: * and ** indicate $p < 0.05$ and $p < 0.01$ respectively by Student's t-test.

signal transduction pathway and is associated with the inflammatory response (Meng et al., 2018). Therefore, we analyzed the levels of *p*-AKT, AKT, *p*-P70S6K and P70S6K in the suitably treated cells. As shown in **Figures 3I–K**, 5-HMF has no significant effect on the LPS-induced phosphorylation of AKT (Ser473) and p70S6K (Thr389). In the *in vivo* ALI model as well, 5-HMF pre-treatment significantly reduced phosphorylation levels of IκBα and p65 in the lung tissues following LPS-challenge compared to that in the untreated mice (**Figures 3N–P**). In conclusion, 5-HMF inhibited NF-κB activation in

LPS-challenged macrophages, which might be the key mechanism underlying its anti-inflammatory effect against ALI.

5-HMF Inhibits NLRP3 Inflammasome Activation in Mouse Macrophages and Human Monocytes

Inflammasomes are critical to the innate immune response and inflammation (Walsh et al., 2014). Herein, we determined the effects of 5-HMF on NLRP3 inflammasome activation in LPS-

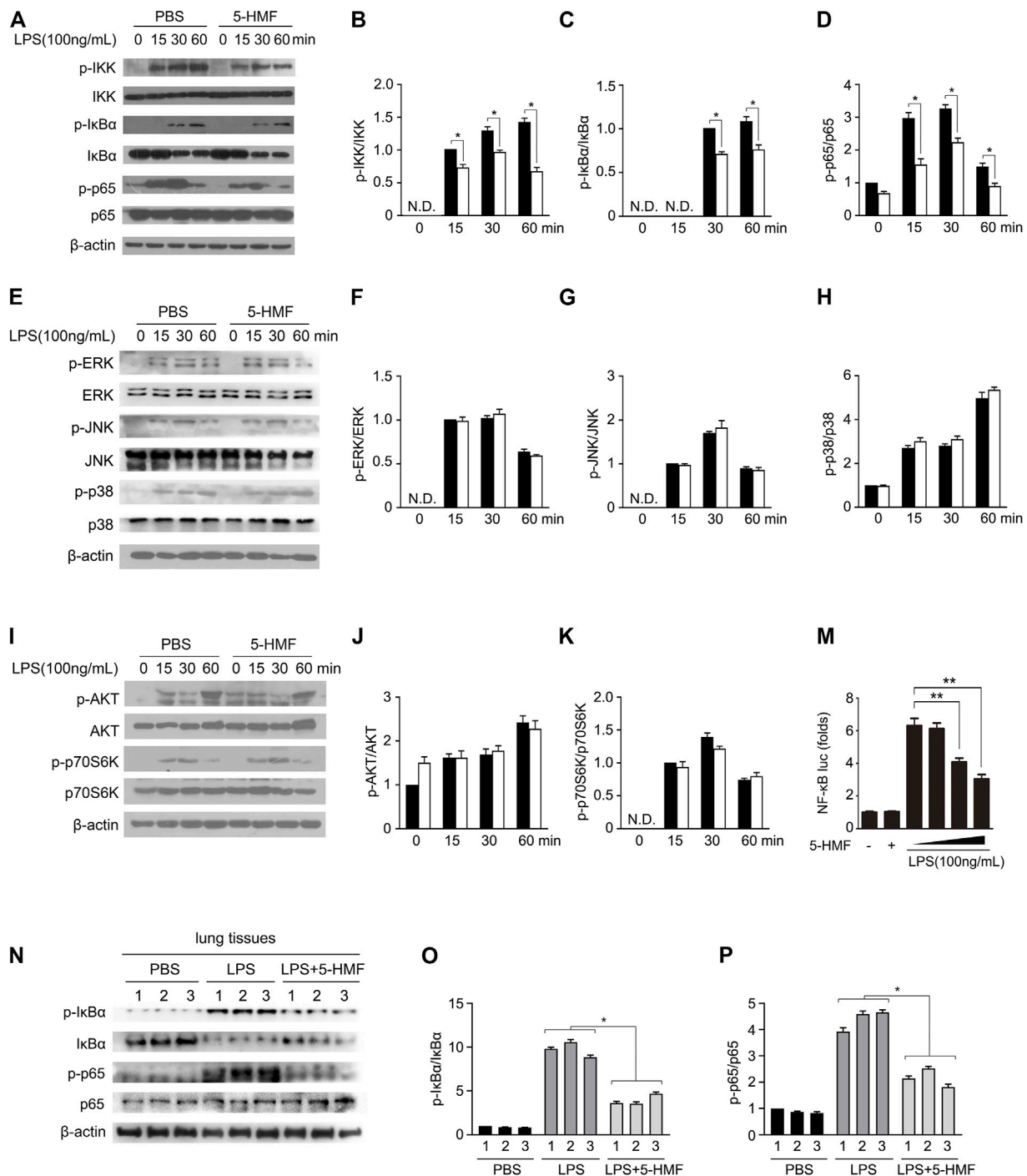


FIGURE 3 | 5-HMF inhibits NF-κB signaling pathway. **(A–K)** BMDMs pretreated with PBS or 5-HMF (50 μg/ml) were subsequently challenged by LPS for varying durations. **(A–D)** Immunoblot showing the expression levels of total and phosphorylated IKK, IκBα and p65 proteins **(A)**. **(B–D)** The relative band densities of the phosphorylation of IKK **(B)**, IκBα **(C)** and p65 **(D)** were measured by ImageJ software, N.D. means non-detected. **(E–H)** Immunoblot showing total and phosphorylated ERK, JNK and p38 proteins **(E)**. **(F–H)** The relative band densities of the phosphorylation of ERK **(F)**, JNK **(G)** and p38 **(H)**. **(I–K)** Immunoblot showing total and phosphorylated AKT and p70S6K proteins **(I)**. **(J, K)** The relative band densities of the phosphorylation of AKT **(J)** and p70S6K **(K)**. **(M)** RAW264.7 cells transfected with pGL3-NF-κB were pretreated with PBS or different concentrations of 5-HMF as indicated, and stimulated with LPS for 6 h. Luciferase activity of the NF-κB-driven promoter in the indicated groups. **(N–P)** Immunoblot showing total and phosphorylated IKK, IκBα and p65 in the lung tissues of mice treated as in **Figure 1A N**. **(O, P)** The relative band densities of the phosphorylation of IκBα **(O)** and p65 **(P)**. Data are the mean ± SD of three independent experiments: * and ** indicate $p < 0.05$ and $p < 0.01$ respectively by Student's t-test.

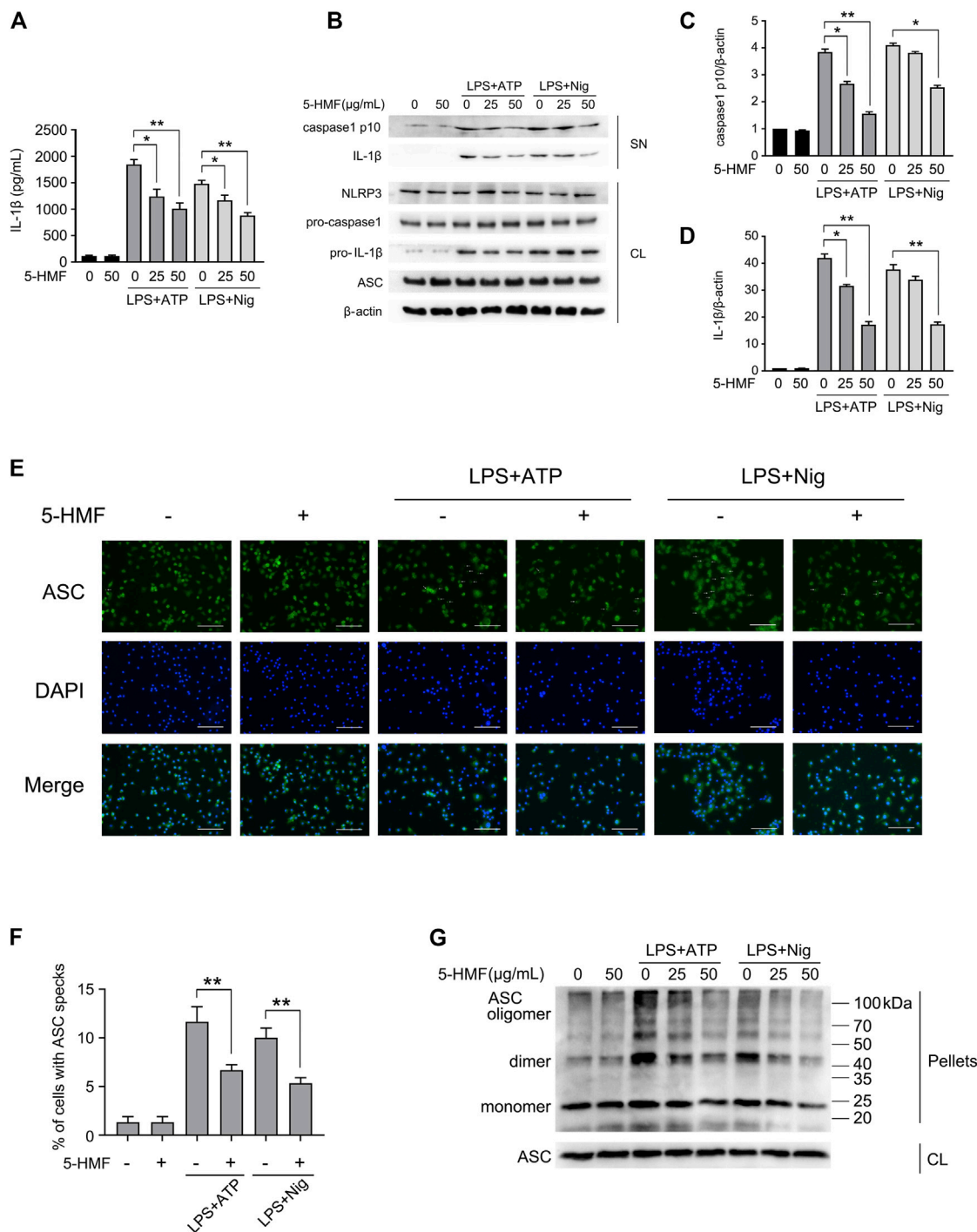


FIGURE 4 | 5-HMF suppresses NLRP3 inflammasome activation. BMDMs were pretreated with different concentrations of 5-HMF for 30 min as indicated, followed by LPS (500 ng/ml) for 6 h and ATP (5 mM) or nigericin (10 μM) for 1 h **(A)** IL-1β levels in the culture supernatants. **(B)** Immunoblot showing levels of indicated proteins in the culture supernatants (SN) and cell lysates (CL). **(C,D)** The relative band densities of IL-1β **(C)**, caspase-1 p10 **(D)** in the supernatant. **(E)** Representative immunofluorescence images showing ASC speck formation (×400), Scale bar, 500 μm. **(F)** The percentage of cells containing ASC-specks as in **(E)**. **(G)** Immunoblot showing ASC oligomerization in pellets cross-linked by DSS.

challenged BMDMs and THP-1 cells following stimulation with ATP or nigericin (Mariathasan et al., 2006). The BMDMs were sequentially exposed to different concentrations of 5-HMF, LPS

and finally ATP or nigericin. 5-HMF inhibited the release of IL-1β from the BMDMs and THP-1 cells (**Figure 4A**, **Supplementary Figure S4A**), and also suppressed the

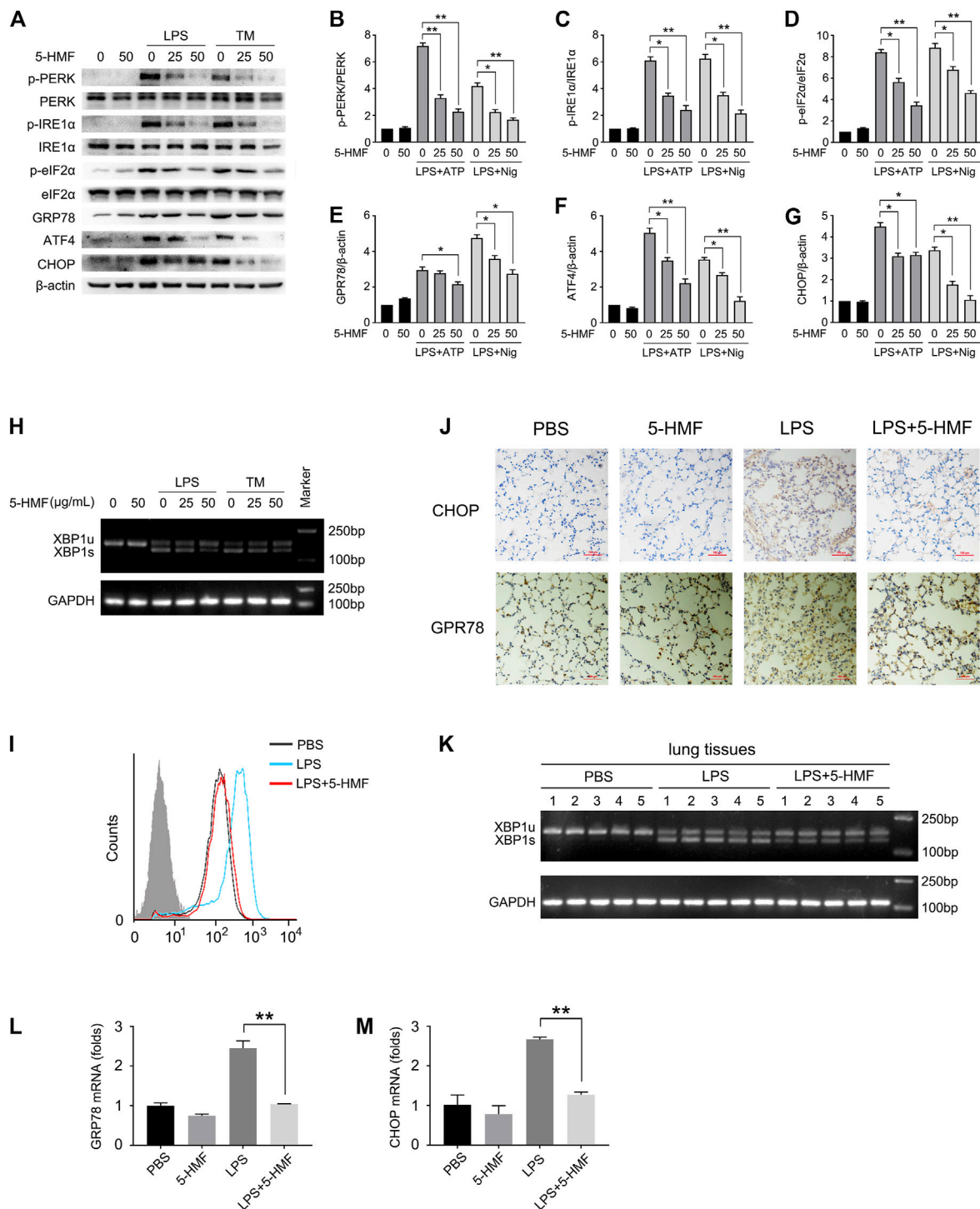


FIGURE 5 | 5-HMF inhibits LPS-triggered ER stress. **(A–K)** BMDMs pretreated with different concentrations of 5-HMF were challenged with LPS (500 ng/ml) for 6 h or tunicamycin (1 μg/ml) for 16 h **(A–G)** Immunoblot showing total and phosphorylated PERK, eIF2α, IRE-1α and expression levels of ATF4, GPR78 and CHOP in BMDMs **(A)**. **(B–G)** The relative band densities of the phosphorylation of PERK **(B)**, IRE1α **(C)** and eIF2α **(D)**, and the expression of GPR78 **(E)** ATF4 **(F)** and CHOP **(G)**. **(H)** RT-PCR analysis of XBP1 splicing in BMDMs cells treated with PBS or 5-HMF, followed by LPS or tunicamycin stimulation as indicated. **(I)** FACS analysis of the intracellular Ca²⁺ concentrations stained by green fluorescence (Fluo-3). **(J)** Representative IHC images showing *in-situ* expression of CHOP and GPR78 in lung tissues of mice treated as in Figure 1A (×200), Scale bar, 100 μm. **(K)** RT-PCR analysis of XBP1 splicing in lung tissues of mice treated with PBS or 5-HMF as in Figure 1A, followed by LPS stimulation. **(L,M)** *Chop* **(L)** and *Gpr78* **(M)** mRNA levels in lung tissues of mice treated as in Figure 1A. Data are the mean ± SD of three independent experiments: * and ** indicate $p < 0.05$ and $p < 0.01$ respectively by Student's t-test.

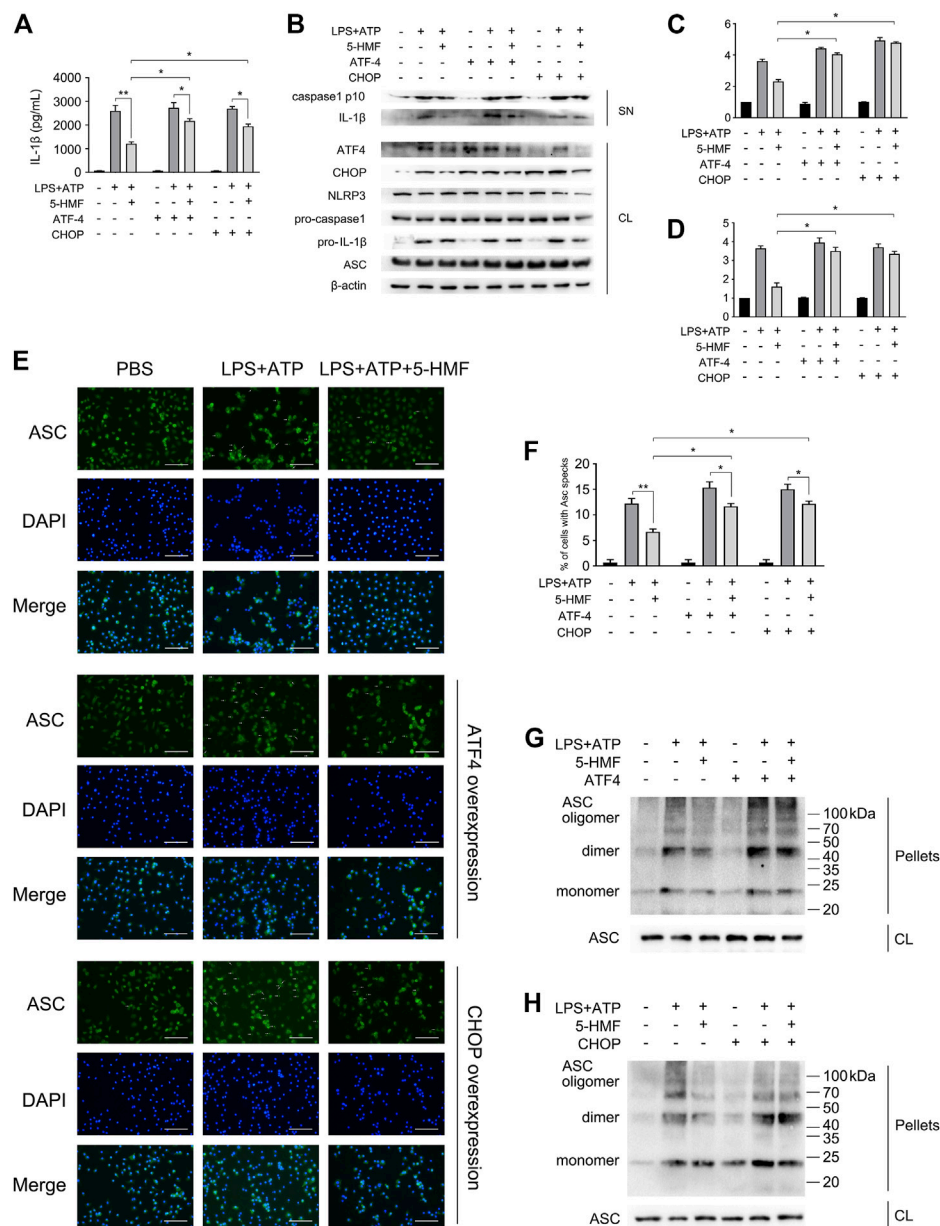


FIGURE 6 | 5-HMF inhibits NLRP3 inflammasome by down-regulating ER stress. BMDM were transfected with ATF4 and CHOP mRNA as indicated. After 48 h, cells were incubated with 5-HMF (50 μg/ml) or PBS for 30 min, followed by LPS (500 ng/ml) for 6 h and ATP (5 mM) for 1 h **(A)** IL-1β levels in culture supernatants. **(B)** Immunoblot showing levels of indicated proteins in the culture supernatants (SN) and cell lysates (CL). **(C,D)** The relative band densities of IL-1β **(C)**, caspase-1 p10 **(D)** in supernatant. **(E)** Representative immunofluorescence images showing ASC speck formation (×400), Scale bar, 500 μm. **(F)** The percentage of cells containing ASC-specks in **(E)**. **(G,H)** Immunoblot showing ASC oligomerization in pellets cross-linked by DSS.

maturation and secretion of cleaved caspase-1p10 and IL-1β in the LPS-primed BMDMs (**Figures 4B–D**) and THP-1 cells (**Supplementary Figures S4B–D**) following stimulation with ATP or nigericin. NLRP3 inflammasome assembly is initiated by the interaction of NLRP3 with ASC (Vajjhala et al., 2012; Cai et al., 2014; Lu et al., 2014). During this step, ASC monomers form large specks in cells via self-challenged oligomerization, which is a marker of NLRP3 inflammasome activation (Elliott and Sutterwala, 2015). Therefore, we surmised that 5-HMF may

inhibit NLRP3 inflammasome activation by suppressing ASC oligomerization. We found that 5-HMF treatment significantly reduced the formation of ASC specks in the BMDMs (**Figures 4E,F**) and THP-1 cells (**Supplementary Figures S4E, F**) stimulated with LPS and ATP or nigericin. Furthermore, 5-HMF also decreased the levels of ASC dimers and oligomers in the DSS-crosslinked pellets of both BMDMs (**Figure 4G**) and THP-1 cells (**Supplementary Figure S4G**) stimulated as above. Taken together, 5-HMF blocks NLRP3 inflammasome activation

in murine macrophages and human monocytes by repressing ASC oligomerization.

5-HMF Inhibits Lipopolysaccharide-Induced ER Stress

Studies increasingly show that ER stress can affect NLRP3 inflammasome activation via the generation of reactive oxygen species (ROS), calcium or lipid metabolism, and the unfolded protein response (UPR) (Chen et al., 2019). To determine whether 5-HMF affected LPS-triggered ER stress in BMDMs, we additionally treated the cells with the ER stress inducer tunicamycin. As shown in **Figures 5A–G**, both LPS and tunicamycin individually increased the phosphorylation of PERK, IRE1 α and eIF2 α in the BMDMs, and upregulated GRP78, ATF4 and CHOP. These mediators of ER stress were markedly attenuated by 5-HMF in a dose-dependent manner (**Figures 5A–G**). Furthermore, 5-HMF also inhibited basal XBP-1 splicing induced by LPS or tunicamycin in BMDMs (**Figure 5H**). The differentially treated BMDMs were then stained with Fluo-3 to measure intracellular Ca²⁺ levels. As shown in **Figure 5I**, LPS significantly increased intracellular Ca²⁺ accumulation, which was remarkably downregulated in the presence of 5-HMF. In line with the *in vitro* findings, 5-HMF reduced XBP1 splicing in the lung tissues of LPS-challenged mice (**Figure 5K**), as well as the *in-situ* expression of CHOP and GPR78 proteins (**Figure 5J**) and mRNAs (**Figures 5L,M**). Altogether, our results suggested that 5-HMF inhibited LPS-induced ER stress both *in vitro* and *in vivo*.

5-HMF Inhibits NLRP3 Inflammasome Activation by Targeting Endoplasmic Reticulum Stress

Given that ER stress activates NLRP3 inflammasome through various mediators (Compan et al., 2015), we next determined whether the inhibitory effect of 5-HMF on NLRP3 inflammasome activation involved the ER stress pathway. To this end, we overexpressed ATF4 or CHOP in the BMDMs by transfecting the respective mRNAs, and stimulated the cells with LPS plus ATP/Nigericin. As shown in **Figure 6B**, the protein levels of ATF4 or CHOP were upregulated after mRNA transfection, respectively. As expected, 5-HMF-driven negative regulation of ER stress-associated NLRP3 activation was reversed by ATF4 or CHOP over-expression (**Figure 6**). Furthermore, ATF4/CHOP overexpression also neutralized the inhibitory effect of 5-HMF on IL-1 β release from the BMDMs following LPS plus ATP/nigericin stimulation (**Figure 6A**). Moreover, ATF4/CHOP overexpression partially abrogated the inhibitory effects of 5-HMF on the maturation and secretion of caspase-1 triggered by LPS plus ATP/nigericin stimulation (**Figures 6B–D**). Since 5-HMF suppressed ASC oligomerization, we also examined whether the attenuation of ER stress affected ASC speck formation and oligomerization. The results showed that overexpression of ATF4/CHOP restored ASC speck formation (**Figures 6E,F**) and ASC oligomerization (**Figures 6G,H**) in the cells stimulated with LPS and ATP even in the presence of 5-HMF.

Taken together, attenuation of ER stress is crucial to the inhibitory effect of 5-HMF on NLRP3 inflammasome activation.

Inhibition of Endoplasmic Reticulum Stress Is Essential for 5-HMF-Mediated Anti-Inflammatory Activity and Amelioration of ALI *In Vivo*

To further explore the role of ER stress to the action mode of 5-HMF in the amelioration of pulmonary dysfunction in the mice model of ALI, we took advantage of tunicamycin (TM), a well-known ER stress inducer in the LPS-triggered ALI mice model to confirm the action of 5-HMF. As shown in **Figure 7**, tunicamycin significantly reversed the protective effects of 5-HMF on LPS-induced inflammation and lung injury. Mice co-treated with tunicamycin displayed more severe signs of LPS-induced lung inflammation and injury compared to the non-treated controls (**Figure 7A**). In addition, the downregulation of CHOP and GPR78 by 5-HMF were reversed by tunicamycin treatment (**Figure 7B**). The total protein level in BALF (**Figure 7C**), MPO activity (**Figure 7D**), and the levels of IL-6, TNF- α , IL-1 β , IL-8/KC and IL-10 in the LPS-challenged mice were exacerbated by tunicamycin pre-treatment compared to mice that received only LPS and 5-HMF (**Figures 7E–I**). To summarize these results, attenuation of ER stress contributed substantially to the inhibition of the NLRP3 inflammasome in the ALI model treated with 5-HMF. Thus, 5-HMF protected against NLRP3 inflammasome-mediated pulmonary dysfunction by modulating ER stress.

DISCUSSION

ALI is a severe lung disease characterized by pulmonary and capillary edema, which eventually leads to acute respiratory failure (Ware and Matthay, 2000). Excessive pulmonary infiltration of inflammatory cells and overproduction of proinflammatory cytokines are the key pathological factors of ALI (Belchamber and Donnelly, 2017). Thus, it is crucial to identify novel anti-inflammatory compounds for the prevention and treatment of inflammation-relevant lung injury. 5-HMF is an active compound commonly found in sugar-rich heat-processed foods, including honey, coffee, dried fruit and fruit juices (Shapla et al., 2018; Zou et al., 2021). Studies show that 5-HMF exerts anti-inflammatory or anti-allergic effects (Zhao et al., 2013; Alizadeh et al., 2017), and can inhibit ROS production and the expression of inflammatory factors such as PGE2, IL-1 β , IL-6 and TNF- α in LPS-stimulated RAW264.7 macrophages (Zhao et al., 2013). In this study, we investigated the effect of 5-HMF on ALI and explored the underlying molecular mechanisms. Our findings indicated that 5-HMF protects against LPS-induced ALI by inhibiting the pro-inflammatory NF- κ B signaling cascade and the activation of NLRP3 inflammasome, which involves attenuation of the ER stress pathway.

The potential mechanisms of ALI have been explored in LPS-stimulated mouse models (Liu et al., 2018). LPS stimulation led to

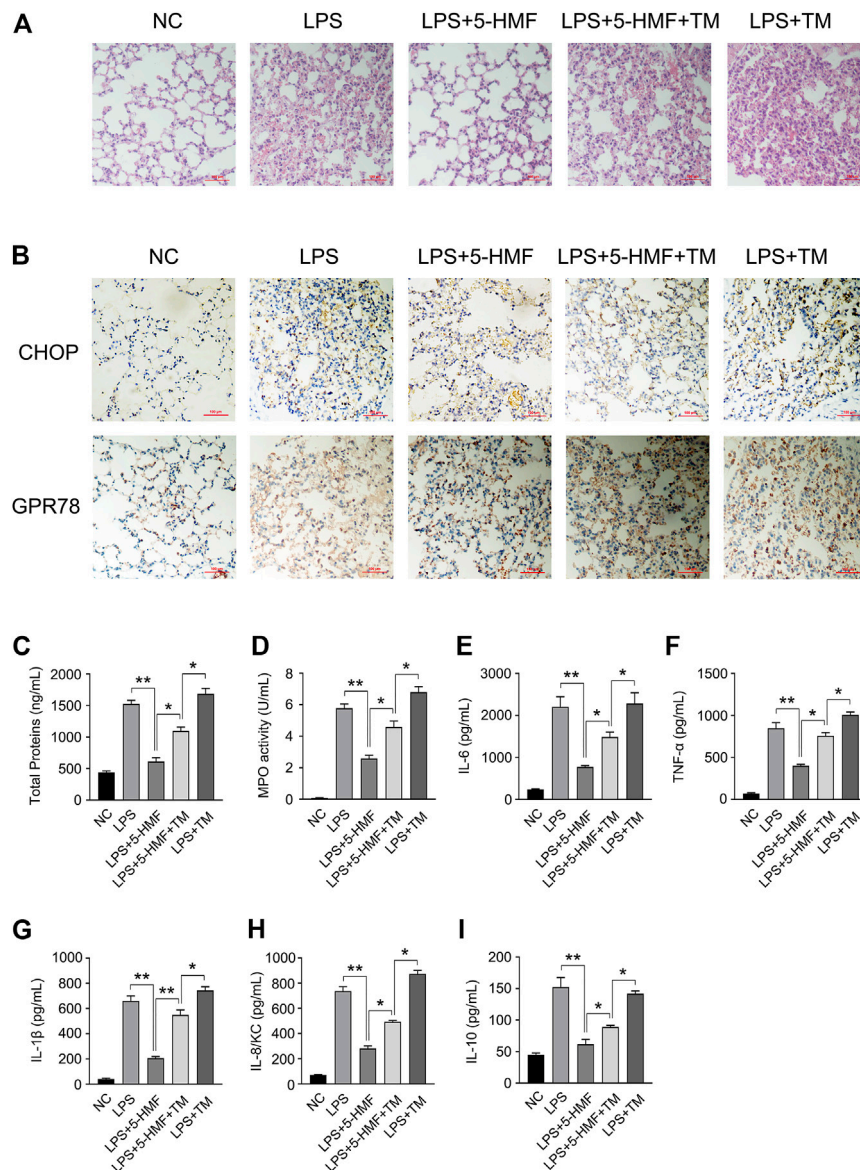


FIGURE 7 | Inhibition of ER stress by 5-HMF mediates amelioration of LPS-induced acute lung injury. C57BL/6J mice (5 mice/group) pretreated with PBS or 5-HMF (12 mg/kg, i. p.) and/or tunicamycin (TM, 0.2 mg/kg, i. p.) were challenged with LPS (1 mg/kg, i. p.). **(A)** Representative images of H&E-stained lung tissue sections from the indicated groups ($\times 200$). Scale bar, 100 μ m. **(B)** Representative IHC images showing *in-situ* expression of CHOP and GPR78 in lung tissues of mice ($\times 200$). Scale bar, 10 μ m. **(C)** Protein content in BALF. **(D)** MPO activity of lung tissues. **(E–I)** IL-6 **(E)**, TNF- α **(F)**, IL-1 β **(G)**, IL-8/KC **(H)** and IL-10 **(I)** levels in sera. All results are expressed as the mean \pm SD; * and ** indicate $p < 0.05$ and $p < 0.01$ respectively by Student's t-test.

significant histological changes such as vascular leakage, neutrophils infiltration, enhanced MPO levels and activity in the BALF, and over-production of various inflammatory cytokines (IL-6, TNF- α and IL-1 β). In our study, we have reported for the first time that exogenous 5-HMF can ameliorate LPS-induced ALI, as indicated by the lower degree of pathological damage (**Figure 1B**) and reduced serum levels of inflammatory cytokines (**Figures 1C–J**). In addition, the survival rate of the LPS-challenged mice was markedly improved after 5-HMF treatment (**Figure 1K**). Activated macrophages play a pivotal role in the early stages of LPS-induced inflammation in

the lungs by secreting large amounts of proinflammatory cytokines such as IL-6 and TNF- α , which in turn activate a complex signaling network that culminates in ALI (Lv et al., 2016). Likewise, human macrophages or monocytes cultured *in vitro* in the presence of LPS also produce significantly higher levels of proinflammatory cytokines (Wang et al., 2019). We found that 5-HMF neutralized LPS-induced production of IL-6, TNF- α and IL-1 β by primary BMDMs or THP-1 monocytes in a dose-dependent manner, and even modulated the mRNA expression of iNOS and the anti-inflammatory cytokine IL-10 (**Figure 2** and **Supplementary**

Figure S2). These results indicated that 5-HMF protects against LPS-induced ALI by reducing the production of proinflammatory cytokines.

To further explore the mechanism underlying the action of 5-HMF, we analyzed its effects on the NF- κ B signaling pathway and NLRP3 inflammasome activation. The NF- κ B pathway plays a crucial role in inflammatory immune responses and is activated in various inflammatory diseases. Inactivation of NF- κ B directly leads to decreased production of IL-6, TNF- α , IL-1 β and other proinflammatory factors, which is capable of relieving LPS-induced ALI (Dang et al., 2016). Several natural compounds present in edible plants and TCM formulations exert anti-inflammatory effects by inhibiting the NF- κ B signal pathway (Seo et al., 2018; Sahukari et al., 2020). Kong et al. have reported that 5-HMF inhibited this pathway in RAW264.7 cells. Consistent with this, we found that 5-HMF inactivated the NF- κ B pathway in primary BMDMs and THP-1 monocytes exposed to LPS (**Figures 3A–D** and **Supplementary Figure S3**), which was confirmed by the luciferase reporter gene assay (**Figure 3M**). In the *in vivo* model as well, 5-HMF downregulated the NF- κ B pathway in the lung tissues of LPS-treated mice (**Figures 3N–P**). The MAPK and AKT signaling pathways are also involved in the production of inflammatory and anti-inflammatory cytokines (Choi et al., 2014; Luo et al., 2019). However, 5-HMF had no significant effect on either MAPK or AKT signaling pathway in LPS-primed BMDMs even at a high concentration of 50 μ g/ml (**Figures 3E–K**). This contradicts a previous report of the modulatory effect of 5-HMF on LPS-induced MAPK and AKT signaling pathway in RAW264.7 cells (Kong et al., 2019). This discrepancy could be due to different cellular models and/or different concentrations of 5-HMF. Nevertheless, our findings indicate that 5-HMF mitigates the inflammatory immune response by targeting the NF- κ B signaling pathway.

The activation of NLRP3 inflammasome is responsible for the release of proinflammatory cytokines such as IL-1 β and IL-18. The NLRP3 inflammasome is activated during the process of lung injury in response to cellular stress (Lee et al., 2016). Studies show that inactivation of the NLRP3 inflammasome due to chemical compounds or genetic mutations can markedly suppress ALI and other inflammatory diseases in animal models (Youm et al., 2015; Coll et al., 2015). However, no study so far has elucidated the regulatory effect of 5-HMF on NLRP3 inflammasome activation. The activation of NLRP3 inflammasome is initiated by the upregulation of NLRP3 and pro-IL-1 β by LPS or other TLR agonists, and is followed by the assembly of NLRP3, caspase-1 and ASC, which was activated in response to various of stimuli, including ATP, nigericin or MSU crystals (Guo et al., 2015). We found that while 5-HMF inhibited the NF- κ B pathway during LPS stimulation, it did not affect NLRP3 or pro-caspase-1 expression in the LPS-primed BMDMs and THP-1 cells. In addition, the expression of pro-IL-1 β was only slightly attenuated by 5-HMF treatment (**Figure 4B**, **Supplementary Figure S4B**). However, 5-HMF did

attenuate the maturation and secretion of IL-1 β and caspase-1 in the LPS-primed primary BMDMs and THP-1 cells stimulated by ATP or nigericin (**Figures 4A–D** and **Supplementary Figures S4A–D**). Furthermore, 5-HMF also blocked ASC speck formation and ASC oligomerization, which precede NLRP3-caspase 1-ASC-complex formation and activation of NLRP3 inflammasome (**Figures 4E–G** and **Supplementary Figures S4E–G**) (Lu et al., 2014). Taken together, 5-HMF may alleviate LPS-induced inflammation and ALI by inactivating the NLRP3 inflammasome.

The ER stress response is closely related to inflammatory diseases such as liver injury, atherosclerosis, diabetes and ALI (Mohan et al., 2019; Lebeaupin et al., 2018). Studies show that the ER stress pathway is involved in the pathological process of lung injury (Endo et al., 2005; Kim et al., 2015b; Leonard et al., 2019). LPS challenge can significantly elevate the expression and/or activation of ER stress mediators including GRP78 protein (Aggarwal et al., 2018), PERK/eIF2- α /ATF4/CHOP pathway (Huang et al., 2020) and the activated splicing of XBP-1 (Zhao et al., 2020). A previous study on LO2 hepatocytes showed that 5-HMF can effectively attenuate ER stress induced by GalN/TNF- α and protect cells against apoptosis (Jiang et al., 2015). To determine whether the protective effect of 5-HMF on LPS-induced ALI depends on the attenuation of ER stress, we analyzed the expression and activation of crucial ER stress mediators. LPS or tunicamycin treatment significantly increased the phosphorylation of PERK, IRE1 α and eIF2 α , as well as the expression of GRP78, ATF4 and CHOP, all of which were inhibited by 5-HMF (**Figures 5A–G**). Consistent with this, we also showed that 5-HMF administration suppressed the significantly increased expression of CHOP and GRP78 induced by LPS in the lung tissues of ALI model mice (**Figures 5J,L,M**). In addition, 5-HMF significantly reduced LPS-induced XBP-1 mRNA splicing in BMDMs and in the murine lung tissues (**Figures 5H,K**). Since ER acts as the most important reservoir of calcium, Ca²⁺ homeostasis is disturbed during ER stress (Krebs et al., 2015; Stewart et al., 2015), resulting in mitochondrial depolarization, overproduction of ROS and induction of inflammatory responses (Rizzuto et al., 2012; Lebeaupin et al., 2018). Thus, treatments that inhibit calcium release from the ER may protect against cell injury and death. We found that 5-HMF suppressed LPS-induced calcium elevation in the cytoplasm of BMDMs (**Figure 5I**), which is consistent with its anti-inflammatory action. Taken together, 5-HMF protects against LPS-induced ALI and alleviates inflammatory responses by alleviating ER stress.

ER stress-mediated UPR is also a key factor involved in the activation of NLRP3 inflammasome, and the subsequent maturation and secretion of IL-1 β (Menu et al., 2012). CHOP is a critical transcriptional factor during the progress of ER stress signaling, and its expression is triggered by three distinct stress signaling cascades. PERK induces CHOP expression by upregulating ATF4 (Ma et al.,

2002), IRE1 α triggers XBP1 mRNA splicing, and the mature XBP1s protein enhances CHOP expression by activating JNK (Dai et al., 2014). In addition, ATF6 directly upregulates CHOP (Yoshida et al., 2000). The overexpression of CHOP induces NLRP3 inflammasome activation, resulting in the maturation and release of IL-1 β , caspase-1 and caspase-11, which eventually leads to pyroptotic cell death (Lebeaupin et al., 2015). Since 5-HMF abrogated LPS-induced ER stress by downregulating ATF4 and CHOP, we overexpressed ATF4 and CHOP mRNA in the BMDMs, and found that increased levels of IL-1 β and caspase 1 were released following LPS and ATP stimulation (Figures 6A–D). This is consistent with the fact that the inhibitory activity of 5-HMF on NLRP3 inflammasome is partially dependent on the down-regulation of PERK/ATF4/CHOP signaling pathway. In addition, the suppression of ASC speck formation and ASC oligomerization by 5-HMF were also rescued upon ectopic expression of ATF4 or CHOP (Figures 6E–H). Thus, 5-HMF prevented NLRP3 activation *in vitro* via suppression of ER stress. In addition, we also demonstrated that 5-HMF-driven suppression of ER stress ameliorated lung injury and decreased inflammatory responses in LPS-induced ALI mice. Consistent with this, the ER stress inducer tunicamycin overcame the ameliorative effects of 5-HMF on LPS-induced pulmonary dysfunction. Tunicamycin also reversed the anti-inflammatory effect of 5-HMF, which mitigated the infiltration of inflammatory cells into the pulmonary alveoli, the MPO activities in BALF and the levels of proinflammatory cytokines in sera (Figure 7). Taken together with the above *in vivo* results, 5-HMF-driven ER stress inhibition is a major mechanism underlying the inactivation of NLRP3 inflammasome and amelioration of pulmonary dysfunction in ALI.

To summarize, our present study demonstrates a novel therapeutic effect of 5-HMF against LPS-induced ALI. 5-HMF not only inhibits the NF- κ B-dependent inflammatory pathway but also inactivates the NLRP3 inflammasome by attenuating ER stress. Thus, 5-HMF should be studied further as a novel anti-inflammation drug. Given that 5-HMF is present in various natural foods and TCM formulations, our study provides a new pharmacological approach for lessening inflammation by using natural occurring compounds.

REFERENCES

- Aggarwal, S., Ahmad, I., Lam, A., Carlisle, M. A., Li, C., Wells, J. M., et al. (2018). Heme Scavenging Reduces Pulmonary Endoplasmic Reticulum Stress, Fibrosis, and Emphysema. *JCI Insight* 3, 1. doi:10.1172/jci.insight.120694
- Alizadeh, M., Khodaei, H., Mesgari Abbasi, M., and Saleh-Ghadimi, S. (2017). Assessing the Effect of 5-hydroxymethylfurfural on Selected Components of Immune Responses in Mice Immunised with Ovalbumin. *J. Sci. Food Agric.* 97, 3979–3984. doi:10.1002/jsfa.8261
- Anese, M., Manzocco, L., Calligaris, S., and Nicoli, M. C. (2013). Industrially Applicable Strategies for Mitigating Acrylamide, Furan, and 5-

DATA AVAILABILITY STATEMENT

The original contributions presented in the study are included in the article/Supplementary Material, further inquiries can be directed to the corresponding authors.

ETHICS STATEMENT

The animal study was reviewed and approved by Animal Ethical and Welfare Committee of Hangzhou Normal University.

AUTHOR CONTRIBUTIONS

HZhang, YK, TX and X-YY conceived and supervised the project. HZhang, RB and X-YY wrote the manuscript. HZhang and YK designed the experiments and analyzed the data. HZhang, ZJ, CS, HZ, ZZ, and KW performed experiments.

FUNDING

This work was supported by the National Natural Science Foundation of China (81,730,108, 81,973,635, 81,900,011, 82,073,686), Zhejiang Provincial Natural Science Foundation of China (LQ19C080001), the Medical Health Science and Technology Project of Zhejiang Provincial Health Commission (2021KY962), Key Project of Hangzhou Ministry of Science and Technology (20212013B03), the Ministry of Science and Technology of China (High-end foreign experts program, G2021017004, G20200217005), Hangzhou's "115" plan to introduce overseas intelligence projects (20,200,215), Hangzhou Normal University startup fund (4125C5021920419), Hangzhou Normal University School of Medicine Teaching Reform Fund (4125b30100112), Project of National Students Platform for Innovation and Entrepreneurship Training Program (201,910,346,035).

SUPPLEMENTARY MATERIAL

The Supplementary Material for this article can be found online at: <https://www.frontiersin.org/articles/10.3389/fcell.2021.782427/full#supplementary-material>

hydroxymethylfurfural in Food. *J. Agric. Food Chem.* 61, 10209–10214. doi:10.1021/jf305085r

- Belchamber, K. B. R., and Donnelly, L. E. (2017). Macrophage Dysfunction in Respiratory Disease. *Results Probl. Cell Differ* 62, 299–313. doi:10.1007/978-3-319-54090-0_12
- Cai, X., Chen, J., Xu, H., Liu, S., Jiang, Q.-X., Halfmann, R., et al. (2014). Prion-like Polymerization Underlies Signal Transduction in Antiviral Immune Defense and Inflammasome Activation. *Cell* 156, 1207–1222. doi:10.1016/j.cell.2014.01.063
- Chen, X., Guo, X., Ge, Q., Zhao, Y., Mu, H., and Zhang, J. (2019). ER Stress Activates the NLRP3 Inflammasome: A Novel Mechanism of Atherosclerosis. *Oxid Med. Cel Longev* 2019, 3462530. doi:10.1155/2019/3462530

- Choi, Y. H., Kim, G.-Y., and Lee, H. H. (2014). Anti-inflammatory Effects of Cordycepin In lipopolysaccharide-Stimulated RAW 264.7 Macrophages through Toll-like Receptor 4-mediated Suppression of Mitogen-Activated Protein Kinases and NF-Kb Signaling Pathways. *Dddt* 8, 1941–1953. doi:10.2147/dddt.s71957
- Coll, R. C., Robertson, A. A. B., Chae, J. J., Higgins, S. C., Muñoz-Planillo, R., Inserra, M. C., et al. (2015). A Small-Molecule Inhibitor of the NLRP3 Inflammasome for the Treatment of Inflammatory Diseases. *Nat. Med.* 21, 248–255. doi:10.1038/nm.3806
- Compan, V., Martín-Sánchez, F., Baroja-Mazo, A., López-Castejón, G., Gomez, A. I., Verkhatsky, A., et al. (2015). Apoptosis-associated Speck-like Protein Containing a CARD Forms Specks but Does Not Activate Caspase-1 in the Absence of NLRP3 during Macrophage Swelling. *J.I.* 194, 1261–1273. doi:10.4049/jimmunol.1301676
- Dai, M. X., Zheng, X. H., Yu, J., Yin, T., Ma, M. J., Zhang, L., et al. (2014). The Impact of Intermittent and Repetitive Cold Stress Exposure on Endoplasmic Reticulum Stress and Instability of Atherosclerotic Plaques. *Cell Physiol Biochem* 34, 393–404. doi:10.1159/000363008
- Dang, Y., Mu, Y., Wang, K., Xu, K., Zhu, Y., Luo, B., et al. (2016). Papaverine Inhibits Lipopolysaccharide-Induced Microglial Activation by Suppressing NF-Kb Signaling Pathway. *Dddt* 10, 851–859. doi:10.2147/dddt.s97380
- Dong, H., Wang, M., Chang, C., Sun, M., Yang, F., Li, L., et al. (2020). Erianin Inhibits the Oncogenic Properties of Hepatocellular Carcinoma via Inducing DNA Damage and Aberrant Mitosis. *Biochem. Pharmacol.* 182, 114266. doi:10.1016/j.bcp.2020.114266
- Elliott, E. I., and Sutterwala, F. S. (2015). Initiation and Perpetuation of NLRP3 Inflammasome Activation and Assembly. *Immunol. Rev.* 265, 35–52. doi:10.1111/imr.12286
- Endo, M., Oyadomari, S., Suga, M., Mori, M., and Gotoh, T. (2005). The ER Stress Pathway Involving CHOP Is Activated in the Lungs of LPS-Treated Mice. *J. Biochem.* 138, 501–507. doi:10.1093/jb/mvi143
- Feng, Y. J., Wang, X. X., Zhuang, P. Y., Zhang, D. Y., Gao, L., Chen, J. M., et al. (2017). Study on Chemical Constituents of Codonopsis Pilosula. *Zhongguo Zhong Yao Za Zhi* 42, 135–139. doi:10.19540/j.cnki.cjcm.20161222.046
- Fukumoto, J., Fukumoto, I., Parthasarathy, P. T., Cox, R., Huynh, B., Ramanathan, G. K., et al. (2013). NLRP3 Deletion Protects from Hyperoxia-Induced Acute Lung Injury. *Am. J. Physiology-Cell Physiol.* 305, C182–C189. doi:10.1152/ajpcell.00086.2013
- Guo, H., Callaway, J. B., and Ting, J. P.-Y. (2015). Inflammasomes: Mechanism of Action, Role in Disease, and Therapeutics. *Nat. Med.* 21, 677–687. doi:10.1038/nm.3893
- Herb, M., Farid, A., Gluscho, A., Kronke, M., and Schramm, M. (2019). Highly Efficient Transfection of Primary Macrophages with *In Vitro* Transcribed mRNA. *J. Vis. Exp.* 153, 1. doi:10.3791/60143
- Huang, C. Y., Deng, J. S., Huang, W. C., Jiang, W. P., and Huang, G. J. (2020). Attenuation of Lipopolysaccharide-Induced Acute Lung Injury by Hispolon in Mice, through Regulating the TLR4/PI3K/Akt/mTOR and Keap1/Nrf2/HO-1 Pathways, and Suppressing Oxidative Stress-Mediated ER Stress-Induced Apoptosis and Autophagy. *Nutrients* 12, 1. doi:10.3390/nu12061742
- Jiang, Z. Q., Ma, Y. X., Li, M. H., Zhan, X. Q., Zhang, X., and Wang, M. Y. (2015). 5-Hydroxymethylfurfural Protects against ER Stress-Induced Apoptosis in GalN/TNF-Alpha-Injured L02 Hepatocytes through Regulating the PERK-eIF2alpha Signaling Pathway. *Chin. J. Nat. Med.* 13, 896–905. doi:10.1016/s1875-5364(15)30095-9
- Kang, Y., Zhang, H., Zhao, Y., Wang, Y., Wang, W., He, Y., et al. (2018). Telomere Dysfunction Disturbs Macrophage Mitochondrial Metabolism and the NLRP3 Inflammasome through the PGC-1 α /TNFAIP3 Axis. *Cel Rep.* 22, 3493–3506. doi:10.1016/j.celrep.2018.02.071
- Kim, H. J., Jeong, J. S., Kim, S. R., Park, S. Y., Chae, H. J., and Lee, Y. C. (2013). Inhibition of Endoplasmic Reticulum Stress Alleviates Lipopolysaccharide-Induced Lung Inflammation through Modulation of NF-Kb/hif-1 α Signaling Pathway. *Sci. Rep.* 3, 1142. doi:10.1038/srep01142
- Kim, H. K., Choi, Y.-W., Lee, E. N., Park, J. K., Kim, S.-G., Park, D.-J., et al. (2011). 5-Hydroxymethylfurfural from Black Garlic Extract Prevents TNF α -Induced Monocytic Cell Adhesion to HUVECs by Suppression of Vascular Cell Adhesion Molecule-1 Expression, Reactive Oxygen Species Generation and NF-Kb Activation. *Phytother. Res.* 25, 965–974. doi:10.1002/ptr.3351
- Kim, S. H., Lee, T. H., Lee, S. M., Park, J. H., Park, K. H., Jung, M., et al. (2015). Cynandione A Attenuates Lipopolysaccharide-Induced Production of Inflammatory Mediators via MAPK Inhibition and NF-Kb Inactivation in RAW264.7 Macrophages and Protects Mice against Endotoxin Shock. *Exp. Biol. Med. (Maywood)* 240, 946–954. doi:10.1177/1535370214558022
- Kim, S. R., Kim, H. J., Kim, D. I., Lee, K. B., Park, H. J., Jeong, J. S., et al. (2015). Blockade of Interplay between IL-17A and Endoplasmic Reticulum Stress Attenuates LPS-Induced Lung Injury. *Theranostics* 5, 1343–1362. doi:10.7150/thno.11685
- Ko, I.-G., Hwang, J. J., Chang, B. S., Kim, S.-H., Jin, J.-J., Hwang, L., et al. (2020). Polydeoxyribonucleotide Ameliorates Lipopolysaccharide-Induced Acute Lung Injury via Modulation of the MAPK/NF- κ B Signaling Pathway in Rats. *Int. Immunopharmacology* 83, 106444. doi:10.1016/j.intimp.2020.106444
- Kong, F., Lee, B. H., and Wei, K. (2019). 5-Hydroxymethylfurfural Mitigates Lipopolysaccharide-Stimulated Inflammation via Suppression of MAPK, NF-Kb and mTOR Activation in RAW 264.7 Cells. *Molecules* 24, 1. doi:10.3390/molecules24020275
- Krebs, J., Agellon, L. B., and Michalak, M. (2015). Ca(2+) Homeostasis and Endoplasmic Reticulum (ER) Stress: An Integrated View of Calcium Signaling. *Biochem. Biophys. Res. Commun.* 460, 114–121. doi:10.1016/j.bbrc.2015.02.004
- Lamkanfi, M., Sarkar, A., Vande Walle, L., Vitari, A. C., Amer, A. O., Wewers, M. D., et al. (2010). Inflammasome-dependent Release of the Alarmin HMGB1 in Endotoxemia. *J.I.* 185, 4385–4392. doi:10.4049/jimmunol.1000803
- Lebeaupin, C., Proics, E., de Bievile, C. H., Rousseau, D., Bonnafous, S., Patouraux, S., et al. (2015). ER Stress Induces NLRP3 Inflammasome Activation and Hepatocyte Death. *Cell Death Dis* 6, e1879. doi:10.1038/cddis.2015.248
- Lebeaupin, C., Vallee, D., Hazari, Y., Hetz, C., Chevet, E., and Bailly-Maitre, B. (2018). Endoplasmic Reticulum Stress Signalling and the Pathogenesis of Non-alcoholic Fatty Liver Disease. *J. Hepatol.* 69, 927–947. doi:10.1016/j.jhep.2018.06.008
- Lee, S., Suh, G.-Y., Ryter, S. W., and Choi, A. M. K. (2016). Regulation and Function of the Nucleotide Binding Domain Leucine-Rich Repeat-Containing Receptor, PIRIN Domain-Containing-3 Inflammasome in Lung Disease. *Am. J. Respir. Cell Mol Biol* 54, 151–160. doi:10.1165/rcmb.2015-0231tr
- Leonard, A., Grose, V., Paton, A. W., Paton, J. C., Yule, D. I., Rahman, A., et al. (2019). Selective Inactivation of Intracellular BIP/GRP78 Attenuates Endothelial Inflammation and Permeability in Acute Lung Injury. *Sci. Rep.* 9, 2096. doi:10.1038/s41598-018-38312-w
- Li, L. Y., Yang, J. F., Rong, F., Luo, Z. P., Hu, S., Fang, H., et al. (2021). ZEB1 Serves an Oncogenic Role in the Tumorigenesis of HCC by Promoting Cell Proliferation, Migration, and Inhibiting Apoptosis via Wnt/beta-Catenin Signaling Pathway. *Acta Pharmacol. Sin* 42 (10), 1676–1689. doi:10.1038/s41401-020-00575-3
- Li, W., Qu, X.-N., Han, Y., Zheng, S.-W., Wang, J., and Wang, Y.-P. (2015). Ameliorative Effects of 5-Hydroxymethyl-2-Furfural (5-HMF) from Schisandra Chinensis on Alcoholic Liver Oxidative Injury in Mice. *Ijms* 16, 2446–2457. doi:10.3390/ijms16022446
- Liu, Y.-y., Shi, Y., Liu, Y., Pan, X.-h., and Zhang, K.-x. (2018). Telomere Shortening Activates TGF- β /Smads Signaling in Lungs and Enhances Both Lipopolysaccharide and Bleomycin-Induced Pulmonary Fibrosis. *Acta Pharmacol. Sin* 39, 1735–1745. doi:10.1038/s41401-018-0007-9
- Lou, J.-S., Zhao, L.-P., Huang, Z.-H., Chen, X.-Y., Xu, J.-T., Tai, W. C.-S., et al. (2021). Ginkgetin Derived from Ginkgo Biloba Leaves Enhances the Therapeutic Effect of Cisplatin via Ferroptosis-Mediated Disruption of the Nrf2/HO-1 axis in EGFR Wild-type Non-small-cell Lung Cancer. *Phytomedicine* 80, 153370. doi:10.1016/j.phymed.2020.153370
- Lu, A., Magupalli, V. G., Ruan, J., Yin, Q., Atianand, M. K., Vos, M. R., et al. (2014). Unified Polymerization Mechanism for the Assembly of ASC-dependent Inflammasomes. *Cell* 156, 1193–1206. doi:10.1016/j.cell.2014.02.008
- Lu, Y.-C., Yeh, W.-C., and Ohashi, P. S. (2008). LPS/TLR4 Signal Transduction Pathway. *Cytokine* 42, 145–151. doi:10.1016/j.cyt.2008.01.006
- Lugrin, J., and Martinon, F. (2017). Detection of ASC Oligomerization by Western Blotting. *Bio Protoc.* 7, 1. doi:10.21769/BioProtoc.2292
- Luo, X., Lin, B., Gao, Y., Lei, X., Wang, X., Li, Y., et al. (2019). Genipin Attenuates Mitochondrial-dependent Apoptosis, Endoplasmic Reticulum Stress, and Inflammation via the PI3K/AKT Pathway in Acute Lung Injury. *Int. Immunopharmacology* 76, 105842. doi:10.1016/j.intimp.2019.105842

- Lv, H., Yu, Z., Zheng, Y., Wang, L., Qin, X., Cheng, G., et al. (2016). Isovotexin Exerts Anti-inflammatory and Anti-oxidant Activities on Lipopolysaccharide-Induced Acute Lung Injury by Inhibiting MAPK and NF-Kb and Activating HO-1/Nrf2 Pathways. *Int. J. Biol. Sci.* 12, 72–86. doi:10.7150/ijbs.13188
- Ma, Y., Brewer, J. W., Diehl, J. A., and Hendershot, L. M. (2002). Two Distinct Stress Signaling Pathways Converge upon the CHOP Promoter during the Mammalian Unfolded Protein Response. *J. Mol. Biol.* 318, 1351–1365. doi:10.1016/s0022-2836(02)00234-6
- Mariathasan, S., Weiss, D. S., Newton, K., McBride, J., O'Rourke, K., Roose-Girma, M., et al. (2006). Cryopyrin Activates the Inflammasome in Response to Toxins and ATP. *Nature* 440, 228–232. doi:10.1038/nature04515
- Meng, L., Li, L., Lu, S., Li, K., Su, Z., Wang, Y., et al. (2018). The Protective Effect of Dexmedetomidine on LPS-Induced Acute Lung Injury through the HMGB1-Mediated TLR4/NF-Kb and PI3K/Akt/mTOR Pathways. *Mol. Immunol.* 94, 7–17. doi:10.1016/j.molimm.2017.12.008
- Menu, P., Mayor, A., Zhou, R., Tardivel, A., Ichijo, H., Mori, K., et al. (2012). ER Stress Activates the NLRP3 Inflammasome via an UPR-independent Pathway. *Cel Death Dis* 3, e261. doi:10.1038/cddis.2011.132
- Mimura, N., Fulciniti, M., Gorgun, G., Tai, Y.-T., Cirstea, D., Santo, L., et al. (2012). Blockade of XBP1 Splicing by Inhibition of IRE1 α Is a Promising Therapeutic Option in Multiple Myeloma. *Blood* 119, 5772–5781. doi:10.1182/blood-2011-07-366633
- Moazed, F., and Calfee, C. S. (2014). Environmental Risk Factors for Acute Respiratory Distress Syndrome. *Clin. Chest Med.* 35, 625–637. doi:10.1016/j.ccm.2014.08.003
- Mohan, S., R. P. R. M., Ayyappan, P., and G. R. K. (2019). Endoplasmic Reticulum Stress: A Master Regulator of Metabolic Syndrome. *Eur. J. Pharmacol.* 860, 172553. doi:10.1016/j.ejphar.2019.172553
- Osowski, C. M., Hara, T., O'Sullivan-Murphy, B., Kanekura, K., Lu, S., Hara, M., et al. (2012). Thioredoxin-Interacting Protein Mediates ER Stress-Induced β Cell Death through Initiation of the Inflammasome. *Cel Metab.* 16, 265–273. doi:10.1016/j.cmet.2012.07.005
- Rizzuto, R., De Stefani, D., Raffaello, A., and Mammucari, C. (2012). Mitochondria as Sensors and Regulators of Calcium Signalling. *Nat. Rev. Mol. Cel Biol* 13, 566–578. doi:10.1038/nrm3412
- Sahukari, R., Punabaka, J., Bhasha, S., Ganjikunta, V. S., Ramudu, S. K., and Kesireddy, S. R. (2020). Plant Compounds for the Treatment of Diabetes, a Metabolic Disorder: NF-Kb as a Therapeutic Target. *Cpd* 26, 4955–4969. doi:10.2174/1381612826666200730221035
- Seo, E.-J., Fischer, N., and Efferth, T. (2018). Phytochemicals as Inhibitors of NF-Kb for Treatment of Alzheimer's Disease. *Pharmacol. Res.* 129, 262–273. doi:10.1016/j.phrs.2017.11.030
- Shapla, U. M., Solayman, M., Alam, N., Khalil, M. I., and Gan, S. H. (2018). 5-Hydroxymethylfurfural (HMF) Levels in Honey and Other Food Products: Effects on Bees and Human Health. *Chem. Cent. J.* 12, 35. doi:10.1186/s13065-018-0408-3
- Stewart, T. A., Yapa, K. T., and Monteith, G. R. (2015). Altered Calcium Signaling in Cancer Cells. *Biochim. Biophys. Acta* 1848, 2502–2511. doi:10.1016/j.bbame.2014.08.016
- Vajjhala, P. R., Mirams, R. E., and Hill, J. M. (2012). Multiple Binding Sites on the Pyrin Domain of ASC Protein Allow Self-Association and Interaction with NLRP3 Protein. *J. Biol. Chem.* 287, 41732–41743. doi:10.1074/jbc.m112.381228
- Walsh, J. G., Muruve, D. A., and Power, C. (2014). Inflammasomes in the CNS. *Nat. Rev. Neurosci.* 15, 84–97. doi:10.1038/nrn3638
- Wang, L., Cao, Y., Gorshkov, B., Zhou, Y., Yang, Q., Xu, J., et al. (2019). Ablation of Endothelial Pfkfb3 Protects Mice from Acute Lung Injury in LPS-Induced Endotoxemia. *Pharmacol. Res.* 146, 104292. doi:10.1016/j.phrs.2019.104292
- Ware, L. B., and Matthay, M. A. (2000). The Acute Respiratory Distress Syndrome. *N. Engl. J. Med.* 342, 1334–1349. doi:10.1056/nejm200005043421806
- Wölkart, G., Schrammel, A., Koyani, C. N., Scherübel, S., Zorn-Pauly, K., Malle, E., et al. (2017). Cardioprotective Effects of 5-hydroxymethylfurfural Mediated by Inhibition of L-type Ca²⁺ currents. *Br. J. Pharmacol.* 174, 3640–3653. doi:10.1111/bph.13967
- Wu, G., Xu, G., Chen, D.-W., Gao, W.-X., Xiong, J.-Q., Shen, H.-Y., et al. (2018). Hypoxia Exacerbates Inflammatory Acute Lung Injury via the Toll-like Receptor 4 Signaling Pathway. *Front. Immunol.* 9, 1667. doi:10.3389/fimmu.2018.01667
- Xu, X., Yin, P., Wan, C., Chong, X., Liu, M., Cheng, P., et al. (2014). Punicalagin Inhibits Inflammation in LPS-Induced RAW264.7 Macrophages via the Suppression of TLR4-Mediated MAPKs and NF-Kb Activation. *Inflammation* 37, 956–965. doi:10.1007/s10753-014-9816-2
- Ye, L., Yang, Y., Zhang, X., Cai, P., Li, R., Chen, D., et al. (2015). The Role of bFGF in the Excessive Activation of Astrocytes Is Related to the Inhibition of TLR4/NFkB Signals. *Int. J. Mol. Sci.* 17, 1. doi:10.3390/ijms17010037
- Yoshida, H., Okada, T., Haze, K., Yanagi, H., Yura, T., Negishi, M., et al. (2000). ATF6 Activated by Proteolysis Binds in the Presence of NF-Y (CBF) Directly to the Cis-Acting Element Responsible for the Mammalian Unfolded Protein Response. *Mol. Cel Biol* 20, 6755–6767. doi:10.1128/mcb.20.18.6755-6767.2000
- Youn, Y.-H., Nguyen, K. Y., Grant, R. W., Goldberg, E. L., Bodogai, M., Kim, D., et al. (2015). The Ketone Metabolite β -hydroxybutyrate Blocks NLRP3 Inflammasome-Mediated Inflammatory Disease. *Nat. Med.* 21, 263–269. doi:10.1038/nm.3804
- Yu, W.-w., Lu, Z., Zhang, H., Kang, Y.-h., Mao, Y., Wang, H.-h., et al. (2014). Anti-inflammatory and Protective Properties of Daphnetin in Endotoxin-Induced Lung Injury. *J. Agric. Food Chem.* 62, 12315–12325. doi:10.1021/jf503667v
- Zeng, M., Sang, W., Chen, S., Chen, R., Zhang, H., Xue, F., et al. (2017). 4-PBA Inhibits LPS-Induced Inflammation through Regulating ER Stress and Autophagy in Acute Lung Injury Models. *Toxicol. Lett.* 271, 26–37. doi:10.1016/j.toxlet.2017.02.023
- Zhang, K., and Kaufman, R. J. (2008). From Endoplasmic-Reticulum Stress to the Inflammatory Response. *Nature* 454, 455–462. doi:10.1038/nature07203
- Zhao, L., Chen, J., Su, J., Li, L., Hu, S., Li, B., et al. (2013). *In Vitro* antioxidant and Antiproliferative Activities of 5-hydroxymethylfurfural. *J. Agric. Food Chem.* 61, 10604–10611. doi:10.1021/jf403098y
- Zhao, Y., Jiang, Y., Chen, L., Zheng, X., Zhu, J., Song, X., et al. (2020). Inhibition of the Endoplasmic Reticulum (ER) Stress-Associated IRE-1/XBP-1 Pathway Alleviates Acute Lung Injury via Modulation of Macrophage Activation. *J. Thorac. Dis.* 12, 284–295. doi:10.21037/jtd.2020.01.45
- Zirbes, L., Nguyen, B. K., de Graaf, D. C., De Meulenaer, B., Reybroeck, W., Haubruge, E., et al. (2013). Hydroxymethylfurfural: a Possible Emergent Cause of Honey Bee Mortality? *J. Agric. Food Chem.* 61, 11865–11870. doi:10.1021/jf403280n
- Zou, H., Wu, T., Wang, Y., Kang, Y., Shan, Q., Xu, L., et al. (2021). 5-Hydroxymethylfurfural Enhances the Antiviral Immune Response in Macrophages through the Modulation of RIG-I-Mediated Interferon Production and the JAK/STAT Signaling Pathway. *ACS Omega.* 6, 28019–28030. doi:10.1021/acsomega.1c03862

Conflict of Interest: The authors declare that the research was conducted in the absence of any commercial or financial relationships that could be construed as a potential conflict of interest.

Publisher's Note: All claims expressed in this article are solely those of the authors and do not necessarily represent those of their affiliated organizations, or those of the publisher, the editors and the reviewers. Any product that may be evaluated in this article, or claim that may be made by its manufacturer, is not guaranteed or endorsed by the publisher.

Copyright © 2021 Zhang, Jiang, Shen, Zou, Zhang, Wang, Bai, Kang, Ye and Xie. This is an open-access article distributed under the terms of the Creative Commons Attribution License (CC BY). The use, distribution or reproduction in other forums is permitted, provided the original author(s) and the copyright owner(s) are credited and that the original publication in this journal is cited, in accordance with accepted academic practice. No use, distribution or reproduction is permitted which does not comply with these terms.



FUNDC1: A Promising Mitophagy Regulator at the Mitochondria-Associated Membrane for Cardiovascular Diseases

Guoyong Li^{1,2,3†}, Junli Li^{1†}, Ruochen Shao^{1,2,3}, Jiahao Zhao^{1,3} and Mao Chen^{2,1*}

¹Laboratory of Heart Valve Disease, West China Hospital, Sichuan University, Chengdu, China, ²Department of Cardiology, West China Hospital, Sichuan University, Chengdu, China, ³West China School of Medicine, Sichuan University, Chengdu, China

OPEN ACCESS

Edited by:

Jianguang Ji,
Lund University, Sweden

Reviewed by:

Danielle Sliter,
Regenxbio Inc., United States
Pooja Jadiya,
Temple University, United States

*Correspondence:

Mao Chen
hmaochen@vip.sina.com

[†]These authors have contributed
equally to this work

Specialty section:

This article was submitted to
Signaling,
a section of the journal
Frontiers in Cell and Developmental
Biology

Received: 03 October 2021

Accepted: 29 November 2021

Published: 16 December 2021

Citation:

Li G, Li J, Shao R, Zhao J and Chen M
(2021) FUNDC1: A Promising
Mitophagy Regulator at the
Mitochondria-Associated Membrane
for Cardiovascular Diseases.
Front. Cell Dev. Biol. 9:788634.
doi: 10.3389/fcell.2021.788634

Mitochondrial autophagy (or mitophagy) regulates the mitochondrial network and function to contribute to multiple cellular processes. The protective effect of homeostatic mitophagy in cardiovascular diseases (CVDs) has attracted increasing attention. FUN14 domain containing 1 (FUNDC1), an identified mitophagy receptor, plays an essential role in CVDs. Different expression levels of FUNDC1 and its phosphorylated state at different sites alleviate or exacerbate hypoxia and ischemia/reperfusion injury, cardiac hypertrophy, or metabolic damage through promotion or inhibition of mitophagy. In addition, FUNDC1 can be enriched at contact sites between mitochondria and the endoplasmic reticulum (ER), determining the formation of mitochondria-associated membranes (MAMs) that regulate cellular calcium (Ca²⁺) homeostasis and mitochondrial dynamics to prevent heart dysfunction. Moreover, FUNDC1 has also been involved in inflammatory cardiac diseases such as septic cardiomyopathy. In this review, we collect and summarize the evidence on the roles of FUNDC1 exclusively in various CVDs, describing its interactions with different cellular organelles, its involvement in multiple cellular processes, and its associated signaling pathways. FUNDC1 may become a promising therapeutic target for the prevention and management of various CVDs.

Keywords: FUNDC1, mitophagy, cardiovascular diseases, LC3, MAM

1 INTRODUCTION

Cardiovascular diseases (CVDs), as a constant public health burden, are the leading cause of morbidity and mortality worldwide. CVD-related mortality has been reduced due to initiative prevention and pharmaceutical and technological improvements. However, the CVD burden remains high due to incomplete adherence to guidelines, difficulties adhering to preventative measures, and the frequency of conditions that increase coronary heart disease risks in patients, including lipid disorders, high blood pressure, and diabetes (Van Camp, 2014). Therefore, clarifying the CVDs' etiology, pathophysiology, and progression underlying mechanisms and potential therapeutic targets is imperative. The occurrence and progression of CVDs involve multiple cellular processes, in which mitochondria are essential (Dai et al., 2012; Bravo-San Pedro et al., 2017; Tian et al., 2019).

Mitochondria are the powerhouse of cardiac cells (they are the heart unit of cells). Mitochondria are essential during cellular activities such as fatty acid oxidation, oxidative phosphorylation, and energy metabolism. Moreover, mitochondria are involved in adenosine triphosphate (ATP) transfer

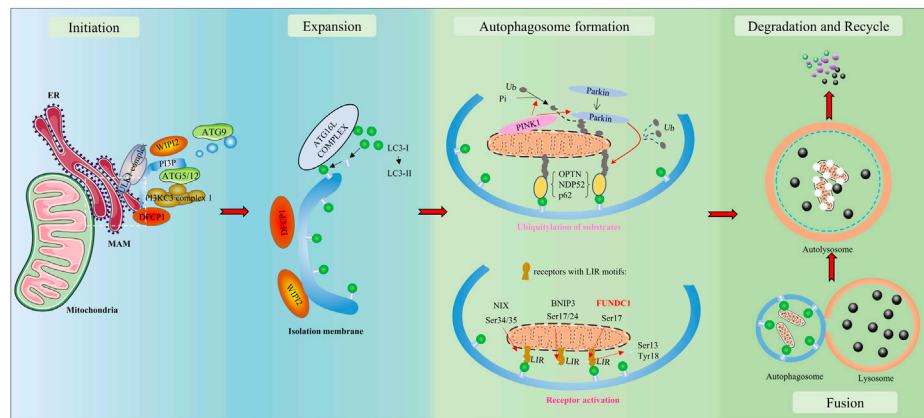


FIGURE 1 | Overview of autophagy/mitophagy. The molecular signals released by damaged mitochondria trigger ubiquitin-mediated and receptor-mediated mitophagy. With the aid of the Unc-51-like kinase 1 (ULK1) complex and class III PI3K (PI3KC3) complex 1, a bilayer lipid membrane enriched in PI3P is formed as part of the endoplasmic reticulum (ER). Then, it could recruit the PI3P effector proteins WD repeat domain phosphoinositide-interacting proteins (WIPIs) and zinc-finger FYVE domain-containing protein 1 (DFCP1), which could attract the autophagy-related protein 8 family (ATG8s), including microtubule-associated protein light chain 3 (LC3) proteins. LC3-I is conjugated to membrane-resident phosphatidylethanolamine (PE) and converted to LC3-II. LC3 has the potential to recognize and engulf labeled proteins and cellular components due to its interaction with LC3-interacting regions (LIRs) of mitophagy receptors. As autophagosomes engulf, they transfer toward and fuse with lysosomes, transforming into autolysosomes. In autolysosomes, the engulfment is degraded and released to the cytosol. Finally, the recycle of nutrients is achieved.

in the contractile apparatus, Ca^{2+} homeostasis modulation, redox status management, and response to cellular and environmental stress regulation in cardiomyocytes (Pecoraro et al., 2019). CVDs such as cardiac hypertrophy, heart failure, and ischemic cardiomyopathy present abnormalities in the mitochondrial organelle structure and function (mitochondrial damage) (Pecoraro et al., 2019). Proper mitochondrial autophagy facilitates the clearance of damaged mitochondria to promote cardiovascular homeostasis (Campos et al., 2017).

Autophagy is a vital catabolic process with tight regulation under various stresses. As depicted in **Figure 1**, a bilayer lipid membrane-formed vesicle (the autophagosome) engulfs aged or damaged cellular organelles such as mitochondria, abnormal proteins, or other cellular components and transfers them toward lysosomes. Fused with a lysosome, the autophagosome transforms into an autolysosome. Autolysosomes degrade engulfed materials and release the products to the cytosol, where nutrient recycling occurs. The UNC51-like Ser/Thr kinase (ULK) complex is required during autophagosome formation to initiate autophagy. Cargo receptors with a cargo-binding domain bind the selected materials to microtubule-associated proteins 1A/1B light chain 3 (LC3) via the LC3-interacting region (LIR) to recruit cargo to autophagosomes (Lamb et al., 2013). To summarize briefly, isolation membranes get expanded to form autophagosomes; these get fused to lysosomes to form autolysosomes, and degradation inside the autolysosomes results in unbroken autophagy (i.e., the autophagic flux) (Lamb et al., 2013). An impaired autophagic flux contributes to multiple CVDs, including ischemia/reperfusion (I/R) injury. Failing hearts are known to present a reduced autophagic flux evidenced by the accumulation of autophagy-related markers (Campos et al., 2017). The infarct size in a heart is significantly increased by lysosomal-associated

transmembrane protein 4B(LAPTM4B) knockdown-induced impairment of the autophagic flux, but it is reversed upon autophagic flux restoration after overexpression (Gu et al., 2020).

Autophagy of mitochondria, a selective form of autophagy that specifically targets damaged mitochondria, is called mitophagy; it is a mechanism to remove impaired or dysfunctional mitochondria and maintain normal mitochondrial morphology and function in cells. Mitophagy is needed for cells to function well because abundant impaired or dysfunctional mitochondria provide an insufficient supply of energy, overproduce excessive reactive oxygen species (ROS), and activate apoptosis pathways by releasing cytochrome C to the cytoplasm (Wang, 2001; Mishra and Chan, 2016; Vásquez-Trincado et al., 2016; Chan, 2020). Many subcellular organelles, including the endoplasmic reticulum (ER), mitochondria-associated membranes (MAMs), lysosomes, and proteins (FUN14 domain containing 1 [FUNDC1], PTEN-induced putative kinase protein-1 [PINK1]/Parkin, selective autophagy adaptor p62/sequestosome 1 [SQSTM1], and LC3) are involved in mitophagy during CVDs (Tagaya and Arasaki, 2017; Yoo and Jung, 2018). MAMs are regions of the ER that mediate communication between the ER and mitochondria and are the platforms of PINK1/Parkin-dependent mitophagy initiation (Yang et al., 2020). As a MAM-localized protein, FUNDC1 maintains homeostasis of MAMs and plays an essential role in receptor-mediated mitophagy.

FUNDC1 was first reported as a novel hypoxia-induced mitophagy receptor in 2012 (Liu et al., 2012a). It is located on the outer mitochondrial membrane (OMM) with an N-terminal LIR (YEVL) exposed to the cytosol that selectively responds to hypoxia/ischemia stimuli (but not to starvation) (Liu et al., 2012a; Kuang et al., 2016). Various upstream phosphorylases or phosphatases change the phosphorylation states at different

FUNDC1 sites to affect the binding affinity of its LIR motif to LC3, thereby promoting or inhibiting mitophagy (Liu et al., 2012a; Feng et al., 2013; Wu et al., 2014a; Chen et al., 2014; Zhou et al., 2018a). In addition, studies have demonstrated that FUNDC1 can tether MAM-specific proteins, facilitate the formation of MAMs, and affect mitochondrial dynamics including the level of Ca^{2+} in the organelle (Wu et al., 2016a; Wu et al., 2016b; Wu et al., 2017). In this review, we collect and summarize the evidence for the roles of FUNDC1 (exclusively on the development of CVDs) describing its interactions with different cellular organelles, its involvement in multiple cellular processes, and its associated signaling pathways.

2 FUNDC1-MEDIATED MITOPHAGY IN CVDs

2.1 Mitophagy in CVDs

Studies have demonstrated at least two major mitophagy pathways: ubiquitin-mediated and receptor-mediated mitophagy (Zimmermann and Reichert, 2017). The ubiquitin-mediated mitophagy pathway is mediated by PINK1/Parkin (Eiyama and Okamoto, 2015; Bingol and Sheng, 2016; Nguyen et al., 2016). PINK1 is a molecular sensor of mitochondrial health that constantly surveys the organelle status. In addition, Parkin is an amplifier of mitophagy. Once mitochondria lose their transmembrane potential, PINK1 accumulates at the OMM of impaired or dysfunctional mitochondria and phosphorylates ubiquitin and Parkin at S65. pS65-Ub (the phosphorylated ubiquitin at S65) binds and activates Parkin by destabilizing Parkin's autoinhibitory interactions and then recruits Parkin from the cytoplasm to the OMM (Nguyen et al., 2016). As E3 ubiquitin ligase, the activated phosphorylated Parkin ubiquitinates various mitochondrial outer-membrane proteins with less specificity. The elongated PINK1 and Parkin proteins form ubiquitin chains that act as molecular signals to further recruit mitophagy receptors, including optineurin (OPTN), nuclear dot protein 52 (NDP52), Tax1-binding protein 1 (TAX1BP1), neighbor of BRCA1 gene 1 (NBR1), and p62, which link ubiquitin chains with LC3 (Dikic and Elazar, 2018). Thus, ubiquitinated proteins in impaired mitochondria can be recognized by cellular mechanisms and get engulfed by autophagosomes to be transferred to lysosomes for degradation.

The known receptor-mediated mitophagy receptors include BCL2 interacting protein 3 such as NIX, also known as (BNIP3L), BCL2 interacting protein 3 (BNIP3), and FUNDC1 in mammalian systems (Liu et al., 2014; Chen et al., 2016). These receptors are integral proteins of the OMM, possessing LIRs, which are the structural basis for LC3 binding to activate mitophagy (Poole and Macleod, 2021). These receptors can be modified by dephosphorylation or phosphorylation under various stresses to affect their affinity for LC3, effectively regulating mitophagy. For instance, BNIP3L-triggered mitophagy can be reversed by PRKA/PKA (protein kinase, AMP-activated)-induced phosphorylation of BNIP3L at Ser212. Activation of the inhibitory phosphorylation site leads to the translocation of BNIP3L from the mitochondria to the

cytosol (da Silva Rosa et al., 2021). Phosphorylation of BNIP3 at Ser17/24 sites or NIX at Ser34/35 sites (Rogov et al., 2017) promotes its binding to LC3 and facilitates subsequent mitophagy (Liu et al., 2014). In the case of FUNDC1, post-transcriptional phosphorylation at Ser17 activates mitophagy, while phosphorylation at Ser13 inhibits the process (Wang et al., 2020a). Thus, mitophagy mediated by these two pathways contributes to the clearance of damaged mitochondria and might be mutually affected.

Proper mitophagy guarantees homeostasis of mitochondria in cells and exerts protective effects on the cardiovascular system, while insufficient or excessive mitophagy may be detrimental. Atherosclerosis, hypertension, ischemia/reperfusion injury, myocardial infarction, cardiac hypertrophy, heart failure, and metabolic cardiomyopathy consistently exhibit mitophagy-involved pathological processes. *In vivo* experiments have shown that knockout of pivotal mitophagy molecules can affect the phenotype and severity of diseases. For example, deletion of PINK1 leads to more severe cardiac hypertrophy and left ventricle dysfunction in mice than those in wild-type and heterozygous mice (Billia et al., 2011), while Parkin-knockout mice are vulnerable to myocardial infarction induced by ligation of the proximal left anterior descending coronary artery and present a low survival rate (Kubli et al., 2013). Similarly, the mammalian target of rapamycin complex 1 (mTORC1) activation in dietary protein-driven atherosclerotic plaques inhibits mitophagy (its downstream effect) and results in a buildup of dysfunctional mitochondria that contribute to a rise in plaque complexity (Zhang et al., 2020). Likewise, the NIX expression has been found to be decreased in human atherosclerosis. Silencing the NIX expression in murine macrophage cells reduced NIX-mediated mitophagy, enhanced oxidized low-density lipoprotein (ox-LDL)-induced macrophage pyroptosis, and led to formation of unstable plaques (Peng et al., 2020). Therefore, numerous chemicals targeting the modulation of mitophagy may alleviate or exacerbate different cardiovascular dysfunctions (Hsu et al., 2015; Ma et al., 2018; Qiao et al., 2018; Yang et al., 2021).

Cardiomyocytes, cardiac fibroblasts (CFs), endothelial cells (ECs), vascular smooth muscle cells (VMSCs), macrophages, and other cell types need to work in an organized manner to keep the cardiovascular system functioning well and maintain a low disease risk. Improper mitophagy can alter the functions of cells and result in the occurrence and progression of diseases. Inhibited mitophagy aggravates lipid accumulation and leads to heart dysfunction (Tong et al., 2019). A mitophagy imbalance renders cardiomyocytes apoptotic under I/R stress (Li et al., 2019a). PINK1/Parkin-mediated mitophagy is upregulated in endothelial cells under metabolic stress to protect mitochondrial integrity and prevent metabolic stress-induced endothelial injury (Wu et al., 2015). The melatonin-induced suppression of mitophagy protects microvascular endothelial cells against I/R injury (Zhou et al., 2017a). In addition, inhibited mitophagy suppresses activation of cardiac fibroblasts but promotes apoptosis (Gao et al., 2020a), while enhanced mitophagy restrains proliferation and apoptosis of

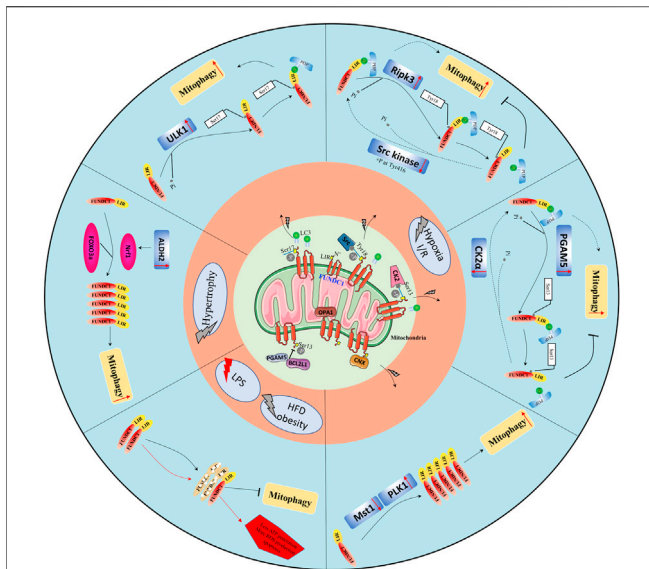


FIGURE 2 | Overview of the protective role of FUNDC1-mediated mitophagy in cardiovascular diseases. Physiologically, FUNDC1 phosphorylation at Ser13 and Tyr18 or dephosphorylation at Ser17; OPA1-FUNDC1 connection, FUNDC1-calnexin association, and the BCL2L1-PGAM5 complex making FUNDC1 dormant. Under abnormal conditions, FUNDC1 could be dephosphorylated at Ser13, Tyr18, and or phosphorylated at Ser17 by various protein kinases such as Src kinase, ULK1, PGAM5, and others remaining to be identified to increase its affinity with LC3 to promote mitophagy.

VMSCs (Swiader et al., 2016; Chen et al., 2020). Thus, mitophagy in various cell types contributes to cardiac function.

2.2 Structure and Post-transcriptional Modification of FUNDC1 for Mitophagy

FUNDC1 is a protein with three α -helix transmembrane domains at the OMM and characteristics similar to those of other mitophagy receptors. Its LIR motif (Y18-E19-V20-L21 at the N-terminal region of FUNDC1 in the cytoplasm) has the classic tetrapeptide W/F/YxxL/I sequence for interaction with LC3, which links it to the ATG5-dependent core autophagic machinery (Liu et al., 2012a; Kuang et al., 2016). Mutants of Y18A, V20A, and L21A or complete deletion of the LIR sequence display a reduced or even abolished affinity of FUNDC1 for LC3 binding that disrupts mitophagy; other FUNDC1 mutations have no effects (Liu et al., 2012a; Kuang et al., 2016). Phosphorylation is the main post-transcriptional modification of FUNDC1 that regulates mitophagy. Three key residues of FUNDC1, Ser13, Ser17, and Tyr18, get phosphorylated and modify the binding affinity of FUNDC1 for LC3 and consequently influence mitophagy (Lv et al., 2017).

Under normal conditions, as depicted in **Figure 2**, FUNDC1 phosphorylation at Ser13 (Chen et al., 2014; Zhou et al., 2018a) and Tyr-18 (Feng et al., 2013; Zhou et al., 2017b) or dephosphorylation at Ser17 (Wu et al., 2014a) both decrease the affinity of FUNDC1 for LC3 by altering its stereochemical properties. The phosphorylation of FUNDC1 at Ser13 and Tyr18

is mediated by casein kinase 2 (CK2) kinases and Src kinase, respectively (Chen et al., 2014). The affinity of the dephosphorylated FUNDC1 peptide (at Ser17) for LC3 (at Lys49) is ~3-fold weaker than that of the phosphorylated FUNDC1 peptide (Lv et al., 2017). The direct optic atrophy 1 (OPA1)-FUNDC1 connection and the FUNDC1-calnexin association block other FUNDC1 interactions, and the BCL2L1 (BH3 domain)-PGAM5L (a member of the phosphoglycerate mutase family) complex inhibits FUNDC1 dephosphorylation at Ser13; all these molecular interactions inhibit FUNDC1 activities (Wu et al., 2014b). Additionally, the membrane-associated RING-CH protein 5 (MARCH5), a mitochondrial E3 ligase, mediates FUNDC1 ubiquitylation and degradation by directly interacting with it at lysine 119. Thus, FUNDC1 is inactivated in healthy hearts. Moderately inactivated FUNDC1 may interact with the F-box protein FBXL2 to maintain the mitochondrial integrity or it may form a complex with heat shock protein 70 (HSC70) to promote the mitochondrial translocation of unfolded cytosolic proteins and maintain the cardiac function (Li et al., 2019b; Ren et al., 2020).

Under abnormal conditions like hypoxia, two pathways regulate FUNDC1 to mediate mitophagy: a kinase-mediated pathway and an interactional protein-regulated pathway. Tyr416-phosphorylated Src enhances Tyr18 dephosphorylation of FUNDC1, increasing its binding ability for LC3 and promoting mitophagy (Feng et al., 2013; Zhou et al., 2017b). Similarly, CK2 dissociates from FUNDC1 and allows PGAM5 to dephosphorylate it at Ser13, strengthening its interaction with LC3 (Chen et al., 2014; Zhou et al., 2018a). ULK1 translocates to mitochondria and activates FUNDC1 by phosphorylating its Ser17, and ULK1 deletion inhibits FUNDC1 activation (Wang et al., 2020a). Under stress, phosphorylated FUNDC1 dissociates from OPA1 and interacts instead with dynamin-related protein 1 (DRP1) to enhance mitochondrial fission and mitophagy (Wu et al., 2016b). During mitophagy under hypoxic conditions, the cytosolic loop of FUNDC1 is exposed (due to an attenuated FUNDC1/calnexin association) and interacts with DRP1 (Wu et al., 2016b). Disorders of mitochondrial dynamics, including imbalanced fission and fusion, are prerequisites for mitophagy. Hypoxia induces BCL2L1 degradation, increases PGAM5 dissociation, and then enhances dephosphorylation of FUNDC1 at Ser13 (Ma et al., 2020). Additionally, the decreased endogenous MARCH5 expression significantly inhibits FUNDC1 degradation and promotes mitophagy (Chen et al., 2017). Other regulators of FUNDC1 have been identified: the Nod-like receptor X1 (NLRX1), in mitochondria, negatively regulates phosphorylated Tyr18 FUNDC1 levels (Li et al., 2021), and the lncRNA MEG3 overexpression induces dephosphorylation of FUNDC1 at Tyr18 by interacting with the 3'UTR of Rac1 to inhibit its expression (Wang et al., 2021a). The transcriptional and post-transcriptional controls of FUNDC1 have also been shown to be important. Under normoxic conditions, the negative regulatory factor microRNA-137 is constitutively expressed; it targets the 3' UTR of the FUNDC1 mRNA suppressing its translation to attenuate FUNDC1-LC3 associations. Under hypoxic conditions, the microRNA-137 is downregulated. At the

transcriptional level, mitophagy is enhanced by the peroxisome proliferator-activated receptor gamma coactivator 1- α (PGC-1 α) protein, which induces the FUNDC1 expression by upregulating the nuclear respiratory factor 1 (NRF1) expression, a factor that binds FUNDC1 at -186/-176 sites (Liu et al., 2021a).

In summary, FUNDC1 is crucial to receptor-mediated mitophagy. Proper mitophagy helps restore cardiac function after hypoxia, I/R, and other stresses. However, a review of FUNDC1-mediated mitophagy in CVDs has not been published.

2.3 FUNDC1-Mediated Mitophagy in CVDs

2.3.1 Hypoxia and I/R

Cardiomyocytes need to generate ATP through oxidative phosphorylation in the respiratory chain of mitochondria, which is highly dependent on oxygen consumption. When hypoxia or ischemia occurs, mitochondria are the first organelles to exhibit extensive fission, loss of membrane potential, and release of proapoptotic signals that eventually led to cell death. I/R injury, which is accompanied by the mitochondrial Ca^{2+} overload, ROS generation, autophagy failure, platelet activation, and microthrombosis (Aghaei et al., 2019; Yang et al., 2019), is a common clinical condition due to rapid revascularization treatments after acute myocardial infarction. Revascularization brings oxygen and nutrition to “suffocated cardiomyocytes,” but it simultaneously promotes cell death (Li et al., 2019a; Wang et al., 2020b). Mitophagy plays a protective role in I/R injury. Under ischemia, mitophagy is thought to be cardioprotective due to its removal of impaired mitochondria, reduction of mitochondrial ROS (mROS) and apoptosis, and reduced inflammation (Yang et al., 2019; Xin and Lu, 2020; Yu et al., 2020). OPA1-induced mitophagy and FUNDC1-dependent mitophagy could offer cardioprotection against ischemia (Li et al., 2018; Xin and Lu, 2020), while the knockout of Parkin causes extensive cardiac injury due to mitochondrial dysfunction and mitophagy inhibition (Kubli et al., 2013). Most other studies have also suggested a cardioprotective role for mitophagy during ischemia. However, mitophagy may exert detrimental effects during the reperfusion phase. According to a published hypothesis, fragmented mitochondria and excessive mitophagy could reduce the necessary ATP supply, leading to cell death (Anzell et al., 2018; Yang et al., 2019). Thus, proper mitophagy guarantees the homeostasis of mitochondria to maintain a normal cellular physiology, but mitophagy dysregulation is pathogenic and even fatal for cells.

Studies have demonstrated that FUNDC1 plays an essential role in mitophagy under hypoxia or I/R conditions. Li et al. reported that the ULK1 signaling pathway mediates FUNDC1 phosphorylation, leading to increased mitophagy levels and cardiac function protection under ischemia (Li et al., 2018). Zhou et al. demonstrated that FUNDC1-mediated mitophagy gets activated to prevent myocardial apoptosis during ischemia, while upregulation of Ripk3 can phosphorylate Tyr18 in FUNDC1 during reperfusion to inhibit FUNDC1-dependent mitophagy and increase necrosis (Zhou et al., 2017b). Zhang et al. found a dual role for mitophagy in platelets, where

FUNDC1-knocked-out platelets presented reduced but sustained mitophagy activity and caused more injuries during the late stages of I/R in the heart (Zhang et al., 2016). The same researchers also generated a cell-penetrating peptide to block mitophagy *in vivo* by intraperitoneal administration to prevent mitochondrial dysfunctions and platelet inactivation, which could become a new strategy potentially applicable in the clinical setting. Zhou et al. studied the association between mitophagy and microvascular permeability and found that under I/R stress, the upregulated nuclear receptor subfamily 4 group A member 1 (NR4A1) induces CK2 α to phosphorylate the mitochondrial fission factor (Mff) and FUNDC1, thereby enhancing mitochondrial fission and inhibiting mitophagy, resulting in microvascular hyperpermeability, endothelial cell apoptosis, and damage (Zhou et al., 2018b). Genetic deletion of CK2 α was also proved by Zhou et al. to protect cardiomyocytes from I/R injury *via* decreased Ser13 phosphorylation of FUNDC1 to promote mitophagy and to prevent mitochondrial damage and apoptosis (Zhou et al., 2018a). In addition, some kinases, such as mammalian STE20-like kinase 1 (Mst1) and polo-like kinase 1 (PLK1), have also been associated with FUNDC1-mediated mitophagy *in vivo* and *in vitro* under I/R stimuli (Yu et al., 2019; Mao et al., 2021).

Interestingly, mitophagy contributes to functional changes in different organs. For example, electroacupuncture preconditioning has a protective effect in patients undergoing heart valve replacement surgery, and this is caused by inhibition of mitophagy mediated by the mTORC1-ULK1-FUNDC1 pathway (Xiao et al., 2020). The protective effect of electroacupuncture pretreatment on cerebral I/R injury also correlates with p-mTORC1 mitophagy (Mao et al., 2020). Moreover, the transient receptor potential cation channel subfamily V member 1 (TRPV1) factor alleviates I/R-induced acute renal injury (Wei et al., 2020). The TRPV1-mediated transient Ca^{2+} influx activates AMP-activated protein kinase (AMPK) and reduces FUNDC1 transcription. This indicates that the Ca^{2+} influx and mitophagy are both regulators during I/R. In addition, FUNDC1-mediated mitophagy (triggered by the activated phosphorylation of AMPK) contributes to the protective effect of the tissue-type plasminogen activator during cerebral I/R injury (Cai et al., 2021). Mitophagy is also considered a key mechanism during intestinal I/R injury. Downregulated NLRX1 promotes phosphorylation of FUNDC1 in intestinal I/R injury (Li et al., 2021). Phosphorylated FUNDC1 decouples from the nitrophenylphosphatase domain and non-neuronal SNAP25-like protein homologs 1 and 2 (NIPSNAP 1 and 2; mitophagy signaling proteins on the outer membrane of damaged mitochondria) and then fails to trigger mitophagy (Li et al., 2021). Similarly, during acute kidney injury, ischemia preconditioning activates FUNDC1 mitophagy (through post-transcriptional phosphorylation at Ser17) to mitigate I/R injury-mediated renal injury (Wang et al., 2020a). Downregulated FUNDC1, the *C. elegans* ortholog of FUNDC1, protects the worm against injury in a model of hypoxia-reoxygenation stress. This protection depends on activation of the transcription factor associated with stress-1 (ATFS-1), the central transcription factor

that regulates the mitochondrial unfolded protein response (Lim et al., 2021). Taken together, most evidence points to FUNDC1-mediated mitophagy being essential against hypoxia and I/R injury; FUNDC1 may be a promising therapeutic target.

2.3.2 Cardiac Hypertrophy and Remodeling

Cardiac hypertrophy is a manifestation of enlargement of individual cardiomyocytes (not an increase in the number of cells) due to various pathological stresses, such as pressure overload, infarction, metabolic disturbances, or structural heart disease, eventually developing into heart failure. Pathological cardiac hypertrophy involves changes in multiple cellular processes, including excessive protein synthesis and inhibition of selective autophagy (Nakamura and Sadoshima, 2018; Zhou et al., 2020). Studies have demonstrated that activated mitophagy can mitigate cardiac hypertrophy. Lysocardiolipin acyltransferase 1 (ALCAT1) deletion upregulates PINK1 and mitigates oxidative stress, insulin resistance, and mitochondrial dysfunction via activation of PINK1-mediated mitophagy and alleviating cardiac hypertrophy (Liu et al., 2012b). Macrophage migration inhibitory factor (MIF) depletion hinders the activation of Parkin-dependent mitophagy by regulating AMPK-mTOR signaling pathways to exacerbate the hypertrophy induced by pressure overload (Xu et al., 2014). In addition, PINK1 autophosphorylation can also recruit Parkin to initiate mitophagy, exerting a protective effect on angiotensin II (ANG II)-induced hypertrophy (Xiong et al., 2018).

FUNDC1-dependent mitophagy has also been shown to play a critical role in cardiac hypertrophy. In a mouse model of cardiac hypertrophy induced by continuous administration of isoproterenol (ISO), Liu et al. reported autophagy inhibition as the LC3II/LC3I ratio decreased, and the FUNDC1 expression was downregulated. This was confirmed by *in vitro* experiments using neonatal rat cardiomyocytes (NRCMs), in which the hypertrophy could be alleviated by baicalein, a flavonoid extracted from the root of *Scutellaria baicalensis* (Liu et al., 2021b). Mechanistically, baicalein binds directly to FOXO3a (a transcription factor) and transactivates FUNDC1. In another study by Li et al., FUNDC1-related mitophagy was associated with cardiac hypertrophy in a mouse model of transaortic constriction (TAC) and an *in vitro* model of NRCMs induced using ANG II (Li et al., 2020). ALDH2 activated by alpha-lipoic acid (α -LA), a well-known antioxidant, governs the activation of Nrf1-FUNDC1. Nrf1, a member of the Cap-N-Collar family of regulatory proteins, binds to the 5' promoter of FUNDC1 to modulate the FUNDC1 expression directly. Thus, the evidence indicates that FUNDC1-mediated mitophagy is involved in cardiac hypertrophy and that interference with the associated signaling pathways could prevent the progression or deterioration of the disease.

2.3.3 FUNDC1-Mediated Mitophagy in Obesity- or High-Fat Diet Intake-Induced Heart Dysfunction

Obesity coexists with reduced autophagy and mitophagy, alongside the inflammation, oxidative stress, lipotoxicity, and apoptosis (Lavallard et al., 2012; Guo et al., 2013; Zhang et al., 2018; Shao et al., 2020) that together may lead to heart dysfunction. Mitophagy markers such as Parkin and BNIP3

are downregulated following HFD feeding (Zeinvand-Lorestani et al., 2018; Thomas et al., 2019). However, a study reported that HFD feeding in mice consistently activates mitophagy, as evaluated with Mito-Keima (Tong et al., 2019). These researchers also found that inhibition of mitophagy by deletion of ATG7 or Parkin in an HFD-induced mouse model can increase lipid accumulation and worsen heart dysfunction, while activation of mitophagy by TB1 (Tat-Becn1) injection exerts the opposite effect (Tong et al., 2019).

Wu et al. found that impaired mitophagy and compromised mitochondrial quality control due to FUNDC1 knockout lead to obesity and insulin resistance in mice via the MAPK/JUN pathway and the inflammatory response (Wu et al., 2019a). In addition, Ren et al. found that FUNDC1 and mitophagy were downregulated in a HFD-induced mouse model and that FUNDC1-knockout mice were more vulnerable to HFD-induced cardiac hypertrophy, fibrosis, and insufficiency, via interaction with FBXL2 in an inositol 1,4,5-trisphosphate receptor type 3 (IP3R3)-dependent manner (Ren et al., 2020). Their study also confirmed that loss of FUNDC1-mediated mitophagy and increased fatty acid synthase acyl-CoA synthetase long-chain 4 (ACSL4)-mediated ferroptosis led to cardiac remodeling and contractile anomaly in FUNDC1-knockout mice under an HFD-induced model (Pei et al., 2021). However, Fu et al. found that skeletal muscle-specific FUNDC1-knockout mice present impaired mitochondrial energetics in the skeletal muscle and exercise performance, but the mice are markedly resistant to HFD-induced obesity with high systemic insulin sensitivity and glucose tolerance (Fu et al., 2018). The mechanism might be that FUNDC1 deficiency upregulated the expression of fibroblast growth factor 21 (FGF21), a peptide hormone that regulates energy homeostasis. Based on the results of these studies, FUNDC1-related mitophagy regulates cardiac metabolism under obesity or HFD stress and may be a potential target to prevent obesity-associated cardiac injury. However, underlying mechanisms remain to be clarified.

3 OTHER ROLES OF FUNDC1 AT MAMS AFFECTING HEART DYSFUNCTION

MAMs are the sites connecting mitochondria and the ER through protein-protein or protein-lipid complex tethers, at which these two subcellular organelles exchange contents and execute fundamental biological processes jointly (Ca^{2+} and lipid exchange, inflammation, and oxidative stress) (Wu and Zou, 2019; Gao et al., 2020b; Silva-Palacios et al., 2020). Emerging evidence has indicated the importance of MAM in CVDs. FUNDC1 is a MAM-related protein important for MAM formation, Ca^{2+} exchange between the ER and mitochondria, and mitochondrial morphology (Wu et al., 2016b; Wu et al., 2017; Wu et al., 2019b).

3.1 FUNDC1 and MAM Formation

FUNDC1 has been found enriched at MAMs under stress and to facilitate ER and mitochondrial tethering by interacting with ER

proteins such as calnexin and IP3R2 (ER-resided inositol 1,4,5-trisphosphate type 2 receptor) (Wu et al., 2016b; Wu et al., 2017; Wu et al., 2019b). Under hypoxia, FUNDC1 accumulates at the MAM and exhibits a dynamic interaction with the MAM-related protein calnexin (Wu et al., 2016b). In cardiomyocyte-specific FUNDC1-knockout mice, the connection between the ER and mitochondria in cardiomyocytes is disrupted, and the mice present few MAMs and MAM-related proteins (IP3R2 and PACS-2 [phosphofurin acidic cluster sorting protein 2]), a picture consistent with that in the H9C2 cell line (Wu et al., 2017). In a high glucose-induced *in vitro* model, the FUNDC1 overexpression promoted MAM formation, and FUNDC1 ablation inhibited it (Wu et al., 2019b). Wang et al. found similar phenotypes in FUNDC1-deleted endothelial cells (EC) and EC-specific FUNDC1-knockout mice (Wang et al., 2021b). Based on the evidence, FUNDC1 is a MAM-related protein that participates in the formation and function of MAMs.

3.2 FUNDC1 and Calcium Homeostasis

During the cardiac cycle, Ca^{2+} is rapidly released to the cytosol from the sarcoplasmic reticulum (SR) and then restored (Gambardella et al., 2018). Appropriate calcium handling is vital for excitation-contraction (EC) coupling of cardiomyocytes, and calcium flux disruption eventually leads to heart dysfunction. Mitochondria can act as Ca^{2+} buffers, and they are also involved in Ca^{2+} reuptake, but Ca^{2+} overload in mitochondria can be harmful and cause heart failure (Brookes et al., 2004; Gambardella et al., 2018). The FUNDC1-mediated MAM is an important structure that regulates intracellular calcium homeostasis. Specific FUNDC1-knockout cardiomyocytes present decreased cytoplasmic and mitochondrial Ca^{2+} and increased ER Ca^{2+} , while FUNDC1-overexpressing cardiomyocytes display the opposite effects (which can be abolished by silencing IP3R2) (Wu et al., 2017). Ablation of FUNDC1 decreases mitochondrial Ca^{2+} (via MAMs induced by high glucose) and also inhibits ROS production and cell apoptosis, preventing cardiac dysfunction *in vivo* (Wu et al., 2019b).

3.3 FUNDC1 and Mitochondrial Dynamics

Studies have reported that deletion of FUNDC1 results in elongated mitochondria in cardiomyocytes (Wu et al., 2016b; Chen et al., 2016; Wu et al., 2017). Wu et al. observed both fewer absolute fission events and a decreased ratio of fission to fusion events in specific FUNDC1-knockout cardiomyocytes *via* time-lapse confocal imaging (Wu et al., 2017). They also found that FUNDC1 loss inhibits the integrity of MAMs, causing increased mitochondrial and intracellular Ca^{2+} concentrations and leading to cardiac dysfunction (Wu et al., 2017). As mentioned, FUNDC1 coordinates mitochondrial dynamics and mitophagy at MAMs by interacting with DRP1 and OPA1. FUNDC1 ablation suppresses the mitochondrial fission 1 protein (Fis1) expression by reducing the binding of the cAMP response element-binding protein (CREB) in the Fis1 promoter and inhibiting mitochondrial fission in cardiomyocytes (Wu et al., 2017). In HeLa cells under hypoxia, FUNDC1 is involved in mitochondrial fission *via* its

Mff interaction (Wu et al., 2016b). In addition, USP19 (an ER-resident deubiquitinase) can bind FUNDC1 and deubiquitinate it at the MAMs leading to DRP1 oligomerization and promotion of mitochondrial division (Chai et al., 2021).

4 FUNDC1 REGULATES THE PRODUCTION OF ROS AND APOPTOSIS IN CVDS

Impaired mitochondria with an altered calcium buffering system generate less ATP and more ROS, eventually leading to mitochondria-related cell apoptosis. Studies have established an association between FUNDC1 and ROS generation and apoptosis (Zhang et al., 2016; Wu et al., 2017; Wu et al., 2019b; Huang et al., 2020; Jiang et al., 2021). Huang et al. found that ablation of FUNDC1 enhances the production of ROS and interleukin 1- β (IL1- β) in macrophages treated with combined lipopolysaccharide (LPS) and nigericin *in vivo* and *in vitro* through the regulation of mitophagy, while the overexpression of FUNDC1 (but not of its Y18A/L21A mutant) can reverse this effect *in vitro* (Huang et al., 2020). In the H9C2 model of septic cardiomyopathy, Jiang et al. found that the ROS generation and apoptosis related to FUNDC1-mediated mitophagy can be attenuated and inhibited by irisin (Jiang et al., 2021). Wang et al. observed similar results in the AC16 human ventricular cardiomyocyte cell line incubated with LPS (Wang et al., 2021c). Wu et al. also confirmed that simple FUNDC1 deletion is sufficient to promote cardiomyocyte apoptosis and heart failure *in vivo* in cardiomyocyte-specific FUNDC1-knockout mice (Wu et al., 2017). However, it is interesting to note that FUNDC1 knockout in Akita mice inhibits excessive ROS production and improves the mitochondrial membrane potential in diabetic hearts compared with the effects in non-FUNDC1-knockout Akita mice (Wu et al., 2019b).

5 CONCLUSION

FUNDC1 (a novel identified receptor of mitophagy at the MAM) plays an important role in mitochondrial homeostasis, MAM-related cellular processes, and mitochondria-mediated apoptosis. We collected evidence demonstrating that FUNDC1 is closely involved with various CVDs. Activated FUNDC1-mediated mitophagy has been proposed to play protective roles in I/R injury, cardiac hypertrophy, and obesity-induced cardiomyopathy. FUNDC1-mediated mitophagy may be stabilized by phosphorylation/dephosphorylation of the three key residues of FUNDC1: Ser13, Ser17, and Tyr18. Thus, these sites are promising therapeutic targets to exploit small molecule drugs that can induce protective mitophagy. This is an enormous challenge that needs to be further explored.

Abundant impaired mitochondria generate high levels of ROS and induce apoptosis, two phenomena that are also affected by FUNDC1. The interaction of FUNDC1 and MAM-located proteins regulates mitochondrial morphology and calcium homeostasis in the cytosol and mitochondria, ensuring cardiac

contractility and normal heart function. Good quality and detailed studies indicate that FUNDC1 and its associated cellular pathways may be a promising therapeutic target for the prevention and management of CVDs. However, the association between FUNDC1 and mROS in CVDs needs clarification.

Some important roles of FUNDC1 in CVDs have been revealed by laboratory experiments, but gaps remain that hamper our understanding of the complex pathophysiological processes at play; more studies are needed before turning laboratory results into effective and safe translational medicine. Many interventional approaches used in the laboratory are not currently available in clinical settings. However, some studies have made excellent attempts at demonstrating their utility. Cell-permeable functional peptides composed of the HIV-1 Tat protein transduction domain have been proven effective to induce FUNDC1-mediated mitophagy activity in cell tests. Similarly, intraperitoneal injection of well-designed synthetic cell-penetrating peptides *in vivo* could lead to satisfactory manipulation of FUNDC1-mediated mitophagy. Unfortunately, in contrast to the many kinases involved in FUNDC1-mediated mitophagy processes tested, no inhibitors

or agonists of those corresponding kinases have been studied *in vivo*. More investigations and innovations are needed before treatments targeting this molecule can be applied in clinical settings.

AUTHOR CONTRIBUTIONS

MC, JL, and GL were responsible for conceptualization and methodology. GL was responsible for original draft preparation and visualization. MC was responsible for supervision. GL, RS, and JZ carried out data curation, software, and validation. JL and MC were responsible for reviewing and editing and funding acquisition.

FUNDING

This study was supported by the National Natural Science Foundation of China (NSFC) projects: 82170375, 81970325, and 11902211 and the Fundamental Research Funds for the Central Universities: 2020SCU12031.

REFERENCES

- Aghaei, M., Motallebnezhad, M., Ghorghanlu, S., Jabbari, A., Enayati, A., Rajaei, M., et al. (2019). Targeting Autophagy in Cardiac Ischemia/reperfusion Injury: A Novel Therapeutic Strategy. *J. Cel Physiol* 234, 16768–16778. doi:10.1002/jcp.28345
- Anzell, A. R., Maizy, R., Przyklenk, K., and Sanderson, T. H. (2018). Mitochondrial Quality Control and Disease: Insights into Ischemia-Reperfusion Injury. *Mol. Neurobiol.* 55, 2547–2564. doi:10.1007/s12035-017-0503-9
- Billia, F., Hauck, L., Konecny, F., Rao, V., Shen, J., and Mak, T. W. (2011). PTEN-inducible Kinase 1 (PINK1)/Park6 Is Indispensable for normal Heart Function. *Proc. Natl. Acad. Sci.* 108, 9572–9577. doi:10.1073/pnas.1106291108
- Bingol, B., and Sheng, M. (2016). Mechanisms of Mitophagy: PINK1, Parkin, USP30 and beyond. *Free Radic. Biol. Med.* 100, 210–222. doi:10.1016/j.freeradbiomed.2016.04.015
- Bravo-San Pedro, J. M., Kroemer, G., and Galluzzi, L. (2017). Autophagy and Mitophagy in Cardiovascular Disease. *Circ. Res.* 120, 1812–1824. doi:10.1161/circresaha.117.311082
- Brookes, P. S., Yoon, Y., Robotham, J. L., Anders, M. W., and Sheu, S.-S. (2004). Calcium, ATP, and ROS: a Mitochondrial Love-Hate triangle. *Am. J. Physiology-Cell Physiol.* 287, C817–C833. doi:10.1152/ajpcell.00139.2004
- Cai, Y., Yang, E., Yao, X., Zhang, X., Wang, Q., Wang, Y., et al. (2021). FUNDC1-dependent Mitophagy Induced by tPA Protects Neurons against Cerebral Ischemia-Reperfusion Injury. *Redox Biol.* 38, 101792. doi:10.1016/j.redox.2020.101792
- Campos, J. C., Quelicini, B. B., Bozi, L. H. M., Bechara, L. R. G., Dourado, P. M. M., Andres, A. M., et al. (2017). Exercise Reestablishes Autophagic Flux and Mitochondrial Quality Control in Heart Failure. *Autophagy* 13, 1304–1317. doi:10.1080/15548627.2017.1325062
- Chai, P., Cheng, Y., Hou, C., Yin, L., Zhang, D., Hu, Y., et al. (2021). USP19 Promotes Hypoxia-Induced Mitochondrial Division via FUNDC1 at ER-Mitochondria Contact Sites. *J. Cel Biol* 220. doi:10.1083/jcb.202010006
- Chan, D. C. (2020). Mitochondrial Dynamics and its Involvement in Disease. *Annu. Rev. Pathol. Mech. Dis.* 15, 235–259. doi:10.1146/annurev-pathmechdis-012419-032711
- Chen, G., Han, Z., Feng, D., Chen, Y., Chen, L., Wu, H., et al. (2014). A Regulatory Signaling Loop Comprising the PGAM5 Phosphatase and CK2 Controls Receptor-Mediated Mitophagy. *Mol. Cel* 54, 362–377. doi:10.1016/j.molcel.2014.02.034
- Chen, M., Chen, Z., Wang, Y., Tan, Z., Zhu, C., Li, Y., et al. (2016). Mitophagy Receptor FUNDC1 Regulates Mitochondrial Dynamics and Mitophagy. *Autophagy* 12, 689–702. doi:10.1080/15548627.2016.1151580
- Chen, Y., Li, S., Guo, Y., Yu, H., Bao, Y., Xin, X., et al. (2020). Astaxanthin Attenuates Hypertensive Vascular Remodeling by Protecting Vascular Smooth Muscle Cells from Oxidative Stress-Induced Mitochondrial Dysfunction[J]. *Oxid Med. Cel Longev* 2020, 4629189. doi:10.1155/2020/4629189
- Chen, Z., Liu, L., Cheng, Q., Li, Y., Wu, H., Zhang, W., et al. (2017). Mitochondrial E3 Ligase MARCH 5 Regulates FUNDC 1 to fine-tune Hypoxic Mitophagy. *EMBO Rep.* 18, 495–509. doi:10.15252/embr.201643309
- da Silva Rosa, S. C., Martens, M. D., Field, J. T., Nguyen, L., Kereliuk, S. M., Hai, Y., et al. (2021). BNIP3L/Nix-induced Mitochondrial Fission, Mitophagy, and Impaired Myocyte Glucose Uptake Are Abrogated by PRKA/PKA Phosphorylation. *Autophagy* 17, 2257–2272. doi:10.1080/15548627.2020.1821548
- Dai, D.-F., Rabinovitch, P. S., and Ungvari, Z. (2012). Mitochondria and Cardiovascular Aging. *Circ. Res.* 110, 1109–1124. doi:10.1161/circresaha.111.246140
- Dikic, I., and Elazar, Z. (2018). Mechanism and Medical Implications of Mammalian Autophagy. *Nat. Rev. Mol. Cel Biol* 19, 349–364. doi:10.1038/s41580-018-0003-4
- Eiyama, A., and Okamoto, K. (2015). PINK1/Parkin-mediated Mitophagy in Mammalian Cells. *Curr. Opin. Cel Biol.* 33, 95–101. doi:10.1016/j.celb.2015.01.002
- Feng, D., Liu, L., Zhu, Y., and Chen, Q. (2013). Molecular Signaling toward Mitophagy and its Physiological Significance. *Exp. Cel Res.* 319, 1697–1705. doi:10.1016/j.yexcr.2013.03.034
- Fu, T., Xu, Z., Liu, L., Guo, Q., Wu, H., Liang, X., et al. (2018). Mitophagy Directs Muscle-Adipose Crosstalk to Alleviate Dietary Obesity. *Cel Rep.* 23, 1357–1372. doi:10.1016/j.celrep.2018.03.127
- Gambardella, J., Trimarco, B., Iaccarino, G., and Santulli, G. (2018). New Insights in Cardiac Calcium Handling and Excitation-Contraction Coupling. *Adv. Exp. Med. Biol.* 1067, 373–385. doi:10.1007/5584_2017_106
- Gao, P., Yan, Z., and Zhu, Z. (2020). Mitochondria-Associated Endoplasmic Reticulum Membranes in Cardiovascular Diseases. *Front. Cel Dev. Biol.* 8, 604240. doi:10.3389/fcell.2020.604240
- Gao, Q. Y., Zhang, H. F., Tao, J., Chen, Z. T., Liu, C. Y., Liu, W. H., et al. (2020). Mitochondrial Fission and Mitophagy Reciprocally Orchestrate Cardiac Fibroblasts Activation. *Front Cel Dev Biol* 8, 629397. doi:10.3389/fcell.2020.629397

- Gu, S., Tan, J., Li, Q., Liu, S., Ma, J., Zheng, Y., et al. (2020). Downregulation of LAPTM4B Contributes to the Impairment of the Autophagic Flux via Unopposed Activation of mTORC1 Signaling during Myocardial Ischemia/Reperfusion Injury. *Circ. Res.* 127, e148–e165. doi:10.1161/CIRCRESAHA.119.316388
- Guo, R., Zhang, Y., Turdi, S., and Ren, J. (2013). Adiponectin Knockout Accentuates High Fat Diet-Induced Obesity and Cardiac Dysfunction: Role of Autophagy. *Biochim. Biophys. Acta (Bba) - Mol. Basis Dis.* 1832, 1136–1148. doi:10.1016/j.bbdis.2013.03.013
- Hsu, P., Liu, X., Zhang, J., Wang, H.-G., Ye, J.-M., and Shi, Y. (2015). Cardiolipin Remodeling by TAZ/tafazzin Is Selectively Required for the Initiation of Mitophagy. *Autophagy* 11, 643–652. doi:10.1080/15548627.2015.1023984
- Huang, J., Zhu, T., Rong, R., You, M., Ji, D., and Li, H. (2020). FUN14 Domain-containing 1-mediated Mitophagy Suppresses Interleukin-1 β Production in Macrophages. *Int. Immunopharmacology* 88, 106964. doi:10.1016/j.intimp.2020.106964
- Jiang, X., Cai, S., Jin, Y., Wu, F., He, J., Wu, X., et al. (2021). Irisin Attenuates Oxidative Stress, Mitochondrial Dysfunction, and Apoptosis in the H9C2 Cellular Model of Septic Cardiomyopathy through Augmenting Fundc1-dependent Mitophagy. *Oxid Med. Cel Longev* 2021, 2989974. doi:10.1155/2021/2989974
- Kuang, Y., Ma, K., Zhou, C., Ding, P., Zhu, Y., Chen, Q., et al. (2016). Structural Basis for the Phosphorylation of FUNDC1 LIR as a Molecular Switch of Mitophagy. *Autophagy* 12, 2363–2373. doi:10.1080/15548627.2016.1238552
- Kubli, D. A., Zhang, X., Lee, Y., Hanna, R. A., Quinsay, M. N., Nguyen, C. K., et al. (2013). Parkin Protein Deficiency Exacerbates Cardiac Injury and Reduces Survival Following Myocardial Infarction. *J. Biol. Chem.* 288, 915–926. doi:10.1074/jbc.M112.411363
- Lamb, C. A., Yoshimori, T., and Tooze, S. A. (2013). The Autophagosome: Origins Unknown, Biogenesis Complex. *Nat. Rev. Mol. Cel Biol* 14, 759–774. doi:10.1038/nrm3696
- Lavallard, V. J., Meijer, A. J., Codogno, P., and Gual, P. (2012). Autophagy, Signaling and Obesity. *Pharmacol. Res.* 66, 513–525. doi:10.1016/j.phrs.2012.09.003
- Li, S., Zhou, Y., Gu, X., Zhang, X., and Jia, Z. (2021). NLRX1/FUNDC1/NIPSNAP1-2 axis Regulates Mitophagy and Alleviates Intestinal Ischaemia/reperfusion Injury[J]. *Cell Prolif* 3, e12986. doi:10.1111/cpr.12986
- Li, W., Yin, L., Sun, X., Wu, J., Dong, Z., Hu, K., et al. (2020). Alpha-lipoic Acid Protects against Pressure Overload-Induced Heart Failure via ALDH2-dependent Nrf1-FUNDC1 Signaling. *Cell Death Dis* 11, 599. doi:10.1038/s41419-020-02805-2
- Li, Y., Liu, Z., Zhang, Y., Zhao, Q., Wang, X., Lu, P., et al. (2018). PEDF Protects Cardiomyocytes by Promoting FUNDC1-mediated Mitophagy via PEDF-R under H₂O₂-induced C-condition. *Int. J. Mol. Med.* 41, 3394–3404. doi:10.3892/ijmm.2018.3536
- Li, Y., Xue, Y., Xu, X., Wang, G., Liu, Y., Wu, H., et al. (2019). A Mitochondrial FUNDC1/HSC70 Interaction Organizes the Proteostatic Stress Response at the Risk of Cell Morbidity. *Embo j* 38. doi:10.15252/embj.201798786
- Li, Y. z., Wu, X. d., Liu, X. h., and Li, P. f. (2019). Mitophagy Imbalance in Cardiomyocyte Ischaemia/reperfusion Injury. *Acta Physiol.* 225, e13228. doi:10.1111/apha.13228
- Lim, Y., Berry, B., Viteri, S., McCall, M., Park, E. C., Rongo, C., et al. (2021). FND-1-mediated Mitophagy and ATFS-1 Coordinate to Protect against Hypoxia-Reoxygenation. *Autophagy* 17, 3389–3401. doi:10.1080/15548627.2021.1872885
- Liu, B.-y., Li, L., Liu, G.-l., Ding, W., Chang, W.-g., Xu, T., et al. (2021). Baicalein Attenuates Cardiac Hypertrophy in Mice via Suppressing Oxidative Stress and Activating Autophagy in Cardiomyocytes. *Acta Pharmacol. Sin* 42, 701–714. doi:10.1038/s41401-020-0496-1
- Liu, L., Li, Y., Wang, J., Zhang, D., Wu, H., Li, W., et al. (2021). Mitophagy Receptor FUNDC1 Is Regulated by PGC-1 α /NRF1 to fine Tune Mitochondrial Homeostasis. *EMBO Rep.* 22, e50629. doi:10.15252/embr.202050629
- Liu, L., Feng, D., Chen, G., Chen, M., Zheng, Q., Song, P., et al. (2012). Mitochondrial Outer-Membrane Protein FUNDC1 Mediates Hypoxia-Induced Mitophagy in Mammalian Cells. *Nat. Cel Biol* 14, 177–185. doi:10.1038/ncb2422
- Liu, L., Sakakibara, K., Chen, Q., and Okamoto, K. (2014). Receptor-mediated Mitophagy in Yeast and Mammalian Systems. *Cell Res* 24, 787–795. doi:10.1038/cr.2014.75
- Liu, X., Ye, B., Miller, S., Yuan, H., Zhang, H., Tian, L., et al. (2012). Ablation of ALCAT1 Mitigates Hypertrophic Cardiomyopathy through Effects on Oxidative Stress and Mitophagy. *Mol. Cel Biol* 32, 4493–4504. doi:10.1128/mcb.01092-12
- Lv, M., Wang, C., Li, F., Peng, J., Wen, B., Gong, Q., et al. (2017). Structural Insights into the Recognition of Phosphorylated FUNDC1 by LC3B in Mitophagy. *Protein Cell* 8, 25–38. doi:10.1007/s13238-016-0328-8
- Ma, K., Zhang, Z., Chang, R., Cheng, H., Mu, C., Zhao, T., et al. (2020). Dynamic PGAM5 Multimers Dephosphorylate BCL-xL or FUNDC1 to Regulate Mitochondrial and Cellular Fate. *Cell Death Differ* 27, 1036–1051. doi:10.1038/s41418-019-0396-4
- Ma, S., Chen, J., Feng, J., Zhang, R., Fan, M., Han, D., et al. (2018). Melatonin Ameliorates the Progression of Atherosclerosis via Mitophagy Activation and NLRP3 Inflammasome Inhibition[J]. *Oxid Med. Cel Longev* 2018, 9286458. doi:10.1155/2018/9286458
- Mao, C., Hu, C., Zhou, Y., Zou, R., Li, S., Cui, Y., et al. (2020). Electroacupuncture Pretreatment against Cerebral Ischemia/Reperfusion Injury through Mitophagy. *Evid. Based Complement. Alternat Med.* 2020, 7486041. doi:10.1155/2020/7486041
- Mao, S., Tian, S., Luo, X., Zhou, M., Cao, Z., and Li, J. (2021). Overexpression of PLK1 Relieved the Myocardial Ischemia-Reperfusion Injury of Rats through Inducing the Mitophagy and Regulating the P-Ampk/fundc1 axis. *Bioengineered* 12, 2676–2687. doi:10.1080/21655979.2021.1938500
- Mishra, P., and Chan, D. C. (2016). Metabolic Regulation of Mitochondrial Dynamics. *J. Cel Biol* 212, 379–387. doi:10.1083/jcb.201511036
- Nakamura, M., and Sadoshima, J. (2018). Mechanisms of Physiological and Pathological Cardiac Hypertrophy. *Nat. Rev. Cardiol.* 15, 387–407. doi:10.1038/s41569-018-0007-y
- Nguyen, T. N., Padman, B. S., and Lazarou, M. (2016). Deciphering the Molecular Signals of PINK1/Parkin Mitophagy. *Trends Cel Biol.* 26, 733–744. doi:10.1016/j.tcb.2016.05.008
- Pecoraro, M., Pinto, A., and Popolo, A. (2019). Mitochondria and Cardiovascular Disease: A Brief Account. *Crit. Rev. Eukaryot. Gene Expr.* 29, 295–304. doi:10.1615/critrevueukaryotgenexpr.2019028579
- Pei, Z., Liu, Y., Liu, S., Jin, W., Luo, Y., Sun, M., et al. (2021). FUNDC1 Insufficiency Sensitizes High Fat Diet Intake-Induced Cardiac Remodeling and Contractile Anomaly through ACSL4-Mediated Ferroptosis. *Metabolism* 122, 154840. doi:10.1016/j.metabol.2021.154840
- Peng, X., Chen, H., Li, Y., Huang, D., Huang, B., and Sun, D. (2020). Effects of NIX-mediated Mitophagy on ox-LDL-induced Macrophage Pyroptosis in Atherosclerosis. *Cell Biol Int* 44, 1481–1490. doi:10.1002/cbin.11343
- Poole, L. P., and Macleod, K. F. (2021). Mitophagy in Tumorigenesis and Metastasis. *Cell. Mol. Life Sci.* 78, 3817–3851. doi:10.1007/s00018-021-03774-1
- Qiao, H., Ren, H., Du, H., Zhang, M., Xiong, X., and Lv, R. (2018). Liraglutide Repairs the Infarcted Heart: The Role of the SIRT1/Parkin/mitophagy Pathway. *Mol. Med. Rep.* 17, 3722–3734. doi:10.3892/mmr.2018.8371
- Ren, J., Sun, M., Zhou, H., Ajoalabady, A., Zhou, Y., Tao, J., et al. (2020). FUNDC1 Interacts with FBXL2 to Govern Mitochondrial Integrity and Cardiac Function through an IP3R3-dependent Manner in Obesity. *Sci. Adv.* 6. doi:10.1126/sciadv.abc8561
- Rogov, V. V., Suzuki, H., Marinković, M., Lang, V., Kato, R., Kawasaki, M., et al. (2017). Phosphorylation of the Mitochondrial Autophagy Receptor Nix Enhances its Interaction with LC3 Proteins. *Sci. Rep.* 7, 1131. doi:10.1038/s41598-017-01258-6
- Shao, D., Kolwicz, S. C., Jr., Wang, P., Roe, N. D., Villet, O., Nishi, K., et al. (2020). Increasing Fatty Acid Oxidation Prevents High-Fat Diet-Induced Cardiomyopathy through Regulating Parkin-Mediated Mitophagy. *Circulation* 142, 983–997. doi:10.1161/circulationaha.119.043319
- Silva-Palacios, A., Zazueta, C., and Pedraza-Chaverri, J. (2020). ER Membranes Associated with Mitochondria: Possible Therapeutic Targets in Heart-Associated Diseases. *Pharmacol. Res.* 156, 104758. doi:10.1016/j.phrs.2020.104758
- Swiader, A., Nahapetyan, H., Faccini, J., D'Angelo, R., Mucher, E., Elbaz, M., et al. (2016). Mitophagy Acts as a Safeguard Mechanism against Human Vascular

- Smooth Muscle Cell Apoptosis Induced by Atherogenic Lipids. *Oncotarget* 7, 28821–28835. doi:10.18632/oncotarget.8936
- Tagaya, M., and Arasaki, K. (2017). Regulation of Mitochondrial Dynamics and Autophagy by the Mitochondria-Associated Membrane. *Adv. Exp. Med. Biol.* 997, 33–47. doi:10.1007/978-981-10-4567-7_3
- Thomas, A., Marek-Iannucci, S., Tucker, K. C., Andres, A. M., and Gottlieb, R. A. (2019). Decrease of Cardiac Parkin Protein in Obese Mice. *Front. Cardiovasc. Med.* 6, 191. doi:10.3389/fcvm.2019.00191
- Tian, R., Colucci, W. S., Arany, Z., Bachschmid, M. M., Ballinger, S. W., Boudina, S., et al. (2019). Unlocking the Secrets of Mitochondria in the Cardiovascular System. *Circulation* 140, 1205–1216. doi:10.1161/circulationaha.119.040551
- Tong, M., Saito, T., Zhai, P., Oka, S.-i., Mizushima, W., Nakamura, M., et al. (2019). Mitophagy Is Essential for Maintaining Cardiac Function during High Fat Diet-Induced Diabetic Cardiomyopathy. *Circ. Res.* 124, 1360–1371. doi:10.1161/circresaha.118.314607
- Van Camp, G. (2014). Cardiovascular Disease Prevention. *Acta Clinica Belgica* 69, 407–411. doi:10.1179/2295333714y.0000000069
- Vásquez-Trincado, C., García-Carvajal, I., Pennanen, C., Parra, V., Hill, J. A., Rothermel, B. A., et al. (2016). Mitochondrial Dynamics, Mitophagy and Cardiovascular Disease. *J. Physiol.* 594, 509–525. doi:10.1113/jp271301
- Wang, C., Dai, X., Wu, S., Xu, W., Song, P., and Huang, K. (2021). FUNDC1-dependent Mitochondria-Associated Endoplasmic Reticulum Membranes Are Involved in Angiogenesis and Neovascularization. *Nat. Commun.* 12, 2616. doi:10.1038/s41467-021-22771-3
- Wang, J., Toan, S., and Zhou, H. (2020). New Insights into the Role of Mitochondria in Cardiac Microvascular Ischemia/reperfusion Injury. *Angiogenesis* 23, 299–314. doi:10.1007/s10456-020-09720-2
- Wang, J., Zhu, P., Li, R., Ren, J., and Zhou, H. (2020). Fundc1-dependent Mitophagy Is Obligatory to Ischemic Preconditioning-Conferred Renoprotection in Ischemic AKI via Suppression of Drp1-Mediated Mitochondrial Fission. *Redox Biol.* 30, 101415. doi:10.1016/j.redox.2019.101415
- Wang, X. (2001). The Expanding Role of Mitochondria in Apoptosis. *Genes Dev.* 15, 2922–2933.
- Wang, Y., Jasper, H., Toan, S., Muid, D., Chang, X., and Zhou, H. (2021). Mitophagy Coordinates the Mitochondrial Unfolded Protein Response to Attenuate Inflammation-Mediated Myocardial Injury. *Redox Biol.* 45, 102049. doi:10.1016/j.redox.2021.102049
- Wang, Z., Xia, P., Hu, J., Huang, Y., Zhang, F., Li, L., et al. (2021). LncRNA MEG3 Alleviates Diabetic Cognitive Impairments by Reducing Mitochondrial-Derived Apoptosis through Promotion of FUNDC1-Related Mitophagy via Rac1-ROS Axis. *ACS Chem. Neurosci.* 12, 2280–2307. doi:10.1021/acscchemneuro.0c00682
- Wei, X., Wei, X., Lu, Z., Li, L., Hu, Y., Sun, F., et al. (2020). Activation of TRPV1 Channel Antagonizes Diabetic Nephropathy through Inhibiting Endoplasmic Reticulum-Mitochondria Contact in Podocytes. *Metabolism* 105, 154182. doi:10.1016/j.metabol.2020.154182
- Wu, H., Wang, Y., Li, W., Chen, H., Du, L., Liu, D., et al. (2019). Deficiency of Mitophagy Receptor FUNDC1 Impairs Mitochondrial Quality and Aggravates Dietary-Induced Obesity and Metabolic Syndrome. *Autophagy* 15, 1882–1898. doi:10.1080/15548627.2019.1596482
- Wu, H., Xue, D., Chen, G., Han, Z., Huang, L., Zhu, C., et al. (2014). The BCL2L1 and PGAM5 axis Defines Hypoxia-Induced Receptor-Mediated Mitophagy. *Autophagy* 10, 1712–1725. doi:10.4161/auto.29568
- Wu, S., Lu, Q., Ding, Y., Wu, Y., Qiu, Y., Wang, P., et al. (2019). Hyperglycemia-Driven Inhibition of AMP-Activated Protein Kinase α 2 Induces Diabetic Cardiomyopathy by Promoting Mitochondria-Associated Endoplasmic Reticulum Membranes *In Vivo*. *Circulation* 139, 1913–1936. doi:10.1161/circulationaha.118.033552
- Wu, S., Lu, Q., Wang, Q., Ding, Y., Ma, Z., Mao, X., et al. (2017). Binding of FUN14 Domain Containing 1 with Inositol 1,4,5-Trisphosphate Receptor in Mitochondria-Associated Endoplasmic Reticulum Membranes Maintains Mitochondrial Dynamics and Function in Hearts *In Vivo*. *Circulation* 136, 2248–2266. doi:10.1161/circulationaha.117.030235
- Wu, S., and Zou, M.-H. (2019). Mitochondria-associated Endoplasmic Reticulum Membranes in the Heart. *Arch. Biochem. Biophys.* 662, 201–212. doi:10.1016/j.abb.2018.12.018
- Wu, W., Xu, H., Wang, Z., Mao, Y., Yuan, L., Luo, W., et al. (2015). PINK1-Parkin-Mediated Mitophagy Protects Mitochondrial Integrity and Prevents Metabolic Stress-Induced Endothelial Injury. *PLoS One* 10, e0132499. doi:10.1371/journal.pone.0132499
- Wu, W., Li, W., Chen, H., Jiang, L., Zhu, R., and Feng, D. (2016). FUNDC1 Is a Novel Mitochondrial-Associated-Membrane (MAM) Protein Required for Hypoxia-Induced Mitochondrial Fission and Mitophagy. *Autophagy* 12, 1675–1676. doi:10.1080/15548627.2016.1193656
- Wu, W., Lin, C., Wu, K., Jiang, L., Wang, X., Li, W., et al. (2016). FUNDC1 Regulates Mitochondrial Dynamics at the ER-mitochondrial Contact Site under Hypoxic Conditions. *Embo j* 35, 1368–1384. doi:10.15252/embj.201593102
- Wu, W., Tian, W., Hu, Z., Chen, G., Huang, L., Li, W., et al. (2014). ULK1 Translocates to Mitochondria and Phosphorylates FUNDC1 to Regulate Mitophagy. *EMBO Rep.* 15, 566–575. doi:10.1002/embr.201438501
- Xiao, Y., Chen, W., Zhong, Z., Ding, L., Bai, H., Chen, H., et al. (2020). Electroacupuncture Preconditioning Attenuates Myocardial Ischemia-Reperfusion Injury by Inhibiting Mitophagy Mediated by the mTORC1-ULK1-FUNDC1 Pathway. *Biomed. Pharmacother.* 127, 110148. doi:10.1016/j.biopha.2020.110148
- Xin, T., and Lu, C. (2020). Irisin Activates Opa1-Induced Mitophagy to Protect Cardiomyocytes against Apoptosis Following Myocardial Infarction. *Aging* 12, 4474–4488. doi:10.18632/aging.102899
- Xiong, W., Hua, J., Liu, Z., Cai, W., Bai, Y., Zhan, Q., et al. (2018). PTEN Induced Putative Kinase 1 (PINK1) Alleviates Angiotensin II-Induced Cardiac Injury by Ameliorating Mitochondrial Dysfunction. *Int. J. Cardiol.* 266, 198–205. doi:10.1016/j.ijcard.2018.03.054
- Xu, X., Hua, Y., Nair, S., Bucala, R., and Ren, J. (2014). Macrophage Migration Inhibitory Factor Deletion Exacerbates Pressure Overload-Induced Cardiac Hypertrophy through Mitigating Autophagy. *Hypertension* 63, 490–499. doi:10.1161/hypertensionaha.113.02219
- Yang, H.-x., Wang, P., Wang, N.-n., Li, S.-d., and Yang, M.-h. (2021). Tongxinluo Ameliorates Myocardial Ischemia-Reperfusion Injury Mainly via Activating Parkin-Mediated Mitophagy and Downregulating Ubiquitin-Proteasome System. *Chin. J. Integr. Med.* 27, 542–550. doi:10.1007/s11655-019-3166-8
- Yang, M., Li, C., Yang, S., Xiao, Y., Xiong, X., Chen, W., et al. (2020). Mitochondria-Associated ER Membranes - the Origin Site of Autophagy. *Front. Cell Dev. Biol.* 8, 595. doi:10.3389/fcell.2020.00595
- Yang, M., Linn, B. S., Zhang, Y., and Ren, J. (2019). Mitophagy and Mitochondrial Integrity in Cardiac Ischemia-Reperfusion Injury. *Biochim. Biophys. Acta (Bba) - Mol. Basis Dis.* 1865, 2293–2302. doi:10.1016/j.bbdis.2019.05.007
- Yoo, S. M., and Jung, Y. K. (2018). A Molecular Approach to Mitophagy and Mitochondrial Dynamics. *Mol. Cell* 41, 18–26. doi:10.14348/molcells.2018.2277
- Yu, W., Sun, S., Xu, H., Li, C., Ren, J., and Zhang, Y. (2020). TBC1D15/RAB7-regulated Mitochondria-Lysosome Interaction Confers Cardioprotection against Acute Myocardial Infarction-Induced Cardiac Injury. *Theranostics* 10, 11244–11263. doi:10.7150/thno.46883
- Yu, W., Xu, M., Zhang, T., Zhang, Q., and Zou, C. (2019). Mst1 Promotes Cardiac Ischemia-Reperfusion Injury by Inhibiting the ERK-CREB Pathway and Repressing FUNDC1-Mediated Mitophagy. *J. Physiol. Sci.* 69, 113–127. doi:10.1007/s12576-018-0627-3
- Zeinvand-Lorestani, M., Kalantari, H., Khodayar, M. J., Teimoori, A., Saki, N., Ahangarpour, A., et al. (2018). Dysregulation of Sqstm1, Mitophagy, and Apoptotic Genes in Chronic Exposure to Arsenic and High-Fat Diet (HFD). *Environ. Sci. Pollut. Res.* 25, 34351–34359. doi:10.1007/s11356-018-3349-4
- Zhang, W., Ren, H., Xu, C., Zhu, C., Wu, H., Liu, D., et al. (2016). Hypoxic Mitophagy Regulates Mitochondrial Quality and Platelet Activation and Determines Severity of I/R Heart Injury[J]. *Elife* 5, e21407. doi:10.7554/eLife.21407
- Zhang, X., Sergin, I., Evans, T. D., Jeong, S.-J., Rodriguez-Velez, A., Kapoor, D., et al. (2020). High-protein Diets Increase Cardiovascular Risk by Activating Macrophage mTOR to Suppress Mitophagy. *Nat. Metab.* 2, 110–125. doi:10.1038/s42255-019-0162-4
- Zhang, Y., Sowers, J. R., and Ren, J. (2018). Targeting Autophagy in Obesity: from Pathophysiology to Management. *Nat. Rev. Endocrinol.* 14, 356–376. doi:10.1038/s41574-018-0009-1
- Zhou, H., Zhang, Y., Hu, S., Shi, C., Zhu, P., Ma, Q., et al. (2017). Melatonin Protects Cardiac Microvasculature against Ischemia/reperfusion Injury via Suppression of Mitochondrial Fission-VDAC1-HK2-mPTP-Mitophagy axis. *J. Pineal Res.* 63. doi:10.1111/jpi.12413

- Zhou, H., He, L., Xu, G., and Chen, L. (2020). Mitophagy in Cardiovascular Disease. *Clinica Chim. Acta* 507, 210–218. doi:10.1016/j.cca.2020.04.033
- Zhou, H., Wang, J., Zhu, P., Zhu, H., Toan, S., Hu, S., et al. (2018). NR4A1 Aggravates the Cardiac Microvascular Ischemia Reperfusion Injury through Suppressing FUNDC1-Mediated Mitophagy and Promoting Mff-Required Mitochondrial Fission by CK2 α . *Basic Res. Cardiol.* 113, 23. doi:10.1007/s00395-018-0682-1
- Zhou, H., Zhu, P., Guo, J., Hu, N., Wang, S., Li, D., et al. (2017). Ripk3 Induces Mitochondrial Apoptosis via Inhibition of FUNDC1 Mitophagy in Cardiac IR Injury. *Redox Biol.* 13, 498–507. doi:10.1016/j.redox.2017.07.007
- Zhou, H., Zhu, P., Wang, J., Zhu, H., Ren, J., and Chen, Y. (2018). Pathogenesis of Cardiac Ischemia Reperfusion Injury Is Associated with CK2 α -Disturbed Mitochondrial Homeostasis via Suppression of FUNDC1-Related Mitophagy. *Cel Death Differ* 25, 1080–1093. doi:10.1038/s41418-018-0086-7
- Zimmermann, M., and Reichert, A. S. (2017). How to Get Rid of Mitochondria: Crosstalk and Regulation of Multiple Mitophagy Pathways. *Biol. Chem.* 399, 29–45. doi:10.1515/hsz-2017-0206

Conflict of Interest: The authors declare that the research was conducted in the absence of any commercial or financial relationships that could be construed as a potential conflict of interest.

Publisher's Note: All claims expressed in this article are solely those of the authors and do not necessarily represent those of their affiliated organizations, or those of the publisher, the editors, and the reviewers. Any product that may be evaluated in this article, or claim that may be made by its manufacturer, is not guaranteed or endorsed by the publisher.

Copyright © 2021 Li, Li, Shao, Zhao and Chen. This is an open-access article distributed under the terms of the Creative Commons Attribution License (CC BY). The use, distribution or reproduction in other forums is permitted, provided the original author(s) and the copyright owner(s) are credited and that the original publication in this journal is cited, in accordance with accepted academic practice. No use, distribution or reproduction is permitted which does not comply with these terms.



MFG-E8 Maintains Cellular Homeostasis by Suppressing Endoplasmic Reticulum Stress in Pancreatic Exocrine Acinar Cells

Yifan Ren^{1,2}, Wuming Liu^{1,3}, Jia Zhang^{1,3}, Jianbin Bi^{1,4}, Meng Fan², Yi Lv^{1,3}, Zheng Wu³, Yuanyuan Zhang^{5*} and Rongqian Wu^{1*}

¹National Local Joint Engineering Research Center for Precision Surgery and Regenerative Medicine, Shaanxi Provincial Center for Regenerative Medicine and Surgical Engineering, First Affiliated Hospital of Xi'an Jiaotong University, Xi'an, China, ²Department of General Surgery, The Second Affiliated Hospital of Xi'an Jiaotong University, Xi'an, China, ³Department of Hepatobiliary Surgery, First Affiliated Hospital of Xi'an Jiaotong University, Xi'an, China, ⁴Department of Oncology, The Second Affiliated Hospital of Xi'an Jiaotong University, Xi'an, China, ⁵Department of Pediatrics, First Affiliated Hospital of Xi'an Jiaotong University, Xi'an, China

OPEN ACCESS

Edited by:

Yongye Huang,
Northeastern University, China

Reviewed by:

Lie Yang,
Sichuan University, China
Wen-bin Zhang,
Renmin Hospital of Wuhan University,
China

*Correspondence:

Yuanyuan Zhang
yuanyuanzhang@xjtu.edu.cn
Rongqian Wu
rwu001@mail.xjtu.edu.cn

Specialty section:

This article was submitted to
Signaling,
a section of the journal
Frontiers in Cell and Developmental
Biology

Received: 28 October 2021

Accepted: 27 December 2021

Published: 14 January 2022

Citation:

Ren Y, Liu W, Zhang J, Bi J, Fan M,
Lv Y, Wu Z, Zhang Y and Wu R (2022)
MFG-E8 Maintains Cellular
Homeostasis by Suppressing
Endoplasmic Reticulum Stress in
Pancreatic Exocrine Acinar Cells.
Front. Cell Dev. Biol. 9:803876.
doi: 10.3389/fcell.2021.803876

Excessive endoplasmic reticulum (ER) stress contributes significantly to the pathogenesis of exocrine acinar damage in acute pancreatitis. Our previous study found that milk fat globule EGF factor 8 (MFG-E8), a lipophilic glycoprotein, alleviates acinar cell damage during AP via binding to $\alpha\beta3/5$ integrins. Ligand-dependent integrin-FAK activation of STAT3 was reported to be of great importance for maintaining cellular homeostasis. However, MFG-E8's role in ER stress in pancreatic exocrine acinar cells has not been evaluated. To study this, thapsigargin, brefeldin A, tunicamycin and cerulein + LPS were used to induce ER stress in rat pancreatic acinar cells *in vitro*. L-arginine- and cerulein + LPS-induced acute pancreatitis in mice were used to study ER stress *in vivo*. The results showed that MFG-E8 dose-dependently inhibited ER stress under both *in vitro* and *in vivo* conditions. MFG-E8 knockout mice suffered more severe ER stress and greater inflammatory response after L-arginine administration. Mechanistically, MFG-E8 increased phosphorylation of FAK and STAT3 in cerulein + LPS-treated pancreatic acinar cells. The presence of specific inhibitors of $\alpha\beta3/5$ integrin, FAK or STAT3 abolished MFG-E8's effect on cerulein + LPS-induced ER stress in pancreatic acinar cells. In conclusion, MFG-E8 maintains cellular homeostasis by alleviating ER stress in pancreatic exocrine acinar cells.

Keywords: pancreatic exocrine acinar cells, endoplasmic reticulum stress, acute pancreatitis, MFG-E8, $\alpha\beta3/5$ integrins, FAK-STAT3 pathway

Abbreviations: AP, Acute Pancreatitis; AR42J, cells of the rat exocrine pancreas; ATF6, Activating Transcription Factor 6; CHOP, C/EBP homologous protein; eIF2 α , eukaryotic initiation factor 2 α ; ELISA, Enzyme-linked immunosorbent assay; ER stress, Endoplasmic Reticulum stress; GRP78, glucose-regulated protein 78; HMGB-1, High Mobility Group Box 1; IkB α , inhibitor of NF- κ B- α ; IL-6, Interleukin-6; IRE1 α , inositol-requiring enzyme 1 α ; KO, knockout; LPS, Lipopolysaccharide; MFG-E8, milk fat globule EGF factor 8; MPO, myeloperoxidase; NF- κ B p65, Nuclear Factor Kappa-B p65; PERK, PKR-like endoplasmic reticulum kinase; SIRS, Systemic Inflammatory Response Syndrome; SAP, severe acute pancreatitis; TNF- α , tumor necrosis factor- α ; UPR, unfolded protein response; WT, wild type.

INTRODUCTION

Endoplasmic reticulum (ER) stress is involved in the damage of pancreatic exocrine acinar cells in acute pancreatitis (Sun et al., 2019; Tan et al., 2020). Inositol-required enzyme 1 (IRE1)-XBP1, PKR-like endoplasmic reticulum kinase (PERK), eukaryotic initiation factor 2 alpha (eIF2 α), activating transcription factor 6 (ATF6), and binding immunoglobulin protein (BIP, also known as glucose-regulated protein 78-kDa, GRP78) are the main signaling pathways that mediate the development of ER stress (Jiang et al., 2010; He, 2021; You et al., 2021). ER stress induced by different causes activates these pathways, respectively or simultaneously, and leads to the unfolded protein response (UPR). UPR participates in the adaptation to various stimuli and restores cellular homeostasis. However, under excessive ER stress conditions, UPR could not further alleviate cellular damage, but instead accelerate cell death by inducing the activation of apoptosis-related molecules transcription factor C/EBP homologous protein (CHOP) and caspase-9 (Gorman et al., 2012). CHOP and caspase-9 reduce the level of Bcl-2 and activate caspase-3 (Li et al., 2014; Datta et al., 2018), which ultimately leads to apoptosis of the cell. When ER stress occurs, IRE1 α recruits TRAF2 into ER and initiates the inflammatory response via activating the NF- κ B pathway (Keestra-Gounder et al., 2016). The storm of the inflammatory response not only sweeps through the affected organs, but also induces systemic damage, resulting in multiple organ injury.

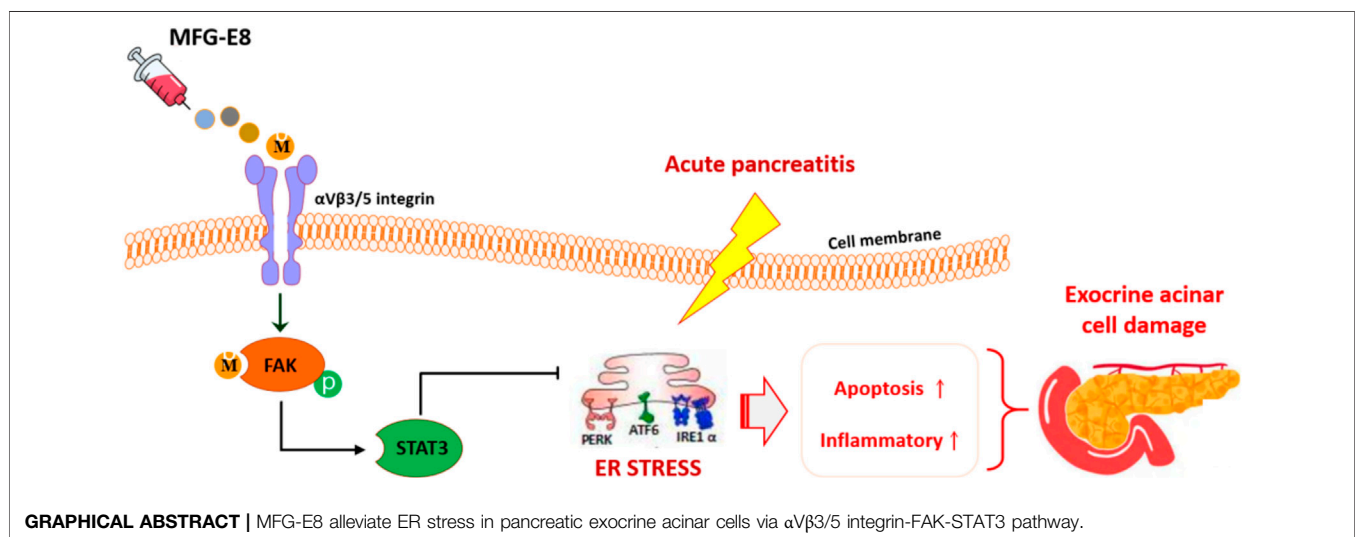
Milk fat globule EGF factor 8 (MFG-E8), a secreted lipophilic glycoprotein, contains an RGD motif and interacts with integrins (Yang et al., 2011; An et al., 2017). It participates in a wide range of cellular communications, such as mediating and maintaining the binding between the sperm and epididymal epithelial cells, repairing intestinal epithelial cells, promoting angiogenesis, and enhancing the phagocytosis and clearance of apoptotic cells by

macrophages (Hanayama et al., 2002; Miksa et al., 2008; Kranich et al., 2010; Aziz et al., 2015). Our previous studies have demonstrated that MFG-E8 alleviates pancreatic tissue damage during acute pancreatitis via binding to α v β 3/5 integrins (Ren et al., 2021a). Ligand-dependent integrin-FAK activation of STAT3 was reported to be of great importance for maintaining cellular homeostasis (Banerjee et al., 2017). However, whether MFG-E8 also has any effects on ER stress in pancreatic exocrine acinar cells remains largely unknown. Therefore, in this study, we aimed to clarify the specific role and molecular mechanism of MFG-E8 in ER stress of pancreatic exocrine acinar cells during acute pancreatitis.

RESULTS

MFG-E8 Alleviates ER Stress in Pancreatic Exocrine Acinar Cells

We used three commonly used ER stress activators thapsigargin, brefeldin A and tunicamycin to induce ER stress in AR42J cells, a rat pancreatic exocrine acinar cell line (Johnson et al., 2009; Misiewicz et al., 2013; Abhari et al., 2019). As shown in **Figures 1A–C**, 2.5 nM thapsigargin slightly increased the expression levels of GRP78, phospho-IRE1 α and CHOP in AR42J cells, 5 nM thapsigargin significantly increased the expression levels of these three ER stress-related proteins in AR42J cells ($p < 0.05$). Similarly, the expression levels of GRP78, phospho-IRE1 α and CHOP in AR42J cells also showing a gradual increase in the increase of tunicamycin ($p < 0.05$, **Figures 1D–F**) and brefeldin A ($p < 0.05$, **Figures 1G–I**) doses. Next, we added 20 ng/ml and 100 ng/ml of recombinant MFG-E8 to AR42J cells treated with 5 nM thapsigargin, 1 μ M tunicamycin, and 6 μ g/ml brefeldin A, respectively. It was observed that exogenous MFG-E8 had a significant inhibitory effect on ER stress induced by three ER stress activators, and the inhibitory effect was dose-dependent ($p < 0.05$, **Figures 1A–I**). Furthermore, the expression level of



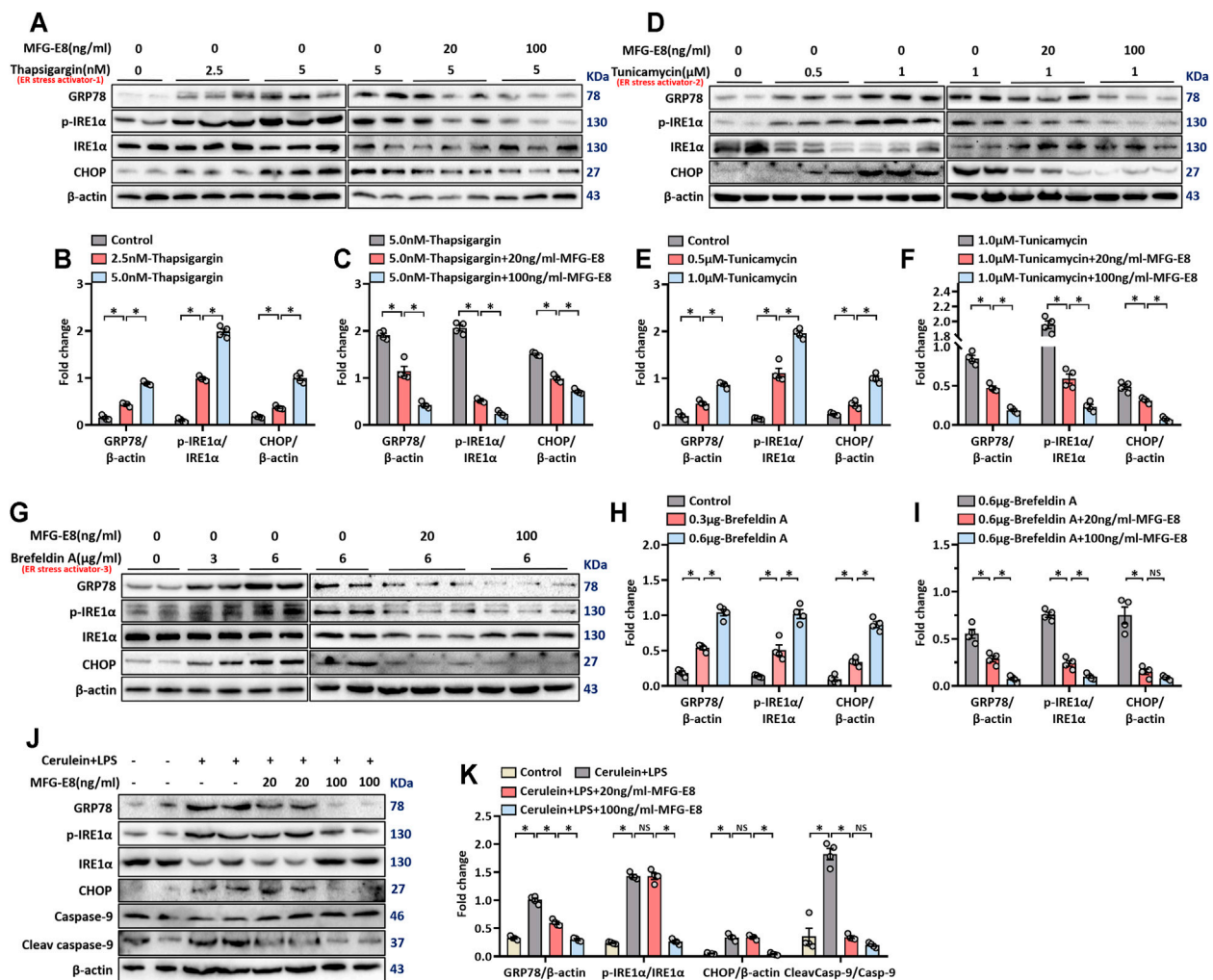


FIGURE 1 | rhMFG-E8 alleviates ER stress in pancreatic exocrine acinar cells. Model 1: Pancreatic AR42J cells (5×10^5 /well) were treated with 2.5 or 5 nM thapsigargin with or without 20 or 100 ng/ml MFG-E8 for 24 h. Model 2: Pancreatic AR42J cells (5×10^5 /well) were treated with 0.5 or 1 μM tunicamycin with or without 20 or 100 ng/ml MFG-E8 for 24 h. Model 3: Pancreatic AR42J cells (5×10^5 /well) were treated with 3 or 6 μg/ml brefeldin A with or without 20 or 100 ng/ml MFG-E8 for 24 h. Model 4: Pancreatic AR42J cells (5×10^5 /well) were treated with 100 nmol/L cerulein and 10 ng/ml LPS with or without 20 or 100 ng/ml MFG-E8 for 24 h. (A–I) Western blot analysis of the expression of GRP78, phospho-IRE1α, IRE1α and CHOP in the AR42J cells; (J,K) Western blot analysis of the expression of GRP78, phospho-IRE1α, IRE1α, CHOP, caspase-9, and cleaved caspase-9 in the AR42J cells. $n = 4$ –6/group, error bars indicate the SEM; * $p < 0.05$ versus Sham group; # $p < 0.05$ versus Vehicle group. MFG-E8, milk fat globule EGF factor 8; GRP78, glucose-regulated protein 78; CHOP, C/EBP homologous protein; LPS, Lipopolysaccharide.

MFG-E8 in AR42J cells decreased with the increase of the dose of the three ER stress activators ($p < 0.05$, **Supplementary Figure S1**).

Cerulein + lipopolysaccharide (LPS) are often used to induce acute pancreatitis in rodents and in cultured pancreatic acinar cells (Fu et al., 2020; Xiao et al., 2020). Our previous study found that treatment of AR42J cells with cerulein + LPS induced an obvious stress response in the ER (Ren et al., 2019a). In this study, cerulein + LPS was also used to induce ER stress in AR42J cells and the effect of exogenous MFG-E8 on ER stress was tested. As shown in **Figures 1J,K**, cerulein + LPS significantly upregulated the expression of GRP78, phospho-IRE1α, CHOP and cleaved-caspase-9, suggesting activation of the ER stress. 100 ng/ml MFG-E8 significantly, while 20 ng/ml MFG-E8 partially, inhibited

cerulein + LPS induced upregulation of these proteins (**Figures 1J,K**).

MFG-E8 Alleviates Pancreatic ER Stress *In Vivo*

L-arginine-induced acute pancreatitis in mice causes extensive ER stress in exocrine acinar cells (Biczko et al., 2018; Ren et al., 2019a; Ren et al., 2021a), and we used this animal model to test whether exogenous MFG-E8 also alleviates ER stress *in vivo*. TEM showed swelling, fragmentation, vacuolization and disintegration of the ER in the pancreatic tissue after L-arginine treatment (**Figure 2A**). Intraperitoneal injection of exogenous MFG-E8 reduced ER damage in pancreatic acinar cells

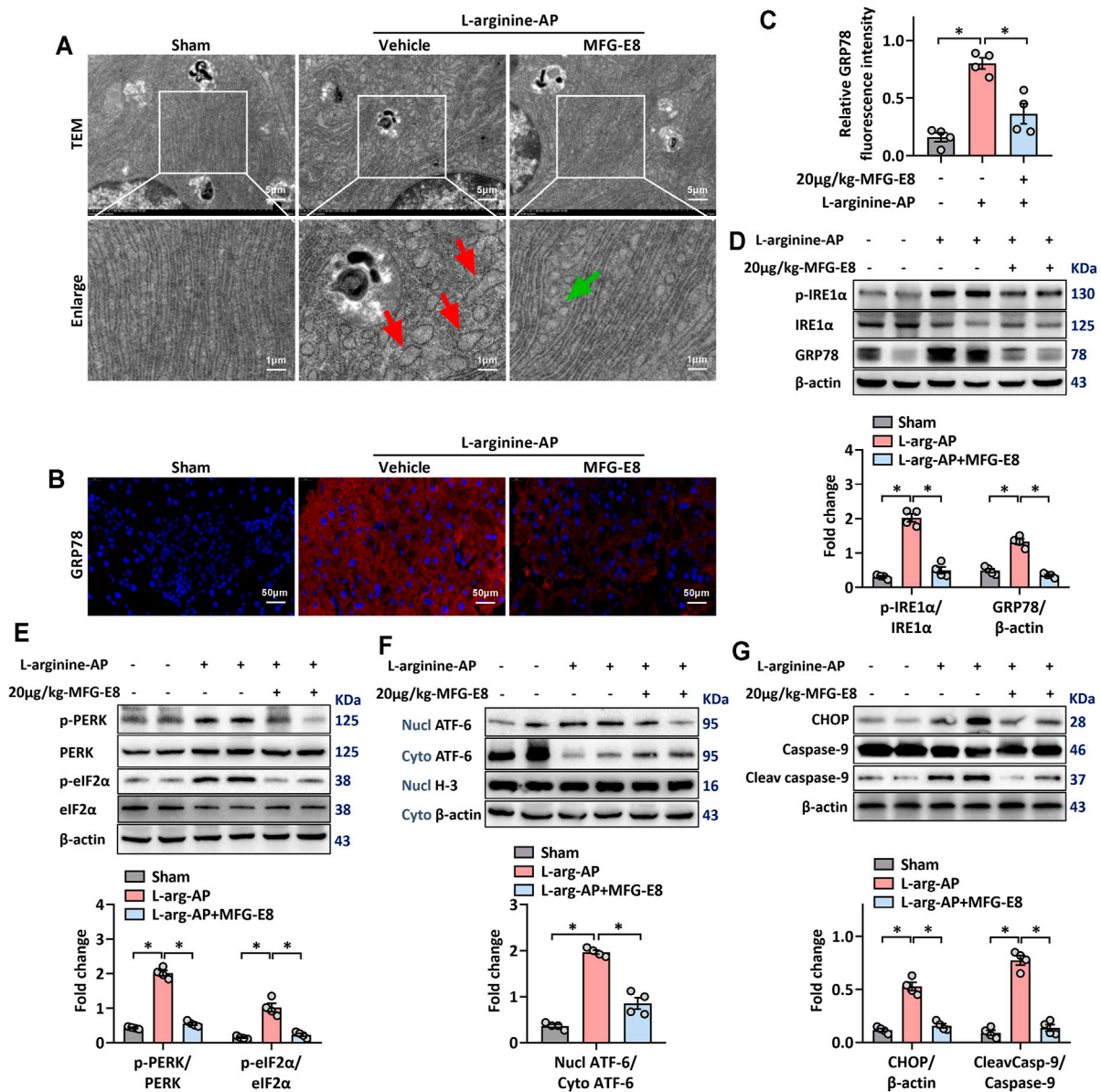


FIGURE 2 | Exogenous MFG-E8 alleviates pancreatic ER stress *in vivo*. In mice, arginine-AP stress was induced by 2 hourly intraperitoneal injections of 4.0 g/kg L-arginine. At 2 h after the last injection of L-arginine, normal saline (vehicle) or 20 μg/kg MFG-E8 were administered through intraperitoneal injection. The animals were sacrificed at 69 h after MFG-E8 treatment (i.e., 72 h after the first injection of L-arginine). Blood and tissue samples were collected. **(A)** Ultrastructural alterations in the pancreas (Transmission electron microscopy); **(B,C)** Representative photos of GRP78 staining and quantitative of GRP78 staining; **(D)** Western blot analysis of the expression of GRP78, phospho-IRE1α and IRE1α in the pancreas; **(E)** Western blot analysis of the expression of phospho-PERK, PERK, phospho-eIF2α and eIF2α in the pancreas; **(F)** Western blot analysis of the expression of nucl-ATF-6, cyto-ATF-6, nucl-H3 and cyto-β-actin in the pancreas; **(G)** Western blot analysis of the expression of CHOP, caspase-9 and cleaved caspase-9 in the pancreas. $n = 4-6$ /group, error bars indicate the SEM; * $p < 0.05$ versus Sham group; # $p < 0.05$ versus Vehicle group. MFG-E8, milk fat globule EGF factor 8; AP, acute pancreatitis; GRP78, glucose-regulated protein 78; eIF2α, eukaryotic initiation factor 2α; ATF-6, Activating Transcription Factor 6; CHOP, C/EBP homologous protein; Nucl, nucleus; Cyto, cytoplasm; H-3, histone-3; PERK, PKR-like endoplasmic reticulum kinase.

of L-arginine-treated mice. Immunofluorescence staining and western blot analysis showed that intraperitoneal injection of 20 μg/kg body weight MFG-E8 significantly reduced the expression of GRP78 in the pancreatic tissue of L-arginine-treated mice (**Figures 2B–D**, $p < 0.05$). The expression of phospho-IRE1α was also decreased after exogenous MFG-E8 injection ($p < 0.05$, **Figure 2D**).

The PERK-eIF2α and ATF-6 pathways are the other two of the three classical pathways of ER stress, phosphorylation of PERK and eIF2α or cytoplasmic ATF-6 translocation into the nucleus indicate activation of these two ER stress pathways (Kubisch et al., 2006). The intraperitoneal injection of 20 μg/ml-MFG-E8 also inhibited the activation of these two pathways in mouse pancreatic tissue, suggesting that exogenous MFG-E8 could effectively inhibit

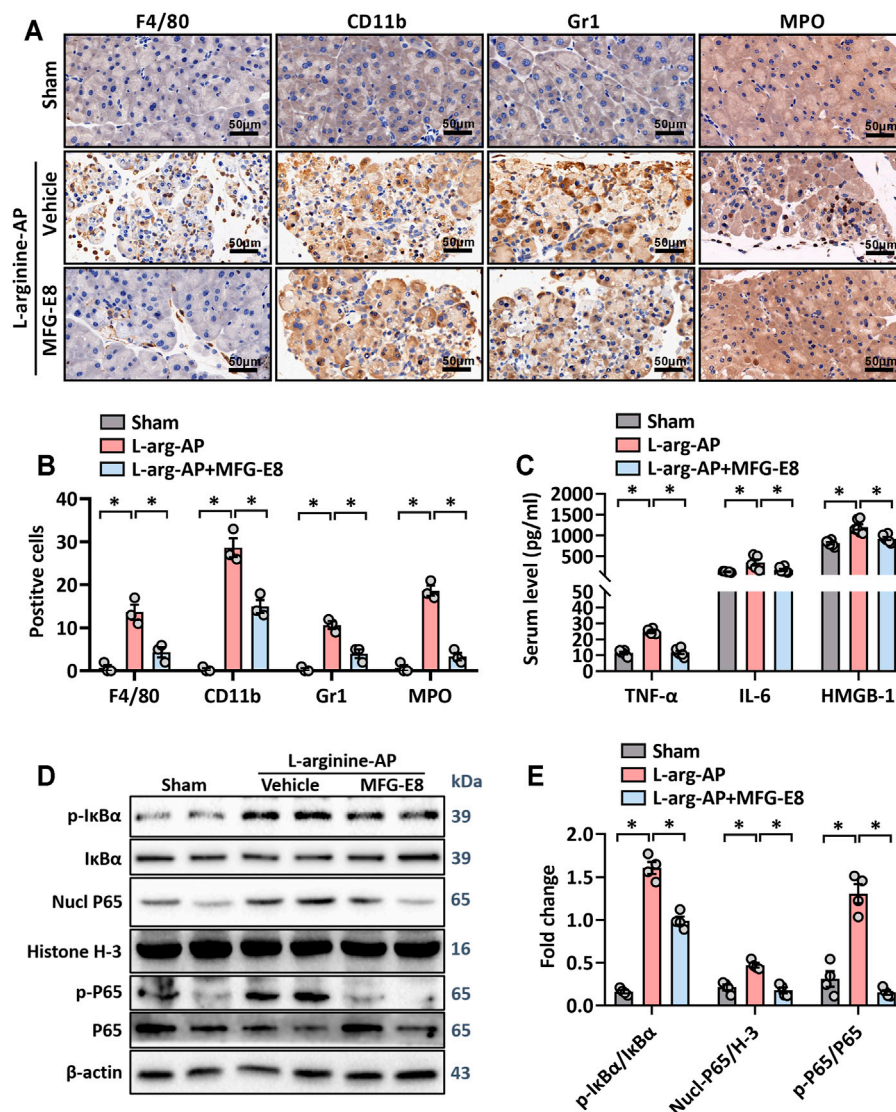


FIGURE 3 | MFG-E8 alleviates the inflammatory response in experimental-AP through NF- κ B signaling pathway. In mice, arginine-AP stress was induced by 2 hourly intraperitoneal injections of 4.0 g/kg L-arginine. At 2 h after the last injection of L-arginine, normal saline (vehicle) or 20 μ g/kg MFG-E8 were administered through intraperitoneal injection. The animals were sacrificed at 69 h after MFG-E8 treatment (i.e., 72 h after the first injection of L-arginine). Blood and tissue samples were collected. **(A)** Representative photos of F4/80, CD11b, Gr1, and MPO staining; **(B)** Quantitative of F4/80, CD11b, Gr1 and MPO staining; **(C)** Serum TNF- α , IL-6, and HMGB-1 levels; **(D,E)** Western blot analysis of the expression of phospho-I κ B α , I κ B α , nucl-P65, P65, p-P65, Histone H3 and β -actin in the pancreas. $n = 4-6$ /group, error bars indicate the SEM; * $p < 0.05$ versus Sham group; # $p < 0.05$ versus Vehicle group. MFG-E8, milk fat globule EGF factor 8; AP, acute pancreatitis; MPO, myeloperoxidase; HMGB-1, High mobility group box 1; Nucl, nucleus; Cyto, cytoplasm; H-3, histone-3; I κ B α , inhibitor of NF- κ B- α ; NF- κ B p65, Nuclear Factor Kappa-B p65.

L-arginine-induced ER stress in pancreatic tissue through multiple pathways ($p < 0.05$, **Figures 2E,F**). Similarly, exogenous MFG-E8 also reduced the expression levels of ER stress-related apoptotic proteins CHOP and cleaved caspase-9 ($p < 0.05$, **Figure 2G**), and the anti-apoptotic effect of MFG-E8 may also be realized through this pathway. Similar to the *in vitro* experiments, the reduction of ER stress in pancreatic tissues of AP mice by exogenous MFG-E8 was also dose-dependent. Compared with 10 μ g/kg, 20 μ g/kg MFG-E8 almost completely inhibited the expression of ER stress-related proteins in pancreatic tissues of AP mice (**Supplementary Figure S2**).

Intraperitoneal injection of 20 μ g/kg MFG-E8 also alleviated ER stress of pancreatic cells in cerulein + LPS-treated mice ($p < 0.05$, **Supplementary Figures S3A-D**).

MFG-E8 Alleviates the Inflammatory Response in Experimental-AP Through NF- κ B Signaling Pathway

Unresolvable ER stress leads to inflammatory responses (Eugene et al., 2020) and inflammation is another pathological feature of L-arginine-induced AP (El Morsy and Ahmed, 2020; Abdelzaher

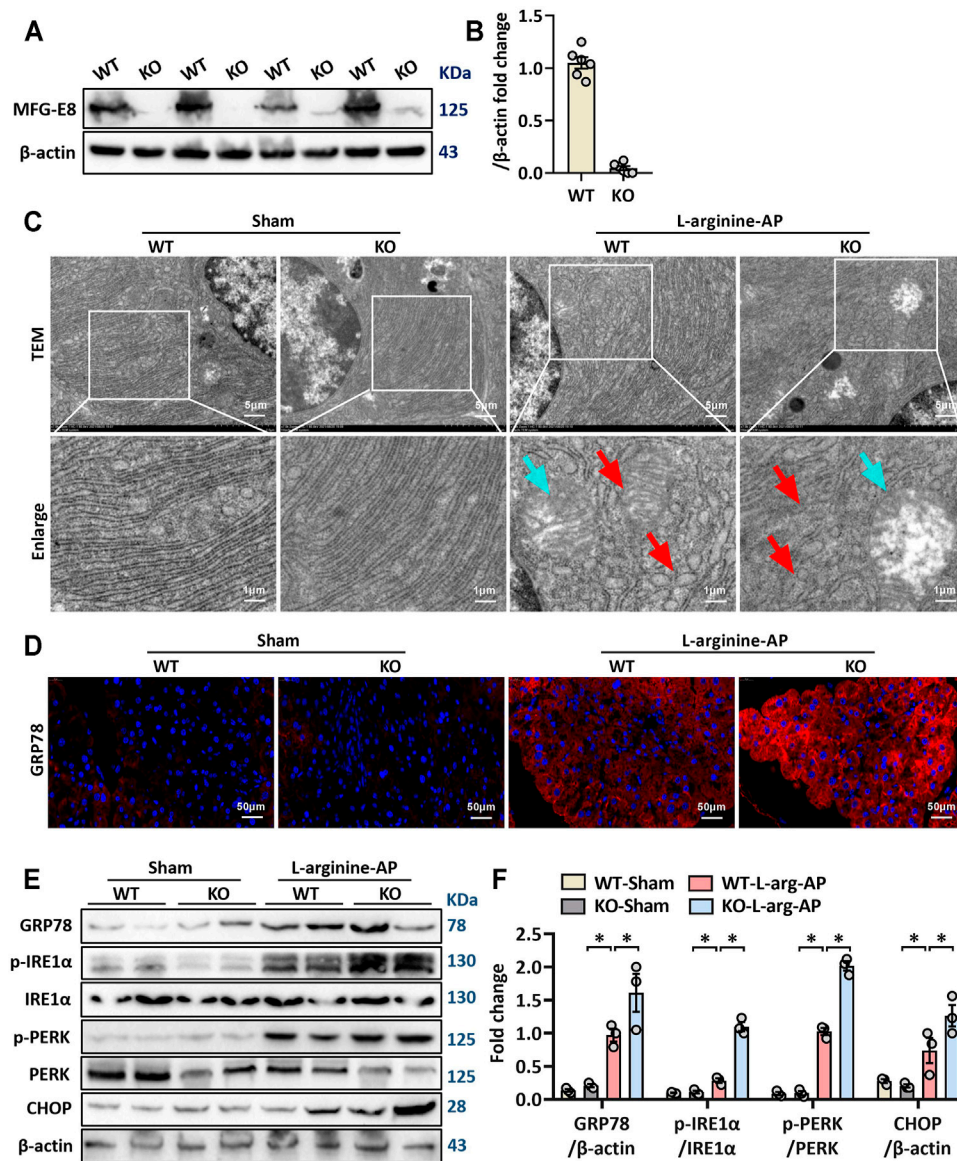


FIGURE 4 | MFG-E8 deficiency aggravated pancreatic ER stress in L-arginine-treated mice. In mice, arginine-AP stress was induced by 2 hourly intraperitoneal injections of 4.0 g/kg L-arginine. At 2 h after the last injection of L-arginine, normal saline (vehicle) or 20 μg/kg MFG-E8 were administered through intraperitoneal injection. The animals were sacrificed at 69 h after MFG-E8 treatment (i.e., 72 h after the first injection of L-arginine). Blood and tissue samples were collected. **(A,B)** Western blot analysis of the expression of MFG-E8 in the pancreas; **(C)** Ultrastructural alterations in the pancreas (Transmission electron microscopy); **(D)** Representative photos of GRP78 staining; **(E,F)** Western blot analysis of the expression of GRP78, phospho-PERK, PERK, phospho-IRE1α, IRE1α and CHOP in the pancreas. $n = 4-6$ /group, error bars indicate the SEM; * $p < 0.05$ versus Sham group; # $p < 0.05$ versus Vehicle group. WT, wild type; KO, knockout; MFG-E8, milk fat globule EGF factor 8; AP, acute pancreatitis; GRP78, glucose-regulated protein 78; CHOP, C/EBP homologous protein; PERK, PKR-like endoplasmic reticulum kinase.

et al., 2021). As shown in **Figures 3A,B**, immunohistochemical staining of F4/80 and CD11b showed that there was a large amount of macrophage infiltration in the pancreatic tissue of L-arginine treated mice, and intraperitoneal injection of 20 μg/kg-MFG-E8 effectively reduced the degree of macrophage infiltration ($p < 0.05$). Gr1 and MPO-labeled neutrophils showed the same trend as macrophages, suggesting that exogenous MFG-E8 effectively reduced the number of inflammatory cells in the pancreatic tissue ($p <$

0.05, **Figures 3A,B**). Serum levels of TNF-α, IL-6 and HMGB1 also indicated that exogenous MFG-E8 had a significant anti-inflammatory effect in experimental-AP ($p < 0.05$, **Figure 3C**).

Activation of IKK leads to the phosphorylation and isolation of inhibitor of NF-κB-α (IκBα), which is bound to Nuclear Factor Kappa-B p65 (NF-κB p65). The dissociated NF-κB p65 is transferred from the cytoplasm to the nucleus and binds with the corresponding inflammation-related genes to initiate the transcription of inflammatory cytokines and induce

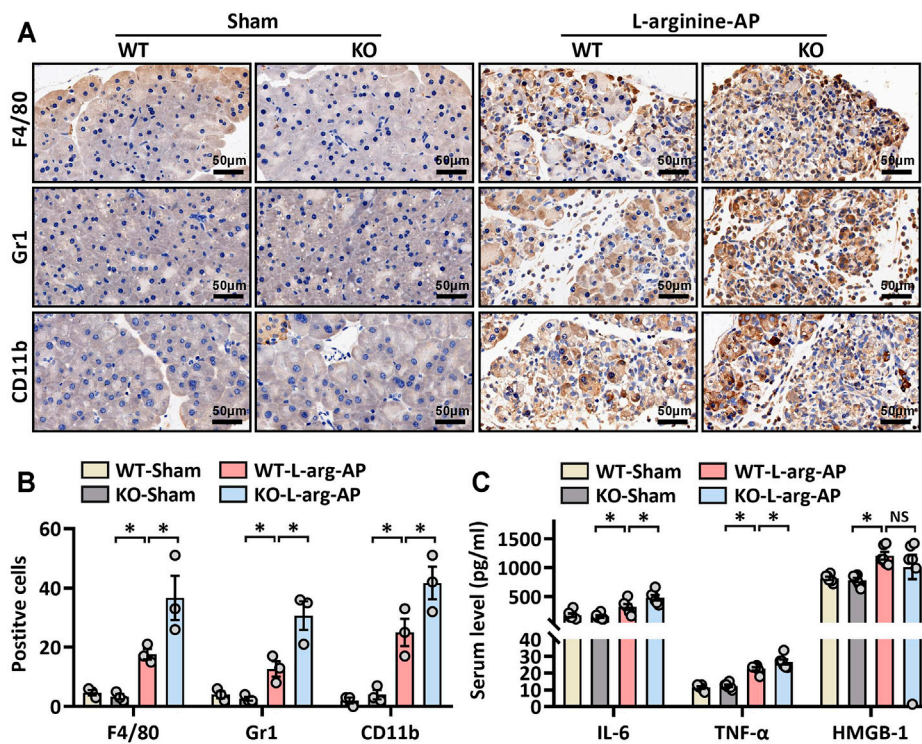


FIGURE 5 | MFG-E8 deficiency aggravated pancreatic inflammatory response in L-arginine-treated mice. In mice, arginine-AP stress was induced by 2 hourly intraperitoneal injections of 4.0 g/kg L-arginine. At 2 h after the last injection of L-arginine, normal saline (vehicle) or 20 μ g/kg MFG-E8 were administered through intraperitoneal injection. The animals were sacrificed at 69 h after MFG-E8 treatment (i.e., 72 h after the first injection of L-arginine). Blood and tissue samples were collected. **(A)** Representative photos of F4/80, CD11b, and Gr1 staining; **(B)** Quantitative of F4/80, CD11b, and Gr1 staining; **(C)** Serum TNF- α , IL-6 and HMGB-1 levels. $n = 4-6$ /group, error bars indicate the SEM; * $p < 0.05$ versus Sham group; # $p < 0.05$ versus Vehicle group. WT, wild type; KO, knockout; MFG-E8, milk fat globule EGF factor 8; AP, acute pancreatitis; HMGB-1, High mobility group box 1.

inflammation (Sun, 2017; Zhang et al., 2017). As shown in **Figures 3D,E**, phospho-I κ B α was significantly increased in L-arginine-treated mice ($p < 0.05$). Accordingly, nucleus NF- κ B p65 and phospho-NF- κ B p65 also increased, suggesting that NF- κ B p65 dissociated and translocated into the nucleus from the cytoplasm in L-arginine-treated mice ($p < 0.05$, **Figures 3D,E**). The intraperitoneal injection of exogenous MFG-E8 significantly reduced the phospho-I κ B α , nucleus NF- κ B p65 and phospho-NF- κ B p65 expression levels in L-arginine-treated mice.

MFG-E8 Deficiency Aggravated Pancreatic ER Stress and Inflammation in L-Arginine-Treated Mice

We then further investigated the role of MFG-E8 in ER stress in pancreatic tissue using MFG-E8 knockout (*mfge8*-KO) mice. As shown in **Figures 4A,B**, compared with the wild-type mice of the same litter, the expression level of MFG-E8 in the pancreas of *mfge8*-KO mice almost completely disappeared ($p < 0.05$). We induced ER stress in mouse pancreatic tissues with L-arginine, and found that MFG-E8 deficiency aggravated ER injury (red arrow) and exacerbated mitochondrial morphological abnormalities (blue arrow) (**Figure 4C**). MFG-E8 deficiency also upregulated GRP78

expression ($p < 0.05$, **Figures 4D-F**, immunofluorescence staining and western blotting). Similarly, phospho-IRE1 α , phospho-PERK, and CHOP were also higher in *mfge8*-KO mice, suggesting that the presence of MFG-E8 in pancreatic tissue plays a role in limiting the severity of ER stress ($p < 0.05$, **Figures 4E,F**). The infiltration level of inflammatory cells in pancreatic tissue (neutrophils labeled by Gr1; macrophages labeled by F4/80 and CD11b) and the number of inflammatory cells released into serum were also significantly higher in *mfge8*-KO mice ($p < 0.05$, **Figures 5A-C**). The above evidence shows that the presence of MFG-E8 has a considerable effect on alleviating L-arginine-induced ER stress and inflammation of pancreatic tissue.

MFG-E8 Alleviates ER Stress Through the Integrin α V β 3/5-FAK-STAT3 Pathway

Our previous study found that the biological effects of exogenous MFG-E8 require binding to the integrin α V β 3/5 receptor (Ren et al., 2021a). Whether MFG-E8 alleviates ER stress also acts on integrin α V β 3/5 remains unknown. Therefore, we utilized cilengitide, a highly effective and specific integrin α V β 3/5 inhibitor (Wang et al., 2020), to test whether the effect of MFG-E8 on ER stress is also mediated by this receptor. As shown in **Figures 6A,B**, the addition of cilengitide

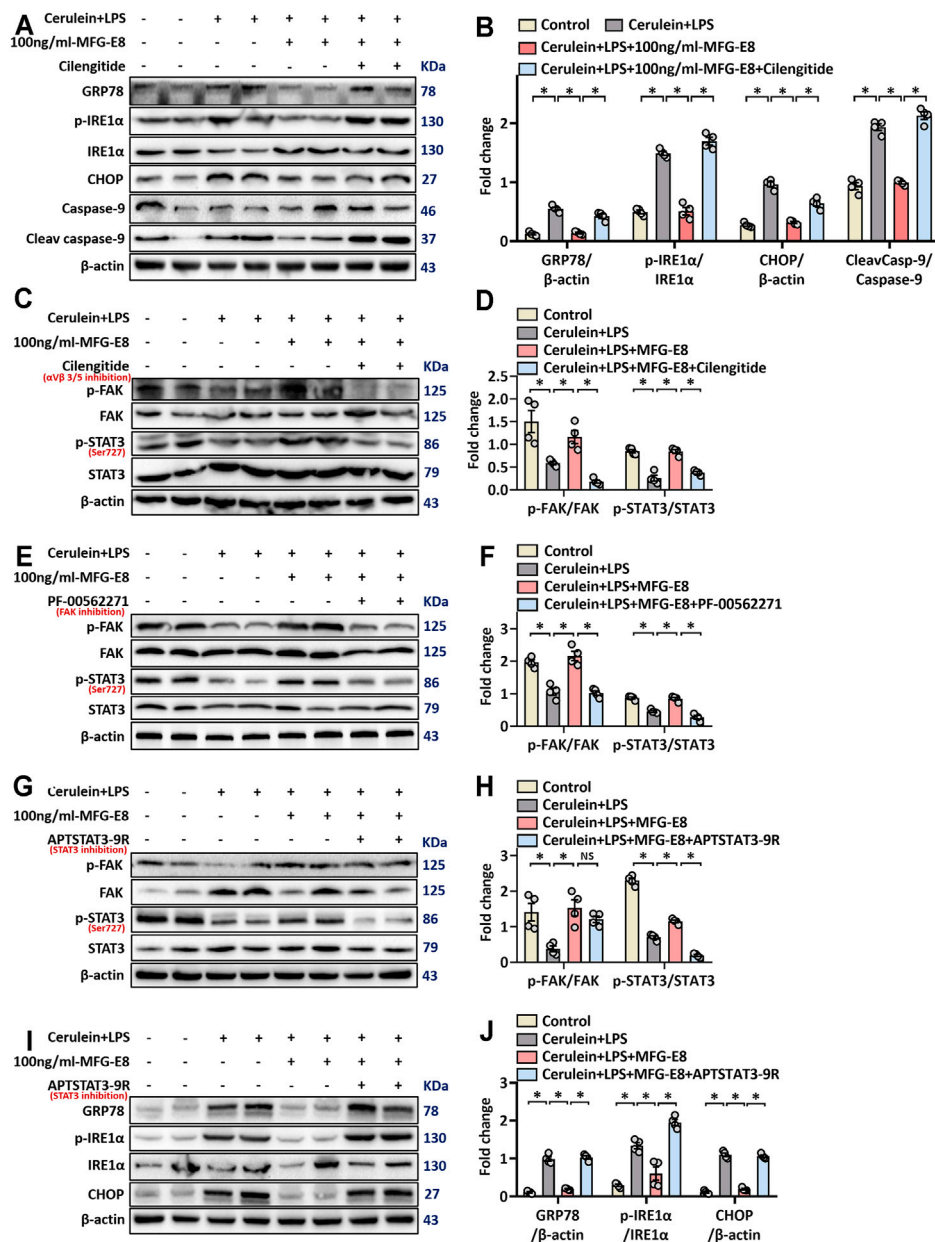


FIGURE 6 | rhMFG-E8 alleviates ER stress in pancreatic exocrine acinar cells through integrin α V β 3/5-FAK-STAT3. Pancreatic AR42J cells (5×10^5 /well) were treated with 100 nmol/L cerulein and 10 ng/ml LPS with or without 100 ng/ml MFG-E8 for 24 h. To determine whether the protective effect of MFG-E8 in ER stress is mediated through integrin α V β 3/5-FAK-STAT3, 5 ng/ml cilengitide, a specific integrin α V β 3/5 antagonist, 1 μ mol/L-PF-00562271, a specific FAK antagonist, 30 μ mol/L-APTSTAT3-9R, a specific STAT3 antagonist, was administered with 100 ng/ml MFG-E8, respectively. **(A,B)** Western blot analysis of the expression of GRP78, phospho-IRE1 α , IRE1 α , CHOP, caspase-9 and cleaved caspase-9 in the AR42J cells; **(C-H)** Western blot analysis of the expression of phospho-FAK, FAK, phospho-STAT3 and STAT3 in the AR42J cells; **(I,J)** Western blot analysis of the expression of GRP78, phospho-IRE1 α , IRE1 α , CHOP, caspase-9 and cleaved caspase-9 in the AR42J cells. $n = 6$ /group, error bars indicate the SEM; * $p < 0.05$ versus Sham group; # $p < 0.05$ versus Vehicle group. MFG-E8, milk fat globule EGF factor 8; GRP78, glucose-regulated protein 78; CHOP, C/EBP homologous protein; LPS, Lipopolysaccharide.

almost completely antagonized the effect of 100 ng/ml MFG-E8 on AR42J cell ER stress ($p < 0.05$).

Ligand-dependent integrin-FAK activation of STAT3 was reported to be of great importance for maintaining cellular homeostasis (Wu et al., 2020). To explore whether the effect of MFG-E8 on ER stress of pancreatic exocrine acinar cells is also

mediated through this pathway, we detected the levels of P-FAK and P-STAT3 in AR42J cells. As shown in **Figures 6C,D**, 100 ng/ml-MFG-E8 effectively restored the decrease of levels of P-FAK and P-STAT3 in AR42J cells induced by cerulein + LPS ($p < 0.05$). The addition of cilengitide antagonized the effect of MFG-E8 on P-FAK and P-STAT3, suggesting that exogenous MFG-E8

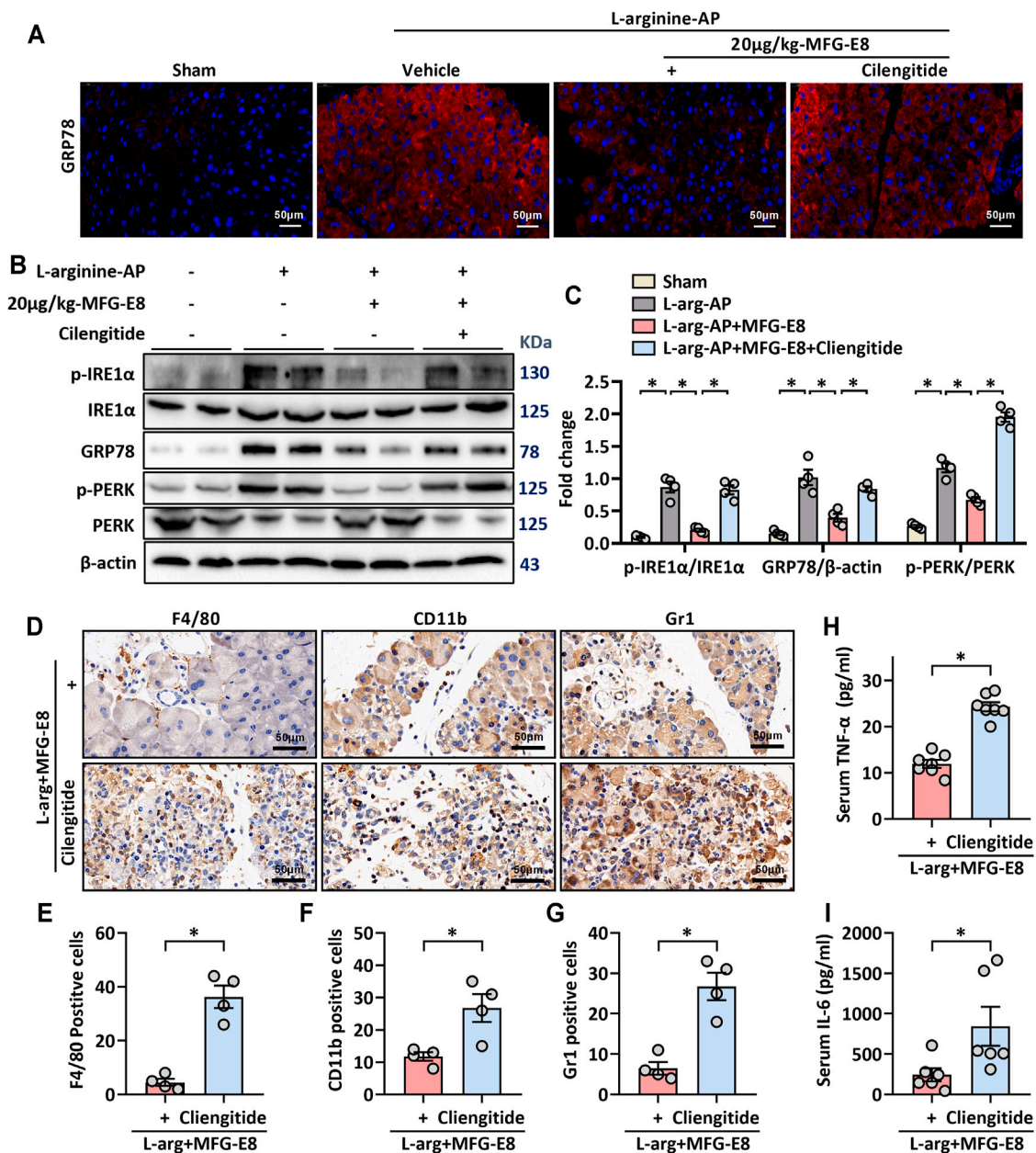


FIGURE 7 | MFG-E8 alleviates ER stress and pancreatic inflammatory response by binding to integrin $\alpha V\beta 3/5$ in experimental AP. In mice, arginine-AP stress was induced by 2 hourly intraperitoneal injections of 4.0 g/kg L-arginine. At 2 h after the last injection of L-arginine, normal saline (vehicle) or 20 µg/kg MFG-E8 were administered through intraperitoneal injection. The animals were sacrificed at 69 h after MFG-E8 treatment (i.e., 72 h after the first injection of L-arginine). Blood and tissue samples were collected. **(A)** Representative photos of GRP78 staining; **(B,C)** Western blot analysis of the expression of GRP78, phospho-PERK, PERK, phospho-IRE1α, IRE1α and CHOP in the pancreas; **(D)** Representative photos of F4/80, CD11b and Gr1 staining; **(E-G)** Quantitative of F4/80, CD11b, and Gr1 staining; **(H)** Serum IL-6 levels; **(I)** Serum IL-6 levels. $n = 4-6$ /group, error bars indicate the SEM; * $p < 0.05$ versus Sham group; # $p < 0.05$ versus Vehicle group. MFG-E8, milk fat globule EGF factor 8; AP, acute pancreatitis; GRP78, glucose-regulated protein 78; CHOP, C/EBP homologous protein; PERK, PKR-like endoplasmic reticulum kinase.

affected phosphorylation of FAK and STAT3 via binding to integrin $\alpha V\beta 3/5$ ($p < 0.05$, **Figures 6C,D**).

To further explore the relationship between FAK and STAT3 signal transduction, we applied specific FAK inhibitors and specific STAT3 inhibitors, respectively. As shown in **Figures 6E-H**, PF-00562271, a specific FAK inhibitor, almost completely antagonized the effects of

MFG-E8 against P-FAK and P-STAT3 ($p < 0.05$). However, APTSTAT3-9R, a specific STAT3 inhibitor, only eliminated the effect of MFG-E8 on P-STAT3, but did not prevent the effect of MFG-E8 on P-FAK ($p > 0.05$). We then examined GRP78, phosphorylated IRE1α, CHOP, and cleaved caspase-9 levels and found that APTSTAT3-9R also inhibited the effect of MFG-E8 on cerulein + LPS-induced ER stress in pancreatic

acinar cells ($p < 0.05$, **Figures 6I,J**). These results suggest that exogenous MFG-E8 suppresses ER stress via activating the integrin $\alpha V\beta 3/5$ -FAK-STAT3 signaling pathway in pancreatic acinar cells.

Consistent with the *in vitro* results, our *in vivo* study also showed that cilengitide antagonized the effect of MFG-E8 on GRP78 ($p < 0.05$, **Figures 7A–C**). Similarly, the effect of MFG-E8 on the reduction of phospho-IRE1 α , phospho-PERK, and CHOP was almost eliminated by cilengitide ($p < 0.05$, **Figures 7B,C**).

The effect of MFG-E8 on inflammatory cell infiltration in pancreatic tissue was also decreased with cilengitide intervention. Immunohistochemical staining showed that the inhibition of MFG-E8 on neutrophils (labeled by Gr1) and macrophages (labeled by F4/80 and CD11b) infiltration in the pancreatic tissue was also blocked by cilengitide ($p < 0.05$, **Figures 7D–G**). And the levels of inflammatory mediators (TNF- α and IL-6) in serum also changed accordingly (**Figures 7H,I**).

DISCUSSION

In this study, we found that MFG-E8 suppresses ER stress of pancreatic exocrine acinar cells under both *in vivo* and *in vitro* conditions. MFG-E8 deficiency, on the other hand, aggravates ER stress in experimental acute pancreatitis. The effect of MFG-E8 on ER stress seems to be achieved through activating the integrin $\alpha V\beta 3/5$ -FAK-STAT3 signaling pathway.

ER stress plays a critical role in the development of acute pancreatitis. Several studies have shown that inhibition of ER stress is beneficial in experimental acute pancreatitis (He et al., 2021; Wu et al., 2021). Thapsigargin, brefeldin A and tunicamycin are commonly used ER stress inducers (Misiewicz et al., 2013; Abhari et al., 2019). In our *in vitro* experiment, we also verified the dose-dependence of rat pancreatic acinar cells on the above three ER stress inducers. Our previous studies have confirmed that administration of cerulein + LPS or L-arginine induces ER stress in pancreatic cells in mice (Ren et al., 2019a; Ren et al., 2021a). In this study, we applied four *in vitro* models and two *in vivo* models to verify the effect of exogenous MFG-E8 on ER stress in pancreatic exocrine acinar cells. It is expected to avoid selection bias as much as possible. These different induction modes cause ER stress through different mechanisms. In this experiment, we found that exogenous MFG-E8 not only inhibited the ER stress of AR42J cells under various *in vitro* conditions in a dose-dependent manner, but also reduced ER stress in L-arginine or cerulein + LPS treated mice.

MFG-E8 is a secreted protein that has been shown to promote apoptotic cell clearance and acts as an anti-inflammatory in a variety of organs (Hanayama et al., 2004; Gao et al., 2021). MFG-E8 deficiency causes the aggravation of systemic sclerosis and increases the degree of skin fibrosis in mice (Fujiwara et al., 2019). Our previous study showed that MFG-E8 activates the FAK-STAT3 signaling pathway and alleviates the extent of mitochondrial damage during acute pancreatitis (Ren et al., 2021a). Mitochondrial dysfunction and ER stress are closely related to each other. Banerjee et al. (2017) reported that inhibition of the FAK-STAT3 signaling pathway contributes to ER

stress-induced mitochondrial dysfunction and death in endothelial cells. Meanwhile, Song et al. (2020) found that the increased p-STAT3 expression during chronic stress may promote splenocyte survival. The results from this study suggest that the inhibitory effect of MFG-E8 on ER stress of pancreatic cells during acute pancreatitis is also mediated by acting on the $\alpha V\beta 3/5$ -FAK-STAT3 signaling axis. Combined with the basis of previous studies, we speculated that exogenous MFG-E8 may alleviate ER stress through activating the FAK-STAT3 signal axis, leading to subsequent improvement of mitochondrial function, reduction of oxygen free radical production, and ultimately protection of pancreatic exocrine acinar cells from damage.

Excessive ER stress activates inflammatory responses (Fritz et al., 2011; Yong et al., 2021). During ER stress, IRE1 α recruits TRAF2 (TNF receptor-associated factor 2) to the ER membrane to initiate inflammatory responses via the NF- κ B pathway (Urano et al., 2000). The activation of the inflammatory response in pancreatic tissue is accompanied by the release of a large number of inflammatory mediators into the blood, resulting in systemic inflammatory response syndrome (SIRS) (Ren et al., 2019b). In the current study, we also examined the effect of exogenous MFG-E8 on the inflammatory response, and found that the level of circulating inflammatory mediators decreased with the treatment of MFG-E8. These results suggest that intraperitoneal injection of exogenous MFG-E8, which was previously found to reduce overall mortality in a mouse model of acute pancreatitis (Ren et al., 2021a), may inhibit local and systemic inflammatory responses via suppressing ER stress. The inhibition of ER stress also reduces oxygen free radical production by improving the function of mitochondria.

Abnormal ER function is a powerful inducer of the transcription factor C/EBP homologous protein (CHOP). All three signaling pathways induced by unfolded protein response eventually induce the expression of CHOP, resulting in the cleavage of procaspase-12 under ER stress conditions and then activate caspases-9 and -3, accelerating cells into the programmed death phase (apoptosis) (Li et al., 2014; Datta et al., 2018). Several studies suggest that inducing apoptosis of damaged acinar cells effectively prevents the release of pancreatic enzymes caused by cell necrosis (Ren et al., 2019c; Zhang et al., 2021). However, excessive cell apoptosis will lead to irreversible loss of pancreatic parenchyma, resulting in more serious consequences (Ren et al., 2021a). Exogenous MFG-E8 not only reduced the expression level of CHOP, but also reduced the amount of apoptosis and necrosis of AR42J cells. These results indicate that MFG-E8 alleviates the cellular and extracellular damage during acute pancreatitis from multiple dimensions. The conclusion of this study is also a strong supplement and improvement of our previous study on exogenous MFG-E8 and mitochondrial injury in acute pancreatitis (Ren et al., 2021a).

There are some limitations of the study. First of all, due to the lack of clinical samples, we were unable to verify our findings in patients with acute pancreatitis. The clinical significance of this study warrants further investigation. In this paper, we reveal that exogenous MFG-E8 reduces the inflammatory response and apoptosis in pancreatic tissue by inhibiting ER stress (Hanayama et al., 2002; Aziz et al., 2011). However, whether the anti-inflammatory effect of MFG-E8 and the promotion of macrophage phagocytosis of apoptotic cells are related to the regulation of ER function remains unknown. Several studies

have shown that MFG-E8 can directly regulate the NF- κ B pathway (Zhao et al., 2019; Gong et al., 2020; Lu et al., 2021). In this study, we also found that MFG-E8 downregulated the NF- κ B pathway. However, whether the NF- κ B pathway plays a major role in MFG-E8-mediated inhibition of ER stress in pancreatic exocrine acinar cells remains to be determined. Therefore, the specific mechanisms of various biological effects of MFG-E8 need to be further explored. On the other hand, our recent study found that MFG-E8 limits the activation of pancreatic stellate cells by inhibiting chaperone-mediated autophagy by controlling unfolded protein response (Ren et al., 2021b). Whether MFG-E8 also improves the autophagy function of pancreatic acinar cells by regulating the ER signaling pathway, and then participates in the repair of acute pancreatitis, remains to be further explored.

CONCLUSION

MFG-E8 maintains cellular homeostasis by alleviating ER stress in pancreatic exocrine acinar cells. The beneficial effects of MFG-E8 appears to be mediated through activating the α V β 3/5 integrin-FAK-STAT3 signaling pathway. These findings may provide a new perspective to reveal the role of MFG-E8 in acute pancreatitis.

MATERIALS AND METHODS

Experimental Animals and *In Vivo* Models

Male adult C57BL/6J mice purchased from Experimental Animal Center of Xi'an Jiaotong University (Xi'an, China) and MFG-E8 knockout (*mfg-e8*-KO) mice purchased from Shanghai Model Organisms Center (Shanghai, China) were used in this study. The *mfg-e8*-KO mice were generated as described previously (Ren et al., 2021a). The mice were fed on a standard laboratory chow diet and housed in a temperature-controlled room on a 12-h light/dark cycle. The study protocol was approved by the Institutional Animal Care and Use Committee of the Ethics Committee of Xi'an Jiaotong University Health Science Center. Mice (8–10 weeks, 20–22 g) were randomly divided into groups with six mice in each group and given intervention at the same time.

Arginine-AP was induced by 2 hourly intraperitoneal injections of 4.0 g/kg L-arginine (Sigma Aldrich, Shanghai, China). Two hours after the last injection of L-arginine, normal saline (vehicle) or 20 μ g/kg MFG-E8 (RD System, Inc. Minnesota, United States) were administered intraperitoneally. The doses of MFG-E8 used in this study were chosen on the basis of our previous publications in acute pancreatitis (Ren et al., 2021a). To determine the role of α V β 3/5 integrin in MFG-E8's effect in ER stress, cilengitide (20 mg/kg, SELLECK, Texas, United States), a specific α V β 3/5 integrin inhibitor (Stupp et al., 2014; Li et al., 2021), were administered through intraperitoneal injection at 1 h after the last injection of L-arginine. At 72 h after the first injection of L-arginine, mice were anesthetized with isoflurane and serum and pancreatic tissue samples were collected.

Cerulein + LPS-AP was induced by 7 hourly injections of cerulein (50 μ g/kg). Lipopolysaccharide (LPS, 10 mg/kg, L8880, Solarbio, Beijing, China) was added to the last

cerulein injection (Liu et al., 2017). 20 μ g/kg-MFG-E8 was intraperitoneally injected into mice 0.5 h after the second injection of cerulein. 4 h after the final injection of cerulein (7th injection), the mice were sacrificed under isoflurane inhalation anesthesia and pancreas tissue was collected.

Cell Culture and *In Vitro* Model

The pancreatic AR42J cells were purchased from Sciencell (zq0145) and cultured in Ham's F-12K medium (PM150910C, Procell) with 20% fetal bovine serum (164210-100, Procell) in a humidified incubator at 37°C with 5% CO₂ (Liu et al., 2017). AR42J cells (5×10^5 /well) were plated into six-well culture plates and incubate for 24 h. The AR42J cells are the most commonly used cell line for *in vitro* studies of acute pancreatitis (Sandoval et al., 2010; Szmola and Sahin-Toth, 2010; Lugea et al., 2017).

In Vitro Model-1

The AR42J cells were treated with 2.5 or 5 nM thapsigargin (S7895, SELLECK, Texas, United States) with or without 20 or 100 ng/ml MFG-E8 (2805-MF, RD System, Inc. Minnesota, United States) for 24 h. Protein homogenate was extracted for subsequent detection.

In Vitro Model-2

The AR42J cells were treated with 0.5 or 1 μ M tunicamycin (B7417, APEX-BIO, Houston, United States) with or without 20 or 100 ng/ml MFG-E8 (2805-MF, RD System, Inc. Minnesota, United States) for 24 h. Protein homogenate was extracted for subsequent detection.

In Vitro Model-3

The AR42J cells were treated with 3 or 6 μ g/ml brefeldin A (S7046, SELLECK, Texas, United States) with or without 20 or 100 ng/ml MFG-E8 (2805-MF, RD System, Inc. Minnesota, United States) for 24 h. Protein homogenate was extracted for subsequent detection.

In Vitro Model-4

The AR42J cells were treated with 100 nmol/L cerulein (C6660, Solarbio, United States) and 10 ng/ml Lipopolysaccharide (LPS) (L-8880, Solarbio, United States) with or without 20 or 100 ng/ml MFG-E8 (2805-MF, RD System, Inc. Minnesota, United States) for 24 h. In additional groups of AR42J cells, Cilengitide (5 ng/ml, SELLECK, Texas, United States), a specific α V β 3/5 integrin inhibitor or PF00562271 (S2672, SELLECK, Texas, United States), a specific FAK inhibitor or APTSTAT3-9R (S8197, SELLECK, Texas, United States), a specific STAT3 antagonist, were administered together with 100 ng/ml MFG-E8.

Statistical Analysis

All measurement data are expressed as the mean \pm standard error (SEM). The *t*-test or one-way ANOVA with the Student-Newman-Keuls test was used to analyze the differences between groups. All analyses were conducted with data statistics software GraphPad Prism version 8.0 (GraphPad Software, Inc., San Diego, CA, United States). *p* < 0.05 represented a significant difference.

Methods for Flow Cytometry Analysis, Enzyme-linked immunosorbent assay (ELISA), GRP78 Staining, Immunohistochemical Staining, Transmission Electron Microscopy and Western Blot Analysis are provided in the **Supplementary Materials**.

DATA AVAILABILITY STATEMENT

The raw data supporting the conclusion of this article will be made available by the authors, without undue reservation.

ETHICS STATEMENT

The animal study was reviewed and approved by Institutional Animal Care and Use Committee of the Ethics Committee of Xi'an Jiaotong University Health Science Center.

AUTHOR CONTRIBUTIONS

YR acquired and analyzed the data, wrote the paper. WL, MF, JZ, and JB participated in data acquirement. ZW and YL interpreted the data. YZ interpreted the data and revised the paper. RW designed and supervised the study and revised the

paper. All authors have read and agreed with the final manuscript.

FUNDING

This work was supported by grants from the National Nature Science Foundation of China (No. 82100685, 81770491), the Innovation Capacity Support Plan of Shaanxi Province (No. 2020TD-040), the Key R&D Program of Shaanxi Province (No. 2021SF-002) and the Science Foundation of First Affiliated Hospital of Xi'an Jiaotong University (No. XJTU1AF-CRF-2020-025).

ACKNOWLEDGMENTS

We appreciate the administrative support provided by Lirong Yuan, Juan Zhao and Hui Yang during data collection.

SUPPLEMENTARY MATERIAL

The Supplementary Material for this article can be found online at: <https://www.frontiersin.org/articles/10.3389/fcell.2021.803876/full#supplementary-material>

REFERENCES

- Abdelzaher, W. Y., Ahmed, S. M., Welson, N. N., Marraiki, N., Batiha, G. E.-S., and Kamel, M. Y. (2021). Vinpocetine Ameliorates L-Arginine Induced Acute Pancreatitis via Sirt1/Nrf2/TNF Pathway and Inhibition of Oxidative Stress, Inflammation, and Apoptosis. *Biomed. Pharmacother.* 133, 110976. doi:10.1016/j.biopha.2020.110976
- Abhari, B. A., McCarthy, N., Le Berre, M., Kilcoyne, M., Joshi, L., Agostinis, P., et al. (2019). Smac Mimetic Suppresses Tunicamycin-Induced Apoptosis via Resolution of ER Stress. *Cell Death Dis* 10, 155. doi:10.1038/s41419-019-1381-z
- An, S. Y., Jang, Y. J., Lim, H.-J., Han, J., Lee, J., Lee, G., et al. (2017). Milk Fat Globule-EGF Factor 8, Secreted by Mesenchymal Stem Cells, Protects against Liver Fibrosis in Mice. *Gastroenterology* 152, 1174–1186. doi:10.1053/j.gastro.2016.12.003
- Aziz, M., Jacob, A., Matsuda, A., and Wang, P. (2011). Review: Milk Fat Globule-EGF Factor 8 Expression, Function and Plausible Signal Transduction in Resolving Inflammation. *Apoptosis* 16, 1077–1086. doi:10.1007/s10495-011-0630-0
- Aziz, M., Yang, W.-L., Corbo, L. M., Chaung, W. W., Matsuo, S., and Wang, P. (2015). MFG-E8 Inhibits Neutrophil Migration through $\alpha\beta3$ -integrin-dependent MAP Kinase Activation. *Int. J. Mol. Med.* 36, 18–28. doi:10.3892/ijmm.2015.2196
- Banerjee, K., Keasey, M. P., Razskazovskiy, V., Visavadiya, N. P., Jia, C., and Hagg, T. (2017). Reduced FAK-STAT3 Signaling Contributes to ER Stress-Induced Mitochondrial Dysfunction and Death in Endothelial Cells. *Cell Signal.* 36, 154–162. doi:10.1016/j.cellsig.2017.05.007
- Biczko, G., Vegh, E. T., Shalbuva, N., Mareninova, O. A., Elperin, J., Lotshaw, E., et al. (2018). Mitochondrial Dysfunction, through Impaired Autophagy, Leads to Endoplasmic Reticulum Stress, Deregulated Lipid Metabolism, and Pancreatitis in Animal Models. *Gastroenterology* 154, 689–703. doi:10.1053/j.gastro.2017.10.012
- Datta, D., Khatri, P., Singh, A., Saha, D. R., Verma, G., Raman, R., et al. (2018). Mycobacterium Fortuitum-Induced ER-Mitochondrial Calcium Dynamics Promotes Calpain/caspase-12/caspase-9 Mediated Apoptosis in Fish Macrophages. *Cell Death Discov.* 4, 30. doi:10.1038/s41420-018-0034-9
- El Morsy, E. M., and Ahmed, M. A. E. (2020). Carvedilol Attenuates L-Arginine Induced Acute Pancreatitis in Rats through Modulation of Oxidative Stress and Inflammatory Mediators. *Chemico-Biological Interactions* 327, 109181. doi:10.1016/j.cbi.2020.109181
- Eugene, S. P., Reddy, V. S., and Trinath, J. (2020). Endoplasmic Reticulum Stress and Intestinal Inflammation: A Perilous Union. *Front. Immunol.* 11, 543022. doi:10.3389/fimmu.2020.543022
- Fritz, T., Niederreiter, L., Adolph, T., Blumberg, R. S., and Kaser, A. (2011). Crohn's Disease: NOD2, Autophagy and ER Stress Converge. *Gut* 60, 1580–1588. doi:10.1136/gut.2009.206466
- Fu, X., Li, P., Yin, W., Ma, L., Zhang, B., Zhen, L., et al. (2020). Overexpression of Nrf2 Protects against Lipopolysaccharide and Cerulein-Induced Pancreatitis *In Vitro* and *In Vivo*. *Pancreas* 49, 420–428. doi:10.1097/mpa.0000000000001501
- Fujiwara, C., Uehara, A., Sekiguchi, A., Uchiyama, A., Yamazaki, S., Ogino, S., et al. (2019). Suppressive Regulation by MFG-E8 of Latent Transforming Growth Factor β -Induced Fibrosis via Binding to αv Integrin: Significance in the Pathogenesis of Fibrosis in Systemic Sclerosis. *Arthritis Rheumatol.* 71, 302–314. doi:10.1002/art.40701
- Gao, Y.-Y., Tao, T., Wu, D., Zhuang, Z., Lu, Y., Wu, L.-Y., et al. (2021). MFG-E8 Attenuates Inflammation in Subarachnoid Hemorrhage by Driving Microglial M2 Polarization. *Exp. Neurol.* 336, 113532. doi:10.1016/j.expneurol.2020.113532
- Gong, Z., Wang, C., Ni, L., Ying, L., Shu, J., Wang, J., et al. (2020). An Injectable Recombinant Human Milk Fat Globule-Epidermal Growth Factor 8-loaded Copolymer System for Spinal Cord Injury Reduces Inflammation through NF- κ B and Neuronal Cell Death. *Cytotherapy* 22, 193–203. doi:10.1016/j.jcyt.2020.01.016
- Gorman, A. M., Healy, S. J. M., Jäger, R., and Samali, A. (2012). Stress Management at the ER: Regulators of ER Stress-Induced Apoptosis. *Pharmacol. Ther.* 134, 306–316. doi:10.1016/j.pharmthera.2012.02.003
- Hanayama, R., Tanaka, M., Miwa, K., Shinohara, A., Iwamatsu, A., and Nagata, S. (2002). Identification of a Factor that Links Apoptotic Cells to Phagocytes. *Nature* 417, 182–187. doi:10.1038/417182a

- Hanayama, R., Tanaka, M., Miyasaka, K., Aozasa, K., Koike, M., Uchiyama, Y., et al. (2004). Autoimmune Disease and Impaired Uptake of Apoptotic Cells in MFG-E8-Deficient Mice. *Science* 304, 1147–1150. doi:10.1126/science.1094359
- He, J., Ma, M., Li, D., Wang, K., Wang, Q., Li, Q., et al. (2021). Sulfiredoxin-1 Attenuates Injury and Inflammation in Acute Pancreatitis through the ROS/ER stress/Cathepsin B axis. *Cel Death Dis* 12, 626. doi:10.1038/s41419-021-03923-1
- He, L. (2021). Alterations of Gut Microbiota by Overnutrition Impact Gluconeogenic Gene Expression and Insulin Signaling. *Int. J. Mol. Sci.* 22. doi:10.3390/ijms22042121
- Jiang, L., Allagnat, F., Nguidjoe, E., Kamagate, A., Pachera, N., Vanderwinden, J.-M., et al. (2010). Plasma Membrane Ca²⁺-ATPase Overexpression Depletes Both Mitochondrial and Endoplasmic Reticulum Ca²⁺ Stores and Triggers Apoptosis in Insulin-Secreting BRIN-BD11 Cells. *J. Biol. Chem.* 285, 30634–30643. doi:10.1074/jbc.m110.116681
- Johnson, C. L., Weston, J. Y., Chadi, S. A., Fazio, E. N., Huff, M. W., Kharitonov, A., et al. (2009). Fibroblast Growth Factor 21 Reduces the Severity of Cerulein-Induced Pancreatitis in Mice. *Gastroenterology* 137, 1795–1804. doi:10.1053/j.gastro.2009.07.064
- Keestra-Gounder, A. M., Byndloss, M. X., Seyffert, N., Young, B. M., Chávez-Arroyo, A., Tsai, A. Y., et al. (2016). NOD1 and NOD2 Signalling Links ER Stress with Inflammation. *Nature* 532, 394–397. doi:10.1038/nature17631
- Kranich, J., Krautler, N. J., Falsig, J., Ballmer, B., Li, S., Hutter, G., et al. (2010). Engulfment of Cerebral Apoptotic Bodies Controls the Course of Prion Disease in a Mouse Strain-dependent Manner. *J. Exp. Med.* 207, 2271–2281. doi:10.1084/jem.20092401
- Kubisch, C. H., Sans, M. D., Arumugam, T., Ernst, S. A., Williams, J. A., and Logsdon, C. D. (2006). Early Activation of Endoplasmic Reticulum Stress Is Associated with Arginine-Induced Acute Pancreatitis. *Am. J. Physiology-Gastrointestinal Liver Physiol.* 291, G238–G245. doi:10.1152/ajpgi.00471.2005
- Li, Y., Gao, Q., Shu, X., Xiao, L., Yang, Y., Pang, N., et al. (2021). Antagonizing $\alpha\text{v}\beta 3$ Integrin Improves Ischemia-Mediated Vascular Normalization and Blood Perfusion by Altering Macrophages. *Front. Pharmacol.* 12, 585778. doi:10.3389/fphar.2021.585778
- Li, Y., Guo, Y., Tang, J., Jiang, J., and Chen, Z. (2014). New Insights into the Roles of CHOP-Induced Apoptosis in ER Stress. *Acta Biochim. Biophys. Sin (Shanghai)* 46, 629–640. doi:10.1093/abbs/gmu048
- Liu, Y., Chen, X.-D., Yu, J., Chi, J.-L., Long, F.-W., Yang, H.-W., et al. (2017). Deletion of XIAP Reduces the Severity of Acute Pancreatitis via Regulation of Cell Death and Nuclear Factor-Kb Activity. *Cel Death Dis* 8, e2685. doi:10.1038/cddis.2017.70
- Lu, Y., Liu, L., Pan, J., Luo, B., Zeng, H., Shao, Y., et al. (2021). MFG-E8 Regulated by miR-99b-5p Protects against Osteoarthritis by Targeting Chondrocyte Senescence and Macrophage Reprogramming via the NF-Kb Pathway. *Cel Death Dis* 12, 533. doi:10.1038/s41419-021-03800-x
- Lugea, A., Gerloff, A., Su, H.-Y., Xu, Z., Go, A., Hu, C., et al. (2017). The Combination of Alcohol and Cigarette Smoke Induces Endoplasmic Reticulum Stress and Cell Death in Pancreatic Acinar Cells. *Gastroenterology* 153, 1674–1686. doi:10.1053/j.gastro.2017.08.036
- Miksa, M., Amin, D., Wu, R., Jacob, A., Zhou, M., Dong, W., et al. (2008). Maturation-induced Down-Regulation of MFG-E8 Impairs Apoptotic Cell Clearance and Enhances Endotoxin Response. *Int. J. Mol. Med.* 22, 743–748.
- Misiewicz, M., Déry, M.-A., Foveau, B., Jodoin, J., Ruths, D., and LeBlanc, A. C. (2013). Identification of a Novel Endoplasmic Reticulum Stress Response Element Regulated by XBP1. *J. Biol. Chem.* 288, 20378–20391. doi:10.1074/jbc.m113.457242
- Ren, Y., Cui, Q., Zhang, J., Liu, W., Xu, M., Lv, Y., et al. (2021). Milk Fat Globule-EGF Factor 8 Alleviates Pancreatic Fibrosis by Inhibiting ER Stress-Induced Chaperone-Mediated Autophagy in Mice. doi:10.3389/fphar.2021.707259
- Ren, Y., Liu, W., Zhang, L., Zhang, J., Bi, J., Wang, T., et al. (2021). Milk Fat Globule EGF Factor 8 Restores Mitochondrial Function via Integrin-Mediated Activation of the FAK-STAT3 Signaling Pathway in Acute Pancreatitis. *Clin. Transl. Med.* 11, e295. doi:10.1002/ctm2.295
- Ren, Y., Qiu, M., Zhang, J., Bi, J., Wang, M., Hu, L., et al. (2019). Low Serum Irisin Concentration Is Associated with Poor Outcomes in Patients with Acute Pancreatitis and Irisin Administration Protects against Experimental Acute Pancreatitis. *Antioxid. Redox Signal.* doi:10.1089/ars.2019.7731
- Ren, Y.-F., Wang, M.-Z., Bi, J.-B., Zhang, J., Zhang, L., Liu, W.-M., et al. (2019). Irisin Attenuates Intestinal Injury, Oxidative and Endoplasmic Reticulum Stress in Mice with L-Arginine-Induced Acute Pancreatitis. *Wjg* 25, 6653–6667. doi:10.3748/wjg.v25.i45.6653
- Ren, Y., Qiu, M., Zhang, J., Bi, J., Wang, M., Hu, L., et al. (2019). Low Serum Irisin Concentration Is Associated with Poor Outcomes in Patients with Acute Pancreatitis, and Irisin Administration Protects against Experimental Acute Pancreatitis. *Antioxid. Redox Signaling* 31, 771–785. doi:10.1089/ars.2019.7731
- Sandoval, J., Pereda, J., Rodriguez, J. L., Escobar, J., Hidalgo, J., Joosten, L. A. B., et al. (2010). Ordered Transcriptional Factor Recruitment and Epigenetic Regulation of Tnf- α in Necrotizing Acute Pancreatitis. *Cell. Mol. Life Sci.* 67, 1687–1697. doi:10.1007/s00018-010-0272-3
- Song, M., Wang, C., Yang, H., Chen, Y., Feng, X., Li, B., et al. (2020). P-STAT3 Inhibition Activates Endoplasmic Reticulum Stress-Induced Splenocyte Apoptosis in Chronic Stress. *Front. Physiol.* 11, 680. doi:10.3389/fphys.2020.00680
- Stupp, R., Hegi, M. E., Gorlia, T., Erridge, S. C., Perry, J., Hong, Y.-K., et al. (2014). Cilengitide Combined with Standard Treatment for Patients with Newly Diagnosed Glioblastoma with Methylated MGMT Promoter (CENTRIC EORTC 26071-22072 Study): a Multicentre, Randomised, Open-Label, Phase 3 Trial. *Lancet Oncol.* 15, 1100–1108. doi:10.1016/s1470-2045(14)70379-1
- Sun, S.-C. (2017). The Non-canonical NF-Kb Pathway in Immunity and Inflammation. *Nat. Rev. Immunol.* 17, 545–558. doi:10.1038/nri.2017.52
- Sun, S., Kelekar, S., Klierer, S. A., and Mangelsdorf, D. J. (2019). The Orphan Nuclear Receptor SHP Regulates ER Stress Response by Inhibiting XBP1s Degradation. *Genes Dev.* 33, 1083–1094. doi:10.1101/gad.326868.119
- Szmola, R., and Sahin-Toth, M. (2010). Pancreatitis-associated Chymotrypsinogen C (CTRC) Mutant Elicits Endoplasmic Reticulum Stress in Pancreatic Acinar Cells. *Gut* 59, 365–372. doi:10.1136/gut.2009.198903
- Tan, J.-h., Cao, R.-c., Zhou, L., Zhou, Z.-t., Chen, H.-j., Xu, J., et al. (2020). EMC6 Regulates Acinar Apoptosis via APAF1 in Acute and Chronic Pancreatitis. *Cel Death Dis* 11, 966. doi:10.1038/s41419-020-03177-3
- Urano, F., Wang, X., Bertolotti, A., Zhang, Y., Chung, P., Harding, H. P., et al. (2000). Coupling of Stress in the ER to Activation of JNK Protein Kinases by Transmembrane Protein Kinase IRE1. *Science* 287, 664–666. doi:10.1126/science.287.5453.664
- Wang, S., Zhang, Q., Tiwari, S. K., Lichinchi, G., Yau, E. H., Hui, H., et al. (2020). Integrin $\alpha\text{v}\beta 5$ Internalizes Zika Virus during Neural Stem Cells Infection and Provides a Promising Target for Antiviral Therapy. *Cel Rep.* 30, 969–983. doi:10.1016/j.celrep.2019.11.020
- Wu, H., Li, H., Wen, W., Wang, Y., Xu, H., Xu, M., et al. (2021). MANF Protects Pancreatic Acinar Cells against Alcohol-Induced Endoplasmic Reticulum Stress and Cellular Injury. *J. Hepatobiliary Pancreat. Sci.*
- Wu, J., Yang, H., Cheng, J., Zhang, L., Ke, Y., Zhu, Y., et al. (2020). Knockdown of Milk-fat Globule EGF Factor-8 Suppresses Glioma Progression in GL261 Glioma Cells by Repressing Microglial M2 Polarization. *J. Cel Physiol* 235, 8679–8690. doi:10.1002/jcp.29712
- Xiao, J., Huang, K., Lin, H., Xia, Z., Zhang, J., Li, D., et al. (2020). Mogroside IIE Inhibits Digestive Enzymes via Suppression of Interleukin 9/Interleukin 9 Receptor Signalling in Acute Pancreatitis. *Front. Pharmacol.* 11, 859. doi:10.3389/fphar.2020.00859
- Yang, C., Hayashida, T., Forster, N., Li, C., Shen, D., Maheswaran, S., et al. (2011). The Integrin $\alpha\text{v}\beta 3$ -5 Ligand MFG-E8 Is a P63/p73 Target Gene in Triple-Negative Breast Cancers but Exhibits Suppressive Functions in ER+ and erbB2+ Breast Cancers. *Cancer Res.* 71, 937–945. doi:10.1158/0008-5472.can-10-1471
- Yong, J., Johnson, J. D., Arvan, P., Han, J., and Kaufman, R. J. (2021). Therapeutic Opportunities for Pancreatic β -cell ER Stress in Diabetes Mellitus. *Nat. Rev. Endocrinol.* 17, 455–467. doi:10.1038/s41574-021-00510-4
- You, K., Wang, L., Chou, C. H., Liu, K., Nakata, T., Jaiswal, A., et al. (2021). QRICH1 Dictates the Outcome of ER Stress through Transcriptional Control of Proteostasis. *Science* 371, 371. doi:10.1126/science.abb6896
- Zhang, Q., Zhao, C., Zhang, L., Sun, K., Yu, L., Wang, X., et al. (2021). Escin Sodium Improves the Prognosis of Acute Pancreatitis via Promoting Cell Apoptosis by Suppression of the ERK/STAT3 Signaling Pathway. *Oxid Med. Cel Longev* 2021, 9921839. doi:10.1155/2021/9921839
- Zhang, Q., Lenardo, M. J., and Baltimore, D. (2017). 30 Years of NF-Kb: A Blossoming of Relevance to Human Pathobiology. *Cell* 168, 37–57. doi:10.1016/j.cell.2016.12.012

Zhao, Y., Wang, Q., and Zang, B. (2019). Milk Fat Globule-Epidermal Growth Factor 8 (MFG-E8) Attenuates Sepsis-Induced Acute Kidney Injury by Inhibiting NF- κ B Signaling Pathway¹. *Acta Cir Bras* 34, e201900209. doi:10.1590/s0102-8650201900209

Conflict of Interest: The authors declare that the research was conducted in the absence of any commercial or financial relationships that could be construed as a potential conflict of interest.

Publisher's Note: All claims expressed in this article are solely those of the authors and do not necessarily represent those of their affiliated organizations, or those of

the publisher, the editors and the reviewers. Any product that may be evaluated in this article, or claim that may be made by its manufacturer, is not guaranteed or endorsed by the publisher.

Copyright © 2022 Ren, Liu, Zhang, Bi, Fan, Lv, Wu, Zhang and Wu. This is an open-access article distributed under the terms of the Creative Commons Attribution License (CC BY). The use, distribution or reproduction in other forums is permitted, provided the original author(s) and the copyright owner(s) are credited and that the original publication in this journal is cited, in accordance with accepted academic practice. No use, distribution or reproduction is permitted which does not comply with these terms.



Deep Learning-Based Morphological Classification of Endoplasmic Reticulum Under Stress

Yuanhao Guo^{1,2†}, Di Shen^{3†}, Yanfeng Zhou^{1,2†}, Yutong Yang^{1†}, Jinzhao Liang¹, Yating Zhou^{1,2}, Ningning Li⁴, Yu Liu³, Ge Yang^{1,2*} and Wenjing Li^{1,2*}

¹Laboratory of Computational Biology and Machine Intelligence, National Laboratory of Pattern Recognition, Institute of Automation, Chinese Academy of Sciences, Beijing, China, ²School of Artificial Intelligence, University of Chinese Academy of Sciences, Beijing, China, ³CAS Key Laboratory of Separation Science for Analytical Chemistry, Dalian Institute of Chemical Physics, Chinese Academy of Sciences, Dalian, China, ⁴Tomas Lindahl Laboratory, The Seventh Affiliated Hospital, Sun Yat-Sen University, Shenzhen, China

OPEN ACCESS

Edited by:

Jianguang Ji,
Lund University, Sweden

Reviewed by:

Stephen H. Howell,
Iowa State University, United States
Rossella Venditti,
Telethon Institute of Genetics and
Medicine (TIGEM), Italy

*Correspondence:

Ge Yang
ge.yang@ia.ac.cn
Wenjing Li
wenjing.li@ia.ac.cn

[†]These authors have contributed
equally to this work and share first
authorship

Specialty section:

This article was submitted to
Signaling,
a section of the journal
Frontiers in Cell and Developmental
Biology

Received: 31 August 2021

Accepted: 31 December 2021

Published: 21 January 2022

Citation:

Guo Y, Shen D, Zhou Y, Yang Y,
Liang J, Zhou Y, Li N, Liu Y, Yang G and
Li W (2022) Deep Learning-Based
Morphological Classification of
Endoplasmic Reticulum Under Stress.
Front. Cell Dev. Biol. 9:767866.
doi: 10.3389/fcell.2021.767866

Endoplasmic reticulum stress (ER stress) is a condition that is defined by abnormal accumulation of unfolded proteins. It plays an important role in maintaining cellular protein, lipid, and ion homeostasis. By triggering the unfolded protein response (UPR) under ER stress, cells restore homeostasis or undergo apoptosis. Chronic ER stress is implicated in many human diseases. Despite extensive studies on related signaling mechanisms, reliable image biomarkers for ER stress remain lacking. To address this deficiency, we have validated a morphological image biomarker for ER stress and have developed a deep learning-based assay to enable automated detection and analysis of this marker for screening studies. Specifically, ER under stress exhibits abnormal morphological patterns that feature ring-shaped structures called whorls (WHs). Using a highly specific chemical probe for unfolded and aggregated proteins, we find that formation of ER whorls is specifically associated with the accumulation of the unfolded and aggregated proteins. This confirms that ER whorls can be used as an image biomarker for ER stress. To this end, we have developed ER-WHs-Analyzer, a deep learning-based image analysis assay that automatically recognizes and localizes ER whorls similarly as human experts. It does not require laborious manual annotation of ER whorls for training of deep learning models. Importantly, it reliably classifies different patterns of ER whorls induced by different ER stress drugs. Overall, our study provides mechanistic insights into morphological patterns of ER under stress as well as an image biomarker assay for screening studies to dissect related disease mechanisms and to accelerate related drug discoveries. It demonstrates the effectiveness of deep learning in recognizing and understanding complex morphological phenotypes of ER.

Keywords: ER stress, morphological classification, image biomarker, deep learning, homeostasis

INTRODUCTION

The endoplasmic reticulum (ER) is a continuous membrane-bound organelle network that plays key roles in protein synthesis and modification, lipid biogenesis, and ionic homeostasis (Friedman and Voeltz, 2011). Dysregulation of protein synthesis and modification caused by intra- and extra-cellular cues leads to excessive accumulation of unfolded proteins, which triggers ER stress (Lee et al.,

2015; Schwarz and Blower, 2016). Unfolded protein response (UPR) often refers to the signal transduction pathway for cellular response to ER stress (Hetz et al., 2020). There are three main UPR transducers: inositol-requiring enzyme 1 (IRE1) (Tirasophon et al., 1998; Wang et al., 1998), protein kinase RNA-like ER kinase (PERK) (Harding et al., 1999), and activating transcription factor 6 (ATF6) (Harding et al., 2000; Ron and Walter, 2007). By orchestrating cellular processes such as mRNA splicing by endoribonuclease IRE1 α (Tirasophon et al., 1998; Wang et al., 1998), translation attenuation by kinases PERK (Harding et al., 1999), and protein folding assistance by chaperone BiP (binding immunoglobulin protein) (Shimizu et al., 2017), the UPR engages different outputs to restore ER protein homeostasis under mild stress conditions or to activate apoptosis under chronic stress conditions (Yoon et al., 2012; Nie et al., 2017; Ramachandran et al., 2021).

ER stress is strongly implicated in the onset and progression of a wide range of human diseases, including neurodegenerative diseases, metabolic diseases, and cancer (Ozcan et al., 2004; Zhang et al., 2005; Wang and Kaufman, 2016). It can cause not only alterations of protein synthesis or folding but also deleterious cellular responses including accumulation of lipids and activation of autophagy. Modulating ER stress shows great potential in the treatment of these diseases. Several compounds, including IRE1 α inhibitor KIRA6 and PERK inhibitor GSK2656157 (Axten et al., 2012; Wang et al., 2012; Ghosh et al., 2014), have been identified in target-based drug screening to modulate ER stress and have shown therapeutic benefits (Nunes et al., 2012; Ghosh et al., 2014; Kitakaze et al., 2019). In comparison to target-based screening, phenotypic screening utilizes readouts that are more observable and physiologically relevant for drug discoveries (Swinney and Anthony, 2011; Moffat et al., 2017). It can accelerate drug discoveries by using cell models of diseases with the support of high-throughput imaging (Zheng et al., 2013; Moffat et al., 2017). However, reliable and sensitive image biomarkers are required for phenotypic screening. Although ER morphology is a key cellular phenotypic feature, it is unclear whether it can serve as an image biomarker for ER stress. In addition, for any image biomarker, a reliable and efficient detection assay is essential for phenotypic screening (Kazama et al., 2018). Such an assay has yet to be developed for ER stress.

Changes in ER morphology correlate well with ER stress (Schuck et al., 2009; Mateus et al., 2018). The classical ER structure consists of a continuous envelope surrounding the nucleus in the perinuclear region and a polygonal network of interconnected tubules and sheets in the peripheral region (Friedman and Voeltz, 2011). In ER-stressed cells, ER membranes are compacted to form ER whorls (Nii et al., 1968; Snapp et al., 2003). Formation of ER whorls provides an effective structural response to prolonged ER stress (Xu et al., 2020). It accompanies the activation of PERK and works together with vesicle transport machinery such as ESCRT (endosomal complexes required for transport) and COPII (coat protein complex II) complex to counter-balance ER stress-induced protein translation and ER expansion (Bernales et al., 2006; Schuck et al., 2014; Schäfer et al., 2020; Xu et al., 2020). ER whorls have been observed in yeast and mammalian cells under ER stress activated by various stimuli, including drugs and herpes

simplex virus infection (Nii et al., 1968; Schäfer et al., 2020). To use ER whorls as an image biomarker for phenotypic drug screening, reliable and automated detection is essential. However, detection of ER whorls within the complex and dense ER network morphology poses a substantial technical challenge (Kazama et al., 2018).

The past decade witnessed the rapid rise of deep learning as a transformative artificial intelligence technique that computes using deep neural networks (DNNs). It has achieved breakthrough performance in many challenging tasks of analyzing natural images (LeCun et al., 2015). It has also achieved breakthrough performance in analyzing cellular images that previously are considered intractable for traditional methods (Moen et al., 2019). Unlike traditional methods, which rely on manually designed features to represent phenotypes in images, deep learning models automatically learn phenotypic features through their supervised training (LeCun et al., 2015). Recently, for example, deep learning models such as ResNet (He et al., 2016) and DenseNet (Huang et al., 2017) have achieved great success in recognizing cell states (Godinez et al., 2017; Sommer et al., 2017) and protein subcellular localization patterns (Kraus et al., 2016; Pärnamaa and Parts, 2017).

In this study, by comparing ER morphology under normal conditions *versus* IRE1 α activation, we found that the formation of ER whorls is initiated specifically when UPR pathways are activated under induced ER stress and that it is dependent on the duration and strength of the induced ER stress. By using a highly specific chemical probe, we found that whorls are tightly associated with unfolded and aggregated proteins. This confirms that ER whorls can serve as an image biomarker for ER stress. To use it as an image biomarker for screening studies, we have developed a deep learning-based image analysis assay, the ER-WHs-Analyzer, that recognizes and localizes ER whorls automatically. It includes a feature recognition module that achieves over 95% accuracy in recognizing ER whorls and classifying their patterns. It also includes a feature localization module that reliably detects regions of ER whorls in a manner consistent with the visual inspection by human experts. Training of deep learning models of ER-WHs-Analyzer requires no manual annotation of precise locations of ER whorls. Through a double-blind experiment, we further confirmed that ER whorls can serve as a reliable image biomarker for ER stress. Importantly, ER-WHs-Analyzer can reliably classify different patterns of ER whorls induced by different ER stress activation reagents. Overall, our study provides mechanistic insights into the relations between unfolded and aggregated proteins and ER whorls. It also provides an image biomarker assay for automated and quantitative analysis of ER stress that is well suited for phenotypic screening for related disease mechanism studies and drug discoveries.

MATERIALS AND METHODS

Induction and Western Blot Analysis of ER Stress in HEK293T Cells

HEK293T cells were treated with DMSO or ER stress induction compounds Thapsigargin (Tg) or Dithiothreitol (DTT) for

various lengths of time based on experimental designs, typically 6 h, then trypsinized, pelleted (800 × g, 4 min, room temperature) and lysed in RIPA buffer (Millipore) with protease inhibitor (Roche) and phosphatase inhibitor on ice. The supernatant was collected by centrifugation (13,000 × g, 15 min, 4°C) and the protein concentration was determined using BCA protein assay (Beyotime). Proteins were resolved by 12% SDS-PAGE, transferred to PVDF membranes, then blocked with 5% non-fat milk in TBST for 1 h at room temperature. The membranes were then washed with TBST (3 × 10 min) and incubated with anti-IRE1 (CST), anti-p-IRE1 (Abcam), or anti-Caspase 3 (CST) overnight at 4°C. Next, the membranes were washed with TBST (3 × 10 min) and incubated with goat-anti-rabbit-HRP or goat-anti-mouse-HRP in TBST for 1 h at room temperature. After washing with TBST for 3 times, the blots were developed using an ECL detection reagent.

Live Cell Imaging

High-resolution images of ER in live cells were acquired under two conditions, i.e., normal ER morphology in control cells and abnormal ER morphology (i.e., with ER whorls) in cells under induced ER stress. HEK293T cells labeled with ER marker GFP-sec61b were treated with DMSO, Tg or DTT for various lengths of time based on experimental designs, typically 6 h. To check abundance and location of ER proteins on whorls, BFP-KDEL was transiently expressed in HEK293T cells to label luminal proteins. And mCherry-Rtn4a, mCherry-ATL3, and GFP-REEP5 were transiently expressed in HEK293T cells to label ER morphology regulator proteins reticulon, atlastin, and REEP5, respectively. Treated cells were then imaged using conventional spinning disk confocal microscopy at ~200 nm resolution (Nikon CSU-W1 under 100× and 1.45 NA, excitation wavelength: 488 nm, emission wavelength: 535 nm) or 3D-SIM at ~70 nm resolution (Nikon N-SIM, 100× SR objective, excitation wavelength: 488 nm, emission wavelength: 535 nm).

Synthesis of the AIEgen Probe for Misfolded and Aggregated Proteins

A 250 ml round bottom flask was charged with isophorone (6.0 ml, 40 mmol), malononitrile (2.9 g, 44 mol) and piperidine (cat.). The mixture was heated to reflux and stirred for 30 h. After cooling to room temperature, the solution was slowly poured into water and the precipitated solid was filtered. Recrystallization from EtOH afforded S1 as a brown solid (2.1 g, 28%). To a 25 ml round bottom flask S1 (186.3 mg, 1.0 mmol), 4-(bis(2-hydroxyethyl)amino) benzaldehyde (313.8 mg, 1.0 mmol) and piperidine (cat.) were stirred in 10 ml EtOH at 85°C for 20 h. The solution was cooled to room temperature, and water was added to the solution. Then the mixture was extracted with DCM (3 × 20 ml). The organic phase was combined and dried over Na₂SO₄. After filtration and concentration in vacuo, the residue was purified *via* flash silica gel chromatography (10–40% EtOAc in hexane) to provide the compound AIEgen as violet solid (231.4 mg, 61.3%) and analyzed by ¹H-NMR (400 MHz, CDCl₃).

In vitro Thermal Shift Assay

AIEgen (25 μM) and 1) WT-DHFR (50 μM), 2) mut-DHFR (50 μM), and 3) sortase (50 μM) were mixed in acidic aggregation buffer (NaOAc 200 mM, KCl 100 mM, acidified by AcOH to pH = 6.23) and incubated at 60°C for 5 min 4) AIEGEN (25 μM) and human Ig (50 μM) were mixed in acidic aggregation buffer (NaOAc 200 mM, KCl 100 mM, acidified by AcOH to pH = 6.23) and incubated at 80°C for 5 min 5) AIEGEN (25 μM) SOD1 (50 μM) were mixed in buffer A (50 mM Tris-HCl, 100 mM NaCl, acidified by HCl to pH = 8.0) and EDTA disodium salt (250 mM). The mixture was incubated at 60°C for 5 min. Spectra were collected with excitation wavelength of 561 nm. All measurements were carried out using Tecan Spark fluorescence plate reader in BeyoGold™ 96-well black opaque plates.

ER-WHS-Analyzer

Image pre-processing and data augmentation – Each of the high-resolution ER images acquired contains multiple cells. Each single cell was first cropped from the acquired full-size images. The cropped images were resized into 256 × 256 pixels with zero padding for its shorter side to keep the original aspect ratio of the single cell. Intensity stretch and histogram equalization were applied to enhance the images. To avoid overfitting when training deep learning models, data augmentation by random flipping and rotation was performed online during training. This produced a considerably diverse data combination. Further details on the image datasets are given in the Results section.

Feature recognition module – It is the module used for recognizing and classifying ER morphological patterns, with or without ER whorls. Two types of representative DNNs, the ResNet (He et al., 2016) and DenseNet (Huang et al., 2017), were chosen as the backbone network of the feature recognition module. The recognition of ER whorls, present or absent, is a standard classification problem. The Softmax function was used to map output of the DNNs into a classification score:

$$p(y^l | \mathbf{x}) = \frac{e^{-f^l}}{\sum_j e^{-f^j}} \quad (1)$$

In Eq. 1, \mathbf{x} denotes the input image; $p(y^l | \mathbf{x})$ denotes the probability that the image \mathbf{x} is classified as in class l ; f is the output of the DNN parameterized by $f = \mathcal{F}(\mathbf{x}; \mathcal{W})$, where \mathcal{F} is the composition of the network parameters and \mathcal{W} represents model weights; f^j is the j -th element in f , which denotes the probability that image \mathbf{x} is classified as in the j -th class. The following Cross-Entropy loss was used for model training:

$$\mathcal{L} = \frac{1}{N} \sum_{i=1}^N -y_i^l \log p(\hat{y}_i | \mathbf{x}_i), \quad (2)$$

where y_i^l is the one-hot coding of the ground-truth for the i -th input image; the l -th element of y_i^l takes the value of 1 for its ground-truth class, and the rest takes the value of 0; $p(\hat{y}_i | \mathbf{x}_i)$ represents the predictions of the network for the input image, which are normalized using Eq. 1; N is the number of training examples. The goal is to minimize the loss by training the DNNs to obtain predictions that best match the ground truth. The

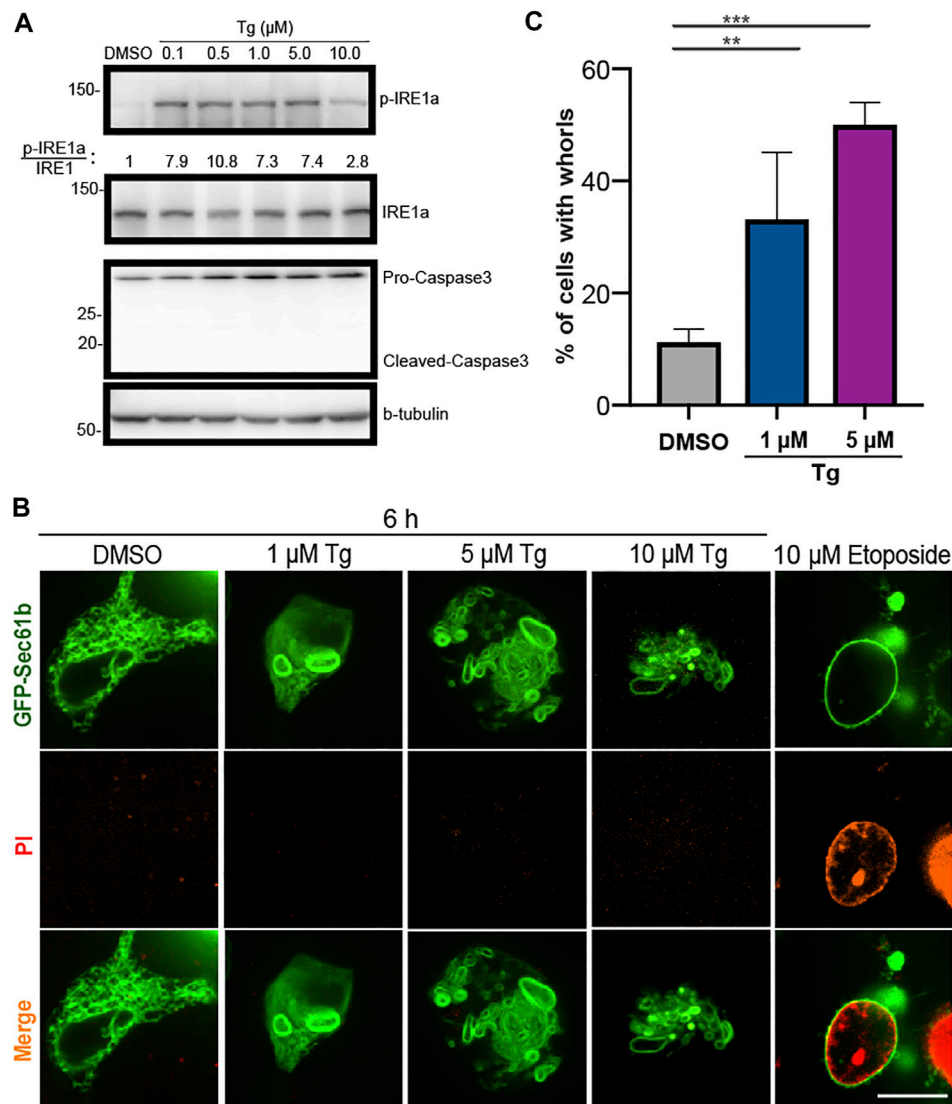


FIGURE 1 | Upregulated ER stress markers and abnormal ER shapes in HEK293T cells treated with Tg at different concentrations. **(A)** Immunoblot analysis of p-IRE1α, IRE1α, caspase3 (pro and cleaved) and β-tubulin from cell lysates after treatment of HEK293T cells with DMSO or Tg at the indicated concentrations for 6 h. The ratio of p-IRE1α to IRE1α is shown for each concentration. **(B)** Representative ER structures labeled with GFP-Sec61β (green) in HEK293T cells treated with Tg at the indicated concentrations for 6 h. PI staining was used to detect cell apoptosis. No substantial PI staining signal was detected in Tg treated cells (second row). Etoposide treated cells were used as a reference and a positive control for PI staining. Scale bar: 10 μm. **(C)** Percentage of HEK293T cells with ER whorls after treatment with DMSO or Tg at different concentrations for 6 h. Error bars indicate standard deviation (SD) calculated from three independent experiments. **: $p < 0.01$, ***: $p < 0.001$.

standard optimization method stochastic gradient descent (SGD) was used in this study.

Training strategies - Two training strategies were used: training from scratch and finetuning from a pre-trained model, i.e., transfer learning (Tan et al., 2018), a widely used approach to stabilize the training of deep learning models. To this end, a large dataset was collected primarily from open-source microscopy images, named as CBMI-Extra, which includes ~70k images from ~120 classes. Some of the images in CBMI-Extra were acquired using imaging protocols similar as those for the ER images in this study. In this way, a

deep learning model pre-trained using CBMI-Extra provided a sound starting point to stabilize its subsequent training using ER images.

Feature localization module - A deep learning model with good performance is expected to capture image features similarly as human experts. The feature visualization tool, Grad-CAM (Selvaraju et al., 2017), was used to check whether the DNN models can correctly recognize features of the ER whorls. Given an input image for a forward pass in a trained network, the feature visualization tool generates a class activation mapping (CAM) in the form of a heatmap, visualizing the importance of each

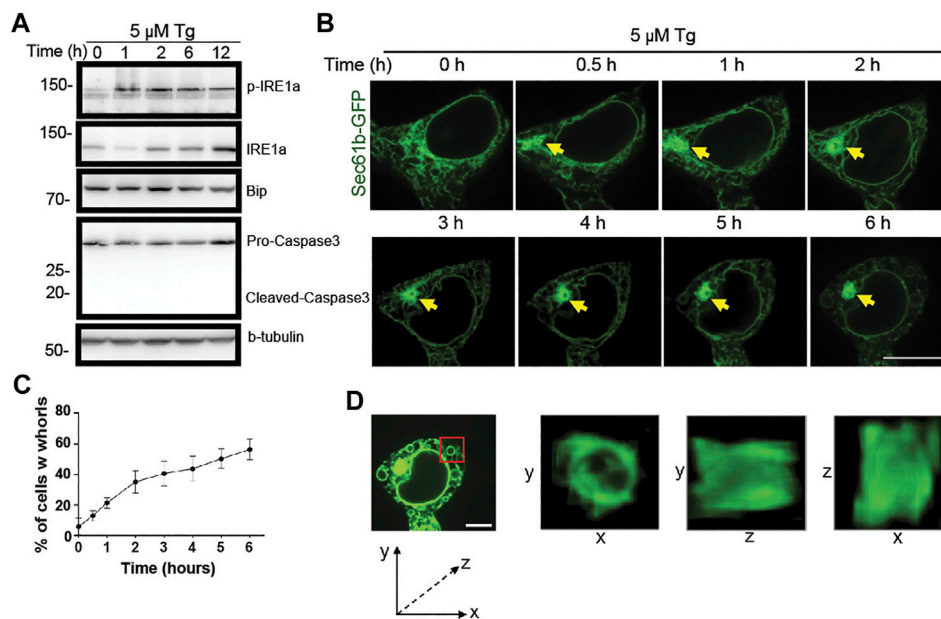


FIGURE 2 | Progressive changes of ER structure under ER stress over time. **(A)** Immunoblot analysis of p-IRE1 α , IRE1 α , caspase3 (pro and cleaved) and β -tubulin from cell lysates after treatment of HEK293T cells with DMSO or 5 μ M Tg for the indicated durations. **(B)** Representative ER structures labeled with GFP-Sec61 β (green) in HEK293T cells treated with 5 μ M Tg for the indicated durations. Yellow arrows point to where initial formation and evolution of an ER whorl occur. Scale bar: 20 μ m. **(C)** Percentages of HEK293T cells with ER whorls after treatment with 5 μ M Tg for the indicated durations. Data were presented as mean \pm SD from three independent experiments. **(D)** 5 \times magnified 3D views of the ring-like ER whorl in the region marked by the red box in the leftmost sub-panel. Scale bar: 10 μ m.

location in the input image in terms of its contribution to the prediction of the network. In this way, the feature visualization tool Grad-CAM constitutes the first part of the feature localization module by identifying up to several hotspots (i.e., clusters with higher scores) in the heatmap. It has been observed that the identified hotspots in the ER images match well with the ER morphological features that a human expert would identify. Based on the hotspots in heatmaps, an image processing-based pipeline was used to detect locations of the regions of ER whorls. This pipeline, which consists of segmentation, instance labeling and bounding-box assignment, constitutes the second part of the feature localization module (**Supplementary Figure S1**).

RESULTS

ER Stress Induces Morphological Deformation That Forms Whorls

We used ER stress activator Thapsigargin (Tg) to set up our experimental assay (Dibdiakova et al., 2019). Because Tg activation of ER stress increases the level of phosphorylated IRE1 α (Han et al., 2009), we used the amount of phosphorylated IRE1 α normalized by the total amount of IRE1 α as an indicator of ER stress. We checked this indicator at different concentrations and durations of Tg treatment (**Figures 1A, 2A**). We found that Tg treatment can reliably activate ER stress at a concentration ranging from 0.1 to 10 μ M and a duration ranging from 6 to 12 h without

affecting cell viability (**Figures 1A, 2A**). Based on these results, we set the concentration and duration of Tg treatment at 5 μ M and 6 h, respectively, for subsequent experiments.

To investigate whether activated ER stress causes morphological changes, ER was labeled by stable expression of GFP-Sec61 β , a subunit of the Sec61 translocon complex located on ER membrane. After activation with Tg, ER morphology in HEK293T cells was examined using spinning disk confocal microscopy at three concentrations for comparison (1, 5, 10 μ M). Consistent with Western blot analysis of IRE1 α , live-cell imaging of ER revealed morphological changes at all three concentrations (**Figures 1B,C**). In control cells treated with only DMSO, ER exhibited an interconnected membrane network that extends from the nuclear envelope (**Figure 1B**). However, under Tg treatment, ER formed multiple whorls that aggregate near the nuclear envelope (**Figure 1B**). Previous studies found that formation of ER whorls is a dynamic and reversible response to strong ER stress (Xu et al., 2020). Consistent with this finding, over $50.0 \pm 5.6\%$ ($n = 3$) of cells treated with 5 μ M Tg for 6 h exhibited the whorl phenotype (**Figure 1C**). In comparison, $11.2 \pm 3.3\%$ ($n = 3$) of control cells treated with DMSO exhibited whorl patterns (**Figure 1C**). Furthermore, Tg treatment at 1 μ M for 6 h induced whorls formation in 33.1% of the treated cells (**Figure 1C**). Together, these results indicate that ER stress induced by Tg treatment drives whorl formation in a dose-dependent manner.

To check whether ER whorls can be induced by drugs other than Tg, we treated HEK293T cells with several reagents reported

in the literature, including MK-28, a PERK activator (Ganz et al., 2020); Palmitic Acid, a long-chain saturated fatty acid (Xu et al., 2020; Harada et al., 2002); Bufalin, a Na^+/K^+ -ATPase inhibitor (Shen et al., 2014); and CB-5083, a p97 inhibitor (Bastola et al., 2016). These reagents are known to induce ER stress *via* different mechanisms (Ganz et al., 2020; Harada et al., 2002; Shen et al., 2014; Bastola et al., 2016). We generally found them to be less effective than DTT and Tg in inducing ER stress and performed all treatments at 1 μM for 12 h. Treatment by these reagents all induced formation of ER whorls (**Supplementary Figure S2**). In addition to these reagents, Cyclopiazonic Acid (CPA) and Lipopolysaccharide (LPS) have also been reported to induce formation of ER whorls in a dose-dependent manner (Xu et al., 2020). Together, these results show that formation of ER whorls is a general hallmark of ER stress rather than a specific outcome of Tg treatment.

Because prolonged ER stress may lead to cell death, we checked whether formation of whorls was caused by cell apoptosis. Using treatment of 10 μM Etoposide to inhibit DNA replication as a positive control, Propidium Iodide (PI) staining found no cell death under the performed Tg treatment (**Figure 1B**). Consistent with this result, cleavage of Caspase-3 was not detected by Western blot analysis (**Figure 1A**). In addition, it was reported that cells treated with Tg for 6 h recovered to exhibit normal ER morphology after Tg was washed out (Xu et al., 2020). Together, these results indicate that formation of whorls results from ER stress rather than cell death.

Dynamic ER Whorl Formation and Structural Deformation

To examine the dynamic formation of ER whorls, we performed time-lapse live cell imaging. Along with the membrane expansion and aggregation under stress, initial formation of ER whorls started approximately 0.5–1 h after Tg treatment. Severe membrane deformation led to further local ER aggregation (**Figure 2B**). Over the next 1–5 h, the number of ER whorls continued to increase while existing whorls became more condensed. After 6 h, the number of whorls and their morphologies generally became stable. The whorls occupied most of the intracellular space, and ER network connections were mostly lost (**Figure 2B**). Quantitative analysis revealed that whorls appeared in ~21.0% of cells after 1 h treatment (**Figure 2C**), and the percentage increased over time (**Figure 2C**). We also examined the three-dimensional structure of whorls (**Figure 2D**) and found that they were composed of warped ER membranes without ER tubules. Expansion and deformation of ER sheets could contribute to whorl formation. Importantly, canonical ER network connections were largely lost due to absence of ER tubules.

To check the abundance and location of ER proteins on the whorls, we examined fluorescently labeled Rtn4a, ATL3, and receptor accessory protein 5 (REEP5) under induced ER stress. We also checked ER luminal proteins by expressing fluorescently labeled lumen marker KDEL (**Supplementary Figure S3A**).

Overall, Rtn4a rarely locates to ER whorls under Tg treatment. Luminal proteins labeled by KDEL locates to ER whorls in ~10% of the treated cells, REEP5 locates to ER whorls in ~20% of the treated cells but ATL3 locates to ER whorls in ~80% of the treated cells (**Supplementary Figure S3B**). Overall, these results reveal differential abundance and location of ER proteins on ER whorls.

Unfolded and Aggregated Proteins are Attached to ER Whorls

The results so far have revealed tight connections between ER whorl formation and ER stress. Unfolded proteins are a key driver of ER stress (Braakman and Bulleid, 2011). To check whether ER whorls may be used as a reliable image biomarker for ER stress, we examined their relations with unfolded proteins using an AIEgen probe. It exhibited highly specific binding affinity to unfolded and aggregated proteins (**Figures 3A–C** and **Supplementary Figure S4**) such as *E. coli* dihydrofolate reductase (DHFR), a model protein for thermal shift assay that detects levels of protein aggregation (**Figure 3C**). The specific binding affinity of the AIEgen probe was further checked in mut-DHFR, sortase, human immunoglobulin, and superoxide dismutase (SOD1). Relative increase of fluorescence intensity ranging from ~2 to ~10 folds was detected, suggesting AIEgen can serve as a general probe for misfolded and aggregated proteins *in vitro* (**Figure 3D**). With illumination by AIEgen, misfolded and aggregated proteins were detected as puncta *in vivo* in live HEK293T cells and were found to be mobile or immobile (**Figure 3E**). The puncta were mostly rounded in shape under Structure Illumination Microscopy (SIM), with a diameter of ~0.5 μm (**Figure 3F**).

In addition to Tg treatment, ER stress can also be activated by Dithiothreitol (DTT) treatment, which causes protein misfolding and aggregation by blocking formation of disulfide bonds. Similar as under Tg treatment, DTT treatment at 10 mM for 6 h induced formation of ER whorls in 75.7% of treated cells (**Figures 4A,B**). In contrast, treatment of HEK293T cells with 1 mM of DTT for 6 h only induced formation of ER whorls in a small percentage (4.3%) of cells (**Supplementary Figures S5A–C**). When the concentration of DTT was increased to 3 mM, formation of ER whorls was detected in 45.3% of treated cells (**Supplementary Figures S5A–C**), indicating ER stress induced by DTT treatment drives whorl formation in a dose-dependent manner. The rate of whorl formation was significantly lower in control experiments, at $1.2 \pm 0.2\%$ (DTT 0 mM, 0 h), $1.2 \pm 0.2\%$ (DTT 0 mM, 6 h), and $0.8 \pm 0.1\%$ (DTT 10 mM, 0 h). In DTT treated cells, $81.7 \pm 2.1\%$ of them showed both puncta of unfolded proteins and ER whorls (**Figures 4B,C**), significantly higher than that of control cells ($11.4 \pm 1.6\%$ in DTT 0 mM 6 h, $3.7 \pm 0.3\%$ in DTT 0 mM 0 h, and $4.1 \pm 0.3\%$ in DTT 10 mM 0 h; $p < 0.0001$; mean \pm SEM; $n = 235$ cells from nine experiments). Interestingly, we noticed that the puncta of unfolded protein were tightly associated with deformed ER (**Figure 4C**). Specifically, $87.5 \pm 0.2\%$ of puncta of unfolded proteins were attached to ER whorls during their formation. They were either attached to outer surfaces of the whorls ($68.3 \pm 0.3\%$) or were wrapped inside the whorls ($19.3 \pm 0.2\%$) (**Figures 4C,D**) (average \pm SEM,

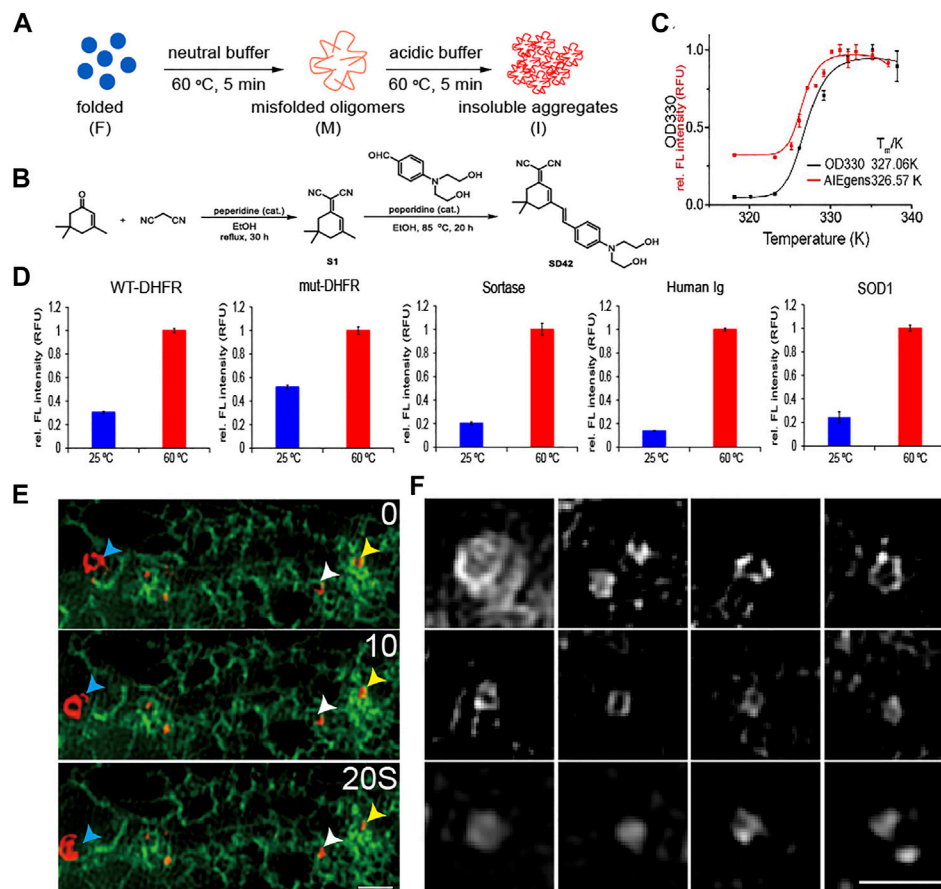


FIGURE 3 | Detecting unfolded and aggregated protein *in vitro* and *in vivo* by AIEgen. **(A)** A cartoon illustration of the formation of misfolded oligomers and insoluble aggregated DHFR model proteins. **(B)** Structural features of the AIEgen. **(C)** Thermal shift assay using OD330 turbidity (black curve) and the fluorescence of the AIEgen (red curve). Fluorescence of AIEgen occurs slightly earlier than the formation of insoluble aggregates measured by OD330 turbidity assay, indicating that the fluorescence originates from misfolded oligomers. **(D)** Fluorescence of AIEgen detecting the folded versus misfolded and aggregated proteins. AIEgen (25 μ M) and WT-DHFR (50 μ M), mut-DHFR (50 μ M), sortase (50 μ M), Human Ig (1 mg/ml) and SOD1 (50 μ M) were mixed in acidic aggregation buffer (NaOAc 200 mM, KCl 100 mM, acidified by AcOH to pH = 6.23) and incubated at 60 °C or 80 °C for 5 min. Spectra were collected with an excitation wavelength of 561 nm. **(E)** Both mobile (blue arrowhead) and immobile (white and yellow arrowheads) unfolded proteins are tightly associated with ER (green). Scale bar = 1 μ m. **(F)** SIM microscopy shows round shapes of unfolded proteins. Scale bar = 1 μ m.

$n = 355$ whorls from 151 cells). Taken together, these results indicate that whorls can serve as a morphological image biomarker for ER stress. The tight attachment of unfolded proteins to ER whorls also suggests a direct role of whorls in isolating misfolded and aggregated proteins.

Development of ER-WHs-Analyzer for Automated Detection of ER Whorls

So far, we have shown that ER whorls can serve as an image biomarker for ER stress. To use it for screening studies, we developed a deep learning-based analysis assay, which we refer to as ER-WHs-Analyzer, for automated detection and analysis of the whorls. The overall workflow of ER-WHs-Analyzer is shown in **Figure 5A**. First, raw images were cropped from acquired full-size ER images. Then, cropped images were standardized in their

sizes and enhanced in their quality through preprocessing. The feature recognition module (DNNs-based classification model) was trained using the preprocessed images along with their binary labels, i.e., WT (wildtype without whorls) or WHs (with whorls) (**Figure 5C**). The trained feature recognition module was then used to detect whether an ER image contains whorls. If ER whorls were detected, the feature localization module was used to generate a heatmap of features learned by the recognition module. Based on the heatmap, regions of whorls were localized by simple thresholding (**Figure 5A**; **Supplementary Figure S1**). Two types of representative DNNs, the ResNet (He et al., 2016) and DenseNet (Huang et al., 2017) (**Supplementary Figures S6, S7**), were used in this study. Their performance was compared using architectures with different depths including ResNet14, ResNet34, ResNet50, ResNet101, DenseNet121, DenseNet161, DenseNet169 and

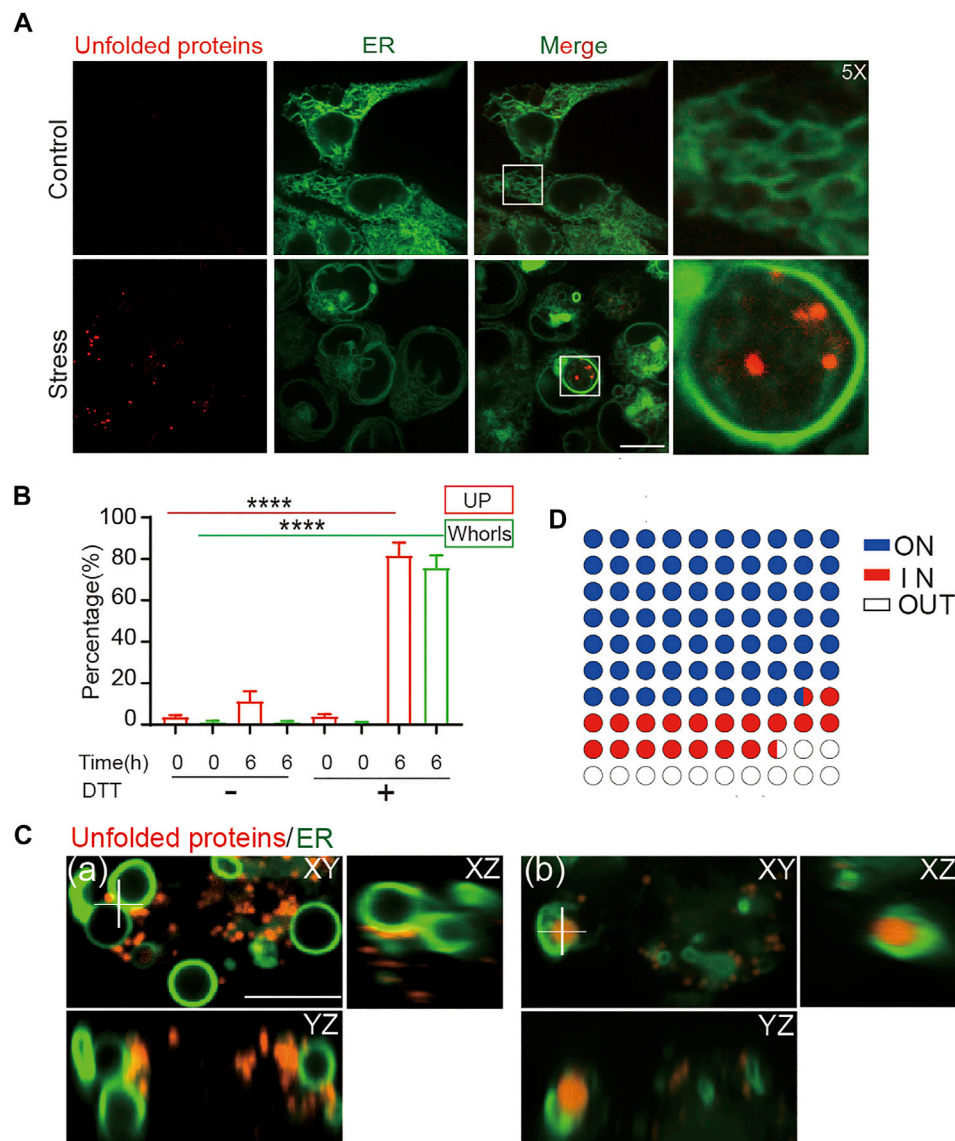


FIGURE 4 | ER whorls tether unfolded proteins under stress. **(A)** ER whorls and unfolded protein (UP) puncta appear only under stress. Scale bar = 10 μ m. **(B)** Quantification of unfolded protein puncta and whorls under stress. A 6-h treatment of 10 mM DTT induced both unfolded protein and whorls formation at a final ratio of $81.7 \pm 2.1\%$ and $75.7 \pm 2.0\%$ (mean \pm SD; from $n = 235$ cells), respectively. ****: $p < 0.0001$. **(C)** 3D view of colocalization of unfolded proteins and whorls. Unfolded proteins may be in contact with the outside surfaces of whorls (a) or exist inside the whorls (b). Scale bar = 1 μ m. **(D)** Quantification of localization of unfolded proteins with respect to whorls, $68.3 \pm 0.3\%$ (mean \pm SD; from $n = 355$) of whorls have UPs attached to the membrane (ON), $19.3 \pm 0.2\%$ of whorls wrapped UPs inside (IN).

DenseNet201, where the numbers indicate the count of trainable model layers (Figure 5B; Supplementary Figure S6).

Training and Testing Deep Learning Models of ER-WHs-Analyzer

For training and testing of the feature recognition module in ER-WHs-Analyzer, we constructed a dataset that we referred to as ER-Stress-A. We collected 490 cell images of normal ER morphology (labeled as WT) or abnormal ER morphology with whorls (labeled as WHs). We split the images into a

training set, a validation set, and a test set (Supplementary Table S1). The training and validation sets were used to finetune training hyper-parameters (Supplementary Table S2). The test set was used for standalone testing. Standard performance metrics for image classification were used, including F1 (F1 score), AUC (area under ROC curve), ACC (accuracy), Spc (specificity), Sen (sensitivity), Pre (precision). The validation set in ER-Stress-A was used to compare performance of different architectural configurations of backbone networks.

Validation results of different configurations of backbone networks are compared in Figure 5B. Several observations can

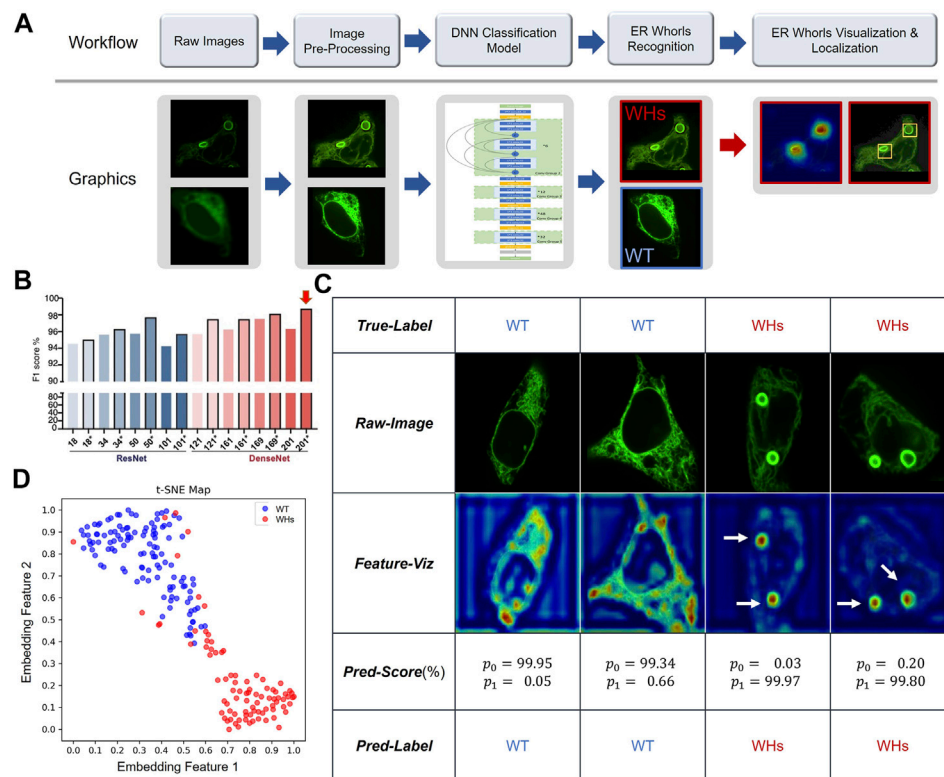


FIGURE 5 | Deep learning-based morphological classification of ER morphology. **(A)** Overall workflow of the proposed ER-WHs-Analyzer. **(B)** Performance evaluation of various DNNs-based classification models in the feature recognition module of ER-WHs-Analyzer. * indicates that the model was finetuned from a pre-trained model. Numbers on X axis indicate different depth of the deep learning models. Red arrow indicates the best performed model, the DenseNet-201 which consists of 201 weights-learnable layers. **(C)** Results of images from the ER-Stress-A dataset processed by ER-WHs-Analyzer-v1, including the raw images, their corresponding feature heat maps, their prediction scores, and their predicted labels. **(D)** Based on the phenotypic features learned, a t-SNE map was used to visualize the distribution of wildtype ER images (WT) and the ER images with whorls (WHs).

be made. First, deeper networks generally provided better performance. For example, ResNet50 with 50 weight-learnable layers obtained a higher F1-score than ResNet34 and ResNet18. And DenseNet generally outperformed ResNet. Second, models pretrained with CBMI-Extra (indicated by *) generally outperformed models without pretraining. The benefit of pretraining was more pronounced for shallow models. For example, the ResNet34 pretrained with CBMI-Extra outperformed DenseNet121 without pretraining. Third, deeper networks such as ResNet101 and DenseNet201 were more prone to overfitting. This problem can be mitigated by finetuning. DenseNet 201 achieves overall the highest rate of recognizing ER whorls (98.78%) (Figure 5B). Other performance metrics are listed in Supplementary Table S5. We chose DenseNet201 with pretraining for the feature recognition module of ER-WHs-Analyzer. In standalone testing, the model achieved excellent performance with F1 = 98.27%, AUC = 99.65%, ACC = 98.54%, Spc = 99.16%, Sen = 97.70%, Pre = 98.84%. In model testing, the ratio of abnormal ER structures labeled by experts was 42.33%, while the ratio detected by ER-WHs-Analyzer is 42.16%, reaching a high level of agreement. After feature recognition, the feature localization

module of ER-WHs-Analyzer determined positions of the regions of whorls based on a heatmap of learned feature and subsequent thresholding (Figure 5A).

Representative images from ER-Stress-A test set and their correct classification labels are shown in the second row and the first row of Figure 5C, respectively. The heatmaps of learning features are shown in the third row of Figure 5C, while their recognition results using the feature recognition module are shown in the fourth and fifth rows, respectively. Together, the results showed that ER-WHs-Analyzer can accurately recognize and localize individual ER whorls (Figure 5C; Supplementary Figure S8). We also used a t-SNE map (Maaten and Hinton, 2008) to visualize the representative features that our method learned to separate morphology of normal ER from ER with whorls (Figure 5D). We found that morphology of ER under normal condition and induced stress can be well differentiated.

Separating Different Sub-Phenotypes of ER Whorls Using ER-WHs-Analyzer

ER stress is induced by treatment of Tg and DTT *via* different mechanisms (Dibdiakova et al., 2019). Tg induces ER stress *via*

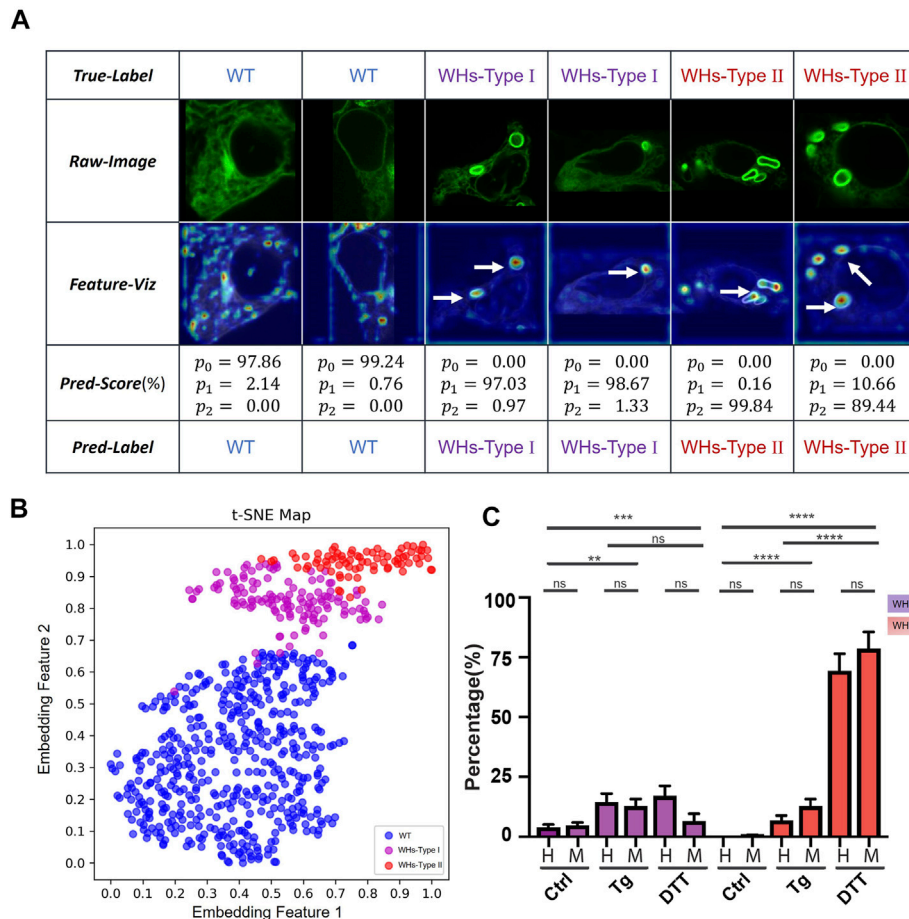


FIGURE 6 | Two sub-phenotypes of ER whorls were identified by ER-WHS-Analyzer-v2. **(A)** Results of images from the ER-Stress-B dataset processed by ER-WHS-Analyzer-v2, including the raw images, their corresponding feature heat maps, their prediction scores, and their predicted labels. **(B)** Based on the phenotypic features learned, a t-SNE map was used to visualize the distribution of wildtype ER images (WT), the ER images with WHs-Type I, and the ER images with WHs-Type II. **(C)** Double-blind testing results between human experts (H) and ER-WHS-Analyzer v2 (M). Purple bars show the distribution of WHs-Type I. Red bars show the distribution of WHs-Type II. Error bars indicate SEM, which was computed from 81 sampled images. **: $p < 0.01$; ***: $p < 0.001$; ****: $p < 0.0001$, ns: not significant.

interfering with calcium ion transport, while DTT induces ER stress by blocking the formation of disulfide bonds required for protein folding (Jiang et al., 2015). Differently from Tg or Tunicamycin (Tm), DTT is also considered as a robust pro-apoptotic ER stress inducer (Labunskyy et al., 2009). As expected, DTT treatment at a concentration of 3 mM caused formation of ER whorls. However, ER whorls induced by DTT (Figure 6A, second row, panels 5–6) showed morphological difference from those induced by Tg treatment (Figure 6A, second row, panels 3–4). Specifically, whorls induced by Tg treatment generally tend to be circular and small whereas whorls induced by DTT treatment tend to be elliptic and large. Cells treated with Tg generally tend to have a low number of whorls, typically one or two. Cells treated with DTT generally tend to have more whorls, typically two or more. We quantitatively analyzed the number and area of whorls in the cells treated by Tg and DTT using feature localization module (Supplementary Figure S1). Overall, DTT treatment induced an average of 2.43 ± 1.36 whorls per cell (mean \pm SD; $n = 112$ cells) and

an average area of whorls of $29.27 \pm 16.75 \mu\text{m}^2$ ($n = 272$ whorls). In contrast, Tg treatment induced an average of 1.37 ± 0.80 whorls per cell ($n = 150$ cells) and an average area of $14.88 \pm 11.79 \mu\text{m}^2$ ($n = 206$ whorls). The differences in whorl number and area between the two treatments are statistically significant ($p < 0.0001$).

To verify whether our ER-WHS-Analyzer can separate these morphological subphenotypes of ER whorls, we constructed another dataset that we refer to as ER-Stress-B. It contains three categories: Wildtype, WHs-Type I and WHs-Type II. WHs-Type I contains one or two whorls and WHs-Type II contains more than two whorls. ER-Stress-B contains a total of 1404 cell images. We partitioned all the images into a training set and a validation set (Supplementary Table S3). We used the same deep learning model and performance metrics as in previous experiments. For this multi-class recognition task, we replaced the previous two-class output layer with a three-class output layer and retrained the models. Again, we compared the performance of our models with and without pretraining with the CBMI-Extra dataset (Supplementary Table

S4). From the results, we observed a similar trend as in previous two-class classification experiments. Overall, DenseNet outperforms ResNet, and models with pretraining (indicated by *) outperform those without. However, differently from previous experiments, DenseNet161 shows overall the best performance, whose F1 score reaches 98.86%. Detailed evaluation metrics are compared in **Supplementary Table S6**. We chose DenseNet161 with pretraining for the feature recognition module and referred to the overall assay as ER-WHs-Analyzer v2.

Next, we checked whether ER-WHs-Analyzer v2 can reliably separate different subphenotypes of ER whorls. **Figure 6A** shows the results, which confirms that ER morphologies of WHs-Type I and WHs-Type II can be reliably differentiated. The t-SNE map (**Figure 6B**) shows that ER-WHs-Analyzer v2 has learned representative features to distinguish the sub-phenotypes of ER whorls.

Finally, we performed a double-blind experiment to compare ER-WHs-Analyzer v2 against human experts in classifying ER images acquired under control, Tg treatment, and DTT treatment respectively. Based on the classification results, we counted the numbers of the cells belonging to different sub-phenotypes for the control group and the two experimental groups. From the results, we have observed clear distribution differences of these three groups of cells (**Figure 6C**). According to classification by human experts, the control group contains $96.1 \pm 7.3\%$ WT, $3.9 \pm 1.2\%$ WHs-Type I and $0.0 \pm 0.0\%$ WHs-Type II. The Tg treatment group contains more WHs-Type I, with $78.7 \pm 4.8\%$ WT, $14.6 \pm 3.5\%$ WHs-Type I, and $6.8 \pm 2.1\%$ WHs-Type II (**Figure 6C**). In contrast, the DTT treatment group contains more WHs-Type II, with $13.6 \pm 6.8\%$ WT, $17.0 \pm 4.2\%$ WHs-Type I, $69.3 \pm 7.1\%$ WHs-Type II (**Figure 6C**). Classification results by ER-WHs-Analyzer v2 generally matched those by human experts ($p > 0.07$, $n > 81$ from seven experiments) (**Figure 6C**). Together, these experimental results suggested that ER-WHs-Analyzer v2 can reliably detect morphological differences of ER whorls induced by different treatments.

DISCUSSION

In this study, we examined morphological patterns of ER under stress and identified ER whorls as an image biomarker of ER stress for screening studies. ER whorls are found in both yeast and mammalian cells, and their formation is considered as an integral part of cellular response to ER stress (Bernales et al., 2006; Schäfer et al., 2020; Xu et al., 2020), an important target of drug development studies for treatment of cancer as well as metabolic and neurodegenerative diseases. Although a wide variety of chemical and genetic tools for assessing ER stress have been developed (Sicari et al., 2020), image biomarkers for efficient phenotypic screening have been lacking. Our study fills this gap.

Monitoring ER stress by detecting and analyzing ER whorls carry some important advantages. Canonical ER stress detection is carried out by Western blot analysis of the expression or phosphorylation of ER stress modulators or their transcription by quantitative reverse transcription polymerase chain reaction (RT-PCR) (Haynes and Wiseman, 2018). These are endpoint

assays that are laborious. More importantly, they cannot measure ER stress in single cells. Another approach to detect ER stress is to monitor the transcription reporters of molecules key to UPR, such as XBP1 and ATF4, by fluorescence. But it is not a real-time approach because of the time delay between initiation of transcription and the illumination of reporter proteins. In comparison, our study shows that ER morphological changes correlate well ER stress, and ER whorls can be used as an image biomarker to detect ER stress. They appear as early as 1 h after stress induction, indicating that they respond quickly to ER stress. Furthermore, high-resolution live-cell imaging of whorls makes real-time and single-cell level monitoring of ER stress possible. Our study combines automated high-resolution ER microscopy with deep learning-based analysis using ER-WHs-Analyzer to achieve high-throughput observation and quantification. This automated monitoring and analysis assay can be used as an effective tool for screening or validation of ER stress-related targets or drugs. It can reliably separate different sub-phenotypes of ER morphology under stress induced by different drugs. It can also be trained for use with other specific image biomarkers for ER stress. However, experimental settings of our study such as concentration and duration of Tg and DTT treatment remain to be further optimized.

The mechanism regulating ER whorl formation is complicated. Although the causal relation between formation of ER whorls and COPII, ESCRT has been established, the relation between formation of ER whorls and PERK signaling remains unclear (Schäfer et al., 2020; Xu et al., 2020). Our study shows that formation of ER whorls accompanies activation of IRE1 α . Therefore, multiple signaling pathways likely contribute to whorl formation. The precise functions of ER whorls are not completely clear either. The oligomerization and *trans*-autophosphorylation are considered as an activation of ER stress sensors. Therefore, whether whorls contribute to the activation of PERK and IRE1 α should be tested. In addition, ER whorls are reported to separate the translocon complex and suppress protein translation (Xu et al., 2020). We have also found that they isolate misfolded and aggregated proteins. However, whether they serve other cellular functions and whether they contribute to cell fate determination under prolonged ER stress remained to be determined. The automated image biomarker assay developed in this study will help address these questions.

DATA AVAILABILITY STATEMENT

The original contributions presented in the study are included in the article/**Supplementary Material**, further inquiries can be directed to the corresponding authors.

AUTHOR CONTRIBUTIONS

YG, WL and GY designed the study and wrote the manuscript. NL contributed to the design of the study. DS and YL synthesized

AI-Eigen probe. YFZ, YTZ and YG developed ER-WHS-Analyzer and analyzed the data. JL, YY and WL performed wet-lab experiments.

FUNDING

This work was supported in part by research grants from the Natural Science Foundation of China (Nos. 91954201, 31971289, and 32101216), the Chinese Academy of Sciences (No.

292019000056), University of Chinese Academy of Sciences (No. 115200M001), and the Beijing Municipal Science & Technology Commission (No. 5202022).

SUPPLEMENTARY MATERIAL

The Supplementary Material for this article can be found online at: <https://www.frontiersin.org/articles/10.3389/fcell.2021.767866/full#supplementary-material>

REFERENCES

- Axten, J. M., Medina, J. R., Feng, Y., Shu, A., Romeril, S. P., Grant, S. W., et al. (2012). Discovery of 7-Methyl-5-(1-[[3-(trifluoromethyl)phenyl]acetyl]-2,3-Dihydro-1H-Indol-5-Yl)-7H-Pyrrolo[2,3-D]pyrimidin-4-Amine (GSK2606414), a Potent and Selective First-In-Class Inhibitor of Protein Kinase R (PKR)-like Endoplasmic Reticulum Kinase (PERK). *J. Med. Chem.* 55 (16), 7193–7207. doi:10.1021/jm300713s
- Bastola, P., Neums, L., Schoenen, F. J., and Chien, J. (2016). VCP Inhibitors Induce Endoplasmic Reticulum Stress, Cause Cell Cycle Arrest, Trigger Caspase-Mediated Cell Death and Synergistically Kill Ovarian Cancer Cells in Combination with Salubrinal. *Mol. Oncol.* 10 (10), 1559–1574. doi:10.1016/j.molonc.2016.09.005
- Bernales, S., McDonald, K. L., and Walter, P. (2006). Autophagy Counterbalances Endoplasmic Reticulum Expansion during the Unfolded Protein Response. *Plos Biol.* 4 (12), e423. doi:10.1371/journal.pbio.0040423
- Braakman, I., and Bulleid, N. J. (2011). Protein Folding and Modification in the Mammalian Endoplasmic Reticulum. *Annu. Rev. Biochem.* 80, 71–99. doi:10.1146/annurev-biochem-062209-093836
- Dibdiakova, K., Saksonova, S., Pilchova, I., Klacanova, K., Tatarkova, Z., and Racay, P. (2019). Both thapsigargin- and Tunicamycin-Induced Endoplasmic Reticulum Stress Increases Expression of Hrd1 in IRE1-dependent Fashion. *Neurol. Res.* 41 (2), 177–188. doi:10.1080/01616412.2018.1547856
- Friedman, J. R., and Voeltz, G. K. (2011). The ER in 3D: a Multifunctional Dynamic Membrane Network. *Trends Cell Biol.* 21 (12), 709–717. doi:10.1016/j.tcb.2011.07.004
- Ganz, J., Shacham, T., Kramer, M., Shenkman, M., Eiger, H., Weinberg, N., et al. (2020). A Novel Specific PERK Activator Reduces Toxicity and Extends Survival in Huntington's Disease Models. *Sci. Rep.* 10 (1), 6875. doi:10.1038/s41598-020-63899-4
- Ghosh, R., Wang, L., Wang, E. S., Perera, B. G. K., Igbaria, A., Morita, S., et al. (2014). Allosteric Inhibition of the IRE1 α RNase Preserves Cell Viability and Function during Endoplasmic Reticulum Stress. *Cell* 158 (3), 534–548. doi:10.1016/j.cell.2014.07.002
- Godinez, W. J., Hossain, I., Lazic, S. E., Davies, J. W., and Zhang, X. (2017). A Multi-Scale Convolutional Neural Network for Phenotyping High-Content Cellular Images. *Bioinformatics* 33 (13), 2010–2019. doi:10.1093/bioinformatics/btx069
- Han, D., Lerner, A. G., Vande Walle, L., Upton, J.-P., Xu, W., Hagen, A., et al. (2009). IRE1 α Kinase Activation Modes Control Alternate Endoribonuclease Outputs to Determine Divergent Cell Fates. *Cell* 138 (3), 562–575. doi:10.1016/j.cell.2009.07.017
- Harada, H., Yamashita, U., Kurihara, H., Fukushi, E., Kawabata, J., and Kamei, Y. (2002). Antitumor Activity of Palmitic Acid Found as a Selective Cytotoxic Substance in a marine Red Alga. *Anticancer Res.* 22 (5), 2587–2590.
- Harding, H. P., Novoa, I., Zhang, Y., Zeng, H., Wek, R., Schapira, M., et al. (2000). Regulated Translation Initiation Controls Stress-Induced Gene Expression in Mammalian Cells. *Mol. Cell* 6 (5), 1099–1108. doi:10.1016/s1097-2765(00)00108-8
- Harding, H. P., Zhang, Y., and Ron, D. (1999). Protein Translation and Folding Are Coupled by an Endoplasmic-Reticulum-Resident Kinase. *Nature* 397 (6716), 271–274. doi:10.1038/16729
- Haynes, C. M., and Wiseman, R. L. (2018). “Coordinating Organismal Physiology through the Unfolded Protein Response Preface,” in *Coordinating Organismal Physiology through the Unfolded Protein Response* (Cham, Switzerland: Springer), 414, V–Vi.
- He, K., Zhang, X., Ren, S., and Sun, J. (2016). “Deep Residual Learning for Image Recognition,” in Proceedings of the IEEE conference on computer vision and pattern recognition, Las Vegas, NV, USA, 27–30 June 2016 (IEEE). doi:10.1109/cvpr.2016.90
- Hetz, C., Zhang, K., and Kaufman, R. J. (2020). Mechanisms, Regulation and Functions of the Unfolded Protein Response. *Nat. Rev. Mol. Cell Biol.* 21 (8), 421–438. doi:10.1038/s41580-020-0250-z
- Huang, G., Liu, Z., Van Der Maaten, L., and Weinberger, K. Q. (2017). “Densely Connected Convolutional Networks,” in Proceedings of the IEEE conference on computer vision and pattern recognition, Honolulu, HI, USA, 21–26 July 2017 (IEEE). doi:10.1109/cvpr.2017.243
- Jiang, H., Zou, J., Zhang, H., Fu, W., Zeng, T., Huang, H., et al. (2015). Unfolded Protein Response Inducers Tunicamycin and Dithiothreitol Promote Myeloma Cell Differentiation Mediated by XBP-1. *Clin. Exp. Med.* 15 (1), 85–96. doi:10.1007/s10238-013-0269-y
- Kazama, H., Hiramoto, M., Miyahara, K., Takano, N., and Miyazawa, K. (2018). Designing an Effective Drug Combination for ER Stress Loading in Cancer Therapy Using a Real-Time Monitoring System. *Biochem. Biophysical Res. Commun.* 501 (1), 286–292. doi:10.1016/j.bbrc.2018.05.001
- Kitakaze, K., Taniuchi, S., Kawano, E., Hamada, Y., Miyake, M., Oyadomari, M., et al. (2019). Cell-based HTS Identifies a Chemical Chaperone for Preventing ER Protein Aggregation and Proteotoxicity. *Elife* 8, e43302. doi:10.7554/elife.43302
- Kraus, O. Z., Ba, J. L., and Frey, B. J. (2016). Classifying and Segmenting Microscopy Images with Deep Multiple Instance Learning. *Bioinformatics* 32 (12), i52–i59. doi:10.1093/bioinformatics/btw252
- Labunsky, V. M., Yoo, M.-H., Hatfield, D. L., and Gladyshev, V. N. (2009). Sep15, a Thioredoxin-like Selenoprotein, Is Involved in the Unfolded Protein Response and Differentially Regulated by Adaptive and Acute ER Stresses. *Biochemistry* 48 (35), 8458–8465. doi:10.1021/bi900717p
- LeCun, Y., Bengio, Y., and Hinton, G. (2015). Deep Learning. *Nature* 521 (7553), 436–444. doi:10.1038/nature14539
- Lee, W., Yoo, W., and Chae, H. (2015). ER Stress and Autophagy. *Curr. Mol. Med.* 15 (8), 735–745. doi:10.2174/1566524015666150921105453
- Maaten, L. v. d., and Hinton, G. (2008). Visualizing Data Using T-SNE. *J. Machine Learn. Res.* 9 (Nov), 2579–2605.
- Mateus, D., Marini, E. S., Progida, C., and Bakke, O. (2018). Rab7a Modulates ER Stress and ER Morphology. *Biochim. Biophys. Acta (Bba) - Mol. Cell Res.* 1865 (5), 781–793. doi:10.1016/j.bbamcr.2018.02.011
- Moen, E., Bannon, D., Kudo, T., Graf, W., Covert, M., and Van Valen, D. (2019). Deep Learning for Cellular Image Analysis. *Nat. Methods* 16 (12), 1233–1246. doi:10.1038/s41592-019-0403-1
- Moffat, J. G., Vincent, F., Lee, J. A., Eder, J., and Prunotto, M. (2017). Opportunities and Challenges in Phenotypic Drug Discovery: an Industry Perspective. *Nat. Rev. Drug Discov.* 16 (8), 531–543. doi:10.1038/nrd.2017.111
- Nie, J., Liu, A., Tan, Q., Zhao, K., Hu, K., Li, Y., et al. (2017). AICAR Activates ER Stress-dependent Apoptosis in Gallbladder Cancer Cells. *Biochem. Biophysical Res. Commun.* 482 (2), 246–252. doi:10.1016/j.bbrc.2016.11.050
- Nii, S., Morgan, C., and Rose, H. M. (1968). Electron Microscopy of Herpes Simplex Virus. *J. Virol.* 2 (5), 517–536. doi:10.1128/jvi.2.5.517-536.1968
- Nunes, A. F., Amaral, J. D., Lo, A. C., Fonseca, M. B., Viana, R. J. S., Callaerts-Vegh, Z., et al. (2012). TUDCA, a Bile Acid, Attenuates Amyloid Precursor Protein

- Processing and Amyloid- β Deposition in APP/PS1 Mice. *Mol. Neurobiol.* 45 (3), 440–454. doi:10.1007/s12035-012-8256-y
- Ozcan, U., Cao, Q., Yilmaz, E., Lee, A. H., Iwakoshi, N. N., Ozdelen, E., et al. (2004). Endoplasmic Reticulum Stress Links Obesity, Insulin Action, and Type 2 Diabetes. *Science* 306 (5695), 457–461. doi:10.1126/science.1103160
- Pärnamaa, T., and Parts, L. (2017). Accurate Classification of Protein Subcellular Localization from High-Throughput Microscopy Images Using Deep Learning. *G3 (Bethesda)* 7 (5), 1385–1392. doi:10.1534/g3.116.033654
- Ramachandran, G., Moharir, S. C., Raghunand, T. R., and Swarup, G. (2021). Optineurin Modulates ER Stress-Induced Signaling Pathways and Cell Death. *Biochem. Biophysical Res. Commun.* 534, 297–302. doi:10.1016/j.bbrc.2020.11.091
- Ron, D., and Walter, P. (2007). Signal Integration in the Endoplasmic Reticulum Unfolded Protein Response. *Nat. Rev. Mol. Cell Biol.* 8 (7), 519–529. doi:10.1038/nrm2199
- Schäfer, J. A., Schessner, J. P., Bircham, P. W., Tsuji, T., Funaya, C., Pajonk, O., et al. (2020). ESCRT Machinery Mediates Selective Microautophagy of Endoplasmic Reticulum in Yeast. *EMBO J.* 39 (2), e102586. doi:10.15252/embj.2019102586
- Schuck, S., Gallagher, C. M., and Walter, P. (2014). ER-phagy Mediates Selective Degradation of Endoplasmic Reticulum Independently of the Core Autophagy Machinery. *J. Cell Sci.* 127 (Pt 18), 4078–4088. doi:10.1242/jcs.154716
- Schuck, S., Prinz, W. A., Thorn, K. S., Voss, C., and Walter, P. (2009). Membrane Expansion Alleviates Endoplasmic Reticulum Stress Independently of the Unfolded Protein Response. *J. Cell Biol.* 187 (4), 525–536. doi:10.1083/jcb.200907074
- Schwarz, D. S., and Blower, M. D. (2016). The Endoplasmic Reticulum: Structure, Function and Response to Cellular Signaling. *Cell. Mol. Life Sci.* 73 (1), 79–94. doi:10.1007/s00018-015-2052-6
- Selvaraju, R. R., Cogswell, M., Das, A., Vedantam, R., Parikh, D., and Batra, D. (2017). “Grad-cam: Visual Explanations from Deep Networks via Gradient-Based Localization,” in Proceedings of the IEEE international conference on computer vision, Venice, Italy, 25 December 2017 (IEEE). doi:10.1109/iccv.2017.74
- Shen, S., Zhang, Y., Wang, Z., Zhang, R., and Gong, X. (2014). Bufalin Induces the Interplay between Apoptosis and Autophagy in Glioma Cells through Endoplasmic Reticulum Stress. *Int. J. Biol. Sci.* 10 (2), 212–224. doi:10.7150/ijbs.8056
- Shimizu, A., Kaira, K., Yasuda, M., Asao, T., and Ishikawa, O. (2017). Clinical and Pathological Significance of ER Stress Marker (BiP/GRP78 and PERK) Expression in Malignant Melanoma. *Pathol. Oncol. Res.* 23 (1), 111–116. doi:10.1007/s12253-016-0099-9
- Sicari, D., Delaunay-Moisan, A., Combettes, L., Chevet, E., and Igbaria, A. (2020). A Guide to Assessing Endoplasmic Reticulum Homeostasis and Stress in Mammalian Systems. *FEBS J.* 287 (1), 27–42. doi:10.1111/febs.15107
- Snapp, E. L., Hegde, R. S., Francolini, M., Lombardo, F., Colombo, S., Pedrazzini, E., et al. (2003). Formation of Stacked ER Cisternae by Low Affinity Protein Interactions. *J. Cell Biol.* 163 (2), 257–269. doi:10.1083/jcb.200306020
- Sommer, C., Hoefler, R., Samwer, M., and Gerlich, D. W. (2017). A Deep Learning and novelty Detection Framework for Rapid Phenotyping in High-Content Screening. *MBoC* 28 (23), 3428–3436. doi:10.1091/mbc.e17-05-0333
- Swinney, D. C., and Anthony, J. (2011). How Were New Medicines Discovered? *Nat. Rev. Drug Discov.* 10 (7), 507–519. doi:10.1038/nrd3480
- Tan, C., Sun, F., Kong, T., Zhang, W., Yang, C., and Liu, C. (2018). “A Survey on Deep Transfer Learning,” in International conference on artificial neural networks, Alghero, Italy, 27 September 2018 (Springer). doi:10.1007/978-3-030-01424-7_27
- Tirasophon, W., Welihinda, A. A., and Kaufman, R. J. (1998). A Stress Response Pathway from the Endoplasmic Reticulum to the Nucleus Requires a Novel Bifunctional Protein Kinase/endoribonuclease (Ire1p) in Mammalian Cells. *Genes Dev.* 12 (12), 1812–1824. doi:10.1101/gad.12.12.1812
- Wang, L., Perera, B. G. K., Hari, S. B., Bhattacharai, B., Backes, B. J., Seeliger, M. A., et al. (2012). Divergent Allosteric Control of the IRE1 α Endoribonuclease Using Kinase Inhibitors. *Nat. Chem. Biol.* 8 (12), 982–989. doi:10.1038/nchembio.1094
- Wang, M., and Kaufman, R. J. (2016). Protein Misfolding in the Endoplasmic Reticulum as a Conduit to Human Disease. *Nature* 529 (7586), 326–335. doi:10.1038/nature17041
- Wang, X.-Z., et al. (1998). Cloning of Mammalian Ire1 Reveals Diversity in the ER Stress Responses. *EMBO J.* 17 (19), 5708–5717. doi:10.1093/emboj/17.19.5708
- Xu, F., Du, W., Zou, Q., Wang, Y., Zhang, X., Xing, X., et al. (2020). COPII Mitigates ER Stress by Promoting Formation of ER Whorls. *Cell Res.* 42, 141–156. doi:10.1038/s41422-020-00416-2
- Yoon, S. O., Park, D. J., Ryu, J. C., Ozer, H. G., Tep, C., Shin, Y. J., et al. (2012). JNK3 Perpetuates Metabolic Stress Induced by A β Peptides. *Neuron* 75 (5), 824–837. doi:10.1016/j.neuron.2012.06.024
- Zhang, K., Wong, H. N., Song, B., Miller, C. N., Scheuner, D., and Kaufman, R. J. (2005). The Unfolded Protein Response Sensor IRE1 α Is Required at 2 Distinct Steps in B Cell Lymphopoiesis. *J. Clin. Invest.* 115 (2), 268–281. doi:10.1172/jci200521848
- Zheng, W., Thorne, N., and McKew, J. C. (2013). Phenotypic Screens as a Renewed Approach for Drug Discovery. *Drug Discov. Today* 18 (21–22), 1067–1073. doi:10.1016/j.drudis.2013.07.001

Conflict of Interest: A patent application related to this study has been approved by the China National Intellectual Property Administration. The number of the approved patent is ZL 2021 1 0150528.7.

Publisher’s Note: All claims expressed in this article are solely those of the authors and do not necessarily represent those of their affiliated organizations, or those of the publisher, the editors, and the reviewers. Any product that may be evaluated in this article, or claim that may be made by its manufacturer, is not guaranteed or endorsed by the publisher.

Copyright © 2022 Guo, Shen, Zhou, Yang, Liang, Zhou, Li, Liu, Yang and Li. This is an open-access article distributed under the terms of the Creative Commons Attribution License (CC BY). The use, distribution or reproduction in other forums is permitted, provided the original author(s) and the copyright owner(s) are credited and that the original publication in this journal is cited, in accordance with accepted academic practice. No use, distribution or reproduction is permitted which does not comply with these terms.



Calcium Signaling Regulated by Cellular Membrane Systems and Calcium Homeostasis Perturbed in Alzheimer's Disease

Dong-Xu Huang¹, Xin Yu¹, Wen-Jun Yu¹, Xin-Min Zhang², Chang Liu³, Hong-Ping Liu³, Yue Sun⁴ and Zi-Ping Jiang^{1*}

¹Department of Hand and Foot Surgery, The First Hospital of Jilin University, Changchun, China, ²Department of Anesthesiology, The First Hospital of Jilin University, Changchun, China, ³Department of Neurology, The First Hospital of Jilin University, Changchun, China, ⁴Department of The First Operating Room, The First Hospital of Jilin University, Changchun, China

OPEN ACCESS

Edited by:

Yongye Huang,
Northeastern University, China

Reviewed by:

Reza Raeisossadati,
Universidade Federal do ABC, Brazil
Kenneth Norman,
Albany Medical College, United States
Linlin Xu,
Shandong University, China

*Correspondence:

Zi-Ping Jiang
waterjzp@jlu.edu.cn

Specialty section:

This article was submitted to
Signaling,
a section of the journal
Frontiers in Cell and Developmental
Biology

Received: 14 December 2021

Accepted: 31 January 2022

Published: 25 February 2022

Citation:

Huang D-X, Yu X, Yu W-J, Zhang X-M,
Liu C, Liu H-P, Sun Y and Jiang Z-P
(2022) Calcium Signaling Regulated by
Cellular Membrane Systems and
Calcium Homeostasis Perturbed in
Alzheimer's Disease.
Front. Cell Dev. Biol. 10:834962.
doi: 10.3389/fcell.2022.834962

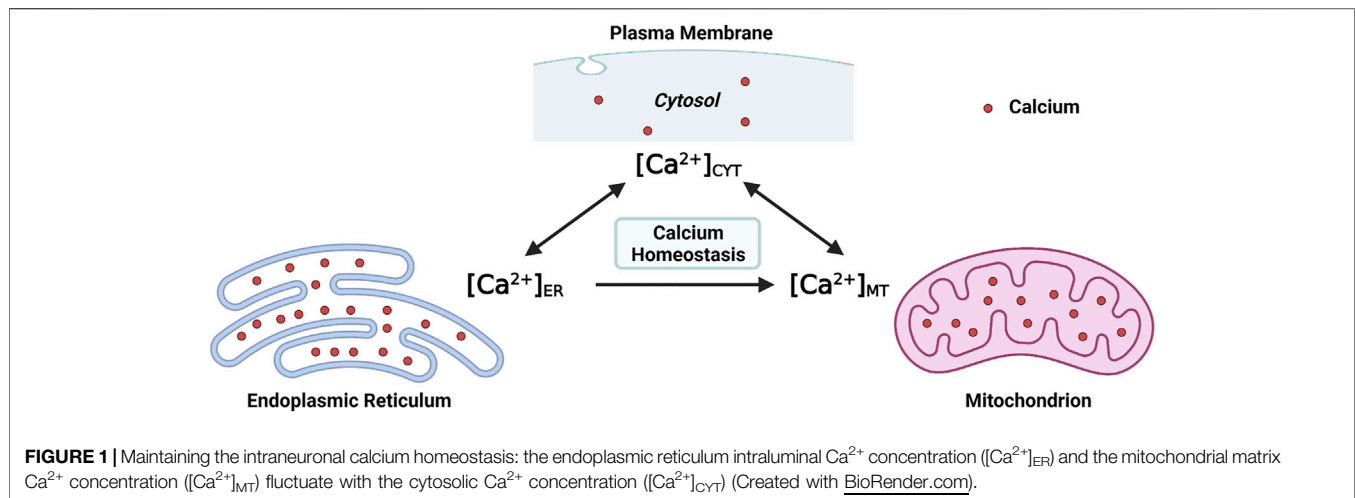
Although anything that changes spatiotemporally could be a signal, cells, particularly neurons, precisely manipulate calcium ion (Ca^{2+}) to transmit information. Ca^{2+} homeostasis is indispensable for neuronal functions and survival. The cytosolic Ca^{2+} concentration ($[\text{Ca}^{2+}]_{\text{CYT}}$) is regulated by channels, pumps, and exchangers on cellular membrane systems. Under physiological conditions, both endoplasmic reticulum (ER) and mitochondria function as intracellular Ca^{2+} buffers. Furthermore, efficient and effective Ca^{2+} flux is observed at the ER-mitochondria membrane contact site (ERMCS), an intracellular membrane juxtaposition, where Ca^{2+} is released from the ER followed by mitochondrial Ca^{2+} uptake in sequence. Hence, the ER intraluminal Ca^{2+} concentration ($[\text{Ca}^{2+}]_{\text{ER}}$), the mitochondrial matrix Ca^{2+} concentration ($[\text{Ca}^{2+}]_{\text{MT}}$), and the $[\text{Ca}^{2+}]_{\text{CYT}}$ are related to each other. Ca^{2+} signaling dysregulation and Ca^{2+} dyshomeostasis are associated with Alzheimer's disease (AD), an irreversible neurodegenerative disease. The present review summarizes the cellular and molecular mechanism underlying Ca^{2+} signaling regulation and Ca^{2+} homeostasis maintenance at ER and mitochondria levels, focusing on AD. Integrating the amyloid hypothesis and the calcium hypothesis of AD may further our understanding of pathogenesis in neurodegeneration, provide therapeutic targets for chronic neurodegenerative disease in the central nervous system.

Keywords: calcium signaling, calcium homeostasis, endoplasmic reticulum, mitochondria, membrane contact site, Alzheimer's disease

INTRODUCTION

The intraneuronal calcium ion (Ca^{2+}) homeostasis is indispensable for neuronal functions and survival, even death (Miller, 1991; Berridge, 1998). Mainly, Ca^{2+} functions as a second messenger: the spatiotemporal change of the cytosolic Ca^{2+} concentration ($[\text{Ca}^{2+}]_{\text{CYT}}$), also known as the Ca^{2+} signal, is one of the ways that cells convey various information either intracellularly or intercellularly (Berridge et al., 1998). Additionally, Ca^{2+} acts as a carrier of positive electrical current, which enters into the cytosol and depolarizes the transmembrane potential (Byrne et al., 2014).

At the molecular level, the $[\text{Ca}^{2+}]_{\text{CYT}}$ is regulated by channels, ATPase pumps, and ion exchangers on cellular membrane systems (the plasma membrane and intracellular membranes),



as well as Ca^{2+} -binding proteins in the cytosol (Byrne et al., 2014). At the subcellular level, at least two organelles, endoplasmic reticulum (ER) and mitochondria, have participated in the regulation of $[\text{Ca}^{2+}]_{\text{CYT}}$ either respectively or interactively (Martonosi, 1984; Miller, 1991; Spät et al., 2008). Structurally, the ER extends into every inner domain in neurons, and mitochondria tend to localize in intraneuronal compartments that consume massive ATPs, such as synapses (Sheng and Cai, 2012; Wu et al., 2017). Functionally, both the ER and mitochondria act as internal Ca^{2+} sources and sinks; namely, both organelles possess the role of buffering the $[\text{Ca}^{2+}]_{\text{CYT}}$ (Miller, 1991; Berridge, 1998; Spät et al., 2008). Collectively, both the endoplasmic reticulum intraluminal Ca^{2+} concentration ($[\text{Ca}^{2+}]_{\text{ER}}$) and the mitochondrial matrix Ca^{2+} concentration ($[\text{Ca}^{2+}]_{\text{MT}}$) fluctuate simultaneously with $[\text{Ca}^{2+}]_{\text{CYT}}$ (Figure 1). Moreover, efficient and effective Ca^{2+} flux is observed at the ER-mitochondria contact site (ERMCS), where the two organelles are intimately apposed (Wu et al., 2018). Briefly, Ca^{2+} is released from the ER lumen followed by mitochondrial Ca^{2+} uptake into the mitochondrial matrix through the outer and inner mitochondrial membranes in sequence (Rizzuto et al., 2012).

Maintaining the physiological level of $[\text{Ca}^{2+}]_{\text{CYT}}$, $[\text{Ca}^{2+}]_{\text{ER}}$, and $[\text{Ca}^{2+}]_{\text{MT}}$ is essential for intraneuronal Ca^{2+} homeostasis. When the neuronal Ca^{2+} signaling is dysregulated, neurons will undergo excitotoxicity or apoptosis (Lipton and Rosenberg, 1994; Berridge et al., 1999). The intraneuronal Ca^{2+} dyshomeostasis contributes to neurodegenerative diseases such as Alzheimer's disease (AD), an irreversible chronic neurodegenerative disease without effective treatment (Pchitskaya et al., 2018). The underlying cellular and molecular mechanisms which regulate Ca^{2+} signaling and maintain intracellular Ca^{2+} homeostasis, particularly by the ER and mitochondria, are summarized in the present review, focusing on AD.

ENDOPLASMIC RETICULAM IS THE CALCIUM SOURCE INSIDE THE NEURON

Subcellular Structures Formed by ER in the Neuron

The ER extends into every portion of the neuron to form an elaborate network, also considered as “a neuron within a neuron” (Berridge, 1998; Wu et al., 2017). The ER membrane, which connects with the nuclear envelope, also connects with the plasma membrane to form various types of specialized regions named the subsurface cisternae (located in the soma and initial dendrites, similar to the triadic junction in myocytes), the cisternae organelle (multilayered subsurface cisternae situated in the initial segment of the axon), the hypolemmal cisternae (located in the axon), and the spine apparatus (located in the dendritic spine) (Berridge, 1998).

Two Primary ER Ca^{2+} Channels: InsP_3R and RyR

Types and Distribution of ER Ca^{2+} Channels

As in other cell types, neuronal ER also contains the inositol 1,4,5-triphosphate receptor (InsP_3R) and the ryanodine receptor (RyR), sharing similar characteristics (Galione et al., 1993; Striggow and Ehrlich, 1996). Structurally, InsP_3Rs are homo- or hetero-tetrameric assemblies that own three isoforms, namely type 1 ($\text{InsP}_3\text{R1}$), type 2 ($\text{InsP}_3\text{R2}$), type 3 ($\text{InsP}_3\text{R3}$) (Taylor, 1998; Spät et al., 2008). Similarly, RyRs are tetrameric proteins that possess three subtypes: RyR1 , the skeletal muscle type; RyR2 , the cardiac muscle type; RyR3 , the brain type (Querfurth et al., 1997; Spät et al., 2008). Functionally, InsP_3Rs and RyRs are chemically-gated Ca^{2+} channels that evoke the regenerative Ca^{2+} wave from the ER lumen to the cytosol, also known as the Ca^{2+} -induced Ca^{2+} release (CICR) (Martonosi, 1984; Berridge, 1998; Spät et al., 2008). Seemingly, InsP_3Rs and RyRs have evolved from the same ancestor owing to the similarities (Berridge, 1997).

Spatially, InsP₃Rs and RyRs share similar but not identical distributions in neurons (Berridge, 1998). From the subcellular perspective, InsP₃Rs spread widely within the neuron, while RyRs localize predominantly in the soma (Walton et al., 1991; Kuwajima et al., 1992; Takei et al., 1992). Concerning mouse hippocampal neurons, both RyRs and InsP₃Rs coexist densely within the soma; but are distributed heterogeneously within dendrites: RyRs are restricted to the proximal region of dendrites, InsP₃Rs are found in the whole region of dendrites (Seymour-Laurent and Barish, 1995). Intriguingly, inspecting dendrites of chicken cerebellum Purkinje cells, there are only InsP₃Rs and no RyRs within the dendritic spine, but there are both InsP₃Rs and RyRs within the dendritic shaft (Walton et al., 1991). From the anatomical perspective, the cardiac muscle type RyR2, which conducts the Ca²⁺-elicited Ca²⁺ release, is detected throughout the brain; nevertheless, the skeletal muscle type RyR1, which performs the depolarization-evoked Ca²⁺ release, is seen exclusively in the cerebellum; the brain type RyR3 is distributed within the hippocampus, cortex, and corpus striatum (Kuwajima et al., 1992; Querfurth et al., 1997).

Elementary and Global Ca²⁺ Signals from ER

Neuronal Ca²⁺ signal initiates with increasing of [Ca²⁺]_{CYT}, which is followed by decreasing of [Ca²⁺]_{CYT} to the resting level (Miller, 1991). Although various types of Ca²⁺ signals are named in different ways, it is less important to focus on the terminology but essential for identifying their characteristics (Berridge et al., 1999).

The elementary Ca²⁺ signals originating from ER Ca²⁺ channel own hierarchical characteristics (Bootman et al., 1997; Berridge et al., 1999). At the fundamental level, the “blip” from InsP₃R and the “quark” from RyR are analogous, both of which are evoked from a single channel (Bootman et al., 1997). At the intermediate level, the “puff” from InsP₃Rs and the “spark” from RyRs are similar, both of which are liberated from clusters of channels (Bootman et al., 1997). These elementary Ca²⁺ signals are characterized by a quick rise period followed by a slow recovery period (Berridge, 1997). The underlying mechanism is that the opening of the channel leads to a plume of Ca²⁺ releasing from ER lumen; after the channel’s closing, the released Ca²⁺ plume dissipates slowly by diffusion (Berridge, 1997).

These elementary Ca²⁺ signals construct the global Ca²⁺ signals, such as waves (at the subcellular level) and oscillations or spikes (at the whole-cell level) (Bootman et al., 1997; Berridge et al., 1999). Ca²⁺ waves propagate by regional Ca²⁺ diffusions and neighbor Ca²⁺ regenerations, based on the CICR, a positive feedback mechanism (Bootman et al., 1997). Furthermore, CICR is regulated by the positive and negative feedback influence of Ca²⁺ on the InsP₃R or RyRs, which are discussed later (Berridge, 1997). Under high, intermediate, low positive feedback CICR, the Ca²⁺ waves, respectively, are continuous, saltatory, and abortive (Bootman et al., 1997).

Regulation of InsP₃R Ca²⁺ Channel

The Ca²⁺-release activity from the opened InsP₃R, at least, is regulated by the InsP₃, [Ca²⁺]_{CYT}, and [Ca²⁺]_{ER}. Under a modest concentration of InsP₃, the opening of InsP₃R is biphasically

regulated by cytosolic Ca²⁺: the low [Ca²⁺]_{CYT} (<1 μM) can activate InsP₃R; in contrast, the high [Ca²⁺]_{CYT} (>1–10 μM) can inhibit the channel (Bootman and Lipp, 1999). Under the circumstance mentioned above, the original graph describing the probability of the InsP₃R opening against the [Ca²⁺]_{CYT} level reveals a bell-shaped curve (Bootman and Lipp, 1999). The ascending portion of the bell-shaped curve yields the positive feedback effect of the [Ca²⁺]_{CYT} on the InsP₃R opening, which allows the localized elementary Ca²⁺ signal to spread regeneratively as Ca²⁺ waves (Berridge, 1997; Sun et al., 1998). The descending portion of the bell-shaped curve represents the negative feedback dependence of the InsP₃R opening on the [Ca²⁺]_{CYT}, which terminates the elementary Ca²⁺ signal (Berridge, 1997; Sun et al., 1998).

Constructively, Adkins and Taylor suggest that InsP₃ acts as a molecular switch that converts the InsP₃R from a condition under which only an inhibitory Ca²⁺-binding site is feasible to one under which only a stimulatory Ca²⁺-binding site is viable (Adkins and Taylor, 1999). Sequentially, two steps are required for opening the InsP₃R: initially, it becomes a liganded InsP₃R by binding with InsP₃; subsequently, it becomes an active InsP₃R by binding with Ca²⁺ at the stimulatory Ca²⁺-binding site (Adkins and Taylor, 1999).

Nevertheless, the bell-shaped dependence of the InsP₃R opening on the [Ca²⁺]_{CYT} is not always expected. If the high [Ca²⁺]_{CYT} (100 μM) is applied secondary to the maximal concentration of InsP₃ (10 μM), the cytosolic Ca²⁺ fails to inhibit the Ca²⁺ release from the liganded InsP₃R; in turn, if the high [Ca²⁺]_{CYT} (100 μM) is given before the InsP₃ (10 μM), the cytosolic Ca²⁺ can entirely inhibit the Ca²⁺ release from the unliganded InsP₃R (Adkins and Taylor, 1999). Moreover, the liganded InsP₃R owns a limited time window beyond which it undergoes intrinsic inactivation, and then the cytosolic Ca²⁺ cannot activate the InsP₃R (Bootman and Lipp, 1999). Notably, although the opening of InsP₃R requires binding with both InsP₃ and Ca²⁺, it might not necessarily need the cytosolic Ca²⁺ (Bootman and Lipp, 1999). When [Ca²⁺]_{ER} is low, the opening of InsP₃R requires both InsP₃ and cytosolic Ca²⁺; however, when [Ca²⁺]_{ER} is high, there is no requirement for cytosolic Ca²⁺, it is enough for InsP₃ itself to open the InsP₃R (Missiaen et al., 1994).

Collectively, at the high InsP₃ level and the low [Ca²⁺]_{ER} level, the high [Ca²⁺]_{CYT} cannot inhibit InsP₃R because most InsP₃Rs are liganded (Adkins and Taylor, 1999). At the low InsP₃ level and the high [Ca²⁺]_{ER} level, the low [Ca²⁺]_{CYT} cannot activate InsP₃R due to InsP₃ alone can open the InsP₃R (Missiaen et al., 1994).

Regulation of RyR Ca²⁺ Channel

The RyR is opened and releases Ca²⁺ into the cytosol by Ca²⁺ binding with the high-affinity stimulatory site; the Ca²⁺ is released until the local [Ca²⁺]_{CYT} rises to the point where the low-affinity inhibitory site is bound, resulting in the RyR closing, which is the mechanism of CICR mediated by RyR (Payne et al., 2013). RyR1 and RyR2 are studied extensively in skeletal myocyte and cardiac myocyte, respectively. Dihydropyridine receptor (DHPR)-coupled RyR1 is opened upon depolarization of the

plasma membrane and then is closed upon repolarization; subsequently, the surrounding uncoupled RyR1 is regeneratively opened under the CICR mechanism (Berridge, 1997). RyR2 is opened by the brief cytosolic Ca^{2+} pulse from DHPR, which is activated upon depolarization of the plasma membrane; approximately four RyR2s together evoke the Ca^{2+} quark, then these quarks turn to sparks, finally to waves (Berridge, 1997). Additionally, the activation of RyR is also regulated by the $[\text{Ca}^{2+}]_{\text{ER}}$ level (Györke and Györke, 1998). Similar to InsP_3R , when $[\text{Ca}^{2+}]_{\text{ER}}$ is overloaded, the Ca^{2+} -release activity of RyR is also significantly potentiated (Cheng et al., 1996).

MITOCHONDRIA ARE CALCIUM BUFFERS INSIDE THE NEURON

Mitochondria-Linked Cytosolic Ca^{2+} Buffering

In addition to synthesizing adenosine triphosphate (ATP), another primary function of mitochondria is buffering intracellular Ca^{2+} (Miller, 1991). Neuronal mitochondria segregate Ca^{2+} under both physiological and pathological conditions (Miller, 1991). The Ca^{2+} buffering ability of mitochondria may lead to the accumulation of abundant Ca^{2+} in a particular domain in neurons (Rizzuto et al., 2012). Mitochondria may function as the last line against the exaggerated $[\text{Ca}^{2+}]_{\text{CYT}}$, which may be fatal for cells when other intracellular Ca^{2+} -regulating mechanisms are exhausted (Martonosi, 1984). It is considered that the majority of mitochondria are generated in the soma, and the dysfunctional mitochondria return to the soma for degradation (Sheng and Cai, 2012).

Mitochondria usually cluster in neuronal domains with high demand for ATP, such as presynaptic and postsynaptic terminals (Tang and Zucker, 1997). In neurons, mitochondria located in proximal to Ca^{2+} channels, such as NMDAR on the postsynaptic density, can accumulate the cytosolic Ca^{2+} and prevent the propagation of Ca^{2+} waves, a global Ca^{2+} signal (Rizzuto et al., 2012). In the post-tetanic potentiation, mitochondria in the presynaptic terminal regulate the $[\text{Ca}^{2+}]_{\text{CYT}}$ by buffering extra intraneuronal Ca^{2+} ; during tetanic stimulation, mitochondria take up Ca^{2+} ; after tetanic stimulation, mitochondria release Ca^{2+} into the cytosol, maintaining the $[\text{Ca}^{2+}]_{\text{CYT}}$ at a relatively high level (Tang and Zucker, 1997).

Mitochondria-Located Ca^{2+} Machinery

Logically, the entrance of Ca^{2+} into the mitochondrial matrix requires passing through two intracellular membranes: the outer mitochondrial membrane (OMM) and the inner mitochondrial membrane (IMM). The OMM is permeable to ions attributed to the massive expression of voltage-dependent anion channels (VDAC) (Rizzuto et al., 2012). The notion that the expression level of VDACs seems to be the bottleneck of mitochondrial Ca^{2+} uptake is supported by the demonstration that over-expression of VDACs potentiates $[\text{Ca}^{2+}]_{\text{MT}}$; in contrast, down-regulation of VDACs attenuates $[\text{Ca}^{2+}]_{\text{MT}}$ (Madesh and Hajnóczky, 2001; Rapizzi et al., 2002). Among three isoforms of VDACs (VDAC1, VDAC2, VDAC3), the VDAC1 isoform selectively

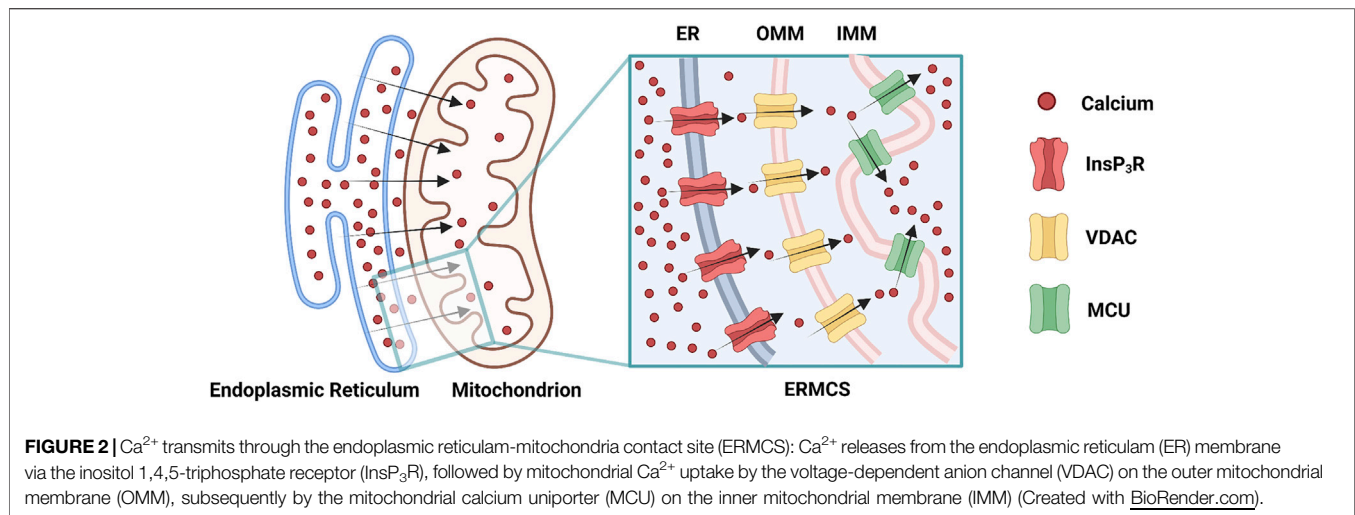
interacted with InsP_3R to transmit Ca^{2+} signal into the mitochondrial matrix that associates with apoptosis (De Stefani et al., 2012). Consistently, in the Chinese hamster ovary cell models that express all three isoforms of InsP_3Rs , the InsP_3R preferentially conducts Ca^{2+} signal into the mitochondria to induce apoptosis (Mendes et al., 2005).

The mitochondrial calcium uniporter (MCU) on the IMM can rapidly accumulate Ca^{2+} into the mitochondria matrix across the electrochemical gradient (Gunter and Gunter, 1994). MCU selectively binds Ca^{2+} with extremely high affinity ($K_D \leq 2 \text{ nM}$) (Kirichok et al., 2004). MCU contains two transmembrane domains and significantly potentiates mitochondrial Ca^{2+} uptake after over-expression (De Stefani et al., 2011). Acidic residues, a binding site for ruthenium red and its analogs (the most potent inhibitors of MCU), reside in the highly conserved motif between the two transmembrane domains and are essential for the entire activity of MCU (Baughman et al., 2011). The mitochondrial calcium uptake 1 (MICU1) protein interacts directly with MCU to regulate the rapid Ca^{2+} uptake of mitochondria (Perocchi et al., 2010).

CALCIUM CROSS-TALK THROUGH ENDOPLASMIC RETICULUM-MITOCHONDRIA CONTACT SITE

The ER has distributed the entire intracellular space from the nucleus to the plasma membrane intertwining all organelles, including mitochondria (Giorgi et al., 2009; Lebiedzinska et al., 2009; Wu et al., 2018). The ER network in which mitochondria are embedded exists in all compartments of neurons (Wu et al., 2017; Wu et al., 2018). The endoplasmic reticulum-mitochondria contact site (ERMCS) is abundant in every neuronal domain from the soma to dendrites and the axon (Wu et al., 2017). The distance between the two membranes in ERMCS is less than 200 nm (Rizzuto et al., 1998). Since the early 1960s, several different contact sites between the opposing membranes have been identified, such as the plasma membrane-ER contact site and the plasma membrane-mitochondria contact site (Lebiedzinska et al., 2009).

Mitochondrial Ca^{2+} uptake can occur at the ERMCS, where a high concentration of Ca^{2+} transports from the ER lumen into the mitochondrial matrix (Rizzuto et al., 2012). Briefly, Ca^{2+} releases from ER membrane via the InsP_3R , followed by mitochondrial Ca^{2+} uptake by the VDAC on OMM, subsequently by the MCU on the IMM (Figure 2) (Rizzuto et al., 2012). Mitochondrial Ca^{2+} uptake can regulate the activity of InsP_3R by decreasing the $[\text{Ca}^{2+}]_{\text{CYT}}$ nearby ER membrane (Rizzuto et al., 2012). During Ca^{2+} absorbing by mitochondria, the $[\text{Ca}^{2+}]_{\text{CYT}}$ near the InsP_3R mouth is not high enough to block the channel; hence the InsP_3R sustain opening, and the Ca^{2+} release from ER is prolonged (Boitier et al., 1999; Hajnóczky et al., 1999; Rizzuto et al., 2012). The increased ERMCS may induce the mitochondrial Ca^{2+} overload following Ca^{2+} release from the ER; conversely, the decreased ERMCS may impair Ca^{2+} -dependent mitochondrial metabolism (Csordás et al., 2006; Lebiedzinska et al., 2009). As mentioned



before, InsP_3R -VDAC1 interaction seems to play a major role in Ca^{2+} fluxion in ERMCS (Mendes et al., 2005; De Stefani et al., 2012). Collectively, $[\text{Ca}^{2+}]_{\text{ER}}$, $[\text{Ca}^{2+}]_{\text{CYT}}$, and $[\text{Ca}^{2+}]_{\text{MT}}$ are simultaneously regulated by ERMCS.

ALZHEIMER'S DISEASE: IRREVERSIBLE NEURODEGENERATION WITHOUT EFFECTIVE THERAPIES

Characteristics of Alzheimer's Disease

Alzheimer's disease (AD), first described in 1907 (Alzheimer et al., 1995), is a type of chronic neurodegenerative disease growing in number, which has brought physical sufferings, psychological stresses, and economic burden to individuals, families, and society (Alzheimer's Association, 2020). Regrettably, there are no available medications for slowing, ceasing, or reversing the neuronal pathological progression that causes neurodegenerative symptoms and makes AD fatal (Alzheimer's Association, 2020). Merely five drugs improving symptoms of AD have been approved by the Food and Drug Administration (FDA): three cholinesterase inhibitors (galantamine, rivastigmine, donepezil); one NMDAR blocker (memantine); one concomitant agent (memantine and donepezil) (Kumar et al., 2015; Atri, 2019; Alzheimer's Association, 2020). Additionally, tacrine, a cholinesterase inhibitor approved once by FDA, is discontinued in the United States due to severe side effects, such as liver damage (Kumar et al., 2015; Alzheimer's Association, 2016). Until 2021, 126 agents are in clinical trials for AD in the United States, and most investigational new drugs target modification of AD (Cummings et al., 2021). Recently, the repurposing and repositioning of conventional drugs is considered an alternative strategy for cancer therapy (Heckman-Stoddard et al., 2017; Huang et al., 2021). The same strategy could facilitate the identification of novel therapy for AD (Ballard et al., 2020).

Pathologically, the senile plaques (also known as β -amyloid plaques or neuritic plaques) and the neurofibrillary tangles (NFT) (also known as tau tangles or dystrophic neurites), observed inside and outside neurons, respectively, are two of several neuropathological features related to AD (Selkoe and Hardy, 2016; Alzheimer's Association, 2020).

Based on the age of morbidity, Alzheimer's disease is divided into two subtypes: the early-onset AD (EOAD), ranging from 30 years to 60 or 65 years; the late-onset AD (LOAD), defined with an onset age later than 60 or 65 years (Bekris et al., 2010). At the inheritance level, EOAD is characterized by the hereditary form, also known as the familial AD (FAD); by contrast, LOAD is typically termed as the sporadic AD (SAD) (Selkoe and Hardy, 2016; Kozlov et al., 2017).

Genetics of Alzheimer's Disease

Mutations in the *amyloid precursor protein* (APP), *presenilin-1* (PSEN1), and *presenilin-2* (PSEN2) genes are genetically associated with FAD (Bekris et al., 2010). The APP gene resides on chromosome 21 (Selkoe, 1994). Indeed, individuals with Down syndrome (DS) have an increased risk of developing AD owing to trisomy 21 (Alzheimer's Association, 2020). The PSEN1 gene, residing in chromosome 14, encodes the presenilin-1 protein of 467 amino acids which contains nine transmembrane domains; the PSEN2 gene, residing in chromosome 1, encodes the presenilin-2 protein of 448 amino acids topologically 67% identical to the presenilin-1 protein (Levy-Lahad et al., 1995; Sherrington et al., 1995; Cook et al., 1996; Leissring et al., 1999a; Laudon et al., 2005; Bekris et al., 2010). Mutations in the APP gene account for less than 5% of all FAD cases, mutations in the PSEN1 gene are responsible for approximately 70% of early-onset FAD (Van Broeckhoven, 1995). Consequently, mutations in the PSEN1 gene are the most common cause of presenile FAD; by contrast, mutations in the PSEN2 gene are a rare cause (Bekris et al., 2010). Mutations in the *apolipoprotein E* (APOE) gene, residing in chromosome 19, fulfill a significant role in SAD (Bertram and Tanzi, 2004; Bekris et al., 2010). Less than one hundred families with mutations in the APP gene, as well as

several hundred families with mutations in the *PSEN1* gene and the *PSEN2* gene have been reported worldwide, hence the FAD cases would occur in less than 1% of all AD cases (Bekris et al., 2010; Castellani and Smith, 2011). More than 90% of individuals with AD would suffer the sporadic type of this disease (Bekris et al., 2010).

INTEGRATING AMYLOID HYPOTHESIS AND CALCIUM HYPOTHESIS OF ALZHEIMER'S DISEASE

Following the “amyloid hypothesis” of AD, initiated by the study of Glenner and Wong in 1984, the accumulation of the amyloid- β (A β) peptide is the predominant force of AD-related pathogenesis, including plaques, tangles, synapse loss, and neuronal death (Glenner and Wong, 1984; Tanzi and Bertram, 2005). Although there are still several controversies (Castellani and Smith, 2011; Kozlov et al., 2017), the amyloid hypothesis, supported by many preclinical and clinical studies, has become the primary model of AD pathogenesis and has provided potential therapeutic targets for AD treatments (Selkoe and Hardy, 2016).

The “calcium hypothesis” of AD, which regards the persistent intraneuronal Ca^{2+} dyshomeostasis as one of the early causes of AD, is first proposed by Khachaturian based on limited direct evidence in the 1980s (Khachaturian, 1994; LaFerla, 2002). Growing lines of evidence have emerged to support the calcium hypothesis (Mattson et al., 2000). Ca^{2+} regulates a series of neuronal functions, such as neurotransmitter release and synaptic plasticity; in turn, neurons own precise mechanisms to sustain the Ca^{2+} homeostasis (LaFerla, 2002). For the intraneuronal Ca^{2+} dyshomeostasis to trigger the AD pathology, the Ca^{2+} signal perturbation must be an initial phenotype of AD, and the Ca^{2+} signaling dysregulation can affect the A β accumulation and the tau protein hyperphosphorylation (LaFerla, 2002). Although the former is still controversial (LaFerla, 2002), the latter is well accepted by viable evidence (Mattson, 1990; Mattson et al., 1993).

The relationship between the amyloid hypothesis and other potential hypotheses of AD may not conflict with one theory against another (Selkoe and Hardy, 2016). Moreover, integrating the amyloid hypothesis (Hardy and Selkoe, 2002; Bekris et al., 2010) and the calcium hypothesis (LaFerla, 2002) may further the understanding of Alzheimer's disease pathogenesis. The calcium hypothesis remains compelling, and targeting selective calcium pathways would be a competitive therapeutic approach for AD (LaFerla, 2002).

AMYLOID-B PEPTIDE IS ASSOCIATED WITH CALCIUM DYSHOMEOSTASIS IN ALZHEIMER'S DISEASE

A β Forms Ca^{2+} -Permeable Channel

A β peptides form Ca^{2+} -permeable channels (also known as A β channels) on the plasma membrane and disrupt Ca^{2+}

homeostasis by rapidly elevating intracellular Ca^{2+} concentration, leading to neuronal death in AD (Figure 3) (Arispe et al., 1993; Arispe et al., 1994b). The physical and chemical characteristics of A β peptides enable the formation of the β -sheet and subsequent aggregation into dimers and, even, large oligomers, which form β -barrel structures for the cation-selective permeability, particularly for Ca^{2+} (Figure 3) (Kagan et al., 2002). The nanomole (nM)-level concentrations of A β_{42} can form Ca^{2+} -permeable channels, which elevate $[\text{Ca}^{2+}]_{\text{CYT}}$ levels and rapidly elicit the degeneration of cultured endothelial cells (Bhatia et al., 2000). When incorporating A β_{40} into the artificial bilayer membrane, Ca^{2+} permeates through the opened A β channels (Arispe et al., 1993). The Ca^{2+} influxes through these channels would prevail due to the most significant electrochemical gradient between extracellular Ca^{2+} concentration and $[\text{Ca}^{2+}]_{\text{CYT}}$ (Arispe et al., 1993; Arispe et al., 1994a). For a neuron with a single A β channel in opening state, the corresponding Ca^{2+} influx would increase the $[\text{Ca}^{2+}]_{\text{CYT}}$ level at a rate of 5 μmol per second (5 $\mu\text{M/s}$), exhausting the neuronal Ca^{2+} buffering capacity rapidly, subsequently leading to the neurotoxicity (Arispe et al., 1993; Arispe et al., 1994a).

A β Activates NMDAR

The N-methyl-D-aspartate receptor (NMDAR) is named by its specific agonist, N-methyl-D-aspartate (NMDA), which does not occur naturally. NMDARs belong to one ionotropic family of glutamate receptors located on the plasma membrane. NMDARs can integrate two extracellular chemical stimuli (glycine and glutamate) and one membrane electrical stimulus (the depolarization of the plasma membrane) into the Ca^{2+} signal (Lipton and Rosenberg, 1994; Furukawa et al., 2005). Structurally, NMDARs constitute three families of subunits: glycine-binding NR1, which owns eight isoforms; glutamate-binding NR2, including NR2A, NR2B, NR2C, and NR2D; glycine-binding NR3, including NR3A and NR3B (Cull-Candy and Leszkiewicz, 2004; Furukawa et al., 2005). Functional NMDARs are tetrameric assemblies composed of two copies of NR1/NR2 heterodimers, sometimes NR1/NR3 heterodimers (Chen and Wyllie, 2006). Moreover, identical or diverse NR2 subunits form di-heteromeric assemblies (such as NR1-NR1-NR2A-NR2A, NR1-NR1-NR2B-NR2B) or tri-heteromeric assemblies (such as NR1-NR1-NR2A-NR2B, NR1-NR1-NR2B-NR2D) (Cull-Candy and Leszkiewicz, 2004; Köhr, 2006). Additionally, massive excitatory and inhibitory neurons encode at least two types of NR2 subunits to give rise to di-heteromeric or tri-heteromeric NMDARs in the same neuron (Köhr, 2006). Speculatively, at least 80 kinds of NMDAR subtypes may exist in the central nervous system (Cull-Candy and Leszkiewicz, 2004).

The overstimulation of NMDARs generates massive Ca^{2+} influxes that overexcite neurons, finally leading to neuronal death (a pathological condition also known as excitotoxicity) (Lipton and Rosenberg, 1994; Lynch and Guttman, 2002). The A β accumulation promotes the persistent Ca^{2+} influx through NMDARs, leading to neuronal excitotoxicity at the early stage AD (Figure 3) (Parameshwaran et al., 2008). Furthermore, the monomeric and oligomeric A β_{42} elevate the $[\text{Ca}^{2+}]_{\text{CYT}}$ level by

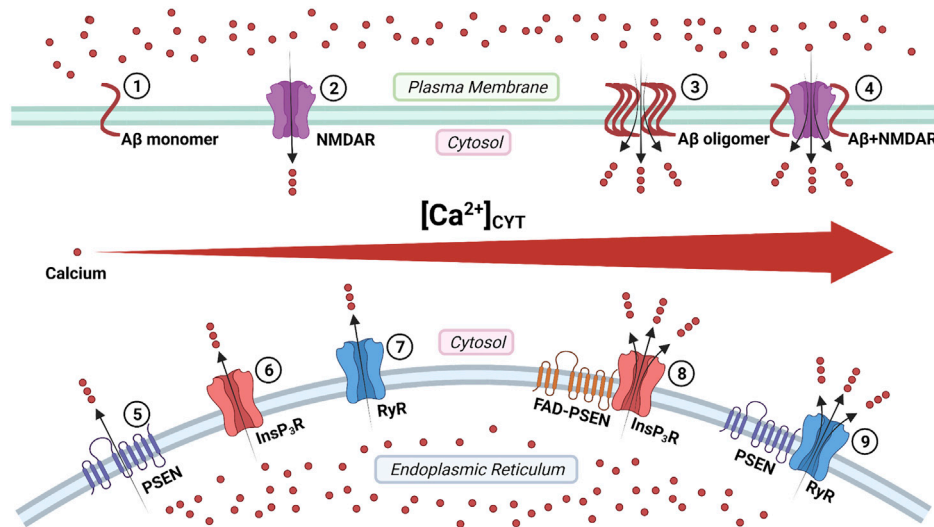


FIGURE 3 | The regulation of calcium signaling by cellular membrane systems: ①③ amyloid- β (A β) peptide monomers aggregate into the oligomer which forms Ca^{2+} -permeable channel; ②④ the A β accumulation promotes the persistent Ca^{2+} signal through the N-methyl-D-aspartate receptor (NMDAR); ⑤ the presenilin (PSEN) holoprotein functions as the endoplasmic reticulum (ER) passive Ca^{2+} leak channel; ⑥⑧ the enhanced Ca^{2+} signal by the familial Alzheimer's disease-causing mutant presenilin (FAD-PSEN) is the inositol 1,4,5-triphosphate receptor (InsP₃R) dependent; ⑦⑨ the interaction between the PSEN and the ryanodine receptor (RyR) regulates the Ca^{2+} signal (Created with [BioRender.com](https://www.biorender.com)).

activating the NR2B subunit of NMDARs in cultured cortical neurons (Ferreira et al., 2012). In turn, prolonged activation of extrasynaptic NMDARs, not synaptic NMDARs, promotes the production of A β in cultured cortical neurons (Lesné et al., 2005; Bordji et al., 2010). It reveals a positive feedback interaction between A β and NMDAR.

NMDAR-Related Mitochondrial Ca^{2+} Uptake

Notably, compared with non-NMDARs or voltage-gated Ca^{2+} channels, NMDAR-related mitochondrial Ca^{2+} uptake is faster and tighter (Peng and Greenamyre, 1998). When neuronal $[\text{Ca}^{2+}]_{\text{CYT}}$ is elevated by NMDARs, the cytosolic Ca^{2+} is segregated by the mitochondrial Ca^{2+} uptake; meanwhile, the mitochondrial Ca^{2+} transient persistently depolarizes the mitochondrial membrane potential ($\Delta\Psi$), causing the opening of the permeability transition pore (PTP) and further depolarizing the $\Delta\Psi$, which parallels with the level of neuronal death (Schinder et al., 1996). Furthermore, under the circumstance in which the $[\text{Ca}^{2+}]_{\text{CYT}}$ elevated vastly, mitochondria divert their function from ATP synthesis to Ca^{2+} accumulation (Lipton and Rosenberg, 1994). Additionally, the lack of ATP synthesis affects Na^+ - K^+ -ATPase activity and results in plasma membrane depolarization, which alleviates the Mg^{2+} block of NMDARs and further activates NMDARs (Greene and Greenamyre, 1996). Mitochondrial Ca^{2+} uptake regulates NMDAR activity under a positive feedback mechanism.

Considering the fundamental role of NMDARs in normal synaptic functions, a complete antagonism of NMDARs generates the majority of side effects, such as severe memory

impairment (Hardingham and Bading, 2010; Mota et al., 2014). Coincidentally, extrasynaptic NMDARs have been largely associated with neuronal excitotoxicity (Hardingham and Bading, 2010), and extrasynaptic NMDARs mainly contain NR2B subunits (Petralia, 2012). Thus, the selective blockage of extrasynaptic NR2B subunits may be a potential strategy to prevent synaptic dysfunction in AD (Mota et al., 2014).

PRESENILINS ARE RELATED TO CALCIUM DYSHOMEOSTASIS IN ALZHEIMER'S DISEASE

PSENs regulate Ca^{2+} signaling, and FAD-causing mutant PSENs perturb Ca^{2+} homeostasis (Leissring et al., 2000; LaFerla, 2002). Spatially, both PSEN1 and PSEN2 are mainly found on the ER membrane (Kovacs et al., 1996) and are widely expressed throughout the central nervous system (Cribbs et al., 1996). A series of FAD-causing mutant PSENs disrupt Ca^{2+} signaling (LaFerla, 2002). PSEN1-deficient neurons also reveal an increased $[\text{Ca}^{2+}]_{\text{CYT}}$ level after exposure to H_2O_2 (Nakajima et al., 2001). Indeed, PSENs do not contain any Ca^{2+} -binding motif, so presenilins may interact with several Ca^{2+} -binding proteins to regulate Ca^{2+} signaling (LaFerla, 2002).

Cleaved Presenilins on the Plasma Membrane Possess γ -secretase Activity

The well-known function of PSENs is to provide the catalytic component of the γ -secretase complex, a membrane-embedded protease for several integral membrane proteins (De Strooper et al., 1998; Wolfe et al., 1999). PSEN has nine transmembrane

domains (TMD) (Laudon et al., 2005). During maturation, PSEN is cleaved into a 30 KDa amino-terminal fragment (NTF) and a 20 KDa carboxy-terminal fragment (CTF) within a cytosol sizeable hydrophilic loop between TMD-6 and TMD-7 by endoproteolysis (Wolfe et al., 1999). Immature (or un-cleaved) presenilin holoproteins are localized on the ER membrane (Annaert et al., 1999). The endoproteolytic cleavage of PSEN holoproteins occurs on the ER membrane (Tandon and Fraser, 2002; Honarnejad and Herms, 2012). The cleaved PSEN (a heterodimer of NTF and CTF), together with anterior pharynx-defective 1 (APH-1), presenilin enhancer 2 (PEN-2), and nicastrin (all are ER transmembrane proteins), form the γ -secretase complex (De Strooper, 2003; Cheung et al., 2010; Honarnejad and Herms, 2012). The γ -secretase complex forms on the ER membrane and subsequently traffics to the Golgi apparatus, finally housed on the plasma membrane to generate A β peptide from APP (De Strooper et al., 2012; Honarnejad and Herms, 2012).

Presenilin Holoproteins on the ER Membrane Function as Ca^{2+} -Leaking Channels

Under the two suppositions that the sarcoplasmic/endoplasmic reticulum Ca^{2+} ATPase (SERCA) acts with 100% efficiency and the $[\text{Ca}^{2+}]_{\text{CYT}}$ level is 0.1 μM , the calculated upper limit value of the $[\text{Ca}^{2+}]_{\text{ER}}$ is 2,400 μM (Tu et al., 2006). In contrast, by directing measurement, the estimated $[\text{Ca}^{2+}]_{\text{ER}}$ level range is from 100 to 500 μM (Hofer, 1999). The leakiness of Ca^{2+} from the ER lumen to cytosol may explain the $[\text{Ca}^{2+}]_{\text{ER}}$ level difference mentioned above (Tu et al., 2006).

Tu and colleagues initially proposed the “presenilin calcium leak channel hypothesis”, in which the un-cleaved PSEN holoprotein functions as an ER passive Ca^{2+} leak channel independently from its γ -secretase activity, based on their sophisticated experiments with PSEN1/PSEN2 double knockout mouse embryonic fibroblasts (DKO-MEFs) (Figure 3) (Tu et al., 2006). The perturbed intracellular Ca^{2+} signaling in DKO-MEFs manifests as the potentiated amplitude of bradykinin-induced Ca^{2+} response, the exaggerated content of ionomycin-sensitive Ca^{2+} pool, and the reduced rate of thapsigargin-induced Ca^{2+} leak, compared with the wild-type control (Tu et al., 2006). Subsequently, in their rescue experiments, the expression of PSEN1_{WT} and PSEN2_{WT} successfully rescue Ca^{2+} signaling abnormalities, but PSEN1_{M146V} and PSEN2_{N141I} do not (Tu et al., 2006). Similarly, in planar lipid bilayers (BLM), the PSEN1_{WT} and PSEN2_{WT} can form a low-conductance divalent-cation-permeable channel, but PSEN1_{M146V} and PSEN2_{N141I} can not (Tu et al., 2006).

Quantitatively, the directly-measured $[\text{Ca}^{2+}]_{\text{ER}}$ level in DKO-MEFs (190 μM) is approximately 2-fold higher than it is in wild-type control (87 μM); moreover, it is calculated that PSENs account for 80% of the ER endogenous Ca^{2+} -leaking ability (Tu et al., 2006). Additionally, PSEN1_{D257A}, a mutation of catalytic aspartate indispensable for γ -secretase activity, forms a channel in BLM and alleviates all Ca^{2+} signaling perturbation in

DKO-MEFs; specifically, PSEN1 _{Δ E9} is a gain-of-function mutation that leads to Ca^{2+} over-leak from ER (Tu et al., 2006), likely contributing to elevated $[\text{Ca}^{2+}]_{\text{CYT}}$ and depleted $[\text{Ca}^{2+}]_{\text{ER}}$ (Bezprozvanny and Mattson, 2008). The presenilin calcium leak channel hypothesis is supported by Bandara and colleagues who investigated the role of PSEN2 in regulating $[\text{Ca}^{2+}]_{\text{ER}}$ using a fluorescence resonance energy transfer (FRET) probe (Bandara et al., 2013). The knockdown of PSEN2 significantly increases the $[\text{Ca}^{2+}]_{\text{ER}}$ level, and the overexpression of PSEN2 decreases the $[\text{Ca}^{2+}]_{\text{ER}}$ level (Bandara et al., 2013).

Adversely, Kasri and colleagues showed opposite conclusions: the increased Ca^{2+} leak from ER and the decreased $[\text{Ca}^{2+}]_{\text{ER}}$ level in the same DKO-MEFs model (Kasri et al., 2006). The presenilin calcium leak channel hypothesis is under suspicion by directly measuring ER Ca^{2+} dynamics (Shilling et al., 2012).

FAD-Causing Mutant Presenilins Increase the Probability of InsP₃R Opening

In 1994, Ito and colleagues first demonstrated that the InsP₃-mediated Ca^{2+} liberation was potentiated in the skin fibroblast from AD patients (later known to harbor the PSEN1_{A246Q} mutation, a FAD-causing mutation) (Ito et al., 1994; LaFerla, 2002). In 1999, Leissring and colleagues found that the InsP₃-mediated Ca^{2+} liberation was enhanced in the *Xenopus oocytes* model, expressing PSEN1_{M146V}, PSEN2_{N141I}, and PSEN2_{M239V}, all of which are FAD-causing mutations (Leissring et al., 1999a; Leissring et al., 1999b). The underlying mechanism is that FAD-causing mutant PSENs (PSEN1_{M146L}, PSEN1_{L166P}, PSEN1_{A246E}, PSEN1_{G384A}, PSEN2_{N141I}) significantly elevate the probability of InsP₃R opening compared with wild-type control (Cheung et al., 2008; Cheung et al., 2010). Interestingly, γ -secretase-eliminated mutant PSENs (PSEN1_{D257A}, PSEN1_{D385A}) also considerably enhance the InsP₃R opening, which indicates that the γ -secretase activity of PSEN is not required for its influence on InsP₃R opening (Cheung et al., 2010). Suppression of InsP₃R1 expression genetically by 50% can normalize the enhanced InsP₃R-mediated Ca^{2+} signaling associated with FAD-causing mutant PSENs (PSEN1_{M146V}) and profoundly decreases both A β accumulation and tau protein hyperphosphorylation in cortical and hippocampal neurons of transgenic mice (Shilling et al., 2014). These lines of evidence support that the enhanced intraneuronal Ca^{2+} signaling by FAD-causing mutant PSENs is InsP₃R dependent, and targeting the InsP₃ signaling pathway could be a potential therapeutic strategy for FAD (Figure 3) (Shilling et al., 2014).

Cytosolic Amino-Terminal Fragment of Presenilins Regulates RyR-Mediated Ca^{2+} Release

Payne and colleagues identified a novel mechanism under which the interaction between the cytosolic amino-terminal fragment of presenilin (PSEN-NTF_{CYT}) and RyR regulates the Ca^{2+} signal from ER (Figure 3) (Payne et al., 2013). Physiological normal Ca^{2+} concentration (10 nM < $[\text{Ca}^{2+}]_{\text{CYT}}$ < 1 μM) and

pathological high Ca^{2+} concentration ($[\text{Ca}^{2+}]_{\text{CYT}} > 10 \mu\text{M}$) are required for the cytosolic amino-terminal fragment residues 1–82 of presenilin-1 (PSEN1-NTF_{CYT1-82}) and the cytosolic amino-terminal fragment residues 1–87 of presenilin-2 (PSEN2-NTF_{CYT1-87}) to bind RyR, respectively (Hayrapetyan et al., 2008; Rybalchenko et al., 2008; Payne et al., 2013). After PSEN1-NTF_{CYT1-82} binding RyR at normal $[\text{Ca}^{2+}]_{\text{CYT}}$, the single RyR opening probability and mean currents are potentiated, causing an increased rate of Ca^{2+} release (Figure 3) (Rybalchenko et al., 2008; Payne et al., 2013). Hence, the whole-neuron net Ca^{2+} release from ER is reduced due to the inhibitory Ca^{2+} concentration being reached in a shorter time (Rybalchenko et al., 2008; Payne et al., 2013). After PSEN2-NTF_{CYT1-87} binding RyR at high $[\text{Ca}^{2+}]_{\text{CYT}}$, the low-affinity inhibitory Ca^{2+} -binding site is blocked, resulting in more elevated $[\text{Ca}^{2+}]_{\text{CYT}}$ is required to close the RyR, which represent a potential feedforward mechanism of Ca^{2+} dysregulation (Hayrapetyan et al., 2008; Payne et al., 2013).

DISCUSSION

For receiving information about the changing environment, cells evolved the ability to signal (Clapham, 2007). Even though the precise definition of the signal is still controversial, it is recently stated that anything that changes could be a signal (Chakravorty, 2018). Ca^{2+} is elegantly manipulated by cells, particularly neurons, as a second messenger (Clapham, 2007). The unequal distribution of ions inside and outside neurons, such as K^+ , Na^+ , and Cl^- , keeps the cellular function by generating the resting membrane potential and holds the neuronal volume by maintaining the osmotic balance (Byrne et al., 2014). It is widely known that the large gradient between extracellular and intracellular Ca^{2+} concentration levels is the most significant among particles with electrical charges. Cells possess numerous molecular machinery to regulate the Ca^{2+} distribution spatially and temporally; simultaneously, numbers of biochemical reactions are controlled by intracellular Ca^{2+} . Therefore, the Ca^{2+} signal can transmit various information throughout the cells, and neurons are no exception (Berridge et al., 2000).

The generation and termination of the Ca^{2+} signal are featured as increasing $[\text{Ca}^{2+}]_{\text{CYT}}$ and decreasing $[\text{Ca}^{2+}]_{\text{CYT}}$, respectively (Miller, 1991). Multiple Ca^{2+} channels exist in the various compartment of neurons to perform separate functions (Berridge et al., 2000). The $[\text{Ca}^{2+}]_{\text{CYT}}$ is changed by extracellular stimuli through directly activating the gated Ca^{2+} channels on the plasma membrane or indirectly triggering the Ca^{2+} -release channels on intracellular Ca^{2+} stores (Takei et al., 1992). In turn, Ca^{2+} , released from ER, can alter transmembrane potential and regulate the excitability of neurons (Berridge, 1998). Spatiotemporally different Ca^{2+} signals modulate a series of neuronal functions, such as neurotransmitter release, post-tetanic potentiation, long-term potentiation (LTP), and long-term depression (LTD) (Purves et al., 2018). For example, large and fast Ca^{2+} signals evoke LTP, and small and slow Ca^{2+} signals trigger LTD (Purves et al., 2018). For neurons under physiological

conditions, $[\text{Ca}^{2+}]_{\text{CYT}}$, $[\text{Ca}^{2+}]_{\text{ER}}$, and $[\text{Ca}^{2+}]_{\text{MT}}$ are at a subtle equilibrium level. Both ER and mitochondria can shape the $[\text{Ca}^{2+}]_{\text{CYT}}$. In addition, the Ca^{2+} in the ER lumen can transmit into the mitochondrial matrix through ERMCS (Wu et al., 2018). Collectively, maintaining the Ca^{2+} homeostasis is vital for neurons.

Dysregulation in Ca^{2+} signaling has been reported in neurodegenerative diseases, such as AD, Parkinson's disease (PD), and Huntington's disease (HD) (Bezprozvanny and Mattson, 2008; Sheng and Cai, 2012; Pchitskaya et al., 2018). The $[\text{Ca}^{2+}]_{\text{ER}}$ is overfilled in AD, whereas depleted in PD and HD (Pchitskaya et al., 2018). In *Caenorhabditis elegans*, mutations in the SEL-12 (the PSEN ortholog) can elevate the $[\text{Ca}^{2+}]_{\text{MT}}$ level, and reducing the Ca^{2+} signal from ER to mitochondria normalizes the $[\text{Ca}^{2+}]_{\text{MT}}$ level and the mitochondrial function (Sarasija et al., 2018). In neurons, mitochondria dysfunction is recognized as a final pathway in neurodegeneration (Friedman et al., 2010; Rizzuto et al., 2012). Area-Gomez and colleagues observed that PSENs are abundant in ERMCS (Area-Gomez et al., 2009), later the same research team demonstrated that mutations in PSEN1, PSEN2, and APP can upregulate the function of ERMCS (Area-Gomez et al., 2012). Moreover, variations in ERMCS likely influence the cellular Ca^{2+} homeostasis (Area-Gomez et al., 2012).

The present review summarizes the intracellular Ca^{2+} signaling regulated by molecular machinery on cellular membrane systems and the Ca^{2+} dyshomeostasis linked to A β and presenilins. Connecting the amyloid hypothesis with the calcium hypothesis may further the understanding of Alzheimer's disease pathogenesis. At ER and mitochondria levels, understanding the regulation of cellular Ca^{2+} signaling and the mechanism underlying neuronal Ca^{2+} dyshomeostasis in AD may provide therapeutic targets for chronic neuronal degeneration disease in the central nervous system.

AUTHOR CONTRIBUTIONS

Z-PJ conceived the project. D-XH, XY, W-JY, X-MZ, CL, H-PL, and YS searched and prepared references. D-XH wrote the manuscript and designed figures.

FUNDING

This work was financially supported by the Natural Science Foundation of Jilin Province (20210101310JC).

ACKNOWLEDGMENTS

Thanks to Dr. Huan-Fa Yi for critical comments and invaluable advice on this manuscript and the Central Laboratory of the First Hospital of Jilin University-the Eastern Division for support. Thanks to the Department of Pathology of the First Hospital of Jilin University-the Eastern Division for supporting this work.

REFERENCES

- Adkins, C. E., and Taylor, C. W. (1999). Lateral Inhibition of Inositol 1,4,5-trisphosphate Receptors by Cytosolic Ca²⁺. *Curr. Biol.* 9 (19), 1115–1118. doi:10.1016/s0960-9822(99)80481-3
- Alzheimer's Association (2016). 2016 Alzheimer's Disease Facts and Figures. *Alzheimer's Dement.* 12 (4), 459–509. doi:10.1016/j.jalz.2016.03.001
- Alzheimer's Association (2020). 2020 Alzheimer's Disease Facts and Figures. *Alzheimers Dement* 16 (3), 391–460. doi:10.1002/alz.12068
- Annaert, W. G., Levesque, L., Craessaerts, K., Dierinck, I., Snellings, G., Westaway, D., et al. (1999). Presenilin 1 Controls γ -Secretase Processing of Amyloid Precursor Protein in Pre-golgi Compartments of Hippocampal Neurons. *J. Cell Biol.* 147 (2), 277–294. doi:10.1083/jcb.147.2.277
- Area-Gomez, E., de Groof, A. J. C., Boldogh, I., Bird, T. D., Gibson, G. E., Koehler, C. M., et al. (2009). Presenilins Are Enriched in Endoplasmic Reticulum Membranes Associated with Mitochondria. *Am. J. Pathol.* 175 (5), 1810–1816. doi:10.2353/ajpath.2009.090219
- Area-Gomez, E., Del Carmen Lara Castillo, M., Tambini, M. D., Guardia-Laguarta, C., de Groof, A. J. C., Madra, M., et al. (2012). Upregulated Function of Mitochondria-Associated ER Membranes in Alzheimer Disease. *Embo j* 31 (21), 4106–4123. doi:10.1038/emboj.2012.202
- Arispe, N., Pollard, H. B., and Rojas, E. (1994b). Beta-Amyloid Ca²⁺-Channel Hypothesis for Neuronal Death in Alzheimer Disease. *Mol. Cell Biochem.* 140 (2), 119–125. doi:10.1007/bf00926750
- Arispe, N., Pollard, H. B., and Rojas, E. (1994a). The Ability of Amyloid β -Protein [A β P (1–40)] to Form Ca²⁺ Channels Provides a Mechanism for Neuronal Death in Alzheimer's Disease. *Ann. N. Y. Acad. Sci.* 747, 256–266. doi:10.1111/j.1749-6632.1994.tb44414.x
- Arispe, N., Rojas, E., and Pollard, H. B. (1993). Alzheimer Disease Amyloid Beta Protein Forms Calcium Channels in Bilayer Membranes: Blockade by Tromethamine and Aluminum. *Proc. Natl. Acad. Sci.* 90 (2), 567–571. doi:10.1073/pnas.90.2.567
- Atri, A. (2019). Current and Future Treatments in Alzheimer's Disease. *Semin. Neurol.* 39 (2), 227–240. doi:10.1055/s-0039-1678581
- Ballard, C., Aarsland, D., Cummings, J., O'Brien, J., Mills, R., Molinuevo, J. L., et al. (2020). Drug Repositioning and Repurposing for Alzheimer Disease. *Nat. Rev. Neurol.* 16 (12), 661–673. doi:10.1038/s41582-020-0397-4
- Bandara, S., Malmersjö, S., and Meyer, T. (2013). Regulators of Calcium Homeostasis Identified by Inference of Kinetic Model Parameters from Live Single Cells Perturbed by siRNA. *Sci. Signal.* 6 (283), ra56. doi:10.1126/scisignal.2003649
- Baughman, J. M., Perocchi, F., Girgis, H. S., Plovnic, M., Belcher-Timme, C. A., Sancak, Y., et al. (2011). Integrative Genomics Identifies MCU as an Essential Component of the Mitochondrial Calcium Uniporter. *Nature* 476 (7360), 341–345. doi:10.1038/nature10234
- Bekris, L. M., Yu, C.-E., Bird, T. D., and Tsuang, D. W. (2010). Review Article: Genetics of Alzheimer Disease. *J. Geriatr. Psychiatry Neurol.* 23 (4), 213–227. doi:10.1177/0891988710383571
- Berridge, M. J., Bootman, M. D., and Lipp, P. (1998). Calcium - a Life and Death Signal. *Nature* 395 (6703), 645–648. doi:10.1038/27094
- Berridge, M. J. (1997). Elementary and Global Aspects of Calcium Signalling. *J. Physiol.* 499 (Pt 2Pt 2), 291–306. doi:10.1113/jphysiol.1997.sp021927
- Berridge, M. J., Lipp, P., and Bootman, M. D. (2000). The Versatility and Universality of Calcium Signalling. *Nat. Rev. Mol. Cell Biol.* 1 (1), 11–21. doi:10.1038/35036035
- Berridge, M. J. (1998). Neuronal Calcium Signaling. *Neuron* 21 (1), 13–26. doi:10.1016/s0896-6273(00)80510-3
- Berridge, M., Lipp, P., and Bootman, M. (1999). Calcium Signalling. *Curr. Biol.* 9 (5), R157–R159. doi:10.1016/s0960-9822(99)80101-8
- Bertram, L., and Tanzi, R. E. (2004). Alzheimer's Disease: One Disorder, Too many Genes? *Hum. Mol. Genet.* 13 Spec No 1, 135R–141R. doi:10.1093/hmg/ddh077
- Bezprozvanny, I., and Mattson, M. P. (2008). Neuronal Calcium Mishandling and the Pathogenesis of Alzheimer's Disease. *Trends Neurosciences* 31 (9), 454–463. doi:10.1016/j.tins.2008.06.005
- Bhatia, R., Lin, H., and Lal, R. (2000). Fresh and Globular Amyloid β Protein (1–42) Induces Rapid Cellular Degeneration: Evidence for A β P Channel-mediated Cellular Toxicity. *FASEB j.* 14 (9), 1233–1243. doi:10.1096/fasebj.14.9.1233
- Boitier, E., Rea, R., and Duchen, M. R. (1999). Mitochondria Exert a Negative Feedback on the Propagation of Intracellular Ca²⁺ Waves in Rat Cortical Astrocytes. *J. Cell Biol.* 145 (4), 795–808. doi:10.1083/jcb.145.4.795
- Bootman, M. D., and Lipp, P. (1999). Calcium Signalling: Ringing Changes to the 'bell-shaped Curve'. *Curr. Biol.* 9 (23), R876–R878. doi:10.1016/s0960-9822(00)80072-x
- Bootman, M., Niggli, E., Berridge, M., and Lipp, P. (1997). Imaging the Hierarchical Ca²⁺ Signalling System in HeLa Cells. *J. Physiol.* 499 (Pt 2), 307–314. doi:10.1113/jphysiol.1997.sp021928
- Bordji, K., Becerril-Ortega, J., Nicole, O., and Buisson, A. (2010). Activation of Extrasynaptic, but Not Synaptic, NMDA Receptors Modifies Amyloid Precursor Protein Expression Pattern and Increases Amyloid- Production. *J. Neurosci.* 30 (47), 15927–15942. doi:10.1523/jneurosci.3021-10.2010
- Broeckhoven, C. V. (1995). Presenilins and Alzheimer Disease. *Nat. Genet.* 11 (3), 230–232. doi:10.1038/ng1195-230
- Byrne, J. H., Heidelberger, R., and Neal Waxham, M. (2014). From Molecules to Networks: An Introduction to Cellular and Molecular Neuroscience. United Kingdom, United States: Academic Press.
- Castellani, R. J., and Smith, M. A. (2011). Compounding Artefacts with Uncertainty, and an Amyloid cascade Hypothesis that Is 'too Big to Fail'. *J. Pathol.* 224 (2), 147–152. doi:10.1002/path.2885
- Chakravorty, P. (2018). What Is a Signal? [Lecture Notes]. *IEEE Signal. Process. Mag.* 35 (5), 175–177. doi:10.1109/MSP.2018.2832195
- Chen, P. E., and Wyllie, D. J. A. (2006). Pharmacological Insights Obtained from Structure-Function Studies of Ionotropic Glutamate Receptors. *Br. J. Pharmacol.* 147 (8), 839–853. doi:10.1038/sj.bjp.0706689
- Cheng, H., Lederer, M. R., Lederer, W. J., and Cannell, M. B. (1996). Calcium sparks and [Ca²⁺]_i Waves in Cardiac Myocytes. *Am. J. Physiology-Cell Physiol.* 270 (1 Pt 1), C148–C159. doi:10.1152/ajpcell.1996.270.1.C148
- Cheung, K.-H., Mei, L., Mak, D.-O. D., Hayashi, I., Iwatsubo, T., Kang, D. E., et al. (2010). Gain-of-Function Enhancement of IP 3 Receptor Modal Gating by Familial Alzheimer's Disease-Linked Presenilin Mutants in Human Cells and Mouse Neurons. *Sci. Signal.* 3 (114), ra22. doi:10.1126/scisignal.2000818
- Cheung, K.-H., Shineman, D., Müller, M., Cárdenas, C., Mei, L., Yang, J., et al. (2008). Mechanism of Ca²⁺ Disruption in Alzheimer's Disease by Presenilin Regulation of InsP3 Receptor Channel Gating. *Neuron* 58 (6), 871–883. doi:10.1016/j.neuron.2008.04.015
- Clapham, D. E. (2007). Calcium Signaling. *Cell* 131 (6), 1047–1058. doi:10.1016/j.cell.2007.11.028
- Cook, D. G., Sung, J. C., Golde, T. E., Felsenstein, K. M., Wojczyk, B. S., Tanzi, R. E., et al. (1996). Expression and Analysis of Presenilin 1 in a Human Neuronal System: Localization in Cell Bodies and Dendrites. *Proc. Natl. Acad. Sci.* 93 (17), 9223–9228. doi:10.1073/pnas.93.17.9223
- Cribbs, D. H., Chen, L. S., Bende, S. M., and LaFerla, F. M. (1996). Widespread Neuronal Expression of the Presenilin-1 Early-Onset Alzheimer's Disease Gene in the Murine Brain. *Am. J. Pathol.* 148 (6), 1797–1806.
- Csorda's, G., Renken, C., Va'rna, P., Walter, L., Weaver, D., Buttle, K. F., et al. (2006). Structural and Functional Features and Significance of the Physical Linkage between ER and Mitochondria. *J. Cell Biol.* 174 (7), 915–921. doi:10.1083/jcb.200604016
- Cull-Candy, S. G., and Leszkiewicz, D. N. (2004). Role of Distinct NMDA Receptor Subtypes at central Synapses. *Sci. STKE* 2004 (255), re16. doi:10.1126/stke.2552004re16
- Cummings, J., Lee, G., Zhong, K., Fonseca, J., and Taghva, K. (2021). Alzheimer's Disease Drug Development Pipeline: 2021. *Alzheimer's Dement. Translational Res. Clin. Interventions* 7 (1), e12179. doi:10.1002/trc2.12179
- De Stefani, D., Bononi, A., Romagnoli, A., Messina, A., De Pinto, V., Pinton, P., et al. (2012). VDAC1 Selectively Transfers Apoptotic Ca²⁺ Signals to Mitochondria. *Cell Death Differ* 19 (2), 267–273. doi:10.1038/cdd.2011.92
- De Stefani, D., Raffaello, A., Teardo, E., Szabó, I., and Rizzuto, R. (2011). A Forty-Kilodalton Protein of the Inner Membrane Is the Mitochondrial Calcium Uniporter. *Nature* 476 (7360), 336–340. doi:10.1038/nature10230
- De Strooper, B. (2003). Aph-1, Pen-2, and Nicastrin with Presenilin Generate an Active γ -Secretase Complex. *Neuron* 38 (1), 9–12. doi:10.1016/s0896-6273(03)00205-8
- De Strooper, B., Iwatsubo, T., and Wolfe, M. S. (2012). Presenilins and -Secretase: Structure, Function, and Role in Alzheimer Disease. *Cold Spring Harbor Perspect. Med.* 2 (1), a006304. doi:10.1101/cshperspect.a006304

- De Strooper, B., Saftig, P., Craessaerts, K., Vanderstichele, H., Guhde, G., Annaert, W., et al. (1998). Deficiency of Presenilin-1 Inhibits the normal Cleavage of Amyloid Precursor Protein. *Nature* 391 (6665), 387–390. doi:10.1038/34910
- Epstein, F. H., Lipton, S. A., and Rosenberg, P. A. (1994). Excitatory Amino Acids as a Final Common Pathway for Neurologic Disorders. *N. Engl. J. Med.* 330 (9), 613–622. doi:10.1056/nejm199403033300907
- Ferreira, I. L., Bajouco, L. M., Mota, S. I., Auberson, Y. P., Oliveira, C. R., and Rego, A. C. (2012). Amyloid Beta Peptide 1-42 Disturbs Intracellular Calcium Homeostasis through Activation of GluN2B-Containing N-Methyl-D-Aspartate Receptors in Cortical Cultures. *Cell Calcium* 51 (2), 95–106. doi:10.1016/j.ceca.2011.11.008
- Friedman, J. R., Webster, B. M., Mastrorade, D. N., Verhey, K. J., and Voeltz, G. K. (2010). ER Sliding Dynamics and ER-Mitochondrial Contacts Occur on Acetylated Microtubules. *J. Cel Biol.* 190 (3), 363–375. doi:10.1083/jcb.200911024
- Furukawa, H., Singh, S. K., Mancusso, R., and Gouaux, E. (2005). Subunit Arrangement and Function in NMDA Receptors. *Nature* 438 (7065), 185–192. doi:10.1038/nature04089
- Galione, A., McDougall, A., Busa, W. B., Willmott, N., Gillot, I., and Whitaker, M. (1993). Redundant Mechanisms of Calcium-Induced Calcium Release Underlying Calcium Waves during Fertilization of Sea Urchin Eggs. *Science* 261 (5119), 348–352. doi:10.1126/science.8392748
- Giorgi, C., De Stefani, D., Bononi, A., Rizzuto, R., and Pinton, P. (2009). Structural and Functional Link between the Mitochondrial Network and the Endoplasmic Reticulum. *Int. J. Biochem. Cel Biol.* 41 (10), 1817–1827. doi:10.1016/j.biocel.2009.04.010
- Glenner, G. G., and Wong, C. W. (1984). Alzheimer's Disease: Initial Report of the Purification and Characterization of a Novel Cerebrovascular Amyloid Protein. *Biochem. Biophysical Res. Commun.* 120 (3), 885–890. doi:10.1016/s0006-291x(84)80190-4
- Greene, J. G., and Greenamyre, J. T. (1996). Manipulation of Membrane Potential Modulates Malonate-Induced Striatal Excitotoxicity *In Vivo*. *J. Neurochem.* 66 (2), 637–643. doi:10.1046/j.1471-4159.1996.66020637.x
- Gunter, K. K., and Gunter, T. E. (1994). Transport of Calcium by Mitochondria. *J. Bioenerg. Biomembr.* 26 (5), 471–485. doi:10.1007/bf00762732
- Györke, I., and Györke, S. (1998). Regulation of the Cardiac Ryanodine Receptor Channel by Luminal Ca²⁺ Involves Luminal Ca²⁺ Sensing Sites. *Biophys. J.* 75 (6), 2801–2810. doi:10.1016/s0006-3495(98)77723-9
- Hajnoczky, G., Hager, R., and Thomas, A. P. (1999). Mitochondria Suppress Local Feedback Activation of Inositol 1,4,5-Trisphosphate Receptors by Ca²⁺. *J. Biol. Chem.* 274 (20), 14157–14162. doi:10.1074/jbc.274.20.14157
- Hardingham, G. E., and Bading, H. (2010). Synaptic versus Extrasynaptic NMDA Receptor Signalling: Implications for Neurodegenerative Disorders. *Nat. Rev. Neurosci.* 11 (10), 682–696. doi:10.1038/nrn2911
- Hardy, J., and Selkoe, D. J. (2002). The Amyloid Hypothesis of Alzheimer's Disease: Progress and Problems on the Road to Therapeutics. *Science* 297 (5580), 353–356. doi:10.1126/science.1072994
- Hayrapetyan, V., Rybalchenko, V., Rybalchenko, N., and Koulen, P. (2008). The N-Terminus of Presenilin-2 Increases Single Channel Activity of Brain Ryanodine Receptors through Direct Protein-Protein Interaction. *Cell Calcium* 44 (5), 507–518. doi:10.1016/j.ceca.2008.03.004
- Heckman-Stoddard, B. M., DeCensi, A., Sahasrabudhe, V. V., and Ford, L. G. (2017). Repurposing Metformin for the Prevention of Cancer and Cancer Recurrence. *Diabetologia* 60 (9), 1639–1647. doi:10.1007/s00125-017-4372-6
- Hofer, A. M. (1999). Measurement of Free [Ca²⁺] Changes in Agonist-Sensitive Internal Stores Using Compartmentalized Fluorescent Indicators. *Methods Mol. Biol.* 114, 249–266. doi:10.1385/1-59259-250-3:249
- Honarnejad, K., and Herms, J. (2012). Presenilins: Role in Calcium Homeostasis. *Int. J. Biochem. Cel Biol.* 44 (11), 1983–1986. doi:10.1016/j.biocel.2012.07.019
- Huang, Y., Zhou, Z., Zhang, J., Hao, Z., He, Y., Wu, Z., et al. (2021). lncRNA MALAT1 Participates in Metformin Inhibiting the Proliferation of Breast Cancer Cell. *J. Cel Mol Med* 25 (15), 7135–7145. doi:10.1111/jcmm.16742
- Ito, E., Oka, K., Etcheberrigaray, R., Nelson, T. J., McPhie, D. L., Tofel-Grehl, B., et al. (1994). Internal Ca²⁺ Mobilization Is Altered in Fibroblasts from Patients with Alzheimer Disease. *Proc. Natl. Acad. Sci.* 91 (2), 534–538. doi:10.1073/pnas.91.2.534
- Kagan, B. L., Hirakura, Y., Azimov, R., Azimova, R., and Lin, M.-C. (2002). The Channel Hypothesis of Alzheimer's Disease: Current Status. *Peptides* 23 (7), 1311–1315. doi:10.1016/s0196-9781(02)00067-0
- Kasri, N. N., Kocks, S. L., Verbert, L., Hébert, S. S., Callewaert, G., Parys, J. B., et al. (2006). Up-regulation of Inositol 1,4,5-trisphosphate Receptor Type 1 Is Responsible for a Decreased Endoplasmic-Reticulum Ca²⁺ Content in Presenilin Double Knock-Out Cells. *Cell Calcium* 40 (1), 41–51. doi:10.1016/j.ceca.2006.03.005
- Khachaturian, Z. S. (1994). Calcium Hypothesis of Alzheimer's Disease and Brain Aging. *Ann. N. Y Acad. Sci.* 747, 1–11. doi:10.1111/j.1749-6632.1994.tb44398.x
- Kirichok, Y., Krapivinsky, G., and Clapham, D. E. (2004). The Mitochondrial Calcium Uniporter Is a Highly Selective Ion Channel. *Nature* 427 (6972), 360–364. doi:10.1038/nature02246
- Köhr, G. (2006). NMDA Receptor Function: Subunit Composition versus Spatial Distribution. *Cell Tissue Res.* 326 (2), 439–446. doi:10.1007/s00441-006-0273-6
- Kovacs, D. M., Fausett, H. J., Page, K. J., Kim, T.-W., Moir, R. D., Merriam, D. E., et al. (1996). Alzheimer-associated Presenilins 1 and 2: Neuronal Expression in Brain and Localization to Intracellular Membranes in Mammalian Cells. *Nat. Med.* 2 (2), 224–229. doi:10.1038/nm0296-224
- Kozlov, S., Afonin, A., Evsyukov, I., and Bondarenko, A. (2017). Alzheimer's Disease: as it Was in the Beginning. *Rev. Neurosci.* 28 (8), 825–843. doi:10.1515/revneuro-2017-0006
- Kumar, A., Singh, A., and Ekavali (2015). A Review on Alzheimer's Disease Pathophysiology and its Management: an Update. *Pharmacol. Rep.* 67 (2), 195–203. doi:10.1016/j.pharep.2014.09.004
- Kuwajima, G., Futatsugi, A., Niinobe, M., Nakanishi, S., and Mikoshiba, K. (1992). Two Types of Ryanodine Receptors in Mouse Brain: Skeletal Muscle Type Exclusively in Purkinje Cells and Cardiac Muscle Type in Various Neurons. *Neuron* 9 (6), 1133–1142. doi:10.1016/0896-6273(92)90071-k
- LaFerla, F. M. (2002). Calcium Dyshomeostasis and Intracellular Signalling in Alzheimer's Disease. *Nat. Rev. Neurosci.* 3 (11), 862–872. doi:10.1038/nrn960
- Laudon, H., Hansson, E. M., Melén, K., Bergman, A., Farmery, M. R., Winblad, B., et al. (2005). A Nine-Transmembrane Domain Topology for Presenilin 1. *J. Biol. Chem.* 280 (42), 35352–35360. doi:10.1074/jbc.M507217200
- Lebiezinska, M., Szabadkai, G., Jones, A. W. E., Duszyński, J., and Wieckowski, M. R. (2009). Interactions between the Endoplasmic Reticulum, Mitochondria, Plasma Membrane and Other Subcellular Organelles. *Int. J. Biochem. Cel Biol.* 41 (10), 1805–1816. doi:10.1016/j.biocel.2009.02.017
- Leissring, M. A., Akbari, Y., Fanger, C. M., Cahalan, M. D., Mattson, M. P., and LaFerla, F. M. (2000). Capacitative Calcium Entry Deficits and Elevated Luminal Calcium Content in Mutant Presenilin-1 Knockin Mice. *J. Cel Biol.* 149 (4), 793–798. doi:10.1083/jcb.149.4.793
- Leissring, M. A., Parker, I., and LaFerla, F. M. (1999a). Presenilin-2 Mutations Modulate Amplitude and Kinetics of Inositol 1,4,5-Trisphosphate-Mediated Calcium Signals. *J. Biol. Chem.* 274 (46), 32535–32538. doi:10.1074/jbc.274.46.32535
- Leissring, M. A., Paul, B. A., Parker, I., Cotman, C. W., and LaFerla, F. M. (1999b). Alzheimer's Presenilin-1 Mutation Potentiates Inositol 1,4,5-Trisphosphate-Mediated Calcium Signaling in *Xenopus*. *J. Neurochem.* 72 (3), 1061–1068. doi:10.1046/j.1471-4159.1999.0721061.x
- Lesne, S., Ali, C., Gabriel, C., Croci, N., MacKenzie, E. T., Glabe, C. G., et al. (2005). NMDA Receptor Activation Inhibits -Secretase and Promotes Neuronal Amyloid- Production. *J. Neurosci.* 25 (41), 9367–9377. doi:10.1523/jneurosci.0849-05.2005
- Levy-Lahad, E., Wijsman, E. M., Nemens, E., Anderson, L., Goddard, K. A. B., Weber, J. L., et al. (1995). A Familial Alzheimer's Disease Locus on Chromosome 1. *Science* 269 (5226), 970–973. doi:10.1126/science.7638621
- Lynch, D. R., and Guttman, R. P. (2002). Excitotoxicity: Perspectives Based on N-Methyl-D-Aspartate Receptor Subtypes. *J. Pharmacol. Exp. Ther.* 300 (3), 717–723. doi:10.1124/jpet.300.3.717
- Madesh, M., and Hajnoczky, G. (2001). VDAC-dependent Permeabilization of the Outer Mitochondrial Membrane by Superoxide Induces Rapid and Massive Cytochrome C Release. *J. Cel Biol.* 155 (6), 1003–1016. doi:10.1083/jcb.200105057
- Martonosi, A. N. (1984). Mechanisms of Ca²⁺ Release from Sarcoplasmic Reticulum of Skeletal Muscle. *Physiol. Rev.* 64 (4), 1240–1320. doi:10.1152/physrev.1984.64.4.1240

- Mattson, M. P. (1990). Antigenic Changes Similar to Those Seen in Neurofibrillary Tangles Are Elicited by Glutamate and Ca^{2+} Influx in Cultured Hippocampal Neurons. *Neuron* 4 (1), 105–117. doi:10.1016/0896-6273(90)90447-n
- Mattson, M. P., LaFerla, F. M., Chan, S. L., Leissring, M. A., Shepel, P. N., and Geiger, J. D. (2000). Calcium Signaling in the ER: its Role in Neuronal Plasticity and Neurodegenerative Disorders. *Trends Neurosciences* 23 (5), 222–229. doi:10.1016/s0166-2236(00)01548-4
- Mattson, M. P., Lovell, M. A., Ehmann, W. D., and Markesbery, W. R. (1993). Comparison of the Effects of Elevated Intracellular Aluminum and Calcium Levels on Neuronal Survival and Tau Immunoreactivity. *Brain Res.* 602 (1), 21–31. doi:10.1016/0006-8993(93)90236-g
- Mendes, C. C. P., Gomes, D. A., Thompson, M., Souto, N. C., Goes, T. S., Goes, A. M., et al. (2005). The Type III Inositol 1,4,5-trisphosphate Receptor Preferentially Transmits Apoptotic Ca^{2+} Signals into Mitochondria. *J. Biol. Chem.* 280 (49), 40892–40900. doi:10.1074/jbc.M506623200
- Miller, R. (1991). The Control of Neuronal Ca^{2+} Homeostasis. *Prog. Neurobiol.* 37 (3), 255–285. doi:10.1016/0301-0082(91)90028-y
- Missiaen, L., De Smedt, H., Parys, J. B., and Casteels, R. (1994). Co-activation of Inositol Trisphosphate-Induced Ca^{2+} Release by Cytosolic Ca^{2+} Is Loading-dependent. *J. Biol. Chem.* 269 (10), 7238–7242. doi:10.1016/s0021-9258(17)37273-3
- Mota, S. I., Ferreira, I. L., and Rego, A. C. (2014). Dysfunctional Synapse in Alzheimer's Disease - A Focus on NMDA Receptors. *Neuropharmacology* 76 A, 16–26. doi:10.1016/j.neuropharm.2013.08.013
- Nakajima, M., Miura, M., Aosaki, T., and Shirasawa, T. (2001). Deficiency of Presenilin-1 Increases Calcium-dependent Vulnerability of Neurons to Oxidative Stress *In Vitro*. *J. Neurochem.* 78 (4), 807–814. doi:10.1046/j.1471-4159.2001.00478.x
- Parameswaran, K., Dhanasekaran, M., and Suppiramaniam, V. (2008). Amyloid Beta Peptides and Glutamatergic Synaptic Dysregulation. *Exp. Neurol.* 210 (1), 7–13. doi:10.1016/j.expneurol.2007.10.008
- Payne, A. J., Gerdes, B. C., Naumchuk, Y., McCalley, A. E., Kaja, S., and Koulen, P. (2013). Presenilins Regulate the Cellular Activity of Ryanodine Receptors Differentially through Isoform-specific N-Terminal Cysteines. *Exp. Neurol.* 250, 143–150. doi:10.1016/j.expneurol.2013.09.001
- Pchitskaya, E., Popugaeva, E., and Bezprozvanny, I. (2018). Calcium Signaling and Molecular Mechanisms Underlying Neurodegenerative Diseases. *Cell Calcium* 70, 87–94. doi:10.1016/j.ceca.2017.06.008
- Peng, T. I., and Greenamyre, J. T. (1998). Privileged Access to Mitochondria of Calcium Influx through N-Methyl-D-Aspartate Receptors. *Mol. Pharmacol.* 53 (6), 974–980.
- Perocchi, F., Gohil, V. M., Girgis, H. S., Bao, X. R., McCombs, J. E., Palmer, A. E., et al. (2010). MICU1 Encodes a Mitochondrial EF Hand Protein Required for Ca^{2+} Uptake. *Nature* 467 (7313), 291–296. doi:10.1038/nature09358
- Petralia, R. S. (2012/2012). Distribution of Extrasynaptic NMDA Receptors on Neurons. *Scientific World J.* 2012, 1–11. doi:10.1100/2012/267120
- Purves, D., Augustine, G. J., Fitzpatrick, D., Hall, W. C., LaMantia, A.-S., Mooney, R. D., et al. (2018). *Neuroscience*. Sunderland, Massachusetts: Oxford University Press.
- Querfurth, H. W., Jiang, J., Geiger, J. D., and Selkoe, D. J. (1997). Caffeine Stimulates Amyloid β -Peptide Release from β -Amyloid Precursor Protein-Transfected HEK293 Cells. *J. Neurochem.* 69 (4), 1580–1591. doi:10.1046/j.1471-4159.1997.69041580.x
- Rapizzi, E., Pinton, P., Szabadkai, G., Wieckowski, M. R., Vandecasteele, G., Baird, G., et al. (2002). Recombinant Expression of the Voltage-dependent Anion Channel Enhances the Transfer of Ca^{2+} Microdomains to Mitochondria. *J. Cell Biol.* 159 (4), 613–624. doi:10.1083/jcb.200205091
- Rizzuto, R., De Stefani, D., Raffaello, A., and Mammucari, C. (2012). Mitochondria as Sensors and Regulators of Calcium Signalling. *Nat. Rev. Mol. Cell Biol.* 13 (9), 566–578. doi:10.1038/nrm3412
- Rizzuto, R., Pinton, P., Carrington, W., Fay, F. S., Fogarty, K. E., Lifshitz, L. M., et al. (1998). Close Contacts with the Endoplasmic Reticulum as Determinants of Mitochondrial Ca^{2+} Responses. *Science* 280 (5370), 1763–1766. doi:10.1126/science.280.5370.1763
- Rybalchenko, V., Hwang, S.-Y., Rybalchenko, N., and Koulen, P. (2008). The Cytosolic N-Terminus of Presenilin-1 Potentiates Mouse Ryanodine Receptor Single Channel Activity. *Int. J. Biochem. Cell Biol.* 40 (1), 84–97. doi:10.1016/j.biocel.2007.06.023
- Sarasija, S., Laboy, J. T., Ashkavand, Z., Bonner, J., Tang, Y., and Norman, K. R. (2018). Presenilin Mutations Deregulate Mitochondrial Ca^{2+} Homeostasis and Metabolic Activity Causing Neurodegeneration in *Caenorhabditis elegans*. *Elife* 7. doi:10.7554/eLife.33052
- Schinder, A. F., Olson, E. C., Spitzer, N. C., and Montal, M. (1996). Mitochondrial Dysfunction Is a Primary Event in Glutamate Neurotoxicity. *J. Neurosci.* 16 (19), 6125–6133. doi:10.1523/jneurosci.16-19-06125.1996
- Selkoe, D. J., and Hardy, J. (2016). The Amyloid Hypothesis of Alzheimer's Disease at 25 Years. *EMBO Mol. Med.* 8 (6), 595–608. doi:10.15252/emmm.201606210
- Selkoe, D. J. (1994). Normal and Abnormal Biology of the Beta-Amyloid Precursor Protein. *Annu. Rev. Neurosci.* 17, 489–517. doi:10.1146/annurev.ne.17.030194.002421
- Seymour-Laurent, K., and Barish, M. (1995). Inositol 1,4,5-trisphosphate and Ryanodine Receptor Distributions and Patterns of Acetylcholine- and Caffeine-Induced Calcium Release in Cultured Mouse Hippocampal Neurons. *J. Neurosci.* 15 (4), 2592–2608. doi:10.1523/jneurosci.15-04-02592.1995
- Sheng, Z.-H., and Cai, Q. (2012). Mitochondrial Transport in Neurons: Impact on Synaptic Homeostasis and Neurodegeneration. *Nat. Rev. Neurosci.* 13 (2), 77–93. doi:10.1038/nrn3156
- Sherrington, R., Rogaev, E. I., Liang, Y., Rogaeva, E. A., Levesque, G., Ikeda, M., et al. (1995). Cloning of a Gene Bearing Missense Mutations in Early-Onset Familial Alzheimer's Disease. *Nature* 375 (6534), 754–760. doi:10.1038/375754a0
- Shilling, D., Mak, D.-O. D., Kang, D. E., and Foskett, J. K. (2012). Lack of Evidence for Presenilins as Endoplasmic Reticulum Ca^{2+} Leak Channels. *J. Biol. Chem.* 287 (14), 10933–10944. doi:10.1074/jbc.M111.300491
- Shilling, D., Muller, M., Takano, H., Daniel Mak, D.-O., Abel, T., Coulter, D. A., et al. (2014). Suppression of InsP3 Receptor-Mediated Ca^{2+} Signaling Alleviates Mutant Presenilin-Linked Familial Alzheimer's Disease Pathogenesis. *J. Neurosci.* 34 (20), 6910–6923. doi:10.1523/jneurosci.5441-13.2014
- Spat, A., Szanda, G., Csordas, G., and Hajnoczky, G. (2008). High- and Low-calcium-dependent Mechanisms of Mitochondrial Calcium Signalling. *Cell Calcium* 44 (1), 51–63. doi:10.1016/j.ceca.2007.11.015
- Stelzmann, R. A., Norman Schnitzlein, H., Reed Murtagh, F., and Murtagh, F. R. (1995). An English translation of alzheimer's 1907 paper, "ber eine eigenartige erkankung der hirnrinde". *Clin. Anat.* 8 (6), 429–431. doi:10.1002/ca.980080612
- Striggo, F., and Ehrlich, B. E. (1996). Ligand-gated Calcium Channels inside and Out. *Curr. Opin. Cell Biol.* 8 (4), 490–495. doi:10.1016/s0955-0674(96)80025-1
- Sun, X.-P., Callamaras, N., Marchant, J. S., and Parker, I. (1998). A Continuum of InsP3-Mediated Elementary Ca^{2+} signalling Events in *Xenopus* oocytes. *J. Physiol.* 509 (Pt 1), 67–80. doi:10.1111/j.1469-7793.1998.067bo.x
- Takei, K., Stukenbrok, H., Metcalf, A., Mignery, G., Sudhof, T., Volpe, P., et al. (1992). Ca^{2+} Stores in Purkinje Neurons: Endoplasmic Reticulum Subcompartments Demonstrated by the Heterogeneous Distribution of the InsP3 Receptor, Ca^{2+} -ATPase, and Calsequestrin. *J. Neurosci.* 12 (2), 489–505. doi:10.1523/jneurosci.12-02-00489.1992
- Tandon, A., and Fraser, P. (2002). The Presenilins. *Genome Biol.* 3 (11), reviews3014.1. doi:10.1186/gb-2002-3-11-reviews3014
- Tang, Y.-g., and Zucker, R. S. (1997). Mitochondrial Involvement in post-tetanic Potentiation of Synaptic Transmission. *Neuron* 18 (3), 483–491. doi:10.1016/s0896-6273(00)81248-9
- Tanzi, R. E., and Bertram, L. (2005). Twenty Years of the Alzheimer's Disease Amyloid Hypothesis: a Genetic Perspective. *Cell* 120 (4), 545–555. doi:10.1016/j.cell.2005.02.008
- Taylor, C. W. (1998). Inositol Trisphosphate Receptors: Ca^{2+} -Modulated Intracellular Ca^{2+} Channels. *Biochim. Biophys. Acta* 1436 (1-2), 19–33. doi:10.1016/s0005-2760(98)00122-2
- Tu, H., Nelson, O., Bezprozvanny, A., Wang, Z., Lee, S.-F., Hao, Y.-H., et al. (2006). Presenilins Form ER Ca^{2+} Leak Channels, a Function Disrupted by Familial Alzheimer's Disease-Linked Mutations. *Cell* 126 (5), 981–993. doi:10.1016/j.cell.2006.06.059
- Walton, P. D., Airey, J. A., Sutko, J. L., Beck, C. F., Mignery, G. A., Südhof, T. C., et al. (1991). Ryanodine and Inositol Trisphosphate Receptors Coexist in Avian Cerebellar Purkinje Neurons. *J. Cell Biol.* 113 (5), 1145–1157. doi:10.1083/jcb.113.5.1145

- Wolfe, M. S., Xia, W., Ostaszewski, B. L., Diehl, T. S., Kimberly, W. T., and Selkoe, D. J. (1999). Two Transmembrane Aspartates in Presenilin-1 Required for Presenilin Endoproteolysis and γ -secretase Activity. *Nature* 398 (6727), 513–517. doi:10.1038/19077
- Wu, H., Carvalho, P., and Voeltz, G. K. (2018). Here, There, and Everywhere: The Importance of ER Membrane Contact Sites. *Science* 361 (6401). doi:10.1126/science.aan5835
- Wu, Y., Whiteus, C., Xu, C. S., Hayworth, K. J., Weinberg, R. J., Hess, H. F., et al. (2017). Contacts between the Endoplasmic Reticulum and Other Membranes in Neurons. *Proc. Natl. Acad. Sci. USA* 114 (24), E4859–e4867. doi:10.1073/pnas.1701078114

Conflict of Interest: The authors declare that the research was conducted in the absence of any commercial or financial relationships that could be construed as a potential conflict of interest.

Publisher's Note: All claims expressed in this article are solely those of the authors and do not necessarily represent those of their affiliated organizations, or those of the publisher, the editors, and the reviewers. Any product that may be evaluated in this article, or claim that may be made by its manufacturer, is not guaranteed or endorsed by the publisher.

Copyright © 2022 Huang, Yu, Yu, Zhang, Liu, Liu, Sun and Jiang. This is an open-access article distributed under the terms of the Creative Commons Attribution License (CC BY). The use, distribution or reproduction in other forums is permitted, provided the original author(s) and the copyright owner(s) are credited and that the original publication in this journal is cited, in accordance with accepted academic practice. No use, distribution or reproduction is permitted which does not comply with these terms.



Intracellular Cholesterol Synthesis and Transport

Qingyang Shi^{1†}, Jiahuan Chen^{2†}, Xiaodong Zou² and Xiaochun Tang^{2,3*}

¹Center of Reproductive Medicine and Center of Prenatal Diagnosis, The First Hospital, Jilin University, Changchun, China,
²Jilin Provincial Key Laboratory of Animal Embryo Engineering, College of Animal Sciences, Jilin University, Changchun, China,
³Chongqing Research Institute of Jilin University, Chongqing, China

Cholesterol homeostasis is related to multiple diseases in humans, including cardiovascular disease, cancer, and neurodegenerative and hepatic diseases. The cholesterol levels in cells are balanced dynamically by uptake, biosynthesis, transport, distribution, esterification, and export. In this review, we focus on *de novo* cholesterol synthesis, cholesterol synthesis regulation, and intracellular cholesterol trafficking. In addition, the progression of lipid transfer proteins (LTPs) at multiple contact sites between organelles is considered.

OPEN ACCESS

Edited by:

Qi Zhao,
University of Science and Technology
Liaoning, China

Reviewed by:

Jie Xu,
University of Michigan, United States
Annette Graham,
Glasgow Caledonian University,
United Kingdom
Cathleen Carlin,
Case Western Reserve University,
United States

*Correspondence:

Xiaochun Tang
xiaochuntang@jlu.edu.cn

[†]These authors have contributed
equally to this work

Specialty section:

This article was submitted to
Signaling,
a section of the journal
Frontiers in Cell and Developmental
Biology

Received: 21 November 2021

Accepted: 01 February 2022

Published: 21 March 2022

Citation:

Shi Q, Chen J, Zou X and Tang X
(2022) Intracellular Cholesterol
Synthesis and Transport.
Front. Cell Dev. Biol. 10:819281.
doi: 10.3389/fcell.2022.819281

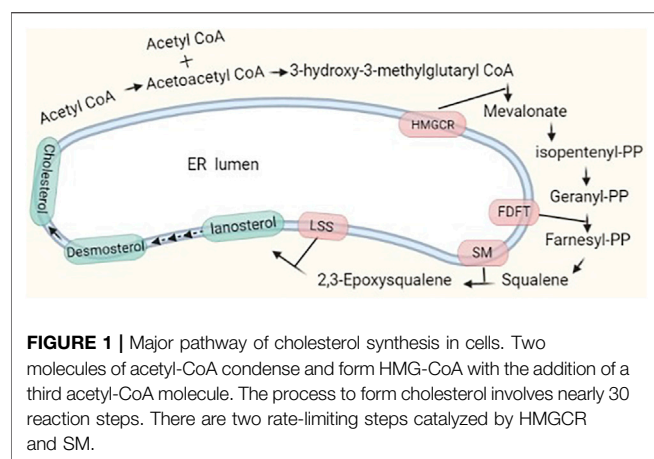
Keywords: cholesterol synthesis, cholesterol trafficking, intracellular, endoplasmic reticulum, sterol regulatory element-binding proteins

INTRODUCTION

The endoplasmic reticulum (ER) produces a number of phospholipids and sterols as well as triglycerides, cholesterol esters, and ceramide. Lipids are exported from the ER to the plasma membrane (PM) and other organelles that lack the ability to synthesize lipids on their own. Despite the extensive transport of lipids and other materials between organelles, these structures exhibit remarkable differences in lipid composition and quantity (Holthuis and Menon, 2014). Cholesterol is an essential component of PMs; it couples with sphingolipid and glycosylphosphatidylinositol (GPI)-anchored proteins to form dynamic and nanoscale domains that are distributed in both inner and outer leaflets of the cell membrane (Lingwood and Simons, 2010; Raghupathy et al., 2015) and participate in the regulation of cellular processes. The proportion of cholesterol compared to that of all lipids in the ER is only 5 mol% but reaches 30–40 mol% in the PM (Van Meer et al., 2008). In this review, we discuss how cholesterol is synthesized in the ER and how the cholesterol is transferred between organelles, especially LTPs, which responsible for bulk transport of cholesterol, and are involved.

Cholesterol Synthesis

Cholesterol levels in cells are regulated dynamically by *de novo* biosynthesis, exogenous uptake, storage, and exportation. Approximately 700–900 mg of cholesterol per day is produced through *de novo* synthesis in humans, while 300–500 mg is taken up from the diet. Approximately 50% of the total synthesized cholesterol comes from the liver. Endogenous and exogenous cholesterol are metabolized into bile acids at approximately 400 mg/day and into steroid hormones at approximately 50 mg/day; the rest is excreted in feces and by the skin (Russell, 1992). The process of cholesterol synthesis is described in the following. In brief, two molecules of acetyl-coenzyme A (CoA) form acetoacetyl-CoA, and the addition of a third molecule to form 3-hydroxy-3-methylglutaryl CoA (HMG-CoA) is catalyzed by HMG-CoA synthase. HMG-CoA is reduced to mevalonate by HMG-CoA reductase, and this reaction is highly regulated at the



transcriptional and posttranslational levels by metabolic intermediates. Mevalonate undergoes extensive phosphorylation and decarboxylation to form isopentenyl pyrophosphate (IPP), and IPP continues to be polymerized to form farnesyl pyrophosphate (FPP) (**Figure 1**). FPP formation is followed by one of three key steps: condensation of two FPP molecules to form squalene, which is processed to cholesterol; combination of a series of condensed IPPs with one molecule of FPP to form a long *trans* polyprenyl derivative, which is a side chain of ubiquinone, and sequential addition of IPP to FPP to form dolichols (Rudney and Sexton, 1986; Russell, 1992). Cholesterol synthesis is completed in the ER membrane, and cholesterol homeostasis is tightly regulated. We briefly review the key players in the regulation of *de novo* cholesterol synthesis.

Regulation of Cholesterol Synthesis

Cholesterol levels are regulated dynamically, and there are three key factors in cholesterol synthesis: sterol regulatory element-binding protein 2 (SREBP2), 3-hydroxy-3-methylglutaryl coenzyme A reductase (HMGCR), and squalene monooxygenase (SM). The regulation occurs in three dimensions: transcriptional, translational, and posttranslational (**Table 1**).

Sterol Regulatory Element-Binding Protein 2

SREBP2 is an isoform of the SREBP transcription factor family and a master regulator of lipid homeostasis that specializes in cholesterol synthesis (Brown and Goldstein, 1997). SREBP2 is synthesized as an inactive precursor that binds to the ER

membrane and is composed of three domains: an N-terminal transactivation domain for DNA binding and dimerization; a hydrophobic transmembrane domain separated by a lumen facing, 30 aa short loop; and a C-terminal regulatory domain responsible for interaction with SREBP cleavage activating protein (SCAP) (Goldstein et al., 2006). To become an active form from a precursor, SREBP2 translocates to the Golgi apparatus from the ER. In the Golgi apparatus, there are two proteases, the site 1 and site 2 proteases (S1P and S2P), that cleave the SREBP2 precursor sequentially to liberate the N-terminus, which enter the nucleus as a homodimer to bind sterol regulatory element (SRE) sequences in the promoter to activate target genes (Brown et al., 2018).

At the transcriptional level, the SREBP2 gene promoter has a 10-bp SRE, 6-bp Sp1 (Sp1 transcription factor), and NF-Y (nuclear transcription factor Y) binding sites, which coincide with other SREBP2-targeted cholesterol synthesis genes. The existence of an SRE binding site means that it is regulated by its activated form nSREBP2 (Sato et al., 1996). SREBP2 transcription is also epigenetically regulated (Tao et al., 2013). There is a FoxO3 (forkhead box O3) binding sequence and insulin response element (IRE) in the promoter. FoxO3 recruits Sirt6 (sirtuin 6), and Sirt6 deacetylates histone H3 and inhibits SREBP2 transcription.

The process of maturation of SREBP2 is triggered by the cholesterol concentration in the ER (**Figure 2**). When the ER cholesterol level is below 5 mol% of all ER lipids, SCAP, an escort of SREBP2, exerts conformational changes to dissociate from insulin-induced gene (Insig)-1, which is complexed with SCAP-SREBP2 in sterol abundance, and binds to COPII coat proteins to transport SREBP2 to the Golgi apparatus *via* vesicles (Nohturfft et al., 2000; Shimano and Sato, 2017). If Insig-1 levels are elevated, the cholesterol concentration that triggers SCAP transport of SREBP2 is lowered to 3 mol% (Radhakrishnan et al., 2008, 2009). After separation with the SCAP-SREBP2 complex under depletion of cholesterol, Insig-1 is ubiquitinated and degraded with a half-life within 30 min (Goldstein et al., 2006). Nuclear SREBP2 targets corresponding genes, including Insig-1, and newly synthesized Insig-1 is degraded continually until the cholesterol level is above 5 mol% in the ER. Stabilized Insig-1 halts the SCAP-SREBP2 complex in the ER membrane, inhibits SREBP2 maturation, and stops cholesterol synthesis. Again, if the ER cholesterol level is below 5 mol% of all ER lipids, feedback regulation is triggered. Insig-2 has similar functions to Insig-1, but it is expressed constitutively at low levels and is not regulated by SREBP2 (Goldstein et al., 2006).

Additional proteins participate in the process of SREBP2 maturation in the ER and Golgi apparatus. Erlins localized to

TABLE 1 | Molecules implicated in SREBP2, HMGCR, and SM regulation.

Regulation	SREBP2	HMGCR	SM
Transcription	Sp1, NF-Y, nSREBP2, FoxO3, SIRT6, SIRT1, MARCH6	SREBP1, nSREBP2, NF-kB, c-Fos, c-Jun, HSP-70, HO-1	NF-1, Sp1, YY1, c-Myc, IRF-1, Mir-133b
Post-translation	Erlins, RNF145, RNF5, TRC8, PCK1, Brg1, POST1, Fbw7, SIRT1, p300, CBP	Gp78, TRC8, RNF145, USP20, UBIAD1	MARCH6, UBE2G2, UBE2J2, Squalene

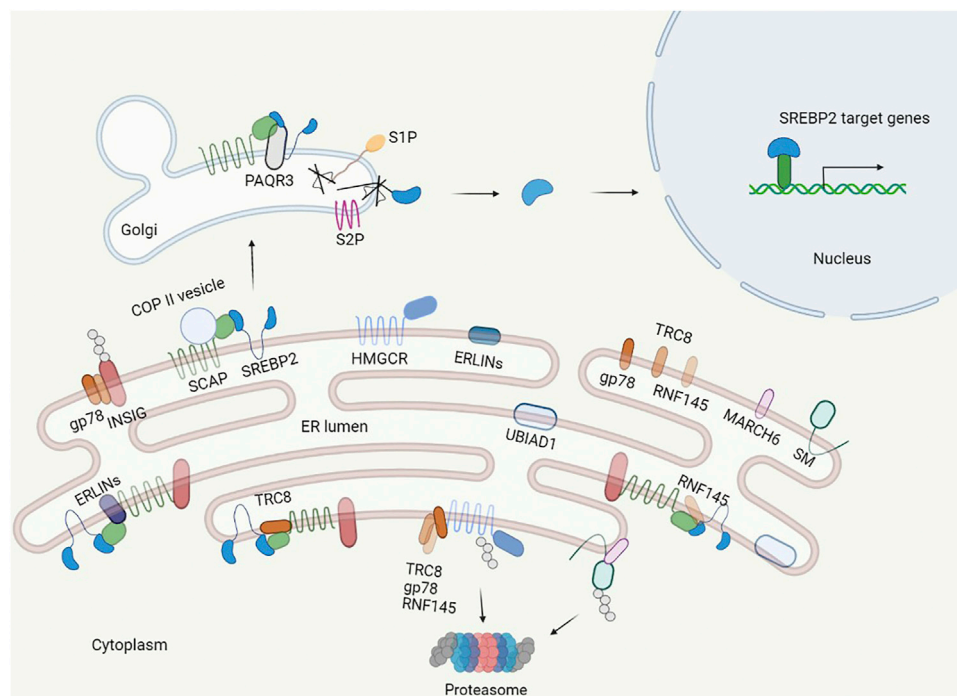


FIGURE 2 | Regulation of cholesterol synthesis. The central transcription factor of cholesterol synthesis in cells is SREBP2, which is regulated in multiple layers and controls the synthesis of key enzymes in cholesterol synthesis. SREBP2 binds to SCAP in the ER. When the cholesterol level is less than 5% of the ER, SCAP binds to the COPII protein and escorts SREBP2 from the ER to the Golgi and anchors via adipoQ receptor 3 (PAQR3) in the Golgi, where site 1 and site 2 proteases (S1P, S2P) cleave the luminal loop of SREBP2 to release the N-terminal domain that enters the nucleus. In the nucleus, SREBP2 activates multiple cholesterol synthesis genes by binding to the SRE. Additionally, the INSIG proteins dissociate from SCAP, and HMGCR and SM are less bound and ubiquitinated by E3 ubiquitin ligase and degraded by the proteasome. When the cholesterol level is more than 5% of the ER, the INSIGs are recruited by SCAP to form the SCAP-SREBP2-INSIG complex, and the complex holds in the ER further by ERLINs and TRC8. Additionally, cholesterol induces the E3 ligase complex to ubiquitinate HMGCR and SM.

the ER lumen with heteromultimeric complexes are cholesterol-binding proteins that interact with Insig-SCAP-SREBP2 to restrict SREBP2 activation in the presence of cholesterol (Huber et al., 2013). RNF145 and RNF5 are ER-anchored E3 ubiquitin ligases; RNF145 ubiquitinates lysine residues of SCAP (K454, K466) and damages binding with COPII protein and Golgi transport (Jiang et al., 2018), and RNF5 binds to the transmembrane domain and ubiquitinates SCAP at K305, regulating the process of SREBP2 maturation (Kuan et al., 2020). TRC8 is also a ubiquitin ligase that binds to the SCAP-SREBP2 complex, and the TRC8-SCAP-SREBP2 complex hinders the interaction of SCAP with COPII proteins independent of its ubiquitin ligase activity (Irisawa et al., 2009). Phosphoenolpyruvate carboxykinase 1 (PCK1), a rate-limiting enzyme in gluconeogenesis, is phosphorylated by AKT in hepatocellular carcinoma (HCC) patients, and phosphorylated PCK1 translocates to the ER and acts as protein kinase to phosphorylates Insig-1 and Insig-2 in the ER (Xu et al., 2020). Phosphorylated Insigs have weak binding ability with sterols and disrupt the SCAP-SREBP2 complex, promoting the translocation of SCAP-SREBP2 to the Golgi from the ER. Although the relationship between phosphorylated PCK1 mediating SREBP2 activation and sterol levels is unknown, more attention needs to be paid to this relationship, especially in nonphysiological conditions. In 2021, Brahma-related gene 1 (Brg1) and partner

of site-1 protease (POST1) were identified as cofactors involved in SREBP2 regulation. Brg1, a chromatin remodeling protein, interacts with Sp1 at the promoter of SCAP, activates the transcription of SCAP, and promotes the maturation of SREBP2 (Kong et al., 2021). On the other hand, Brg1 is recruited to the promoters of cholesterol genes by SREBP2. In turn, Brg1 recruits the H3K9 methyltransferase KDM3A to promote the transcription of related genes, and deficiency of Brg1 in the liver reduces cholesterol levels in mice (Fan et al., 2020). POST1 was discovered by a genome-wide CRISPR/Cas9 knockout screen; it controls S1P maturation, and ablation of POST1 decreases nuclear SREBP2 and the corresponding target gene expression (Xiao et al., 2021).

After maturation, the activated form of nSREBP2 can be phosphorylated by GSK-3 at T426 and S430, the surrounding sequence called phosphodegion. Fbw7, which is a substrate receptor of SCF ubiquitin ligase, interacted with the phosphodegion to degrade it and decrease the expression of SREBP2 target genes (Sundqvist et al., 2005). Simultaneously, p300 and CBP acetylate the N-terminus of SREBP2, is stabilized and enhances the expression of SREBP2 target genes (Giandomenico et al., 2003). Accordingly, the acetylation of SREBP2 by SIRT1 inhibition also increases SREBP2 stability and transcriptional activity. Moreover, SREBP2 can be phosphorylated by ERK, MAPK, AMPK, and mTORC1 and SUMOylated to

regulate stability, transcriptional activity, and trafficking (Arito et al., 2008; Mohamed et al., 2018; Liu et al., 2020).

3-Hydroxy-3-Methylglutaryl Coenzyme A Reductase

HMGCR is a membrane protein located in the ER that contains a transmembrane domain in the N-terminus and a hydrophilic C-terminus facing the cytosol. The cytosol-facing C-terminal domain is responsible for mevalonate formation, and the transmembrane domain includes an SSD, like SCAP, that senses sterol levels in the ER. *HMGCR* transcription is stimulated by nSREBP2, similar to other cholesterol-related genes. To date, HMGCR posttranslational regulation, including ubiquitination and phosphorylation, has been extensively studied.

HMGCR can be ubiquitinated by the intermediates of mevalonate and cholesterol derivatives, such as lanosterol, 24, 25-dihydrolanosterol, and 25- and 27-hydroxycholesterol (Song et al., 2005; Chen et al., 2019). However, cholesterol itself has a minor degradation effect. In addition to the cholesterol pathway, γ - and δ -tocotrienols also mimic sterols but not nonsterol isoprenoids, promoting the degradation of HMGCR (Song and DeBose-Boyd, 2006).

HMGCR ubiquitination and degradation induced by sterol requires Insig binding. The second transmembrane helix of HMGCR contains a YIYF sequence, which also exists in the SSD of SCAP and is responsible for Insig binding and ubiquitination. Mutation of tetrapeptide YIYF abolishes Insig binding of HMGCR, as in SCAP, and destroys sterol-induced endoplasmic reticulum-associated degradation (ERAD) (Jiang et al., 2018). Substitution of lysine 248 with arginine in HMGCR abolishes ubiquitination and delays degradation but does not affect Insig binding (Sever et al., 2003). Another substitution at lysine 89 further delays degradation in the absence of lysine 248 but has little effect on its own. Lysine 248 is near the C-terminal catalytic domain and localizes to the juxtamembrane; this position may facilitate ubiquitin transfer to HMGCR by membrane-bound ubiquitin transferase and subsequent ERAD.

The ubiquitination of HMGCR is mediated by membrane-bound E3 ubiquitin ligase. At least three E3 ligases have been reported to be related to Insigs. Gp78, known as AMFR, is an ER membrane-anchored ubiquitin ligase that mediates HMGCR ubiquitination by interacting with Insigs. When cholesterol is abundant, gp78 is transferred to the HMGCR-Insig complex, causing the ubiquitination of HMGCR and degradation and suppressing cholesterol synthesis; when cholesterol is depleted, HMGCR is free from the Insig-gp78 complex and stabilized, increasing cholesterol synthesis (Jo et al., 2011b; Liu et al., 2012). Another ubiquitin ligase is TRC8, known as RNF139. Insig binding to HMGCR recruits Trc8 to facilitate its ubiquitination. Either gp78 or TRC8 knockdown in cells inhibits sterol-induced degradation by approximately 50%–60%, and combined knockdown of the two E3 ubiquitin ligases inhibits the degradation of HMGCR by up to 90% (Jo et al., 2011a). RNF145 is an E3 ubiquitin ligase that interacts with Insigs to ubiquitinate HMGCR. Knockdown of both RNF145 and gp78 abrogates HMGCR degradation, but RNF145 itself has little effect on HMGCR stability (Menzies et al., 2018). RNF145 also contains

a YIYF sequence in the SSD, which is essential for its binding with Insigs, and in the RING finger domain, the Cys537 residue is responsible for RNF145 activity (Jiang et al., 2018). Why multiple E3 ubiquitin ligases are involved in HMGCR degradation and which ligases are responsible for HMGCR ubiquitination under certain conditions need further investigation. In contrast to ubiquitination, HMGCR is deubiquitinated by mTORC1-phosphorylated USP20, which preferentially hydrolyzes K48 and K63 linkages, and stabilized HMGCR increases cholesterol synthesis in the feeding state (Lu et al., 2020).

After ubiquitination of HMGCR, energy produced from VCP/p97-mediated hydrolysis of ATP powers ubiquitinated HMGCR extraction from the ER membrane (Stevenson et al., 2016). The extracted HMGCR is transferred to the cytosol from the ER membrane by the 19S regulatory subunit of the proteasome. Subsequently, it is delivered to the proteolytic core of the 20S proteasome for degradation. Both VCP and the 19S regulatory subunit have AAA + ATPase activity (Meyer et al., 2012). The extraction process is enhanced by geranylgeraniol, which is a derivative of isoprenoid geranylgeranyl pyrophosphate (GGpp). In the presence of a substrate of GGpp, UBIAD1, which binds with HMGCR and blocks its membrane extraction, is transported to the Golgi and removes the inhibition of HMGCR degradation. UBIAD1 is a membrane prenyltransferase that can catalyze the transfer of isoprenyl groups to aromatic acceptors and produce ubiquinones, hemes, chlorophylls, vitamin E, and vitamin K. UBIAD1 knockout in mice is embryonic lethal, and the phenotype can be rescued by knocking in HMGCR, which is a resistant mutant (Schumacher et al., 2015; Jo et al., 2020). Therefore, HMGCR levels can be regulated with nonsterol mevalonate pathway products.

Another posttranslational regulation of HMGCR is phosphorylation. The Ser872 residue in the C-terminal catalytic domain of HMGCR is phosphorylated by AMPK, and phosphorylation at Ser872 disrupts HMGCR activity and restricts the flux of the mevalonate pathway rapidly but does not affect sterol-induced ubiquitination and subsequent degradation (Clarke and Hardie, 1990).

Squalene Monooxygenase

SM catalyzes the first oxygenation step in cholesterol synthesis; it introduces an epoxide group to squalene, converts alkene squalene into squalene epoxide, and is proposed to be a rate-limiting step in cholesterol synthesis.

There are three SREs in the SM promoter: two adjacent SREs near the initiation site that partially respond to sterol via SREBP2 and a third SRE that is sterol independent. Other transcriptional cofactors and factors, including NF-Y, Sp1, YY1, c-Myc, and IRF-1, participate in the regulation of SM transcription (Chua et al., 2020). Mir-133b is reported to promote SM mRNA degradation (Qin et al., 2017).

The focus of SM regulation, similar to that of HMGCR, is posttranslational. SM can be ubiquitinated and degraded under cholesterol abundance. The phenomenon of cholesterol-induced squalene accumulation suggests that SM, similar to HMGCR, is another flux-controlling enzyme (Gill et al., 2011).

The N-terminal 100 residues of SM contain a cholesterol-sensitive amphipathic helix and a reentrant loop; the

amphipathic helix binds membranes with absent cholesterol, the affinity is reduced upon cholesterol addition, and the released helix forms a disordered sequence (Chua et al., 2017; Prinz, 2017). MARCH6, an E3 ligase that physically interacts with conformationally changed SM (Zelcer et al., 2014), combines with two E2 enzymes, UBE2G2 and UBE2J2, for ubiquitination and subsequent degradation in the presence of cholesterol. In contrast to cholesterol-induced SM degradation, the accumulated substrate squalene binds to the N-terminal 100 residues of SM, altering the recognition of MARCH6, and stabilizing SM on the ER membrane (Yoshioka et al., 2020). In addition to ubiquitination, MARCH6 can regulate SREBP2 at the transcriptional level; thus, HMGCR and SM are controlled. During ERAD, SM is truncated by N-terminal degradation, which results in defects in sterol sensing. Truncated SM has similar abundance and is constitutively active. The distinction of SM and truncated SM function needs further investigation in detail.

Intracellular Cholesterol Transport

Cholesterol is distributed unevenly in cellular membranes. The PM is the membrane most enriched with cholesterol and accounts for approximately 30–40 mol% of total cholesterol in cells; cholesterol is also abundant in the endocytic recycling compartment and *trans*-Golgi facing side (Lange, 1991; Pomorski et al., 2001; Ikonen, 2008). The ER, mitochondria, and lysosomes are characterized by small amounts of cholesterol (Maxfield and Wüstner, 2002). To achieve compositional heterogeneity, cholesterol needs to be transported in cells in a dedicated manner.

The synthesized cholesterol in the ER is transported to organelles immediately, and this cholesterol transport is primarily coupled with the transport and metabolism of phosphoinositide, phosphatidylserine (PtdSer), and sphingolipids (Holthuis and Menon, 2014). Cholesterol trafficking is mediated by vesicular and nonvesicular trafficking systems (Prinz, 2010; Luo et al., 2019). Vesicular transport plays an important role in the response to trafficking of proteins in extracellular and endocytic pathways, and along with protein transport, cholesterol can traffic between organelles in the secretory pathway continuously (Holthuis and Menon, 2014). However, a number of lines of evidence support that there is an alternative nonvesicular transport response for rapid and bulk cholesterol exchanges in the secretory pathway that do not receive vesicular trafficking.

The nonvesicular transport system includes cholesterol traveling spontaneously between membranes at a low rate of desorption and movement, horizontal movement in continuous membranes, and movement in two leaflets of the membranes. *In vitro* investigations have demonstrated that the spontaneous exchange of cholesterol is related to aqueous-phase solubility and membrane curvature. Cholesterol exchanges rapidly from donors of small vesicles that have higher membrane curvature than large vesicles (Lev, 2010). However, cholesterol interacts with sphingolipid and GPI-anchored proteins to form condensed complexes in the bilayer, and the nanostructure decreases the desorption of cholesterol from membranes. Lipid transfer proteins (LTPs) have been identified to accelerate the transport of lipids, including cholesterol (Wong et al., 2019).

The contacts of the ER with the PM, mitochondria, endosomes, peroxisomes, Golgi, and lipid droplets are mediated by membrane contact sites (MCSs), which are membrane microdomains formed between two organelles close to each other (~10–30 nm) (Wang and Dehesh, 2018; Martello et al., 2020). Many LTPs are localized to MCSs and undergo conformational changes from open bridges to closed tubes to facilitate the transfer of lipids (Figure 3). To date, at least 27 protein families have been found in lipid trafficking.

Regulation of Cholesterol Transport From the Endoplasmic Reticulum

Most newly synthesized cholesterol is transported to the *trans*-Golgi network (TGN), which is a sorting site for lipids, to maintain a low concentration in the ER. Oxysterol-binding protein (OSBP), a bridge between the ER and Golgi membranes, and has been observed to mediate cholesterol transfer. OSBP contains three conserved domains: the N-terminal pH domain, the central FFAT motif, and the C-terminal OSBP-related domain (ORD), which recognize PI(4)P and small GTPase ADP-ribosylation factor (Arf1) in the Golgi, target the VAP-A protein in the ER, and bind sterols, respectively. The architecture of OSBP supports cholesterol export (Antonny et al., 2018). In detail, first, the membranes are tethered between Golgi and ER by the pH domain and FFAT motif of OSBP; second, sterols that bind to the ORD are transferred to the Golgi; third, at the Golgi, the ORD of OSBP transfers PI(4)P, which is synthesized by phosphatidylinositol 4-kinase (PI4K) III β , back to the ER; and fourth, PI(4)P is dephosphorylated to PI *via* Sac1, which is an ER-localized phosphatase. The low ratio of PI(4)P to sterols in the ER makes the phosphorylation and dephosphorylation cycle move continuously to fuel cholesterol export. The exchange between cholesterol in the ER and PI(4)P in the Golgi is maintained by PI4KIII β and Sac1 (Antonny et al., 2018). Intriguingly, Sac1 also acts in *trans* on 4-phosphatase on PI(4)P in a manner mediated by FAPP1 when the concentration of PI(4)P is elevated in the TGN (Venditti et al., 2019). The two modes of Sac1 activity may coexist in cells such that when the concentration of PI(4)P reaches a threshold, the *trans*-phosphatase activity of Sac1 is enhanced and coordinated with the *cis* phosphatase activity to lower PI(4)P levels in the TGN. Moreover, the *cis* activity of Sac1 is required for contact sites between the PM and the ER or the late endosomes (LEs) and the ER (Del Bel and Brill, 2018). A recent study found that in cholesterol-fed cells, the ER-anchored cholesterol escort SCAP interacts with the VAP-OSBP complex *via* Sac1. Deletion of SCAP inhibits PI(4)P transport and carriers of the Golgi network to the cell surface (CARTS) (Wakana et al., 2021). Whether cholesterol perturbation causes disruption of the cycle between PI(4)P and cholesterol is unclear.

Mitochondria are important organelles in cells that can synthesize phosphatidylglycerol, cardiolipin, and phosphatidylethanolamine but must import phosphatidylcholine, phosphatidylinositol, PtdSer, and sterols from other organelles to maintain normal function (Flis and Daum, 2013; Horvath and Daum, 2013). The

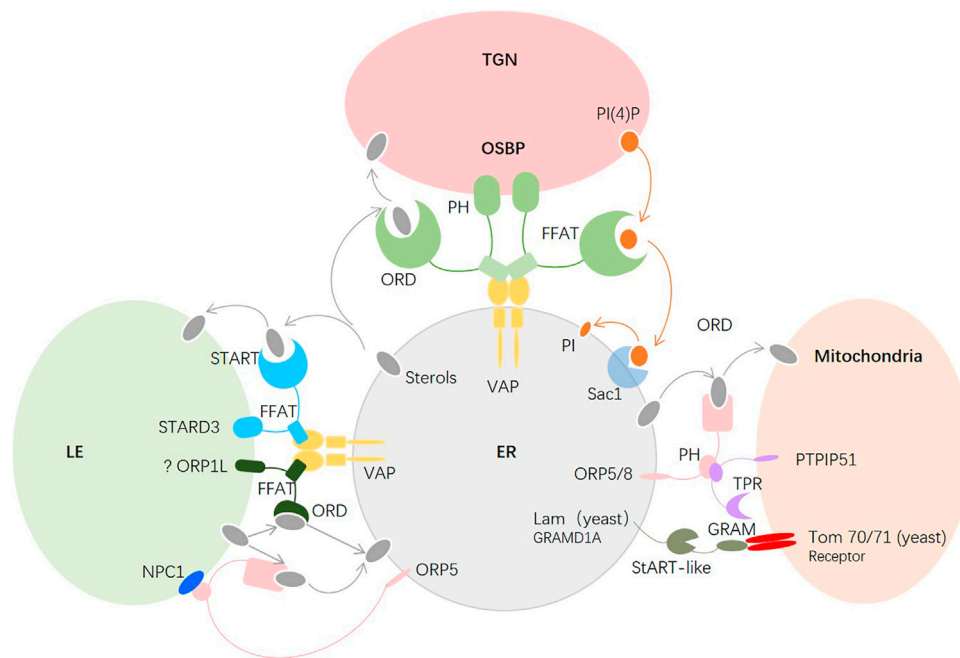


FIGURE 3 | Major molecules in intracellular cholesterol transport. Between the ER and the TGN, OSBP bridges the two membranes, sterols of the ER that bind to the ORD are transferred to the TGN, and the ORD of OSBP transfers PI(4)P of the TGN back to the ER. Between the ER and the mitochondria, ORP5/ORP8 of the ER and PTPIP51 of the mitochondria tether the two organelles at the MAM, and the ORD of ORP5/8 transfers the sterols of the ER to the mitochondria. In yeast, Lam6p located in the ER facilitates the sterol transfer by interacting with Tom70/71 in the OMM. The conserved mammalian ortholog of Lam6p is GRAMD1A, which is proposed to interact with the receptor of the mitochondria to transfer sterols.

inner mitochondrial membrane (IMM) has abundant proteins and only 20% lipids, while the outer mitochondrial membrane (OMM) is lipid rich in mammalian cells. The ER and mitochondria are physically connected at the mitochondria-associated membrane (MAM). Most cholesterol transfer from the ER to mitochondria takes place on the MCSs of MAMs (Giordano, 2018). There are three families of LTPs conserved in yeast and mammals as tethers, lipid sensors, or transporters at the MCSs between the ER and mitochondria. The first is the ORP family; specifically, ORP5 and ORP8 interact with tyrosine phosphatase-interacting protein 51 (PTPIP51) at the MCSs and mediate ER-mitochondrial contact as well as at the PM-ER to facilitate sterol transport in mammalian cells (Chung et al., 2015; Galmes et al., 2016). The second is the START family, which is responsible for cholesterol transport from the OMM to the IMM under hormonal stimulation, after which the cholesterol in the IMM is transformed into pregnenolone for production of steroids or bile acid in hepatic cells (Elustondo et al., 2017). The third is the LAM-GRAM family, which was recently discovered in yeast and includes Lam6 and Lct1, which are ER-anchored proteins located in the ER-mitochondria MCSs that bind with the mitochondrial import receptors Tom70 and Tom71 in yeast (Murley et al., 2015). The conserved orthologs in mammals are GRAMD1A and GRAMD1C, which are involved in lipid transfer in the PM (Naito et al., 2019; Ercan et al., 2021; Ikonen and Zhou, 2021), but their localization and function remain to be elucidated. Thus, we know little about cholesterol transfer at the ER-mitochondria MCSs in mammals at present. The discovery of new sterol transfer molecules will further

illustrate the important roles of cholesterol and MCSs in mitochondria.

Endosomes also have abundant contact sites with the ER, and cholesterol is transferred from the ER to late endosomes (LEs) and lysosomes (LYs) via MCSs in cells. StAR-related lipid transfer protein 3 (STARD3), also known as MLN64, contains a conserved FFAT-like motif that interacts with VAPs in the ER membrane, mediates MCS formation between the ER and LE and transfers newly synthesized cholesterol from the ER to endosomes via a sterol-binding domain (Wilhelm et al., 2016). Similar to another sterol transfer protein, ORP1L, which responds to cholesterol transfer from endosomes to the ER, STARD3 binds VAP to form a tether between the ER and endosome (Ridgway and Zhao, 2018). Whether these proteins compete with each other for VAP binding and how the major molecule that binds with VAP is regulated needs further investigation.

Regulation of Cholesterol Transport From Late Endosomes/Lysosomes

Cholesteryl esters (CEs) carried by low-density lipoprotein (LDL) are absorbed by LDL receptors (LDLRs) at the membrane and hydrolyzed by acid lipase in LEs. The released free cholesterol is transferred to other organelles: ER, PM, mitochondria, TGN, and peroxisomes. This transfer of cholesterol from LEs/LYs is also mediated by sterol transfer proteins (STPs) at MCSs. ORP1L and ORP5 respond to cholesterol transfer from LEs/LYs to the ER (Ridgway and Zhao, 2018). Additionally, ORP5 is responsible for the cycling of PS in the ER and PI(4)P in the PM to maintain the low

level of PI(4,5)P₂ in the PM (Ghai et al., 2017). During the movement of cholesterol from LEs/LYs to mitochondria, STARD3 also plays an important role by accepting NPC2-bound LDL-C to directly bypass NPC1 and transfer the LDL-C to the mitochondrial membrane *in vitro* (Charman et al., 2010). Peroxisomes, as sites of lipid metabolism, play an important role in the cholesterol trafficking pathway. Synaptotagmin VII (Syt7) of lysosomes and PI(4, 5)P₂ of peroxisomes is located at MCSs that form between the two organelles. Either Syt7 or PI(4, 5)P₂ is essential to the formation of the MCSs and to cholesterol export from LYs (Chu et al., 2015). Syt7 has been reported to be a potential oncogenic target and to be involved in synaptic transmission as a calcium sensor (Turecek et al., 2017; Fu et al., 2021). Thus, further side effects need to be studied intensively when targeting Syt7 to cure disease.

DISCUSSION

Cholesterol is an essential lipid that serves as a precursor of steroid hormones, bile acids, and oxysterols in special mammalian tissues. Disturbed cholesterol homeostasis in humans is related to cardiovascular disease, cancer, neurodegenerative disease, and congenital disease. Thus, the *de novo* synthesis of cholesterol in cells and regulation, coordination between intracellular syntheses, import of exogenous cholesterol, biological distribution in organelles, transport of cholesterol in and out of cells, trafficking of intracellular cholesterol, and how to coordinate all the above processes precisely need to be researched continuously.

Because of the central role of SREBP2 in cholesterol homeostasis, numerous dysregulations of the gene in certain disease phenotypes are connected to cholesterol homeostasis. Some investigations have revealed that SREBP2 can function independently in addition to regulating cholesterol synthesis. For example, in circulating melanoma cells, SREBP2 contributes to ferroptosis resistance by inducing transcription of the ion carrier transferrin (TF) (Hong et al., 2021); in coronary artery endothelial cells, high-mobility group box 1 (HMGB1) attenuates LDL transcytosis by inhibiting SREBP2 (Ghaffari et al., 2021); and in idiopathic pulmonary fibrosis (IPF) patients, SREBP2 is markedly increased, and overexpressed SREBP2 in endothelial cells (ECs) enhances the TGF and Wnt pathways and mesenchymal genes *in vitro* and exacerbates vascular remodeling *in vivo* (Martin et al., 2021). Therefore, SREBP2, as a transcription factor, not only plays a key role in cholesterol homeostasis but also exerts multifunctional effects in pathophysiology. The additional functions and related mechanisms need further investigation.

The newly synthesized cholesterol and the released free cholesterol hydrolyzed from endocytosis LDL-C need to be distributed rapidly to maintain the normal functions of cells. Although more LTPs are identified and closely connect with MCSs in membranes, the detailed mechanisms by which they facilitate cholesterol transfer, and whether they have other pathophysiological roles and can be inhibited as drug targets, are still not well known.

For example, the well-known function of STARD3 is to tether the ER and endosome and facilitate cholesterol transfer from the ER to the endosome. Recent findings indicate that high STARD3 levels are associated with worse overall survival (OS), relapse-free survival

(RFS), and disease metastasis-free survival (MFS). STARD3 expression is associated with HER2+ breast cancers (BCs); thus, STARD3 has the potential to be a diagnostic and predictive marker of HER2+ BC (Asif et al., 2021). Moreover, increased STARD1 expression is found in Alzheimer's disease (AD) and Down syndrome (DS), and AD and DS patients exhibit lysosomal cholesterol accumulation within hippocampal astrocytes (Arenas et al., 2020). Thus, STARD1 could be a preclinical marker of AD at early stages. In alcoholic liver disease (ALD), STARD1 not only acts as a sterol transporter but also serves as a UPR and ER stress gene, which is stimulated by alcohol and facilitates ALD development (Marí et al., 2014). Moreover, STARD1 is expressed in many extra-adrenal and extra-gonadal organs, cells, and malignancies, including brain, eye, liver, vasculature, macrophages, heart, lung, skin cells, and so on. In liver, STARD1 involved in bile acid formation *via* the "alternative acidic" pathway, in which the translocated cholesterol in IMM is catalyzed into oxysterols, including 27,24,25-hydroxycholesterol, activated liver X receptors (LXRs) to facilitate bile acid production (Anuka et al., 2013). In addition, in macrophages, STARD1 also facilitated the cholesterol efflux by activate LXRs (Taylor et al., 2010; Manna et al., 2015). The functions of STARD1 in extra-endocrine tissues need more attention in future research.

The functional ORD of ORP5 interacts with mTOR1 and participates in cancer cell invasion and tumor progression. ORP5 depletion impairs mTOR localization to lysosomes, abolishes mTORC1 activity, and inhibits cell proliferation in HeLa cells (Du et al., 2018). The oncogenic gene KRAS is anchored on PM to maintain biological activity. The C-terminal of KRAS binds with specificity to PtdSer in the PM. Both ORP5 and ORP8 are responsible for exchanging PtdSer in the ER and phosphatidyl-4-phosphate in the PM. Depletion of ORP5 or ORP8 reduces PtdSer in the PM, causes KRAS mislocalization *in vitro*, and attenuates KRAS signaling *in vivo*; in addition, it reduces cell proliferation of KRAS-dependent cancer cells (Kattan et al., 2019).

GRAMD1A, which facilitates lipid transfer between the mitochondria and the ER, similar to ORP5, promotes HCC self-renewal, tumor growth, and resistance to chemotherapy. The effects of GRAMD1A are mediated by STAT5 (Fu et al., 2016). In addition, during autophagosome biogenesis, GRAMD1A is bound by autogamins on its StART domain, causing accumulation of GRAMD1A at the sites of autophagosome initiation (Laraia et al., 2019).

As indicated for the above-mentioned molecules, although alterations in both cholesterol and its related genes are observed in certain pathological conditions simultaneously, the exact functions of the molecules aside from cholesterol regulation need to be further investigated.

The most extensive application of lipid-lowering drugs in the clinic is antiatherogenic to reduce the morbidity and mortality of cardiovascular disease. Targets in the clinical and preclinical stages include HMGCR, proprotein convertase subtilisin/kexin type 9 (PCSK9), apolipoprotein B (Apo B), apolipoprotein C-III (Apo CIII), angiopoietin-like 3 (ANGPTL3), lipoprotein(a) (LPA), and Niemann-Pick C1-Like 1 (NPC1L1) (Table 2); among these, only statins for HMGCR inhibition are in the cholesterol synthesis pathway, while the others are associated with the assembly, transport and absorption of low-density lipoprotein cholesterol (LDL-C), and the inhibition of triglyceride synthesis.

TABLE 2 | Targets in lipid homeostasis for cardiovascular disease

Target	Full name	Mechanisms
HMGCR inhibitor: Statins	3-hydroxy-3-methylglutaryl coenzyme A reductase (HMGCR)	Reduces cholesterol synthesis
NPC1L1 inhibitor: Ezetimibe	Niemann–Pick C1-like 1 (NPC1L1)	Reduces intestinal absorption
PPAR α agonist: Fibrates pemafibrate	Peroxisome proliferator activated receptor α (PPAR α)	Reduces triglyceride in Liver
Bile acid sequestering agents	Bile acids	Reduce acids reabsorption and cholesterol levels
PCSK9 inhibitor antibodies/ASOs	Proprotein convertase Subtilisin/Kexin type 9 (PCSK9)	Reduces LDLR and LDL-C endocytosis
Apo B inhibitor Mipomersen (ASO)	Apolipoprotein B (ApoB)	Inhibits Apo B synthesis, LDL-C assembly
ACLY inhibitor: Bempedoic acid SB-204990 ETC-1002	ATP-citrate lyase (ACLY)	Inhibits ACLY caused decrease Acetyl-CoA and inhibit cholesterol synthesis
MTP inhibitor: Lomitapide	Microsomal triglyceride transfer protein (MTP)	Reduces Apo B-containing lipoproteins
Apo A inhibitor: AMG 890 AKCEA-APO(a)-LRx (ASO) IONIS-APO(a) Rx (ASO)	Apolipoprotein(a) (Apo A)/lipoprotein(a) [Lp(a)]	Reduces Lp(a) levels
CETP inhibitor: Evacetrapib anacetrapib	Cholesteryl ester transfer protein (CETP)	Increases HDL level and decrease LDL-C level
Apo C-III inhibitor Volanesorsen (ASO) ISIS 304801 (ASO)	Apolipoprotein C-III (Apo C-III)	Decrease triglyceride levels
Apolipoprotein A-I mimetic peptides: 4F	Apolipoprotein A-I (Apo A-I)	Increases HDLs
ANGPTL3 inhibitor: BE-Angptl3 Gln135 (gene editing) IONIS-ANGPTL3-LRx (ASO) Evinacumab	Angiopoietin like-3 (ANGPTL3)	Increase lipoprotein lipase (LPL) and EL activity
ANGPTL4 inhibitor 14D12	Angiopoietin like-4 (ANGPTL4)	Increases LPL activity

Aside from cardiovascular disease, increasing evidence indicates that dysregulation of cholesterol homeostasis or some related genes correlates with cancers (Kopecka et al., 2020), neurodegenerative disease (Dai et al., 2021), fibrosis (Ioannou, 2016), and viral infection (Koçar et al., 2021). For example, cholesterol- and lipid-mediated innate immune memory induces COVID-19-related cytokine storms (Sohrabi et al., 2021), and decreased cholesterol synthesis of invariant natural killer T cells reduces IFN- γ production in the tumor microenvironment (Fu et al., 2020). In AD, AD brains retain significantly more cholesterol than age-matched nondementia control (ND) brains; the APP acts as a lipid-sensing peptide on cholesterol and forms MAMs in the ER, causing extracellular cholesterol internalization in the ER (Montesinos et al., 2020). In addition to the antiatherogenic drugs approved by the Food and Drug Administration (FDA), several molecules in the mevalonate pathway have emerged as promising drug targets for cancer and AD. For example, *SC4MOL* and *NSDHL* inactivation sensitizes tumor cells to EGFR inhibitors (Sukhanova et al., 2013), and *DHCR24* heterozygous knockout in mice reduces cholesterol levels without causing health problems (Horvat et al., 2011). Therefore, further genetic screening of drug targets in the mevalonate pathway and cholesterol homeostasis for cancers and neurodegenerative disease therapy or prevention are essential. Targeting the mevalonate pathway or cholesterol homeostasis combined with medicine used in the clinic may benefit disease therapy.

In recent years, additional traditional Chinese medicines have been observed to have cholesterol-lowering effects, including aloe-

emodin (Su et al., 2020), apigenin (Wu et al., 2021b), Dingxin recipe IV (Zhang et al., 2021), and ZeXie decoction (Wu et al., 2021a). The mechanisms of some of these medicines involve SREBP2 transcription and maturation processes. Therefore, it is worth testing additional traditional Chinese medicines based on the present medicinal knowledge.

Along with the increasing understanding of cholesterol homeostasis, more regulator molecules have been identified to be involved in pathological conditions. Targeting of related molecules has been demonstrated to ameliorate certain symptoms; however, more research is needed to assess the side effects. Aside from cholesterol itself, intermediates of the mevalonate pathway, lipid transfer proteins, and metabolites of cholesterol all warrant further research.

AUTHOR CONTRIBUTIONS

QS and JC wrote the manuscript. XZ drew the Figures and edited the review. XT provided thoughts and corrected the review. All authors contributed to the article and approved the submitted manuscript.

ACKNOWLEDGMENTS

We acknowledge the support of Jilin Province science and technology development plan (20200703007ZP).

REFERENCES

- Antonny, B., Bigay, J., and Mesmin, B. (2018). The Oxysterol-Binding Protein Cycle: Burning off PI(4)P to Transport Cholesterol. *Annu. Rev. Biochem.* 87, 809–837. doi:10.1146/annurev-biochem-061516-044924
- Anuka, E., Gal, M., Stocco, D. M., and Orly, J. (2013). Expression and Roles of Steroidogenic Acute Regulatory (StAR) Protein in 'non-Classical', Extra-

- adrenal and Extra-gonadal Cells and Tissues. *Mol. Cell Endocrinol.* 371, 47–61. doi:10.1016/j.mce.2013.02.003
- Arenas, F., Castro, F., Nuñez, S., Gay, G., Garcia-Ruiz, C., and Fernandez-Checa, J. C. (2020). STARD1 and NPC1 Expression as Pathological Markers Associated with Astroglialosis in post-mortem Brains from Patients with Alzheimer's Disease and Down Syndrome. *Aging* 12, 571–592. doi:10.18632/aging.102641
- Arito, M., Horiba, T., Hachimura, S., Inoue, J., and Sato, R. (2008). Growth Factor-Induced Phosphorylation of Sterol Regulatory Element-Binding Proteins

- Inhibits Sumoylation, Thereby Stimulating the Expression of Their Target Genes, Low Density Lipoprotein Uptake, and Lipid Synthesis. *J. Biol. Chem.* 283, 15224–15231. doi:10.1074/jbc.M800910200
- Asif, K., Memeo, L., Palazzolo, S., Frión-Herrera, Y., Parisi, S., Caligiuri, I., et al. (2021). Stard3: A Prospective Target for Cancer Therapy. *Cancers* 13, 4693. doi:10.3390/cancers13184693
- Brown, M. S., and Goldstein, J. L. (1997). The SREBP Pathway: Regulation of Cholesterol Metabolism by Proteolysis of a Membrane-Bound Transcription Factor. *Cell* 89, 331–340. doi:10.1016/S0092-8674(00)80213-5
- Brown, M. S., Radhakrishnan, A., and Goldstein, J. L. (2018). Retrospective on Cholesterol Homeostasis: The Central Role of Scap. *Annu. Rev. Biochem.* 87, 783–807. doi:10.1146/annurev-biochem-062917-011852
- Charman, M., Kennedy, B. E., Osborne, N., and Karten, B. (2010). MLN64 Mediates Egress of Cholesterol from Endosomes to Mitochondria in the Absence of Functional Niemann-Pick Type C1 Protein. *J. Lipid Res.* 51, 1023–1034. doi:10.1194/jlr.M002345
- Chen, L., Ma, M.-Y., Sun, M., Jiang, L.-Y., Zhao, X.-T., Fang, X.-X., et al. (2019). Endogenous Sterol Intermediates of the Mevalonate Pathway Regulate HMGCR Degradation and SREBP-2 Processing. *J. Lipid Res.* 60, 1765–1775. doi:10.1194/jlr.RA119000201
- Chu, B.-B., Liao, Y.-C., Qi, W., Xie, C., Du, X., Wang, J., et al. (2015). Cholesterol Transport through Lysosome-Peroxisome Membrane Contacts. *Cell* 161, 291–306. doi:10.1016/j.cell.2015.02.019
- Chua, N. K., Coates, H. W., and Brown, A. J. (2020). Squalene Monooxygenase: a Journey to the Heart of Cholesterol Synthesis. *Prog. Lipid Res.* 79, 101033. doi:10.1016/j.plipres.2020.101033
- Chua, N. K., Howe, V., Jatana, N., Thukral, L., and Brown, A. J. (2017). A Conserved Degron Containing an Amphipathic helix Regulates the Cholesterol-Mediated Turnover of Human Squalene Monooxygenase, a Rate-Limiting Enzyme in Cholesterol Synthesis. *J. Biol. Chem.* 292, 19959–19973. doi:10.1074/jbc.M117.794230
- Chung, J., Torta, F., Masai, K., Lucast, L., Czapl, H., Tanner, L. B., et al. (2015). PI4P/ phosphatidylserine Countertransport at ORP5- and ORP8-Mediated ER-Plasma Membrane Contacts. *Science* 349, 428–432. doi:10.1126/science.aab1370
- Clarke, P. R., and Hardie, D. G. (1990). Regulation of HMG-CoA Reductase: Identification of the Site Phosphorylated by the AMP-Activated Protein Kinase *In Vitro* and in Intact Rat Liver. *EMBO J.* 9, 2439–2446. doi:10.1002/j.1460-2075.1990.tb07420.x
- Dai, L., Zou, L., Meng, L., Qiang, G., Yan, M., and Zhang, Z. (2021). Cholesterol Metabolism in Neurodegenerative Diseases: Molecular Mechanisms and Therapeutic Targets. *Mol. Neurobiol.* 58, 2183–2201. doi:10.1007/s12035-020-02232-6
- Del Bel, L. M., and Brill, J. A. (2018). Sac1, a Lipid Phosphatase at the Interface of Vesicular and Nonvesicular Transport. *Traffic* 19, 301–318. doi:10.1111/tra.12554
- Du, X., Zadoorian, A., Lukmantara, I. E., Qi, Y., Brown, A. J., and Yang, H. (2018). Oxysterol-binding Protein-Related Protein 5 (ORP5) Promotes Cell Proliferation by Activation of mTORC1 Signaling. *J. Biol. Chem.* 293, 3806–3818. doi:10.1074/jbc.RA117.001558
- Elustondo, P., Martin, L. A., and Karten, B. (2017). Mitochondrial Cholesterol Import. *Biochim. Biophys. Acta (Bba) - Mol. Cell Biol. Lipids* 1862, 90–101. doi:10.1016/j.bbalip.2016.08.012
- Ercan, B., Naito, T., Koh, D. H. Z., Dharmawan, D., Saheki, Y., and Dharmawan, D. (2021). Molecular Basis of Accessible Plasma Membrane Cholesterol Recognition by the GRAM Domain of GRAMD1b. *EMBO J.* 40, 1–26. doi:10.15252/embj.2020106524
- Fan, Z., Kong, M., Li, M., Hong, W., Fan, X., and Xu, Y. (2020). Brahma Related Gene 1 (Brg1) Regulates Cellular Cholesterol Synthesis by Acting as a Co-factor for SREBP2. *Front. Cell Dev. Biol.* 8, 1–14. doi:10.3389/fcell.2020.00259
- Flis, V. V., and Daum, G. (2013). Lipid Transport between the Endoplasmic Reticulum and Mitochondria. *Cold Spring Harbor Perspect. Biol.* 5, a013235. doi:10.1101/cshperspect.a013235
- Fu, B., Meng, W., Zhao, H., Zhang, B., Tang, H., Zou, Y., et al. (2016). GRAM Domain-Containing Protein 1A (GRAMD1A) Promotes the Expansion of Hepatocellular Carcinoma Stem Cell and Hepatocellular Carcinoma Growth through STAT5. *Sci. Rep.* 6, 1–10. doi:10.1038/srep31963
- Fu, S., He, K., Tian, C., Sun, H., Zhu, C., Bai, S., et al. (2020). Impaired Lipid Biosynthesis Hinders Anti-tumor Efficacy of Intratumoral iNKT Cells. *Nat. Commun.* 11, 1–15. doi:10.1038/s41467-020-14332-x
- Fu, Y., Tian, G., Zhang, Z., and Yang, X. (2021). SYT7 Acts as an Oncogene and a Potential Therapeutic Target and Was Regulated by ΔNp63α in HNSCC. *Cancer Cell Int* 21, 1–14. doi:10.1186/s12935-021-02394-w
- Galmes, R., Houcine, A., Vliet, A. R., Agostinis, P., Jackson, C. L., and Giordano, F. (2016). ORP5/ORP8 Localize to Endoplasmic Reticulum-Mitochondria Contacts and Are Involved in Mitochondrial Function. *EMBO Rep.* 17, 800–810. doi:10.15252/embr.201541108
- Ghaffari, S., Jang, E., Nabi, F. N., Sanwal, R., Khosraviani, N., Wang, C., et al. (2021). Endothelial HMGB1 Is a Critical Regulator of LDL Transcytosis via an SREBP2-SR-BI Axis. *Atvb* 41, 200–216. doi:10.1161/ATVBAHA.120.314557
- Ghai, R., Du, X., Wang, H., Dong, J., Ferguson, C., Brown, A. J., et al. (2017). ORP5 and ORP8 Bind Phosphatidylinositol-4, 5-bisphosphate (PtdIns(4,5)P₂) and Regulate its Level at the Plasma Membrane. *Nat. Commun.* 8, 1. doi:10.1038/s41467-017-00861-5
- Giandomenico, V., Simonsson, M., Grönroos, E., and Ericsson, J. (2003). Coactivator-Dependent Acetylation Stabilizes Members of the SREBP Family of Transcription Factors. *Mol. Cell. Biol.* 23, 2587–2599. doi:10.1128/mcb.23.7.2587-2599.2003
- Gill, S., Stevenson, J., Kristiana, I., and Brown, A. J. (2011). Cholesterol-dependent Degradation of Squalene Monooxygenase, a Control point in Cholesterol Synthesis beyond HMG-CoA Reductase. *Cell Metab.* 13, 260–273. doi:10.1016/j.cmet.2011.01.015
- Giordano, F. (2018). Non-vesicular Lipid Trafficking at the Endoplasmic Reticulum-Mitochondria Interface. *Biochem. Soc. Trans.* 46, 437–452. doi:10.1042/BST20160185
- Goldstein, J. L., DeBose-Boyd, R. A., and Brown, M. S. (2006). Protein Sensors for Membrane Sterols. *Cell* 124, 35–46. doi:10.1016/j.cell.2005.12.022
- Holthuis, J. C. M., and Menon, A. K. (2014). Lipid Landscapes and Pipelines in Membrane Homeostasis. *Nature* 510, 48–57. doi:10.1038/nature13474
- Hong, X., Roh, W., Sullivan, R. J., Wong, K. H. K., Wittner, B. S., Guo, H., et al. (2021). The Lipogenic Regulator Srebp2 Induces Transferrin in Circulating Melanoma Cells and Suppresses Ferroptosis. *Cancer Discov.* 11, 678–695. doi:10.1158/2159-8290.CD-19-1500
- Horvat, S., McWhir, J., and Rozman, D. (2011). Defects in Cholesterol Synthesis Genes in Mouse and in Humans: Lessons for Drug Development and Safer Treatments. *Drug Metab. Rev.* 43, 69–90. doi:10.3109/03602532.2010.540580
- Horvath, S. E., and Daum, G. (2013). Lipids of Mitochondria. *Prog. Lipid Res.* 52, 590–614. doi:10.1016/j.plipres.2013.07.002
- Huber, M. D., Vesely, P. W., Datta, K., and Gerace, L. (2013). Erlins Restrict SREBP Activation in the ER and Regulate Cellular Cholesterol Homeostasis. *J. Cell Biol.* 203, 427–436. doi:10.1083/jcb.201305076
- Ikonen, E. (2008). Cellular Cholesterol Trafficking and Compartmentalization. *Nat. Rev. Mol. Cell Biol.* 9, 125–138. doi:10.1038/nrm2336
- Ikonen, E., and Zhou, X. (2021). Cholesterol Transport between Cellular Membranes: A Balancing Act between Interconnected Lipid Fluxes. *Dev. Cell* 56, 1430–1436. doi:10.1016/j.devcel.2021.04.025
- Ioannou, G. N. (2016). The Role of Cholesterol in the Pathogenesis of NASH. *Trends Endocrinol. Metab.* 27, 84–95. doi:10.1016/j.tem.2015.11.008
- Irisawa, M., Inoue, J., Ozawa, N., Mori, K., and Sato, R. (2009). The Sterol-Sensing Endoplasmic Reticulum (ER) Membrane Protein TRC8 Hampers ER to Golgi Transport of Sterol Regulatory Element-Binding Protein-2 (SREBP-2)/SREBP Cleavage-Activated Protein and Reduces SREBP-2 Cleavage. *J. Biol. Chem.* 284, 28995–29004. doi:10.1074/jbc.M109.041376
- Jiang, L.-Y., Jiang, W., Tian, N., Xiong, Y.-N., Liu, J., Wei, J., et al. (2018). Ring finger Protein 145 (RNF145) Is a Ubiquitin Ligase for Sterol-Induced Degradation of HMG-CoA Reductase. *J. Biol. Chem.* 293, 4047–4055. doi:10.1074/jbc.RA117.001260
- Jo, Y., Kim, S. S., Garland, K., Fuentes, I., Dicarlo, L. M., Ellis, J. L., et al. (2020). Enhanced ER-Associated Degradation of Hmg Coa Reductase Causes Embryonic Lethality Associated with Ubiad1 Deficiency. *Elife* 9, 1–18. doi:10.7554/eLife.54841
- Jo, Y., Lee, P. C. W., Sguigna, P. V., and DeBose-Boyd, R. A. (2011a). Sterol-induced Degradation of HMG CoA Reductase Depends on Interplay of Two Insigns and Two Ubiquitin Ligases, Gp78 and Trc8. *Proc. Natl. Acad. Sci.* 108, 20503–20508. doi:10.1073/pnas.1112831108
- Jo, Y., Sguigna, P. V., and DeBose-Boyd, R. A. (2011b). Membrane-associated Ubiquitin Ligase Complex Containing Gp78 Mediates Sterol-Accelerated Degradation of 3-Hydroxy-3-Methylglutaryl-Coenzyme A Reductase. *J. Biol. Chem.* 286, 15022–15031. doi:10.1074/jbc.M110.211326

- Kattan, W. E., Chen, W., Ma, X., Lan, T. H., Van Der Hoeven, D., Van Der Hoeven, R., et al. (2019). Targeting Plasma Membrane Phosphatidylserine Content to Inhibit Oncogenic KRAS Function. *Life Sci. Alliance* 2, e201900431–12. doi:10.26508/lsa.201900431
- Kočar, E., Režen, T., and Rozman, D. (2021). Cholesterol, Lipoproteins, and COVID-19: Basic Concepts and Clinical Applications. *Biochim. Biophys. Acta (Bba) - Mol. Cell Biol. Lipids* 1866, 158849. doi:10.1016/j.bbalip.2020.158849
- Kong, M., Zhu, Y., Shao, J., Fan, Z., and Xu, Y. (2021). The Chromatin Remodeling Protein BRG1 Regulates SREBP Maturation by Activating SCAP Transcription in Hepatocytes. *Front. Cell Dev. Biol.* 9, 1–13. doi:10.3389/fcell.2021.622866
- Kopecka, J., Trouillas, P., Gašparović, A. Č., Gazzano, E., Assaraf, Y. G., and Riganti, C. (2020). Phospholipids and Cholesterol: Inducers of Cancer Multidrug Resistance and Therapeutic Targets. *Drug Resist. Updates* 49, 100670. doi:10.1016/j.drug.2019.100670
- Kuan, Y.-C., Takahashi, Y., Maruyama, T., Shimizu, M., Yamauchi, Y., Sato, R., et al. (2020). Ring finger Protein 5 Activates Sterol Regulatory Element-Binding Protein 2 (SREBP2) to Promote Cholesterol Biosynthesis via Inducing Polyubiquitination of SREBP Chaperone SCAP. *J. Biol. Chem.* 295, 3918–3928. doi:10.1074/jbc.RA119.011849
- Lange, Y. (1991). Disposition of Intracellular Cholesterol in Human Fibroblasts. *J. Lipid Res.* 32, 329–339. doi:10.1016/S0022-2275(20)42093-0
- Laraia, L., Friese, A., Corkery, D. P., Konstantinidis, G., Erwin, N., Hofer, W., et al. (2019). The Cholesterol Transfer Protein GRAMD1A Regulates Autophagosome Biogenesis. *Nat. Chem. Biol.* 15, 710–720. doi:10.1038/s41589-019-0307-5
- Lev, S. (2010). Non-vesicular Lipid Transport by Lipid-Transfer Proteins and beyond. *Nat. Rev. Mol. Cell Biol.* 11, 739–750. doi:10.1038/nrm2971
- Lingwood, D., and Simons, K. (2010). Lipid Rafts as a Membrane-Organizing Principle. *Science* 327, 46–50. doi:10.1126/science.1174621
- Liu, S., Gao, Y., Zhang, L., Yin, Y., and Zhang, W. (2020). Rsp1/Rsp3-LGR4 Signaling Inhibits Hepatic Cholesterol Synthesis through the AMPK α -SREBP2 Pathway. *FASEB J.* 34, 14946–14959. doi:10.1096/fj.202001234R
- Liu, T.-F., Tang, J.-J., Li, P.-S., Shen, Y., Li, J.-G., Miao, H.-H., et al. (2012). Ablation of Gp78 in Liver Improves Hyperlipidemia and Insulin Resistance by Inhibiting SREBP to Decrease Lipid Biosynthesis. *Cell Metab.* 16, 213–225. doi:10.1016/j.cmet.2012.06.014
- Lu, X.-Y., Shi, X.-J., Hu, A., Wang, J.-Q., Ding, Y., Jiang, W., et al. (2020). Feeding Induces Cholesterol Biosynthesis via the mTORC1-USP20-HMGCR axis. *Nature* 588, 479–484. doi:10.1038/s41586-020-2928-y
- Luo, J., Jiang, L.-Y., Yang, H., and Song, B.-L. (2019). Intracellular Cholesterol Transport by Sterol Transfer Proteins at Membrane Contact Sites. *Trends Biochem. Sci.* 44, 273–292. doi:10.1016/j.tibs.2018.10.001
- Manna, P. R., Sennoune, S. R., Martinez-Zaguilan, R., Slominski, A. T., and Pruitt, K. (2015). Regulation of Retinoid Mediated Cholesterol Efflux Involves Liver X Receptor Activation in Mouse Macrophages. *Biochem. Biophysical Res. Commun.* 464, 312–317. doi:10.1016/j.bbrc.2015.06.150
- Mari, M., Morales, A., Colell, A., García-Ruiz, C., and Fernández-Checa, J. C. (2014). Mitochondrial Cholesterol Accumulation in Alcoholic Liver Disease: Role of ASMase and Endoplasmic Reticulum Stress. *Redox Biol.* 3, 100–108. doi:10.1016/j.redox.2014.09.005
- Martello, A., Platt, F. M., and Eden, E. R. (2020). Staying in Touch with the Endocytic Network: The Importance of Contacts for Cholesterol Transport. *Traffic* 21, 354–363. doi:10.1111/tra.12726
- Martin, M., Zhang, J., Miao, Y., He, M., Kang, J., Huang, H.-Y., et al. (2021). Role of Endothelial Cells in Pulmonary Fibrosis via SREBP2 Activation. *JCI Insight* 6, 1. doi:10.1172/jci.insight.125635
- Maxfield, F. R., and Wüstner, D. (2002). Intracellular Cholesterol Transport. *J. Clin. Invest.* 110, 891–898. doi:10.1172/JCI0216500
- Menzies, S. A., Volkmar, N., van den Boomen, D. J., Timms, R. T., Dickson, A. S., Nathan, J. A., et al. (2018). The Sterol-Responsive RNF145 E3 Ubiquitin Ligase Mediates the Degradation of HMG-CoA Reductase Together with Gp78 and Hrd1. *Elife* 7, 1–30. doi:10.7554/eLife.40009
- Meyer, H., Bug, M., and Bremer, S. (2012). Emerging Functions of the VCP/p97 AAA-ATPase in the Ubiquitin System. *Nat. Cell Biol.* 14, 117–123. doi:10.1038/ncb2407
- Mohamed, A., Viveiros, A., Williams, K., and Posse de Chaves, E. (2018). A β Inhibits SREBP-2 Activation through Akt Inhibition. *J. Lipid Res.* 59, 1–13. doi:10.1194/jlr.M076703
- Montesinos, J., Pera, M., Larrea, D., Guardia-Laguarta, C., Agrawal, R. R., Velasco, K. R., et al. (2020). The Alzheimer's Disease-associated C99 Fragment of APP Regulates Cellular Cholesterol Trafficking. *EMBO J.* 39, 1–16. doi:10.15252/embj.2019103791
- Murley, A., Sarsam, R. D., Toulmay, A., Yamada, J., Prinz, W. A., and Nunnari, J. (2015). Itc1 Is an ER-Localized Sterol Transporter and a Component of ER-Mitochondria and ER-Vacuole Contacts. *J. Cell Biol.* 209, 539–548. doi:10.1083/jcb.201502033
- Naito, T., Ercan, B., Krshnan, L., Triebl, A., Koh, D. H. Z., Wei, F.-Y., et al. (2019). Movement of Accessible Plasma Membrane Cholesterol by the GRAMD1 Lipid Transfer Protein Complex. *Elife* 8, 1–42. doi:10.7554/eLife.51401
- Nohturfft, A., Yabe, D., Goldstein, J. L., Brown, M. S., and Espenshade, P. J. (2000). Regulated Step in Cholesterol Feedback Localized to Budding of SCAP from ER Membranes. *Cell* 102, 315–323. doi:10.1016/S0092-8674(00)00037-4
- Pomorski, T., Hrafnisdóttir, S., Devaux, P. F., and Meer, G. v. (2001). Lipid Distribution and Transport across Cellular Membranes. *Semin. Cell Dev. Biol.* 12, 139–148. doi:10.1006/scdb.2000.0231
- Prinz, W. A. (2017). A Cholesterol-Sensing Mechanism Unfolds. *J. Biol. Chem.* 292, 19974–19975. doi:10.1074/jbc.H117.74230
- Prinz, W. A. (2010). Lipid Trafficking Sans Vesicles: where, Why, How? *Cell* 143, 870–874. doi:10.1016/j.cell.2010.11.031
- Qin, Y., Zhang, Y., Tang, Q., Jin, L., and Chen, Y. a. (2017). SQLE Induces Epithelial-To-Mesenchymal Transition by Regulating of MIR-133b in Esophageal Squamous Cell Carcinoma. *Acta Biochim. Biophys. Sin* 49, 138–148. doi:10.1093/abbs/gmw127
- Radhakrishnan, A., Goldstein, J. L., McDonald, J. G., and Brown, M. S. (2009). Switch-like Control of SREBP-2 Transport Triggered by Small Changes in ER Cholesterol: a Delicate Balance. *Cell Metab.* 8, 512–521. doi:10.1016/j.cmet.2008.10.008.Switch-like
- Radhakrishnan, A., Goldstein, J. L., McDonald, J. G., and Brown, M. S. (2008). Switch-like Control of SREBP-2 Transport Triggered by Small Changes in ER Cholesterol: A Delicate Balance. *Cell Metab.* 8, 512–521. doi:10.1016/j.cmet.2008.10.008
- Raghupathy, R., Anilkumar, A. A., Polley, A., Singh, P. P., Yadav, M., Johnson, C., et al. (2015). Transbilayer Lipid Interactions Mediate Nanoclustering of Lipid-Anchored Proteins. *Cell* 161, 581–594. doi:10.1016/j.cell.2015.03.048
- Ridgway, N. D., and Zhao, K. (2018). Cholesterol Transfer at Endosomal-Organelle Membrane Contact Sites. *Curr. Opin. Lipidol.* 29, 212–217. doi:10.1097/MOL.0000000000000506
- Rudney, H., and Sexton, R. C. (1986). Regulation of Cholesterol Biosynthesis. *Annu. Rev. Nutr.* 6, 245–272. doi:10.1146/annurev.nu.06.070186.001333
- Russell, D. W. (1992). Cholesterol Biosynthesis and Metabolism. *Cardiovasc. Drug Ther.* 6, 103–110. doi:10.1007/BF00054556
- Sato, R., Inoue, J., Kawabe, Y., Kodama, T., Takano, T., and Maeda, M. (1996). Sterol-dependent Transcriptional Regulation of Sterol Regulatory Element-Binding Protein-2. *J. Biol. Chem.* 271, 26461–26464. doi:10.1074/jbc.271.43.26461
- Schumacher, M. M., Elsabrouty, R., Seemann, J., Jo, Y., and DeBose-Boyd, R. A. (2015). The Prenyltransferase UBIAD1 Is the Target of Geranylgeraniol in Degradation of HMG CoA Reductase. *Elife* 4, 1–21. doi:10.7554/eLife.05560
- Sever, N., Song, B.-L., Yabe, D., Goldstein, J. L., Brown, M. S., and DeBose-Boyd, R. A. (2003). Insig-dependent Ubiquitination and Degradation of Mammalian 3-Hydroxy-3-Methylglutaryl-CoA Reductase Stimulated by Sterols and Geranylgeraniol. *J. Biol. Chem.* 278, 52479–52490. doi:10.1074/jbc.M310053200
- Shimano, H., and Sato, R. (2017). SREBP-regulated Lipid Metabolism: Convergent Physiology - Divergent Pathophysiology. *Nat. Rev. Endocrinol.* 13, 710–730. doi:10.1038/nrendo.2017.91
- Sohrabi, Y., Reinecke, H., and Godfrey, R. (2021). Altered Cholesterol and Lipid Synthesis Mediates Hyperinflammation in COVID-19. *Trends Endocrinol. Metab.* 32, 132–134. doi:10.1016/j.tem.2021.01.001
- Song, B.-L., and DeBose-Boyd, R. A. (2006). Insig-dependent Ubiquitination and Degradation of 3-Hydroxy-3-Methylglutaryl Coenzyme A Reductase Stimulated by δ - and γ -Tocotrienols. *J. Biol. Chem.* 281, 25054–25061. doi:10.1074/jbc.M605575200
- Song, B.-L., Javitt, N. B., and DeBose-Boyd, R. A. (2005). Insig-mediated Degradation of HMG CoA Reductase Stimulated by Lanosterol, an

- Intermediate in the Synthesis of Cholesterol. *Cell Metab.* 1, 179–189. doi:10.1016/j.cmet.2005.01.001
- Stevenson, J., Huang, E. Y., and Olzmann, J. A. (2016). Endoplasmic Reticulum-Associated Degradation and Lipid Homeostasis. *Annu. Rev. Nutr.* 36, 511–542. doi:10.1146/annurev-nutr-071715-051030
- Su, Z.-L., Hang, P.-z., Hu, J., Zheng, Y.-y., SunqiGuo, H. J., Guo, J., et al. (2020). Aloe-emodin Exerts Cholesterol-Lowering Effects by Inhibiting Proprotein Convertase Subtilisin/kexin Type 9 in Hyperlipidemic Rats. *Acta Pharmacol. Sin.* 41, 1085–1092. doi:10.1038/s41401-020-0392-8
- Sukhanova, A., Gorin, A., Serebriiskii, I. G., Gabitova, L., Zheng, H., Restifo, D., et al. (2013). Targeting C4-Demethylating Genes in the Cholesterol Pathway Sensitizes Cancer Cells to EGF Receptor Inhibitors via Increased EGF Receptor Degradation. *Cancer Discov.* 3, 96–111. doi:10.1158/2159-8290.CD-12-0031
- Sundqvist, A., Bengoechea-Alonso, M. T., Ye, X., Lukiyanchuk, V., Jin, J., Harper, J. W., et al. (2005). Control of Lipid Metabolism by Phosphorylation-dependent Degradation of the SREBP Family of Transcription Factors by SCFFbw7. *Cell Metab.* 1, 379–391. doi:10.1016/j.cmet.2005.04.010
- Tao, R., Xiong, X., DePinho, R. A., Deng, C.-X., and Dong, X. C. (2013). Hepatic SREBP-2 and Cholesterol Biosynthesis Are Regulated by FoxO3 and Sirt6. *J. Lipid Res.* 54, 2745–2753. doi:10.1194/jlr.M039339
- Taylor, J. M. W., Borthwick, F., Bartholomew, C., and Graham, A. (2010). Overexpression of Steroidogenic Acute Regulatory Protein Increases Macrophage Cholesterol Efflux to Apolipoprotein AI. *Cardiovasc. Res.* 86, 526–534. doi:10.1093/cvr/cvq015
- Turecek, J., Jackman, S. L., and Regehr, W. G. (2017). Synaptotagmin 7 Confers Frequency Invariance onto Specialized Depressing Synapses. *Nature* 551, 503–506. doi:10.1038/nature24474
- Van Meer, G., Voelker, D. R., and Feigenson, G. W. (2008). Membrane Lipids: Where They Are and How They Behave. *Nat. Rev. Mol. Cell Biol.* 9, 112–124. doi:10.1038/nrm2330
- Venditti, R., Masone, M. C., Rega, L. R., Di Tullio, G., Santoro, M., Polishchuk, E., et al. (2019). The Activity of Sac1 across ER-TGN Contact Sites Requires the Four-Phosphate-Adaptor-Protein-1. *J. Cell Biol.* 218, 783–797. doi:10.1083/jcb.201812021
- Wakana, Y., Hayashi, K., Nemoto, T., Watanabe, C., Taoka, M., Angulo-Capel, J., et al. (2021). The ER Cholesterol Sensor SCAP Promotes CARTS Biogenesis at ER-Golgi Membrane Contact Sites. *J. Cell Biol.* 220. doi:10.1083/jcb.202002150
- Wang, J.-Z., and Dehesh, K. (2018). ER: the Silk Road of Interorganellar Communication. *Curr. Opin. Plant Biol.* 45, 171–177. doi:10.1016/j.pbi.2018.07.012
- Wilhelm, L. P., Tomasetto, C., and Alpy, F. (2016). Touché! STARD3 and STARD3NL Tether the ER to Endosomes. *Biochem. Soc. Trans.* 44, 493–498. doi:10.1042/BST20150269
- Wong, L. H., Gatta, A. T., and Levine, T. P. (2019). Lipid Transfer Proteins: the Lipid Commute via Shuttles, Bridges and Tubes. *Nat. Rev. Mol. Cell Biol.* 20, 85–101. doi:10.1038/s41580-018-0071-5
- Wu, J., Zhang, F., Ruan, H., Chang, X., Wang, J., Li, Z., et al. (2021a). Integrating Network Pharmacology and RT-qPCR Analysis to Investigate the Mechanisms Underlying ZeXie Decoction-Mediated Treatment of Non-alcoholic Fatty Liver Disease. *Front. Pharmacol.* 12, 1–18. doi:10.3389/fphar.2021.722016
- Wu, L., Guo, T., Deng, R., Liu, L., and Yu, Y. (2021b). Apigenin Ameliorates Insulin Resistance and Lipid Accumulation by Endoplasmic Reticulum Stress and SREBP-1c/SREBP-2 Pathway in Palmitate-Induced HepG2 Cells and High-Fat Diet-Fed Mice. *J. Pharmacol. Exp. Ther.* 377, 146–156. doi:10.1124/jpet.120.000162
- Xiao, J., Xiong, Y., Yang, L.-T., Wang, J.-Q., Zhou, Z.-M., Dong, L.-W., et al. (2021). POST1/C12ORF49 Regulates the SREBP Pathway by Promoting Site-1 Protease Maturation. *Protein Cell* 12, 279–296. doi:10.1007/s13238-020-00753-3
- Xu, D., Wang, Z., Xia, Y., Shao, F., Xia, W., Wei, Y., et al. (2020). The Gluconeogenic Enzyme PCK1 Phosphorylates INSIG1/2 for Lipogenesis. *Nature* 580, 530–535. doi:10.1038/s41586-020-2183-2
- Yoshioka, H., Coates, H. W., Chua, N. K., Hashimoto, Y., Brown, A. J., and Ohgane, K. (2020). A Key Mammalian Cholesterol Synthesis Enzyme, Squalene Monooxygenase, Is Allosterically Stabilized by its Substrate. *Proc. Natl. Acad. Sci. USA* 117, 7150–7158. doi:10.1073/pnas.1915923117
- Zelcer, N., Sharpe, L. J., Loregger, A., Kristiana, I., Cook, E. C. L., Phan, L., et al. (2014). The E3 Ubiquitin Ligase MARCH6 Degrades Squalene Monooxygenase and Affects 3-Hydroxy-3-Methyl-Glutaryl Coenzyme A Reductase and the Cholesterol Synthesis Pathway. *Mol. Cell. Biol.* 34, 1262–1270. doi:10.1128/mcb.01140-13
- Zhang, Y., Gu, Y., Chen, Y., Huang, Z., Li, M., Jiang, W., et al. (2021). Dingxin Recipe IV Attenuates Atherosclerosis by Regulating Lipid Metabolism through LXR-A/srebp1 Pathway and Modulating the Gut Microbiota in ApoE^{-/-} Mice Fed with HFD. *J. Ethnopharmacology* 266, 113436. doi:10.1016/j.jep.2020.113436

Conflict of Interest: The authors declare that the research was conducted in the absence of any commercial or financial relationships that could be construed as a potential conflict of interest.

Publisher's Note: All claims expressed in this article are solely those of the authors and do not necessarily represent those of their affiliated organizations, or those of the publisher, the editors, and the reviewers. Any product that may be evaluated in this article, or claim that may be made by its manufacturer, is not guaranteed or endorsed by the publisher.

Copyright © 2022 Shi, Chen, Zou and Tang. This is an open-access article distributed under the terms of the Creative Commons Attribution License (CC BY). The use, distribution or reproduction in other forums is permitted, provided the original author(s) and the copyright owner(s) are credited and that the original publication in this journal is cited, in accordance with accepted academic practice. No use, distribution or reproduction is permitted which does not comply with these terms.

GLOSSARY

ER	endoplasmic reticulum	OSBP	oxysterol-binding protein
PM	plasma membrane	ORD	OSBP-related domainOSBP-related domain
GPI	glycosylphosphatidylinositol	Arf1	ADP-ribosylation factor
HMG-CoA	3-hydroxy-3-methylglutaryl CoA	PI4K	phosphatidylinositol 4-kinase
IPP	isopentenyl pyrophosphate	PTPIP51	phosphatase-interacting protein 51
FPP	farnesyl pyrophosphate	IMM	inner mitochondrial membrane
HMGCR	3-hydroxy-3-methylglutaryl coenzyme A reductase	OMM	outer mitochondrial membrane
SM	squalene monooxygenase	MAM	mitochondria-associated membrane
DFT	farnesyl-diphosphate farnesyltransferase	GRAMD1	GRAM domain-containing 1
LSS	lanosterol synthase	LEs	late endosomes
PP	pyrophosphate	LYs	lysosomes
SREBP2	sterol regulatory element-binding protein 2	STARD3	StAR-related lipid transfer protein
S1P	site 1 protease	CEs	cholesteryl esters
S2P	site 2 protease	LDLR	low-density lipoprotein receptor
SRE	sterol regulatory element	STPs	sterol transfer proteins
IRE	insulin response element	Syt7	synaptotagmin VII
Insig	insulin-induced gene	TF	transferrin
SCAP	SREBP cleavage-activating protein	HMGB1	high-mobility group box 1
PCK1	phosphoenolpyruvate carboxykinase 1	IPF	idiopathic pulmonary fibrosis
HCC	hepatocellular carcinoma	ECs	endothelial cells
Brp1	Brahma-related gene 1	OS	overall survival
POST1	partner of site-1 protease	RFS	relapse-free survival
ERAD	endoplasmic reticulum-associated degradation	MFS	metastasis-free survival
RNF145	ring finger protein 145	BCs	breast cancers
ORP	OSBP-related protein	DS	Down syndrome
USP20	ubiquitin carboxyl-terminal hydrolase 20	ALD	alcoholic liver disease
VCP	valosin-containing protein	ORD	OSBP-related domainOSBP-related domain
GGpp	isoprenoid geranylgeranyl pyrophosphate	PC	phosphatidylcholine
UBIAD1	UbiA prenyltransferase domain-containing protein 1	PtdSer	phosphatidylserine
MARCH	membrane-associated ring-CH-type finger	PI	phosphatidylinositol
UBE2G2	ubiquitin-conjugating enzyme E2 G2	PCSK9	proprotein convertase subtilisin/kexin type 9
UBE2J2	ubiquitin-conjugating enzyme E2 J2	Apo B	apolipoprotein B
PAQR3	adipoQ receptor 3	Apo CIII	apolipoprotein C-III
LTPs	lipid transfer proteins	ANGPTL3	angiopoietin-like 3
MCs	membrane contact sites	LPA	lipoprotein(a)
		NPC1L1	Niemann-Pick C1-like 1



Mitochondrial ROS in *Slc4a11* KO Corneal Endothelial Cells Lead to ER Stress

Rajalekshmy Shyam*, Diego G. Ogando and Joseph A. Bonanno

Vision Science Program, School of Optometry, Indiana University, Bloomington, IN, United States

OPEN ACCESS

Edited by:

Yongye Huang,
Northeastern University, China

Reviewed by:

Beatriz San-Miguel,
University of León, Spain
Manish Bodas,
University of Oklahoma Health
Sciences Center, United States
Huizhen Zhang,
Department of Environmental Health,
College of Public Health, Zhengzhou
University, China

*Correspondence:

Rajalekshmy Shyam
rashyam@iu.edu

Specialty section:

This article was submitted to
Signaling,
a section of the journal
Frontiers in Cell and Developmental
Biology

Received: 18 February 2022

Accepted: 30 March 2022

Published: 26 April 2022

Citation:

Shyam R, Ogando DG and
Bonanno JA (2022) Mitochondrial ROS
in *Slc4a11* KO Corneal Endothelial
Cells Lead to ER Stress.
Front. Cell Dev. Biol. 10:878395.
doi: 10.3389/fcell.2022.878395

Recent studies from *Slc4a11*^{-/-} mice have identified glutamine-induced mitochondrial dysfunction as a significant contributor toward oxidative stress, impaired lysosomal function, aberrant autophagy, and cell death in this Congenital Hereditary Endothelial Dystrophy (CHED) model. Because lysosomes are derived from endoplasmic reticulum (ER)—Golgi, we asked whether ER function is affected by mitochondrial ROS in *Slc4a11* KO corneal endothelial cells. In mouse *Slc4a11*^{-/-} corneal endothelial tissue, we observed the presence of dilated ER and elevated expression of ER stress markers BIP and CHOP. *Slc4a11* KO mouse corneal endothelial cells incubated with glutamine showed increased aggresome formation, BIP and GADD153, as well as reduced ER Ca²⁺ release as compared to WT. Induction of mitoROS by ETC inhibition also led to ER stress in WT cells. Treatment with the mitochondrial ROS quencher MitoQ, restored ER Ca²⁺ release and relieved ER stress markers in *Slc4a11* KO cells *in vitro*. Systemic MitoQ also reduced BIP expression in *Slc4a11* KO endothelium. We conclude that mitochondrial ROS can induce ER stress in corneal endothelial cells.

Keywords: corneal endothelial cells, ROS—reactive oxygen species, er stress, ERAD (ER associated protein degradation), MitoQ, SLC4A11 ammonia transporter

INTRODUCTION

Congenital Hereditary Endothelial Dystrophy (CHED) is a rare recessive blinding disease that affects 3 out of 100,000 newborns each year. In this disease, the corneal endothelial layer malfunctions resulting in corneal edema (Aldave et al., 2007). This progressive disease arises during infancy and has no cure, and the current treatment involves corneal transplantation (Aldave et al., 2013). Loss of function of a membrane protein, SLC4A11, leads to CHED (Vithana et al., 2006; Han et al., 2013). Recent studies from our lab and others indicate that in the absence of *Slc4a11*, glutamine-induced mitochondrial Reactive Oxygen Species (ROS) production results in lysosomal dysfunction, autophagy impairment, and aberrant master regulator of oxidative stress response Nrf2 signaling resulting in cell death (Guha et al., 2017; Ogando et al., 2019; Shyam et al., 2021).

In eukaryotes, lysosomes are formed from the budding off of acidic proteases from the ER-Golgi network. Since *Slc4a11* KO lysosomes are dysfunctional, we asked if there was Endoplasmic Reticulum (ER) stress as well. ER is the primary organelle in which protein biosynthesis, folding, and modifications occur. ER can also identify misfolded proteins and deploy them for ER-associated degradation (ERAD). The canonical ERAD system is characterized by the proteasome-mediated degradation of misfolded proteins, whereas autophagy is activated in the non-canonical mode (Ren et al., 2021). When the rate of misfolded protein formation saturates ERAD, a signaling cascade known as Unfolded Protein Response (UPR) is triggered leading to ER

stress (Ren et al., 2021). In Fuchs Endothelial Corneal Dystrophy, ER stress (Jun et al., 2012) and activation of the unfolded protein response (Okumura et al., 2017b) are present. In addition, some mutations in *Slc4a11* that are associated with CHED and FECD results in ER retention of the misfolded protein (Loganathan and Casey, 2014). The protein folding process in the ER is affected by several internal and external cues, including $[Ca^{2+}]$ and oxidative stress (Xu et al., 2012). Since elevated mitochondrial oxidative stress (Guha et al., 2017; Ogando et al., 2019) and dysfunctional lysosomes are present in the CHED mouse endothelium (Shyam et al., 2021), we asked whether ER function is affected in this disease model.

In *Slc4a11*^{-/-} corneal endothelium, we observed alterations in ER morphology and elevated expression of UPR associated proteins. In addition, we found that glutamine-induced mitochondrial ROS is the cause of ER stress in *Slc4a11*^{-/-} corneal endothelial cells.

MATERIALS AND METHODS

Animal Model

Slc4a11^{-/-} (KO) mice were originally provided by Dr. Eranga Vithana (Singapore Eye Research Institute) (Vithana et al., 2006). *Slc4a11*^{+/+} (Normal, Wild Type, WT) and KO mice were housed and maintained in pathogen-free conditions. Animals were used in the experiments in accordance with institutional guidelines and the current regulations of the National Institutes of Health, the United States Department of Health and Human Services, the United States Department of Agriculture and Association for Research in Vision and Ophthalmology (ARVO) Statement for the Use of Animals in Ophthalmic and Vision Research.

Cell Culture Experiments

Conditionally immortalized mouse corneal endothelial cells (MCEC) *Slc4a11*^{+/+} and *Slc4a11*^{-/-} were generated and maintained in our lab (Zhang et al., 2017b). Cells were cultured in Complete Media, which contains OptiMEM-I medium (#51985; Thermo Fisher Scientific, Canoga Park, CA, United States), 14 mM Glucose and 4 mM L-Alanyl Glutamine supplemented with 8% heat-inactivated fetal bovine serum (FBS) (#10082139; Thermo Fisher Scientific), EGF 5 ng/ml (#01-107 Millipore, Darmstadt, Germany), pituitary extract 100 µg/ml (Hyclone 15 Laboratories, Logan, UT, United States), calcium chloride 200 mg/L, 0.08% chondroitin sulfate (#G6737; SigmaAldrich Corp., St. Louis, MO, United States), gentamicin 50 µg/ml (#15710072; Thermo Fisher Scientific), antibiotic/antimycotic solution diluted 1:100 (#15240062; Thermo Fisher Scientific), and 44 units/mL IFN-γ (#485-MI; R&D Systems, Minneapolis, MN, United States).

For experiments, cells were incubated in Assay Media, which contained Dulbecco's Modified Eagle Medium (no glutamine, no sodium pyruvate, no phenol red, contains 5.5 mM glucose) (#11054001; Thermo Fisher Scientific), supplemented with 0.5 mM glutamine (#250030-081, Thermo Fisher Scientific) and 0.5% dialyzed FBS (#26400-036; Thermo Fisher Scientific) at 33°C for 16 h. Corneal

TABLE 1 | Primer sequences used in this study.

m-sXBP1-F	CTGAGTCCGAATCAGGTGCAG
m-sXBP1-R	GTCCATGGGAAGATGTTCTGG
m-usXBP1-F	CAGCACTCAGACTATGTGCA
m-usXBP1-R	GTCCATGGGAAGATGTTCTGG
m-Total XBP1-F	TGGCCGGGTCTGCTGAGTCCG
m-Total XBP1-R	GTCCATGGGAAGATGTTCTGG

endothelium is exposed to 0.5 mM glutamine *in vivo* (Langford et al., 2007), therefore this concentration was used in our experiments. Drug treatments, 2 µM MitoQ (#317102, Medkoo Biosciences, Morrisville, NC, United States), or 0.1 µM Thapsigargin (SML 1845, Sigma Aldrich) were added into the assay media for 16 h. All drug treatments were carried out in assay media. Significant elevation in mitochondrial ROS was observed after 16 h treatment of cells in assay media (Shyam et al., 2021).

Real Time PCR

Total RNA was isolated using RNA mini kit (#74104, Qiagen, Germantown, Maryland, United States). 1 µg of RNA was used to prepare cDNA using a high capacity RNA to DNA kit (#4388950, Thermo Fisher Scientific). Previously published primer designs were used to amplify XBP1, us-XBP1, s-XBP1, and β-actin (Yoon et al., 2019). NCBI primer designing tool was used to design all other primers used for this study. List of primers used can be found in **Table 1**. Real time PCR was conducted using SYBR green dye using a BioRad CFX96 system. Relative quantitation was performed using 2^{-ΔΔCt} method against housekeeping gene. Fold Change (FC) is calculated as 2^{-ΔΔCt}. Data is plotted on Log10 scale.

Cytosolic Calcium Measurement

Immortalized *Slc4a11*^{+/+} (WT) and *Slc4a11*^{-/-} (KO) corneal endothelial cells were cultured on fibronectin pre-coated 25-mm diameter glass coverslips (GG-25-pdl; Neuvitro Corporation, Vancouver, WA, United States) for 24 h in Assay media with or without glutamine. 1 mM stock of Fura 2-AM (#F1221, ThermoFisher Scientific) was prepared in DMSO. 5 µL of Fura stock solution along with 5 µL of 20% Pluronic F-127 solution in DMSO (#P3000MP, ThermoFisher Scientific) were mixed in 1 ml Hanks Balanced Salt Solution (HBSS) to obtain a final Fura 2-AM concentration of 5 µM. Cells were loaded with Fura-2AM for 30 min at 37°C. Cover slips were washed in HBSS for 30 min at room temperature, before they were mounted into a perfusion chamber, connected to a stage warmer (37°C) of an inverted microscope (Eclipse TE200; Nikon, Tokyo, Japan). Cells were perfused with HBSS containing 500 µM non-cell permeant BAPTA for 50 s to establish baseline. After establishing the fluorescence baseline, cells were perfused with HBSS containing 50 µM Ionomycin (#2092, Tocris, Minneapolis, MN, United States). Perfusing solutions were adjusted to pH 7.5 using NaOH, and kept at 37°C in a warming box. The flow of the perfusate (~0.5 ml/min) was by gravity. Osmolarity of all solutions was adjusted to 295 mOsm with sucrose. Cells were

imaged with a 40x oil-immersion objective (Nikon). Cells loaded with Fura-2AM were excited at 340 and 380 nm and the emission was collected at 505 nm to measure changes in cytosolic calcium. Ca^{2+} bound Fura-2 has an excitation maximum of 340 nm, while Ca^{2+} free Fura-2 has its excitation maximum of 380 nm. In both states, the emission maximum is 510 nm. The 340/380 nm excitation ratio for Fura-2 is a measure of intracellular $[\text{Ca}^{2+}]$.

Electron Microscopy

Endothelium-Descemet's tissue samples from WT and KO mice were fixed with 2.5% glutaraldehyde (#16020, Electron Microscopy Sciences, Hatfield, PA, United States), 4% paraformaldehyde (#15710, Electron Microscopy Sciences), in 0.1 M sodium cacodylate buffer, pH 7.2 at 4°C and post-fixed with 1% osmium tetroxide (#19150, Electron Microscopy Sciences) in 0.1 M sodium cacodylate buffer (#12300, Electron Microscopy Sciences), pH 7.2 at 4°C. Samples were dehydrated in a graded ethanol series to 100% ethanol, transitioned to propylene oxide (#20401, Electron Microscopy Sciences), and infiltrated with Embed 812 resin (#14120, Electron Microscopy Sciences). Infiltrated samples were placed in flat embedding molds and polymerized at 65°C for 18 h. Resin blocks were cut with a diamond knife using a Leica Ultracut UCT ultramicrotome (Leica Systems, Buffalo Grove, IL). Sections were placed on 300 mesh copper TEM grids (#0300-CU, Electron Microscopy Sciences) and stained with saturated uranyl acetate in aqueous solution, and lead citrate. Stained sections were viewed with a JEM-1010 TEM (JEOL, Peabody, MA, United States) at 80 kV and photographed with a Gatan MegaScan 794 CCD camera or JEM-1400plus TEM (JEOL) with a Gatan OneView CMOS digital camera.

Protein Simple—Simple Western Wes Immunoassay for Protein Expression

Corneal endothelial cell layer was removed from dissected corneas. Protein lysates were prepared by pooling the tissues from two animals, using radioimmunoprecipitation (RIPA) lysis buffer containing protease and phosphatase inhibitors. Equal amounts of protein (1.5 µg) were loaded into 12–230 kDa separation module kit, and analyzed using the Protein Simple Wes System (Protein Simple, San Jose, CA, United States) following the manufacturer's instructions as previously described (Shyam et al., 2021). Antibodies used are BIP (#3177, Cell Signaling technologies, Danvers, MA, United States), GADD153 (#NB600-1,335, Novus, Centennial, CO, United States), and α -tubulin (#NB100-690, Novus).

Wes immunoassay was carried out since it is challenging to obtain sufficient total protein from corneal endothelial peelings to conduct traditional western blots. Our lab has used this approach in several recent studies to quantify changes in protein expression (Ogando et al., 2021; Shyam et al., 2021; Shyam et al., 2022; Ogando and Bonanno, 2022).

Mitochondrial ROS Induction

Slc4a11^{+/+} corneal endothelial cells were treated with 0.25 µM Antimycin A (#A8674, Sigma-Aldrich), 0.5 µM Rotenone (#R8875, Sigma-Aldrich), or 0.25 µM Antimycin A+ Rotenone

in assay media for 18 h. Control cells were cultured in assay media for the same duration.

Flow Cytometry for Mitochondrial ROS and Apoptosis

Slc4a11^{+/+} corneal endothelial cells were trypsinized and stained in triplicate with Pacific Blue Annexin V kit with PI (#640928, BioLegend, San Diego, CA, United States) or MitoSOX (#M36008, Thermo Fisher Scientific) following manufacturer's instructions. Cells were collected in 2 ml micro centrifuge tubes following filtration using CellTrics Filters (#04-004-2,327, Sysmex, Gorlitz, Germany). Flow cytometry analysis was conducted on MACSQuant VYB (Miltenyi Biotech, Germany). 10,000 cells were collected for each acquisition. Data were analyzed using FCS Express (De Novo software, Pasadena, CA, United States).

Aggresome Quantification

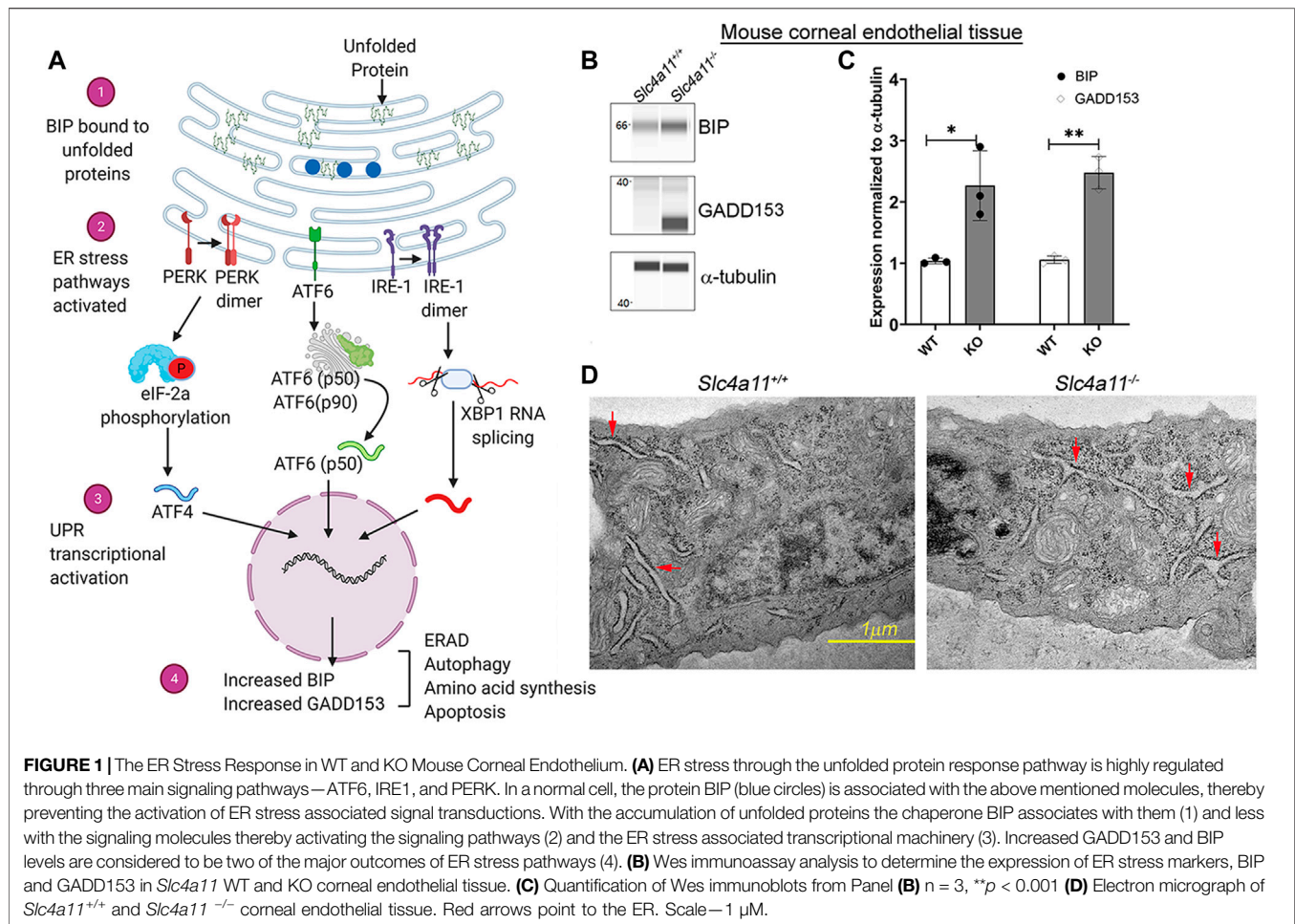
MCEC cultures in 12-well format were trypsinized, washed and fixed using 4% Paraformaldehyde. Following permeabilization, cells were stained for aggresomes using the Aggresome detection kit (#ENZ51035, Enzo Life Sciences, NY) following manufacturer's instructions. The aggresome detection reagent emits strong fluorescence when bound by misfolded proteins but not in solution. Therefore, the increase in fluorescence intensity is indicative of the levels of protein aggregates present in the cells. After filtration using 50 µm sterile CellTrics Filters flow cytometry analysis was conducted on MACSQuant VYB. 10,000 cells were collected per acquisition. Cells treated with ER stress inducer, Thapsigargin (#1138, Tocris, Minneapolis, MN, United States), served as a positive control, unstained cells were used as negative control. Data were analyzed with FCS Express.

MitoQ Injections

MitoQ, 1 mM (#317102; Medkoo Biosciences) was prepared in equal volume of ethanol: distilled sterile water mixture. 100 µL of this solution containing 68 µg of MitoQ was injected intraperitoneally into *Slc4a11*^{-/-} mice on alternate days. Littermate control mice were injected with equal volume of vehicle for the same duration at the same time/day. To prevent stress induced weight loss due to increased handling, animals were provided with a vet-approved supplement. One tablespoon of commercially available peanut butter was provided to both control animals and experimental animals, once a day immediately after handling.

Statistical Analysis

All experiments were performed at least three times on different days. Error bars represent mean \pm SD. Statistical significance was calculated using unpaired t-tests when two groups were involved. ANOVA with Tukey's multiple comparisons test was used to determine statistical significance if more than two groups were analyzed. Statistical analyses were conducted using Graph Pad Prism software (La Jolla, CA, United States).



Model Figures

The model figures were created with the aid of BioRender.com.

RESULTS

Activation of Unfolded Protein Response in *Slc4a11*^{-/-} Corneal Endothelium

ER is the major site for protein folding in eukaryotes. When the protein folding machinery is overwhelmed by the influx of nascent polypeptides, ER stress ensues. The Unfolded Protein Response (UPR) pathway is activated during ER stress to promote cell survival through three distinct pathways (Figure 1A). However, chronic UPR activation leads to ER-stress-induced apoptosis (Adams et al., 2019; Bartoszewska and Collawn, 2020).

Misfolded proteins trigger the unfolded protein response (UPR) through three primary sensors, Inositol-Requiring Enzyme 1 α (IRE1- α), Protein kinase R-like Endoplasmic Reticulum Kinase (PERK), and Activating transcription factor 6 (ATF6). Activation of UPR leads to increased expression of ER chaperone protein BIP (Binding Immunoglobulin Protein) and chronic ER stress induces apoptosis through ER-related apoptosis protein GADD153 (Growth Arrest DNA Damage protein153,

also known as CHOP) (Figure 1A) (Qi et al., 2017). In the mouse corneal endothelium, we observed increased BIP and GADD153 expression in 10 week old *Slc4a11*^{-/-} animals but not in the age-matched *Slc4a11*^{+/+} animals (Figures 1B,C). Another established characteristic of ER stress is the presence of dilated ER lumen (Bernales et al., 2006; Despa, 2009; Hartley et al., 2010; Schönthal, 2012). Therefore, we conducted electron microscopy to determine whether there are any structural changes in the ER of the corneal endothelia of *Slc4a11*^{-/-} mice. Ten-week old *Slc4a11*^{-/-} mice corneal endothelia reveal the presence of dilated ER lumen that was not observed in WT samples of age-matched animals (Figure 1D).

Glutamine Induced Activation of UPR in *Slc4a11*^{-/-} Corneal Endothelial Cells

Glutamine-induced mitochondrial ROS is the primary cellular stress in *Slc4a11*^{-/-} corneal endothelium (Ogando et al., 2019). To determine its contribution toward ER stress, we treated *Slc4a11*^{+/+} and *Slc4a11*^{-/-} immortalized corneal endothelial cells with or without glutamine. Flow cytometry analysis showed a significant increase in misfolded protein aggregates (aggresomes) in *Slc4a11*^{-/-} compared to WT cells in glutamine

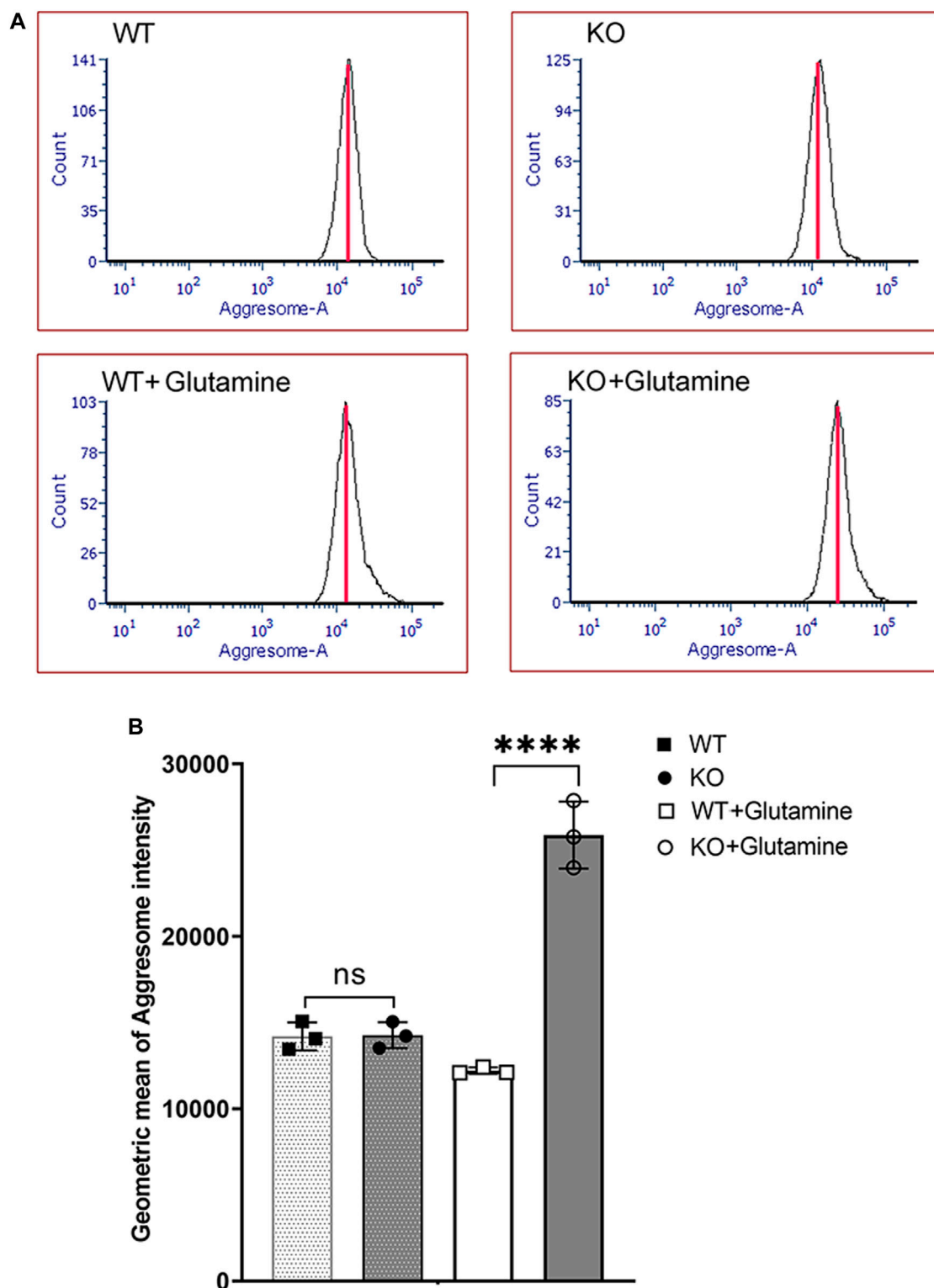
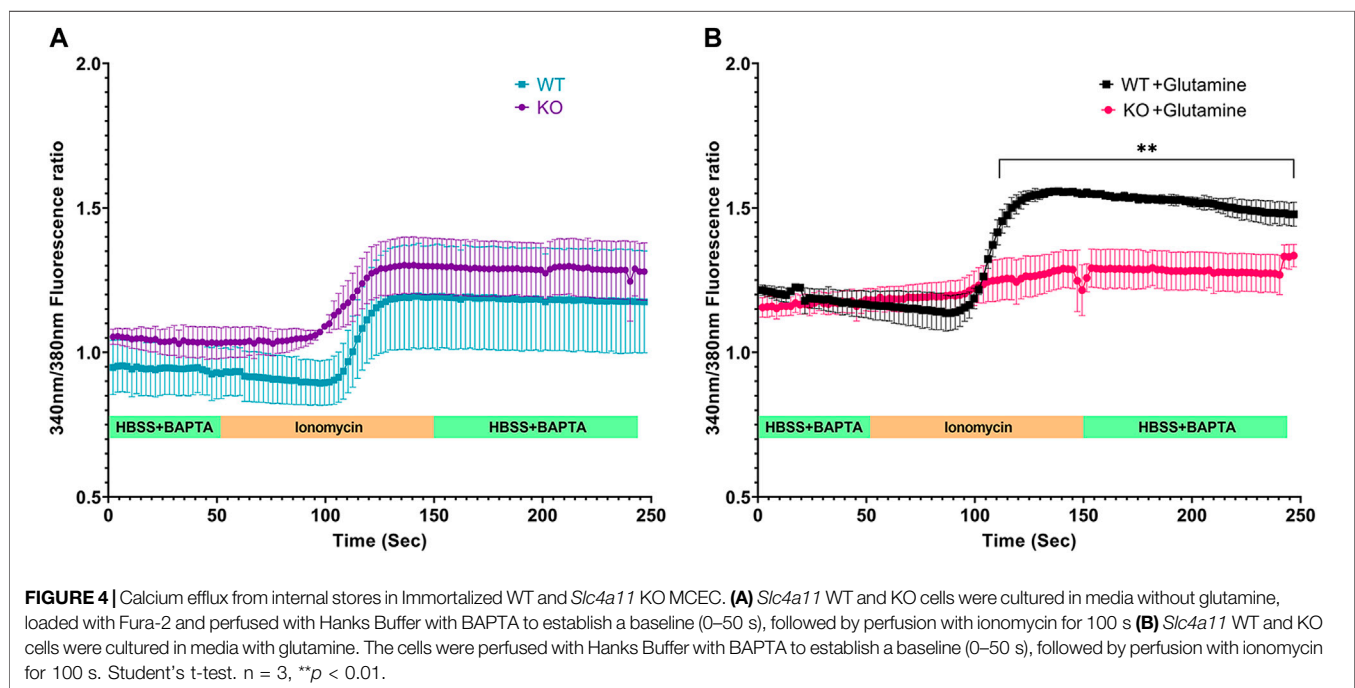
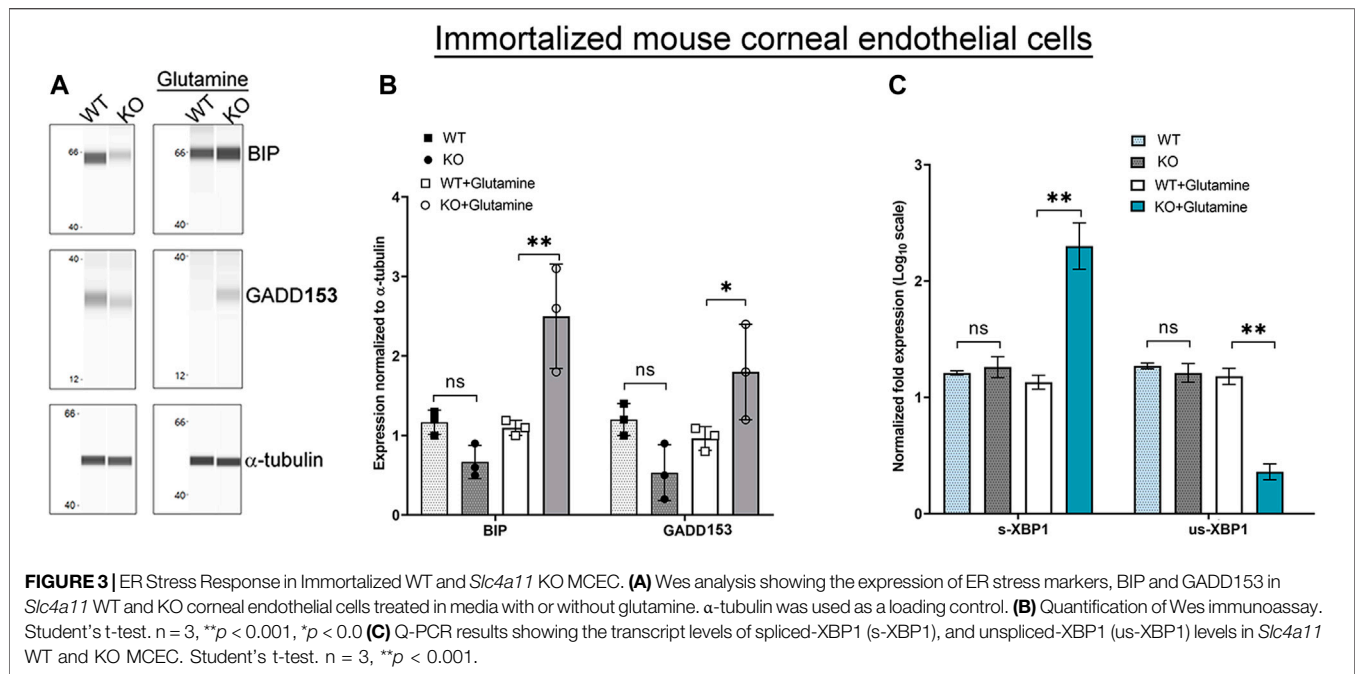


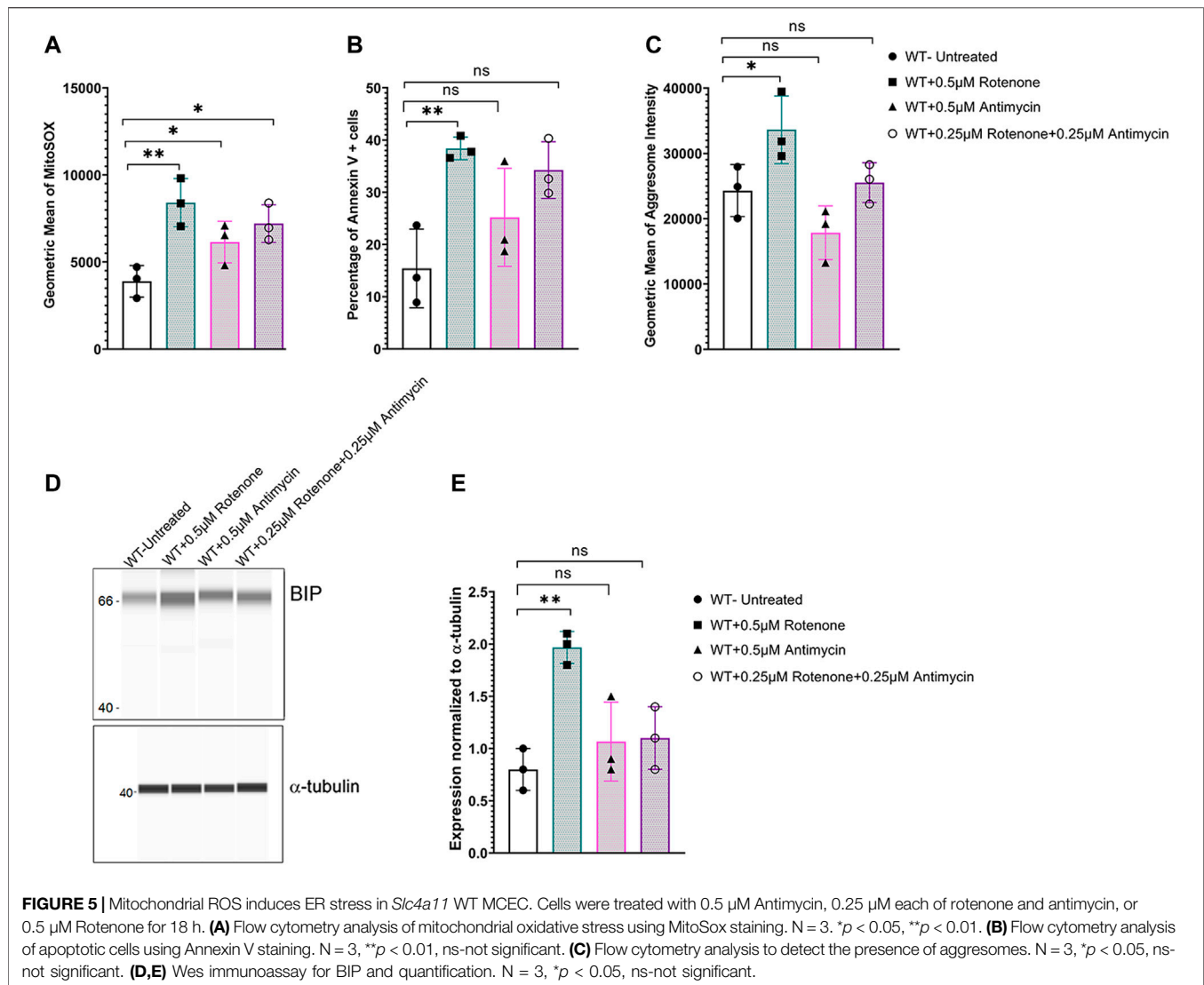
FIGURE 2 | Aggresome Formation in Immortalized WT and *Slc4a11* KO MCEC. **(A)** Flow cytometry analysis of *Slc4a11* WT and KO MCEC to determine the presence of aggresomes (marker for unfolded proteins in the ER). **(B)** Quantification of the Geometric mean of Aggresome Intensity. Students t-test. $n = 3$, **** $p < 0.0001$.



media (Figures 2A,B). Unstained cells were used as negative control, and cells treated with the ER stress inducer Thapsigargin, was used as positive control for aggregates formation (Supplementary Figure S1).

Glutamine incubation also elevated expression of UPR associated proteins, BIP and GADD153 in *Slc4a11*^{-/-} cells consistent with the accumulation of misfolded proteins as an outcome of ER stress (Figures 3A,B). Splicing of X-Box Binding Protein-1 (XBP1) mRNA occurs in response to the IRE-1 α

pathway (Figure 1A). Therefore, if there is ER stress and IRE-1 α is activated we expect an increase in the levels of spliced XBP1, but not the unspliced version. Using primers (Table 1) that can bind to unspliced XBP1, and spliced XBP1 (Yoon et al., 2019), we conducted real-time PCR. *Slc4a11*^{-/-} cells in the presence of glutamine had increased levels of the spliced XBP1 transcripts (Figure 3C), whereas the unspliced XBP1 levels were decreased. This result is consistent with ER stress induced activation of IRE-1 α pathway.

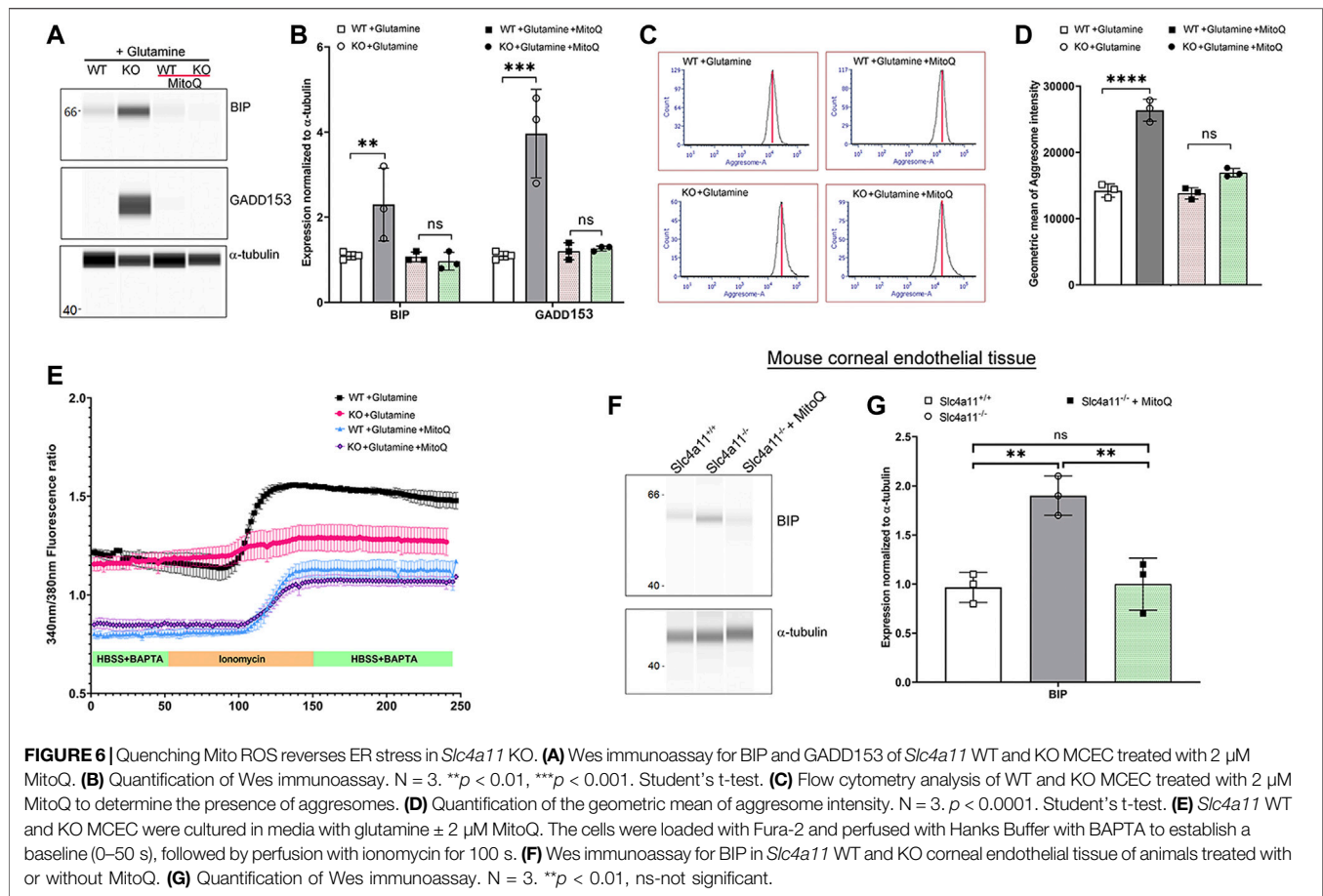


Glutamine Decreased ER $[Ca^{2+}]$ Release in *Slc4a11*^{-/-} Corneal Endothelial Cells

ER is the largest reservoir of Ca^{2+} in eukaryotic cells. We used the calcium indicator dye, Fura-2, to measure cytosol $[Ca^{2+}]$. A baseline fluorescence ratio was established using Hanks Balanced Saline Solution (HBSS) containing calcium chelator BAPTA so that extracellular calcium was minimal. Following this, the cells were perfused with the calcium ionophore ionomycin, which under these conditions releases Ca^{2+} from ER intracellular stores. Live-cell microscopy revealed similar baseline and ionomycin stimulated change in cytosolic $[Ca^{2+}]$ for both *Slc4a11*^{+/+} and *Slc4a11*^{-/-} cells when perfused without glutamine (Figure 4A). However in the presence of glutamine, ionomycin released significantly less calcium into the cytosol of *Slc4a11*^{-/-} cells indicating that the ER calcium store is deficient (Figure 4B).

Mitochondrial ROS Increases ER Stress in Wild-type Corneal Endothelial Cells

To determine if oxidative stress was sufficient to induce ER stress, WT corneal endothelial cells were treated with mitochondrial ROS inducers - rotenone (mitochondrial electron transport chain complex I inhibitor) or antimycin A (mitochondrial electron transport chain complex III inhibitor) or a combination of both drugs. Flow cytometry analysis of MitoSOX indicated that all three treatment conditions increased mitochondrial oxidative stress (Figure 5A), while significant apoptotic cell death was evident only with 0.5 μ M rotenone treatment (Figure 5B). Significant increase in aggresome levels (Figure 5C) as well as elevation in ER stress marker, BIP (Figures 5D,E), were observed with 0.5 μ M Rotenone treatment indicating that mitochondrial oxidative stress alone is sufficient to cause ER stress and that it is not simply due to the lack of *Slc4a11*.



MitoQ Reduced ER Stress and Improved ER Ca^{2+} Release in *Slc4a11*^{-/-} Cells

In the absence of the ammonia sensitive mitochondrial uncoupling by *Slc4a11*, glutamine catabolism leads to mitochondrial membrane hyperpolarization that elevates mitochondrial ROS in corneal endothelial cells (Ogando et al., 2019). Since we now show that glutamine is causing ER stress, we asked whether quenching mitochondrial ROS can decrease ER stress in *Slc4a11*^{-/-} cells. *Slc4a11*^{-/-} corneal endothelial cells were incubated with 2 μ M MitoQ for 24 h in assay media, which was previously shown to significantly reduce mitochondrial ROS (Shyam et al., 2021). **Figures 6A,B** show that this treatment significantly reduced BIP and GADD153 expression, and aggresome levels in KO cells (**Figures 6C,D**). Interestingly, **Figure 6E** shows that MitoQ in the presence of glutamine lowered baseline calcium in both WT and KO corneal endothelial cells and restored the release of calcium from internal stores by ionomycin in KO cells to a level similar to that observed in glucose alone (see **Figure 4A**).

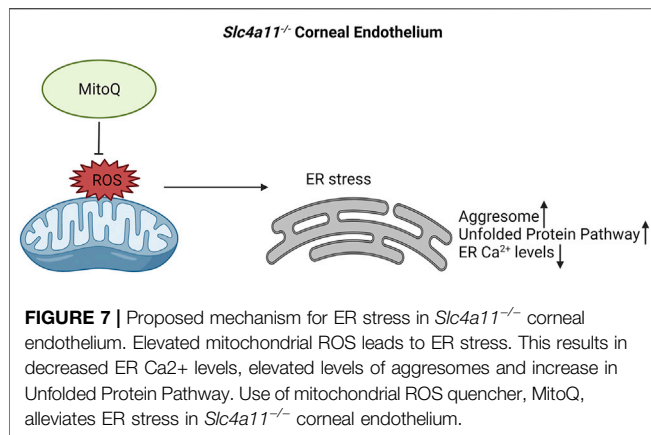
To determine whether MitoQ was sufficient to improve ER stress *in vivo*, 8-week old *Slc4a11*^{-/-} animals were injected with this drug on alternate days over the course of 4 weeks (Shyam et al., 2021). Following MitoQ treatment, BIP expression in dissected corneal endothelium was determined using Wes immunoassay. Significant reduction in BIP levels were observed in *Slc4a11*^{-/-} animals

compared to littermate controls when treated with MitoQ (**Figures 6F,G**). These observations are consistent with our previous findings in which MitoQ treatment alleviated autophagy and lysosomal dysfunction in *Slc4a11*^{-/-} animals (Shyam et al., 2021).

DISCUSSION

In addition to glucose, glutamine has been established as an important metabolite used by corneal endothelium (Zhang et al., 2017a; Zhang et al., 2017b; Ogando et al., 2019; Hamuro et al., 2020; Jin et al., 2020; Ogando and Bonanno, 2022). Moreover, the high expression of *Slc4a11* in mitochondria of corneal endothelial cells reduces glutamine-induced generation of superoxide and oxidative damage (Ogando et al., 2019). In the current study, we show that glutamine (*in vivo* or *in vitro*) in the absence of *Slc4a11* leads to ER stress that can be reversed by quenching mitochondrial ROS. Mitochondrial ROS also triggers lysosomal dysfunction with autophagy impairment in *Slc4a11*^{-/-} corneal endothelial cells (Shyam et al., 2021). Since lysosomes are derived from ER-Golgi, our findings suggest that ROS induced ER stress is an important trigger for cellular dysfunction in the *Slc4a11* KO model.

In many pathological conditions, ER stress manifests when the capacity of this organelle to fold proteins becomes saturated, thereby leading to the accumulation of misfolded proteins (Ren



et al., 2021). Evolutionarily conserved unfolded protein response acts as an ER to nucleus signal to trigger signaling pathways that can circumvent cell death. Even though proteasomal degradation of unfolded proteins is the canonical ER-associated clearance mechanism (Ren et al., 2021), recent evidence indicates that ER stress can activate autophagy as a cell survival mechanism (Bernales et al., 2006; Yorimitsu et al., 2006; Rashid et al., 2015). Cross-talk between ROS, ER stress and autophagy is well-documented in other cell types (Senft and Ronai, 2015) and it is possible that ROS-mediated ER stress may activate autophagy in CHED. However, ROS induced lysosomal dysfunction prevents the degradation of autophagosome contents (Shyam et al., 2021). Together, these studies indicate the effect of elevated mitochondrial ROS on multiple organelle functions in corneal endothelial cells and suggest that dysfunctional lysosomes may stem from ER stress.

ER is the major reservoir of Ca²⁺ in the cell. In the presence of glutamine, both *Slc4a11*^{+/+} and *Slc4a11*^{-/-} cells showed slightly elevated cytosolic [Ca²⁺]; however, we noticed a significant decrease in ionomycin induced calcium efflux from internal stores in *Slc4a11*^{-/-} cells in glutamine. These results suggest that ER stress induced by glutamine in *Slc4a11*^{-/-} cells causes reduced Ca²⁺ release either due to impaired ER Ca²⁺ loading and/or dysfunctional release mechanisms. That treatment with MitoQ, which is known to reduce ROS levels in *Slc4a11*^{-/-} cells (Shyam et al., 2021) improved Ca²⁺ efflux from the internal stores, supports the notion that ER stress is caused by mitochondrial ROS production. Interestingly, glutamine significantly raised cytosolic Ca²⁺ in both WT and KO cells and MitoQ lowered cytosolic Ca²⁺ levels. This suggests that mitochondrial activity and ROS production (high in KO and lower in WT) influence mitochondrial and/or ER Ca²⁺ levels (Feno et al., 2019; Delierneux et al., 2020).

Elevated ROS (Guha et al., 2017; Ogando et al., 2019), dysfunctional autophagy (Shyam et al., 2021), and ER stress are characteristics of loss of *Slc4a11*. Similar to the CHED model, increased ROS (Ong Tone et al., 2020) and ER distress (Okumura et al., 2017a) are present in FECD. Whether ROS

induces ER stress in FECD is not known. With the evidence of organelle crosstalk in corneal endothelial cells, it is plausible that ER stress may result from elevated ROS in FECD.

CONCLUSION

Mitochondrial ROS increases ER stress, decreases ER Ca²⁺ stores and upregulates the unfolded protein response pathway in *Slc4a11*^{-/-} corneal endothelium. Our study is the first to determine the presence of ER stress in an animal model of CHED and provide evidence that this is attributable to mitochondrial ROS (Figure 7).

DATA AVAILABILITY STATEMENT

The original contributions presented in the study are included in the article/Supplementary Material, further inquiries can be directed to the corresponding author.

ETHICS STATEMENT

The animal study was reviewed and approved by the National Institutes of Health United States Department of Health and Human Services United States Department of Agriculture Association for Research in Vision and Ophthalmology (ARVO) Statement for the Use of Animals in Ophthalmic and Vision Research.

AUTHOR CONTRIBUTIONS

RS—Funding procurement, experimental design, carried out experiments, the first draft of the manuscript DO—Carried out experiments JB—Funding procurement, Experimental design, project oversight, Manuscript editing.

ACKNOWLEDGMENTS

The authors are thankful to Bonanno lab members; Dr. Shimin Li, Dr. Moonjung Choi, and Mr. Edward Kim for suggestions on experimental design and data analysis. We thank Ms. Christiane Hassel, Indiana University Flow Cytometry Core Facility, Mr. Barry Stein IUB Electron Microscopy facility, and Prof. Catherine Cheng (Indiana University Bloomington) for the use of Protein Simple Wes machine.

SUPPLEMENTARY MATERIAL

The Supplementary Material for this article can be found online at: <https://www.frontiersin.org/articles/10.3389/fcell.2022.878395/full#supplementary-material>

REFERENCES

- Adams, C. J., Kopp, M. C., Larburu, N., Nowak, P. R., and Ali, M. M. U. (2019). Structure and Molecular Mechanism of ER Stress Signaling by the Unfolded Protein Response Signal Activator IRE1. *Front. Mol. Biosci.* 6, 11. doi:10.3389/fmolb.2019.00011
- Aldave, A. J., Han, J., and Frausto, R. F. (2013). Genetics of the Corneal Endothelial Dystrophies: an Evidence-Based Review. *Clin. Genet.* 84, 109–119. doi:10.1111/cge.12191
- Aldave, A. J., Yellore, V. S., Bourla, N., Momi, R. S., Khan, M. A., Salem, A. K., et al. (2007). Autosomal Recessive CHED Associated with Novel Compound Heterozygous Mutations in SLC4A11. *Cornea* 26, 896–900. doi:10.1097/ICO.0b013e318074bb01
- Bartoszewski, S., and Collawn, J. F. (2020). Unfolded Protein Response (UPR) Integrated Signaling Networks Determine Cell Fate during Hypoxia. *Cell. Mol. Biol. Lett.* 25, 18. doi:10.1186/s11658-020-00212-1
- Bernales, S., McDonald, K. L., and Walter, P. (2006). Autophagy Counterbalances Endoplasmic Reticulum Expansion during the Unfolded Protein Response. *Plos Biol.* 4, e423. doi:10.1371/journal.pbio.0040423
- Delierneux, C., Kouba, S., Shanmughapriya, S., Potier-Cartereau, M., Trebak, M., and Hempel, N. (2020). Mitochondrial Calcium Regulation of Redox Signaling in Cancer. *Cells* 9, 432. doi:10.3390/cells9020432
- Despa, F. (2009). Dilatation of the Endoplasmic Reticulum in Beta Cells Due to Molecular Overcrowding? *Biophysical Chem.* 140, 115–121. doi:10.1016/j.bpc.2008.12.003
- Feno, S., Butera, G., Vecellio Reane, D., Rizzuto, R., and Raffaello, A. (2019). Crosstalk between Calcium and ROS in Pathophysiological Conditions. *Oxidative Med. Cell Longevity* 2019, 1–18. doi:10.1155/2019/9324018
- Guha, S., Chaurasia, S., Ramachandran, C., and Roy, S. (2017). SLC4A11 Depletion Impairs NRF2 Mediated Antioxidant Signaling and Increases Reactive Oxygen Species in Human Corneal Endothelial Cells during Oxidative Stress. *Sci. Rep.* 7, 4074. doi:10.1038/s41598-017-03654-4
- Hamuro, J., Deguchi, H., Fujita, T., Ueda, K., Tokuda, Y., Hiramoto, N., et al. (2020). Polarized Expression of Ion Channels and Solute Carrier Family Transporters on Heterogeneous Cultured Human Corneal Endothelial Cells. *Invest. Ophthalmol. Vis. Sci.* 61, 47. doi:10.1167/iovs.61.5.47
- Han, S. B., Ang, H.-P., Poh, R., Chaurasia, S. S., Peh, G., Liu, J., et al. (2013). Mice with a Targeted Disruption of SLC4A11 Model the Progressive Corneal Changes of Congenital Hereditary Endothelial Dystrophy. *Invest. Ophthalmol. Vis. Sci.* 54, 6179–6189. doi:10.1167/iovs.13-12089
- Hartley, T., Siva, M., Lai, E., Teodoro, T., Zhang, L., and Volchuk, A. (2010). Endoplasmic Reticulum Stress Response in an INS-1 Pancreatic β -cell Line with Inducible Expression of a Folding-Deficient Proinsulin. *BMC Cell Biol* 11, 59. doi:10.1186/1471-2121-11-59
- Jin, M., Wang, Y., Wang, Y., Li, Y., Wang, G., Liu, X., et al. (2020). Protective Effects On corneal Endothelium during Intracameral Irrigation Using N-(2)-l-alanyl-l-glutamine. *Front. Pharmacol.* 11, 369. doi:10.3389/fphar.2020.00369
- Jun, A. S., Meng, H., Ramanan, N., Matthaei, M., Chakravarti, S., Bonshek, R., et al. (2012). An Alpha 2 Collagen VIII Transgenic Knock-In Mouse Model of Fuchs Endothelial Corneal Dystrophy Shows Early Endothelial Cell Unfolded Protein Response and Apoptosis. *Hum. Mol. Genet.* 21, 384–393. doi:10.1093/hmg/ddr473
- Langford, M. P., Gosslee, J. M., Liang, C., Chen, D., Redens, T. B., and Welbourne, T. C. (2007). Apical Localization of Glutamate in GLAST-1, Glutamine Synthetase Positive Ciliary Body Nonpigmented Epithelial Cells. *Clin. Ophthalmol.* 1, 43–53.
- Loganathan, S. K., and Casey, J. R. (2014). Corneal Dystrophy-Causing SLC4A11 Mutants: Suitability for Folding-Correction Therapy. *Hum. Mutat.* 35, 1082–1091. doi:10.1002/humu.22601
- Ogando, D. G., and Bonanno, J. A. (2022). RNA Sequencing Uncovers Alterations in Corneal Endothelial Metabolism, Pump and Barrier Functions of Slc4a11 KO Mice. *Exp. Eye Res.* 214, 108884. doi:10.1016/j.exer.2021.108884
- Ogando, D. G., Choi, M., Shyam, R., Li, S., and Bonanno, J. A. (2019). Ammonia Sensitive SLC4A11 Mitochondrial Uncoupling Reduces Glutamine Induced Oxidative Stress. *Redox Biol.* 26, 101260. doi:10.1016/j.redox.2019.101260
- Ogando, D. G., Shyam, R., Kim, E. T., Wang, Y.-C., Liu, C.-Y., and Bonanno, J. A. (2021). Inducible Slc4a11 Knockout Triggers Corneal Edema through Perturbation of Corneal Endothelial Pump. *Invest. Ophthalmol. Vis. Sci.* 62, 28. doi:10.1167/iovs.62.7.28
- Okumura, N., Hashimoto, K., Kitahara, M., Okuda, H., Ueda, E., Watanabe, K., et al. (2017a). Activation of TGF- β Signaling Induces Cell Death via the Unfolded Protein Response in Fuchs Endothelial Corneal Dystrophy. *Sci. Rep.* 7, 6801. doi:10.1038/s41598-017-06924-3
- Okumura, N., Kitahara, M., Okuda, H., Hashimoto, K., Ueda, E., Nakahara, M., et al. (2017b). Sustained Activation of the Unfolded Protein Response Induces Cell Death in Fuchs' Endothelial Corneal Dystrophy. *Invest. Ophthalmol. Vis. Sci.* 58, 3697. doi:10.1167/iovs.16-21023
- Ong Tone, S., Kocaba, V., Böhm, M., Wylegala, A., White, T. L., and Jurkunas, U. V. (2021). Fuchs Endothelial Corneal Dystrophy: The Vicious Cycle of Fuchs Pathogenesis. *Prog. Retin. Eye Res.* 80, 100863. doi:10.1016/j.preteyeres.2020.100863
- Qi, L., Tsai, B., and Arvan, P. (2017). New Insights into the Physiological Role of Endoplasmic Reticulum-Associated Degradation. *Trends Cell Biol.* 27, 430–440. doi:10.1016/j.tcb.2016.12.002
- Rashid, H.-O., Yadav, R. K., Kim, H.-R., and Chae, H.-J. (2015). ER Stress: Autophagy Induction, Inhibition and Selection. *Autophagy* 11, 1956–1977. doi:10.1080/15548627.2015.1091141
- Ren, H., Zhai, W., Lu, X., and Wang, G. (2021). The Cross-Links of Endoplasmic Reticulum Stress, Autophagy, and Neurodegeneration in Parkinson's Disease. *Front. Aging Neurosci.* 13, 691881. doi:10.3389/fnagi.2021.691881
- Schönthal, A. H. (2012). Endoplasmic Reticulum Stress: Its Role in Disease and Novel Prospects for Therapy. *Scientifica* 2012, 1–26. doi:10.6064/2012/857516
- Senft, D., and Ronai, Z. e. A. (2015). UPR, Autophagy, and Mitochondria Crosstalk Underlies the ER Stress Response. *Trends Biochem. Sci.* 40, 141–148. doi:10.1016/j.tibs.2015.01.002
- Shyam, R., Ogando, D. G., Choi, M., Liton, P. B., and Bonanno, J. A. (2021). Mitochondrial ROS Induced Lysosomal Dysfunction and Autophagy Impairment in an Animal Model of Congenital Hereditary Endothelial Dystrophy. *Invest. Ophthalmol. Vis. Sci.* 62, 15. doi:10.1167/iovs.62.12.15
- Shyam, R., Ogando, D. G., Kim, E. T., Murugan, S., Choi, M., and Bonanno, J. A. (2022). Rescue of the Congenital Hereditary Endothelial Dystrophy Mouse Model by Adeno-Associated Virus-Mediated Slc4a11 Replacement. *Ophthalmol. Sci.* 2, 100084. doi:10.1016/j.xops.2021.100084
- Vithana, E. N., Morgan, P., Sundaresan, P., Ebenezer, N. D., Tan, D. T. H., Mohamed, M. D., et al. (2006). Mutations in Sodium-Borate Cotransporter SLC4A11 Cause Recessive Congenital Hereditary Endothelial Dystrophy (CHED2). *Nat. Genet.* 38, 755–757. doi:10.1038/ng1824
- Xu, J., Zhou, Q., Xu, W., and Cai, L. (2012). Endoplasmic Reticulum Stress and Diabetic Cardiomyopathy. *Exp. Diabetes Res.* 2012, 1–12. doi:10.1155/2012/827971
- Yoon, S.-B., Park, Y.-H., Choi, S.-A., Yang, H.-J., Jeong, P.-S., Cha, J.-J., et al. (2019). Real-time PCR Quantification of Spliced X-Box Binding Protein 1 (XBP1) Using a Universal Primer Method. *PLoS One* 14, e0219978. doi:10.1371/journal.pone.0219978
- Yorimitsu, T., Nair, U., Yang, Z., and Klionsky, D. J. (2006). Endoplasmic Reticulum Stress Triggers Autophagy. *J. Biol. Chem.* 281, 30299–30304. doi:10.1074/jbc.M607007200
- Zhang, W., Li, H., Ogando, D. G., Li, S., Feng, M., Price, F. W., et al. (2017a). Glutaminolysis Is Essential for Energy Production and Ion Transport in Human Corneal Endothelium. *EBioMedicine* 16, 292–301. doi:10.1016/j.ebiom.2017.01.004
- Zhang, W., Ogando, D. G., Kim, E. T., Choi, M.-J., Li, H., Tenessen, J. M., et al. (2017b). Conditionally Immortal Slc4a11 $^{-/-}$ Mouse Corneal Endothelial Cell Line Recapitulates Disrupted Glutaminolysis Seen in Slc4a11 $^{-/-}$ Mouse Model. *Invest. Ophthalmol. Vis. Sci.* 58, 3723–3731. doi:10.1167/iovs.17-21781

Conflict of Interest: The authors declare that the research was conducted in the absence of any commercial or financial relationships that could be construed as a potential conflict of interest.

Publisher's Note: All claims expressed in this article are solely those of the authors and do not necessarily represent those of their affiliated organizations, or those of the publisher, the editors and the reviewers. Any product that may be evaluated in this article, or claim that may be made by its manufacturer, is not guaranteed or endorsed by the publisher.

Copyright © 2022 Shyam, Ogando and Bonanno. This is an open-access article distributed under the terms of the Creative Commons Attribution License (CC BY). The use, distribution or reproduction in other forums is permitted, provided the original author(s) and the copyright owner(s) are credited and that the original publication in this journal is cited, in accordance with accepted academic practice. No use, distribution or reproduction is permitted which does not comply with these terms.



The ER-Mitochondria Interface as a Dynamic Hub for T Cell Efficacy in Solid Tumors

Elizabeth G. Hunt^{1,2}, Alex M. Andrews^{3,4}, Sydney R. Larsen⁵ and Jessica E. Thaxton^{1,2*}

¹Immunotherapy Program, Lineberger Comprehensive Cancer Center, University of North Carolina, Chapel Hill, NC, United States, ²Department of Cell Biology and Physiology, School of Medicine, University of North Carolina, Chapel Hill, NC, United States, ³Hollings Cancer Center, Charleston, SC, United States, ⁴Department of Orthopedics and Physical Medicine, Medical University of South Carolina, Charleston, SC, United States, ⁵Amherst College, Amherst, MA, United States

OPEN ACCESS

Edited by:

Yongye Huang,
Northeastern University, China

Reviewed by:

Patrick Legembre,
University of Limoges, France
Ulises Ahumada-Castro,
University of Chile, Chile
Roberto Bravo-Sagua,
University of Chile, Chile

*Correspondence:

Jessica E. Thaxton
jess_thaxton@med.unc.edu

Specialty section:

This article was submitted to
Signaling,
a section of the journal
Frontiers in Cell and Developmental
Biology

Received: 01 February 2022

Accepted: 28 March 2022

Published: 27 April 2022

Citation:

Hunt EG, Andrews AM, Larsen SR and
Thaxton JE (2022) The ER-
Mitochondria Interface as a Dynamic
Hub for T Cell Efficacy in Solid Tumors.
Front. Cell Dev. Biol. 10:867341.
doi: 10.3389/fcell.2022.867341

The endoplasmic reticulum (ER) is a large continuous membranous organelle that plays a central role as the hub of protein and lipid synthesis while the mitochondria is the principal location for energy production. T cells are an immune subset exhibiting robust dependence on ER and mitochondrial function based on the need for protein synthesis and secretion and metabolic dexterity associated with foreign antigen recognition and cytotoxic effector response. Intimate connections exist at mitochondrial-ER contact sites (MERCs) that serve as the structural and biochemical platforms for cellular metabolic homeostasis through regulation of fission and fusion as well as glucose, Ca^{2+} , and lipid exchange. Work in the tumor immunotherapy field indicates that the complex interplay of nutrient deprivation and tumor antigen stimulation in the tumor microenvironment places stress on the ER and mitochondria, causing dysfunction in organellar structure and loss of metabolic homeostasis. Here, we assess prior literature that establishes how the structural interface of these two organelles is impacted by the stress of solid tumors along with recent advances in the manipulation of organelle homeostasis at MERCs in T cells. These findings provide strong evidence for increased tumor immunity using unique therapeutic avenues that recharge cellular metabolic homeostasis in T cells.

Keywords: endoplasmic reticulum (ER), ER stress, metabolism, cancer immunotherapy, T cell, tumor microenvironment, MERCs

PRIMER: IMMUNOTHERAPY AND T CELL BIOLOGY

The adaptive immune system plays a substantial role in antitumor response with tumor infiltrating T lymphocytes (TILs) serving as the foundation for targeted cancer immunotherapies as they are responsible for penetrating tumors, recognizing tumor antigen, and directly killing malignant cells. High concentrations of CD8⁺ TILs are correlated with increased survival in multiple solid tumor types (Nakano et al., 2001; Sato et al., 2005; Sharma et al., 2007; Nguyen et al., 2016; Vihervuori et al., 2019), highlighting the critical role T cells play in cancer control. Due to diminished toxicity and robust response rates, development of immunotherapies utilizing TILs has swept the cancer care field. Initial immunotherapy efforts aimed to expand patient TILs *ex vivo* with high dose cytokines in order to infuse the cell product back to a donor, leading to increased tumor control in comparison to systemic treatment with IL-2 (Rosenberg et al., 1988). Since these initial studies, efforts in adoptive cellular therapy (ACT) have aimed to improve durability of the cellular product. Chimeric antigen receptor (CAR) T cell therapy improved upon traditional ACT by imbuing patient-derived T cells with specific,

engineered antigen receptors that bypass the need for major histocompatibility complex (MHC) presentation and coactivation while targeting molecules expressed on malignant cells, allowing T cells to more efficiently attack tumor (Mohanty et al., 2019).

Upon encounter with tumor antigen, both infused and endogenous tumor-specific T cells quickly exhibit exhaustion and undergo apoptosis, leading to loss of tumor control (Long et al., 2015; Davoodzadeh Gholami et al., 2017). Exhaustion is a phenotype defined by reduced proliferation and expression of inhibitory or checkpoint molecules marked by compromised cytotoxic cytokine production (Wherry and Kurachi, 2015). Programmed cell death protein 1 (PD1) is a specific checkpoint molecule enriched on antigen-specific T cells (Petrovas et al., 2006) that binds programmed cell death ligand 1 (PDL1) on tumor cells (Keir et al., 2008). Tumor cells expressing PDL1 evade the immune system through PD1-PDL1 ligation that leads to silenced effector cell function (Freeman et al., 2000) of the antigen-enriched TIL pool. Impairing PD1-PDL1 ligation through deletion of PD1 promotes clearance of tumors expressing PDL1 (Chen and Han, 2015) and monoclonal antibodies that target the interaction to overturn PDL1-mediated inhibition of TILs have revolutionized cancer care.

Naïve CD8+ T cells are exposed to tumor antigen *via* major histocompatibility complex I (MHCI) located on antigen-presenting cells (APCs) and subsequent costimulatory signals induce activation and clonal expansion, resulting in a pool of antigen-specific cells (van Stipdonk et al., 2001). Within the CD8+ TIL pool, subsets of effector and memory cells are capable of development, differing in terms of longevity of antigen response, cytotoxicity, and proliferative ability (Gerlach et al., 2010). The effector subset is highly cytotoxic with a short half-life and low capacity for long-term persistence, defined by interferon- γ (IFN- γ), granzyme B, and perforin secretion. Effector CD8+ T cells have high proliferative capability due in part to autocrine secretion of interleukin-2 (IL-2), but are short-lived upon re-exposure to antigen and subsequent cytotoxicity, dying through activation-induced cell death (Oshima et al., 1976; Smith et al., 1989; Schultz-Cherry et al., 2001; Joshi et al., 2007). From the initial phase of clonal expansion and contraction, a small pool of T cells survives – undergoing molecular changes to generate immunological memory, providing long-lived antigen recognition and rapid recall upon rechallenge (Opferman et al., 1999; Veiga-Fernandes et al., 2000; Kaech and Ahmed, 2001; Kaech et al., 2002).

A seminal discovery for the immunotherapy field was that central memory cells exhibit robust and durable tumor control, often promoting tumor clearance in comparison to effectors (Klebanoff et al., 2005). Similarly, infusion of memory T cells has proven beneficial for CAR T cell therapy, resulting in increased proliferation *in vivo* and vigorous tumor control (Gattinoni et al., 2005; Berger et al., 2008; Wang et al., 2012a; Sommermeyer et al., 2016). Effector and memory T cells are notably defined by their divergent metabolic programs. Prior to activation, naïve T cells exhibit low energy demand marked by high oxidative phosphorylation (OXPHOS) and fatty acid oxidation (FAO) (Pearce et al., 2013; Bantug et al., 2018b).

Upon antigen exposure, differentiation into the effector state requires ATP for expansion, forcing a shift toward aerobic glycolysis (Wieman et al., 2007). In this state of metabolic activation, glucose and amino acid transporters are upregulated, glutaminolysis pathways engage, and FAO is suppressed by upregulation of transcription factor c-Myc (Frauwirth et al., 2002; Wang et al., 2011a; Sinclair et al., 2013). The memory cell metabolic profile opposes that of effectors in displaying sustained OXPHOS and FAO, with the majority of ATP content derived from mitochondrial metabolism (Pearce et al., 2009). Other studies indicate that a source of glucose for memory T cells is stored glycogen produced by an enhanced gluconeogenic cycle. Glycogen catabolism reinforces memory T cell antioxidant capability through generation of reduced glutathione equivalents that prolong survival while imbuing a cell intrinsic source of glucose (Ma et al., 2018).

The distinct metabolic programs of effector and memory cells are the likely cause for their differential antitumor efficacy. The tumor microenvironment (TME) presents a metabolic assault on CD8+ TILs including pH imbalance dysregulating metabolites, amino acid and glucose deprivation (Gajewski et al., 2013), and hypoxia (Petrova et al., 2018), all of which severely undermine the antitumor capability of effector TILs. For example, amino acid availability is crucial for T cell survival and metabolic fitness. Arginine deficiency in the TME compromises T cell tumor control, and L-arginine supplementation in T cells prompts a metabolic shift toward OXPHOS, resulting in therapeutic T cells (Geiger et al., 2016). Glucose deprivation in the TME similarly impairs gene expression events and cytotoxic functions in effector cells (Qiu et al., 2019), but metabolic remodeling of T cells away from glucose dependence drives memory formation and enhances T cell tumor control (Sukumar and Gattinoni, 2014). Also, a picture is emerging that effector cells are disproportionately affected by hypoxia as low oxygen drives abnormal proliferation, forcing increased glucose dependence (Xu et al., 2016) and enhancing terminal exhaustion in the endogenous CD8+ TIL pool (Yu et al., 2020). In contrast, the presence of memory T cells in the tumor bed is often linked to positive immunotherapy outcomes. For example, in the context of checkpoint therapies, memory markers on the TIL pool predict efficacy of treatment (Vanmeerbeek et al., 2021). In order to design successful novel immunotherapies, it is imperative to gain an understanding of the mechanisms through which memory TILs sustain function in the stress of the TME, resisting death, promoting long-lived tumor control.

Tumor Stress Undermines Endoplasmic Reticulum Homeostasis in T Cells

The exquisite persistence of memory T cells in solid tumors is indicative of an intrinsic resistance to the metabolic stress presented by the TME. Perturbations to metabolic homeostasis such as amino acid deprivation, glucose starvation, and hypoxia promote the induction of the unfolded protein response (UPR) (Pan et al., 2003; Bi et al., 2005; Qiu et al., 2010; Bobak et al., 2016; Zanetti et al., 2022) in the endoplasmic reticulum (ER) of cells. As the hub of protein translation, the ER is equipped with three stress sensors, protein kinase RNA-like endoplasmic reticulum kinase

(PERK), inositol-requiring enzyme 1 (IRE1 α), and activating transcription factor 6 (ATF6) poised to sense a burden of unfolded/misfolded proteins in the ER lumen (ER stress) or other challenges to ER function such as lipid dysregulation (Hetz, 2012). The stress sensors initiate signaling pathways collectively referred to as the UPR that promote translational and transcriptional remodeling aimed to restore accurate protein synthesis and folding for re-establishment of cell homeostasis. Where ER stress pervades, pro-apoptotic signaling is enacted through the UPR, linking cell fate to duration and extent of ER stress (Cunha et al., 2012). Effector CD8+ TILs in mouse and human tumors experience ER stress mediated by PERK (Hurst et al., 2019a) and IRE1 α (Song et al., 2018; Yu et al., 2020) and T cell-specific deletion of stress sensors contributes to improved tumor immunity. We have focused on the stress sensor PERK, demonstrating that memory T cells harbor diminished PERK protein relative to effectors (Hurst et al., 2019a) replete with robust reduction of the chronic PERK axis (Hurst et al., 2019a) characterized by transcription factors *Atf4*, *Ddit3* (C/EBP homologous protein (CHOP)) and their downstream transcriptional target *Ero1l* (Han and Kaufman, 2017). Similarly, the IRE1 α -regulated transcription factor X-box-binding protein 1 (XBP1s) was found to contribute to terminal differentiation of antigen-specific T cells, reducing the formation of memory cells (Kamimura and Bevan, 2008). Together, the studies indicate that stress sensors may be differentially regulated among T cell lineages.

Diminished expression of stress sensors could serve to protect memory TILs from metabolic stress in the TME that engage the ER stress response, undermining CD8+ TIL antitumor function. In the TME, CD8+ TILs encounter glucose deprivation, a stress that immediately engages the UPR in glucose-dependent cells (Wengrod et al., 2015). In this context, PERK arrests global cap-dependent translation through phosphorylation of eIF2 α subunit (p-eIF2 α) in an effort to restore cellular proteostasis (Harding et al., 1999). Our data indicate that translation attenuation in effector CD8+ TILs directed by robust upregulation of p-eIF2 α undermines T cell ability to control tumor growth. In contrast, memory-like T cells express diminished p-eIF2 α upon culture in TME conditions, sustaining protein translation and tumor control (Hurst et al., 2020; Riesenberger et al., 2022). In solid tumors, CD8+ TILs encounter lipid stress mediated by exposure to high levels of exogenous tumor-derived cholesterol. Exposure to cholesterol was found to induce terminal exhaustion in CD8+ TILs in a process linked to IRE1 α activation. Inhibition of XBP1s diminished T cell exhaustion and augmented tumor control (Ma et al., 2019). In ovarian cancers, ascites fluid from ovarian cancer patients prohibited glucose uptake by T cells, ultimately leading to IRE1 α -XBP1 activation that repressed mitochondrial respiration. IRE1 α -XBP1 activation was found to prohibit the compensatory mechanism of glutamine uptake needed to maintain mitochondrial respiration in glucose deprived states. The study elegantly demonstrated that XBP1-deficient T cells enriched effector function in mouse models of ovarian cancer, providing evidence for the IRE1 α axis as an immunotherapeutic target in cancer (Song et al., 2018). Together the data suggest that

T cells endowed with mechanisms to support intrinsic resistance to TME metabolic stress exhibit heightened tumor killing capacity.

Tumor Stress Impairs Mitochondrial Function in T Cells

Mitochondrial regulation has largely been the focus of CD8+ TIL immunometabolic study as the intratumoral subset exhibits severe alterations in mitochondrial morphology (Yu et al., 2020). T cells in solid tumors experience diminished mitochondrial biogenesis marked by reduced mitochondrial mass and hypopolarization. Mitochondrial biogenesis, growth, and replication of mitochondria increases mitochondrial mass and metabolic capacities that are crucial for T cell activation, proliferation, and ATP production (Desdin-Mico et al., 2018). Increased biogenesis through overexpression of PPAR- γ coactivator 1 α (PGC1 α) enriches mitochondrial mass and supports T cell tumor control (Scharping et al., 2016). In line with these data, it was discovered that memory T cells have enriched mitochondrial mass relative to effectors, illustrating an intrinsic advantage for stress resistance in the TME (Buck et al., 2016). PD-1 (+) (exhausted) TILs display a reduction and shortening of mitochondrial cristae (Ogando et al., 2019) with disrupted membranes and low mitochondrial activity per unit of mitochondrial mass. Hypoxia was identified as a TME condition that represses PGC1 α expression in PD-1 TILs as hypoxic exposure coupled with persistent antigen stimulation in the TME drove mitochondrial dysfunction marked by excessive mitochondrial reactive oxygen species (ROS), exacerbating the terminal exhaustion state (Yu et al., 2020). Thus, stimulation of mitochondria through ROS signaling or PGC1 α activators augmented the efficacy of T cell response to a-PDL1 therapy (Chamoto et al., 2017). Together, these data illustrate gross dysregulation of mitochondrial biology in CD8+ T cells in tumors.

ENDOPLASMIC RETICULUM-MITOCHONDRIA INTERFACE UNDER PRESSURE

Potential Impacts of Endoplasmic Reticulum-Mitochondrial Interaction in T Cells

The role of the ER in the paradigm of mitochondrial dysfunction in TILs has not been explored. However, studies are emerging that associate CD8+ TIL dysfunction with distress between the two organelles. RNA-seq indicated that exhausted CD8+ TILs experience heightened ER stress relative to other CD8+ TIL subsets, indicative of a profound misfolded protein burden in this T cell pool. Along with exacerbated ER stress, this TIL pool exhibits elevated alterations in mitochondrial morphology characterized by ineffective elimination of damaged mitochondria (mitophagy), abnormal mitochondrial membrane structure, and fewer, shorter cristae compared to autologous splenic T cells (Yu et al., 2020). The data corroborate our previous finding that severe (chronic) ER stress mediated by the PERK axis disproportionately affects exhausted

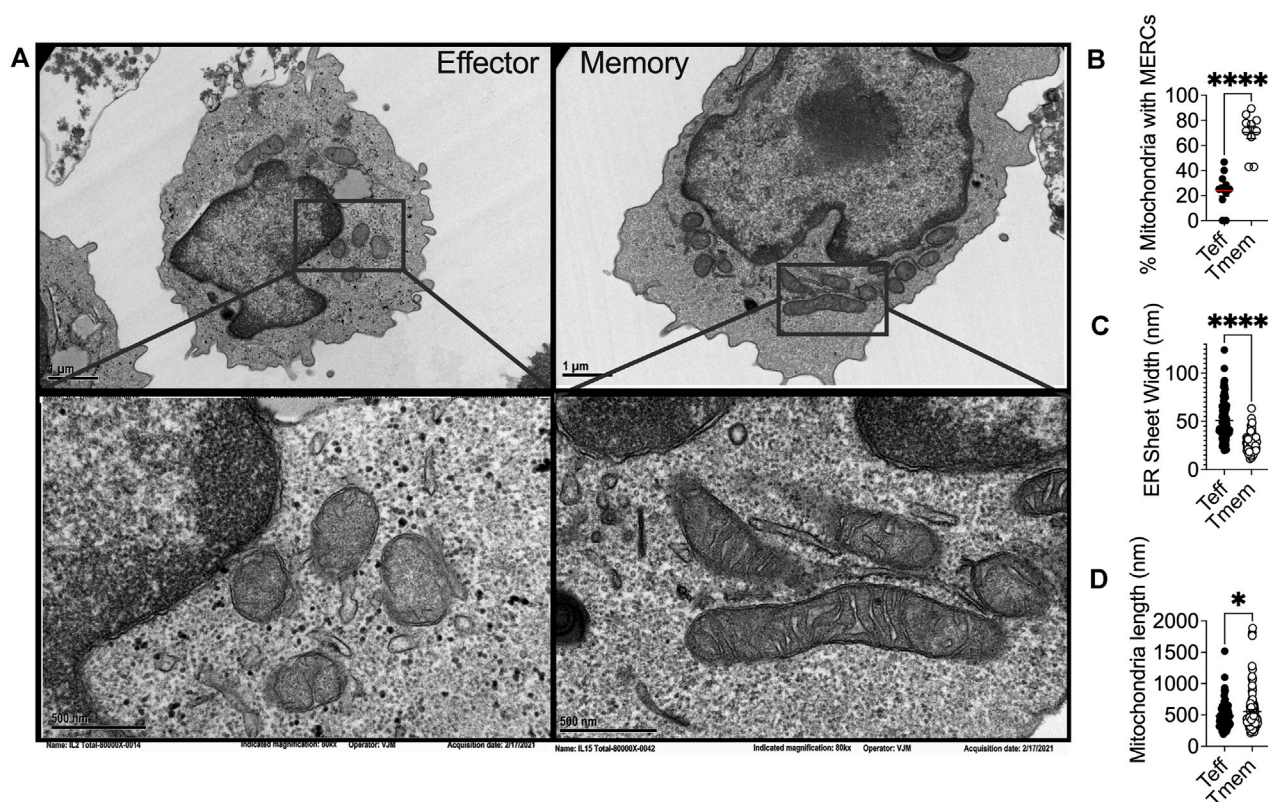


FIGURE 1 | (A) Representative transmission electron microscopy of IL2 and IL15-derived effector and memory-like T cells, respectively, illustrating differential ER and mitochondrial biology in T cell subsets in alignment with previous reports that elucidated the phenomenon. *Ex vivo* expanded OT-1 T cells activated and expanded for 3 days with OVA peptide were conditioned for four more days in IL2 (200U) or IL15 (50 ng/ml) and **(B)** percentage of mitochondria possessing MERCs **(C)** ER luminal width and **(D)** mitochondrial length were quantified.

CD8+ TILs, replete with mitochondria dysfunction marked by excessive ROS generation (Hurst et al., 2019a). Together, a picture is emerging that links ER stress to impaired TIL mitochondrial homeostasis, bringing into question the interaction between the two organelles in tumor immunity.

Stress-Mediated Fission and Fusion at Mitochondrial-Endoplasmic Reticulum Contact Sites

ER stress is associated with mitochondrial dysfunction in multiple disease pathologies (Giacomello and Pellegrini, 2016) and physical interactions between the ER and mitochondria often preclude organellar dysfunction. The ER and mitochondria are physically tethered at close distances of ~10–25 nm (Giacomello and Pellegrini, 2016). These mitochondrial-ER contact sites (MERCs) are unique structures responsible for maintaining physical proximity and biomolecular signals between the two organelles. To this point, over 100 proteins have been identified at these sites as mediators of architecture or biochemical exchange, regulating fission, fusion, calcium (Ca^{2+}), glucose, and lipid metabolism. MERCs may comprise up to 20% of the outer mitochondrial membrane (OMM) (Rizzuto et al., 1998). Though MERCs have not been studied in depth in CD8+TILs, transmission electron microscopy

has been used to demonstrate that memory T cells display enhanced MERCs relative to effectors (Buck et al., 2016) (Figures 1A,B). These findings align with a study conducted on effector memory T cells where, upon activation, effector memory cells displayed increased MERCs compared to naïve counterparts, relying on contact sites to modulate mitochondrial function and rapid generation of IFN- γ (Bantug et al., 2018a).

Endoplasmic Reticulum-Mediated Mitochondrial Fission

MERCs have been identified to play a role in regulating the dynamics of both the ER and mitochondria (Friedman et al., 2010; Friedman et al., 2011). Mitochondria undergo frequent fusion and fission to maintain organellar quality and cell homeostasis (Westermann, 2010) and the process is perceived to be regulated at MERCs. Mitochondrial fission is driven by the dynamin-related GTPase dynamin related protein 1 (Drp1), the fission protein which is recruited to the mitochondrial OMM and forms homo-oligomers around the mitochondria, constricting until one mitochondrion is severed in two (Macdonald et al., 2016). Live-cell imaging demonstrated that ER tubules mediate constriction of mitochondrial membranes, inducing fission in yeast and mammalian cells (Friedman et al., 2011). ER tubules

physically wrap around mitochondria, forming MERCs, as the ER protein inverted formin 2 (INF2) recruits Drp1 from the cytosol to initiate fission. These data implicate MERCs and ER morphology in regulation of fission (Korobova et al., 2013) (Lee et al., 2016). Moreover, INF2 impacts ER-localized actin polymerization, enhancing MERCs formation, inter-organelle Ca^{2+} trafficking, and constriction of the inner mitochondrial membrane (IMM) (Chakrabarti et al., 2018). If MERCs are disrupted by ER tubule reorganization, mitochondrial fission and apoptotic signaling are similarly disturbed (Yedida et al., 2019). This regulation at MERCs may be reciprocal in nature, with disruption of Drp1 leading to disturbed ER morphology as well (Pitts et al., 1999; Westermann, 2011), as Drp1 overexpression can lead to both structural ER changes and mitochondrial fragmentation (Wikstrom et al., 2013; Kobayashi et al., 2020).

In yeast treated with ER stressors, both the ER and the mitochondria displayed expanded membranes prompting ER-mitochondria encounter structures and fission (Kojima et al., 2019). Upon induction of ER stress, the fission protein Drp1 is increased, resulting in mitochondrial fission and fragmentation (Li et al., 2015). ER stress increases MERCs formation, allowing for excessive Ca^{2+} transfer from the ER to mitochondria (Wanget al., 2021b), leading to mitochondrial fission and impaired bioenergetics (Kaddour-Djebbar et al., 2010; Glancy and Balaban, 2012). These data indicate the interconnectivity between chronic ER stress and mitochondrial fragmentation. ER stress can also induce apoptosis through the mitochondria, specifically through remodeling of cristae junctions for cytochrome c release (Zhang et al., 2008; Pinkaew et al., 2017). In response to ROS-induced ER stress, PERK stabilizes MERCs that relay ROS signals between the organelles, and sustains CHOP that induces mitochondrial apoptosis (Verfaillie et al., 2012). The data illuminate chronic ER stress as a driver of mitochondrial morphological changes, fission dynamics, and apoptotic signaling and could explain our previous finding that effector T cells with fragmented mitochondria express dramatically elevated PERK, failing to possess the resiliency and antitumor capabilities of their memory counterparts, expressing fused mitochondria (Figures 1A,D) (Buck et al., 2016) and diminished PERK (Hurst et al., 2019a).

Endoplasmic Reticulum-Associated Mitochondrial Fusion

Differential mitochondrial biogenesis patterns impact T cell differentiation and immunotherapeutic efficacy. The major fusion proteins of mammalian mitochondria are the OMM GTPases mitofusin 1 and 2 (Mfn1/2) and the IMM GTPase optic atrophy 1 (OPA1) (Gao and Hu, 2021). These proteins serve to facilitate the two sequential steps of mitochondrial fusion at the OMM and IMM, respectfully. Mfn2 has been associated with MERCs formation and stabilization. Mfn2 deletion leads to decreased association between the ER and mitochondria, altering organellar morphology, reducing mitochondrial Ca^{2+} uptake (de Brito and Scorrano, 2008; Rizzuto et al., 2012). Similar to what has been observed in fission dynamics, the

position at which mitochondria fusion occurs is marked by ER tubules (Abrisch et al., 2020), once again indicating that ER-mitochondrial interface acts on mitochondrial fission/fusion dynamics. Of note, memory T cells display fused mitochondrial networks (Figures 1A,D) with greater expression of Mfn2 and OPA1 (Buck et al., 2016). In contrast, effector cells require Drp1 for differentiation, with Drp1^{-/-} T cells displaying memory-like phenotype (Simula et al., 2018). Treatment of effector cells with fusion promoter M1 or Drp-1 inhibitor Mdivi-1 enforced fusion, leading to memory T cell development replete with heightened tumor immunity to murine lymphoma (Buck et al., 2016). Increased fusion is associated with organized cristae morphology (Varanita et al., 2015), enhanced oxidative phosphorylation (Rossignol et al., 2004; Simula et al., 2017), and increased mitochondrial mass (Buck et al., 2016), factors that contribute to enhanced persistence and tumor rejection by CD8+ TILs.

In contrast to chronic stress, acute stress in the ER followed by resolution of the unfolded protein burden promotes fusion of mitochondrial membranes. The PERK arm of the UPR is multifaceted in that it attenuates translation to resolve protein stress (Walter and Ron, 2011) and acutely serves to protect mitochondria homeostasis (Rainbolt et al., 2014). PERK localization to MERCs is required for maintenance of MERCs structure, with PERK^{-/-} mouse embryonic fibroblasts (MEFs) displaying decreased association between ER and mitochondrial proteins, fragmented ER morphology (Verfaillie et al., 2012), and fissioned mitochondria (Lebeau et al., 2018). These data indicate that PERK plays a role in modulating mitochondrial fusion and morphology. PERK is critical to production of phosphatidic acid (PA) (Bobrovnikova-Marjon et al., 2012), a lipid responsible for facilitating fusion (Baba et al., 2014), potentially linking resolution of ER stress to mitochondria fusion dynamics through PERK. A direct correlation between PERK activation and mitochondrial dynamics was shown, with PERK-driven phosphorylation of eIF2 α being required for mitochondrial hyperfusion in MEFs treated acutely (6–12 h) with ER stress enhancer Thapsigargin (Tg). However, longer treatments with Tg led to increased mitochondrial fragmentation, supporting the concept that chronic ER stress drives fission (Lebeau et al., 2018). Therefore, it is possible that among T cells, memory cells possess the ability to cope with and resolve ER stress, suggesting a cell intrinsic stress resistance that could explain sustained function in the TME.

Stress-Induced Disruption of Endoplasmic Reticulum Dynamics

Disruption of ER structural homeostasis has been shown to directly impact mitochondrial morphology. The peripheral ER is a dynamic structure that interacts with and regulates numerous organelles including mitochondria and must be continuously remodeled to accommodate various demands such as protein production and folding. T cells are highly secretory and the rough ER acts as the primary site where secreted proteins are translated. Of similar importance in T cells, the smooth ER is the primary site of lipid synthesis (Higgins, 1974) and is the principal storage site

for cellular Ca^{2+} ions (Schwarz and Blower, 2016). As a result of the diverse functions that the rough and smooth ER carry out, the ER is comprised of different sub-structures of sheets and tubules, respectively, that branch out to form a complex network consisting of the luminal compartment (Westrate et al., 2015). The distinct domains remain dynamic and undergo rapid changes (West et al., 2011) with the dense network of ER tubules extending to far edges of the cell enabling the ER to interact with other organelles including mitochondria.

In response to the stress of a protein burden in the ER lumen, the ER expands through proliferation of ER sheets to create increased volume for protein folding demand (Bernales et al., 2006). Cytoskeleton-linking membrane protein (Climp63) is the luminal protein that orchestrates ER expansion. Acting as a spacing protein, Climp63 determines the luminal width of ER sheets with depletion and overexpression resulting in decreased and increased luminal width, respectively (Voeltz et al., 2006; Shibata et al., 2010). In response to ER stress, Climp63 expression is upregulated coincident with UPR signaling (Schuck et al., 2009). Overexpression of Climp63 leads to impaired mitochondrial replication and reduced segregation of mtDNA during fission (Lewis et al., 2016). The impact of Climp63 on the mitochondria solidifies a connection between ER morphological proteins and mitochondrial dynamics and function. ER morphology has not been studied in T cell subsets, nor in the context of immunotherapy. Using transmission electron microscopy, we found that the ER of effector T cells displays expansion in comparison to that of memory cells, quantified by ER luminal width (Figures 1A,C). The data identify for the first time the possibility of differential ER morphology between T cell lineages and raise intrigue surrounding the potential impact of ER structure as a feature of T cell tumor immunity.

BIOCHEMICAL EXCHANGE AT MITOCHONDRIAL-ENDOPLASMIC RETICULUM CONTACT SITES: METABOLIC HUBS

Ca^{2+} , A Matter of Life and Death

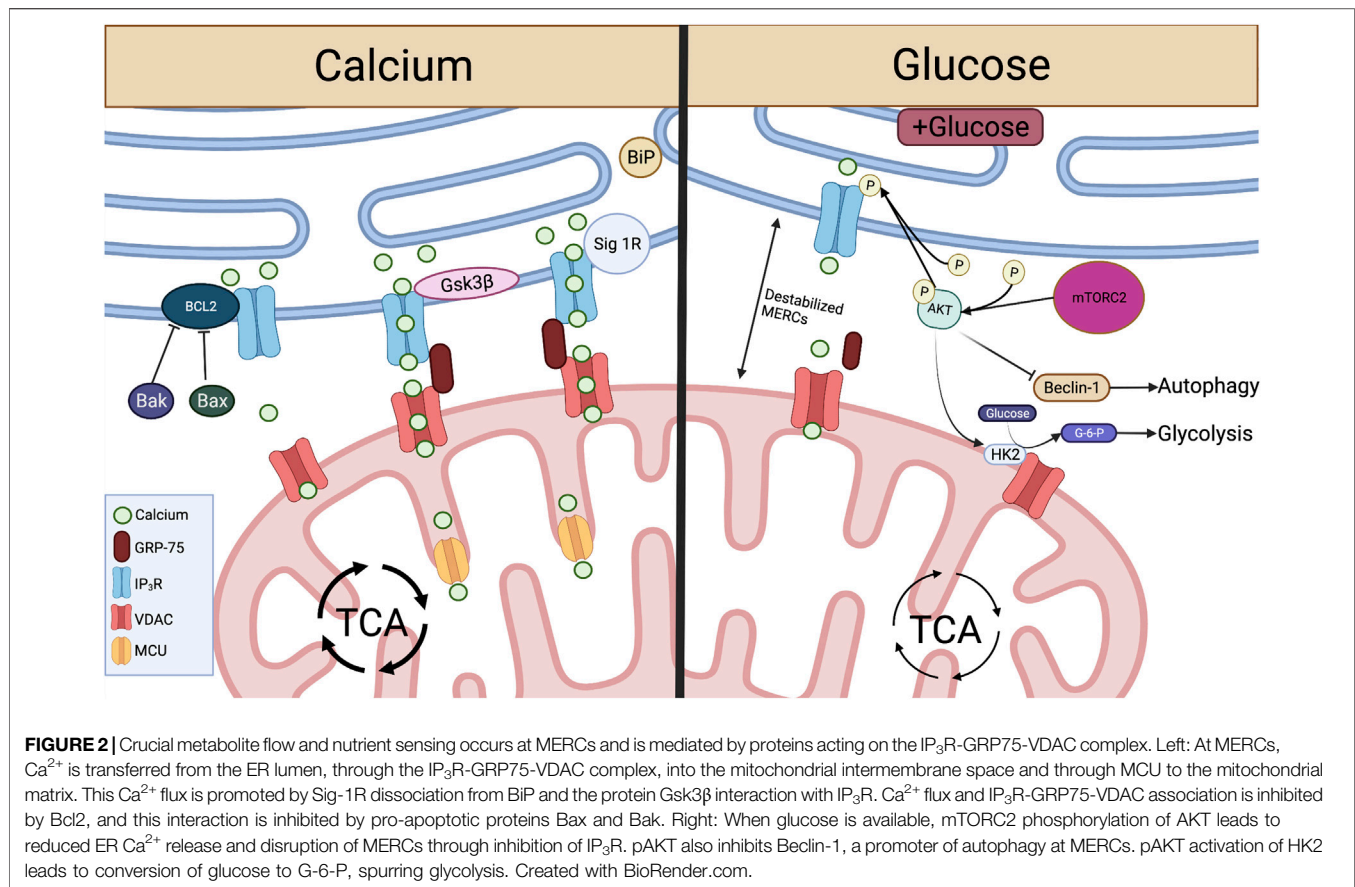
MERCs not only serve to shape structural outcomes between the ER and mitochondria, but are conduits for biochemical exchange, serving to facilitate cellular metabolic programming. Ca^{2+} is a key second messenger regulating apoptosis, exocytosis, and gene transcription (Clapham, 2007), whose exchange is centralized at MERCs. Ca^{2+} metabolism is paramount in T cells given that T cell receptor (TCR) engagement by antigen results in robust release of ER Ca^{2+} to tune the process of T cell activation and lineage fate. When the MHC-antigen complex interacts with the TCR, phospholipase C- γ is phosphorylated leading to cleavage of phosphatidyl inositol, yielding diacylglycerol (DAG) and inositol 1,4,5-triphosphate (IP_3) (Putney, 1986). Upon cleavage, IP_3 binds IP_3 Rs, causing Ca^{2+} release from the ER lumen to cytosol, inducing nuclear factor of activated T-cells (NFAT) transcription (Fenninger and Jefferies, 2019; Hunt et al., 2020; Xiang et al., 2020), followed by IL2 production, T cell

proliferation, and disease control (Klein-Hessling et al., 2017). The ER serves as the largest intracellular Ca^{2+} ion store, relying on Ca^{2+} signaling for normal protein folding and other homeostatic processes (Groenendyk et al., 2021). The ER Ca^{2+} gradient is dependent on import of Ca^{2+} from the cytosol into the ER lumen via sarcoendoplasmic reticulum Ca^{2+} ATPase pump (SERCA). In T cells, prolonged inhibition of SERCA through overexpression of the enzyme phosphoenolpyruvate carboxykinase 1 (Pck1) resulted in increased cytosolic Ca^{2+} that extended NFAT signaling, promoting effector function in tumors (Ho et al., 2015).

Specific microdomains known as “hotspots” have been identified where Ca^{2+} is concentrated around IP_3 R and mitochondria in close contact with the ER (Rizzuto et al., 1993), introducing the concept that transmission of Ca^{2+} between the ER and mitochondria occurs at MERCs. It was later demonstrated that interactions between the ER and mitochondria are regulated by the formation of a molecular bridge comprised of IP_3 R on the ER membrane, voltage dependent anion channels (VDACs) embedded in the OMM, and the chaperone 75-kDa Glucose Regulated Protein (GRP75), which facilitates the physical interaction between the two channels (Marchi et al., 2018). Upon IP_3 binding, Ca^{2+} is released from IP_3 R at the ER and travels through the OMM into the mitochondrial intermembrane space by way of VDAC Ca^{2+} transfer. This interaction and subsequent Ca^{2+} transfer between IP_3 R and VDAC is mediated by appropriate MERCs formation (Honrath et al., 2017; Wang et al., 2021c). As Ca^{2+} enters the mitochondria and accumulates in the intermembrane space it passes through the mitochondrial Ca^{2+} uniporter (MCU) on the IMM to enter the matrix (Raffaello et al., 2016). There, Ca^{2+} activates dehydrogenases crucial for NADH production via the tricarboxylic acid (TCA) cycle (Figure 2), spurring mitochondrial respiration and ATP production (Vinnakota et al., 2016).

MERCs-facilitated Ca^{2+} flux from ER to mitochondria can be enhanced through direct protein-protein interactions with IP_3 R. Glycogen synthase kinase-3 β (Gsk3 β) is responsible for direct phosphorylation of IP_3 R, leading to increased Ca^{2+} transfer through the IP_3 R/GRP75/VDAC complex (Figure 2). However, over enrichment of this interaction drives cell susceptibility to apoptotic Ca^{2+} signaling (Gomez et al., 2016). In T cells targeting tumor, overactivity of Gsk3 β has been linked to poor tumor control. Initial studies demonstrated that Gsk3 β inhibition arrested T cell products prepared for adoptive cell therapy of melanomas in a stem-like state, enabling prolonged self-renewal and impairing differentiation (Gattinoni et al., 2009). The concept translated to the CAR T cell therapy field as Gsk3 β inhibition diminished exhaustion hallmarks in CAR T cells transferred to glioblastomas, resulting in prolonged tumor control (Sengupta et al., 2018). Both studies identified a memory T cell phenotype in the T cell populations characterized by Bcl2^{high} expression, identifying a Ca^{2+} buffering effect by the antiapoptotic protein.

In contrast to enhanced Ca^{2+} flow from the ER to the mitochondria, the Bcl2 protein protects against mitochondria-mediated cell death by stabilizing Ca^{2+} flow through interactions with IP_3 R. Bcl2 is responsible for



inhibition of excessive IP₃R-mediated Ca²⁺ release, protecting cells from apoptotic Ca²⁺ signaling (Rong et al., 2008). Bcl2 also serves to protect cells from excessive ER Ca²⁺ buildup through enhancing IP₃R sensitivity to low levels of IP₃, leading to appropriate Ca²⁺ flow and increased mitochondrial bioenergetics (Eckenrode et al., 2010; White et al., 2005). Conversely, pro-apoptotic proteins Bax and Bak inhibit Bcl2-mediated IP₃R stabilization, leading to reduced IP₃R sensitivity and buildup of ER Ca²⁺, enabling robust Ca²⁺ release to the mitochondria, initiating programmed cell death (Oakes et al., 2005) (**Figure 2**).

The Bcl2 family of proteins are well-known for control of T cell antitumor efficacy. During development, Bcl2 expression is low in immature thymocytes. As T cells mature Bcl2 is increased as it is required for thymocytes to survive, protecting cells from programmed cell death (Shanmuganad et al., 2022). Across different T cell subsets, expression of Bcl2 family members differs, with naïve and memory CD8⁺ T cells expressing elevated Bcl2 in comparison to effectors (Grayson et al., 2000). Moreover, memory differentiation relies on Bcl2 expression as formation is impaired upon Bcl2 inhibition (Kurtulus et al., 2011). The data suggest that Bcl2 is a factor in long-term maintenance of immunity. Overexpression of Bcl2 in tumor-specific T cells promoted cell survival and therapeutic efficacy of adoptively transferred T cells infiltrating mouse melanomas (Charo et al.,

2005; Kalbasi et al., 2010). Other studies of constitutive expression of Bcl2 in CAR-T cells resulted in prolonged T cell survival and tumor control in murine lymphomas (Wang et al., 2021a). Together, these data illustrate the importance of mediated Ca²⁺ flux by Bcl2 in T cell differentiation, longevity, and tumor control.

In addition to protein folding functions, ER chaperone proteins also play a role in control of Ca²⁺ flux and cell survival at MERCs. In a homeostatic state, the ER chaperone protein Sigma-1 Receptor (Sig-1R) localizes to MERCs and complexes with another chaperone, BiP (Grp78). ER Ca²⁺ depletion results in Sig-1R dissociation from BiP and subsequent interaction with IP₃Rs, enabling prolonged influx of Ca²⁺ to the mitochondria. Therefore, overexpression of Sig-1R protects from cellular apoptosis, while depletion enhances cell death (Hayashi and Su, 2007) (**Figure 2**). These studies illustrate the role MERCs play as Ca²⁺ signaling hubs. Though knockout of IP₃Rs leads to diminished ATP and loss of ER-mitochondrial contact maintenance (Cardenas et al., 2010; Bartok et al., 2019), we found that inhibition of IP₃R in antigen-stimulated T cells promotes viability and memory formation. The resultant T cell pool showed enriched mitochondrial ATP reserves and robust capability to control murine melanomas (Thaxton et al., 2017), indicating that modulation of Ca²⁺ flux through IP₃R tuning is intimately tied to T cell metabolism and tumor control.

Glucose, Competing for Control

Ca^{2+} homeostasis is tightly connected to programming of glucose metabolism. Glucose is an essential nutrient for all mammalian cells, serving as a precursor for fatty acids, amino acids, and nucleotides (Navale and Paranjape, 2016). To sustain the energy demands of effector cells, CD8+ T cells shift metabolism from oxidative phosphorylation (OXPHOS) to aerobic glycolysis (Frauwirth et al., 2002; Jones and Thompson, 2007) and this is marked by an increase in glycolytic enzymes, lactate production, and glucose consumption (MacIver et al., 2013; Buck et al., 2015). Glucose is taken up directly by glucose transporters (GLUTs) that reside in the plasma membrane (Navale and Paranjape, 2016) and is phosphorylated by hexokinase 2 (HK2) to form glucose-6-phosphate (G-6-P) which is further broken down *via* glycolysis to pyruvate (Hay, 2016). In the cytosol, pyruvate can be converted to lactate or imported to the mitochondria through VDAC to fuel the Krebs cycle and electron transport chain. Mammalian target of rapamycin complex 1 (mTORC1) is the energy sensing complex that stimulates glycolysis, supporting protein synthesis and cell growth (Mao and Zhang, 2018). In T cells, deletion of negative mTORC1 regulator tuberous sclerosis complex 2 (TSC2) yielded highly differentiated hyper proliferative effector T cells with enhanced glycolytic dependence. T cells with TSC2 deletion resulted in a pool of robust antitumor T cells, but memory formation was impaired *in vivo* (Pollizzi et al., 2015). This study illustrated the importance of mTORC1 to produce the initial wave of effector response for tumor immunity, and the significance of mTORC1 to hinder memory cell metabolism and development of cellular longevity.

In response to glucose limitation, cells induce autophagy, a process by which cell components are catabolized to sustain cell function and viability (Yang and Klionsky, 2010; Dall'Armi et al., 2013). Autophagy has been shown to be critical for memory T cell formation (Xu et al., 2014). Active mTORC1 and glycolysis limit autophagy through disruption of a phosphorylation event carried out by energy deprivation sensor AMP-activated protein kinase (AMPK) (Kim et al., 2011), providing a mechanism to impede cellular degradation in nutrient replete settings. Upon induction of autophagy, a vesicular sac is formed enclosing cytoplasmic contents, resulting in a double membranous autophagosome that fuses with a lysosome to degrade contents (Lamb et al., 2013). Amino acids degraded from the process can be used to sustain translation and energy generation (Onodera and Ohsumi, 2005; Guo et al., 2016). A set of autophagy-related (Atg) proteins carries out the autophagic process and the protein light chain 3 (LC3) is widely observed on autophagosome membranes, thus this often serves as a ubiquitous marker for the process (Kabeya et al., 2000; Mizushima et al., 2004; Maruyama et al., 2014; Schaaf et al., 2016). During viral infection, autophagy was rapidly induced at the peak of effector T cell response, with virus-specific T cells exhibiting robust upregulation of LC3 proteins. T cell-specific gene deletion of the Atg7 or Atg5 proteins resulted in defective autophagy at the peak of effector response and impaired memory cell survival leading to faulty virus control (Xu et al., 2014). These data suggest that T cells with excessive mTORC1 activity and inability to form

memory responses are likely defective in the initiation of autophagy due to abundant glycolysis.

MERCs play a dominant role in glucose sensing for cells to reprogram metabolism during fluctuations in nutrient availability (Tubbs et al., 2014; Theurey et al., 2016). MERCs were first implicated in nutrient-dependent autophagy by Hailey et al. (2010), who found that starvation-induced autophagy was inhibited after disruption of MERCs by Mfn2 deletion. Accumulation of autophagic proteins Atg14L and Atg5 and subsequent autophagosome formation occurred at MERCs in a starvation-dependent manner (Hamasaki et al., 2013). The process was found to be controlled by mammalian target of rapamycin complex 2 (mTORC2), a protein implicated in cell growth and metabolic function. Specifically, mTORC2-driven activation of the protein kinase AKT inhibits autophagy-promoting protein Beclin-1 (Wang et al., 2012b), resulting in suppression of autophagy. In nutrient deprivation, activation of AKT is inhibited (Betz et al., 2013), leading to induction of autophagy at MERCs through recruitment of Beclin-1 (Gelmetti et al., 2017).

MERCs were further linked to nutrient sensing when it was shown that hepatocytes of fasted mice display increased MERC lengths relative to fed counterparts (Sood et al., 2014). In contrast, hepatocytes from fed mice showed increased mitochondrial fragmentation as a result of decreased MERCs association through disrupted IP3R/VDAC1 interaction (Theurey et al., 2016). With increased pAKT and mTORC2 found at MERCs of fed mice (Betz et al., 2013; Tubbs et al., 2014), it has been hypothesized that this MERC disruption is a result of mTORC2 activation of AKT, resulting in inhibition of IP₃R-VDAC interactions at MERCs (Szado et al., 2008; Betz et al., 2013). Glucose serves as the major determinant of these nutrient-dependent changes, with exposure to glucose disrupting MERC interaction both *in vitro* and *in vivo*, leading to increased mitochondrial fission and impaired respiration (Theurey et al., 2016). This can be attributed to mTORC2-AKT signaling, which promotes glucose uptake through activation of glucose transporters (Beg et al., 2017) and stimulates HK2-VDAC interactions, enabling conversion of glucose to G-6-P and therefore glycolysis (Stiles, 2009; Betz et al., 2013) (Figure 2). This AKT-dependent glycolytic switch is particularly important in memory T cells and has been shown to promote rapid effector function upon restimulation with antigen.

Two critical studies have offered insight to the necessity of autophagy in antitumor T cells. The studies draw divergent conclusions, highlighting the need for further study. DeVorkin et al. (2019) showed that T cell autophagy was disadvantageous to tumor control as mice deficient in autophagy genes Atg5, Atg14, and Atg16L1 displayed rejection of prostate, breast, and colorectal tumors. The effect was found to be immune-mediated based on diminished tumor growth in wild type mice reconstituted with Atg5^{-/-} bone marrow, and adoptively transferred tumor antigen-specific Atg5^{-/-} T cells demonstrated impaired antitumor immunity. Mechanistically, autophagy was responsible for metabolic dependence on OXPHOS; thus, limiting autophagy increased glycolysis and supported effector function—promoting tumor control (DeVorkin et al., 2019). This contrasts with a study conducted by Vodnala et al. (2019) T cell exposure to extracellular [K⁺], a cation enriched in the TME, limited

T cell nutrient uptake and induced autophagy, diminishing acetylation of effector genes, promoting proliferation and self-renewal, indicative of stem-like T cells. K⁺-treated T cells were autophagy enriched and represented a pool of T cells with potent cytotoxicity and persistence in the TME that produced tumor clearance (Vodnala et al., 2019). However, the direct contribution of T cell-specific autophagy as a necessity or hindrance for rejection of solid tumors was not addressed. These studies illustrate the need to investigate the role of autophagy in CD8⁺ TIL metabolism and phenotypic modulation, as autophagy could serve as an avenue to enhance T cell-based immunotherapies.

The balance between glucose dependence and autophagy that facilitates memory T cell development is an intriguing concept for understanding how to program effective T cell tumor immunity. On one hand hyperglycolytic T cells are powerful effectors for tumor control. On the other hand, T cells experience glucose deprivation in the TME that undermines their ability to persist as effectors (Ho et al., 2015). Interestingly, chronic low glucose conditioning (Klein Geltink et al., 2020) or long-term inhibition of glycolysis (Sukumar and Gattinoni, 2014) reprogrammed T cells toward a memory phenotype, likely as a result of autophagy induction. These data are intriguing in light of our recent discovery that acute glucose deprivation in T cells in the TME induces acute translation arrest through activation of the ER stress response (PERK-p-eIF2 α), undermining sustained tumor control. We found that metabolic reprogramming of cells toward a memory lineage alleviated the stress response, abrogating p-eIF2 α expression and restoring translation and tumor control to T cells in nutrient deprived environments (Riesenberg et al., 2022). The data raise the possibility that memory cells could use selective autophagy to eliminate stressed ER as a protective measure.

Endoplasmic Reticulum-Associated Signaling and Structures in Autophagy

The ER is a crucial organelle in the autophagic process. ER stress induces autophagy as treatment of cells with nutrient deprivation or ER stressor Tg forced expression of LC3 proteins and formation of autophagosomes. The process appears to be IRE1 α -dependent as deletion of IRE1 α leads to diminished autophagosome formation and impaired cell survival in response to ER stress (Ogata et al., 2006). This ER stress-mediated regulation of autophagy has not been well-studied in T cells, but IRE1 α signaling has generally been found to be detrimental to T cell development and control of tumor growth. While ER stress instigates autophagy, structural entities derived in the ER are crucial components to orchestrate the autophagic response. Both omegasomes, a subdomain of the ER containing a lipid bilayer enriched for phosphatidylinositol 3-phosphate [PI(3)P], and ER-generated lipid droplets (LDs), are integral to initiation of autophagy. Premature phagophores that eventually mature into autophagosomes initiate from the omegasome and their formation accelerates with starvation (Lamb et al., 2013). LDs are organelles originating from ER membranes encapsulated by a phospholipid monolayer, comprised of a neutral lipid core containing triacylglycerols (TAGs) and cholesterol esters (Walther and Farese, 2012; Hashemi and Goodman, 2015; Olzmann and Carvalho, 2019). In this way, LDs are a stored resource of fatty acids (FAs), providing a lipid rich nutrient source that can be released to the mitochondria

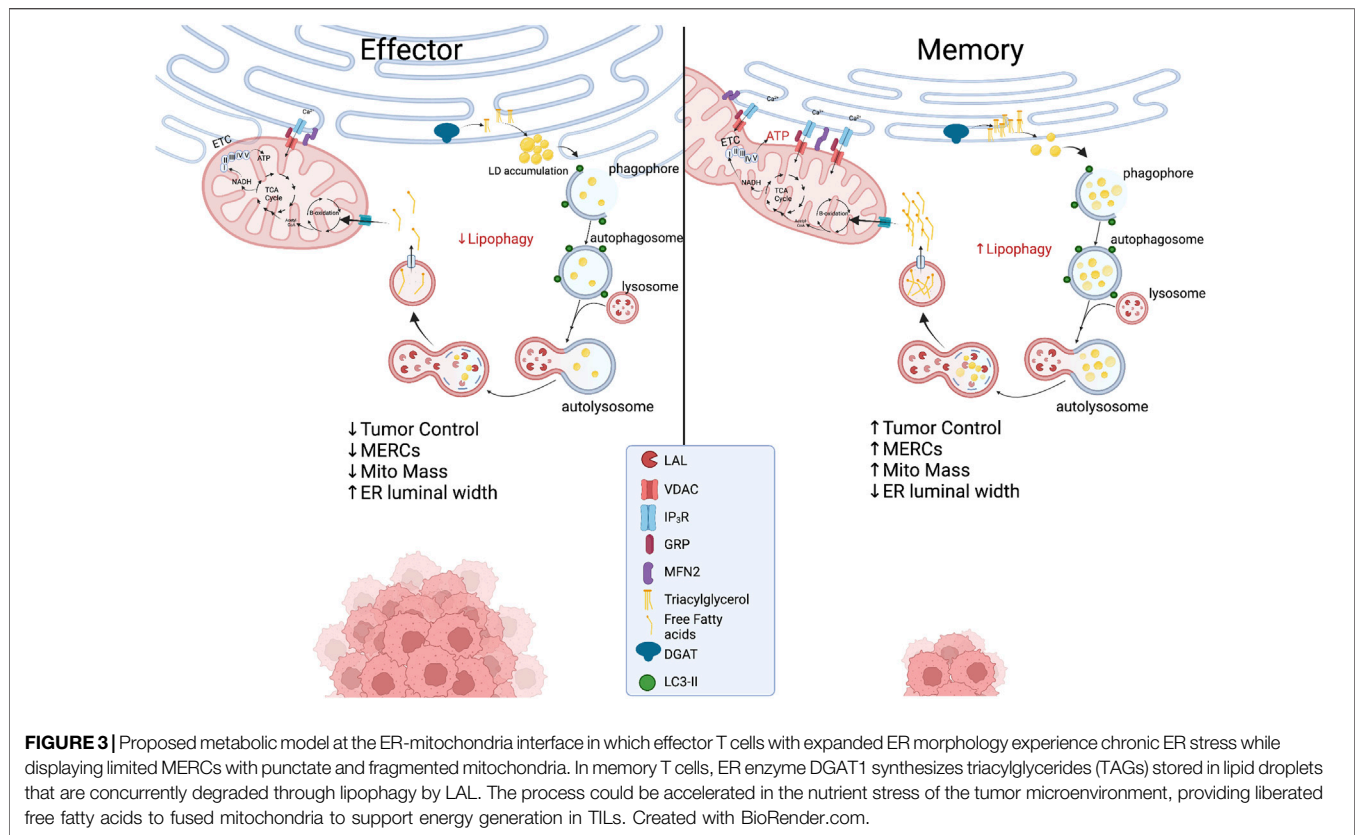
upon nutrient limitation (Yan et al., 2019). In response to autophagy induction, LD formation is accelerated in the ER and LDs can be found in close proximity to the mitochondria, acting as a buffer from chronic ER stress (Velazquez et al., 2016) and supporting FAO-mediated OXPHOS through MERCs (Saito et al., 2019) (Figure 3). In acute myeloid leukemia cells, disruption of MERCs through VDAC1 or Mfn2 depletion diminished lipolysis, autophagosome development, and OXPHOS, highlighting the importance of MERCs to regulate lipid metabolism to support autophagy and survival in cells adapting to stress.

Endoplasmic Reticulum-Associated Signaling and Structures in Lipophagy

As previously discussed, MERCs and autophagy appear to be enriched in memory T cells. A link between ER and mitochondria lipolysis to support autophagy in T cells in tumor stress has not been investigated; however, using pharmacological inhibition, it was discovered that ER-resident diacylglycerol acyltransferases 1/2 (DGAT1/2) that catalyze TAG synthesis sustained FAO and OXPHOS in memory T cells (O'Sullivan et al., 2018). Moreover, overexpression of DGAT1 rescued immunological memory in T cells deficient in TAG synthesis (Cui et al., 2015). Given that LDs were not detected in memory cells, it was discovered that FAs were directly liberated from lysosomes, as the lysosomal acid lipase (LAL) was elevated in memory T cells relative to effectors, proving necessary for cell survival *in vivo* (O'Sullivan et al., 2018). Thus, it is likely that memory cells use lipophagy to access internal lipid stores and this aligns with their superior function and persistence in nutrient deplete settings. Together, the questions remain: Do memory T cells access ER-derived lipid stores to fuel FAO in the stress of solid tumors? If so, is the process dependent on lipophagy and can the process be facilitated through increased interactions at MERCs (Figure 3)? Understanding lipid dynamics could allow for successful design of potent immunotherapies.

Endoplasmic Reticulum-Phagy

A final intriguing concept for tumor immunotherapy is that of ER-phagy, the orchestrated removal of damaged ER. In solid tumors mitophagy, the selective degradation of marred mitochondria, is impaired and results in persistence of dysmorphic mitochondria in CD8⁺ TILs. Similarly, cell stress conditions promote ER-stress induced autophagy as well as the process of selective ER-phagy. ER turnover is enabled by recruitment of autophagic machinery to sections of the ER exposed to extreme ER stress. Retreg1 (*Fam134b*) is among the most researched ER-phagy receptors and binds the LC3/GABARAP protein complex on the autophagosomal membrane mediated by a LC3-containing region (LIR) domain. In mice, disruption of *Fam134b* led to ER expansion, loss of ER turnover, and diminished ER stress resistance resulting in cell death (Khaminets et al., 2015). Nutrient deprivation induces ER degradation (Hamasaki et al., 2005) and in *Fam134b* competent MEFs, starvation induced degradation of Retreg1 was accompanied by loss of Climp63 expression. In contrast, in *Fam134b*^{-/-} MEFs



Climp63 expression remained elevated during nutrient starvation (Khaminets et al., 2015), indicating the paramount role of ER-phagy to promote regulation of ER dynamics in nutrient stress. These findings are intriguing, as they highlight the crucial process of maintaining ER homeostasis in cells through membrane remodeling, but this process has yet to be studied in the context of TILs or ER-mitochondrial interactions.

CONCLUDING REMARKS

MERCs have emerged as regulatory hubs for maintenance of cellular function and survival. The contacts serve as regulatory points in eukaryotic cells, facilitating metabolite exchange and organelle morphology in order to promote cell survival, differentiation, and proliferation. The importance of MERCs is widely recognized in the fields of metabolism and cell biology, but the profound effects of ER-mitochondrial signaling in T cell differentiation and immune function in the suppressive TME are understudied. Our observations indicate that T cell subsets likely display altered ER morphology that could lead to differential MERC formation and mitochondrial morphology. The variability in MERCs likely impacts metabolic signaling, stress response, and autophagic

patterns in T cells, ultimately facilitating the efficacy of an immune response in the TME. Now, we emphasize the need for more comprehensive studies on this topic to elucidate the role of ER-mitochondria interactions responding to cell stress, defining organelle structure, and function in nutrient deprivation in order to help bolster future T cell-based cancer immunotherapies.

AUTHOR CONTRIBUTIONS

Idea and conceptualization by JT and EH. Figures by EH. Writing and original draft preparation by EH, AA, SL, and JT. Visualization and supervision by JT.

FUNDING

1R01CA248359-01 (JET), 1R01CA244361-01A1 (JET), T32 CA 193201 (AMA).

ACKNOWLEDGMENTS

We are grateful to R. Luke Wiseman, PhD for careful critique and review of the manuscript.

REFERENCES

- Abrisch, R. G., Gumbin, S. C., Wisniewski, B. T., Lackner, L. L., and Voeltz, G. K. (2020). Fission and Fusion Machineries Converge at Er Contact Sites to Regulate Mitochondrial Morphology. *J. Cell Biol.* 219. doi:10.1083/jcb.201911122
- Adams, J. M., and Cory, S. (2018). The Bcl-2 Arbiters of Apoptosis and Their Growing Role as Cancer Targets. *Cell Death Differ.* 25, 27–36. doi:10.1038/cdd.2017.161
- Baba, T., Kashiwagi, Y., Arimitsu, N., Kogure, T., Edo, A., Maruyama, T., et al. (2014). Phosphatidic Acid (Pa)-Preferring Phospholipase A1 Regulates Mitochondrial Dynamics. *J. Biol. Chem.* 289, 11497–11511. doi:10.1074/jbc.m113.531921
- Bantug, G. R., Fischer, M., Grählert, J., Balmer, M. L., Unterstab, G., Develioglul, L., et al. (2018a). Mitochondria-Endoplasmic Reticulum Contact Sites Function as Immunometabolic Hubs that Orchestrate the Rapid Recall Response of Memory CD8+ T Cells. *Immunity* 48, 542–555. doi:10.1016/j.immuni.2018.02.012
- Bantug, G. R., Galluzzi, L., Kroemer, G., and Hess, C. (2018b). The Spectrum of T Cell Metabolism in Health and Disease. *Nat. Rev. Immunol.* 18, 19–34. doi:10.1038/nri.2017.99
- Bartok, A., Weaver, D., Golenár, T., Nichtova, Z., Katona, M., Bánsági, S., et al. (2019). Ip3 Receptor Isoforms Differently Regulate Er-Mitochondrial Contacts and Local Calcium Transfer. *Nat. Commun.* 10, 3726. doi:10.1038/s41467-019-11646-3
- Beg, M., Abdullah, N., Thowfeik, F. S., Altorki, N. K., and McGraw, T. E. (2017). Distinct Akt Phosphorylation States Are Required for Insulin Regulated Glut4 and Glut1-Mediated Glucose Uptake. *Elife* 6. doi:10.7554/eLife.26896
- Bental, M., and Deutsch, C. (1993). Metabolic Changes in Activated T Cells: An Nmr Study of Human Peripheral Blood Lymphocytes. *Magn. Reson. Med.* 29, 317–326. doi:10.1002/mrm.1910290307
- Berger, C., Jensen, M. C., Lansdorp, P. M., Gough, M., Elliott, C., and Riddell, S. R. (2008). Adoptive Transfer of Effector Cd8+ T Cells Derived from Central Memory Cells Establishes Persistent T Cell Memory in Primates. *J. Clin. Invest.* 118, 294–305. doi:10.1172/jci32103
- Bernales, S., McDonald, K. L., and Walter, P. (2006). Autophagy Counterbalances Endoplasmic Reticulum Expansion during the Unfolded Protein Response. *Plos Biol.* 4, E423. doi:10.1371/journal.pbio.0040423
- Betz, C., Stracka, D., Prescianotto-Baschong, C., Frieden, M., Demareux, N., and Hall, M. N. (2013). mTOR Complex 2-Akt Signaling at Mitochondria-Associated Endoplasmic Reticulum Membranes (MAM) Regulates Mitochondrial Physiology. *Proc. Natl. Acad. Sci. U.S.A.* 110, 12526–12534. doi:10.1073/pnas.1302455110
- Bi, M., Naczki, C., Koritzinsky, M., Fels, D., Blais, J., Hu, N., et al. (2005). Er Stress-Regulated Translation Increases Tolerance to Extreme Hypoxia and Promotes Tumor Growth. *Embo J.* 24, 3470–3481. doi:10.1038/sj.emboj.7600777
- Bobak, Y., Kurlishchuk, Y., Vynnytska-Myronovska, B., Grydzuk, O., Shuvayeva, G., Redowicz, M. J., et al. (2016). Arginine Deprivation Induces Endoplasmic Reticulum Stress in Human Solid Cancer Cells. *Int. J. Biochem. Cell Biol.* 70, 29–38. doi:10.1016/j.biocel.2015.10.027
- Bobrovnikova-Marjon, E., Pytel, D., Riese, M. J., Vaites, L. P., Singh, N., Koretzky, G. A., et al. (2012). Perk Utilizes Intrinsic Lipid Kinase Activity to Generate Phosphatidic Acid, Mediate Akt Activation, and Promote Adipocyte Differentiation. *Mol. Cell Biol.* 32, 2268–2278. doi:10.1128/mcb.00063-12
- Brunelle, J. K., and Letai, A. (2009). Control of Mitochondrial Apoptosis by the Bcl-2 Family. *J. Cell Sci.* 122, 437–441. doi:10.1242/jcs.031682
- Buck, M. D., O'Sullivan, D., Klein Geltink, R. I., Curtis, J. D., Chang, C.-H., Sanin, D. E., et al. (2016). Mitochondrial Dynamics Controls T Cell Fate through Metabolic Programming. *Cell* 166, 63–76. doi:10.1016/j.cell.2016.05.035
- Buck, M. D., O'Sullivan, D., and Pearce, E. L. (2015). T Cell Metabolism Drives Immunity. *J. Exp. Med.* 212, 1345–1360. doi:10.1084/jem.20151159
- Cárdenas, C., Miller, R. A., Smith, I., Bui, T., Molgó, J., Müller, M., et al. (2010). Essential Regulation of Cell Bioenergetics by Constitutive Insp3 Receptor Ca2+ Transfer to Mitochondria. *Cell* 142, 270–283. doi:10.1016/j.cell.2010.06.007
- Carreras-Sureda, A., Pihán, P., and Hetz, C. (2018). Calcium Signaling at the Endoplasmic Reticulum: Fine-Tuning Stress Responses. *Cell Calcium* 70, 24–31. doi:10.1016/j.ceca.2017.08.004
- Chakrabarti, R., Ji, W.-K., Stan, R. V., De Juan Sanz, J., Ryan, T. A., and Higgs, H. N. (2018). Inf2-Mediated Actin Polymerization at the Er Stimulates Mitochondrial Calcium Uptake, Inner Membrane Constriction, and Division. *J. Cell Biol.* 217, 251–268. doi:10.1083/jcb.201709111
- Cham, C. M., Driessens, G., O'keefe, J. P., and Gajewski, T. F. (2008). Glucose Deprivation Inhibits Multiple Key Gene Expression Events and Effector Functions in Cd8+ T Cells. *Eur. J. Immunol.* 38, 2438–2450. doi:10.1002/eji.200838289
- Cham, C. M., and Gajewski, T. F. (2005). Glucose Availability Regulates IFN- γ Production and p70S6 Kinase Activation in CD8+ Effector T Cells. *J. Immunol.* 174, 4670–4677. doi:10.4049/jimmunol.174.8.4670
- Chami, M., Oulès, B., Szabadkai, G., Tacine, R., Rizzuto, R., and Paterlini-Bréchet, P. (2008). Role of Serca1 Truncated Isoform in the Proapoptotic Calcium Transfer from Er to Mitochondria during Er Stress. *Mol. Cell* 32, 641–651. doi:10.1016/j.molcel.2008.11.014
- Chamoto, K., Chowdhury, P. S., Kumar, A., Sonomura, K., Matsuda, F., Fagarasan, S., et al. (2017). Mitochondrial Activation Chemicals Synergize with Surface Receptor Pd-1 Blockade for T Cell-dependent Antitumor Activity. *Proc. Natl. Acad. Sci. U S A.* 114, E761–E770. doi:10.1073/pnas.1620433114
- Chang, C.-H., Qiu, J., O'Sullivan, D., Buck, M. D., Noguchi, T., Curtis, J. D., et al. (2015). Metabolic Competition in the Tumor Microenvironment Is A Driver of Cancer Progression. *Cell* 162, 1229–1241. doi:10.1016/j.cell.2015.08.016
- Charo, J., Finkelstein, S. E., Grewal, N., Restifo, N. P., Robbins, P. F., and Rosenberg, S. A. (2005). Bcl-2 Overexpression Enhances Tumor-specific T-Cell Survival. *Cancer Res.* 65, 2001–2008. doi:10.1158/0008-5472.can-04-2006
- Chen, L., and Han, X. (2015). Anti-Pd-1/Pd-L1 Therapy of Human Cancer: Past, Present, and Future. *J. Clin. Invest.* 125, 3384–3391. doi:10.1172/jci80011
- Cho, B. K., Wang, C., Sugawa, S., Eisen, H. N., and Chen, J. (1999). Functional Differences between Memory and Naive Cd8 T Cells. *Proc. Natl. Acad. Sci. U.S.A.* 96, 2976–2981. doi:10.1073/pnas.96.6.2976
- Chonghaile, T. N., Gupta, S., John, M., Szegezdi, E., Logue, S. E., and Samali, A. (2015). Bcl-2 Modulates the Unfolded Protein Response by Enhancing Splicing of X-Box Binding Protein-1. *Biochem. Biophysical Res. Commun.* 466, 40–45. doi:10.1016/j.bbrc.2015.08.100
- Clapham, D. E. (2007). Calcium Signaling. *Cell* 131, 1047–1058. doi:10.1016/j.cell.2007.11.028
- Cousens, L. P., Orange, J. S., and Biron, C. A. (1995). Endogenous Il-2 Contributes to T Cell Expansion and Ifn-Gamma Production during Lymphocytic Choriomeningitis Virus Infection. *J. Immunol.* 155, 5690–5699.
- Csordás, G., Renken, C., Várnai, P., Walter, L., Weaver, D., Buttle, K. F., et al. (2006). Structural and Functional Features and Significance of the Physical Linkage between Er and Mitochondria. *J. Cell Biol.* 174, 915–921. doi:10.1083/jcb.200604016
- Cui, G., Staron, M. M., Gray, S. M., Ho, P.-C., Amezcua, R. A., Wu, J., et al. (2015). Il-7-Induced Glycerol Transport and Tag Synthesis Promotes Memory Cd8+ T Cell Longevity. *Cell* 161, 750–761. doi:10.1016/j.cell.2015.03.021
- Cunha, D. A., Igoillo-Esteve, M., Gurzov, E. N., Germano, C. M., Naamane, N., Marhfour, I., et al. (2012). Death Protein 5 and P53-Upregulated Modulator of Apoptosis Mediate the Endoplasmic Reticulum Stress-Mitochondrial Dialog Triggering Lipotoxic Rodent and Human β -Cell Apoptosis. *Diabetes* 61, 2763–2775. doi:10.2337/db12-0123
- Dall'Armi, C., Devereaux, K. A., and Di Paolo, G. (2013). The Role of Lipids in the Control of Autophagy. *Curr. Biol.* 23, R33–R45. doi:10.1016/j.cub.2012.10.041
- Davoodzadeh Gholami, M., Kardar, G. A., Saeedi, Y., Heydari, S., Garssen, J., and Falak, R. (2017). Exhaustion of T Lymphocytes in the Tumor Microenvironment: Significance and Effective Mechanisms. *Cell Immunol.* 322, 1–14. doi:10.1016/j.cellimm.2017.10.002
- de Brito, O. M., and Scorrano, L. (2008). Mitofusin 2 Tethers Endoplasmic Reticulum to Mitochondria. *Nature* 456, 605–610. doi:10.1038/nature07534
- Degenhardt, K., Sundararajan, R., Lindsten, T., Thompson, C., and White, E. (2002). Bax and Bak Independently Promote Cytochrome cRelease from Mitochondria. *J. Biol. Chem.* 277, 14127–14134. doi:10.1074/jbc.m109939200
- Desdín-Micó, G., Soto-Herederó, G., and Mittelbrunn, M. (2018). Mitochondrial Activity in T Cells. *Mitochondrion* 41, 51–57. doi:10.1016/j.mito.2017.10.006

- DeVorkin, L., Pavey, N., Carleton, G., Comber, A., Ho, C., Lim, J., et al. (2019). Autophagy Regulation of Metabolism Is Required for CD8+ T Cell Anti-tumor Immunity. *Cell Rep.* 27, 502–513. doi:10.1016/j.celrep.2019.03.037
- Eckenrode, E. F., Yang, J., Velmurugan, G. V., Foscett, J. K., and White, C. (2010). Apoptosis Protection by Mcl-1 and Bcl-2 Modulation of Inositol 1,4,5-Trisphosphate Receptor-dependent Ca²⁺ Signaling. *J. Biol. Chem.* 285, 13678–13684. doi:10.1074/jbc.M109.096040
- Fanger, C. M., Hoth, M., Crabtree, G. R., and Lewis, R. S. (1995). Characterization of T Cell Mutants with Defects in Capacitative Calcium Entry: Genetic Evidence for the Physiological Roles of Crac Channels. *J. Cell Biol.* 131, 655–667. doi:10.1083/jcb.131.3.655
- Fenninger, F., and Jefferies, W. A. (2019). What's Bred in the Bone: Calcium Channels in Lymphocytes. *J. I.* 202, 1021–1030. doi:10.4049/jimmunol.1800837
- Frauwirth, K. A., Riley, J. L., Harris, M. H., Parry, R. V., Rathmell, J. C., Plas, D. R., et al. (2002). The Cd28 Signaling Pathway Regulates Glucose Metabolism. *Immunity* 16, 769–777. doi:10.1016/s1074-7613(02)00323-0
- Freeman, G. J., Long, A. J., Iwai, Y., Bourque, K., Chernova, T., Nishimura, H., et al. (2000). Engagement of the Pd-1 Immunoinhibitory Receptor by A Novel B7 Family Member Leads to Negative Regulation of Lymphocyte Activation. *J. Exp. Med.* 192, 1027–1034. doi:10.1084/jem.192.7.1027
- Fridman, W. H., Pagès, F., Sautès-Fridman, C., and Galon, J. (2012). The Immune Contexture in Human Tumours: Impact on Clinical Outcome. *Nat. Rev. Cancer* 12, 298–306. doi:10.1038/nrc3245
- Friedman, J. R., Lackner, L. L., West, M., Dibenedetto, J. R., Nunnari, J., and Voeltz, G. K. (2011). Er Tubules Mark Sites of Mitochondrial Division. *Science* 334, 358–362. doi:10.1126/science.1207385
- Friedman, J. R., Webster, B. M., Mastronarde, D. N., Verhey, K. J., and Voeltz, G. K. (2010). Er Sliding Dynamics and Er-Mitochondrial Contacts Occur on Acetylated Microtubules. *J. Cell Biol.* 190, 363–375. doi:10.1083/jcb.200911024
- Gajewski, T. F., Schreiber, H., and Fu, Y.-X. (2013). Innate and Adaptive Immune Cells in the Tumor Microenvironment. *Nat. Immunol.* 14, 1014–1022. doi:10.1038/ni.2703
- Gao, S., and Hu, J. (2021). Mitochondrial Fusion: The Machineries in and Out. *Trends Cell Biol.* 31, 62–74. doi:10.1016/j.tcb.2020.09.008
- Gattinoni, L., Klebanoff, C. A., Palmer, D. C., Wrzesinski, C., Kerstann, K., Yu, Z., et al. (2005). Acquisition of Full Effector Function *In Vitro* Paradoxically Impairs the *In Vivo* Antitumor Efficacy of Adoptively Transferred Cd8+ T Cells. *J. Clin. Invest.* 115, 1616–1626. doi:10.1172/jci24480
- Gattinoni, L., Zhong, X.-S., Palmer, D. C., Ji, Y., Hinrichs, C. S., Yu, Z., et al. (2009). Wnt Signaling Arrests Effector T Cell Differentiation and Generates Cd8+ Memory Stem Cells. *Nat. Med.* 15, 808–813. doi:10.1038/nm.1982
- Geiger, R., Rieckmann, J. C., Wolf, T., Basso, C., Feng, Y., Fuhrer, T., et al. (2016). L-arginine Modulates T Cell Metabolism and Enhances Survival and Anti-tumor Activity. *Cell* 167, 829–842. doi:10.1016/j.cell.2016.09.031
- Gelmetti, V., De Rosa, P., Torosantucci, L., Marini, E. S., Romagnoli, A., Di Rienzo, M., et al. (2017). Pink1 and Becn1 Relocalize at Mitochondria-Associated Membranes during Mitophagy and Promote Er-Mitochondria Tethering and Autophagosome Formation. *Autophagy* 13, 654–669. doi:10.1080/15548627.2016.1277309
- Gerlach, C., Van Heijst, J. W. J., Swart, E., Sie, D., Armstrong, N., Kerkhoven, R. M., et al. (2010). One Naive T Cell, Multiple Fates in Cd8+ T Cell Differentiation. *J. Exp. Med.* 207, 1235–1246. doi:10.1084/jem.20091175
- Giacomello, M., and Pellegrini, L. (2016). The Coming of Age of the Mitochondria-Er Contact: A Matter of Thickness. *Cell Death Differ* 23, 1417–1427. doi:10.1038/cdd.2016.52
- Glancy, B., and Balaban, R. S. (2012). Role of Mitochondrial Ca²⁺ in the Regulation of Cellular Energetics. *Biochemistry* 51, 2959–2973. doi:10.1021/bi2018909
- Gomez, L., Thiebaut, P.-A., Paillard, M., Ducreux, S., Abrial, M., Crola Da Silva, C., et al. (2016). The SR/ER-mitochondria Calcium Crosstalk Is Regulated by GSK3 β during Reperfusion Injury. *Cell Death Differ* 23, 313–322. doi:10.1038/cdd.2015.101
- Gratiot-Deans, J., Merino, R., Nuñez, G., and Turka, L. A. (1994). Bcl-2 Expression during T-Cell Development: Early Loss and Late Return Occur at Specific Stages of Commitment to Differentiation and Survival. *Proc. Natl. Acad. Sci. U.S.A.* 91, 10685–10689. doi:10.1073/pnas.91.22.10685
- Grayson, J. M., Zajac, A. J., Altman, J. D., and Ahmed, R. (2000). Cutting Edge: Increased Expression of Bcl-2 in Antigen-specific Memory Cd8+ T Cells. *J. Immunol.* 164, 3950–3954. doi:10.4049/jimmunol.164.8.3950
- Groenendyk, J., Agellon, L. B., and Michalak, M. (2021). Calcium Signaling and Endoplasmic Reticulum Stress. *Int. Rev. Cell Mol Biol* 363, 1–20. doi:10.1016/bs.ircmb.2021.03.003
- Guo, J. Y., Teng, X., Laddha, S. V., Ma, S., Van Nostrand, S. C., Yang, Y., et al. (2016). Autophagy Provides Metabolic Substrates to Maintain Energy Charge and Nucleotide Pools in Ras-Driven Lung Cancer Cells. *Genes Dev.* 30, 1704–1717. doi:10.1101/gad.283416.116
- Hailey, D. W., Rambold, A. S., Satpute-Krishnan, P., Mitra, K., Sougrat, R., Kim, P. K., et al. (2010). Mitochondria Supply Membranes for Autophagosome Biogenesis during Starvation. *Cell* 141, 656–667. doi:10.1016/j.cell.2010.04.009
- Hales, C. N., Luzio, J. P., Chandler, J. A., and Herman, L. (1974). Localization of Calcium in the Smooth Endoplasmic Reticulum of Rat Isolated Fat Cells. *J. Cell Sci* 15, 1–15. doi:10.1242/jcs.15.1.1
- Hamasaki, M., Furuta, N., Matsuda, A., Nezu, A., Yamamoto, A., Fujita, N., et al. (2013). Autophagosomes Form at Er-Mitochondria Contact Sites. *Nature* 495, 389–393. doi:10.1038/nature11910
- Hamasaki, M., Noda, T., Baba, M., and Ohsumi, Y. (2005). Starvation Triggers the Delivery of the Endoplasmic Reticulum to the Vacuole via Autophagy in Yeast. *Traffic* 6, 56–65. doi:10.1111/j.1600-0854.2004.00245.x
- Han, J., and Kaufman, R. J. (2017). Physiological/Pathological Ramifications of Transcription Factors in the Unfolded Protein Response. *Genes Dev.* 31, 1417–1438. doi:10.1101/gad.297374.117
- Harding, H. P., Zhang, Y., and Ron, D. (1999). Protein Translation and Folding Are Coupled by an Endoplasmic-Reticulum-Resident Kinase. *Nature* 397, 271–274. doi:10.1038/16729
- Hashemi, H. F., and Goodman, J. M. (2015). The Life Cycle of Lipid Droplets. *Curr. Opin. Cell Biol.* 33, 119–124. doi:10.1016/j.cob.2015.02.002
- Hay, N. (2016). Reprogramming Glucose Metabolism in Cancer: Can it Be Exploited for Cancer Therapy? *Nat. Rev. Cancer* 16, 635–649. doi:10.1038/nrc.2016.77
- Hayashi, T., and Su, T.-P. (2007). Sigma-1 Receptor Chaperones at the ER-Mitochondrion Interface Regulate Ca²⁺ Signaling and Cell Survival. *Cell* 131, 596–610. doi:10.1016/j.cell.2007.08.036
- Hetz, C. (2012). The Unfolded Protein Response: Controlling Cell Fate Decisions under Er Stress and beyond. *Nat. Rev. Mol. Cell Biol* 13, 89–102. doi:10.1038/nrm3270
- Higgins, J. A. (1974). Studies on the Biogenesis of Smooth Endoplasmic Reticulum Membranes in Hepatocytes of Phenobarbital-Treated Rats. *J. Cell Biol* 62, 635–646. doi:10.1083/jcb.62.3.635
- Ho, P.-C., Bihuniak, J. D., Macintyre, A. N., Staron, M., Liu, X., Amezcua, R., et al. (2015). Phosphoenolpyruvate Is a Metabolic Checkpoint of Anti-tumor T Cell Responses. *Cell* 162, 1217–1228. doi:10.1016/j.cell.2015.08.012
- Honrath, B., Metz, I., Bendridi, N., Rieusset, J., Culmsee, C., and Dolga, A. M. (2017). Glucose-Regulated Protein 75 Determines Er-Mitochondrial Coupling and Sensitivity to Oxidative Stress in Neuronal Cells. *Cell Death Discov.* 3, 17076. doi:10.1038/cddiscovery.2017.76
- Hsieh, W.-C., Sutter, B. M., Ruess, H., Barnes, S. D., Malladi, V. S., and Tu, B. P. (2022). Glucose Starvation Induces A Switch in the Histone Acetylome for Activation of Gluconeogenic and Fat Metabolism Genes. *Mol. Cell* 82, 60–74. doi:10.1016/j.molcel.2021.12.015
- Hunt, H., Tilunaité, A., Bass, G., Soeller, C., Roderick, H. L., Rajagopal, V., et al. (2020). Ca²⁺ Release via IP3 Receptors Shapes the Cardiac Ca²⁺ Transient for Hypertrophic Signaling. *Biophysical J.* 119, 1178–1192. doi:10.1016/j.bpj.2020.08.001
- Hurst, K. E., Lawrence, K. A., Reyes Angeles, L., Ye, Z., Zhang, J., Townsend, D. M., et al. (2019b). Endoplasmic Reticulum Protein Disulfide Isomerase Shapes T Cell Efficacy for Adoptive Cellular Therapy of Tumors. *Cells* 8. doi:10.3390/cells8121514
- Hurst, K. E., Lawrence, K. A., Essman, M. T., Walton, Z. J., Leddy, L. R., and Thaxton, J. E. (2019a). Endoplasmic Reticulum Stress Contributes to Mitochondrial Exhaustion of CD8+ T Cells. *Cancer Immunol. Res.* 7, 476–486. doi:10.1158/2326-6066.cir-18-0182
- Hurst, K. E., Lawrence, K. A., Robino, R. A., Ball, L. E., Chung, D., and Thaxton, J. E. (2020). Remodeling Translation Primes CD8+ T-Cell Antitumor Immunity. *Cancer Immunol. Res.* 8, 587–595. doi:10.1158/2326-6066.cir-19-0516
- Ingerman, E., Perkins, E. M., Marino, M., Mears, J. A., Mccaffery, J. M., Hinshaw, J. E., et al. (2005). Dnm1 Forms Spirals that Are Structurally

- Tailored to Fit Mitochondria. *J. Cell Biol* 170, 1021–1027. doi:10.1083/jcb.200506078
- Ishihara, N., Fujita, Y., Oka, T., and Mihara, K. (2006). Regulation of Mitochondrial Morphology through Proteolytic Cleavage of Opa1. *Embo J.* 25, 2966–2977. doi:10.1038/sj.emboj.7601184
- Iwai, Y., Ishida, M., Tanaka, Y., Okazaki, T., Honjo, T., and Minato, N. (2002). Involvement of Pd-L1 on Tumor Cells in the Escape from Host Immune System and Tumor Immunotherapy by Pd-L1 Blockade. *Proc. Natl. Acad. Sci. U.S.A.* 99, 12293–12297. doi:10.1073/pnas.192461099
- Janikiewicz, J., Szymański, J., Malinska, D., Patalas-Krawczyk, P., Michalska, B., Duszyński, J., et al. (2018). Mitochondria-Associated Membranes in Aging and Senescence: Structure, Function, and Dynamics. *Cell Death Dis* 9, 332. doi:10.1038/s41419-017-0105-5
- Jones, R. G., and Thompson, C. B. (2007). Revving the Engine: Signal Transduction Fuels T Cell Activation. *Immunity* 27, 173–178. doi:10.1016/j.immuni.2007.07.008
- Joshi, N. S., Cui, W., Chandele, A., Lee, H. K., Urso, D. R., Hagman, J., et al. (2007). Inflammation Directs Memory Precursor and Short-Lived Effector CD8+ T Cell Fates via the Graded Expression of T-Bet Transcription Factor. *Immunity* 27, 281–295. doi:10.1016/j.immuni.2007.07.010
- Kabeya, Y., Mizushima, N., Ueno, T., Yamamoto, A., Kirisako, T., Noda, T., et al. (2000). Lc3, A Mammalian Homologue of Yeast Apg8p, Is Localized in Autophagosome Membranes after Processing. *Embo J.* 19, 5720–5728. doi:10.1093/emboj/19.21.5720
- Kaddour-Djebbar, I., Choudhary, V., Brooks, C., Ghazaly, T., Lakshmikanthan, V., Dong, Z., et al. (2010). Specific Mitochondrial Calcium Overload Induces Mitochondrial Fission in Prostate Cancer Cells. *Int. J. Oncol.* 36, 1437–1444. doi:10.3892/ijo.00000629
- Kaech, S. M., and Ahmed, R. (2001). Memory CD8+ T Cell Differentiation: Initial Antigen Encounter Triggers a Developmental Program in Naïve Cells. *Nat. Immunol.* 2, 415–422. doi:10.1038/87720
- Kaech, S. M., Hemby, S., Kersh, E., and Ahmed, R. (2002). Molecular and Functional Profiling of Memory CD8 T Cell Differentiation. *Cell* 111, 837–851. doi:10.1016/s0092-8674(02)01139-x
- Kalbasi, A., Shirmali, R. K., Chinnasamy, D., and Rosenberg, S. A. (2010). Prevention of Interleukin-2 Withdrawal-Induced Apoptosis in Lymphocytes Retrovirally Cotransduced with Genes Encoding an Antitumor T-Cell Receptor and an Antiapoptotic Protein. *J. Immunother.* 33, 672–683. doi:10.1097/cji.0b013e3181e475cd
- Kamimura, D., and Bevan, M. J. (2008). Endoplasmic Reticulum Stress Regulator Xbp-1 Contributes to Effector Cd8+ T Cell Differentiation during Acute Infection. *J. Immunol.* 181, 5433–5441. doi:10.4049/jimmunol.181.8.5433
- Keir, M. E., Butte, M. J., Freeman, G. J., and Sharpe, A. H. (2008). Pd-1 and its Ligands in Tolerance and Immunity. *Annu. Rev. Immunol.* 26, 677–704. doi:10.1146/annurev.immunol.26.021607.090331
- Khaminets, A., Heinrich, T., Mari, M., Grumati, P., Huebner, A. K., Akutsu, M., et al. (2015). Regulation of Endoplasmic Reticulum Turnover by Selective Autophagy. *Nature* 522, 354–358. doi:10.1038/nature14498
- Kim, J., Kundu, M., Viollet, B., and Guan, K.-L. (2011). Ampk and Mtor Regulate Autophagy through Direct Phosphorylation of Ulk1. *Nat. Cell Biol* 13, 132–141. doi:10.1038/ncb2152
- Klebanoff, C. A., Gattinoni, L., Torabi-Parizi, P., Kerstann, K., Cardones, A. R., Finkelstein, S. E., et al. (2005). Central Memory Self/tumor-Reactive CD8 + T Cells Confer superior Antitumor Immunity Compared with Effector Memory T Cells. *Proc. Natl. Acad. Sci. U.S.A.* 102, 9571–9576. doi:10.1073/pnas.0503726102
- Klein Geltink, R. I., Edwards-Hicks, J., Apostolova, P., O'Sullivan, D., Sanin, D. E., Patterson, A. E., et al. (2020). Metabolic Conditioning of CD8+ Effector T Cells for Adoptive Cell Therapy. *Nat. Metab.* 2, 703–716. doi:10.1038/s42255-020-0256-z
- Klein-Hessling, S., Muhammad, K., Klein, M., Pusch, T., Rudolf, R., Flöter, J., et al. (2017). NFATc1 Controls the Cytotoxicity of CD8+ T Cells. *Nat. Commun.* 8, 511. doi:10.1038/s41467-017-00612-6
- Kobayashi, S., Zhao, F., Zhang, Z., Kobayashi, T., Huang, Y., Shi, B., et al. (2020). Mitochondrial Fission and Mitophagy Coordinately Restrict High Glucose Toxicity in Cardiomyocytes. *Front. Physiol.* 11, 604069. doi:10.3389/fphys.2020.604069
- Kojima, R., Kakimoto, Y., Shinmyo, M., Kurokawa, K., Nakano, A., Endo, T., et al. (2019). A Non-canonical Unfolded Protein Response Pathway and Mitochondrial Dynamics Control the Number of Er-Mitochondria Contact Sites. Cold Spring Harbor, NY: Biorxiv, 684753.
- Korobova, F., Ramabhadran, V., and Higgs, H. N. (2013). An Actin-dependent Step in Mitochondrial Fission Mediated by the Er-Associated Formin Inf2. *Science* 339, 464–467. doi:10.1126/science.1228360
- Kurtulus, S., Tripathi, P., Moreno-Fernandez, M. E., Sholl, A., Katz, J. D., Grimes, H. L., et al. (2011). Bcl-2 Allows Effector and Memory Cd8+ T Cells to Tolerate Higher Expression of Bim. *J. I.* 186, 5729–5737. doi:10.4049/jimmunol.1100102
- Lamb, C. A., Yoshimori, T., and Tooze, S. A. (2013). The Autophagosome: Origins Unknown, Biogenesis Complex. *Nat. Rev. Mol. Cell Biol* 14, 759–774. doi:10.1038/nrm3696
- Lebeau, J., Saunders, J. M., Moraes, V. W. R., Madhavan, A., Madrazo, N., Anthony, M. C., et al. (2018). The Perk Arm of the Unfolded Protein Response Regulates Mitochondrial Morphology during Acute Endoplasmic Reticulum Stress. *Cell Rep.* 22, 2827–2836. doi:10.1016/j.celrep.2018.02.055
- Lee, J. E., Westrate, L. M., Wu, H., Page, C., and Voeltz, G. K. (2016). Multiple Dynamin Family Members Collaborate to Drive Mitochondrial Division. *Nature* 540, 139–143. doi:10.1038/nature20555
- Levine, B., Sinha, S. C., and Kroemer, G. (2008). Bcl-2 Family Members: Dual Regulators of Apoptosis and Autophagy. *Autophagy* 4, 600–606. doi:10.4161/auto.6260
- Lewis, S. C., Uchiyama, L. F., and Nunnari, J. (2016). Er-Mitochondria Contacts Couple Mtdna Synthesis with Mitochondrial Division in Human Cells. *Science* 353, Aaf5549. doi:10.1126/science.aaf5549
- Li, J., Wang, Y., Wang, Y., Wen, X., Ma, X.-N., Chen, W., et al. (2015). Pharmacological Activation of Ampk Prevents Drp1-Mediated Mitochondrial Fission and Alleviates Endoplasmic Reticulum Stress-Associated Endothelial Dysfunction. *J. Mol. Cell Cardiol.* 86, 62–74. doi:10.1016/j.yjmcc.2015.07.010
- Loh, C., Shaw, K. T.-Y., Carew, J., Viola, J. P. B., Luo, C., Perrino, B. A., et al. (1996). Calcineurin Binds the Transcription Factor Nfat1 and Reversibly Regulates its Activity. *J. Biol. Chem.* 271, 10884–10891. doi:10.1074/jbc.271.18.10884
- Long, A. H., Haso, W. M., Shern, J. F., Wanhainen, K. M., Murgai, M., Ingaramo, M., et al. (2015). 4-1bb Costimulation Ameliorates T Cell Exhaustion Induced by Tonic Signaling of Chimeric Antigen Receptors. *Nat. Med.* 21, 581–590. doi:10.1038/nm.3838
- Ma, R., Ji, T., Zhang, H., Dong, W., Chen, X., Xu, P., et al. (2018). A Pck1-Directed Glycogen Metabolic Program Regulates Formation and Maintenance of Memory CD8+ T Cells. *Nat. Cell Biol* 20, 21–27. doi:10.1038/s41556-017-0002-2
- Ma, X., Bi, E., Lu, Y., Su, P., Huang, C., Liu, L., et al. (2019). Cholesterol Induces CD8+ T Cell Exhaustion in the Tumor Microenvironment. *Cell Metab.* 30, 143–156. doi:10.1016/j.cmet.2019.04.002
- Ma, Y., and Hendershot, L. M. (2003). Delineation of A Negative Feedback Regulatory Loop that Controls Protein Translation during Endoplasmic Reticulum Stress. *J. Biol. Chem.* 278, 34864–34873. doi:10.1074/jbc.m301107200
- Macdonald, P. J., Francy, C. A., Stepanyants, N., Lehman, L., Baglio, A., Mears, J. A., et al. (2016). Distinct Splice Variants of Dynamin-Related Protein 1 Differentially Utilize Mitochondrial Fission Factor as an Effector of Cooperative Gtpase Activity. *J. Biol. Chem.* 291, 493–507. doi:10.1074/jbc.m115.680181
- MacIver, N. J., Michalek, R. D., and Rathmell, J. C. (2013). Metabolic Regulation of T Lymphocytes. *Annu. Rev. Immunol.* 31, 259–283. doi:10.1146/annurev-immunol-032712-095956
- Mao, Z., and Zhang, W. (2018). Role of Mtor in Glucose and Lipid Metabolism. *Int. J. Mol. Sci.* 19. doi:10.3390/ijms19072043
- Marchi, S., Patergnani, S., Missiroli, S., Morciano, G., Rimessi, A., Wieckowski, M. R., et al. (2018). Mitochondrial and Endoplasmic Reticulum Calcium Homeostasis and Cell Death. *Cell Calcium* 69, 62–72. doi:10.1016/j.ceca.2017.05.003
- Maruyama, Y., Sou, Y.-S., Kageyama, S., Takahashi, T., Ueno, T., Tanaka, K., et al. (2014). Lc3b Is Indispensable for Selective Autophagy of P62 but Not Basal Autophagy. *Biochem. Biophysical Res. Commun.* 446, 309–315. doi:10.1016/j.bbrc.2014.02.093
- Mizushima, N., Yamamoto, A., Matsui, M., Yoshimori, T., and Ohsumi, Y. (2004). In Vivo Analysis of Autophagy in Response to Nutrient Starvation Using Transgenic Mice Expressing A Fluorescent Autophagosome Marker. *MBoC* 15, 1101–1111. doi:10.1091/mbc.e03-09-0704

- Mohanty, R., Chowdhury, C. R., Arega, S., Sen, P., Ganguly, P., and Ganguly, N. (2019). Car T Cell Therapy: A New Era for Cancer Treatment (Review). *Oncol. Rep.* 42, 2183–2195. doi:10.3892/or.2019.7335
- Morris, J. L., Gillet, G., Prudent, J., and Popgeorgiev, N. (2021). Bcl-2 Family of Proteins in the Control of Mitochondrial Calcium Signalling: An Old Chap with New Roles. *Int. J. Mol. Sci.* 22. doi:10.3390/ijms22073730
- Nakano, O., Sato, M., Naito, Y., Suzuki, K., Orikasa, S., Aizawa, M., et al. (2001). Proliferative Activity of Intratumoral Cd8(+) T-Lymphocytes as A Prognostic Factor in Human Renal Cell Carcinoma: Clinicopathologic Demonstration of Antitumor Immunity. *Cancer Res.* 61, 5132–5136.
- Navale, A. M., and Paranjape, A. N. (2016). Glucose Transporters: Physiological and Pathological Roles. *Biophys. Rev.* 8, 5–9. doi:10.1007/s12551-015-0186-2
- Nguyen, H. H., Kim, T., Song, S. Y., Park, S., Cho, H. H., Jung, S.-H., et al. (2016). Naïve CD8+ T Cell Derived Tumor-specific Cytotoxic Effectors as a Potential Remedy for Overcoming TGF- β Immunosuppression in the Tumor Microenvironment. *Sci. Rep.* 6, 28208. doi:10.1038/srep28208
- Nichols, B. A., Setzer, P. Y., and Bainton, D. F. (1984). Glucose-6-Phosphatase as A Cytochemical Marker of Endoplasmic Reticulum in Human Leukocytes and Platelets. *J. Histochem. Cytochem.* 32, 165–171. doi:10.1177/32.2.6319482
- O'Sullivan, D., Van Der Windt, G. J. W., Huang, S. C., Curtis, J. D., Chang, C. H., Buck, M. D., et al. (2018). Memory CD8+ T Cells Use Cell-Intrinsic Lipolysis to Support the Metabolic Programming Necessary for Development. *Immunity* 49, 375–376. doi:10.1016/j.immuni.2018.07.018
- Oakes, S. A., Scorrano, L., Opferman, J. T., Bassik, M. C., Nishino, M., Pozzan, T., et al. (2005). Proapoptotic Bax and Bak Regulate the Type 1 Inositol Trisphosphate Receptor and Calcium Leak from the Endoplasmic Reticulum. *Proc. Natl. Acad. Sci. U.S.A.* 102, 105–110. doi:10.1073/pnas.0408352102
- Ogando, J., Sáez, M. E., Santos, J., Nuevo-Tapióles, C., Gut, M., Esteve-Codina, A., et al. (2019). PD-1 Signaling Affects Cristae Morphology and Leads to Mitochondrial Dysfunction in Human CD8+ T Lymphocytes. *J. Immunotherapy Cancer* 7, 151. doi:10.1186/s40425-019-0628-7
- Ogata, M., Hino, S.-i., Saito, A., Morikawa, K., Kondo, S., Kanemoto, S., et al. (2006). Autophagy Is Activated for Cell Survival after Endoplasmic Reticulum Stress. *Mol. Cell Biol* 26, 9220–9231. doi:10.1128/mcb.01453-06
- Olzmann, J. A., and Carvalho, P. (2019). Dynamics and Functions of Lipid Droplets. *Nat. Rev. Mol. Cell Biol* 20, 137–155. doi:10.1038/s41580-018-0085-z
- Onodera, J., and Ohsumi, Y. (2005). Autophagy Is Required for Maintenance of Amino Acid Levels and Protein Synthesis under Nitrogen Starvation. *J. Biol. Chem.* 280, 31582–31586. doi:10.1074/jbc.m506736200
- Opferman, J. T., Ober, B. T., and Ashton-Rickardt, P. G. (1999). Linear Differentiation of Cytotoxic Effectors into Memory T Lymphocytes. *Science* 283, 1745–1748. doi:10.1126/science.283.5408.1745
- Oshima, T., Uenishi, N., and Imahori, K. (1976). Simple Assay Methods for Ribonuclease T 1, T 2, and Nuclease P 1. *Anal. Biochem.* 71, 632–634. doi:10.1016/s0003-2697(76)80039-5
- Owen, O. E., Reichard, G. A., Jr., Patel, M. S., and Boden, G. (1979). Energy Metabolism in Feasting and Fasting. *Adv. Exp. Med. Biol.* 111, 169–188. doi:10.1007/978-1-4757-0734-2_8
- Pan, Y., Chen, H., Siu, F., and Kilberg, M. S. (2003). Amino Acid Deprivation and Endoplasmic Reticulum Stress Induce Expression of Multiple Activating Transcription Factor-3 Mrna Species that, when Overexpressed in Hepg2 Cells, Modulate Transcription by the Human Asparagine Synthetase Promoter. *J. Biol. Chem.* 278, 38402–38412. doi:10.1074/jbc.m304574200
- Pearce, E. L., Poffenberger, M. C., Chang, C.-H., and Jones, R. G. (2013). Fueling Immunity: Insights into Metabolism and Lymphocyte Function. *Science* 342, 1242454. doi:10.1126/science.1242454
- Pearce, E. L., Walsh, M. C., Cepas, P. J., Harms, G. M., Shen, H., Wang, L.-S., et al. (2009). Enhancing Cd8 T-Cell Memory by Modulating Fatty Acid Metabolism. *Nature* 460, 103–107. doi:10.1038/nature08097
- Petrova, V., Annicchiarico-Petruzzelli, M., Melino, G., and Amelio, I. (2018). The Hypoxic Tumour Microenvironment. *Oncogenesis* 7, 10. doi:10.1038/s41389-017-0011-9
- Petrovas, C., Casazza, J. P., Brenchley, J. M., Price, D. A., Gostick, E., Adams, W. C., et al. (2006). Pd-1 Is A Regulator of Virus-specific Cd8+ T Cell Survival in Hiv Infection. *J. Exp. Med.* 203, 2281–2292. doi:10.1084/jem.20061496
- Pinkaew, D., Chattopadhyay, A., King, M. D., Chunhacha, P., Liu, Z., Stevenson, H. L., et al. (2017). Fortilin Binds IRE1 α and Prevents ER Stress from Signaling Apoptotic Cell Death. *Nat. Commun.* 8, 18. doi:10.1038/s41467-017-00029-1
- Pitts, K. R., Yoon, Y., Krueger, E. W., and Mcniven, M. A. (1999). The Dynamin-like Protein Dlp1 Is Essential for Normal Distribution and Morphology of the Endoplasmic Reticulum and Mitochondria in Mammalian Cells. *MBoC* 10, 4403–4417. doi:10.1091/mbc.10.12.4403
- Pollizzi, K. N., Patel, C. H., Sun, I.-H., Oh, M.-H., Waickman, A. T., Wen, J., et al. (2015). mTORC1 and mTORC2 Selectively Regulate CD8+ T Cell Differentiation. *J. Clin. Invest.* 125, 2090–2108. doi:10.1172/jci77746
- Putney, J. W., Jr. (1986). A Model for Receptor-Regulated Calcium Entry. *Cell Calcium* 7, 1–12. doi:10.1016/0143-4160(86)90026-6
- Qiu, J., Villa, M., Sanin, D. E., Buck, M. D., O'Sullivan, D., Ching, R., et al. (2019). Acetate Promotes T Cell Effector Function during Glucose Restriction. *Cell Rep.* 27, 2063–2074. doi:10.1016/j.celrep.2019.04.022
- Qiu, Y., Mao, T., Zhang, Y., Shao, M., You, J., Ding, Q., et al. (2010). A Crucial Role for Rack1 in the Regulation of Glucose-Stimulated Ire1alpha Activation in Pancreatic Beta Cells. *Sci. Signal.* 3, Ra7. doi:10.1126/scisignal.2000514
- Raffaello, A., Mammucari, C., Gherardi, G., and Rizzuto, R. (2016). Calcium at the Center of Cell Signaling: Interplay between Endoplasmic Reticulum, Mitochondria, and Lysosomes. *Trends Biochem. Sci.* 41, 1035–1049. doi:10.1016/j.tibs.2016.09.001
- Rainbolt, T. K., Saunders, J. M., and Wiseman, R. L. (2014). Stress-Responsive Regulation of Mitochondria through the Er Unfolded Protein Response. *Trends Endocrinol. Metab.* 25, 528–537. doi:10.1016/j.tem.2014.06.007
- Riesenberg, B. P., Hunt, E. G., Tennant, M. D., Hurst, K. E., Andrews, A. M., Leddy, L. R., et al. (2022). Stress-Mediated Attenuation of Translation Undermines T Cell Tumor Control. Cold Spring Harbor, NY: Biorxiv.
- Rines, A. K., Sharabi, K., Tavares, C. D. J., and Puigserver, P. (2016). Targeting Hepatic Glucose Metabolism in the Treatment of Type 2 Diabetes. *Nat. Rev. Drug Discov.* 15, 786–804. doi:10.1038/nrd.2016.151
- Rizzuto, R., Brini, M., Murgia, M., and Pozzan, T. (1993). Microdomains with High Ca²⁺ Close to IP₃-Sensitive Channels that Are Sensed by Neighboring Mitochondria. *Science* 262, 744–747. doi:10.1126/science.8235595
- Rizzuto, R., De Stefani, D., Raffaello, A., and Mammucari, C. (2012). Mitochondria as Sensors and Regulators of Calcium Signalling. *Nat. Rev. Mol. Cell Biol* 13, 566–578. doi:10.1038/nrm3412
- Rizzuto, R., Pinton, P., Carrington, W., Fay, F. S., Fogarty, K. E., Lifshitz, L. M., et al. (1998). Close Contacts with the Endoplasmic Reticulum as Determinants of Mitochondrial Ca²⁺ Responses. *Science* 280, 1763–1766. doi:10.1126/science.280.5370.1763
- Robey, R. B., and Hay, N. (2006). Mitochondrial Hexokinases, Novel Mediators of the Antiapoptotic Effects of Growth Factors and Akt. *Oncogene* 25, 4683–4696. doi:10.1038/sj.onc.1209595
- Rong, Y.-P., Aromolaran, A. S., Bultynck, G., Zhong, F., Li, X., Mccoll, K., et al. (2008). Targeting Bcl-2-Ip3 Receptor Interaction to Reverse Bcl-2's Inhibition of Apoptotic Calcium Signals. *Mol. Cell* 31, 255–265. doi:10.1016/j.molcel.2008.06.014
- Rosenberg, S. A., Packard, B. S., Aebersold, P. M., Solomon, D., Topalian, S. L., Toy, S. T., et al. (1988). Use of Tumor-Infiltrating Lymphocytes and Interleukin-2 in the Immunotherapy of Patients with Metastatic Melanoma. *N. Engl. J. Med.* 319, 1676–1680. doi:10.1056/nejm19881223192527
- Rossignol, R., Gilkerson, R., Aggeler, R., Yamagata, K., Remington, S. J., and Capaldi, R. A. (2004). Energy Substrate Modulates Mitochondrial Structure and Oxidative Capacity in Cancer Cells. *Cancer Res.* 64, 985–993. doi:10.1158/0008-5472.can-03-1101
- Saito, T., Kuma, A., Sugiura, Y., Ichimura, Y., Obata, M., Kitamura, H., et al. (2019). Autophagy Regulates Lipid Metabolism through Selective Turnover of Ncor1. *Nat. Commun.* 10, 1567. doi:10.1038/s41467-019-08829-3
- Santel, A., and Fuller, M. T. (2001). Control of Mitochondrial Morphology by A Human Mitofusin. *J. Cell Sci* 114, 867–874. doi:10.1242/jcs.114.5.867
- Sato, E., Olson, S. H., Ahn, J., Bundy, B., Nishikawa, H., Qian, F., et al. (2005). Intraepithelial CD8 + Tumor-Infiltrating Lymphocytes and a High CD8 +/regulatory T Cell Ratio Are Associated with Favorable Prognosis in Ovarian Cancer. *Proc. Natl. Acad. Sci. U.S.A.* 102, 18538–18543. doi:10.1073/pnas.0509182102
- Satoh, T., Ross, C. A., Villa, A., Supattapone, S., Pozzan, T., Snyder, S. H., et al. (1990). The Inositol 1,4,5,-Trisphosphate Receptor in Cerebellar

- Purkinje Cells: Quantitative Immunogold Labeling Reveals Concentration in an Er Subcompartment. *J. Cell Biol* 111, 615–624. doi:10.1083/jcb.111.2.615
- Schaaf, M. B. E., Keulers, T. G., Vooijs, M. A., and Rouschop, K. M. A. (2016). LC3/GABARAP Family Proteins: Autophagy-(un)related Functions. *FASEB J.* 30, 3961–3978. doi:10.1096/fj.201606098r
- Scharping, N. E., Menk, A. V., Moreci, R. S., Whetstone, R. D., Dadey, R. E., Watkins, S. C., et al. (2016). The Tumor Microenvironment Represses T Cell Mitochondrial Biogenesis to Drive Intratumoral T Cell Metabolic Insufficiency and Dysfunction. *Immunity* 45, 374–388. doi:10.1016/j.immuni.2016.07.009
- Schluns, K. S., Kieper, W. C., Jameson, S. C., and Lefrançois, L. (2000). Interleukin-7 Mediates the Homeostasis of Naïve and Memory CD8 T Cells *In Vivo*. *Nat. Immunol.* 1, 426–432. doi:10.1038/80868
- Schluns, K. S., Williams, K., Ma, A., Zheng, X. X., and Lefrançois, L. (2002). Cutting Edge: Requirement for IL-15 in the Generation of Primary and Memory Antigen-specific Cd8 T Cells. *J. Immunol.* 168, 4827–4831. doi:10.4049/jimmunol.168.10.4827
- Schuck, S., Prinz, W. A., Thorn, K. S., Voss, C., and Walter, P. (2009). Membrane Expansion Alleviates Endoplasmic Reticulum Stress Independently of the Unfolded Protein Response. *J. Cell Biol* 187, 525–536. doi:10.1083/jcb.200907074
- Schultz-Cherry, S., Dybdahl-Sissoko, N., Neumann, G., Kawaoka, Y., and Hinshaw, V. S. (2001). Influenza Virus Ns1 Protein Induces Apoptosis in Cultured Cells. *J. Virol.* 75, 7875–7881. doi:10.1128/jvi.75.17.7875-7881.2001
- Schwarz, D. S., and Blower, M. D. (2016). The Endoplasmic Reticulum: Structure, Function and Response to Cellular Signaling. *Cell. Mol. Life Sci.* 73, 79–94. doi:10.1007/s00018-015-2052-6
- Sengupta, S., Katz, S. C., Sengupta, S., and Sampath, P. (2018). Glycogen Synthase Kinase 3 Inhibition Lowers Pd-1 Expression, Promotes Long-Term Survival and Memory Generation in Antigen-specific Car-T Cells. *Cancer Lett.* 433, 131–139. doi:10.1016/j.canlet.2018.06.035
- Shamas-Din, A., Brahmabhatt, H., Leber, B., and Andrews, D. W. (2011). Bh3-Only Proteins: Orchestrators of Apoptosis. *Biochim. Biophys. Acta (Bba) - Mol. Cell Res.* 1813, 508–520. doi:10.1016/j.bbamer.2010.11.024
- Shanmuganad, S., Hummel, S. A., Varghese, V., and Hildeman, D. A. (2022). Bcl-2 Is Necessary to Counteract Bim and Promote Survival of TCRαβ+CD8αα+ Intraepithelial Lymphocyte Precursors in the Thymus. *J.I.* 208, 651–659. doi:10.4049/jimmunol.2100975
- Sharma, P., Shen, Y., Wen, S., Yamada, S., Jungbluth, A. A., Gnjatich, S., et al. (2007). Cd8 Tumor-Infiltrating Lymphocytes Are Predictive of Survival in Muscle-Invasive Urothelial Carcinoma. *Proc. Natl. Acad. Sci. U.S.A.* 104, 3967–3972. doi:10.1073/pnas.0611618104
- Shaw, J., Utz, P., Durand, D., Toole, J., Emmel, E., and Crabtree, G. (1988). Identification of A Putative Regulator of Early T Cell Activation Genes. *Science* 241, 202–205. doi:10.1126/science.3260404
- Shibata, Y., Shemesh, T., Prinz, W. A., Palazzo, A. F., Kozlov, M. M., and Rapoport, T. A. (2010). Mechanisms Determining the Morphology of the Peripheral Er. *Cell* 143, 774–788. doi:10.1016/j.cell.2010.11.007
- Simula, L., Nazio, F., and Campello, S. (2017). The Mitochondrial Dynamics in Cancer and Immune-Surveillance. *Semin. Cancer Biol.* 47, 29–42. doi:10.1016/j.semcancer.2017.06.007
- Simula, L., Pacella, I., Colamatteo, A., Procaccini, C., Cancila, V., Bordi, M., et al. (2018). Drp1 Controls Effective T Cell Immune-Surveillance by Regulating T Cell Migration, Proliferation, and Cmyc-dependent Metabolic Reprogramming. *Cell Rep.* 25, 3059–3073. doi:10.1016/j.celrep.2018.11.018
- Sinclair, L. V., Rolf, J., Emslie, E., Shi, Y.-B., Taylor, P. M., and Cantrell, D. A. (2013). Control of Amino-Acid Transport by Antigen Receptors Coordinates the Metabolic Reprogramming Essential for T Cell Differentiation. *Nat. Immunol.* 14, 500–508. doi:10.1038/ni.2556
- Smith, C. A., Williams, G. T., Kingston, R., Jenkinson, E. J., and Owen, J. J. T. (1989). Antibodies to Cd3/T-Cell Receptor Complex Induce Death by Apoptosis in Immature T Cells in Thymic Cultures. *Nature* 337, 181–184. doi:10.1038/337181a0
- Sommermeier, D., Hudecek, M., Kosasih, P. L., Gogishvili, T., Maloney, D. G., Turtle, C. J., et al. (2016). Chimeric Antigen Receptor-Modified T Cells Derived from Defined Cd8+ and Cd4+ Subsets Confer Superior Antitumor Reactivity *In Vivo*. *Leukemia* 30, 492–500. doi:10.1038/leu.2015.247
- Song, M., Sandoval, T. A., Chae, C.-S., Chopra, S., Tan, C., Rutkowski, M. R., et al. (2018). IRE1α-XBP1 Controls T Cell Function in Ovarian Cancer by Regulating Mitochondrial Activity. *Nature* 562, 423–428. doi:10.1038/s41586-018-0597-x
- Sood, A., Jeyaraju, D. V., Prudent, J., Caron, A., Lemieux, P., McBride, H. M., et al. (2014). A Mitofusin-2-dependent Inactivating Cleavage of Opa1 Links Changes in Mitochondria Cristae and Er Contacts in the Postprandial Liver. *Proc. Natl. Acad. Sci. U.S.A.* 111, 16017–16022. doi:10.1073/pnas.1408061111
- Stiles, B. L. (2009). PI-3-K and AKT: Onto the Mitochondria☆. *Adv. Drug Deliv. Rev.* 61, 1276–1282. doi:10.1016/j.addr.2009.07.017
- Streb, H., Irvine, R. F., Berridge, M. J., and Schulz, I. (1983). Release of Ca2+ from A Nonmitochondrial Intracellular Store in Pancreatic Acinar Cells by Inositol-1,4,5-Trisphosphate. *Nature* 306, 67–69. doi:10.1038/306067a0
- Su, E. W., Moore, C. J., Soriano, S., Johnson, C. B., Songalia, N., Patterson, A., et al. (2015). IL-2Ra Mediates Temporal Regulation of IL-2 Signaling and Enhances Immunotherapy. *Sci. Transl. Med.* 7, 311ra170. doi:10.1126/scitranslmed.aac8155
- Sukumar, M., and Gattinoni, L. (2014). The Short and Sweet of T-Cell Therapy: Restraining Glycolysis Enhances the Formation of Immunological Memory and Antitumor Immune Responses. *Oncoimmunology* 3, E27573. doi:10.4161/onci.27573
- Szabadkai, G., Bianchi, K., Va'rneai, P., De Stefani, D., Wieckowski, M. R., Cavagna, D., et al. (2006). Chaperone-Mediated Coupling of Endoplasmic Reticulum and Mitochondrial Ca2+ Channels. *J. Cell Biol* 175, 901–911. doi:10.1083/jcb.200608073
- Szado, T., Vanderheyden, V., Parys, J. B., De Smedt, H., Rietdorf, K., Kotelevets, L., et al. (2008). Phosphorylation of Inositol 1,4,5-trisphosphate Receptors by Protein Kinase B/Akt Inhibits Ca 2+ Release and Apoptosis. *Proc. Natl. Acad. Sci. U.S.A.* 105, 2427–2432. doi:10.1073/pnas.0711324105
- Thaxton, J. E., Wallace, C., Riesenberger, B., Zhang, Y., Paulos, C. M., Beeson, C. C., et al. (2017). Modulation of Endoplasmic Reticulum Stress Controls CD4+ T-Cell Activation and Antitumor Function. *Cancer Immunol. Res.* 5, 666–675. doi:10.1158/2326-6066.cir-17-0081
- Theurey, P., Tubbs, E., Vial, G., Jacquemetton, J., Bendridi, N., Chauvin, M.-A., et al. (2016). Mitochondria-Associated Endoplasmic Reticulum Membranes Allow Adaptation of Mitochondrial Metabolism to Glucose Availability in the Liver. *J. Mol. Cell Biol* 8, 129–143. doi:10.1093/jmcb/mjw004
- Tubbs, E., Theurey, P., Vial, G., Bendridi, N., Bravard, A., Chauvin, M.-A., et al. (2014). Mitochondria-Associated Endoplasmic Reticulum Membrane (Mam) Integrity Is Required for Insulin Signaling and Is Implicated in Hepatic Insulin Resistance. *Diabetes* 63, 3279–3294. doi:10.2337/db13-1751
- van Stipdonk, M. J. B., Lemmens, E. E., and Schoenberger, S. P. (2001). Naïve CTLs Require a Single Brief Period of Antigenic Stimulation for Clonal Expansion and Differentiation. *Nat. Immunol.* 2, 423–429. doi:10.1038/87730
- Vanmeerbeek, I., Borras, D. M., Sprooten, J., Bechter, O., Tejpar, S., and Garg, A. D. (2021). Early Memory Differentiation and Cell Death Resistance in T Cells Predicts Melanoma Response to Sequential Anti-ctla4 and Anti-pd1 Immunotherapy. *Genes Immun.* 22, 108–119. doi:10.1038/s41435-021-00138-4
- Varanita, T., Soriano, M. E., Romanello, V., Zaglia, T., Quintana-Cabrera, R., Semenzato, M., et al. (2015). The Opa1-dependent Mitochondrial Cristae Remodeling Pathway Controls Atrophic, Apoptotic, and Ischemic Tissue Damage. *Cell Metab.* 21, 834–844. doi:10.1016/j.cmet.2015.05.007
- Veiga-Fernandes, H., Walter, U., Bourgeois, C., Mclean, A., and Rocha, B. (2000). Response of Naïve and Memory CD8+ T Cells to Antigen Stimulation *In Vivo*. *Nat. Immunol.* 1, 47–53. doi:10.1038/76907
- Velázquez, A. P., Tatsuta, T., Ghillebert, R., Drescher, I., and Graef, M. (2016). Lipid Droplet-Mediated Er Homeostasis Regulates Autophagy and Cell Survival during Starvation. *J. Cell Biol* 212, 621–631. doi:10.1083/jcb.201508102
- Verfaillie, T., Rubio, N., Garg, A. D., Bultynck, G., Rizzuto, R., Decuypere, J.-P., et al. (2012). Perk Is Required at the Er-Mitochondrial Contact Sites to Convey Apoptosis after Ros-Based Er Stress. *Cell Death Differ* 19, 1880–1891. doi:10.1038/cdd.2012.74
- Vihervuori, H., Autere, T. A., Repo, H., Kurki, S., Kallio, L., Lintunen, M. M., et al. (2019). Tumor-infiltrating Lymphocytes and CD8+ T Cells Predict Survival of Triple-Negative Breast Cancer. *J. Cancer Res. Clin. Oncol.* 145, 3105–3114. doi:10.1007/s00432-019-03036-5
- Vinnakota, K. C., Singhal, A., Van den Bergh, F., Bagher-Oskouei, M., Wiseman, R. W., and Beard, D. A. (2016). Open-Loop Control of Oxidative Phosphorylation in Skeletal and Cardiac Muscle Mitochondria by Ca2+. *Biophysical J.* 110, 954–961. doi:10.1016/j.bpj.2015.12.018

- Vodnala, S. K., Eil, R., Kishton, R. J., Sukumar, M., Yamamoto, T. N., Ha, N. H., et al. (2019). T Cell Stemness and Dysfunction in Tumors Are Triggered by A Common Mechanism. *Science* 363. doi:10.1126/science.aau0135
- Voeltz, G. K., Prinz, W. A., Shibata, Y., Rist, J. M., and Rapoport, T. A. (2006). A Class of Membrane Proteins Shaping the Tubular Endoplasmic Reticulum. *Cell* 124, 573–586. doi:10.1016/j.cell.2005.11.047
- Walter, P., and Ron, D. (2011). The Unfolded Protein Response: From Stress Pathway to Homeostatic Regulation. *Science* 334, 1081–1086. doi:10.1126/science.1209038
- Walther, T. C., and Farese, R. V., Jr. (2012). Lipid Droplets and Cellular Lipid Metabolism. *Annu. Rev. Biochem.* 81, 687–714. doi:10.1146/annurev-biochem-061009-102430
- Wang, A., Chandran, S., Shah, S. A., Chiu, Y., Paria, B. C., Aghamolla, T., et al. (2012a). The Stoichiometric Production of IL-2 and IFN- γ mRNA Defines Memory T Cells that Can Self-Renew after Adoptive Transfer in Humans. *Sci. Transl. Med.* 4, 149ra120. doi:10.1126/scitranslmed.3004306
- Wang, H., Han, P., Qi, X., Li, F., Li, M., Fan, L., et al. (2021a). Bcl-2 Enhances Chimeric Antigen Receptor T Cell Persistence by Reducing Activation-Induced Apoptosis. *Cancers (Basel)* 13. doi:10.3390/cancers13020197
- Wang, N., Wang, C., Zhao, H., He, Y., Lan, B., Sun, L., et al. (2021b). The Mams Structure and its Role in Cell Death. *Cells* 10, 10. doi:10.3390/cells10030657
- Wang, R. C., Wei, Y., An, Z., Zou, Z., Xiao, G., Bhagat, G., et al. (2012b). Akt-Mediated Regulation of Autophagy and Tumorigenesis through Beclin 1 Phosphorylation. *Science* 338, 956–959. doi:10.1126/science.1225967
- Wang, R., Dillon, C. P., Shi, L. Z., Milasta, S., Carter, R., Finkelstein, D., et al. (2011a). The Transcription Factor Myc Controls Metabolic Reprogramming upon T Lymphocyte Activation. *Immunity* 35, 871–882. doi:10.1016/j.immuni.2011.09.021
- Wang, S. F., Fouquet, S., Chapon, M., Salmon, H., Regnier, F., Labroquère, K., et al. (2011b). Early T Cell Signalling Is Reversibly Altered in Pd-1+ T Lymphocytes Infiltrating Human Tumors. *Plos One* 6, E17621. doi:10.1371/journal.pone.0017621
- Wang, Y., Zhang, X., Wen, Y., Li, S., Lu, X., Xu, R., et al. (2021c). Endoplasmic Reticulum-Mitochondria Contacts: A Potential Therapy Target for Cardiovascular Remodeling-Associated Diseases. *Front. Cell Dev. Biol.* 9, 774989. doi:10.3389/fcell.2021.774989
- Wei, F., Zhong, S., Ma, Z., Kong, H., Medvec, A., Ahmed, R., et al. (2013). Strength of Pd-1 Signaling Differentially Affects T-Cell Effector Functions. *Proc. Natl. Acad. Sci. U S A* 110, E2480–E2489. doi:10.1073/pnas.1305394110
- Wengrod, J., Wang, D., Weiss, S., Zhong, H., Osman, I., and Gardner, L. B. (2015). Phosphorylation of eIF2 α Triggered by mTORC1 Inhibition and PP6C Activation Is Required for Autophagy and Is Aberrant in PP6C-Mutated Melanoma. *Sci. Signal.* 8, Ra27. doi:10.1126/scisignal.aaa0899
- Wentworth, L., Meyers, J. V., Alam, S., Russ, A. J., Suresh, M., and Cho, C. S. (2013). Memory T Cells Are Uniquely Resistant to Melanoma-Induced Suppression. *Cancer Immunol. Immunother.* 62, 149–159. doi:10.1007/s00262-012-1326-1
- Wesselborg, S., Fruman, D. A., Sagoo, J. K., Bierer, B. E., and Burakoff, S. J. (1996). Identification of A Physical Interaction between Calcineurin and Nuclear Factor of Activated T Cells (Nfatp). *J. Biol. Chem.* 271, 1274–1277. doi:10.1074/jbc.271.3.1274
- West, M., Zurek, N., Hoenger, A., and Voeltz, G. K. (2011). A 3d Analysis of Yeast Er Structure Reveals How Er Domains Are Organized by Membrane Curvature. *J. Cell Biol* 193, 333–346. doi:10.1083/jcb.201011039
- Westermann, B. (2010). Mitochondrial Fusion and Fission in Cell Life and Death. *Nat. Rev. Mol. Cell Biol* 11, 872–884. doi:10.1038/nrm3013
- Westermann, B. (2011). Organelle Dynamics: Er Embraces Mitochondria for Fission. *Curr. Biol.* 21, R922–R924. doi:10.1016/j.cub.2011.10.010
- Westrate, L. M., Lee, J. E., Prinz, W. A., and Voeltz, G. K. (2015). Form Follows Function: The Importance of Endoplasmic Reticulum Shape. *Annu. Rev. Biochem.* 84, 791–811. doi:10.1146/annurev-biochem-072711-163501
- Wherry, E. J., and Kurachi, M. (2015). Molecular and Cellular Insights into T Cell Exhaustion. *Nat. Rev. Immunol.* 15, 486–499. doi:10.1038/nri3862
- White, C., Li, C., Yang, J., Petrenko, N. B., Madesh, M., Thompson, C. B., et al. (2005). The Endoplasmic Reticulum Gateway to Apoptosis by Bcl-XL Modulation of the InsP3R. *Nat. Cell Biol* 7, 1021–1028. doi:10.1038/ncb1302
- Wieman, H. L., Wofford, J. A., and Rathmell, J. C. (2007). Cytokine Stimulation Promotes Glucose Uptake via Phosphatidylinositol-3 Kinase/Akt Regulation of Glut1 Activity and Trafficking. *MBoC* 18, 1437–1446. doi:10.1091/mbc.e06-07-0593
- Wikstrom, J. D., Israeli, T., Bachar-Wikstrom, E., Swisa, A., Ariav, Y., Waiss, M., et al. (2013). AMPK Regulates ER Morphology and Function in Stressed Pancreatic β -Cells via Phosphorylation of DRP1. *Mol. Endocrinol.* 27, 1706–1723. doi:10.1210/me.2013-1109
- Xiang, X., Cao, N., Chen, F., Qian, L., Wang, Y., Huang, Y., et al. (2020). Polysaccharide of Atractylodes Macrocephala Koidz (PAMK) Alleviates Cyclophosphamide-Induced Immunosuppression in Mice by Upregulating CD28/IP3R/PLC γ -1/AP-1/NFAT Signal Pathway. *Front. Pharmacol.* 11, 529657. doi:10.3389/fphar.2020.529657
- Xu, X., Araki, K., Li, S., Han, J.-H., Ye, L., Tan, W. G., et al. (2014). Autophagy Is Essential for Effector CD8+ T Cell Survival and Memory Formation. *Nat. Immunol.* 15, 1152–1161. doi:10.1038/ni.3025
- Xu, Y., Chaudhury, A., Zhang, M., Savoldo, B., Metelitsa, L. S., Rodgers, J., et al. (2016). Glycolysis Determines Dichotomous Regulation of T Cell Subsets in Hypoxia. *J. Clin. Invest.* 126, 2678–2688. doi:10.1172/jci85834
- Yan, Y., Wang, H., Wei, C., Xiang, Y., Liang, X., Phang, C.-W., et al. (2019). Hdac6 Regulates Lipid Droplet Turnover in Response to Nutrient Deprivation via P62-Mediated Selective Autophagy. *J. Genet. Genomics* 46, 221–229. doi:10.1016/j.jgg.2019.03.008
- Yang, Z., and Klionsky, D. J. (2010). Eaten Alive: A History of Macroautophagy. *Nat. Cell Biol* 12, 814–822. doi:10.1038/ncb0910-814
- Yedida, G., Milani, M., Cohen, G. M., and Varadarajan, S. (2019). Apogossypol-Mediated Reorganisation of the Endoplasmic Reticulum Antagonises Mitochondrial Fission and Apoptosis. *Cell Death Dis* 10, 521. doi:10.1038/s41419-019-1759-y
- Yu, Y.-R., Imrichova, H., Wang, H., Chao, T., Xiao, Z., Gao, M., et al. (2020). Disturbed Mitochondrial Dynamics in CD8+ TILs Reinforce T Cell Exhaustion. *Nat. Immunol.* 21, 1540–1551. doi:10.1038/s41590-020-0793-3
- Zanetti, M., Xian, S., Dosset, M., and Carter, H. (2022). The Unfolded Protein Response at the Tumor-Immune Interface. *Front. Immunol.* 13, 823157. doi:10.3389/fimmu.2022.823157
- Zhang, D., Lu, C., Whiteman, M., Chance, B., and Armstrong, J. S. (2008). The Mitochondrial Permeability Transition Regulates Cytochrome C Release for Apoptosis during Endoplasmic Reticulum Stress by Remodeling the Cristae Junction. *J. Biol. Chem.* 283, 3476–3486. doi:10.1074/jbc.m707528200

Conflict of Interest: The authors declare that the research was conducted in the absence of any commercial or financial relationships that could be construed as a potential conflict of interest.

Publisher's Note: All claims expressed in this article are solely those of the authors and do not necessarily represent those of their affiliated organizations, or those of the publisher, the editors and the reviewers. Any product that may be evaluated in this article, or claim that may be made by its manufacturer, is not guaranteed or endorsed by the publisher.

Copyright © 2022 Hunt, Andrews, Larsen and Thaxton. This is an open-access article distributed under the terms of the Creative Commons Attribution License (CC BY). The use, distribution or reproduction in other forums is permitted, provided the original author(s) and the copyright owner(s) are credited and that the original publication in this journal is cited, in accordance with accepted academic practice. No use, distribution or reproduction is permitted which does not comply with these terms.



Mitochondrial-Dependent and Independent Functions of PINK1

Xiusheng Chen, Qi Wang, Shihua Li, Xiao-Jiang Li and Weili Yang*

Guangdong Key Laboratory of Non-human Primate Research, Guangdong-Hongkong-Macau Institute of CNS Regeneration, Jinan University, Guangzhou, China

PINK1 has been characterized as a mitochondrial kinase that can target to damaged mitochondria to initiate mitophagy, a process to remove unhealthy mitochondria for protecting neuronal cells. Mutations of the human *PINK1* gene are also found to cause early onset Parkinson's disease, a neurodegenerative disorder with the pathological feature of mitochondrial dysfunction. Despite compelling evidence from *in vitro* studies to support the role of PINK1 in regulation of mitochondrial function, there is still lack of strong *in vivo* evidence to validate PINK1-mediated mitophagy in the brain. In addition, growing evidence indicates that PINK1 also executes function independent of mitochondria. In this review, we discuss the mitochondrial dependent and independent functions of PINK1, aiming at elucidating how PINK1 functions differentially under different circumstances.

Keywords: PINK1, mitophagy, mitochondria, Parkinson's disease (PD), parkin (PARK2)

OPEN ACCESS

Edited by:

Yongye Huang,
Northeastern University, China

Reviewed by:

Eszter Dombi,
University of Oxford, United Kingdom
Xiangnan Zhang,
Zhejiang University, China
François Singh,
University of Dundee, United Kingdom

*Correspondence:

Weili Yang
weiliyang12@jnu.edu.cn

Specialty section:

This article was submitted to
Signaling,
a section of the journal
Frontiers in Cell and Developmental
Biology

Received: 27 May 2022

Accepted: 16 June 2022

Published: 08 July 2022

Citation:

Chen X, Wang Q, Li S,
Li X-J and Yang W (2022)
Mitochondrial-Dependent and
Independent Functions of PINK1.
Front. Cell Dev. Biol. 10:954536.
doi: 10.3389/fcell.2022.954536

INTRODUCTION

The PTEN-induced kinase 1 (PINK1) is a serine/threonine kinase whose function has been well characterized by biochemical studies and protein structural analysis (Kane et al., 2014; Kumar et al., 2017; Gan et al., 2022). A large amount of *in vitro* studies have shown that PINK1 works with Parkin, an E3 ubiquitin ligase, in coordination to target damaged mitochondria for removing unhealthy mitochondria by the lysosome, a process called mitophagy (Matsuda et al., 2010; Kane et al., 2014; Koyano et al., 2014; Ivankovic et al., 2016). In support of the role of PINK1/Parkin in mitochondria, mutations in the *PINK1* and *Parkin* genes are found to cause early onset of Parkinson's disease that is also associated with mitochondrial dysfunction (Valente et al., 2004; Ishihara-Paul et al., 2008; McLelland et al., 2014; Ham et al., 2020). Identification of the involvement of PINK1/Parkin in mitophagy has expanded the roles of mitochondrial dysfunction and mitophagy in a variety of pathological conditions and diseases. As a result, extensive studies of the function of PINK1/Parkin related to mitochondrial function continue to provide a wealth of information about how PINK1/Parkin govern mitochondria homeostasis.

Despite the prevalent theory that PINK1 is a mitochondrial kinase and its mitochondrial-dependent function plays a critical role in the pathogenesis of PD, there have been unclear and important issues that need to be addressed. First, there is lack of strong *in vivo* evidence for PINK1/Parkin-mediated mitophagy in animal models. Second, non-mitochondrial dependent function of PINK1 has been reported, but whether this function is related to PD pathogenesis or other pathological conditions remains elusive. In this review, we will discuss the mitochondrial-dependent and non-dependent functions of PINK1, aiming at elucidating how PINK1 functions *in vivo* and how its dysfunction is involved in PD and other diseases.

Parkinson's Disease Is Associated With Mitochondrial Defects

Parkinson's disease (PD) is the second most common neurodegenerative disorder (less prevalent than Alzheimer's disease) and is characterized by age-dependent and progressive loss of neurons, especially dopamine neurons in the basal ganglia (Tolosa et al., 2006; Bloem et al., 2021). As a result of this selective neurodegeneration, PD is mainly manifested by motor dysfunction, accompanied by cognitive impairment and psychiatric abnormalities (Kalia and Lang, 2015). Pathologically, PD is featured by loss of dopamine neurons in the substantia nigra pars compacta region in the brain and accumulation of α -synuclein positive inclusions (Lewy bodies) (Bloem et al., 2021). The selective neurodegeneration in PD is thought to associate with mitochondrial dysfunction, which is supported by the discovery that mitochondrial toxins, such as 1-methyl-4-phenyl-1,2,3,6-tetrahydropyridine (MPTP), induce selective nigral degeneration in humans and animals (Fornai et al., 2005). Also, postmortem PD patient brain tissue display defects in mitochondrial bioenergetic capacity and function (Schapira et al., 1989; Schapira et al., 1990; Mallach et al., 2019).

Evidence to support the role of PINK1 in mitochondrial homeostasis also includes the association of genetic mutations of the *PINK1* gene with PD. Although most of PD patients start to develop symptoms when they reach the age over 50, early onset PD cases were also found in less than 10% of individuals with PD (Golbe, 1991). Most of these early onset cases are caused by genetic mutations, of which the autosomal recessive mutations in the *PINK1* gene were identified in early onset PD (Valente et al., 2004; Bonifati et al., 2005; Zhao et al., 2020). Biochemical analysis of PINK1 uncovers its function as a kinase that phosphorylates Parkin. Consistently, recessive mutations in the human Parkin gene were also found to cause early onset PD (Matsumine et al., 1997; Kitada et al., 1998). Furthermore, genetic studies of *Drosophila* harboring Pink1 mutations demonstrate that mitochondrial pathology caused by loss of Pink1 could be rescued by Parkin (Yang et al., 2006), establishing the theory that PINK1/Parkin act in the same pathway to protect mitochondria. Moreover, PINK1 deficiency in cellular models of PD has been reported to cause a loss of mitochondrial complex I reductive activity (Morais et al., 2014). Loss of functional mitochondrial complex I has been proved to be associated with dopaminergic cell death in PD (Surmeier et al., 2017; González-Rodríguez et al., 2021). However, complex I dysfunction is also implicated in sporadic PD, suggesting that complex I dysfunction can occur independent of PINK1 mutations.

Mitochondrial Dependent Function of PINK1

The first *in vivo* evidence indicating that PINK1 is involved in regulating mitochondrial quality control came from genetic studies in *Drosophila*, which revealed that PINK1 null mutant flies showed apoptotic muscle degeneration, mitochondrial defects, and male sterility (Clark et al., 2006). Subsequently, a

large body of biochemical studies have proved that PINK1 functions as a mitochondrial kinase. PINK1 is a 581 amino acid protein consisting of an N-terminal mitochondrial targeting motif that contains a transmembrane domain (110 amino acids long), a highly conserved kinase domain with three insertions in the N lobe, and a C-terminal autoregulatory sequence (Beilina et al., 2005; Cardona et al., 2011; Kumar et al., 2017). Mounting evidence from biochemical and *in vitro* studies indicates that PINK1 and Parkin work together in the same signaling pathway, as both proteins target damaged mitochondria to the lysosomes for clearance of the unhealthy mitochondria, a process called mitophagy (Pickrell and Youle, 2015; Ivankovic et al., 2016; Nguyen et al., 2016). The most compelling evidence to support the role of PINK1/Parkin in mitophagy is that PINK1 is targeted to mitochondria when cultured cells are under mitochondrial stress induced by the mitochondria-depolarizing agent such as CCCP (carbonyl cyanide *m*-chlorophenylhydrazine). Once PINK1 is localized on mitochondria, it phosphorylates Parkin and ubiquitin to recruit them to the damaged mitochondria, leading to the ubiquitination of mitochondrial proteins. Then the autophagic adaptor proteins such as p62/SQSTM1/sequestosome-1 were recruited to the damaged mitochondria and mediate the removal of damaged mitochondria by lysosomes (Nguyen et al., 2016). During this process, PINK1 acts as a key sensor of mitochondrial damage whereas Parkin amplifies this damage signal by facilitating the formation of ubiquitin chains, which recruit more Parkin to the damaged mitochondria (Harper et al., 2018). Further, analysis of the crystal structure of insect PINK1 bound to ubiquitin provides a structural base for the interactions of PINK1 with Parkin and ubiquitin (Kumar et al., 2017; Schubert et al., 2017; Gan et al., 2022). All these findings generate important insights into the function of PINK1 and strongly support the theory that PINK1 functions as a mitochondrial kinase and plays a pivotal role in mitophagy, an important intracellular process that is involved in a variety of cellular functions. Consistently, several lines of evidence indicate that PINK1 confers protection against mitochondria dependent apoptosis induced by both intrinsic stress and environmental insults (Gautier et al., 2008; Wang et al., 2011; Huang et al., 2017).

Investigation of the function of PINK1 for mitophagy also yield important finding that endogenous PINK1 is synthesized constitutively in the cytosol as a full-length precursor (~63–68 kDa). Upon import into mitochondria, PINK1 is proteolytically cleaved to produce its mature form (~52–55 kDa) that is subsequently re-translocated to the cytosol, resulting in a rapid turnover and low steady state levels (Liu et al., 2017). Indeed, N-terminal region of PINK1, which is responsible for targeting PINK1 to the mitochondria, contains proteolytic sites that can be cleaved by MPP (mitochondrial processing peptidase) and PARL (presenilin-associated rhomboid-like protease) successively (Jin et al., 2010; Deas et al., 2011). These cleavages release PINK1 from mitochondria to produce a cytosolic form containing the kinase domain (**Figure 1**). However, when mitochondria are damaged, PINK1 is stabilized on the mitochondrial membrane, which can

also be activated by kinetin that can amplify the catalytic activity of PINK1 (Hertz et al., 2013), to phosphorylate Parkin and ubiquitin to initiate mitophagy (Kane et al., 2014). All these findings convincingly demonstrate the mitochondrial-dependent function of PINK1 in cells. Since PINK1-mediated mitophagy is dependent on its targeting to mitochondria whereas cleavage of PINK1 via proteases can dissociate PINK1 from mitochondria and therefore inhibit PINK1's function on mitophagy, suppressing proteases activity to cleave PINK1 is presumably able to enhance PINK1-dependent mitophagy process. In this regard, small-molecule inhibitors of the mitochondrial protease PARL that can cleave PINK1 could potentially enhance the activity of PINK1-dependent mitophagy (Parsons et al., 2021).

Lack of *in vivo* evidence for PINK1-mediated mitophagy

However, most of studies of PINK1 used cultured cells or *in vitro* systems to investigate mitochondrial-dependent function of full-length PINK1 in the field. Several groups have established PINK1 KO mouse models, aiming at identifying phenotypes associated with loss of PINK1 (Table 1). However, all these rodent KO models do not recapitulate the neurodegeneration seen in PD patient brains (Kitada et al., 2007; Akundi et al., 2011; Ge et al., 2020). Although rat PINK1 KO model was initially report to show DA neuronal degeneration (Dave et al., 2014), this phenotype is not severe as that in PD patient brain and was unable to be confirmed later by a different group (de Haas et al., 2019). Although PINK1/Parkin knockout mouse models are unable to show typical PD phenotypes, Parkin knockout could increase the vulnerability of dopaminergic neurons to exhaustive exercise via STING, a central regulator of the type I interferon response to cytosolic DNA (Sliter et al., 2018), suggesting that loss of Parkin alone is not sufficient to induce neurodegeneration in mice. To rigorously investigate the *in vivo* function of PINK1 for mitophagy, a knock-in mouse model, in which the codon encoding Parkin Ser65 was mutated to Ala65 to prevent its phosphorylation by PINK1, was established but this model still showed no clear neurodegeneration or nigrostriatal mitophagy impairment (McWilliams et al., 2018a).

Another strong evidence indicating that loss of PINK1 does not impact mitochondria homeostasis is the lack of influence of PINK1 on the basal mitophagy activity in *Drosophila* and mice (McWilliams et al., 2018b; Lee et al., 2018). In the PINK1 null fly and mice, *in vivo* mitophagy assay, which was performed using mito-QC or mt-Keima as a mitophagy reporter, did not show alteration as compared with wild type animals. Although the complex I subunit NDUFA10 was found to be phosphorylated by PINK1, transgenic overexpression of NDUFA10 can rescue *Drosophila* pink1 mutants independent of mitophagy (Pogson et al., 2014). Apart from these findings, mass spectrometry analysis of PINK1 knockout rodent did not show significant alterations in the expression levels of mitochondrial proteins (Stauch et al., 2016). As for mitochondrial function studies, inconsistent or mild alterations, at least not striking as *in vitro* findings, were found among the PINK1 KO animal models (Zhuang et al., 2016; Yamada et al., 2019). Also, PINK1/

Parkin axis is not only the signaling pathway to regulate mitophagy, as growing evidence indicates the presence of PINK1/Parkin-independent mitophagy under *in vivo* or physiological conditions (Munson et al., 2021; Munson et al., 2022; Terešák et al., 2022). All these raise an important issue of whether PINK1 acts differentially *in vitro* and *in vivo* to mediate mitochondrial-dependent and independent functions.

Our recent studies using non-human primate model demonstrate for the first time that loss of PINK1 in the mammalian brain can cause neuronal loss (Table 1). We found that the deletion of the large PINK1 DNA fragment by CRISPR/Cas9 can induce neuronal loss in the developing and adult monkey brains (Yang et al., 2019a; Yang et al., 2022). The homozygous deletion of a large region of the PINK1 gene has not been found in humans, perhaps because such deletion is embryonic lethal in humans. However, CRISPR/Cas9-mediated deletion of the monkey PINK1 gene can completely eliminate the expression of PINK1 to elicit severe neurodegeneration in the non-human primate brain (Yang et al., 2019a), which also suggests that PINK1 point mutations found in patients with PD may partially impair PINK1 function to cause age-dependent neurodegeneration. One of the important findings from the non-human primate models is the striking neuronal loss without significant impact on mitochondria homeostasis (Yang et al., 2022). Also, the severe neuronal loss in the monkey brain is in clear contrast to the absence of neurodegeneration in mouse models that have completely deleted the *Pink1* gene, suggesting that PINK1's function is species-dependent.

Mitochondria Independent Function of PINK1

Although PINK1 is known to be cleaved to a truncated form by removing its N-terminal mitochondrial targeting domain, the functions of this cytosolic form of PINK1 have not been well characterized, and most of investigation focuses on the mitochondrial-dependent function of full-length PINK1 in the field. However, emerging evidence indicates that cytosolic PINK1 functions in many aspects to regulate cellular functions. In addition to PINK1-mediated phosphorylation of Parkin and ubiquitin (Eiyama and Okamoto, 2015), growing evidence indicates that the kinase activity of PINK1 spans to other substrates, including Drp1 (Han et al., 2020), TRAP1 (Pridgeon et al., 2007), Mfn2 (Chen et al., 2013), Miro (Wang et al., 2011), Bcl-xL (Arena et al., 2013), complex I subunit Ndufa10 (Morais et al., 2014), and HtrA2 (Plun-Favreau et al., 2007). Phosphorylation of these signaling molecules appears to be independent of mitochondria but important for cell survival. In line with this idea, cytosolic PINK1 can mediate neuroprotection, since PINK1 lacking the mitochondrial targeting sequences, which can be produced by proteolytic process via N-end rule pathway, protects against MPTP-induced toxicity in mice (Haque et al., 2008). In addition, cytosolic PINK1 cannot promote mitophagy (Geisler et al., 2010; Narendra et al., 2010), suggesting that the pro-survival activity of PINK1 is not related to the mitophagy-inducing activity.

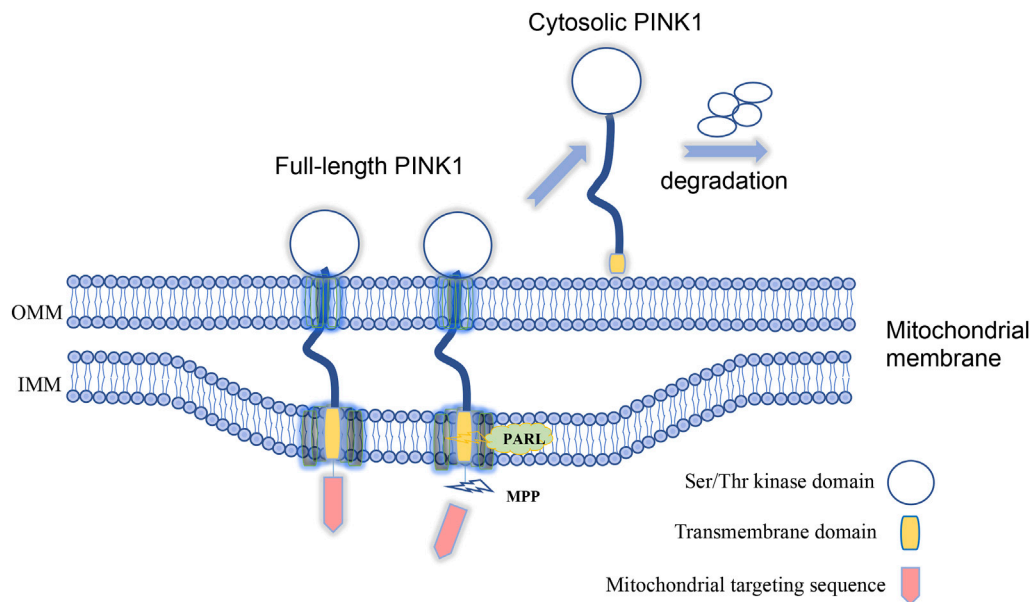
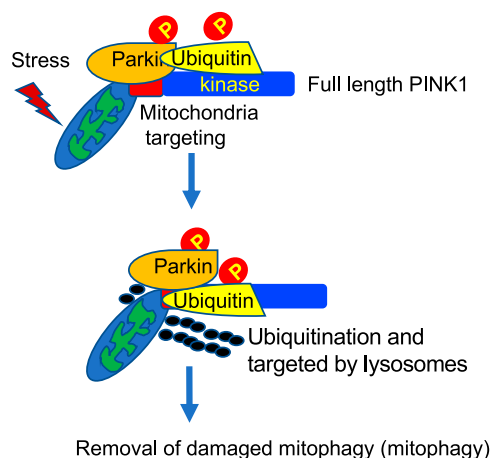


FIGURE 1 | Full-length PINK1 is able to target to mitochondria and is cleaved by proteases to generate cytosolic form of PINK1 upon mitochondria damage. Lack of *in vivo* evidence for PINK1-mediated mitophagy.

Mitochondrial dependent



Mitochondrial independent

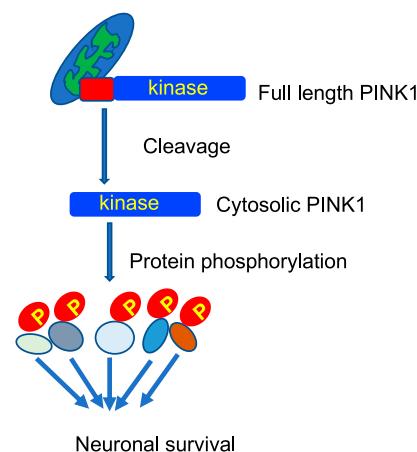


FIGURE 2 | Mitochondrial-dependent and independent functions of PINK1. In the primate brain, PINK1 can phosphorylate a large number of proteins, including those for regulating mitochondrial function, to maintain neuronal survival.

Investigation of PINK1-targeted monkey models also strongly supports the notion that PINK1 functions as a kinase *in vivo*, at least in the primate brains. Loss of PINK1 leads to marked decrease in phosphorylation of proteins that are important for neuronal survival (Yang et al., 2022). In support of this finding, the major form of PINK1 seen in the primate brain is the cytosolic form (55 kD) that lacks N-terminal region (Yang et al., 2022). This form of PINK1 contains the intact kinase domain and is presumably able to

phosphorylate proteins in a mitochondrial independent manner. Earlier studies have revealed that cytosolic PINK1 promotes neuronal plasticity and differentiation, as PINK1-deficient cortical and midbrain neurons display defective dendritic morphology, and overexpression of truncated and cytosolic PINK1 could rescue this phenotype and also induce neuronal differentiation in SH-SH5Y neuronal cells (Dagda et al., 2014). The role of PINK1 in regulating neuronal differentiation is also supported by the finding from

TABLE 1 | PINK1 knock out animal models

Model	Loss of dopaminergic neuron	Motor deficits	Mitophagy impairment	Reference
Mice	–	ND	ND	(Kitada et al., 2007)
Mice	–	ND	ND	(Akundi et al., 2011)
Rat	+	+	ND	(Dave et al., 2014)
Rat	–	+	ND	(de Haas et al., 2019)
Mice ^a	–	+	–	(McWilliams et al., 2018a)
Mice	ND	ND	–	(McWilliams et al., 2018b)
<i>Drosophila</i>	+	+	–	(Lee et al., 2018)
Rat	ND	ND	–	(Stauch et al., 2016)
Mice	ND	ND	–	(Yamada et al., 2019)
Pig	ND	ND	ND	(Zhou et al., 2015)
Pig	ND	–	ND	(Wang et al., 2016)
Monkey	+	+	–	(Yang et al., 2019a,b; Yang et al., 2022)
Monkey ^b (adult)	+	+	ND	(Li et al., 2021)

ND: not detected

^aThis model was generated by Parkin Ser65Ala (S65A) knock-in to mimic PINK1 deficiency.

^bThis model was generated by co-editing PINK1 and DJ-1.

zebrafish and human organoid models that PINK1 deficiency impedes dopaminergic neuron neurogenesis (Brown et al., 2021).

PINK1's function seems to be not restricted to the brain, as PINK1 is also upregulated in breast, colorectal, and endometrial cancer tissues, whereas PINK1 inhibition reduces cancer cell proliferation (Zhang et al., 2017). The cytosolic PINK1 has been implicated in signaling cascades critical to cell growth and survival, including the PI3-kinase (PI3K)/Akt, valosin-containing protein (VCP), and protein kinase A (PKA) pathways (Akundi et al., 2012; Soutar et al., 2018; Wang et al., 2018; Boonying et al., 2019). PINK1 deficiency in *Drosophila* is found to cause multiple growth defects independent of Parkin (Han et al., 2021). Along with the mitochondrial function of PINK1, the role of PINK1 in regulating cell cycle has also been reported, which is more likely to relate to tumor and cancer cells in which PINK1 expression is noticeably altered (O'Flanagan et al., 2015; Leites and Morais, 2018). PINK1 was initially identified as a downstream effector of phosphatase and tensin homolog (PTEN), a tumor suppressor that is frequently mutated in various types of human cancers (Unoki and Nakamura, 2001). Thus, more studies are required to investigate the mitochondrial-independent function of PINK1 and the relevance of this function to physiological and pathological scenarios.

Questions That Need to Be Addressed

The above description of mitochondrial-dependent and independent functions of PINK1 clearly indicates that PINK1 functions differently under different circumstances (Figure 2). It is difficult to reconcile the well-characterized mitophagy function of PINK1 and the absence of *in vivo* evidence for PINK1-mediated mitophagy in some animal models. It should be noted that most of *in vitro* studies of mitochondrial-dependent function of PINK1 involve overexpression of PINK1 or

exogenously transfected PINK1 in combination with a mitochondrial depolarizing agent. It has been well recognized in the field that endogenous PINK1 is unstable and is very difficult to be detected in the rodent animals. This would explain that the intrinsically very low level of endogenous PINK1 is unable to recapitulate the *in vitro* function that is induced by overexpressed PINK1 with acute or extraordinary stress on mitochondria. On the other hand, endogenous PINK1 is more abundant in the primate brain and mainly functions as a kinase to phosphorylate neuronal proteins for maintaining the survival of primate neuronal cells. Thus, expression levels of PINK1 *in vivo* and *in vitro* are highly likely to account for different functions of PINK1. Also, as full-length PINK1 is more likely to act as a mitochondrial kinase whereas its cleaved products exist in the cytosol to function independent of mitochondria, the proteolytic processing of PINK1 determines the specific function of different PINK1 forms.

PINK1 seems to be a multifaceted protein acting at the crossroads of various pathways critical for cell survival, mitochondria quality control, and cell cycle regulation. The various functions of PINK1 raise many important issues that need to be well addressed and also pose challenges to our understanding of how these functions are regulated. First, why is there species-dependent expression of PINK1, for example, why is PINK1 undetectable in mice but abundant in the primates? The regulation of PINK1 expression is more likely mediated at translational and/or protein stability level, as *PINK1* mRNA is ubiquitously and abundantly expressed across different species (Blackinton et al., 2007). However, rigorous investigation of mechanisms underlying PINK1 protein expression and cleavage *in vivo* remains to be conducted. Lack of detectable expression of PINK1 in the rodent models makes it difficult to use small mammals to explore this important issue. Large animal models have been found to provide new insights into the pathogenesis of neurodegenerative diseases (Sun et al., 2022; Yin et al.,

2022). However, the absent phenotypes of pig models that have deleted the *PINK1* gene (Zhou et al., 2015; Wang et al., 2016) suggest that endogenous PINK1 may also be expressed at a low level in the swine species. Thus, identification of the abundant expression of PINK1 kinase in the primate brains and the phenotypes due to PINK1 deficiency in the monkey model indicates that the non-human primates would be a suitable animal model for delineating the *in vivo* regulation of PINK1 expression and function.

Second, to what extent does PINK1 mitochondrial-dependent function play a role *in vivo*, especially under pathological conditions? Mitophagy has been well documented and characterized for its protection against cell death. There is no doubt that PINK1/Parkin mediates mitophagy in cultured cells, but an important and outstanding question is whether this occurs *in vivo* when PINK1/Parkin are expressed at the endogenous level and under physiological conditions. Is full-length PINK1, which is able to localize to mitochondria, or cytosolic PINK1, which loses the ability to associate with mitochondria, more important for cell survival and function, and how do these different forms of PINK1 coordinate their functions *in vivo*?

Lastly, how important is PINK1's function beyond mitochondria? Cytosolic PINK1 is evidently able to function as a kinase independent of mitochondria. Most kinases are key regulators of multiple cellular processes, and their functions and expressions are regulated by complex and sophisticated

mechanisms whereas dysregulation of their expression can lead to diseases (Burke, 2018). If PINK1's kinase function is critical for neuronal survival and differentiation, can improving its catalytic activity reduce neurodegeneration that is resulted from loss of PINK1 function? On the other hand, because PINK1 is upregulated in many tumor cells, can inhibition of its kinase activity suppress abnormal cell proliferation to treat tumorigenesis? Continued study of PINK1 beyond its mitochondrial functions may potentially shed light on novel therapeutic approaches.

AUTHOR CONTRIBUTIONS

X-JL, WY, and XC wrote the manuscript. QW and SL edited the manuscript. All discussed and approved the overall structure of the review.

FUNDING

This work was supported by The National Natural Science Foundation of China (32070534, 81830032, 31872779, 82071421, and 81873736); Guangzhou Key Research Program on Brain Science (202007030008), Department of Science and Technology of Guangdong Province (2018B030337001, 2021ZT09Y007; 2020B121201006).

REFERENCES

- Akundi, R. S., Huang, Z., Eason, J., Pandya, J. D., Zhi, L., Cass, W. A., et al. (2011). Increased Mitochondrial Calcium Sensitivity and Abnormal Expression of Innate Immunity Genes Precede Dopaminergic Defects in Pink1-Deficient Mice. *PLoS One* 6 (1), e16038. doi:10.1371/journal.pone.0016038
- Akundi, R. S., Zhi, L., and Büeler, H. (2012). PINK1 Enhances Insulin-like Growth Factor-1-dependent Akt Signaling and Protection against Apoptosis. *Neurobiol. Dis.* 45 (1), 469–478. doi:10.1016/j.nbd.2011.08.034
- Arena, G., Gelmetti, V., Torosantucci, L., Vignone, D., Lamorte, G., De Rosa, P., et al. (2013). PINK1 Protects against Cell Death Induced by Mitochondrial Depolarization, by Phosphorylating Bcl-xL and Impairing its Pro-apoptotic Cleavage. *Cell. Death Differ.* 20 (7), 920–930. doi:10.1038/cdd.2013.19
- Beilina, A., Van Der Brug, M., Ahmad, R., Kesavapany, S., Miller, D. W., Petsko, G. A., et al. (2005). Mutations in PTEN-Induced Putative Kinase 1 Associated with Recessive Parkinsonism Have Differential Effects on Protein Stability. *Proc. Natl. Acad. Sci. U.S.A.* 102 (16), 5703–5708. doi:10.1073/pnas.0500617102
- Blackinton, J. G., Anvret, A., Beilina, A., Olson, L., Cookson, M. R., and Galter, D. (2007). Expression of PINK1 mRNA in Human and Rodent Brain and in Parkinson's Disease. *Brain Res.* 1184, 10–16. doi:10.1016/j.brainres.2007.09.056
- Bloem, B. R., Okun, M. S., and Klein, C. (2021). Parkinson's Disease. *Lancet* 397 (10291), 2284–2303. doi:10.1016/s0140-6736(21)00218-x
- Bonifati, V., Rohe, C. F., Breedveld, G. J., Fabrizio, E., De Mari, M., Tassorelli, C., et al. (2005). Early-onset Parkinsonism Associated with PINK1 Mutations: Frequency, Genotypes, and Phenotypes. *Neurology* 65 (1), 87–95. doi:10.1212/01.wnl.0000167546.39375.82
- Boonying, W., Joselin, A., Huang, E., Qu, D., Safarpour, F., Iyirhiaro, G. O., et al. (2019). Pink1 regulatesFKBP5 Interaction withAKT/PHLPPand Protects Neurons from Neurotoxin Stress Induced byMPP+. *J. Neurochem.* 150 (3), 312–329. doi:10.1111/jnc.14683
- Brown, S. J., Boussaad, I., Jarazo, J., Fitzgerald, J. C., Antony, P., Keatinge, M., et al. (2021). PINK1 Deficiency Impairs Adult Neurogenesis of Dopaminergic Neurons. *Sci. Rep.* 11 (1), 6617. doi:10.1038/s41598-021-84278-7
- Burke, J. E. (2018). Structural Basis for Regulation of Phosphoinositide Kinases and Their Involvement in Human Disease. *Mol. Cell.* 71 (5), 653–673. doi:10.1016/j.molcel.2018.08.005
- Cardona, F., Sánchez-Mut, J. V., Dopazo, H., and Pérez-Tur, J. (2011). Phylogenetic and In Silico Structural Analysis of the Parkinson Disease-related Kinase PINK1. *Hum. Mutat.* 32 (4), 369–378. doi:10.1002/humu.21444
- Chen, Y., Dorn, G. W., and 2nd (2013). PINK1-phosphorylated Mitofusin 2 Is a Parkin Receptor for Culling Damaged Mitochondria. *Science* 340 (6131), 471–475. doi:10.1126/science.1231031
- Clark, I. E., Dodson, M. W., Jiang, C., Cao, J. H., Huh, J. R., Seol, J. H., et al. (2006). Drosophila Pink1 Is Required for Mitochondrial Function and Interacts Genetically with Parkin. *Nature* 441 (7097), 1162–1166. doi:10.1038/nature04779
- Dagda, R. K., Pien, I., Wang, R., Zhu, J., Wang, K. Z. Q., Callio, J., et al. (2014). Beyond the Mitochondrion: Cytosolic PINK1 Remodels Dendrites through Protein Kinase A. *J. Neurochem.* 128 (6), 864–877. doi:10.1111/jnc.12494
- Dave, K. D., De Silva, S., Sheth, N. P., Ramboz, S., Beck, M. J., Quang, C., et al. (2014). Phenotypic Characterization of Recessive Gene Knockout Rat Models of Parkinson's Disease. *Neurobiol. Dis.* 70, 190–203. doi:10.1016/j.nbd.2014.06.009
- de Haas, R., Heltzel, L. C. M. W., Tax, D., van den Broek, P., Steenbreker, H., Verheij, M. M. M., et al. (2019). To Be or Not to Be Pink(1): Contradictory Findings in an Animal Model for Parkinson's Disease. *Brain Commun.* 1 (1), fc2016. doi:10.1093/braincomms/fcz016
- Deas, E., Plun-Favreau, H., Gandhi, S., Desmond, H., Kjaer, S., Loh, S. H. Y., et al. (2011). PINK1 Cleavage at Position A103 by the Mitochondrial Protease PARL. *Hum. Mol. Genet.* 20 (5), 867–879. doi:10.1093/hmg/ddq526
- Eiyama, A., and Okamoto, K. (2015). PINK1/Parkin-mediated Mitophagy in Mammalian Cells. *Curr. Opin. Cell. Biol.* 33, 95–101. doi:10.1016/j.ccb.2015.01.002
- Fornai, F., Schlüter, O. M., Lenzi, P., Gesi, M., Ruffoli, R., Ferrucci, M., et al. (2005). Parkinson-like Syndrome Induced by Continuous MPTP Infusion: Convergent Roles of the Ubiquitin-Proteasome System and α -synuclein. *Proc. Natl. Acad. Sci. U.S.A.* 102 (9), 3413–3418. doi:10.1073/pnas.0409713102

- Gan, Z. Y., Callegari, S., Cobbald, S. A., Cotton, T. R., Mlodzianoski, M. J., Schubert, A. F., et al. (2022). Activation Mechanism of PINK1. *Nature* 602 (7896), 328–335. doi:10.1038/s41586-021-04340-2
- Gautier, C. A., Kitada, T., and Shen, J. (2008). Loss of PINK1 Causes Mitochondrial Functional Defects and Increased Sensitivity to Oxidative Stress. *Proc. Natl. Acad. Sci. U.S.A.* 105 (32), 11364–11369. doi:10.1073/pnas.0802076105
- Ge, P., Dawson, V. L., and Dawson, T. M. (2020). PINK1 and Parkin Mitochondrial Quality Control: a Source of Regional Vulnerability in Parkinson's Disease. *Mol. Neurodegener.* 15 (1), 20. doi:10.1186/s13024-020-00367-7
- Geisler, S., Holmström, K. M., Skujat, D., Fiesel, F. C., Rothfuss, O. C., Kahle, P. J., et al. (2010). PINK1/Parkin-mediated Mitophagy Is Dependent on VDAC1 and p62/SQSTM1. *Nat. Cell. Biol.* 12 (2), 119–131. doi:10.1038/ncb2012
- Golbe, L. I. (1991). Young-onset Parkinson's Disease. *Neurology* 41 (2Pt 1), 168. doi:10.1212/wnl.41.2_part_1.168
- González-Rodríguez, P., Zampese, E., Stout, K. A., Guzman, J. N., Ilijic, E., Yang, B., et al. (2021). Disruption of Mitochondrial Complex I Induces Progressive Parkinsonism. *Nature* 599 (7886), 650–656. doi:10.1038/s41586-021-04059-0
- Ham, S. J., Lee, D., Yoo, H., Jun, K., Shin, H., and Chung, J. (2020). Decision between Mitophagy and Apoptosis by Parkin via VDAC1 Ubiquitination. *Proc. Natl. Acad. Sci. U.S.A.* 117 (8), 4281–4291. doi:10.1073/pnas.1909814117
- Han, H., Tan, J., Wang, R., Wan, H., He, Y., Yan, X., et al. (2020). PINK 1 Phosphorylates Drp1 S616 to Regulate Mitophagy-independent Mitochondrial Dynamics. *EMBO Rep.* 21 (8), e48686. doi:10.15252/embr.201948686
- Han, Y., Zhuang, N., and Wang, T. (2021). Roles of PINK1 in Regulation of Systemic Growth Inhibition Induced by Mutations of PTEN in *Drosophila*. *Cell. Rep.* 34 (12), 108875. doi:10.1016/j.celrep.2021.108875
- Haque, M. E., Thomas, K. J., D'Souza, C., Callaghan, S., Kitada, T., Slack, R. S., et al. (2008). Cytoplasmic Pink1 Activity Protects Neurons from Dopaminergic Neurotoxin MPTP. *Proc. Natl. Acad. Sci. U.S.A.* 105 (5), 1716–1721. doi:10.1073/pnas.0705363105
- Harper, J. W., Ordureau, A., and Heo, J.-M. (2018). Building and Decoding Ubiquitin Chains for Mitophagy. *Nat. Rev. Mol. Cell. Biol.* 19 (2), 93–108. doi:10.1038/nrm.2017.129
- Hertz, N. T., Berthet, A., Sos, M. L., Thorn, K. S., Burlingame, A. L., Nakamura, K., et al. (2013). A Neo-Substrate that Amplifies Catalytic Activity of Parkinson's-Disease-Related Kinase PINK1. *Cell* 154 (4), 737–747. doi:10.1016/j.cell.2013.07.030
- Huang, E., Qu, D., Huang, T., Rizzi, N., Boonying, W., Krolak, D., et al. (2017). PINK1-mediated Phosphorylation of LETM1 Regulates Mitochondrial Calcium Transport and Protects Neurons against Mitochondrial Stress. *Nat. Commun.* 8 (1), 1399. doi:10.1038/s41467-017-01435-1
- Ishihara-Paul, L., Hulihan, M. M., Kachergus, J., Upmanyu, R., Warren, L., Amouri, R., et al. (2008). PINK1 Mutations and Parkinsonism. *Neurology* 71 (12), 896–902. doi:10.1212/01.wnl.0000323812.40708.1f
- Ivankovic, D., Chau, K. Y., Schapira, A. H. V., and Gegg, M. E. (2016). Mitochondrial and Lysosomal Biogenesis Are Activated Following PINK 1/ parkin-mediated Mitophagy. *J. Neurochem.* 136 (2), 388–402. doi:10.1111/jnc.13412
- Jin, S. M., Lazarou, M., Wang, C., Kane, L. A., Narendra, D. P., and Youle, R. J. (2010). Mitochondrial Membrane Potential Regulates PINK1 Import and Proteolytic Destabilization by PARL. *J. Cell. Biol.* 191 (5), 933–942. doi:10.1083/jcb.201008084
- Kalia, L. V., and Lang, A. E. (2015). Parkinson's Disease. *Lancet* 386 (9996), 896–912. doi:10.1016/s0140-6736(14)61393-3
- Kane, L. A., Lazarou, M., Fogel, A. I., Li, Y., Yamano, K., Sarraf, S. A., et al. (2014). PINK1 Phosphorylates Ubiquitin to Activate Parkin E3 Ubiquitin Ligase Activity. *J. Cell. Biol.* 205 (2), 143–153. doi:10.1083/jcb.201402104
- Kitada, T., Asakawa, S., Hattori, N., Matsumine, H., Yamamura, Y., Minoshima, S., et al. (1998). Mutations in the Parkin Gene Cause Autosomal Recessive Juvenile Parkinsonism. *Nature* 392 (6676), 605–608. doi:10.1038/33416
- Kitada, T., Pisani, A., Porter, D. R., Yamaguchi, H., Tschertner, A., Martella, G., et al. (2007). Impaired Dopamine Release and Synaptic Plasticity in the Striatum of PINK1-deficient Mice. *Proc. Natl. Acad. Sci. U.S.A.* 104 (27), 11441–11446. doi:10.1073/pnas.0702171104
- Koyano, F., Okatsu, K., Kosako, H., Tamura, Y., Go, E., Kimura, M., et al. (2014). Ubiquitin Is Phosphorylated by PINK1 to Activate Parkin. *Nature* 510 (7503), 162–166. doi:10.1038/nature13392
- Kumar, A., Tamjar, J., Waddell, A. D., Woodroof, H. I., Raimi, O. G., Shaw, A. M., et al. (2017). Structure of PINK1 and Mechanisms of Parkinson's Disease-Associated Mutations. *Elife* 6. doi:10.7554/eLife.29985
- Lee, J. J., Sanchez-Martinez, A., Zarate, A. M., Benincá, C., Mayor, U., Clague, M. J., et al. (2018). Basal Mitophagy Is Widespread in *Drosophila* but Minimally Affected by Loss of Pink1 or Parkin. *J. Cell. Biol.* 217 (5), 1613–1622. doi:10.1083/jcb.201801044
- Leites, E. P., and Morais, V. A. (2018). Mitochondrial Quality Control Pathways: PINK1 Acts as a Gatekeeper. *Biochem. Biophysical Res. Commun.* 500 (1), 45–50. doi:10.1016/j.bbrc.2017.06.096
- Li, H., Wu, S., Ma, X., Li, X., Cheng, T., Chen, Z., et al. (2021). Co-editing PINK1 and DJ-1 Genes via Adeno-Associated Virus-Delivered CRISPR/Cas9 System in Adult Monkey Brain Elicits Classical Parkinsonian Phenotype. *Neurosci. Bull.* 37 (9), 1271–1288. doi:10.1007/s12264-021-00732-6
- Liu, Y., Guardia-Laguarta, C., Yin, J., Erdjument-Bromage, H., Martin, B., James, M., et al. (2017). The Ubiquitination of PINK1 Is Restricted to its Mature 52-kDa Form. *Cell. Rep.* 20 (1), 30–39. doi:10.1016/j.celrep.2017.06.022
- Mallach, A., Weinert, M., Arthur, J., Geric, D., Tierney, T. S., and Alavian, K. N. (2019). Post Mortem Examination of Parkinson's Disease Brains Suggests Decline in Mitochondrial Biomass, Reversed by Deep Brain Stimulation of Subthalamic Nucleus. *FASEB J.* 33 (6), 6957–6961. doi:10.1096/fj.201802628R
- Matsuda, N., Sato, S., Shiba, K., Okatsu, K., Saisho, K., Gautier, C. A., et al. (2010). PINK1 Stabilized by Mitochondrial Depolarization Recruits Parkin to Damaged Mitochondria and Activates Latent Parkin for Mitophagy. *J. Cell. Biol.* 189 (2), 211–221. doi:10.1083/jcb.200910140
- Matsumine, H., Saito, M., Shimoda-Matsubayashi, S., Tanaka, H., Ishikawa, A., Nakagawa-Hattori, Y., et al. (1997). Localization of a Gene for an Autosomal Recessive Form of Juvenile Parkinsonism to Chromosome 6q25.2-27. *Am. J. Hum. Genet.* 60 (3), 588–596.
- McLelland, G.-L., Soubannier, V., Chen, C. X., McBride, H. M., and Fon, E. A. (2014). Parkin and PINK1 Function in a Vesicular Trafficking Pathway Regulating Mitochondrial Quality Control. *Embo J.* 33 (4), a–n. doi:10.1002/emboj.201385902
- McWilliams, T. G., Barini, E., Pohjolan-Pirhonen, R., Brooks, S. P., Singh, F., Burel, S., et al. (2018a). Phosphorylation of Parkin at Serine 65 Is Essential for its Activation *In Vivo*. *Open Biol.* 8 (11), 180108. doi:10.1098/rsob.180108
- McWilliams, T. G., Prescott, A. R., Montava-Garriga, L., Ball, G., Singh, F., Barini, E., et al. (2018b). Basal Mitophagy Occurs Independently of PINK1 in Mouse Tissues of High Metabolic Demand. *Cell. Metab.* 27 (2), 439–449. e435. doi:10.1016/j.cmet.2017.12.008
- Morais, V. A., Haddad, D., Craessaerts, K., De Bock, P.-J., Swerts, J., Vilain, S., et al. (2014). PINK1 Loss-Of-Function Mutations Affect Mitochondrial Complex I Activity via Ndufa10 Ubiquinone Uncoupling. *Science* 344 (6180), 203–207. doi:10.1126/science.1249161
- Munson, M. J., Mathai, B. J., Ng, M. Y. W., Trachsel-Moncho, L., de la Ballina, L. R., Schultz, S. W., et al. (2021). GAK and PRKCD Are Positive Regulators of PRKN-independent Mitophagy. *Nat. Commun.* 12 (1), 6101. doi:10.1038/s41467-021-26331-7
- Munson, M. J., Mathai, B. J., Ng, M. Y. W., Trachsel-Moncho, L., de la Ballina, L. R., and Simonsen, A. (2022). GAK and PRKCD Kinases Regulate Basal Mitophagy. *Autophagy* 18 (2), 467–469. doi:10.1080/15548627.2021.2015154
- Narendra, D. P., Jin, S. M., Tanaka, A., Suen, D.-F., Gautier, C. A., Shen, J., et al. (2010). PINK1 Is Selectively Stabilized on Impaired Mitochondria to Activate Parkin. *PLoS Biol.* 8 (1), e1000298. doi:10.1371/journal.pbio.1000298
- Nguyen, T. N., Padman, B. S., and Lazarou, M. (2016). Deciphering the Molecular Signals of PINK1/Parkin Mitophagy. *Trends Cell. Biol.* 26 (10), 733–744. doi:10.1016/j.tcb.2016.05.008
- O'Flanagan, C. H., Bowers, L. W., and Hursting, S. D. (2015). A Weighty Problem: Metabolic Perturbations and the Obesity-Cancer Link. *Horm. Mol. Biol. Clin. Invest.* 23 (2), 47–57. doi:10.1515/hmbci-2015-0022
- Parsons, W. H., Rutland, N. T., Crainic, J. A., Cardozo, J. M., Chow, A. S., Andrews, C. L., et al. (2021). Development of Succinimide-Based Inhibitors for the Mitochondrial Rhomboid Protease PARL. *Bioorg. Med. Chem. Lett.* 49, 128290. doi:10.1016/j.bmcl.2021.128290
- Pickrell, A. M., and Youle, R. J. (2015). The Roles of PINK1, Parkin, and Mitochondrial Fidelity in Parkinson's Disease. *Neuron* 85 (2), 257–273. doi:10.1016/j.neuron.2014.12.007

- Plun-Favreau, H., Klupsch, K., Moiso, N., Gandhi, S., Kjaer, S., Frith, D., et al. (2007). The Mitochondrial Protease HtrA2 Is Regulated by Parkinson's Disease-Associated Kinase PINK1. *Nat. Cell. Biol.* 9 (11), 1243–1252. doi:10.1038/ncb1644
- Pogson, J. H., Ivatt, R. M., Sanchez-Martinez, A., Tufi, R., Wilson, E., Mortiboys, H., et al. (2014). The Complex I Subunit NDUFA10 Selectively Rescues *Drosophila* Pink1 Mutants through a Mechanism Independent of Mitophagy. *PLoS Genet.* 10 (11), e1004815. doi:10.1371/journal.pgen.1004815
- Pridgeon, J. W., Olzmann, J. A., Chin, L.-S., and Li, L. (2007). PINK1 Protects against Oxidative Stress by Phosphorylating Mitochondrial Chaperone TRAP1. *PLoS Biol.* 5 (7), e172. doi:10.1371/journal.pbio.0050172
- Schapira, A. H. V., Cooper, J. M., Dexter, D., Jenner, P., Clark, J. B., and Marsden, C. D. (1989). Mitochondrial Complex I Deficiency in Parkinson's Disease. *Lancet* 333 (8649), 1269. doi:10.1016/s0140-6736(89)92366-0
- Schapira, A. H. V., Holt, I. J., Sweeney, M., Harding, A. E., Jenner, P., and Marsden, C. D. (1990). Mitochondrial DNA Analysis in Parkinson's Disease. *Mov. Disord.* 5 (4), 294–297. doi:10.1002/mds.870050406
- Schubert, A. F., Gladkova, C., Pardon, E., Wagstaff, J. L., Freund, S. M. V., Steyaert, J., et al. (2017). Structure of PINK1 in Complex with its Substrate Ubiquitin. *Nature* 552 (7683), 51–56. doi:10.1038/nature24645
- Sliter, D. A., Martinez, J., Hao, L., Chen, X., Sun, N., Fischer, T. D., et al. (2018). Parkin and PINK1 Mitigate STING-Induced Inflammation. *Nature* 561 (7722), 258–262. doi:10.1038/s41586-018-0448-9
- Soutar, M. P. M., Kempthorne, L., Miyakawa, S., Annuario, E., Melandri, D., Harley, J., et al. (2018). AKT Signalling Selectively Regulates PINK1 Mitophagy in SHSY5Y Cells and Human iPSC-Derived Neurons. *Sci. Rep.* 8 (1), 8855. doi:10.1038/s41598-018-26949-6
- Stauch, K. L., Villeneuve, L. M., Purnell, P. R., Pandey, S., Guda, C., and Fox, H. S. (2016). SWATH-MS Proteome Profiling Data Comparison of DJ-1, Parkin, and PINK1 Knockout Rat Striatal Mitochondria. *Data Brief* 9, 589–593. doi:10.1016/j.dib.2016.09.031
- Sun, Z., Ye, J., and Yuan, J. (2022). PINK1 Mediates Neuronal Survival in Monkey. *Protein Cell.* 13 (1), 4–5. doi:10.1007/s13238-021-00889-w
- Surmeier, D. J., Obeso, J. A., and Halliday, G. M. (2017). Selective Neuronal Vulnerability in Parkinson Disease. *Nat. Rev. Neurosci.* 18 (2), 101–113. doi:10.1038/nrn.2016.178
- Terešák, P., Lapao, A., Subic, N., Boya, P., Elazar, Z., and Simonsen, A. (2022). Regulation of PRKN-independent Mitophagy. *Autophagy* 18 (1), 24–39. doi:10.1080/15548627.2021.1888244
- Tolosa, E., Wenning, G., and Poewe, W. (2006). The Diagnosis of Parkinson's Disease. *Lancet Neurology* 5 (1), 75–86. doi:10.1016/s1474-4422(05)70285-4
- Unoki, M., and Nakamura, Y. (2001). Growth-suppressive Effects of BPOZ and EGR2, Two Genes Involved in the PTEN Signaling Pathway. *Oncogene* 20 (33), 4457–4465. doi:10.1038/sj.onc.1204608
- Valente, E. M., Abou-Sleiman, P. M., Caputo, V., Muqit, M. M. K., Harvey, K., Gispert, S., et al. (2004). Hereditary Early-Onset Parkinson's Disease Caused by Mutations in PINK1. *Science* 304 (5674), 1158–1160. doi:10.1126/science.1096284
- Wang, K. Z. Q., Steer, E., Otero, P. A., Bateman, N. W., Cheng, M. H., Scott, A. L., et al. (2018). PINK1 Interacts with VCP/p97 and Activates PKA to Promote NSF1/Cp47 Phosphorylation and Dendritic Arborization in Neurons. *eNeuro* 5 (6), 0466–518. doi:10.1523/eneuro.0466-18.2018
- Wang, X., Cao, C., Huang, J., Yao, J., Hai, T., Zheng, Q., et al. (2016). One-step Generation of Triple Gene-Targeted Pigs Using CRISPR/Cas9 System. *Sci. Rep.* 6, 20620. doi:10.1038/srep20620
- Wang, X., Winter, D., Ashrafi, G., Schlehe, J., Wong, Y. L., Selkoe, D., et al. (2011). PINK1 and Parkin Target Miro for Phosphorylation and Degradation to Arrest Mitochondrial Motility. *Cell.* 147 (4), 893–906. doi:10.1016/j.cell.2011.10.018
- Yamada, T., Dawson, T. M., Yanagawa, T., Iijima, M., and Sesaki, H. (2019). SQSTM1/p62 Promotes Mitochondrial Ubiquitination Independently of PINK1 and PRKN/parkin in Mitophagy. *Autophagy* 15 (11), 2012–2018. doi:10.1080/15548627.2019.1643185
- Yang, W., Guo, X., Tu, Z., Chen, X., Han, R., Liu, Y., et al. (2022). PINK1 Kinase Dysfunction Triggers Neurodegeneration in the Primate Brain without Impacting Mitochondrial Homeostasis. *Protein Cell.* 13 (1), 26–46. doi:10.1007/s13238-021-00888-x
- Yang, W., Li, S., and Li, X.-J. (2019a). A CRISPR Monkey Model Unravels a Unique Function of PINK1 in Primate Brains. *Mol. Neurodegener.* 14 (1), 17. doi:10.1186/s13024-019-0321-9
- Yang, W., Liu, Y., Tu, Z., Xiao, C., Yan, S., Ma, X., et al. (2019b). CRISPR/Cas9-mediated PINK1 Deletion Leads to Neurodegeneration in Rhesus Monkeys. *Cell. Res.* 29 (4), 334–336. doi:10.1038/s41422-019-0142-y
- Yang, Y., Gehrke, S., Imai, Y., Huang, Z., Ouyang, Y., Wang, J.-W., et al. (2006). Mitochondrial Pathology and Muscle and Dopaminergic Neuron Degeneration Caused by Inactivation of *Drosophila* Pink1 Is Rescued by Parkin. *Proc. Natl. Acad. Sci. U.S.A.* 103 (28), 10793–10798. doi:10.1073/pnas.0602493103
- Yin, P., Li, S., Li, X. J., Yang, W., et al. (2022). New Pathogenic Insights from Large Animal Models of Neurodegenerative Diseases. *Protein Cell.* doi:10.1007/s13238-022-00912-8
- Zhang, R., Gu, J., Chen, J., Ni, J., Hung, J., Wang, Z., et al. (2017). High Expression of PINK1 Promotes Proliferation and Chemoresistance of NSCLC. *Oncol. Rep.* 37 (4), 2137–2146. doi:10.3892/or.2017.5486
- Zhao, Y., Qin, L., Pan, H., Liu, Z., Jiang, L., He, Y., et al. (2020). The Role of Genetics in Parkinson's Disease: a Large Cohort Study in Chinese Mainland Population. *Brain* 143 (7), 2220–2234. doi:10.1093/brain/awaa167
- Zhou, X., Xin, J., Fan, N., Zou, Q., Huang, J., Ouyang, Z., et al. (2015). Generation of CRISPR/Cas9-mediated Gene-Targeted Pigs via Somatic Cell Nuclear Transfer. *Cell. Mol. Life Sci.* 72 (6), 1175–1184. doi:10.1007/s00018-014-1744-7
- Zhuang, N., Li, L., Chen, S., and Wang, T. (2016). PINK1-dependent Phosphorylation of PINK1 and Parkin Is Essential for Mitochondrial Quality Control. *Cell. Death Dis.* 7 (12), e2501. doi:10.1038/cddis.2016.396

Conflict of Interest: The authors declare that the research was conducted in the absence of any commercial or financial relationships that could be construed as a potential conflict of interest.

Publisher's Note: All claims expressed in this article are solely those of the authors and do not necessarily represent those of their affiliated organizations, or those of the publisher, the editors and the reviewers. Any product that may be evaluated in this article, or claim that may be made by its manufacturer, is not guaranteed or endorsed by the publisher.

Copyright © 2022 Chen, Wang, Li, Li and Yang. This is an open-access article distributed under the terms of the Creative Commons Attribution License (CC BY). The use, distribution or reproduction in other forums is permitted, provided the original author(s) and the copyright owner(s) are credited and that the original publication in this journal is cited, in accordance with accepted academic practice. No use, distribution or reproduction is permitted which does not comply with these terms.

Advantages of publishing in Frontiers



OPEN ACCESS

Articles are free to read
for greatest visibility
and readership



FAST PUBLICATION

Around 90 days
from submission
to decision



HIGH QUALITY PEER-REVIEW

Rigorous, collaborative,
and constructive
peer-review



TRANSPARENT PEER-REVIEW

Editors and reviewers
acknowledged by name
on published articles

Frontiers

Avenue du Tribunal-Fédéral 34
1005 Lausanne | Switzerland

Visit us: www.frontiersin.org

Contact us: frontiersin.org/about/contact



REPRODUCIBILITY OF RESEARCH

Support open data
and methods to enhance
research reproducibility



DIGITAL PUBLISHING

Articles designed
for optimal readership
across devices



FOLLOW US

@frontiersin



IMPACT METRICS

Advanced article metrics
track visibility across
digital media



EXTENSIVE PROMOTION

Marketing
and promotion
of impactful research



LOOP RESEARCH NETWORK

Our network
increases your
article's readership